

CONTRIBUTORS TO THIS VOLUME

M. J. Atherton

R. P. Burns

J. H. Holloway

H. Donald B. Jenkins

C. A. McAuliffe

Joan Mason

Kenneth F. Pratt

Reg H. Prince

H. W. Roesky

G. Stedman

Advances in
INORGANIC CHEMISTRY
AND
RADIOCHEMISTRY

EDITORS

H. J. EMELÉUS

A. G. SHARPE

*University Chemical Laboratory
Cambridge, England*

VOLUME 22

1979

ACADEMIC PRESS



New York San Francisco London

A Subsidiary of Harcourt Brace Jovanovich, Publishers

COPYRIGHT © 1979, BY ACADEMIC PRESS, INC.

ALL RIGHTS RESERVED.

NO PART OF THIS PUBLICATION MAY BE REPRODUCED OR
TRANSMITTED IN ANY FORM OR BY ANY MEANS, ELECTRONIC
OR MECHANICAL, INCLUDING PHOTOCOPY, RECORDING, OR ANY
INFORMATION STORAGE AND RETRIEVAL SYSTEM, WITHOUT
PERMISSION IN WRITING FROM THE PUBLISHER.

ACADEMIC PRESS, INC.

111 Fifth Avenue, New York, New York 10003

United Kingdom Edition published by
ACADEMIC PRESS, INC. (LONDON) LTD.
24/28 Oval Road, London NW1 7DX

LIBRARY OF CONGRESS CATALOG CARD NUMBER: 59-7692

ISBN 0-12-023622-2

PRINTED IN THE UNITED STATES OF AMERICA

79 80 81 82 9 8 7 6 5 4 3 2 1

LIST OF CONTRIBUTORS

Numbers in parentheses indicate the pages on which the authors' contributions begin.

- M. J. ATHERTON (171), *Springfields, British Nuclear Fuels Limited, Salwick, Preston PR4 0XN, Lancashire, England*
- R. P. BURNS (303), *Department of Chemistry, University of Manchester, Institute of Sciences and Technology, Manchester M60 1QD, United Kingdom*
- J. H. HOLLOWAY (171), *Department of Chemistry, The University, Leicester LE1 7RH, England*
- H. DONALD B. JENKINS (1), *Department of Molecular Sciences, University of Warwick, Coventry CV4 7AL, Warwickshire, United Kingdom*
- C. A. MCAULIFFE (303), *Department of Chemistry, University of Manchester, Institute of Sciences and Technology, Manchester M60 1QD, United Kingdom*
- JOAN MASON (199), *Open University, Milton Keynes MK7 6AA, Buckinghamshire, England*
- KENNETH F. PRATT (1), *Department of Molecular Sciences, University of Warwick, Coventry CV4 7AL, Warwickshire, United Kingdom*
- REG H. PRINCE (349), *University Chemical Laboratory, Cambridge, United Kingdom*
- H. W. ROESKY (239), *Institute of Inorganic Chemistry, University of Frankfurt, Frankfurt, West Germany*
- G. STEDMAN (113), *Department of Chemistry, University College of Swansea, Singleton Park, Swansea SA2 8PP, England*

LATTICE ENERGIES AND THERMOCHEMISTRY OF HEXAHALOMETALLATE(IV) COMPLEXES, A_2MX_6 , WHICH POSSESS THE ANTIFLUORITE STRUCTURE

H. DONALD B. JENKINS AND KENNETH F. PRATT

Department of Molecular Sciences, University of Warwick, Coventry, Warwickshire, U.K.

I. Introduction	2
A. Thermochemical Cycle.	2
B. Bond Strength	6
C. Scope of Review	7
II. Rigorous Lattice-Energy Calculation for A_2MX_6 Salts	10
A. Theory	10
B. Charge Distribution in MX_6^{2-} Ions	17
III. Estimated Lattice Energies	17
IV. Thermochemical Data	22
V. Computations of Lattice Energies and Associated Data	24
A. Format	24
B. Titanium(IV), Zirconium(IV), and Hafnium(IV) Salts	25
C. Niobium(IV) and Tantalum(IV) Salts	36
D. Chromium(IV), Molybdenum(IV), and Tungsten(IV) Salts	40
E. Manganese(IV), Technetium(IV), and Rhenium(IV) Salts	48
F. Ruthenium(IV), Osmium(IV), Cobalt(IV), Iridium(IV), Nickel(IV), Palladium(IV), and Platinum(IV) Salts	56
G. Silicon(IV), Germanium(IV), Tin(IV), and Lead(IV) Salts	70
H. Antimony(IV) Salts	84
1. Selenium(IV), Tellurium(IV), and Polonium(IV) Salts	84
VI. Summary Tabulation of Rigorous Calculations	93
VII. Summary Tabulation of Derived Estimates	93
VIII. Discussion	93
A. Introduction	93
B. Charge Distributions	94
C. Comparison of Lattice Energies Generated with Literature Values	95
D. Enthalpies of Formation of Ions from Standard States, $\Delta H_f(MX_6^{2-})(g)$	96
E. Enthalpies of Hydration of Ions, $\Delta H_{hyd}^0(MX_6^{2-})(g)$	100
F. Halide Ion Affinities	101
G. Bond Strengths	103
IX. Concluding Remarks	104
References	105

X. Appendix	107
Appendix References	111

I. Introduction

Salts having the general formula A_2MX_6 are formed by both transition and main-group elements (M) in the formal oxidation state (IV), where A is an alkali metal, thallium, or ammonium and X is a halogen. Accordingly, a study of such salts, in this chapter confined to those having the antiferite (K_2PtCl_6) structure, generates interesting data embracing a wide section of the periodic table. This chapter concerns the role lattice energy plays in the thermochemistry of these salts.

Since this chapter went to press a similar study of the lattice energies of salts of general formula A_2MX_6 possessing noncubic structures has been made and will appear shortly (40a).

This study describes the attention that lattice energies of A_2MX_6 salts have received to date in the literature, reports some recent studies from this laboratory of the lattice energies of such salts as calculated using a new minimization procedure (38, 39), and, on the basis of these latter results, also presents estimates of the lattice energies of A_2MX_6 salts where M = Hf, Nb, Ta, Ru, and Sb to complete the study. All the salts considered (with the exception of a handful for which we estimate the lattice energy from thermochemical data) for which we have carried out an accurate evaluation of the lattice energy possess the antiferite (K_2PtCl_6) structure, having a unit cell length a_0 and an M—X bond distance d ($d = u.a_0$) as the only variants from structure to structure.

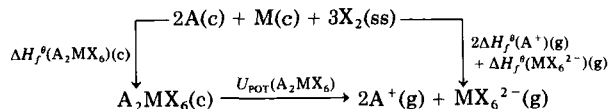
Lattice energies have been the subject of isolated studies (16, 19, 22, 29, 36, 40, 51, 53, 68–70) for isolated salts over the last decade and a half. Figure 1 represents the situation prior to the study that is the main subject of this article.

Figure 1 gives the salts, in periodic order, for which lattice energies had been reported prior to the commencement of this present study.

Table I gives the detailed results and references associated with Fig. 1 and indicates the type of calculation used to establish the lattice of the twenty-two A_2MX_6 salts considered.

A. THERMOCHEMICAL CYCLE

Incorporating the lattice energy into the Born–Fajans–Haber cycle:



							IVB	VB	VIB
IVA	VA	VIA	VIIA	← VIII →					
							Cs ₂ GeCl ₆		
K ₂ ZrCl ₆	K ₂ NbCl ₆ Rb ₂ NbCl ₆ Cs ₂ NbCl ₆	Na ₂ MoCl ₆ K ₂ MoCl ₆ Rb ₂ MoCl ₆ Cs ₂ NbCl ₆				K ₂ PdCl ₆	K ₂ SnCl ₆ Rb ₂ SnCl ₆		Rb ₂ TeCl ₆
K ₂ HfCl ₆	K ₂ TaCl ₆ Rb ₂ TaCl ₆ Cs ₂ TaCl ₆		K ₂ ReCl ₆ Cs ₂ ReCl ₆ Cs ₂ ReBr ₆		(NH ₄) ₂ IrCl ₆	K ₂ PtCl ₆ K ₂ PtBr ₆ K ₂ PtI ₆ Cs ₂ PtCl ₆ (NH ₄) ₂ PtCl ₆ (NH ₄) ₂ PtBr ₆	Rb ₂ PbCl ₆		

FIG. 1. Calculated and estimated lattice energies for A₂MX₆ salts: pre-1977.

TABLE I

LATTICE ENERGY CALCULATIONS FOR A_2MX_6 SALTS, PRE-1977. ENERGIES IN kJ mol^{-1a}

4	Complex Ion	Counter Ion	Webster	Efimov	Tsintsius	Hartley		Lister (53) <i>et al.</i>						Welsh	Lal	Gelbman	Jenkins	Burgess	De	Jenkins	Makhija
			and Collins (69) 1963 (j)	and Belorukova (19) 1967 (g)	and Smirnova (68) 1969 (g)	(29) 1972 (b)	(c)	(d)	(e)	(e)	(f)	(c)	(g)	<i>et al.</i> (70) 1974 (j)	West- land (51) 1974 (c)	and West- land (22) 1975 (a)	and Smith (40) 1975 (k)	and Cart- wright (10a) 1975 (b)	Jonge (16) 1976 (e)	(36) 1976 (h)	and Westland (54a) 1977 (c)
	ZrCl ₆ ²⁻	K ⁺	—	—	—	—	—	—	—	—	—	—	—	—	(1571)	—	—	—	—	—	
	ZrBr ₆ ²⁻	K ⁺	—	—	—	—	—	—	—	—	—	—	—	—	—	—	—	—	—	1501	
		Cs ⁺	—	—	—	—	—	—	—	—	—	—	—	—	—	—	—	—	—	1464	
	HfCl ₆ ²⁻	K ⁺	—	—	—	—	—	—	—	—	—	—	—	—	(1574)	—	—	—	—	—	
	HfBr ₆ ²⁻	Cs ⁺	—	—	—	—	—	—	—	—	—	—	—	—	—	—	—	—	—	1464	
	NbCl ₆ ²⁻	K ⁺	—	—	—	—	—	—	—	—	—	—	—	1586	—	—	—	—	—	—	
		Rb ⁺	—	—	—	—	—	—	—	—	—	—	—	1569	—	—	—	—	—	—	
		Cs ⁺	—	—	—	—	—	—	—	—	—	—	—	1540	—	—	—	—	—	—	
	TaCl ₆ ²⁻	K ⁺	—	—	1582	—	—	—	—	—	—	—	—	1586	—	—	—	—	—	—	
		Rb ⁺	—	—	1565	—	—	—	—	—	—	—	—	1569	—	—	—	—	—	—	
		Cs ⁺	—	—	1540	—	—	—	—	—	—	—	—	1540	—	—	—	—	—	—	
	MoCl ₆ ²⁻	Na ⁺	—	1638	—	—	—	—	—	—	—	—	—	—	—	—	—	—	—	—	
		K ⁺	—	1602	—	—	—	—	—	—	—	—	—	—	—	—	—	—	—	—	
		Rb ⁺	—	1567	—	—	—	—	—	—	—	—	—	—	—	—	—	—	—	—	
		Cs ⁺	—	1537	—	—	—	—	—	—	—	—	—	—	—	—	—	—	—	—	
	ReCl ₆ ²⁻	K ⁺	—	—	—	—	—	1448	1231	1170	1437	1555	1508	—	—	—	1506	—	—	—	
		Cs ⁺	—	—	—	—	—	—	—	—	—	—	—	—	—	—	1453	—	—	—	

ReBr ₆ ²⁻	Cs ⁺	—	—	—	—	—	—	—	—	—	—	—	—	—	—	—	1399	—	—	—
IrCl ₆ ²⁻	NH ₄ ⁺	—	—	—	—	—	—	—	—	—	—	—	—	—	—	—	1505	—	—	—
PdCl ₆ ²⁻	K ⁺	—	—	—	1519	1573	—	—	—	—	—	—	—	—	—	—	—	—	—	—
PtCl ₆ ²⁻	K ⁺	—	—	—	1540	1598	1461	1327	1274	1450	1572	1521	—	—	—	—	1521	{1323 ^b	—	—
	Cs ⁺	—	—	—	—	—	—	—	—	—	—	—	—	—	—	—	1459	{1337	1468	—
	NH ₄ ⁺	—	—	—	—	—	—	—	—	—	—	—	—	—	—	—	1507	—	—	—
PtBr ₆ ²⁻	K ⁺	—	—	—	1452	1506	1388	—	1301	1377	1498	1445	—	—	—	—	1451	1299	—	—
	NH ₄	—	—	—	—	—	—	—	—	—	—	—	—	—	—	—	1439	—	—	—
PtI ₆ ²⁻	K ⁺	—	—	—	—	—	1264	—	—	—	1421	1317	—	—	—	—	—	—	—	—
GeCl ₆ ²⁻	Cs ⁺	—	—	—	—	—	—	—	—	—	—	—	1404	—	—	—	—	—	—	—
SnCl ₆ ²⁻	K ⁺	—	—	—	—	—	1425	—	—	1414	1533	1484	1370	—	(1586)	—	—	—	—	—
	Rb ⁺	1551	—	—	—	—	—	—	—	—	—	—	—	—	—	1259	—	—	—	—
SnBr ₆ ²⁻	K ⁺	—	—	—	—	—	—	—	—	—	—	—	—	—	—	—	—	—	—	1505
PbCl ₆ ²⁻	Kb ⁺	—	—	—	—	—	—	—	—	—	—	—	1335	—	—	—	—	—	—	—
TeCl ₆ ²⁻	Rb ⁺	1578	—	—	—	—	—	—	—	—	—	—	—	—	—	1197	—	—	—	—

^a Column heads: (a) Estimated from lattice energies calculated in reference 51 using relationships proposed in Gelbman and Westland (22). (b) Born-Mayer equation (6). (c) Kapustinskii equation (46). (d) Empirical. (e) Extended Born-Lande equation (5). (f) Simple Born-Lande equation (5). (g) Alternative Kapustinskii equation (46). (h) Direct minimization equation (35). (j) Wood's method (2, 18, 21, 72, 73). (k) Extended Huggins and Mayer equation (33).

^b As corrected by DeJonge (17).

where (ss) indicates standard state (for $A = \text{NH}_4$ we must replace $U_{\text{POT}}(A_2\text{MX}_6)$ by $\{U_{\text{POT}}[(\text{NH}_4)_2\text{MX}_6] + 3RT\}$, the following equations are generated:

$$U_{\text{POT}}(A_2\text{MX}_6) = 2\Delta H_f^\theta(A^+)(g) + \Delta H_f^\theta(\text{MX}_6^{2-})(g) - \Delta H_f^\theta(A_2\text{MX}_6)(c) \quad (1)$$

for salts where $A = \text{K}, \text{Rb}, \text{Cs}, \text{Tl}, \text{and Ag}$, and

$$U_{\text{POT}}((\text{NH}_4)_2\text{MX}_6) = 2\Delta H_f^\theta(\text{NH}_4^+)(g) + \Delta H_f^\theta(\text{MX}_6^{2-})(g) - \Delta H_f^\theta((\text{NH}_4)_2\text{MX}_6)(c) - 3RT \quad (2)$$

for the ammonium salts.

We use these equations and the relationships:

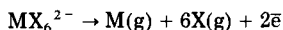
$$\Delta H_f^\theta(\text{MX}_6^{2-})(g) = \Delta H_f^\theta(\text{MX}_6^{2-})(\text{aq}) - 2\Delta H_f^\theta(\text{H}^+)(g) - 2\Delta H_{\text{hyd}}^\theta(\text{H}^+)(g) - \Delta H_{\text{hyd}}^\theta(\text{MX}_6^{2-})(g) \quad (3)$$

$$\overline{\Delta H}_{\text{X(ss)}} = \Delta H_f^\theta(\text{MX}_6^{2-})(g) - 2\Delta H_f^\theta(\text{X}^-)(g) - \Delta H_f^\theta(\text{MX}_4)(\text{ss}) \quad (4)$$

to obtain enthalpies of hydration, $\Delta H_{\text{hyd}}^\theta(\text{MX}_6^{2-})(g)$, and enthalpies of formation, $\Delta H_f^\theta(\text{MX}_6^{2-})(g)$, for the gaseous ions as well as halide (X^-) ion affinities for MX_4 in the state (ss), where (ss) = (g), (l), or (c).

B. BOND STRENGTH

We can define the metal-halogen bond strength in the MX_6^{2-} ion in two ways. First, with reference to the homolytic fission of the bond:



in which case the enthalpy change, $-\Delta H_f^\theta(\text{MX}_6^{2-})(g)$ of the reaction above can be employed as a measure of the average (homolytic) bond energy, $\overline{E}(\text{M} - \text{X})_{\text{hom}}$, defined as:

$$\overline{E}(\text{M} - \text{X})_{\text{hom}} = -\frac{1}{6} \Delta H_f^\theta(\text{MX}_6^{2-})(g) \quad (5)$$

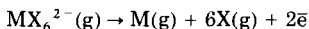
Second, with reference to the heterolytic fission of the bond:



we can define an average (heterolytic) bond energy, $\overline{E(M-X)}_{het}$, using the enthalpy change, $-\Delta H_f^i(MX_6^{2-})(g)$ of the reaction thus:

$$\overline{E(M-X)}_{het} = -\frac{1}{6} \Delta H_f^i(MX_6^{2-})(g) \quad (6)$$

This latter bond energy has been referred to by Basolo and Pearson (1) as the coordinate bond energy and is recommended by them as the more informative for the study of ions of the type MX_6^{2-} on the grounds (i) that in common substitution reactions it is heterolytic, rather than homolytic fission, that occurs in the M-X bonds, (ii) that no process corresponding to:



really exists, and (iii) that the ionic nature of the metal halogen bonds makes it natural to think of complexes dissociating into ions. However, at high temperature the homolytic fission occurs, and thus for consideration of reactions at high temperature and in certain redox reactions involving atom-transfer mechanisms, the former $\overline{E(M-X)}_{hom}$ definition may be more appropriate. Consequently we have chosen to cite both bond energies in what follows, although coordinate (heterolytic) bond energies, $\overline{E(M-X)}_{het}$, for the most part feature in our discussion.

The "total coordinate bond energy" (c.b.e.) defined by Pearson and Mawby (58) is defined as $6\overline{E(M-X)}_{het} = \text{c.b.e. for } MX_6^{2-} \text{ ions}$.

Figure 2 gives the energy diagram related to the above definitions.

C. SCOPE OF REVIEW

Figure 1 presented details of the calculations of the lattice energies of A_2MX_6 salts prior to the main studies reported here. Figure 3 shows the compounds that have received attention as a result of our *recent* minimization method in addition to values that have been estimated from these studies. Deriving from these lattice energies, using ancillary thermochemical data where available, we have computed halide ion affinities as defined in Eq. (4), and these have been obtained for the compounds $MX_4(ss)$ as indicated in Fig. 4.

The bond strengths of the metal-halogen bonds indicated in Fig. 5 have been obtained using the approach described in Section I,B above.

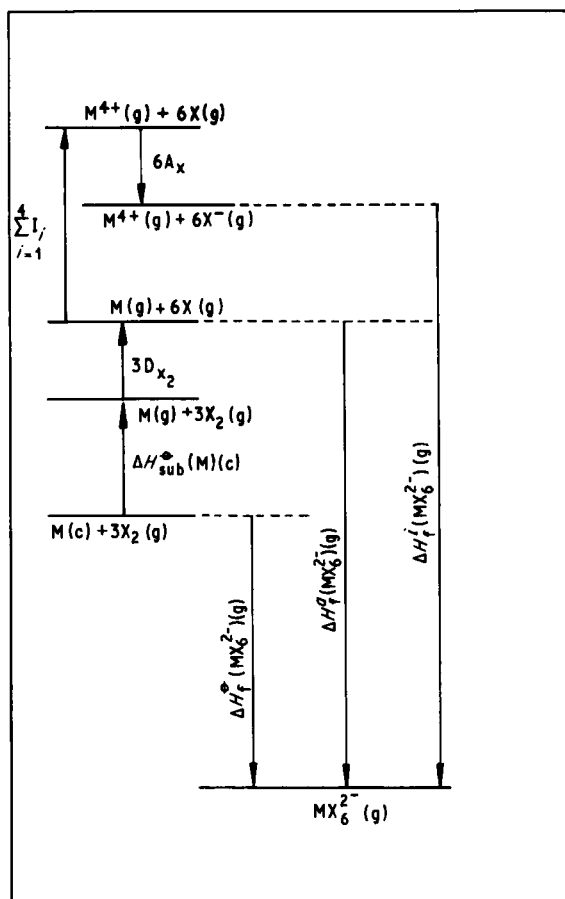


FIG. 2. Energy-thermodynamic correlation for bond-energy definitions.

We proceed now to a discussion of the method which is the main source of the lattice energies referred to in this chapter. The results are discussed in Section VIII and classified by ion type in periodic order in Section V. The lattice energies fall into three categories: (i) those derived from our new approach; (ii) those estimated on the basis of the results in (i); (iii) those obtained by other workers.

The study on the whole adds up to the generation of a systematic scheme for the examination of bond energies and other thermochemical properties across the periodic table to an extent not previously achieved.

						IVB	VB	VIB
						K_2SiF_6 Rb_2SiF_6 Cs_2SiF_6 $(NH_4)_2SiF_6$		
IVA	VA	VIA	VIIA	VIII				
K_2TiCl_6 K_2TiBr_6 Rb_2TiCl_6 Rb_2TiBr_6 Cs_2TiCl_6 Cs_2TiBr_6 $(NH_4)_2TiCl_6$		Cs_2CrF_6	K_2MnCl_6 Rb_2MnF_6 Rb_2MnCl_6 Cs_2MnF_6 Cs_2MnCl_6 $(NH_4)_2MnCl_6$		Rb_2CoF_6 Cs_2CoF_6	K_2NiF_6 Rb_2NiF_6	Cs_2GeCl_6	K_2SeBr_6 Rb_2SeCl_6 Cs_2SeCl_6 $(NH_4)_2SeCl_6$ $(NH_4)_2SeBr_6$
K_2ZrCl_6 Rb_2ZrCl_6 Cs_2ZrCl_6	K_2NbCl_6 Rb_2NbCl_6 Cs_2NbCl_6	Na_2MoCl_6 K_2MoCl_6 Rb_2MoCl_6 Cs_2MoCl_6	K_2TeCl_6 Rb_2TeCl_6	K_2RuCl_6		K_2PdCl_6 Rb_2PdCl_6 Cs_2PdCl_6 $(NH_4)_2PdCl_6$	K_2SnCl_6 Rb_2SnCl_6 Rb_2SnBr_6 Rb_2SnI_6 Cs_2SnCl_6 Cs_2SnBr_6 Cs_2SnI_6 $(NH_4)_2SnCl_6$ $(NH_4)_2SnBr_6$	K_2TeCl_6 Rb_2TeCl_6 Cs_2TeCl_6 Cs_2TeBr_6 Cs_2TeI_6 $(NH_4)_2TeCl_6$ $(NH_4)_2TeBr_6$
K_2HfCl_6	K_2TaCl_6 Rb_2TaCl_6 Cs_2TaCl_6	K_2WCl_6 K_2WBr_6 Rb_2WCl_6 Rb_2WBr_6 Cs_2WCl_6 Cs_2WBr_6	K_2ReCl_6 K_2ReBr_6 Rb_2ReCl_6 Cs_2ReCl_6 $(NH_4)_2ReCl_6$	K_2OsCl_6 K_2OsBr_6 Cs_2OsCl_6 $(NH_4)_2OsCl_6$	$(NH_4)_2IrCl_6$	K_2PtCl_6 K_2PtBr_6 Rb_2PtCl_6 Cs_2PtCl_6 $(NH_4)_2PtCl_6$	Rb_2PbCl_6 Cs_2PbCl_6 $(NH_4)_2PbCl_6$	Cs_2PoBr_6 $(NH_4)_2PoCl_6$ $(NH_4)_2PoBr_6$

FIG. 3. Calculated and estimated lattice energies for A_2MX_6 salts: 1977.

						IVB	VB	VIB
						SiF_4		
IVA	VA	VIA	VIIA	VIII				
$TiCl_4$ $TiBr_4$					NiF_4	GeF_4 $GeCl_4$		
$ZrCl_4$	$NbCl_4$	$MoCl_4$				$PdCl_4$	$SnCl_4$	$TeCl_4$ $TeBr_4$
$HfCl_4$	$TaCl_4$	WCl_4 WBr_4	$ReCl_4$ $ReBr_4$	$OsCl_4$	$IrCl_4$	$PtCl_4$ $PtBr_4$	$PbCl_4$	

FIG. 4. Calculated halide ion affinities for MX_4 compounds.

							IVB	VB	VIB
							Si-F		
IVA	VA	VIA	VIIA	VIII \longleftrightarrow					
Ti-Cl Ti-Br						Ni-F	Ge-F Ge-Cl		
Zr-Cl	Nb-Cl	Mo-Cl				Pd-Cl	Sn-Cl		Te-Cl Te-Br
Hf-Cl	Ta-Cl	W-Cl W-Br	Re-Cl Re-Br	Os-Cl	Ir-Cl	Pt-Cl Pt-Br	Pb-Cl		

Fig. 5. Calculated metal-halogen bond strengths.

II. Rigorous Lattice-Energy Calculation for A_2MX_6 Salts

A. THEORY

In the present study we have assigned a charge distribution (see Section II,B) in all cases to the MX_6^{2-} ion, based where possible on experimental data already available. Within a given ion MX_6^{2-} we have six atoms X bearing a charge q_X surrounding a central metal atom M bearing a charge q_M where:

$$q_M + 6q_X = -2 \quad (7)$$

The lattice potential energy of a salt A_2MX_6 , $U_{\text{POT}}(A_2MX_6)$ is given by the sum of the electrostatic (U_{ELEC}), dipole-dipole dispersion (U_{dd}), dipole-quadrupole dispersion (U_{qd}), and repulsion (U_{R}) energies:

$$U_{\text{POT}}(A_2MX_6) = U_{\text{ELEC}} + U_{\text{dd}} + U_{\text{qd}} - U_{\text{R}} \quad (8)$$

and the condition that:

$$\left(\frac{\partial U_{\text{POT}}(A_2MX_6)}{\partial a} \right)_{a=a_0} = 0 \quad (9)$$

is used, and hence:

$$\left(\frac{\partial U_R}{\partial a}\right)_{a=a_0} = \left(\frac{\partial U_{\text{ELEC}}}{\partial a}\right)_{a=a_0} + \left(\frac{\partial U_{\text{dd}}}{\partial a}\right)_{a=a_0} + \left(\frac{\partial U_{\text{qd}}}{\partial a}\right)_{a=a_0} \quad (10)$$

If, for a salt A_2MX_6 , we regard it as consisting of two A^+ ions and an approximately spherical MX_6^{2-} complex ion, the approach of Huggins and Mayer (33) renders a parametric form for the repulsion energy:

$$\begin{aligned} U_R = & \frac{1}{2}bC_{++} \exp\left(\frac{2\bar{r}_{A^+}}{\rho}\right) \left[2 \sum_{\substack{\text{all ions} \\ A_i^+}} \exp\left(\frac{-R_{A^+A_i^+}}{\rho}\right) \right] \\ & + bC_{+-} \exp\left(\frac{\bar{r}_{A^+} + \bar{r}_{MX_6^{2-}}}{\rho}\right) \left[2 \sum_{\substack{\text{all ions} \\ MX_{6i}^{2-}}} \exp\left(\frac{-R_{A^+MX_{6i}^{2-}}}{\rho}\right) \right] \\ & + \frac{1}{2}bC_{--} \exp\left(\frac{2\bar{r}_{MX_6^{2-}}}{\rho}\right) \left[\sum_{\substack{\text{all ions} \\ MX_{6i}^{2-}}} \exp\left(\frac{-R_{MX_6^{2-}MX_{6i}^{2-}}}{\rho}\right) \right] \end{aligned} \quad (11)$$

applicable for this salt, where $C_{++} = 1.25$, $C_{+-} = 0.875$, and $C_{--} = 0.50$. All the distances involved in the summations are expressible as functions of a , the unit cell parameter, thus:

$$R_{ij} = a[(h + x_i - x_j)^2 + (k + y_i - y_j)^2 + (l + z_i - z_j)^2]^{1/2} = ak_{ij} \quad (12)$$

and hence U_R is differentiable and takes the form:

$$\begin{aligned} \left(\frac{\partial U_R}{\partial a}\right)_{a=a_0} = & -\frac{1}{2}bC_{++} \exp\left(\frac{2\bar{r}_{A^+}}{\rho}\right) \left[2 \sum_{\substack{\text{all ions} \\ A_i^+}} \left(\frac{k_{A^+A_i^+}}{\rho}\right) \exp\left(\frac{-R_{A^+A_i^+}}{\rho}\right) \right] \\ & - bC_{+-} \exp\left(\frac{\bar{r}_{A^+} + \bar{r}_{MX_6^{2-}}}{\rho}\right) \left[2 \sum_{\substack{\text{all ions} \\ MX_{6i}^{2-}}} \left(\frac{k_{A^+MX_{6i}^{2-}}}{\rho}\right) \right. \\ & \left. \exp\left(\frac{-R_{A^+MX_{6i}^{2-}}}{\rho}\right) \right] \\ & - \frac{1}{2}bC_{--} \exp\left(\frac{2\bar{r}_{MX_6^{2-}}}{\rho}\right) \\ & \left[\sum_{\substack{\text{all ions} \\ MX_{6i}^{2-}}} \left(\frac{k_{MX_6^{2-}MX_{6i}^{2-}}}{\rho}\right) \exp\left(\frac{-R_{MX_6^{2-}MX_{6i}^{2-}}}{\rho}\right) \right] \end{aligned} \quad (13)$$

Herzig *et al.* (32) have expanded U_{ELEC} , the electrostatic energy for these salts, as a function of the cell length a , and an internal distance, d (corresponding to the M—X distance in the salt), and the charge distribution q_X on the terminal halogen atoms of the complex ion.

$$U_{\text{ELEC}} = K/a \left\{ \alpha_0 + \left[\sum_{\substack{n=2 \\ \text{even}}}^{\infty} \alpha_n (d/a)^n \right] q_X + \left[\sum_{\substack{n=2 \\ \text{even}}}^{\infty} \beta_n (d/a)^n \right] q_X^2 \right\} \quad (14)$$

whereupon

$$\left(\frac{\partial U_{\text{ELEC}}}{\partial a} \right)_{a=a_0} = \frac{K}{a_0} \left[\left(\frac{\partial M_{\text{ELEC}}}{\partial a} \right)_{a=a_0} - \frac{M_{\text{ELEC}}}{a_0} \right] \quad (15)$$

$$= -\frac{K}{a_0^2} \left[\alpha_0 + \sum_{\substack{n=2 \\ \text{even}}}^{\infty} (n+1) \alpha_n \left(\frac{d}{a_0} \right)^n q_X + \sum_{\substack{n=2 \\ \text{even}}}^{\infty} (n+1) \beta_n \left(\frac{d}{a_0} \right)^n q_X^2 \right] \quad (16)$$

where M_{ELEC} is the electrostatic Madelung constant based on a_0 . The derivatives $(\partial U_{\text{dd}}/\partial a)_{a=a_0}$ and $(\partial U_{\text{qd}}/\partial a)_{a=a_0}$ are evaluated using the polarizabilities of Pirenne and Kartheuser (59), treating the ions MX_6^{2-} as though they could be regarded as being comprised of six halide ions. The electron numbers were taken as 8, apart from the case where $M = \text{Tl}$, in which case the Herzfeld and Woolf formula (31) was employed. The summations necessary for the evaluation of the above derivatives took the form:

$$S_L^{A^+A^+} = 2 \left[\sum_{\substack{\text{all ions} \\ A_i^+}}^{AA} (R_{A^+A_i^+})^{-L} \right] \quad (17)$$

$$S_L^{A^+X^-} = 2 \left[\sum_{\substack{\text{all ions} \\ X_i^-}}^{AX} (R_{A^+X_i^-})^{-L} \right] \quad (18)$$

$$S_L^{X^-X^-} = 6 \left[\sum_{\substack{\text{all ions} \\ X_i^-}}^{XX} (R_{X^-X_i^-})^{-L} - 4(R_{X^-X_{\text{cis}}^-})^{-L} - (R_{X^-X_{\text{trans}}^-})^{-L} \right] \quad (19)$$

where $R_{X^-X_{\text{cis}}^-}$ and $R_{X^-X_{\text{trans}}^-}$ are the halogen-halogen nearest and next-nearest neighbor distances in the same ion, MX_6^{2-} , and

$$U_{\text{dd}} = \frac{1}{2} [c_{++} S_6^{++} + c_{--} S_6^{--}] + c_{+-} S_6^{+-} \quad (20)$$

$$U_{\text{qd}} = \frac{1}{2} [d_{++} S_8^{++} + d_{--} S_8^{--}] + d_{+-} S_8^{+-} \quad (21)$$

where

$$c_{ij} = (2e^4 Q_i Q_j) / 3(\epsilon_i + \epsilon_j) \quad (22)$$

$$d_{ij} = \frac{3}{2} c_{ij} [Q_i / p_i + Q_j / p_j] \quad (23)$$

$$Q_i = (3\alpha_i \epsilon_i) / 2e^2 \quad (24)$$

α_i , ϵ_i , and p_i are the polarizability, characteristic energy, and electron number of the ion i and e is the electronic charge and, since

$$\left(\frac{\partial S_L^{ij}}{\partial a} \right)_{a=a_0} = - \sum_{\text{all } j} k_{ij} L R_{ij}^{-(L+1)} = \frac{-L S_L^{ij}}{a_0} \quad (25)$$

we have

$$\left(\frac{\partial U_{dd}}{\partial a} \right)_{a=a_0} = - \frac{6U_{dd}}{a_0} \quad (26)$$

and

$$\left(\frac{\partial U_{qd}}{\partial a} \right)_{a=a_0} = - \frac{8U_{qd}}{a_0} \quad (27)$$

Substitution of Eqs. (13), (16), (26), and (27) into Eq. (10) gives us an equation of the form:

$$\theta_1 \exp\left(\frac{2\bar{r}_{MX_6^{2-}}}{\rho}\right) + \theta_2 \exp\left(\frac{\bar{r}_{A^+} + \bar{r}_{MX_6^{2-}}}{\rho}\right) + \theta_3 \exp\left(\frac{2\bar{r}_{A^+}}{\rho}\right) = \theta_4 \quad (28)$$

where

$$\theta_1 = \left\{ -\frac{1}{2} b C_{--} \left[\sum_{\substack{\text{all ions} \\ MX_6^{2-}}} \left(\frac{k_{MX_6^{2-} - MX_6^{2-}}}{\rho} \right) \exp\left(-\frac{R_{MX_6^{2-} - MX_6^{2-}}}{\rho}\right) \right] \right\} \quad (29)$$

$$\theta_2 = \left[-2b C_{+-} \sum_{\substack{\text{all ions} \\ MX_6^{2-}}} \left(\frac{k_{A^+ - MX_6^{2-}}}{\rho} \right) \exp\left(-\frac{R_{A^+ - MX_6^{2-}}}{\rho}\right) \right] \quad (30)$$

$$\theta_3 = \left[-b C_{++} \sum_{\substack{\text{all ions} \\ A_i^+}} \left(\frac{k_{A^+ - A_i^+}}{\rho} \right) \exp\left(-\frac{R_{A^+ - A_i^+}}{\rho}\right) \right] \quad (31)$$

$$\theta_4 = \left[\frac{1}{a_0} \left(U_{\text{ELEC}} + 6U_{dd} + 8U_{qd} - K \left(\frac{\partial M_{\text{ELEC}}}{\partial a} \right)_{a=a_0} \right) \right] \quad (32)$$

In a particular salt, A_2MX_6 , since we *know* the "basic" radius for the cation, A^+ , \bar{r}_{A^+} ($A = K, Rb, Cs, Tl, NH_4$), Eq. (28) becomes

$$\theta_1 \exp(2\bar{r}_{MX_6^{2-}}/\rho) + \eta_2 \exp(\bar{r}_{MX_6^{2-}}/\rho) + \eta_3 = 0 \quad (33)$$

where

$$\eta_2 = [\theta_2 \exp(\bar{r}_{A^+}/\rho)] \quad (34)$$

$$\eta_3 = [\theta_3 \exp(2\bar{r}_{A^+}/\rho) - \theta_4] \quad (35)$$

and hence we can solve Eq. (33) for $\bar{r}_{MX_6^{2-}}$:

$$\exp\left(\frac{\bar{r}_{MX_6^{2-}}}{\rho}\right) = \left[\frac{-\eta_2 \pm (\eta_2^2 - 4\theta_1\eta_3)^{1/2}}{2\theta_1} \right] \quad (36)$$

for a range of charge distributions on the MX_6^{2-} ion as represented by q_X , θ_4 being itself a function of q_X by virtue of Eq. (21).

$$\theta_4 = \sum_{i=0}^2 A_i q_X^i \quad (37)$$

and hence

$$\bar{r}_{MX_6^{2-}} = \rho \ln \left[\phi_0 + \left(\sum_{j=1}^3 \phi_j q_X^{(j-1)} \right)^{1/2} \right] \quad (38)$$

where

$$\phi_3 = 4\theta_1 A_2 \quad (39)$$

$$\phi_2 = 4\theta_1 A_1 \quad (40)$$

$$\phi_1 = \eta_2^2 - 4\theta_1\theta_3 [\exp(2\bar{r}_{A^+}/\rho) - A_0] \quad (41)$$

and

$$\phi_0 = (-\eta_2/2\theta_1) \quad (42)$$

In the present work, admitting a variable ρ parameter would introduce complications and, in the absence of compressibility data, makes the calculation of U_R difficult. Assumption that ρ is constant (taking the value to be 0.345 Å) within the framework of the present method is made prior to the solution of Eq. (38) and hence errors introduced by such an assumption will be minimized since $\bar{r}_{MX_6^{2-}}$, which is determined in the study, has a close parametric relationship with ρ . From

Eq. (38), it will be seen that

$$\exp\left(\frac{\bar{r}_{MX_6^{2-}}}{\rho}\right) = \left[\phi_0 + \left(\sum_{j=1}^3 \phi_j q_X^{(j-1)} \right)^{1/2} \right] \quad (43)$$

and hence in Eq. (11), the charge dependence can be expressed as

$$U_R = U_R^{++} + U_R^{+-} + U_R^{--} \quad (44)$$

$$= U_R^{++} + \delta_0 \left[\phi_0 + \left(\sum_{j=1}^3 \phi_j q_X^{(j-1)} \right)^{1/2} \right] + \delta_1 \left[\phi_0 + \left(\sum_{j=1}^3 \phi_j q_X^{(j-1)} \right)^{1/2} \right]^2 \quad (45)$$

where

$$\delta_0 = 2bC_{+-} \exp\left(\frac{\bar{r}_{A^+}}{\rho}\right) \sum_{\substack{\text{all ions} \\ MX_6^{2-}}} \exp\left(-\frac{R_{A^+MX_6^{2-}}}{\rho}\right) = \left[U_R^{+-} / \exp\left(\frac{\bar{r}_{MX_6^{2-}}}{\rho}\right) \right] \quad (46)$$

and

$$\delta_1 = \frac{1}{2} bC_{--} \sum_{\substack{\text{all ions} \\ MX_6^{2-}}} \exp\left(-\frac{R_{MX_6^{2-}MX_6^{2-}}}{\rho}\right) = \left[U_R^{--} / \exp\left(\frac{2\bar{r}_{MX_6^{2-}}}{\rho}\right) \right] \quad (47)$$

and hence

$$U_R = [U_R^{++} + \delta_0 \phi_0 + \delta_1 \phi_0^2 + \delta_1 \phi_1] + [\delta_1 \phi_2] q_X + [\delta_1 \phi_3] q_X^2 + [\delta_0 + 2\phi_0 \delta_1] (\phi_1 + \phi_2 q_X + \phi_3 q_X^2)^{1/2} \quad (48)$$

U_{dd} and U_{qd} are charge independent, and U_{ELEC} can be written:

$$U_{ELEC} = \sum_{k=0}^2 \gamma_k q_X^k \quad (49)$$

Hence the charge dependence of U_{POT} , as defined by Eq. (8) is given by

$$U_{POT} = \sum_{k=0}^2 \gamma_k q_X^k - [U_R^{++} + \delta_0 \phi_0 + \delta_1 \phi_0^2 + \delta_1 \phi_1] - \delta_1 \phi_2 q_X - \delta_1 \phi_3 q_X^2 - (\delta_0 + 2\phi_0 \delta_1) (\phi_1 + \phi_2 q_X + \phi_3 q_X^2)^{1/2} + U_{dd} + U_{gd} \quad (50)$$

$$U_{POT} = [\gamma_0 - U_R^{++} + U_{dd} + U_{qd} - \delta_0 \phi_0 - \delta_1 \phi_0^2 - \delta_1 \phi_1] + q_X [\gamma_1 - \delta_1 \phi_2] + q_X^2 [\gamma_2 - \delta_1 \phi_3] - (\delta_0 + 2\phi_0 \delta_1) (\phi_1 + \phi_2 q_X + \phi_3 q_X^2)^{1/2} \quad (51)$$

TABLE II
CHARGE DISTRIBUTIONS ON MX_6^{2-} IONS FROM LITERATURE SOURCES^a

Group	Ion MX_6^{2-}	Calculated q_X			Experimental q_X			
		Jørgensen (42-45)	Jørgensen with Madelung correction (42-45)	Average	Cotton and Harris (12)	Kubo and Nakamura (50)	Brown <i>et al.</i> (9)	Adopted value q_X
IVA	TiCl_6^{2-}	-0.44	-0.79	-0.61	—	—	—	-0.61
	TiBr_6^{2-}	-0.44	-0.74	-0.59	—	—	—	-0.59
	ZrCl_6^{2-}	-0.42	-0.91	-0.66	—	—	—	-0.66
	HfCl_6^{2-}	—	—	—	—	—	—	(-0.66) ^b
VA	NbCl_6^{2-}	-0.40	-0.89 ^d	-0.65	—	—	—	-0.65
	TaCl_6^{2-}	—	—	—	—	—	—	(-0.65) ^b
VIA	CrF_6^{2-}	-0.42	-0.88	-0.65	—	—	—	-0.65
	MoCl_6^{2-}	-0.40	-0.81	-0.60	—	—	—	-0.60
	WCl_6^{2-}	—	—	—	—	-0.43	-0.62	-0.62
	WBr_6^{2-}	—	—	—	—	—	—	(-0.55) ^b
VIIA	MnF_6^{2-}	-0.40	-0.86	-0.63	—	—	—	-0.63
	MnCl_6^{2-}	-0.40	-0.71	-0.55	—	—	—	-0.55
	ToCl_6^{2-}	-0.35	-0.64	-0.49	—	—	—	-0.49
	ReCl_6^{2-}	—	—	—	-0.55	-0.45	-0.56	-0.56
VIII	ReBr_6^{2-}	—	—	—	—	-0.39	—	(-0.5) ^c
	OsCl_6^{2-}	—	—	—	-0.53	-0.47	-0.51	-0.51
	OsBr_6^{2-}	—	—	—	—	—	—	(-0.45) ^b
	CoF_6^{2-}	-0.40	-0.79	-0.59	—	—	—	-0.59
	IrCl_6^{2-}	—	—	—	-0.48	-0.47	-0.47	-0.47
	NiF_6^{2-}	-0.40	-0.75	-0.57	—	—	—	-0.57
	PdCl_6^{2-}	-0.36	-0.63	-0.49	—	-0.43	—	-0.43
	PdBr_6^{2-}	-0.35	-0.60 ^d	-0.48	—	-0.37	—	-0.37
IVB	PtCl_6^{2-}	-0.34	-0.68	-0.51	-0.45	-0.44	-0.45	-0.44 ^d
	PtBr_6^{2-}	-0.33	-0.63	-0.48	—	-0.38	—	-0.38
	SiF_6^{2-}	-0.36	-1.33	-0.84	—	—	—	-0.84
	GeF_6^{2-}	-0.36	-1.21	-0.78	—	—	—	-0.78
	GeCl_6^{2-}	-0.35	-1.10	-0.73	—	—	—	-0.73
	SnCl_6^{2-}	-0.36	-1.01	-0.74	—	-0.66	—	-0.66
	SnBr_6^{2-}	-0.35	-0.90	-0.63	—	-0.60	—	-0.60
	SnI_6^{2-}	-0.33	-0.80	-0.56	—	-0.55	—	-0.55
VIB	PbCl_6^{2-}	—	—	—	—	-0.63	—	-0.63
	SeCl_6^{2-}	-0.31	-0.60	-0.45	—	-0.56	—	-0.56
	SeBr_6^{2-}	-0.30	-0.55	-0.42	—	-0.47	—	-0.47
	TeCl_6^{2-}	-0.32	-0.69	-0.50	—	-0.68	—	-0.68
	TeBr_6^{2-}	-0.30	-0.64	-0.47	—	-0.58	—	-0.58
	TeI_6^{2-}	-0.29	-0.53	-0.41	—	-0.48	—	-0.48
	PoCl_6^{2-}	—	—	—	—	—	—	(-0.7) ^b
	PoBr_6^{2-}	—	—	—	—	—	—	(-0.6) ^b

^a Values adopted in the current work are given in the right-hand column of the table.

^b Estimated

^c Kubo and Nakamura (50) disagree with the adopted value for ReCl_6^{2-} , and so this value is estimated.

^d As used in reference (38a).

^e $d = u \cdot a_0$ has been estimated in the absence of data for the purposes of using Jørgensen's approach to calculate q_X .

B. CHARGE DISTRIBUTION IN MX_6^{2-} IONS

Ideally with precise crystal structures and precise calculations, from plots of $\bar{r}_{MX_6^{2-}}$ against the charge q_X on the terminal halogen atom we ought to be able to determine q_X uniquely for a given ion. However, as in our previous work, in order to obtain a reliable discriminant for such a determination we really require to include in a study such as this, salts that exhibit at least two differing crystal structures within the series of different cations studied. This inclusion will be made later, (40a) but the present work is limited in that it includes only salts with the antifluorite structure, and consequently no estimate of the charge distribution in the complex ions can be gained from the plots of $\bar{r}_{MX_6^{2-}}$ versus q_X . Accordingly we have to resort to other studies to estimate the value of q_X for a given ion, uncertain though such estimates may be.

Jørgensen *et al.* (42–45) have detailed a method for the estimation of ionicities in complex ions MX_6^{2-} , both with and without a Madelung correction, using differential ionization energies as a measure of the electronegativities of the atoms involved. They claim that the calculations having the correction give the better results, but, as Table II indicates, this does not appear to be borne out when the Jørgensen charges (which we calculated using his method) are compared to the experimental estimates of Kubo and Nakamura (50) or Brown *et al.* (9). In fact an average of the two Jørgensen charges seems more appropriate, and we have chosen such an average when no experimental determination of q_X was available. The right-hand column of Table II, which lists the various determinations, gives the value of q_X we have used in this study. Having selected q_X for an ion in question, we determine from Eq. (38) a radius $\bar{r}_{MX_6^{2-}}$ for each salt A_2MX_6 , which should be (and usually is found to be) practically constant for a given ion. We can calculate U_R corresponding to this "basic" radius $\bar{r}_{MX_6^{2-}}$ for the complex ion and hence determine the total lattice potential energy $U_{POT}(A_2MX_6)$ for each salt.

III. Estimated Lattice Energies

The vast majority of lattice energies cited in this chapter have been rigorously evaluated; however, a few are estimated in three different ways. The first takes known $\Delta H_f^\circ(A_2MX_6)(c)$ data for the salt A_2MX_6 (for which no lattice energy has been calculated) in conjunction with $\Delta H_f^\circ(MX_6^{2-})(g)$ data derived from salts for which the lattice potential energy and enthalpy of formation are known, to give an estimate of $U_{POT}(A_2MX_6)$. The results for these lattice energies are quoted in parentheses in Table III. The second method of estimation takes into

TABLE III
SUMMARY TABLE OF LATTICE ENERGY VALUES FOR A_2MX_6 SALTS AS
CALCULATED BY THE NEW MINIMIZATION APPROACH DEVELOPED IN
THIS CHAPTER AND JENKINS AND PRATT (39)

MX_6^{2-}	A^+	\AA		Adopted q_X	kJ mol^{-1}					\AA $r_{MX_6^{2-}}$
		a_0	d		U_{ELEC}	U_{dd}	U_{qd}	U_{R}	U_{POT}	
$TiCl_6^{2-}$	K^+	9.792	2.35	-0.61	1370	116	10	84	1412	2.48
	Rb^+	9.922	2.33	-0.61	1374	127	11	76	1415	2.47
	Cs^+	10.219	2.35	-0.61	1354	145	15	112	1402	2.50
	NH_4^+ (Tl^+)	9.89	2.37	-0.61	1356	140	13	96	1413	2.50 (1560)
$TiBr_6^{2-}$	Rb^+	10.39	2.60	-0.59	1255	155	15	84	1341	2.62
	Cs^+	10.57	2.64	-0.59	1235	182	20	98	1339	2.61
	(K^+)			-0.59						(1379)
$ZrCl_6^{2-}$	Rb^+	10.178	2.44	-0.66	1292	113	10	67	1348	2.45
	Cs^+	10.407	2.45	-0.66	1287	133	14	86	1348	2.49
$HfCl_6^{2-}$	Cs^+	10.42	2.60	-0.66	1225	141	15	66	1315	2.37
CrF_6^{2-}	Cs^+	9.02	1.73	-0.65	1656	92	10	155	1603	2.08
$MoCl_6^{2-}$	K^+	9.85	2.30	-0.60	1393	107	8	90	1418	2.54
	(Na^+)			-0.60						(1526)
	(Rb^+)			-0.60						(1399)
	(Cs^+)			-0.60						(1347)
WCl_6^{2-}	K^+	9.875	2.36	-0.62	1358	110	9	79	1398	2.50
	Rb^+	10.00	2.36	-0.62	1354	122	11	90	1397	2.47
	Cs^+	10.27	2.36	-0.62	1343	141	15	107	1392	2.51
WBr_6^{2-}	Rb^+	10.50	2.48	-0.55	1321	130	11	101	1361	2.73
	Cs^+	10.70	2.48	-0.55	1310	152	16	116	1362	2.72
	(K^+)			-0.55						(1408)
MnF_6^{2-}	Rb^+	8.43	1.69	-0.63	1752	87	8	159	1688	1.99
	Cs^+	8.92	1.74	-0.63	1670	99	11	160	1620	2.05
$MnCl_6^{2-}$	K^+	9.644	2.28	-0.55	1438	123	10	109	1462	2.51
	Rb^+	9.838	2.28	-0.55	1426	132	12	117	1451	2.50
	NH_4^+	9.82	2.24	-0.55	1440	136	13	126	1464	2.56
$TcCl_6^{2-}$	K^+	9.83	2.35	-0.49	1429	113	9	108	1443	2.59
$ReCl_6^{2-}$	K^+	9.84	2.35	-0.56	1386	111	9	90	1416	2.54
$ReBr_6^{2-}$	K^+	10.385	2.48	-0.5	1348	119	10	102	1375	2.81
$OsCl_6^{2-}$	K^+	9.729	2.36	-0.51	1419	124	10	106	1447	2.54
$OsBr_6^{2-}$	K^+	10.30	2.51	-0.45	1366	130	11	111	1396	2.80
CoF_6^{2-}	Rb^+	8.46	1.7	-0.59	1755	86	8	161	1688	2.00
	Cs^+	8.914	1.7	-0.59	1692	98	11	169	1632	2.07
$IrCl_6^{2-}$	NH_4^+	9.87	2.47	-0.47	1394	151	15	118	1442	2.56
NiF_6^{2-}	K^+	8.1088	1.78	-0.57	1774	84	7	144	1721	1.94
	Rb^+	8.462	1.71	-0.57	1757	86	8	163	1688	2.01
$PdCl_6^{2-}$	NH_4^+	9.84	2.30	-0.43	1470	138	13	140	1481	2.61
$PtCl_6^{2-}$	K^+	9.755	2.34	-0.44	1461	119	10	122	1468	2.60
	Rb^+	9.901	2.33	-0.44	1455	129	11	131	1464	2.56
	Cs^+	10.215	2.35	-0.44	1424	146	16	141	1444	2.58
	NH_4^+	9.858	2.37	-0.44	1446	142	13	134	1468	2.62
	Tl^+	9.779	2.30	-0.44	1473	247	27	201	1546	2.60
	(Ag^+) (Ba^{2+})			-0.44 -0.44					(1773) (2047)	

TABLE III (Continued)

MX ₆ ²⁻	A ⁺	Å		Adopted <i>q</i>	kJ mol ⁻¹					Å $\bar{r}_{\text{MX}_6^{2-}}$
		<i>a</i> ₀	<i>d</i>		<i>U</i> _{ELEC}	<i>U</i> _{dd}	<i>U</i> _{qd}	<i>U</i> _R	<i>U</i> _{POT}	
PtPr ₆ ²⁻	K ⁺	10.293	2.46	-0.38	1414	125	11	127	1423	2.85
	(Ag ⁺)			-0.38					(1791)	
SiF ₆ ²⁻	K ⁺	8.133	1.75	-0.84	1676	81	6	93	1670	1.79
	Rb ⁺	8.452	1.69	-0.84	1688	86	8	113	1639	1.87
	Cs ⁺	8.919	1.69	-0.84	1639	98	11	144	1604	2.01
	Tl ⁺	8.568	1.71	-0.84	1665	173	20	183	1675	2.05
	NH ₄ ⁺	8.395	1.72	-0.84	1676	97	10	126	1657	1.94
	NH ₄ ⁺	8.395	1.69	-0.84	1694	96	9	134	1665	1.96
GeF ₆ ²⁻	Cs ⁺	9.021	1.80	-0.78	1598	93	11	129	1573	2.02
	NH ₄ ⁺	8.46	1.72	-0.78	1691	92	9	135	1657	1.99
GeCl ₆ ²⁻	Cs ⁺	10.21	2.35	-0.73	1305	146	16	92	1375	2.43
SnCl ₆ ²⁻	K ⁺	10.002	2.45	-0.66	1289	107	9	53	1352	2.41
	K ⁺	9.982	2.41	-0.66	1310	105	8	60	1363	2.45
	Rb ⁺	10.118	2.43	-0.66	1300	117	10	69	1358	2.43
	Rb ⁺	10.096	2.42	-0.66	1303	119	10	71	1361	2.43
	Cs ⁺	10.381	2.44	-0.66	1291	135	14	88	1352	2.48
	Cs ⁺	10.355	2.42	-0.66	1298	137	14	91	1358	2.48
	Tl ⁺	9.97	2.39	-0.66	1319	224	24	130	1437	2.55
	NH ₄ ⁺	10.060	2.41	-0.66	1307	126	11	75	1369	2.49
	NH ₄ ⁺	10.044	2.42	-0.66	1304	128	12	74	1370	2.48
	Rb ⁺	10.64	2.61	-0.60	1244	128	11	74	1309	2.69
SnBr ₆ ²⁻	Cs ⁺	10.81	2.65	-0.60	1224	154	16	88	1306	2.67
	NH ₄ ⁺	10.59	2.59	-0.60	1250	136	13	80	1319	2.74
SnI ₆ ²⁻	Rb ⁺	11.60	2.84	-0.55	1165	126	11	76	1226	3.11
	Cs ⁺	11.63	2.85	-0.55	1162	156	16	91	1243	3.03
PbCl ₆ ²⁻	Rb ⁺	10.197	2.49	-0.63	1283	115	10	65	1343	2.45
	Cs ⁺	10.415	2.50	-0.63	1278	136	14	84	1344	2.48
	NH ₄ ⁺	10.135	2.48	-0.63	1289	125	11	70	1355	2.50
SeCl ₆ ²⁻	Rb ⁺	9.978	2.39	-0.56	1369	127	11	98	1409	2.50
	Cs ⁺	10.266	2.41	-0.56	1350	145	15	113	1397	2.52
	NH ₄ ⁺	9.935	2.38	-0.56	1375	136	13	104	1420	2.55
SeBr ₆ ²⁻	K ⁺	10.363	2.54	-0.47	1345	127	11	104	1379	2.81
	NH ₄ ⁺	10.46	2.56	-0.47	1332	147	14	113	1380	2.81
TeCl ₆ ²⁻	Rb ⁺	10.233	2.51	-0.68	1249	113	10	51	1321	2.38
	Rb ⁺	10.233	2.53	-0.68	1239	115	10	48	1316	2.35
	Cs ⁺	10.447	2.51	-0.68	1249	132	13	71	1323	2.44
	Tl ⁺	10.107	2.48	-0.68	1264	211	22	105	1392	2.54
	NH ₄ ⁺	10.178	2.54	-0.68	1227	126	11	46	1318	2.37
	NH ₄ ⁺	10.20	2.53	-0.68	1237	122	11	50	1320	2.41
TeBr ₆ ²⁻	Cs ⁺	10.91	2.62	-0.58	1243	141	14	92	1306	2.73
	Cs ⁺	10.918	2.69	-0.58	1214	147	15	84	1292	2.70
	NH ₄ ⁺	10.728	2.68	-0.58	1222	132	12	72	1294	2.76
TeI ₆ ²⁻	Cs ⁺	11.721	2.91	-0.48	1175	152	15	96	1246	3.10
PoCl ₆ ²⁻	NH ₄ ⁺	10.35	2.38	-0.7	1300	100	8	70	1338	2.60
PoBr ₆ ²⁻	Cs ⁺	11.01	2.64	-0.6	1223	134	13	83	1286	2.74
	NH ₄ ⁺	10.84	2.60	-0.6	1242	114	10	74	1292	2.83

account the approximate equality of the lattice energies,

$$U_{\text{POT}}(\text{K}_2\text{MX}_6) \simeq U_{\text{POT}}((\text{NH}_4)_2\text{MX}_6) \quad (52)$$

and estimates the lattice energy of a potassium salt from that of an ammonium salt and vice versa; again they are quoted in parentheses in Table III. This subterfuge is resorted to only in cases where we stand to generate extra thermochemical data that could not otherwise be obtained. The third approach stems from the apparent rectilinear relationships (Figs. 6–9) between our calculated $U_{\text{POT}}(\text{A}_2\text{MX}_6)$ values and

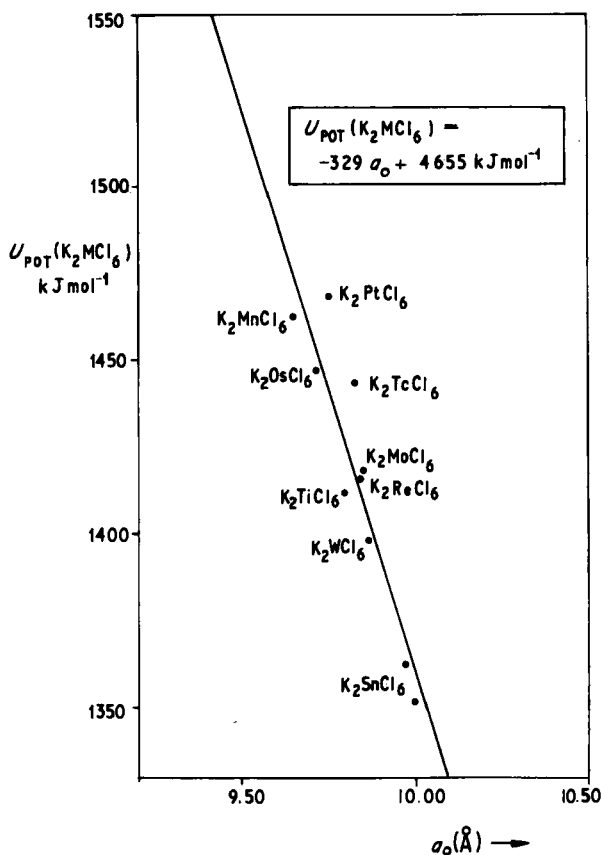


FIG. 6. Calculated lattice energy for potassium salts, K_2MCl_6 , as a function of the cubic cell parameter, a_0 . The relationship $U_{\text{POT}}(\text{K}_2\text{MCl}_6) = -329a_0 + 4655 \text{ kJ mol}^{-1}$ is found.

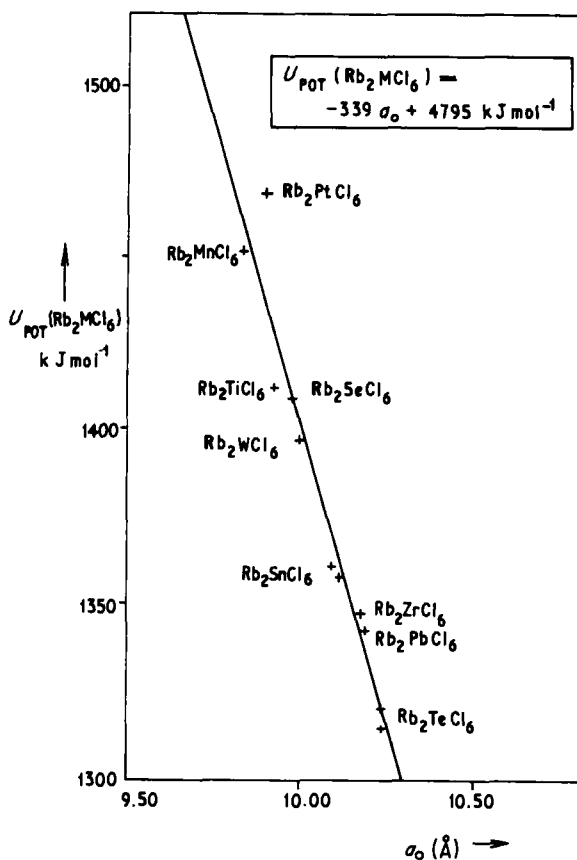


FIG. 7. Calculated lattice energy for rubidium salts, Rb_2MCl_6 , as a function of the cubic cell parameter, a_0 . The relationship $U_{\text{POT}}(\text{Rb}_2\text{MCl}_6) = -339a_0 + 4795 \text{ kJ mol}^{-1}$ is found.

the cell constant a_0 for a particular cation A, for which the following parametric relationships (least-square fits) are obtained:

$$U_{\text{POT}}(\text{K}_2\text{MCl}_6) = -329a_0 + 4655 \text{ kJ mol}^{-1} \quad (53)$$

$$U_{\text{POT}}(\text{Rb}_2\text{MCl}_6) = -339a_0 + 4795 \text{ kJ mol}^{-1} \quad (54)$$

$$U_{\text{POT}}(\text{Cs}_2\text{MCl}_6) = -348a_0 + 4969 \text{ kJ mol}^{-1} \quad (55)$$

$$U_{\text{POT}}((\text{NH}_4)_2\text{MCl}_6) = -309a_0 + 4486 \text{ kJ mol}^{-1} \quad (56)$$

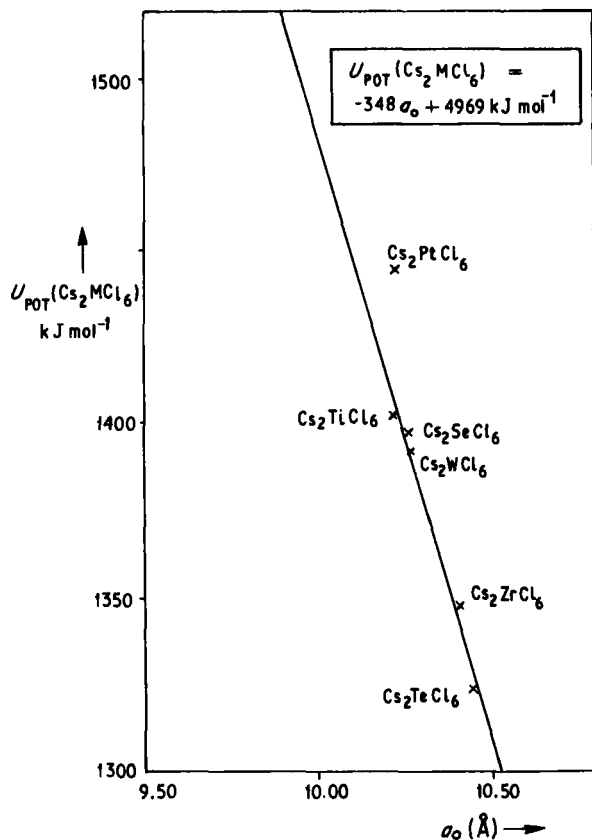


FIG. 8. Calculated lattice energy for cesium salts, Cs_2MCl_6 , as a function of the cubic cell parameter, a_0 . The relationship $U_{\text{POT}}(\text{Cs}_2\text{MCl}_6) = -348a_0 + 4969 \text{ kJ mol}^{-1}$ is found.

Equations (53)–(56) are used in cases where no u parameter is available for the antifuorite structure. (This is the case where only powder diffraction work has been carried out.)

IV. Thermochemical Data

The following standard thermodynamic data are used consistently throughout this study.

$$\Delta H_f^\theta(\text{K}^+)(\text{g}) = 514.2 \text{ kJ mol}^{-1} \text{ (34)*} \quad (57)$$

$$\Delta H_f^\theta(\text{Rb}^+)(\text{g}) = 494.9 \text{ kJ mol}^{-1} \text{ (61)} \quad (58)$$

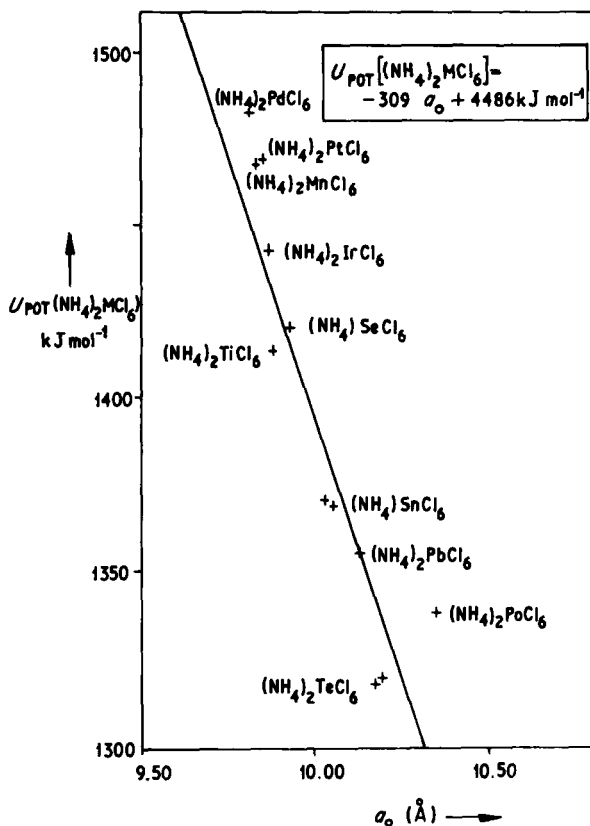


FIG. 9. Calculated lattice energy for ammonium salts, $(NH_4)_2MCl_6$, as a function of the cubic cell parameter, a_0 . The relationship $U_{POT}[(NH_4)_2MCl_6] = -309a_0 + 4486$ kJ mol $^{-1}$ is found.

$$\Delta H_f^\theta(Cs^+)(g) = 452.3 \text{ kJ mol}^{-1} \quad (34) \quad (59)$$

$$\Delta H_f^\theta(Tl^+)(g) = 777.7 \text{ kJ mol}^{-1} \quad (56) \quad (60)$$

$$\Delta H_f^\theta(NH_4^+)(g) = 630.2 \text{ kJ mol}^{-1} \quad (37) \quad (61)$$

$$\Delta H_f^\theta(F^-)(g) = -270.7 \text{ kJ mol}^{-1} \quad (11) \quad (62)$$

$$\Delta H_f^\theta(Cl^-)(g) = -246.0 \text{ kJ mol}^{-1} \quad (11) \quad (63)$$

$$\Delta H_f^\theta(Br^-)(g) = -233.9 \text{ kJ mol}^{-1} \quad (11) \quad (64)$$

$$\Delta H_f^\theta(\text{H}^+)(\text{g}) = 1536.2 \text{ kJ mol}^{-1} \quad (56) \quad (65)$$

$$\Delta H_{\text{hyd}}^\theta(\text{H}^+)(\text{g}) = -1100.6 \text{ kJ mol}^{-1} \quad (37) \quad (66)$$

Other thermochemical data used in the course of this study are cited at the relevant point in the text; the above data are the more general and heavily used data.

V. Computations of Lattice Energies and Associated Data

A. FORMAT

This chapter cites data extracted from the literature (structural information, standard enthalpies of formation, etc.), and from these data much new thermodynamic information is derived. To make the immediate distinction between these two sets of data, we have adopted the policy of enclosing within boxes the *derived* data included in this study.

The entry for a given ion is divided where appropriate into three subsections. The subsection "*Recent Studies*" give the results obtained by Jenkins and Pratt using their recently proposed (39) minimization technique (Section II,A) for lattice energies and the associated thermochemical values. The new data derived from such calculations are enclosed in boxes. Using the accurately computed lattice energies from subsections *a*, we can derive the plots given in Fig. 6-9 [and the associated least squares-fit equations, (53)-(56)] from which, in cases where only a_0 is known for an antiferroite structure, $U_{\text{POT}}(\text{A}_2\text{MX}_6)$ can be interpolated. The subsection which lists these results is headed "*Derived Estimates*." We give in Table I the numerical values of the lattice energy, etc., as derived from other work and we list thermochemical values cited in these studies in subsections headed "*Previous Calculations*."

The numerical results from subsections *a*, *b*, and *c* are collected in Tables III, IV, and I, respectively.

Absence of a subsection for a given ion implies that the appropriate section was not relevant to that particular ion, usually because of lack of the necessary data.

The compounds are dealt with in periodic order. A standard format for the presentation of the results is established for TiCl_6^{2-} , and the results for the ions subsequently dealt with are presented in an abbreviated but similar fashion.

TABLE IV
DERIVED ESTIMATES FOR LATTICE ENERGIES USING
EQUATIONS (53)–(56) IN THE TEXT

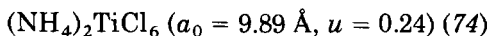
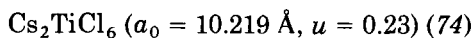
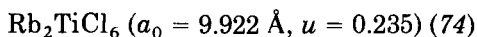
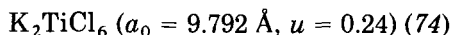
MX_6^{2-}	A^+	a_0 (Å)	$U_{\text{POT}}(A_2MX_6)$ (kJ mol ⁻¹)
ZrCl ₆ ²⁻	K ⁺	10.08	1339
HfCl ₆ ²⁻	K ⁺	10.06	1345
NbCl ₆ ²⁻	K ⁺	9.97	1375
	Rb ⁺	10.10	1371
	Cs ⁺	10.31	1381
TaCl ₆ ²⁻	K ⁺	9.96	1378
	Rb ⁺	10.11	1368
	Cs ⁺	10.32	1378
MoCl ₆ ²⁻	Rb ⁺	9.99	1408
	Cs ⁺	10.27	1395
MnCl ₆ ²⁻	Cs ⁺	10.17	1430
TcCl ₆ ²⁻	Rb ⁺	9.965	1417
ReCl ₆ ²⁻	Rb ⁺	9.974	1414
	Cs ⁺	10.26	1398
	NH ₄ ⁺	9.98	1402
	NH ₄ ⁺	10.07	1374
RuCl ₆ ²⁻	K ⁺	9.738	1451
OsCl ₆ ²⁻	Cs ⁺	10.230	1409
	NH ₄ ⁺	9.881	1433
PdCl ₆ ²⁻	K ⁺	9.74	1450
	Rb ⁺	9.87	1449
	Cs ⁺	10.18	1426
SbCl ₆ ²⁻	Rb ⁺	10.14	1357
TeCl ₆ ²⁻	K ⁺	10.143	1318

B. TITANIUM(IV), ZIRCONIUM(IV), AND HAFNIUM(IV) SALTS

1. TiCl₆²⁻: Hexachlorotitinate Ion

a. Recent Studies

i. *Structures.* The hexachlorotitanates that possess the antiferroite structure and for which complete structural information is available are



ii. *Charge distribution in ion.* We use, in the absence of experimental data, the method of Jørgensen (42–45) to establish

$$q_{\text{Cl}} = -0.61$$

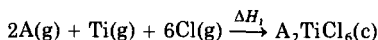
iii. *Lattice energies.* Based on a charge distribution above, we calculate the total lattice potential energies of the salts concerned to be

$$\begin{aligned} U_{\text{POT}}(\text{K}_2\text{TiCl}_6) &= 1412 \text{ kJ mol}^{-1} \\ U_{\text{POT}}(\text{Rb}_2\text{TiCl}_6) &= 1415 \text{ kJ mol}^{-1} \\ U_{\text{POT}}(\text{Cs}_2\text{TiCl}_6) &= 1402 \text{ kJ mol}^{-1} \\ U_{\text{POT}}[(\text{NH}_4)_2\text{TiCl}_6] &= 1413 \text{ kJ mol}^{-1} \end{aligned}$$

iv. *"Basic" radius.* The values of $\bar{r}_{\text{TiCl}_6^{2-}}$ given in Fig. 10 and corresponding to $q_{\text{Cl}} = -0.61$ are 2.48 Å (K_2TiCl_6); 2.47 Å (Rb_2TiCl_6); 2.50 Å (Cs_2TiCl_6), and 2.50 Å $[(\text{NH}_4)_2\text{TiCl}_6]$. They average to:

$$\bar{r}_{\text{TiCl}_6^{2-}} = 2.48 \text{ Å}$$

v. *Enthalpy of formation of gaseous TiCl_6^{2-} ion.* Korol'kov and Efimov (48) have reported the enthalpies of formation of A_2MX_6 salts ($\text{A} = \text{K, Rb, Cs}$; $\text{M} = \text{Ti}$; $\text{X} = \text{Cl}$) from their gaseous atoms, ΔH_1 :



This enthalpy is related to $\Delta H_f^\theta(\text{A}_2\text{TiCl}_6)(\text{c})$ by the equation:

$$\Delta H_f^\theta(\text{A}_2\text{TiCl}_6)(\text{c}) = \Delta H_1 + 2\Delta H_f^\theta(\text{A})(\text{g}) + \Delta H_f^\theta(\text{Ti})(\text{g}) + 6\Delta H_f^\theta(\text{Cl})(\text{g}) \quad (67)$$

where: $\Delta H_f^\theta(\text{K})(\text{g}) = 89.16 \text{ kJ mol}^{-1}$ (34), $\Delta H_f^\theta(\text{Rb})(\text{g}) = 85.8 \text{ kJ mol}^{-1}$ (61), $\Delta H_f^\theta(\text{Cs})(\text{g}) = 76.65 \text{ kJ mol}^{-1}$ (34), $\Delta H_f^\theta(\text{Ti})(\text{g}) = 473 \text{ kJ mol}^{-1}$ (34), and $\Delta H_f^\theta(\text{Cl})(\text{g}) = 121.01 \text{ kJ mol}^{-1}$ (34); and we find that

$$\begin{aligned} \Delta H_f^\theta(\text{K}_2\text{TiCl}_6)(\text{c}) &= -1747 \text{ kJ mol}^{-1} \\ \Delta H_f^\theta(\text{Rb}_2\text{TiCl}_6)(\text{c}) &= -1767 \text{ kJ mol}^{-1} \\ \Delta H_f^\theta(\text{Cs}_2\text{TiCl}_6)(\text{c}) &= -1797 \text{ kJ mol}^{-1} \end{aligned}$$

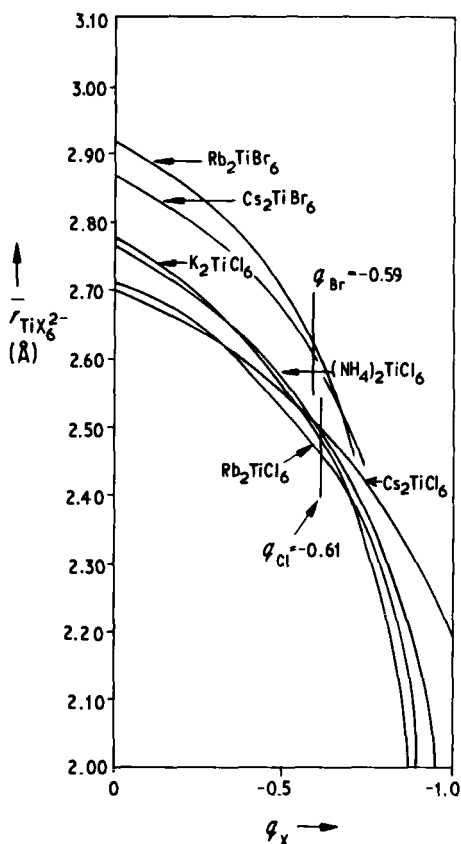


FIG. 10. Basic radius of $TiCl_6^{2-}$ and $TiBr_6^{2-}$ ions, corresponding to lattice potential energy minima, as a function of the charge, q_X , on the halogen atom.

Using the standard data at the end of the last section in Eq. (1) with the computed values of $U_{POT}(A_2TiCl_6)$, we can plot $\Delta H_f^\theta(TiCl_6^{2-})(g)$ as a function of q_{Cl} (Fig. 11). We find that $\Delta H_f^\theta(TiCl_6^{2-})(g) = -1361 \text{ kJ mol}^{-1}$ (K_2TiCl_6), $-1342 \text{ kJ mol}^{-1}$ (Rb_2TiCl_6) and $-1300 \text{ kJ mol}^{-1}$ (Cs_2TiCl_6), giving an estimated average value:

$$\Delta H_f^\theta(TiCl_6^{2-})(g) = -1330 \pm 30 \text{ kJ mol}^{-1}$$

vi. *Enthalpy of hydration of the gaseous $TiCl_6^{2-}$ ion.* No aqueous data exist for these salts.

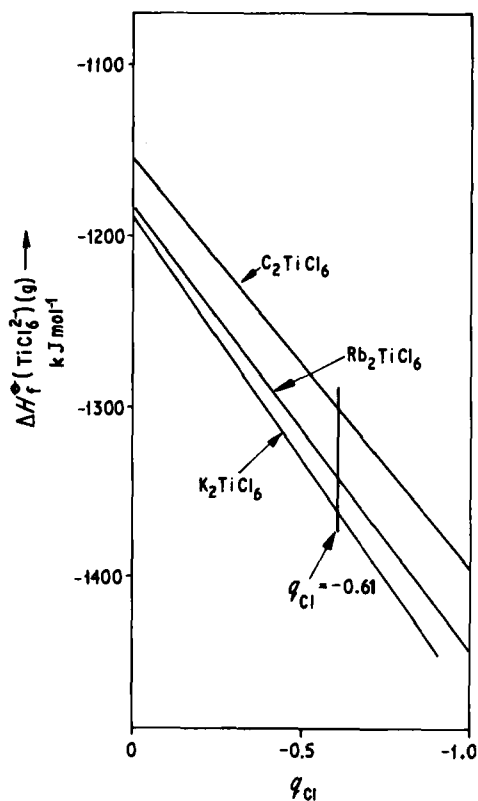


FIG. 11. Enthalpy of formation, $\Delta H_f^\circ(\text{TiCl}_6^{2-})(g)$ corresponding to lattice potential energy minimum as a function of the charge, q_{Cl} on the chlorine atoms.

vii. *Halide ion affinities.* Taking $\Delta H_f^\circ(\text{TiCl}_4)(g) = -763.2 \text{ kJ mol}^{-1}$ (56); $\Delta H_f^\circ(\text{TiCl}_4)(l) = -804.2 \text{ kJ mol}^{-1}$ (56), we find:

$$\begin{aligned} \Delta H_{\text{Cl}(g)} &= -76 \pm 30 \text{ kJ mol}^{-1} \\ \Delta H_{\text{Cl}(l)} &= -36 \pm 30 \text{ kJ mol}^{-1} \end{aligned}$$

for the chloride ion affinities of $\text{TiCl}_4(g)$ and $\text{TiCl}_4(l)$, respectively.

viii. *Prediction of lattice energies.* Taking

$$\Delta H_f^\circ(\text{Ti}_2\text{TiCl}_6)(c) = -1330 \text{ kJ mol}^{-1} \text{ (56),}$$

we calculate:

$$U_{\text{POT}}(\text{Ti}_2\text{TiCl}_6) = 1560 \pm 30 \text{ kJ mol}^{-1}$$

2. TiBr_6^{2-} : Hexabromotitanate Ion

a. Recent Studies

i. Structure

$$\text{Rb}_2\text{TiBr}_6 (a_0 = 10.39 \text{ \AA}, u = 0.25) (48)$$

$$\text{Cs}_2\text{TiBr}_6 (a_0 = 10.57 \text{ \AA}, u = 0.25) (48)$$

ii. Charge distribution

$$q_{\text{Br}} = -0.59$$

iii. Lattice energies

$$U_{\text{POT}}(\text{Rb}_2\text{TiBr}_6) = 1341 \text{ kJ mol}^{-1}$$

$$U_{\text{POT}}(\text{Cs}_2\text{TiBr}_6) = 1339 \text{ kJ mol}^{-1}$$

iv. "Basic" radius of ion (Fig. 10)

$$\bar{r}_{\text{TiBr}_6^{2-}} = 2.61 \text{ \AA}$$

v. Enthalpy of formation of gaseous ion (Fig. 12)

Ancillary data:

$$\Delta H_f^\theta(\text{K}_2\text{TiBr}_6)(\text{c}) = -1493 \text{ kJ mol}^{-1} (48);$$

$\Delta H_f^\theta(\text{Rb}_2\text{TiBr}_6)(\text{c}) = -1517 \text{ kJ mol}^{-1} (48)$, $-1505 \text{ kJ mol}^{-1} (68a)$ or $-1612 \text{ kJ mol}^{-1} (64)$, $(62a)$ and $\Delta H_f^\theta(\text{Cs}_2\text{TiBr}_6)(\text{c}) = -1553 \text{ kJ mol}^{-1} (48)$, $-1644 \text{ kJ mol}^{-1} (62a)$ or $-1641 \text{ kJ mol}^{-1} (64)$. Where two values are given, the former has been calculated by us from the $\Delta H_f^\theta(\text{A}_2\text{MBr}_6)(\text{c})$ data of Korol'kov and Efimov using $\Delta H_f^\theta(\text{Br})(\text{g}) = 111.9 \text{ kJ mol}^{-1} (34)$, similar to the case of the corresponding chlorides, A_2MCl_6 . We have chosen to use these formation data because they were recorded two years later than the alternative data available.

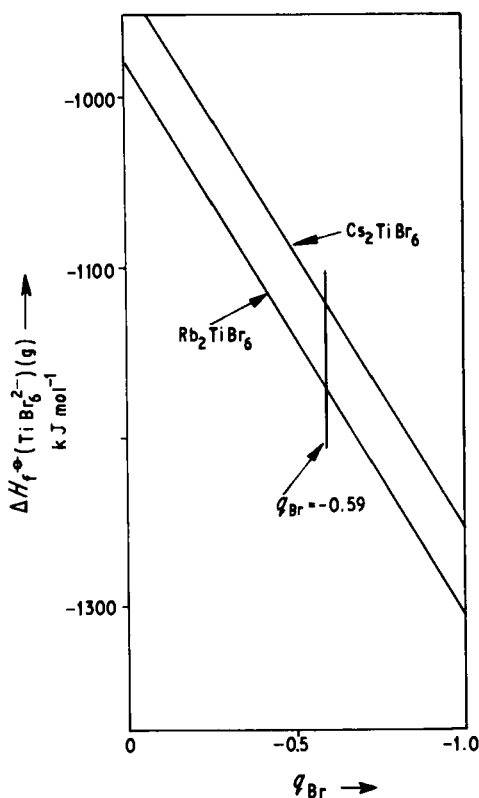


FIG. 12. Enthalpy of formation, $\Delta H_f^\theta(\text{TiBr}_6^{2-})(\text{g})$, corresponding to lattice potential energy minimum, as a function of the charge, q_{Br} , on the bromine atom.

Assigned value:

$$\Delta H_f^\theta(\text{TiBr}_6^{2-})(\text{g}) = -1142 \pm 32 \text{ kJ mol}^{-1}$$

vi. *Halide ion affinities*

Ancillary data:

$$\Delta H_f^\theta(\text{TiBr}_4)(\text{c}) = -616.7 \text{ kJ mol}^{-1} \text{ (56)}$$

and

$$\Delta H_f^\theta(\text{TiBr}_4)(\text{g}) = -549.3 \text{ kJ mol}^{-1} \text{ (56)}.$$

Assigned value:

$$\begin{aligned}\Delta H_{\text{Br(c)}} &= -58 \pm 32 \text{ kJ mol}^{-1} \\ \Delta H_{\text{Br(g)}} &= -125 \pm 32 \text{ kJ mol}^{-1}\end{aligned}$$

vii. *Prediction of lattice energies*

Ancillary data:

$$\Delta H_f^\theta(\text{K}_2\text{TiBr}_6)(\text{c}) = -1493 \text{ kJ mol}^{-1} \quad (48)$$

and

$$\Delta H_f^\theta(\text{TiBr}_6^{2-})(\text{g}) = -1142 \pm 32 \text{ kJ mol}^{-1}.$$

Assigned value:

$$U_{\text{POT}}(\text{K}_2\text{TiBr}_6) = 1379 \pm 32 \text{ kJ mol}^{-1}$$

3. ZrCl_6^{2-} : Hexachlorozirconate Ion

a. Recent Studies

i. Structures

$$\text{Rb}_2\text{ZrCl}_6 \quad (a_0 = 10.178 \text{ \AA}, u = 0.24) \quad (74)$$

$$\text{Cs}_2\text{ZrCl}_6 \quad (a_0 = 10.407 \text{ \AA}, u = 0.235) \quad (74)$$

ii. Charge distribution

$$q_{\text{Cl}} = -0.66$$

iii. Lattice energy

$$U_{\text{POT}}(\text{Rb}_2\text{ZrCl}_6) = 1348 \text{ kJ mol}^{-1}$$

$$U_{\text{POT}}(\text{Cs}_2\text{ZrCl}_6) = 1348 \text{ kJ mol}^{-1}$$

iv. "Basic" radius of ion (Fig. 13)

$$\bar{r}_{\text{ZrCl}_6^{2-}} = 2.47 \text{ \AA}$$

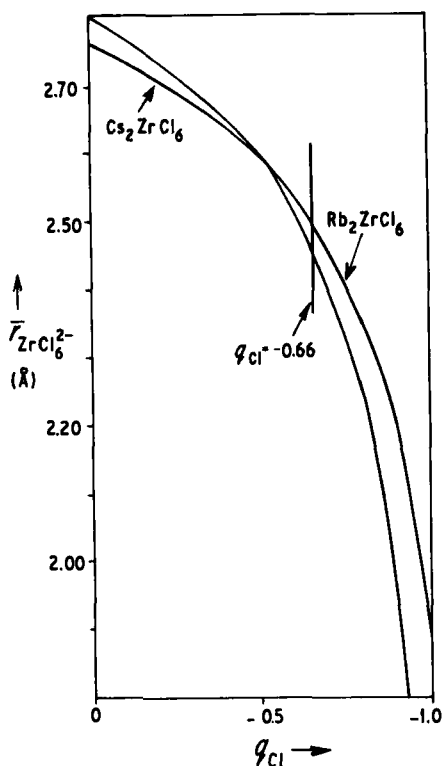


FIG. 13. Basic radius of ZrCl_6^{2-} ion, corresponding to lattice potential energy minimum, as a function of the charge, q_{Cl} , on the chlorine atoms.

v. *Enthalpy of formation of gaseous ion*

Ancillary data: $\Delta H_f^\circ(\text{Zr})(\text{g}) = 620 \text{ kJ mol}^{-1}$ (34), together with Korol'kov and Efimov's (48) estimate of the enthalpy of formation of Cs_2ZrCl_6 to be $-3445 \text{ kJ mol}^{-1}$ (from gaseous atoms)

Assigned value:

$$\Delta H_f^\circ(\text{ZrCl}_6^{2-})(\text{g}) = -1503 \text{ kJ mol}^{-1}$$

Gelbman and Westland (22) have reported $\Delta H_f^\circ(\text{Cs}_2\text{ZrCl}_6)(\text{c}) = -1992 \pm 4 \text{ kJ mol}^{-1}$ and combining this with the calculated lattice energy above we obtain a value: $\Delta H_f^\circ(\text{ZrCl}_6^{2-})(\text{g}) = -1549 \text{ kJ mol}^{-1}$.

Further using Gelbman and Westland's (22) value for

$$\Delta H_f^\circ(\text{K}_2\text{ZrCl}_6)(\text{c}) = -1932 \pm 4 \text{ kJ mol}^{-1}$$

in conjunction with the lattice energy $U_{\text{POT}}(\text{K}_2\text{ZrCl}_6)$ estimated below, we find:

$$\Delta H_f^\theta(\text{ZrCl}_6^{2-})(\text{g}) \simeq -1621 \text{ kJ mol}^{-1}$$

$$\Delta H_f^\theta(\text{ZrCl}_6^{2-})(\text{g}) = -1526 + 32 \text{ kJ mol}^{-1}$$

vi. *Halide ion affinities*

Ancillary data:

$$\Delta H_f^\theta(\text{ZrCl}_4)(\text{c}) = -980.5 \text{ kJ mol}^{-1} \text{ (22, 56)}$$

and

$$\Delta H_f^\theta(\text{ZrCl}_4)(\text{g}) = -870.3 \text{ kJ mol}^{-1} \text{ (56)}.$$

Assigned values:

$$\overline{\Delta H}_{\text{Cl(c)}} = -54 \text{ kJ mol}^{-1}$$

$$\overline{\Delta H}_{\text{Cl(g)}} = -164 \text{ kJ mol}^{-1}$$

b. Derived Estimates. The above calculations are derived from our accurate approach to the treatment of lattice energies. In addition, on the basis of partial structural details:

$$\text{K}_2\text{ZrCl}_6 \text{ (} a_0 = 10.08 \text{ \AA) (54)}$$

we can use Eq. (53) to estimate

$$U_{\text{POT}}(\text{K}_2\text{ZrCl}_6) \simeq 1339 \text{ kJ mol}^{-1}$$

c. Previous Calculations. Gelbman and Westland (22) have cited the relationship:

$$\overline{\Delta H}_{\text{Cl(g)}} = -1597 \pm 5 + U_{\text{POT}}(\text{K}_2\text{ZrCl}_6) \text{ kJ mol}^{-1} \quad (68)$$

In his previous work (51) with Lal, Westland quoted:

$$U_{\text{POT}}(\text{K}_2\text{NbCl}_6) = 1586 \text{ kJ mol}^{-1}$$

and in the present work (22) he quotes:

$$U_{\text{POT}}(\text{K}_2\text{NbCl}_6) - U_{\text{POT}}(\text{K}_2\text{ZrCl}_6) \simeq 15 \text{ kJ mol}^{-1} \quad (69)$$

on the basis of Kapustinskii's equation (46) whereupon:

$$U_{\text{POT}}(\text{K}_2\text{ZrCl}_6) \simeq 1571 \text{ kJ mol}^{-1}$$

and hence a chloride ion affinity for $\text{ZrCl}_4(\text{g})$ of

$$\overline{\Delta H}_{\text{Cl}(\text{g})} = -26 \pm 5 \text{ kJ mol}^{-1}$$

is predicted.

4. ZrBr_6^{2-} : Hexabromozirconate Ion

c. Previous Calculations. Makhija and Westland (54a) have cited the relationships:

$$\overline{\Delta H}_{\text{Br}(\text{g})} = -1510 + U_{\text{POT}}(\text{K}_2\text{ZrBr}_6) \text{ kJ mol}^{-1} \quad (70)$$

$$\overline{\Delta H}_{\text{Br}(\text{g})} = -1465 + U_{\text{POT}}(\text{Cs}_2\text{ZrBr}_6) \text{ kJ mol}^{-1} \quad (71)$$

Using their lattice energies cited in Table I they obtain:

$$\overline{\Delta H}_{\text{Br}(\text{g})} = -9 \text{ or } -1 \text{ kJ mol}^{-1}$$

5. HfCl_6^{2-} : Hexachlorohafnate Ion

a. Recent Studies.

i. Structures

$$\text{Cs}_2\text{HfCl}_6 (a_0 = 10.42 \text{ \AA}, u = 0.25) \quad (54c)$$

ii. Charge distribution

$$q_{\text{Cl}} = -0.66$$

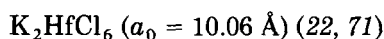
iii. Lattice energies

$U_{\text{POT}}(\text{Cs}_2\text{HfCl}_6) = 1315 \text{ kJ mol}^{-1}$

iv. "Basic" radius of ion

$$\bar{r}_{\text{HfCl}_6^{2-}} = 2.37 \text{ \AA}$$

No thermochemical data exists for this salt.

b. *Derived Estimates*i. *Structures*ii. *Prediction of lattice energies*

Assigned value:

$$U_{\text{TOT}}(\text{K}_2\text{HfCl}_6) \simeq 1345 \text{ kJ mol}^{-1}$$

iii. *Enthalpy of formation of gaseous ion*

Ancillary data:

$$\Delta H_f^\theta(\text{K}_2\text{HfCl}_6)(\text{c}) = -1957 \pm 12 \text{ kJ mol}^{-1} (22)$$

Assigned value:

$$\Delta H_f^\theta(\text{HfCl}_6^{2-})(\text{g}) = -1640 \pm 12 \text{ kJ mol}^{-1}$$

iv. *Halide ion affinities*

Ancillary data:

$$\Delta H_f^\theta(\text{HfCl}_4)(\text{c}) = -990 \pm 10 \text{ kJ mol}^{-1} (56), -992 \text{ kJ mol}^{-1} (20b)$$

and

$$\Delta H_f^\theta(\text{HfCl}_4)(\text{g}) = -889 \pm 12 \text{ kJ mol}^{-1} (56).$$

Assigned value:

$$\bar{\Delta H}_{\text{Cl}(\text{c})} = -158 \text{ kJ mol}^{-1}$$

$$\bar{\Delta H}_{\text{Cl}(\text{g})} = -259 \text{ kJ mol}^{-1}$$

c. *Previous Calculations.* Gelbman and Westland (22) have cited the relationship

$$\overline{\Delta H}_{\text{Cl(g)}} = -1611 \pm 14 + U_{\text{POT}}(\text{K}_2\text{HfCl}_6) \text{ kJ mol}^{-1} \quad (72)$$

and the lattice energy relationship

$$U_{\text{POT}}(\text{K}_2\text{HfCl}_6) - U_{\text{POT}}(\text{K}_2\text{ZrCl}_6) \simeq 3 \text{ kJ mol}^{-1} \quad (73)$$

Using the lattice energy of K_2ZrCl_6 , which they obtained ($\simeq 1571 \text{ kJ mol}^{-1}$) (22), they would assign

$$U_{\text{POT}}(\text{K}_2\text{HfCl}_6) \simeq 1574 \text{ kJ mol}^{-1}$$

and

$$\overline{\Delta H}_{\text{Cl(g)}} \simeq -37 \pm 14 \text{ kJ mol}^{-1}$$

6. HfBr_6^{2-} : Hexabromohafnate Ion

c. *Previous Calculations:* Makhija and Westland (54a) have given the relationship:

$$\overline{\Delta H}_{\text{Br(g)}} = -1510 = U_{\text{POT}}(\text{Cs}_2\text{HfBr}_6) \text{ kJ mol}^{-1} \quad (74)$$

Using their lattice energy given in Table I:

$$\overline{\Delta H}_{\text{Br(g)}} = -46 \text{ kJ mol}^{-1}$$

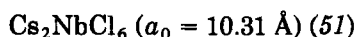
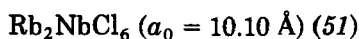
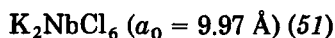
C. NIOBIUM(IV) AND TANTALUM(IV) SALTS

1. NbCl_6^{2-} Hexachloroniobate Ion

a. *Recent Studies.* No crystal structure data are available.

b. *Derived Estimates*

i. *Structures*



ii. *Prediction of lattice energies*

Assigned values:

$$\begin{aligned} U_{\text{POT}}(\text{K}_2\text{NbCl}_6) &= 1375 \text{ kJ mol}^{-1} \\ U_{\text{POT}}(\text{Rb}_2\text{NbCl}_6) &= 1371 \text{ kJ mol}^{-1} \\ U_{\text{POT}}(\text{Cs}_2\text{NbCl}_6) &= 1381 \text{ kJ mol}^{-1} \end{aligned}$$

iii. *Enthalpy of formation of gaseous ion*

Ancillary data:

$$\Delta H_f^\theta(\text{K}_2\text{NbCl}_6)(\text{c}) = -1594 \text{ kJ mol}^{-1} \text{ (51),}$$

$$\Delta H_f^\theta(\text{Rb}_2\text{NbCl}_6)(\text{c}) = -1619 \text{ kJ mol}^{-1} \text{ (51),}$$

and

$$\Delta H_f^\theta(\text{Cs}_2\text{NbCl}_6)(\text{c}) = -1663 \text{ kJ mol}^{-1} \text{ (51).}$$

Assigned value:

$$\Delta H_f^\theta(\text{NbCl}_6^{2-})(\text{g}) = -1224 \pm 32 \text{ kJ mol}^{-1}$$

iv. *Halide ion affinities*

Ancillary data:

$$\Delta H_f^\theta(\text{NbCl}_4)(\text{c}) = -694 \text{ kJ mol}^{-1} \text{ (34)}$$

and

$$\Delta H_f^\theta(\text{NbCl}_4)(\text{g}) = -561 \text{ kJ mol}^{-1} \text{ (34).}$$

Assigned value:

$$\begin{aligned} \overline{\Delta H}_{\text{Cl}(\text{c})} &= -38 \quad 32 \text{ kJ mol}^{-1} \\ \overline{\Delta H}_{\text{Cl}(\text{g})} &= -171 \pm 32 \text{ kJ mol}^{-1} \end{aligned}$$

c. *Previous Calculations.* Lal and Westland (51) have cited the relationship.

$$\overline{\Delta H}_{\text{Cl}(\text{g})} = -1571 + U_{\text{POT}}(\text{K}_2\text{NbCl}_6) \quad (75)$$

together with the following lattice energies obtained from the Kapustinskii (46) equation:

$$U_{\text{POT}}(\text{K}_2\text{NbCl}_6) = 1586 \text{ kJ mol}^{-1}$$

$$U_{\text{POT}}(\text{Rb}_2\text{NbCl}_6) = 1569 \text{ kJ mol}^{-1}$$

$$U_{\text{POT}}(\text{CsNbCl}_6) = 1540 \text{ kJ mol}^{-1}$$

Using the first of these values in Eq. (76), the predicted chloride ion affinity of niobium(IV) chloride is therefore:

$$\overline{\Delta H}_{\text{Cl(g)}} = +15 \text{ kJ mol}^{-1}$$

2. TaCl_6^{2-} : Hexachlorotantalate Ion

a. *Recent Studies.* No crystal structure data are available.

b. *Derived Estimates*

i. *Structures*

$$\text{K}_2\text{TaCl}_6 (a_0 = 9.96 \text{ \AA}) (51)$$

$$\text{Rb}_2\text{TaCl}_6 (a_0 = 10.11 \text{ \AA}) (51)$$

$$\text{Cs}_2\text{TaCl}_6 (a_0 = 10.32 \text{ \AA}) (51)$$

ii. *Prediction of lattice energies*

Assigned value:

$$U_{\text{POT}}(\text{K}_2\text{TaCl}_6) = 1378 \text{ kJ mol}^{-1}$$

$$U_{\text{POT}}(\text{Rb}_2\text{TaCl}_6) = 1368 \text{ kJ mol}^{-1}$$

$$U_{\text{POT}}(\text{Cs}_2\text{TaCl}_6) = 1378 \text{ kJ mol}^{-1}$$

iii. *Enthalpy of formation of gaseous ion*

Ancillary data:

$$\Delta H_f^\theta(\text{K}_2\text{TaCl}_6)(\text{c}) = -1648 \text{ kJ mol}^{-1} (51) \quad \text{or} \quad -1707 \text{ kJ mol}^{-1} (68),$$

$$\Delta H_f^\theta(\text{Rb}_2\text{TaCl}_6)(\text{c}) = -1669 \text{ kJ mol}^{-1} (51),$$

and

$$\Delta H_f^\theta(\text{Cs}_2\text{TaCl}_6)(\text{c}) = -1711 \text{ kJ mol}^{-1} (51).$$

Assigned value:

$$\Delta H_f^\theta(\text{TaCl}_6^{2-})(g) = -1296 \pm 49 \text{ kJ mol}^{-1}$$

iv. *Halide ion affinities*

Ancillary data:

$$\Delta H_f^\theta(\text{TaCl}_4)(c) = -702 \text{ kJ mol}^{-1} (34)^*, -860 \text{ kJ mol}^{-1} (20a)$$

and

$$\Delta H_f^\theta(\text{TaCl}_4)(g) = -561 \text{ kJ mol}^{-1} (34).$$

Assigned value:

$$\begin{aligned} \overline{\Delta H}_{\text{Cl}(c)} &= -102 \pm 49 \text{ kJ mol}^{-1} \\ \overline{\Delta H}_{\text{Cl}(g)} &= -243 \pm 49 \text{ kJ mol}^{-1} \end{aligned}$$

c. *Previous Calculations.* Tsintsius and Smirnova (68) have calculated that:

$$\Delta H_f^\theta(\text{TaCl}_6^{2-})(g) = -1268 \text{ kJ mol}^{-1}$$

from lattice energies obtained from the extended Kapustinskii (46) equation:

$$U_{\text{POT}}(\text{K}_2\text{TaCl}_6) = 1582 \text{ kJ mol}^{-1}$$

$$U_{\text{POT}}(\text{Rb}_2\text{TaCl}_6) = 1565 \text{ kJ mol}^{-1}$$

$$U_{\text{POT}}(\text{Cs}_2\text{TaCl}_6) = 1540 \text{ kJ mol}^{-1}$$

Lal and Westland (51) have cited the relationship

$$\overline{\Delta H}_{\text{Cl}(g)} = -1609 + U_{\text{POT}}(\text{K}_2\text{TaCl}_6) \quad (76)$$

together with the following lattice energies obtained from the Kapustinskii (46) relationship:

$$U_{\text{POT}}(\text{K}_2\text{TaCl}_6) = 1586 \text{ kJ mol}^{-1}$$

$$U_{\text{POT}}(\text{Rb}_2\text{TaCl}_6) = 1569 \text{ kJ mol}^{-1}$$

$$U_{\text{POT}}(\text{Cs}_2\text{TaCl}_6) = 1540 \text{ kJ mol}^{-1}$$

* Preferred value.

Using the first of these values in Eq. (77), the predicted chloride ion affinity of tantalum(IV) chloride is therefore:

$$\overline{\Delta H}_{\text{Cl(g)}} = -23 \text{ kJ mol}^{-1}$$

D. CHROMIUM(IV), MOLYBDENUM(IV) AND TUNGSTEN(IV) SALTS

1. CrF_6^{2-} : Hexafluorochromate Ion

a. Recent Studies

i. Structure

$$\text{Cs}_2\text{CrF}_6 \ (a_0 = 9.02 \text{ \AA}, u = 0.192) \ (74)$$

ii. Charge distribution

$$q_{\text{F}} = -0.65$$

iii. *Lattice energies.* The equation for the lattice potential energy of Cs_2CrF_6 as a function of the charge q_{F} takes the rectilinear form:

$$U_{\text{POT}}(\text{Cs}_2\text{CrF}_6) \simeq 120 q_{\text{F}} + 1681 \text{ kJ mol}^{-1}$$

and corresponding to $q_{\text{F}} = -0.65$,

$$U_{\text{POT}}(\text{Cs}_2\text{CrF}_6) = 1603 \text{ kJ mol}^{-1}$$

iv. "Basic" radius of ion

$$\bar{r}_{\text{CrF}_6^{2-}} = 2.08 \text{ \AA}$$

No thermochemical data exist for A_2CrF_6 salts.

2. MoCl_6^{2-} : Hexachloromolybdate Ion

a. Recent Studies

i. Structure

$$\text{K}_2\text{MoCl}_6 \ (a_0 = 9.85 \text{ \AA}, u = 0.234) \ (74)$$

ii. *Charge distribution*

$$q_{\text{Cl}} = -0.60$$

iii. *Lattice energies*

$$U_{\text{TOT}}(\text{K}_2\text{MoCl}_6) = 1418 \text{ kJ mol}^{-1}$$

iv. "Basic" radius of ion

$$\bar{r}_{\text{MoCl}_6^{2-}} = 2.54 \text{ \AA}$$

v. *Enthalpy of formation of gaseous ion*

Ancillary data:

$$\Delta H_f^\theta(\text{K}_2\text{MoCl}_6)(\text{c}) = -1475 \text{ kJ mol}^{-1} (11), -1465 \text{ kJ mol}^{-1} (48)$$

or

$$-1469 \text{ kJ mol}^{-1} (19).$$

Assigned value:

$$\Delta H_f^\theta(\text{MoCl}_6^{2-})(\text{g}) = -1070 \pm 5 \text{ kJ mol}^{-1}$$

iv. *Halide ion affinities*

Ancillary data:

$$\Delta H_f^\theta(\text{MoCl}_4)(\text{c}) = -475.8 \text{ kJ mol}^{-1} (11)$$

and

$$\Delta H_f^\theta(\text{MoCl}_4)(\text{g}) = -386.3 \text{ kJ mol}^{-1} (11)$$

Assigned value:

$$\begin{aligned} \overline{\Delta H}_{\text{Cl}(\text{c})} &= -102 \pm 5 \text{ kJ mol}^{-1} \\ \overline{\Delta H}_{\text{Cl}(\text{g})} &= -192 \pm 5 \text{ kJ mol}^{-1} \end{aligned}$$

vii. *Prediction of lattice energies*

Ancillary data:

$$\Delta H_f^\theta(\text{Rb}_2\text{MoCl}_6)(\text{c}) = -1479 \text{ kJ mol}^{-1} \text{ (48)}$$

or $-1495 \text{ kJ mol}^{-1}$ (19);

$$\Delta H_f^\theta(\text{Cs}_2\text{MoCl}_6)(\text{c}) = -1512 \text{ kJ mol}^{-1} \text{ (48)}$$

or $-1527 \text{ kJ mol}^{-1}$ (19); and

$$\Delta H_f^\theta(\text{Na}_2\text{MoCl}_6)(\text{c}) = -1376 \text{ kJ mol}^{-1} \text{ (11)}$$

or $-1372 \text{ kJ mol}^{-1}$ (19).

Assigned values:

$$U_{\text{POT}}(\text{Rb}_2\text{MoCl}_6) = 1399 \text{ kJ mol}^{-1} \text{ or } 1383 \text{ kJ mol}^{-1}$$

$$U_{\text{POT}}(\text{Cs}_2\text{MoCl}_6) = 1347 \text{ kJ mol}^{-1} \text{ or } 1332 \text{ kJ mol}^{-1}$$

$$U_{\text{POT}}(\text{Na}_2\text{MoCl}_6) = 1526 \text{ kJ mol}^{-1} \text{ or } 1530 \text{ kJ mol}^{-1}$$

depending on the source used for $\Delta H_f^\theta(\text{A}_2\text{MoCl}_6)(\text{c})$.b. *Derived Values*i. *Structures*

$$\text{Rb}_2\text{MoCl}_6 \text{ (} a_0 = 9.99 \text{ \AA) (74)}$$

$$\text{Cs}_2\text{MoCl}_6 \text{ (} a_0 = 10.27 \text{ \AA) (74)}$$

ii. *Prediction of lattice energies*

Assigned value:

$$U_{\text{POT}}(\text{Rb}_2\text{MoCl}_6) = 1408 \text{ kJ mol}^{-1}$$

$$U_{\text{POT}}(\text{Cs}_2\text{MoCl}_6) = 1395 \text{ kJ mol}^{-1}$$

iii. *Enthalpy of formation of gaseous ion*

Ancillary data:

$$\Delta H_f^\theta(\text{Rb}_2\text{MoCl}_6)(\text{c}) = -1479 \text{ kJ mol}^{-1} \text{ (48)}$$

or $-1495 \text{ kJ mol}^{-1}$ (19); and

$$\Delta H_f^\theta(\text{Cs}_2\text{MoCl}_6)(\text{c}) = -1512 \text{ kJ mol}^{-1} \text{ (48)}$$

or $-1527 \text{ kJ mol}^{-1}$ (19).

Assigned value:

$$\Delta H_f^\theta(\text{MoCl}_6^{2-})(\text{g}) = -1041 \pm 28 \text{ kJ mol}^{-1}$$

iv. *Halide ion affinities*

Ancillary data:

$$\Delta H_f^\theta(\text{MoCl}_4)(\text{c}) = -475.8 \text{ kJ mol}^{-1} \text{ (11)}$$

and

$$\Delta H_f^\theta(\text{MoCl}_4)(\text{g}) = -386.3 \text{ kJ mol}^{-1} \text{ (11)}.$$

Assigned value:

$$\begin{aligned} \overline{\Delta H}_{\text{Cl}(\text{c})} &= -73 \pm 28 \text{ kJ mol}^{-1} \\ \overline{\Delta H}_{\text{Cl}(\text{g})} &= -163 \pm 28 \text{ kJ mol}^{-1} \end{aligned}$$

c. *Previous Calculations.* Efimov and Belorukova (19), using the extended Kapustinskii equation, have obtained:

$$U_{\text{POT}}(\text{Na}_2\text{MoCl}_6) = 1638 \text{ kJ mol}^{-1}$$

$$U_{\text{POT}}(\text{K}_2\text{MoCl}_6) = 1602 \text{ kJ mol}^{-1}$$

$$U_{\text{POT}}(\text{Rb}_2\text{MoCl}_6) = 1567 \text{ kJ mol}^{-1}$$

$$U_{\text{POT}}(\text{Cs}_2\text{MoCl}_6) = 1537 \text{ kJ mol}^{-1}$$

from which they obtained:

$$\Delta H_f^\theta(\text{MoCl}_6^{2-})(\text{g}) = -1023 \text{ kJ mol}^{-1}$$

3. WCl_6^{2-} : Hexachlorotungstate Ion

a. Recent Studies

i. Structures

$$\text{K}_2\text{WCl}_6 (a_0 = 9.875 \text{ \AA}, u = 0.239) \text{ (47, 57)}$$

$$\text{Rb}_2\text{WCl}_6 (a_0 = 10.0 \text{ \AA}, u = 0.236) \text{ (47, 57)}$$

$$\text{Cs}_2\text{WCl}_6 (a_0 = 10.27 \text{ \AA}, u = 0.230) \text{ (47, 57)}$$

ii. Charge distribution

$$q_{\text{Cl}} = -0.62$$

iii. Lattice energies

$$\begin{aligned} U_{\text{POT}}(\text{K}_2\text{WCl}_6) &= 1398 \text{ kJ mol}^{-1} \\ U_{\text{POT}}(\text{Rb}_2\text{WCl}_6) &= 1397 \text{ kJ mol}^{-1} \\ U_{\text{POT}}(\text{Cs}_2\text{WCl}_6) &= 1392 \text{ kJ mol}^{-1} \end{aligned}$$

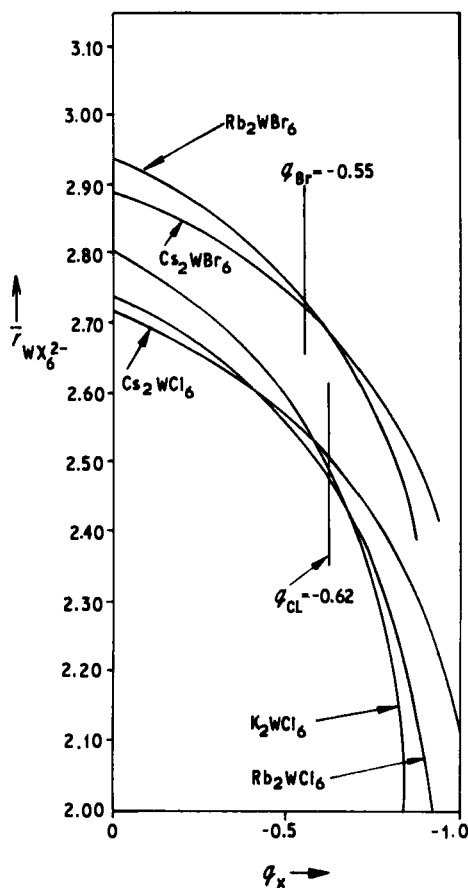


FIG. 14. Basic radii for ions WCl_6^{2-} and WBr_6^{2-} , corresponding to lattice potential energy minima, as a function of the charge, q_x , on the halogen atoms.

iv. "Basic" radius of ion (Fig. 14)

$$\bar{r}_{\text{WCl}_6^{2-}} = 2.49 \text{ \AA}$$

v. Enthalpy of formation of gaseous ion (Fig. 15)

Ancillary data:

$$\Delta H_f^\theta(\text{K}_2\text{WCl}_6)(c) = -1380 \text{ kJ mol}^{-1} (57),$$

and

$$-1359 \text{ kJ mol}^{-1} (11, 49), \Delta H_f^\theta(\text{Rb}_2\text{WCl}_6)(c) = -1429 \text{ kJ mol}^{-1} (11, 49),$$

$$\Delta H_f^\theta(\text{Cs}_2\text{WCl}_6)(c) = -1446 \text{ kJ mol}^{-1} (11, 49).$$

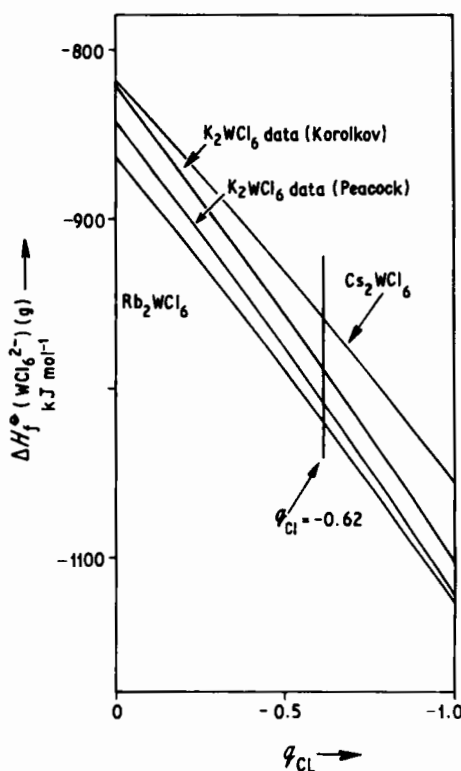


FIG. 15. Enthalpy of formation, $\Delta H_f^\theta(\text{WCl}_6^{2-})(g)$, corresponding to the lattice potential energy minima, as a function of the charge q_{Cl} on the chlorine atom.

Assigned value:

$$\Delta H_f^\theta(\text{WCl}_6^{2-})(g) = -985 \pm 35 \text{ kJ mol}^{-1}$$

vi. *Halide ion affinities*

Ancillary data:

$$\Delta H_f^\theta(\text{WCl}_4)(c) = -447 \text{ kJ mol}^{-1} (11)$$

or -469 kJ mol^{-1} (56) and

$$\Delta H_f^\theta(\text{WCl}_4)(g) = -341 \text{ kJ mol}^{-1} (11)$$

or -305 kJ mol^{-1} (56).

Assigned values:

$$\begin{aligned} \overline{\Delta H}_{\text{Cl}(c)} &= -46 \pm 35 \text{ kJ mol}^{-1} \\ \overline{\Delta H}_{\text{Cl}(g)} &= -152 \pm 35 \text{ kJ mol}^{-1} \end{aligned}$$

The values above correspond to the CATCH (11) data, taken since it emerges from a later tabulation.

vii. *Prediction of electron affinity of WCl₆(g):* Taking

$$\Delta H_f^\theta(\text{WCl}_6)(g) = -499 \text{ kJ mol}^{-1} (11),$$

we can calculate the electron affinity of WCl₆(g) for two electrons and find it to be:

$$A_{\text{WCl}_6} = -486 \pm 35 \text{ kJ mol}^{-1}$$

4. WBr₆²⁻: Hexabromotungstate ion

a. *Recent Studies*

i. *Structures*

$$\text{Rb}_2\text{WBr}_6 (a_0 = 10.50 \text{ \AA}, u = 0.236) (47, 57)$$

$$\text{Cs}_2\text{WBr}_6 (a_0 = 10.70 \text{ \AA}, u = 0.232) (47, 57)$$

ii. *Charge distribution*

$$q_{\text{Br}} = -0.55$$

iii. *Lattice energies*

$$U_{\text{POT}}(\text{Rb}_2\text{WBr}_6) = 1361 \text{ kJ mol}^{-1}$$

$$U_{\text{POT}}(\text{Cs}_2\text{WBr}_6) = 1362 \text{ kJ mol}^{-1}$$

iv. "Basic" radius of ion (Fig. 14)

$$\bar{r}_{\text{WBr}_6^{2-}} = 2.72 \text{ \AA}$$

v. *Enthalpy of formation of gaseous ion* (Fig. 16)

Ancillary data:

$$\Delta H_f^\circ(\text{Rb}_2\text{WBr}_6)(\text{c}) = -1106 \text{ kJ mol}^{-1} \quad (57)$$

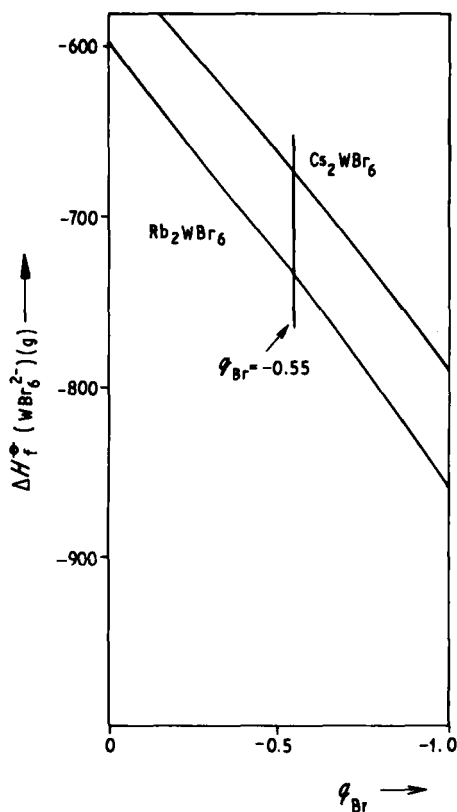


FIG. 16. Enthalpy of formation, $\Delta H_f^\circ(\text{WBr}_6^{2-})(\text{g})$, corresponding to the lattice potential energy minima, as a function of the charge, q_{Br} , on the bromine atom.

and

$$\Delta H_f^\theta(\text{Cs}_2\text{WBr}_6)(\text{c}) = -1132 \text{ kJ mol}^{-1} \text{ (57)}$$

Assigned value:

$$\Delta H_f^\theta(\text{WBr}_6^{2-})(\text{g}) = -705 + 30 \text{ kJ mol}^{-1}$$

vi. *Halide ion affinities*

Ancillary data:

$$\Delta H_f^\theta(\text{WBr}_4)(\text{c}) = -146 \text{ kJ mol}^{-1} \text{ (61)}$$

Assigned value:

$$\overline{\Delta H}_{\text{Br}(\text{c})} = -91 \pm 30 \text{ kJ mol}^{-1}$$

vii. *Prediction of lattice energies*

Ancillary data:

$$\Delta H_f^\theta(\text{K}_2\text{WBr}_6) = -1085 \text{ kJ mol}^{-1} \text{ (57)}$$

Assigned value:

$$U_{\text{POT}}(\text{K}_2\text{WBr}_6) = 1408 \pm 30 \text{ kJ mol}^{-1}$$

viii. *Prediction of electron affinity of WBr₆(c).* In the absence of $\Delta H_f^\theta(\text{WBr}_6)(\text{g})$ data we have a value for $\Delta H_f^\theta(\text{WBr}_6)(\text{c})$ (11) and find the enthalpy change for the conversion of $\text{WBr}_6(\text{c})$ to $\text{WBr}_6^{2-}(\text{g})$ to be $-359 \pm 30 \text{ kJ mol}^{-1}$.

E. MANGANESE(IV), TECHNIUM(IV), AND RHENIUM(IV) SALTS

1. MnF_6^{2-} : Hexafluoromanganate ion

a. *Recent Studies*

i. *Structures*

$$\text{Rb}_2\text{MnF}_6 (a_0 = 8.43 \text{ \AA}, u = 0.20) \text{ (74)}$$

$$\text{Cs}_2\text{MnF}_6 (a_0 = 8.92 \text{ \AA}, u = 0.195) \text{ (74)}$$

ii. *Charge distribution*

$$q_F = -0.63$$

iii. *Lattice energies.* The curves of $U_{\text{POT}}(A_2\text{MnF}_6)$ versus q_F show a rectilinear relationship over the range $0.0 \geq q_F \geq -1.0$ and, to within 5 kJ mol^{-1} , fit the equations

$$U_{\text{POT}}(\text{Rb}_2\text{MnF}_6) \simeq 143q_F + 1778$$

$$U_{\text{POT}}(\text{Cs}_2\text{MnF}_6) \simeq 128q_F + 1701$$

For a charge of $q_F = -0.63$, we find:

$U_{\text{POT}}(\text{Rb}_2\text{MnF}_6) = 1688 \text{ kJ mol}^{-1}$ $U_{\text{POT}}(\text{Cs}_2\text{MnF}_6) = 1620 \text{ kJ mol}^{-1}$

iv. "Basic" radius of ion (Fig. 17)

$\bar{r}_{\text{MnCl}_6^{2-}} = 2.02 \text{ \AA}$

No thermochemical data exist for these salts.

2. MnCl_6^{2-} : Hexachloromanganate iona. *Recent Studies*i. *Structures*

$$\text{K}_2\text{MnCl}_6 (a_0 = 9.6445 \text{ \AA}, u = 0.236) (55)$$

$$\text{Rb}_2\text{MnCl}_6 (a_0 = 9.838 \text{ \AA}, u = 0.232) (52)$$

$$(\text{NH}_4)_2\text{MnCl}_6 (a_0 = 9.82 \text{ \AA}, u = 0.228) (52)$$

ii. *Charge distribution*

$$q_{\text{Cl}} = -0.55$$

iii. *Lattice energies.* The curves of $U_{\text{POT}}(A_2\text{MnCl}_6)$ versus charge are not linear and vary over the range $0.0 \geq q_{\text{Cl}} \geq -1.0$ between the limits:

$$1606 \geq U_{\text{POT}}(\text{K}_2\text{MnCl}_6) \geq 1336 \text{ kJ mol}^{-1}$$

$$1583 \geq U_{\text{POT}}(\text{Rb}_2\text{MnCl}_6) \geq 1333 \text{ kJ mol}^{-1}$$

$$1588 \geq U_{\text{POT}}(\text{Cs}_2\text{MnCl}_6) \geq 1355 \text{ kJ mol}^{-1}$$

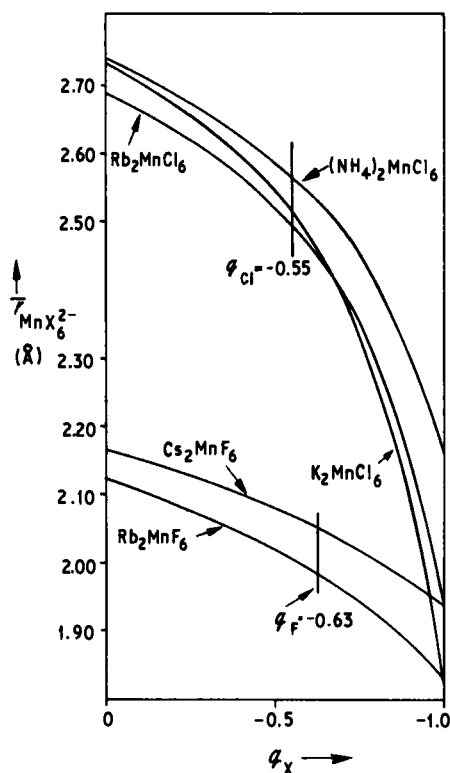


FIG. 17. Basic radii for the ions MnF_6^{2-} and MnCl_6^{2-} , corresponding to lattice potential energy minima, as a function of the charge, q_X , on the halogen atoms.

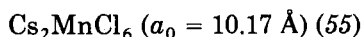
and assigning, on the basis that $q_{\text{Cl}} = -0.55$, we find:

$$\begin{aligned} U_{\text{POT}}(\text{K}_2\text{MnCl}_6) &= 1462 \text{ kJ mol}^{-1} \\ U_{\text{POT}}(\text{Rb}_2\text{MnCl}_6) &= 1451 \text{ kJ mol}^{-1} \\ U_{\text{POT}}((\text{NH}_4)_2\text{MnCl}_6) &= 1464 \text{ kJ mol}^{-1} \end{aligned}$$

iv. "Basic" radius of ion (Fig. 17)

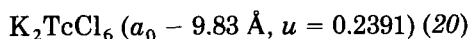
$$\bar{r}_{\text{MnCl}_6^{2-}} = 2.52 \text{ \AA}$$

No thermochemical data exist for these salts.

b. *Derived Estimates*i. *Structures*ii. *Prediction of lattice energies*

Assigned value:

$$U_{\text{POT}}(Cs_2MnCl_6) = 1430 \text{ kJ mol}^{-1}$$

3. $TcCl_6^{2-}$: *Hexachlorotechnetate Ion*a. *Recent Studies*i. *Structure*ii. *Charge distribution*

$$q_{Cl} = -0.49$$

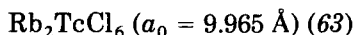
iii. *Lattice energies.* Over the range $0.0 \geq q_{Cl} \geq -0.9$ [Eq. (38) has no roots at $q_{Cl} = -1.0$] we find that $U_{\text{POT}}(K_2TcCl_6)$ varies from 1322 kJ mol⁻¹ to 1575 kJ mol⁻¹ and the "basic" radius of the ion varies from 1.8 Å to 2.8 Å. At a charge distribution corresponding to $q_{Cl} = -0.49$, we find by interpolation:

$$U_{\text{POT}}(K_2TcCl_6) = 1443 \text{ kJ mol}^{-1}$$

iv. *"Basic" radius of ion*

$$\bar{r}_{TcCl_6^{2-}} = 2.59 \text{ \AA}$$

No thermochemical data exist for these salts.

b. *Derived Estimates*i. *Structures*

ii. *Prediction of lattice energies*

Assigned value:

$$U_{\text{POT}}(\text{Rb}_2\text{TcCl}_6) = 1417 \text{ kJ mol}^{-1}$$

4. ReCl_6^{2-} : *Hexachlororhenate Ion*a. *Recent Studies*i. *Structure*

$$\text{K}_2\text{ReCl}_6 \ (a_0 = 9.84 \text{ \AA}, u = 0.2391) \ (27)$$

ii. *Charge distribution*

$$q_{\text{Cl}} = -0.55$$

iii. *Lattice energies*

$$U_{\text{POT}}(\text{K}_2\text{ReCl}_6) = 1416 \text{ kJ mol}^{-1}$$

iv. *"Basic" radius of ion* (Fig. 18)

$$\bar{r}_{\text{ReCl}_6^{2-}} = 2.54 \text{ \AA}$$

v. *Enthalpy of formation of gaseous ion*

Ancillary data:

$$\Delta H_f^\theta(\text{K}_2\text{ReCl}_6)(\text{c}) = -1333 \text{ kJ mol}^{-1} \ (56), -1331 \text{ kJ mol}^{-1} \ (10b);$$

$$\Delta H_f^\theta(\text{(NH}_4)_2\text{ReCl}_6)(\text{c}) = -1056.5 \text{ kJ mol}^{-1} \ (23).$$

Assigned value:

$$\Delta H_f^\theta(\text{ReCl}_6^{2-})(\text{g}) = -919 \pm 26 \text{ kJ mol}^{-1}$$

vi. *Enthalpy of hydration of gaseous ion*

Ancillary data:

$$\Delta H_f^\theta(\text{ReCl}_6^{2-})(\text{aq}) = -761 \text{ kJ mol}^{-1} \ (56), -766 \text{ kJ mol}^{-1} \ (10b).$$

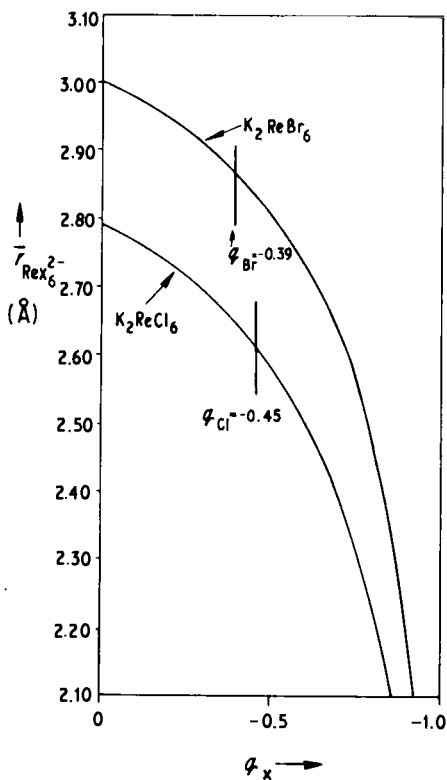


FIG. 18. Basic radii for the ions, ReCl_6^{2-} and ReBr_6^{2-} , corresponding to lattice potential energy minima, as functions of charge distributions, q_x , on the halogen atom.

Assigned value

$$\Delta H_{\text{hyd}}^{\theta}(\text{ReCl}_6^{2-})(\text{g}) = -709 \pm 26 \text{ kJ mol}^{-1}$$

vii. *Halide ion affinities*

Ancillary data:

$$\Delta H_f^{\theta}(\text{ReCl}_4)(\text{c}) = -361 \text{ kJ mol}^{-1} \text{ (57).}$$

Assigned value:

$$\overline{\Delta H}_{\text{Cl(c)}} = -66 \pm 26 \text{ kJ mol}^{-1}$$

viii. *Prediction of lattice energies*

Ancillary data:

$$U_{\text{POT}}(\text{K}_2\text{ReCl}_6) = 1416 \text{ kJ mol}^{-1},$$

assuming

$$U_{\text{POT}}(\text{K}_2\text{ReCl}_6) \simeq U_{\text{POT}}((\text{NH}_4)_2\text{ReCl}_6).$$

Assigned value

$U_{\text{POT}}((\text{NH}_4)_2\text{ReCl}_6) \simeq 1416 \text{ kJ mol}^{-1}$
--

b. *Derived Estimates*i. *Structures*

$$\text{Rb}_2\text{ReCl}_6 (a_0 = 9.974 \text{ \AA}) (4)$$

$$\text{Cs}_2\text{ReCl}_6 (a_0 = 10.26 \text{ \AA}) (4)$$

$$(\text{NH}_4)_2\text{ReCl}_6 (a_0 = 9.98 \text{ \AA}) (13)$$

$$(\text{NH}_4)_2\text{ReCl}_6 (a_0 = 10.07 \text{ \AA}) (10)$$

ii. *Prediction of lattice energies*

$U_{\text{POT}}(\text{Rb}_2\text{ReCl}_6) = 1414 \text{ kJ mol}^{-1}$

$U_{\text{POT}}(\text{Cs}_2\text{ReCl}_6) = 1398 \text{ kJ mol}^{-1}$

$U_{\text{POT}}((\text{NH}_4)_2\text{ReCl}_6) = 1402 \text{ kJ mol}^{-1}$

$U_{\text{POT}}((\text{NH}_4)_2\text{ReCl}_6) = 1374 \text{ kJ mol}^{-1}$

c. *Previous Calculations.* Lister *et al.* (53) tabulated values of the lattice energy obtained for K_2ReCl_6 in 1974; these are listed in Table I. The values that should correspond most closely to those we obtain in this present study, in that they recognize a distributed charge on the ReCl_6^{2-} ion, are the ones given in column e of Table I.

Burgess and Cartwright (10a) have obtained the enthalpy of solution of Cs_2ReCl_6 as $+88 \text{ kJ mol}^{-1}$ and obtain:

$$\Delta H_{\text{hyd}}^\theta(\text{ReCl}_6^{2-})(\text{g}) = -845 \text{ kJ mol}^{-1}$$

Busey, Dearman and Bevan (10b) have determined the enthalpy of solution of K_2ReCl_6 as $+43.5 \text{ kJ mol}^{-1}$ from which Burgess and Cartwright calculate:

$$\Delta H_{\text{hyd}}^{\theta}(ReCl_6^{2-})(g) = -827 \text{ kJ mol}^{-1}$$

A mean value:

$$\Delta H_{\text{hyd}}^{\theta}(ReCl_6^{2-})(g) = -836 \text{ kJ mol}^{-1}$$

is proposed. They use Kapustinskii's equation to obtain:

$$U_{\text{POT}}(Cs_2ReCl_6) = 1453 \text{ kJ mol}^{-1}$$

$$U_{\text{POT}}(K_2ReCl_6) = 1459 \text{ kJ mol}^{-1}$$

5. $ReBr_6^{2-}$: Hexabromorhenate Ion

a. Recent Calculations

i. Structure

$$K_2ReBr_6 (a_0 = 10.385 \text{ \AA}, u = 0.2391) (27)$$

ii. Charge distribution

$$q_{Br} = -0.5$$

iii. Lattice energies

$$U_{\text{POT}}(K_2ReBr_6) = 1375 \text{ kJ mol}^{-1}$$

iv. "Basic" radius of ion (Fig. 18)

$$\bar{r}_{ReBr_6^{2-}} = 2.81 \text{ \AA}$$

v. Enthalpy of formation of gaseous ion

Ancillary data:

$$\Delta H_f^{\theta}(K_2ReBr_6)(c) = -1036 \text{ kJ mol}^{-1} (57).$$

Assigned value:

$$\Delta H_f^{\theta}(ReBr_6^{2-})(g) = -689 \text{ kJ mol}^{-1}$$

vi. *Halide ion affinities*

Ancillary data:

$$\Delta H_f^\theta(\text{ReBr}_4)(\text{c}) = -303 \text{ kJ mol}^{-1} \text{ (57).}$$

Assigned value:

$\overline{\Delta H}_{\text{Br(c)}} = +82 \text{ kJ mol}^{-1}$
--

b. Previous Calculations. Burgess and Cartwright (10a) have assigned:

$$\Delta H_{\text{hyd}}^\theta(\text{ReBr}_6^{2-})(\text{g}) = -784 \text{ kJ mol}^{-1}$$

using lattice energies derived from Kapustinskii's equation giving:

$$U_{\text{POT}}(\text{Cs}_2\text{ReBr}_6) = 1399 \text{ kJ mol}^{-1}$$

F. RUTHENIUM(IV), OSMIUM(IV), COBALT(IV),
IRIDIUM(IV), NICKEL(IV), PALLADIUM(IV), AND
PLATINUM(IV) SALTS

1. RuCl_6^{2-} ; *Hexachlororuthenate Ion*

a. Recent Studies. No crystal structure data are available.

b. Derived Estimates

i. *Structure*

$$\text{K}_2\text{RuCl}_6 \text{ (} a_0 = 9.738 \text{ \AA) (74)}$$

ii. *Prediction of lattice energies*

$U_{\text{POT}}(\text{K}_2\text{RuCl}_6) = 1451 \text{ kJ mol}^{-1}$
--

2. OsCl_6^{2-} ; *Hexachloroosmate Ion*

a. Recent Studies

i. *Structures*

$$\text{K}_2\text{OsCl}_6 \text{ (} a_0 = 9.729 \text{ \AA, } u = 0.243 \text{) (74)}$$

ii. Charge distribution

$$q_{Cl} = -0.51$$

iii. Lattice energies

$$U_{\text{POT}}(\text{K}_2\text{OsCl}_6) = 1447 \text{ kJ mol}^{-1}$$

iv. "Basic" radius of ion (Fig. 19)

$$\bar{r}_{\text{OsCl}_6^{2-}} = 2.54 \text{ \AA}$$

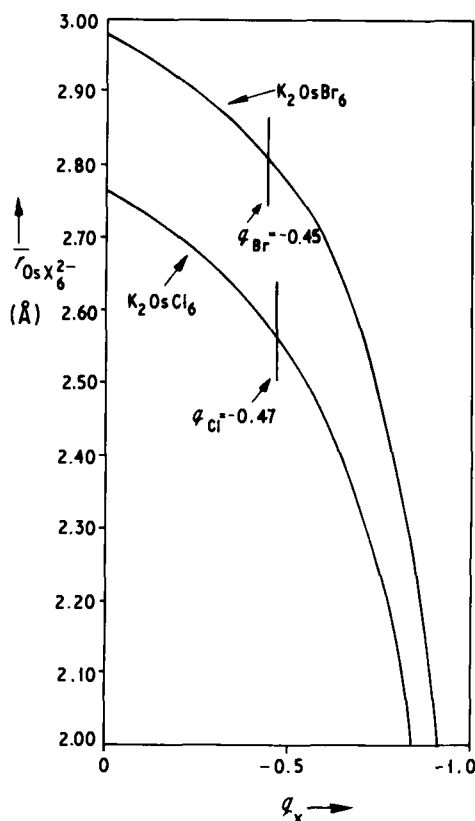


FIG. 19. Basic radius for the ions OsCl_6^{2-} and OsBr_6^{2-} , corresponding to lattice energy minima, as functions of the charge, q_X , on the halogen atom.

v. *Enthalpy of formation of gaseous ion*

Ancillary data:

$$\Delta H_f^\circ(\text{K}_2\text{OsCl}_6)(\text{c}) = -1171 \text{ kJ mol}^{-1} \text{ (61)}$$

Assigned value:

$$\Delta H_f^\circ(\text{OsCl}_6^{2-})(\text{g}) = -752 \text{ kJ mol}^{-1}$$

vi. *Halide ion affinities*

Ancillary data:

$$\Delta H_f^\circ(\text{OsCl}_4)(\text{c}) = -255 \text{ kJ mol}^{-1} \text{ (56)}$$

and

$$\Delta H_f^\circ(\text{OsCl}_4)(\text{g}) = -79 \text{ kJ mol}^{-1} \text{ (56)}.$$

Assigned value:

$$\Delta \bar{H}_{\text{Cl}(\text{c})} = -5 \text{ kJ mol}^{-1}$$

$$\Delta \bar{H}_{\text{Cl}(\text{g})} = -181 \text{ kJ mol}^{-1}$$

b. *Derived Estimates*i. *Structures*

$$\text{Cs}_2\text{OsCl}_6 \text{ (} a_0 = 10.230 \text{ \AA) (66)}$$

$$(\text{NH}_4)_2\text{OsCl}_6 \text{ (} a_0 = 9.881 \text{ \AA) (67)}$$

ii. *Prediction of lattice energies*

$$U_{\text{POT}}(\text{Cs}_2\text{OsCl}_6) = 1409 \text{ kJ mol}^{-1}$$

$$U_{\text{POT}}((\text{NH}_4)_2\text{OsCl}_6) = 1433 \text{ kJ mol}^{-1}$$

3. OsBr_6^{2-} : *Hexabromoosmate Ion*a. *Recent Studies*i. *Structures*

$$\text{K}_2\text{OsBr}_6 \text{ (} a_0 = 10.30 \text{ \AA, } u = 0.244) \text{ (74)}$$

ii. *Charge distribution*

$$q_{Br} = -0.45$$

iii. *Lattice energies*

$$U_{\text{POT}}(\text{K}_2\text{OsBr}_6) = 1396 \text{ kJ mol}^{-1}$$

iv. "Basic" radius of ion (Fig. 19)

$$\bar{r}_{\text{OsBr}_6^{2-}} = 2.80 \text{ \AA}$$

No thermodynamic data exist for these salts.

4. CoF_6^{2-} : Hexafluorocobaltate Iona. *Recent Studies*i. *Structures*

$$\text{Rb}_2\text{CoF}_6 (a_0 = 8.46 \text{ \AA}, u = 0.2009) (60)$$

$$\text{Cs}_2\text{CoF}_6 (a_0 = 8.914 \text{ \AA}, u = 0.1907) (60)$$

u was assigned on basis of $\text{Co-F} \sim 1.7 \text{ \AA}$ as reported.

ii. *Charge distribution*

$$q_F = -0.59$$

iii. *Lattice energies*

$$U_{\text{POT}}(\text{Rb}_2\text{CoF}_6) = 1688 \text{ kJ mol}^{-1}$$

$$U_{\text{POT}}(\text{Cs}_2\text{CoF}_6) = 1632 \text{ kJ mol}^{-1}$$

iv. "Basic" radius of ion (Fig. 20)

$$\bar{r}_{\text{CoF}_6^{2-}} = 2.04 \text{ \AA}$$

No thermodynamic data exist for these salts.

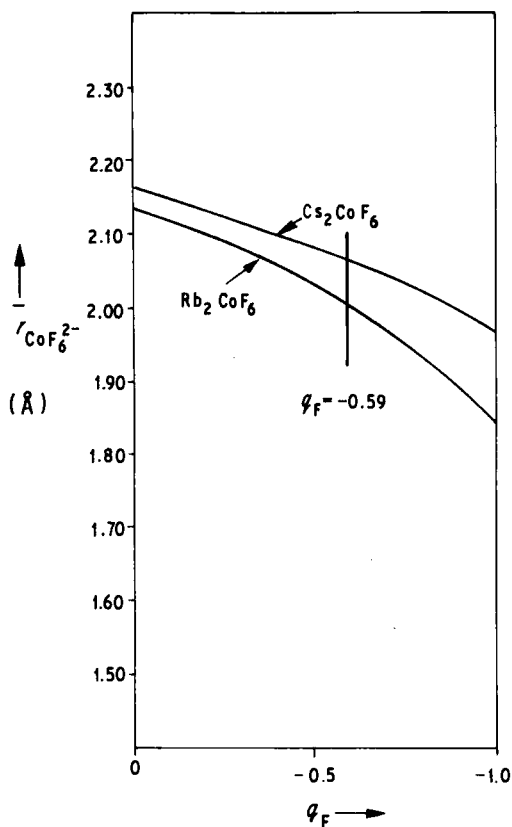
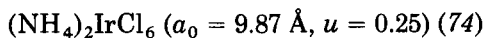


FIG. 20. Basic radius of CoF_6^{2-} ion, corresponding to lattice potential energy minima, as a function of q_F , the charge on the fluorine atoms.

5. IrCl_6^{2-} : Hexachloroiridate Ion

a. Recent Studies

i. Structures



ii. Charge distribution

$$q_{\text{Cl}} = -0.47$$

iii. Lattice energies

$$U_{\text{POT}}((\text{NH}_4)_2\text{IrCl}_6) = 1442 \text{ kJ mol}^{-1}$$

iv. "Basic" radius of ion

$$\bar{r}_{\text{IrCl}_6^{2-}} = 2.56 \text{ \AA}$$

v. *Enthalpy of formation of gaseous ion*

Ancillary data:

$$\Delta H_f^\theta(\text{K}_2\text{IrCl}_6)(\text{c}) = -1197 \text{ kJ mol}^{-1} (61), -1176 \text{ kJ mol}^{-1} (68a)$$

assuming that

$$\begin{aligned} U_{\text{POT}}(\text{K}_2\text{IrCl}_6) &\simeq U_{\text{POT}}((\text{NH}_4)_2\text{IrCl}_6), \Delta H_f^\theta(\text{Rb}_2\text{IrCl}_6)(\text{c}) \\ &= -1180 \text{ kJ mol}^{-1} (68a). \end{aligned}$$

Assigned value:

$$\Delta H_f^\theta(\text{IrCl}_6^{2-})(\text{g}) \sim -785 \text{ kJ mol}^{-1}$$

vi. *Enthalpy of hydration of gaseous ion*

Ancillary data:

$$\Delta H_f^\theta(\text{IrCl}_6^{2-})(\text{aq}) = -619.7 \text{ kJ mol}^{-1} (61).$$

Assigned value:

$$\Delta H_{\text{hyd}}^\theta(\text{IrCl}_6^{2-})(\text{g}) = -706 \text{ kJ mol}^{-1}$$

vii. *Prediction of lattice energies*

Ancillary data:

$$U_{\text{POT}}(\text{K}_2\text{IrCl}_6) \approx U_{\text{POT}}((\text{NH}_4)_2\text{IrCl}_6).$$

Assigned value:

$$U_{\text{POT}}(\text{K}_2\text{IrCl}_6) \simeq 1442 \text{ kJ mol}^{-1}$$

b. *Previous Calculations.* Burgess and Cartwright (10a) have estimated:

$$\Delta H_{\text{hyd}}^\theta(\text{IrCl}_6^{2-})(\text{g}) = -834 \text{ kJ mol}^{-1}$$

from a lattice energy:

$$U_{\text{POT}}((\text{NH}_4)_2\text{IrCl}_6) = 1505 \text{ kJ mol}^{-1}$$

6. NiF_6^{2-} : Hexafluoronickalate Ion

a. Recent Studies

i. Structures

$$\text{K}_2\text{NiF}_6 (a_0 = 8.1088 \text{ \AA}, u = 0.219) (74)$$

$$\text{Rb}_2\text{NiF}_6 (a_0 = 8.462 \text{ \AA}, u = 0.202) (74)$$

ii. Charge distribution

$$q_{\text{F}} = -0.57$$

iii. Lattice energies

$$U_{\text{POT}}(\text{K}_2\text{NiF}_6) = 1721 \text{ kJ mol}^{-1}$$

$$U_{\text{POT}}(\text{Rb}_2\text{NiF}_6) = 1688 \text{ kJ mol}^{-1}$$

iv. "Basic" radius of ion (Fig. 21)

$$\bar{r}_{\text{NiF}_6^{2-}} = 1.97 \text{ \AA}$$

v. Enthalpy of formation of gaseous ion

Ancillary data:

$$\Delta H_f^\circ(\text{K}_2\text{NiF}_6)(\text{c}) = -2021 \pm 12 \text{ kJ mol}^{-1} (32a).$$

Assigned value:

$$\Delta H_f^\circ(\text{NiF}_6^{2-})(\text{g}) = -1328 \pm 12 \text{ kJ mol}^{-1}$$

7. PdCl_6^{2-} : Hexachloropalladate Ion

a. Recent Studies

i. Structures

$$(\text{NH}_4)_2\text{PdCl}_6 (a_0 = 9.84 \text{ \AA}, u = 0.2337) (3)$$

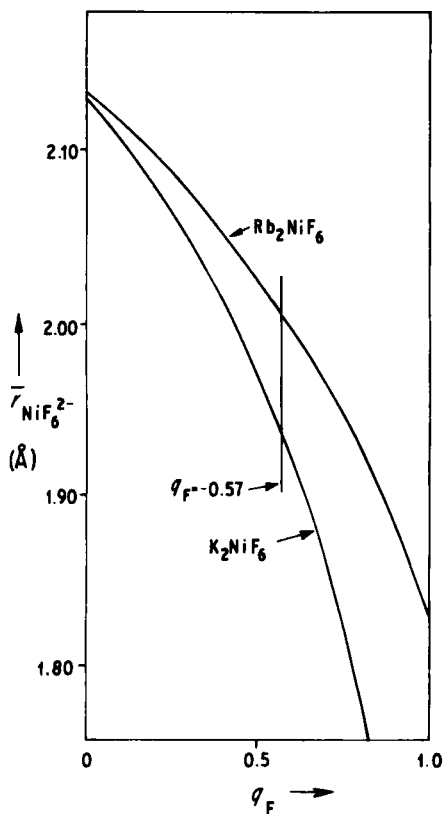


FIG. 21. Basic radius of the ion NiF_6^{2-} , corresponding to a lattice potential energy minima, as a function of the charge, q_F , on the fluorine atoms.

ii. *Charge distribution*

$$q_{\text{Cl}} = -0.43$$

iii. *Lattice energies*

$$U_{\text{POT}}[(\text{NH}_4)_2\text{PdCl}_6] = 1481 \text{ kJ mol}^{-1}$$

iv. *"Basic" radius of ion*

$$\bar{r}_{\text{PdCl}_6^{2-}} = 2.61 \text{ \AA}$$

v. *Enthalpy of formation of gaseous ion*

Ancillary data:

$$\Delta H_f^\theta(\text{K}_2\text{PdCl}_6)(\text{c}) = -1187 \text{ kJ mol}^{-1} \text{ (61)}$$

and assuming

$$U_{\text{POT}}(\text{K}_2\text{PdCl}_6) \approx U_{\text{POT}}((\text{NH}_4)_2\text{PdCl}_6).$$

Assigned value:

$\Delta H_f^\theta(\text{PdCl}_6^{2-})(\text{g}) = -734 \text{ kJ mol}^{-1}$
--

vi. *Enthalpy of hydration of gaseous ion*

Ancillary data:

$$\Delta H_f^\theta(\text{PdCl}_6^{2-})(\text{aq}) = -598 \text{ kJ mol}^{-1} \text{ (56)}.$$

Assigned value:

$\Delta H_{\text{hyd}}^\theta(\text{PdCl}_6^{2-})(\text{g}) = -735 \text{ kJ mol}^{-1}$

b. *Derived Estimates*i. *Structures*

$$\text{K}_2\text{PdCl}_6 \text{ (} a_0 = 9.74 \text{ \AA) (74)}$$

$$\text{Rb}_2\text{PdCl}_6 \text{ (} a_0 = 9.87 \text{ \AA) (74)}$$

$$\text{Cs}_2\text{PdCl}_6 \text{ (} a_0 = 10.18 \text{ \AA) (74)}$$

ii. *Prediction of lattice energies*

$U_{\text{POT}}(\text{K}_2\text{PdCl}_6) = 1450 \text{ kJ mol}^{-1}$
--

$U_{\text{POT}}(\text{Rb}_2\text{PdCl}_6) = 1449 \text{ kJ mol}^{-1}$

$U_{\text{POT}}(\text{Cs}_2\text{PdCl}_6) = 1426 \text{ kJ mol}^{-1}$

iii. *Enthalpy of formation of gaseous ion*

Ancillary data:

$$\Delta H_f^\theta(\text{K}_2\text{PdCl}_6)(\text{c}) = -1187 \text{ kJ mol}^{-1} \text{ (61)}.$$

Assigned value:

$$\Delta H_f^\theta(\text{PdCl}_6^{2-})(g) = -765 \text{ kJ mol}^{-1}$$

c. Previous Calculations. Hartley (29) has used both the Born-Mayer (6) equation and the Kapustinskii (46) equation to estimate the lattice energy of K_2PtCl_6 ; his results are given in Table I.

8. PtCl_6^{2-} : Hexachloroplatinate Ion

a. Recent Studies

i. Structures

$$\text{K}_2\text{PtCl}_6 \ (a_0 = 9.755 \text{ \AA}, u = 0.24) \ (74)$$

$$\text{Rb}_2\text{PtCl}_6 \ (a_0 = 9.901 \text{ \AA}, u = 0.235) \ (74)$$

$$\text{Cs}_2\text{PtCl}_6 \ (a_0 = 10.215 \text{ \AA}, u = 0.23) \ (74)$$

$$(\text{NH}_4)_2\text{PtCl}_6 \ (a_0 = 9.858 \text{ \AA}, u = 0.24) \ (74)$$

$$\text{Ti}_2\text{PtCl}_6 \ (a_0 = 9.799 \text{ \AA}, u = 0.235) \ (74)$$

ii. Charge distribution

$$q_{\text{Cl}} = -0.44$$

iii. Lattice energies

$$U_{\text{POT}}(\text{K}_2\text{PtCl}_6) = 1468 \text{ kJ mol}^{-1}$$

$$U_{\text{POT}}(\text{Rb}_2\text{PtCl}_6) = 1464 \text{ kJ mol}^{-1}$$

$$U_{\text{POT}}(\text{Cs}_2\text{PtCl}_6) = 1444 \text{ kJ mol}^{-1}$$

$$U_{\text{POT}}((\text{NH}_4)_2\text{PtCl}_6) = 1468 \text{ kJ mol}^{-1}$$

$$U_{\text{POT}}(\text{Ti}_2\text{PtCl}_6) = 1546 \text{ kJ mol}^{-1}$$

iv. "Basic" radius of ion (Fig. 22)

$$\bar{r}_{\text{PtCl}_6^{2-}} = 2.59 \text{ \AA}$$

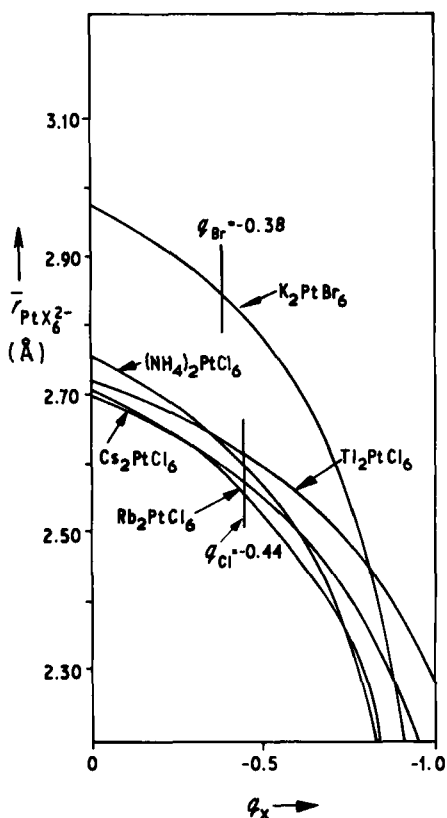


FIG. 22. Basic radii of the ions, PtCl_6^{2-} and PtBr_6^{2-} , corresponding to lattice energy minima, as functions of the charge, q_x , on the halogen atoms.

v. *Enthalpy of formation of gaseous ion*

Ancillary data:

$$\Delta H_f^\theta(\text{PtCl}_6^{2-})(\text{aq}) = -678 \pm 4 \text{ kJ mol}^{-1} \text{ (24)}$$

$$\begin{aligned} \Delta H_f^\theta(\text{K}_2\text{PtCl}_6)(\text{c}) &= -1235 \text{ kJ mol}^{-1} \text{ (68a)}, \Delta H_f^\theta(\text{Rb}_2\text{PtCl}_6)(\text{c}) \\ &= -1251 \text{ kJ mol}^{-1} \text{ (68a)} \end{aligned}$$

Assigned value:

$$\Delta H_f^\theta(\text{PtCl}_6^{2-})(\text{g}) = -792 \text{ kJ mol}^{-1}$$

vi. *Enthalpy of hydration of gaseous ion*

Ancillary data:

$$\Delta H_{\text{soln}}^{\theta}(\text{K}_2\text{PtCl}_6)(\text{c}) = 56.5 \text{ kJ mol}^{-1} \text{ (14)}$$

and

$$\Delta H_{\text{soln}}^{\theta}((\text{NH}_4)_2\text{PtCl}_6)(\text{c}) = 49.8 \text{ kJ mol}^{-1} \text{ (65)}$$

Assigned value:

$\Delta H_{\text{hyd}}^{\theta}(\text{PtCl}_6^{2-})(\text{g}) = -757 \pm 6 \text{ kJ mol}^{-1}$

vii. *Halide ion affinities*

Ancillary data:

$$\Delta H_f^{\theta}(\text{PtCl}_4)(\text{c}) = -263.2 \text{ kJ mol}^{-1} \text{ (56)}$$

Assigned value:

$\overline{\Delta H}_{\text{Cl(c)}} = -37 \text{ kJ mol}^{-1}$
--

viii. *Prediction of lattice energies*

Ancillary data:

$$\Delta H_f^{\theta}(\text{Ag}_2\text{PtCl}_6)(\text{c}) = -527 \text{ kJ mol}^{-1} \text{ (24),}$$

$$\Delta H_f^{\theta}(\text{BaPtCl}_6)(\text{c}) = -1180 \text{ kJ mol}^{-1} \text{ (24).}$$

Assigned value:

$U_{\text{POT}}(\text{Ag}_2\text{PtCl}_6) = 1773 \text{ kJ mol}^{-1}$

$U_{\text{POT}}(\text{BaPtCl}_6) = 2047 \text{ kJ mol}^{-1}$
--

c. *Previous Calculations.* Hartley (29), Lister *et al.* (53), DeJonge (16), and Jenkins (36) have all studied the lattice potential energies. All the approaches used have differed from the present one and, aside from the simple Born–Lande approach of Lister *et al.* (53), only the calculated value of Jenkins approaches the present value. The results are tabulated in Table I.

Burgess and Cartwright (10a) have estimated:

$$U_{\text{POT}}(\text{K}_2\text{PtCl}_6) = 1521 \text{ kJ mol}^{-1}$$

$$U_{\text{POT}}(\text{Cs}_2\text{PtCl}_6) = 1459 \text{ kJ mol}^{-1}$$

$$U_{\text{POT}}((\text{NH}_4)_2\text{PtCl}_6) = 1507 \text{ kJ mol}^{-1}$$

leading to:

$$\Delta H_{\text{hyd}}^\theta(\text{PtCl}_6^{2-})(\text{g}) = -844 \text{ kJ mol}^{-1}$$

9. PtBr_6^{2-} : Hexabromoplatinate Ion

a. Recent Studies

i. Structures

$$\text{K}_2\text{PtBr}_6 \ (a_0 = 10.293 \text{ \AA}, u = 0.2391) \ (3)$$

ii. Charge distribution

$$q_{\text{Br}} = -0.38$$

iii. Lattice energies

$$U_{\text{POT}}(\text{K}_2\text{PtBr}_6) = 1423 \text{ kJ mol}^{-1}$$

iv. "Basic" radius of ion (Fig. 22)

$$\bar{r}_{\text{PtBr}_6^{2-}} = 2.85 \text{ \AA}$$

v. Enthalpy of formation of gaseous ion

Ancillary data:

$$\Delta H_f^\theta(\text{K}_2\text{PtBr}_6)(\text{c}) = -1040 \text{ kJ mol}^{-1} \ (6I).$$

Assigned value:

$$\Delta H_f^\theta(\text{PtBr}_6^{2-})(\text{g}) = -645 \text{ kJ mol}^{-1}$$

vi. *Enthalpy of hydration of gaseous ion*

Ancillary data:

$$\Delta H_f^\theta(\text{PtBr}_6^{2-})(\text{aq}) = -477 \text{ kJ mol}^{-1} (56).$$

Assigned value:

$$\Delta H_{\text{hyd}}^\theta(\text{PtBr}_6^{2-})(\text{g}) = -703 \text{ kJ mol}^{-1}$$

vii. *Halide ion affinities*

Ancillary data:

$$\Delta H_f^\theta(\text{PtBr}_4)(\text{c}) = -159 \text{ kJ mol}^{-1} (56).$$

Assigned value:

$$\Delta H_{\text{Br(c)}} = -18 \text{ kJ mol}^{-1}$$

viii. *Prediction of lattice energies*

Ancillary data:

$$\Delta H_f^\theta(\text{Ag}_2\text{PtBr}_6)(\text{c}) = -398 \text{ kJ mol}^{-1} (56).$$

Assigned value:

$$U_{\text{POT}}(\text{Ag}_2\text{PtBr}_6) = 1791 \text{ kJ mol}^{-1}$$

c. *Previous Calculations.* Hartley (29), Lister *et al.* (53), and DeJonge (16) have all calculated the lattice energy of K_2PtBr_6 , and the results are given in Table I. Hartley (29) and DeJonge (16) have estimated the Pt—Br bond strength.

Burgess and Cartwright (10a) have calculated:

$$U_{\text{POT}}(\text{K}_2\text{PtBr}_6) = 1451 \text{ kJ mol}^{-1}$$

$$U_{\text{POT}}((\text{NH}_4)_2\text{PtBr}_6) = 1439 \text{ kJ mol}^{-1}$$

from which they estimate:

$$\Delta H_{\text{hyd}}^\theta(\text{PtBr}_6^{2-})(\text{g}) = -769 \text{ kJ mol}^{-1}$$

G. SILICON(IV), GERMANIUM(IV), TIN(IV), AND
LEAD(IV) SALTS

1. SiF_6^{2-} : *Hexafluorosilicate Ion*

a. *Recent Studies*

i. *Structures*

$$\text{K}_2\text{SiF}_6 \ (a_0 = 8.133 \text{ \AA}, u = 0.215) \ (74)$$

$$\text{Rb}_2\text{SiF}_6 \ (a_0 = 8.452 \text{ \AA}, u = 0.20) \ (74)$$

$$\text{Cs}_2\text{SiF}_6 \ (a_0 = 8.919 \text{ \AA}, u = 0.19) \ (74)$$

$$\text{Tl}_2\text{SiF}_6 \ (a_0 = 8.568 \text{ \AA}, u = 0.20) \ (74)$$

$$(\text{NH}_4)_2\text{SiF}_6 \ (a_0 = 8.395 \text{ \AA}, u = 0.205) \text{ or } (a_0 = 8.395 \text{ \AA}, u = 0.2011) \ (28, 62)$$

ii. *Charge distribution*

$$q_{\text{F}} = -0.84$$

iii. *Lattice energies*

$$U_{\text{POT}}(\text{K}_2\text{SiF}_6) = 1670 \text{ kJ mol}^{-1}$$

$$U_{\text{POT}}(\text{Rb}_2\text{SiF}_6) = 1639 \text{ kJ mol}^{-1}$$

$$U_{\text{POT}}(\text{Cs}_2\text{SiF}_6) = 1604 \text{ kJ mol}^{-1}$$

$$U_{\text{POT}}(\text{Tl}_2\text{SiF}_6) = 1675 \text{ kJ mol}^{-1}$$

$$U_{\text{POT}}((\text{NH}_4)_2\text{SiF}_6) = 1657 \text{ kJ mol}^{-1} \text{ or } 1665 \text{ kJ mol}^{-1}$$

iv. “Basic” radius of ion (Fig. 23)

$$\bar{r}_{\text{SiF}_6^{2-}} = 1.94 \text{ \AA}$$

v. *Enthalpy of formation of gaseous ion* (Fig. 24)

Ancillary data:

$$\Delta H_f^\theta(\text{K}_2\text{SiF}_6)(\text{c}) = -2807 \text{ kJ mol}^{-1} \ (61), -2966 \text{ kJ mol}^{-1} \ (68a)$$

$$\Delta H_f^\theta(\text{Rb}_2\text{SiF}_6)(\text{c}) = -2838 \text{ kJ mol}^{-1} \ (61), -2911.6 \text{ kJ mol}^{-1} \ (68a)$$

$$\Delta H_f^\theta(\text{Cs}_2\text{SiF}_6)(\text{c}) = -2801 \text{ kJ mol}^{-1} \ (61),$$

$$\Delta H_f^\theta((\text{NH}_4)_2\text{SiF}_6)(\text{c}) = -2681 \text{ kJ mol}^{-1} \ (56).$$

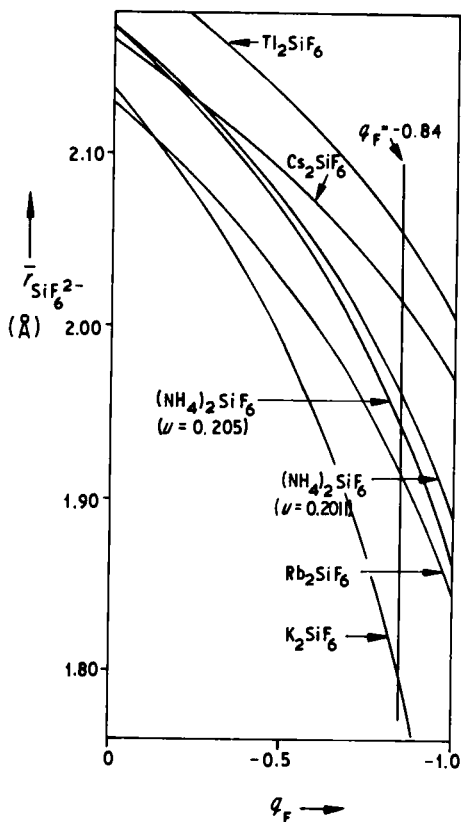


FIG. 23. Basic radius of the ion, SiF_6^{2-} , corresponding to lattice potential energy minima, as a function of the charge distribution, q_F , on the fluorine atom.

Assigned value:

$$\Delta H_f^\theta(\text{SiF}_6^{2-})(g) = -2198 \pm 75 \text{ kJ mol}^{-1}*$$

vi. *Enthalpy of hydration of gaseous ion*

Ancillary data:

$$\Delta H_f^\theta(\text{SiF}_6^{2-})(aq) = -2389 \text{ kJ mol}^{-1} (56).$$

* Assigned in noncubic salt calculations also (Ref. 40a).

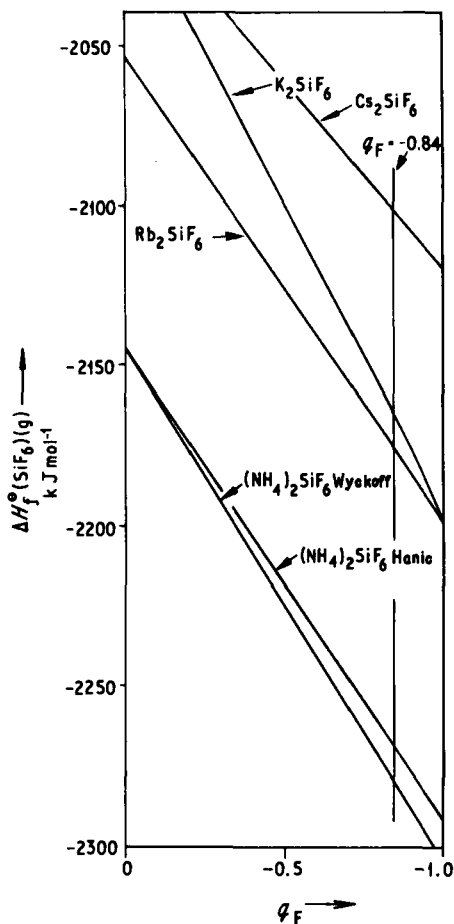


FIG. 24. Enthalpy of formation, $\Delta H_f^\circ(\text{SiF}_6^{2-})(g)$, corresponding to lattice potential energy minima, as a function of the charge distribution q_F , on the fluorine atom.

Assigned value:

$$\Delta H_{\text{hyd}}^\circ(\text{SiF}_6^{2-})(g) = -1071 \pm 75 \text{ kJ mol}^{-1}$$

vii. *Halide ion affinities*

Ancillary data:

$$\Delta H_f^\circ(\text{SiF}_4)(g) = -1615 \text{ kJ mol}^{-1} (56).$$

Assigned value:

$$\overline{\Delta H}_{F(g)} = -42 \pm 75 \text{ kJ mol}^{-1*}$$

2. GeF_6^{2-} : Hexafluorogermanate ion

a. Recent Studies

i. Structures

$$\text{Cs}_2\text{GeF}_6 \ (a_0 = 9.021 \text{ \AA}, u = 0.20) \ (74)$$

$$(\text{NH}_4)_2\text{GeF}_6 \ (a_0 = 8.46 \text{ \AA}, u = 0.203) \ (74)$$

ii. Charge distribution

$$q_F = -0.78$$

iii. Lattice energies

$$U_{\text{POT}}(\text{Cs}_2\text{GeF}_6) = 1573 \text{ kJ mol}^{-1}$$

$$U_{\text{POT}}((\text{NH}_4)_2\text{GeF}_6) = 1657 \text{ kJ mol}^{-1}$$

iv. "Basic" radius of ion (Fig. 25)

$$\bar{r}_{\text{GeF}_6^{2-}} = 2.01 \text{ \AA}$$

v. Enthalpy of formation of gaseous ion

Ancillary data:

$$U_{\text{POT}}[(\text{NH}_4)_2\text{GeF}_6] \simeq U_{\text{POT}}(\text{K}_2\text{GeF}_6);$$

$$\Delta H_f^\theta(\text{K}_2\text{GeF}_6)(c) = -2600 \pm 8 \text{ kJ mol}^{-1} \ (32a).$$

Assigned value:

$$\Delta H_f^\theta(\text{GeF}_6^{2-})(g) = -1971 \text{ kJ mol}^{-1}$$

* Assigned in noncubic salt calculations also (Ref. 40a).

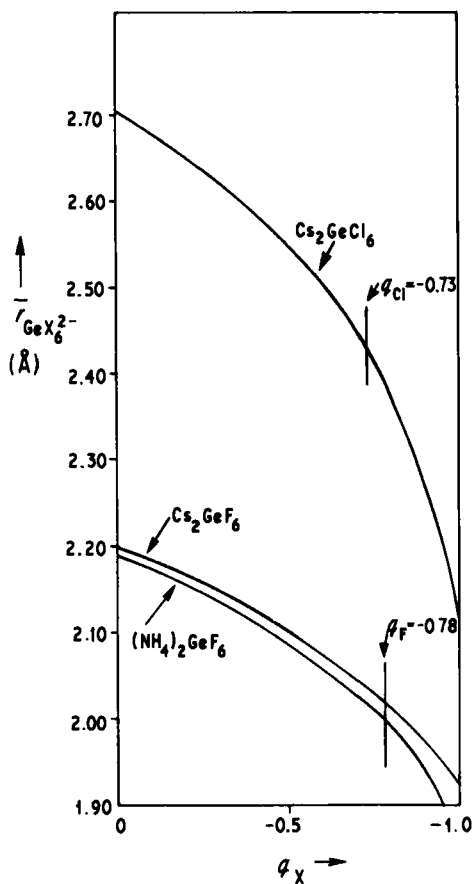


FIG. 25. Basic radii of the ions GeF_6^{2-} and GeCl_6^{2-} corresponding to lattice potential energy minima, as a function of the charge, q_X on the halogen atom.

vi. *Halide Ion Affinity:*

Ancillary Data:

$$\Delta H_f^\theta(\text{GeF}_4)(\text{g}) = -1190 \text{ kJ mol}^{-1} \quad (26a)$$

Assigned value:

$$\overline{\Delta H}_{F(\text{g})} = -240 \text{ kJ mol}^{-1}$$

3. GeCl_6^{2-} : Hexachlorogermanate ion

a. Recent Studies

i. Structures

$$\text{Cs}_2\text{GeCl}_6 \ (a_0 = 10.21 \text{ \AA}, u = 0.23) \ (74)$$

ii. Charge distribution

$$q_{\text{Cl}} = -0.73$$

iii. Lattice energies

$$U_{\text{TOT}}(\text{Cs}_2\text{GeCl}_6) \approx 1375 \text{ kJ mol}^{-1}$$

iv. "Basic" radius of ion (Fig. 25)

$$\bar{r}_{\text{GeCl}_6^{2-}} = 2.43 \text{ \AA}$$

v. Enthalpy of formation of gaseous ion

Ancillary data:

$$\Delta H_f^\theta(\text{Rb}_2\text{GeCl}_6)(\text{c}) = -1464 \text{ kJ mol}^{-1} \ (68a)$$

$$\Delta H_f^\theta(\text{Cs}_2\text{GeCl}_6)(\text{c}) = -1451.8 \text{ kJ mol}^{-1} \ (70).$$

Assigned value:

$$\Delta H_f^\theta(\text{GeCl}_6^{2-})(\text{g}) = -981 \text{ kJ mol}^{-1}$$

vi. Halide ion affinities

Ancillary data:

$$\Delta H_f^\theta(\text{GeCl}_4)(\text{l}) = -532 \text{ kJ mol}^{-1} \ (56),$$

$$\Delta H_f^\theta(\text{GeCl}_4)(\text{g}) = -496 \text{ kJ mol}^{-1} \ (56).$$

Assigned values:

$$\Delta \bar{H}_{\text{Cl}(\text{l})} = +43 \text{ kJ mol}^{-1}$$

$$\Delta \bar{H}_{\text{Cl}(\text{g})} = +7 \text{ kJ mol}^{-1}$$

c. Previous Calculations. Welsh *et al.* (70) have calculated the lattice energy of Cs_2GeCl_6 using Wood's method (2, 18, 21, 72, 73). They obtained the results given in Table I together with the following thermochemical data:

$$\Delta H_f^\theta(\text{GeCl}_6^{2-})(g) = -956 \pm 84 \text{ kJ mol}^{-1}$$

$$\overline{\Delta H}_{\text{Cl}(g)} = +32 \pm 84 \text{ kJ mol}^{-1}$$

this latter term being referred to as the donor-acceptor bond energy, aside from a sign reversal.

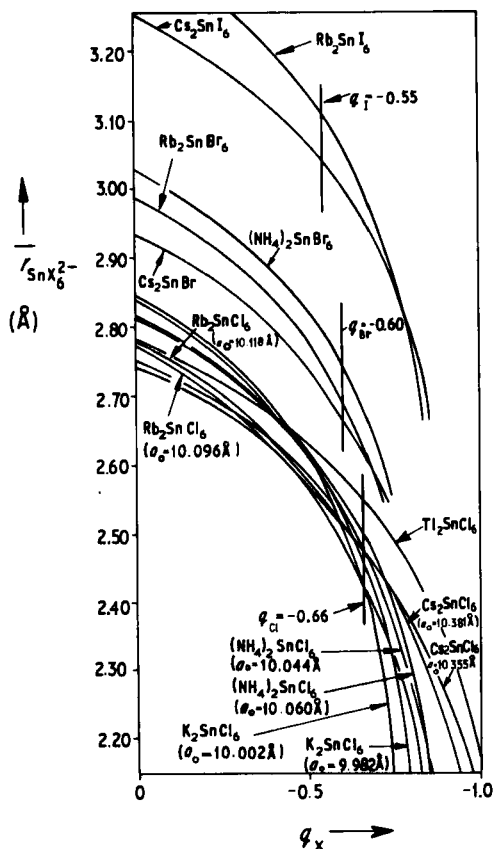


FIG. 26. Basic radii for ions SnCl_6^{2-} , SnBr_6^{2-} , and SnI_6^{2-} , corresponding to lattice potential energy minima, as a function of the charge distributions, q_X , on the halogen atoms.

4. SnCl_6^{2-} : *Hexachlorostannate Ion*a. *Recent Studies*i. *Structures*

K_2SnCl_6 ($a_0 = 10.002 \text{ \AA}$, $u = 0.245$) (74) or ($a_0 = 9.982 \text{ \AA}$, $u = 0.2415$) (7)

Rb_2SnCl_6 ($a_0 = 10.118 \text{ \AA}$, $u = 0.24$) (74) or ($a_0 = 10.096 \text{ \AA}$, $u = 0.2399$) (7)

Cs_2SnCl_6 ($a_0 = 10.381 \text{ \AA}$, $u = 0.235$) (74) or ($a_0 = 10.355 \text{ \AA}$, $u = 0.234$) (7)

Ti_2SnCl_6 ($a_0 = 9.97 \text{ \AA}$, $u = 0.24$) (74)

$(\text{NH}_4)_2\text{SnCl}_6$ ($a_0 = 10.060 \text{ \AA}$, $u = 0.24$) (74) or ($a_0 = 10.044 \text{ \AA}$, $u = 0.2411$) (7)

Recently Lerbscher and Trotter have redetermined the structure of

$$\text{K}_2\text{SnCl}_6 (a_0 = 9.990 \text{ \AA}, u = 0.2411) (52a)$$

$$(\text{NH}_4)_2\text{SnCl}_6 (a_0 = 10.038 \text{ \AA}, u = 0.2412) (52a)$$

these are very similar to the structures of reference (7).

ii. *Charge distribution*

$$q_{\text{Cl}} = -0.66$$

iii. *Lattice energies*

$$U_{\text{POT}}(\text{K}_2\text{SnCl}_6) = 1352 \text{ kJ mol}^{-1} \text{ or } 1363 \text{ kJ mol}^{-1}$$

$$U_{\text{POT}}(\text{Rb}_2\text{SnCl}_6) = 1358 \text{ kJ mol}^{-1} \text{ or } 1361 \text{ kJ mol}^{-1}$$

$$U_{\text{POT}}(\text{Cs}_2\text{SnCl}_6) = 1352 \text{ kJ mol}^{-1} \text{ or } 1358 \text{ kJ mol}^{-1}$$

$$U_{\text{POT}}(\text{Ti}_2\text{SnCl}_6) = 1437 \text{ kJ mol}^{-1}$$

$$U_{\text{POT}}((\text{NH}_4)_2\text{SnCl}_6) = 1369 \text{ kJ mol}^{-1} \text{ or } 1370 \text{ kJ mol}^{-1}$$

iv. *"Basic" radius of ion* (Fig. 26)

$$\bar{r}_{\text{SnCl}_6^{2-}} = 2.47 \text{ \AA}$$

v. *Enthalpy of formation of gaseous ion* (Fig. 27)

Ancillary data:

$$\Delta H_f^\theta(\text{K}_2\text{SnCl}_6)(\text{c}) = -1518 \text{ kJ mol}^{-1} (61), -1485 \text{ kJ mol}^{-1} (70), \\ -1481.7 \text{ kJ mol}^{-1} (62a);$$

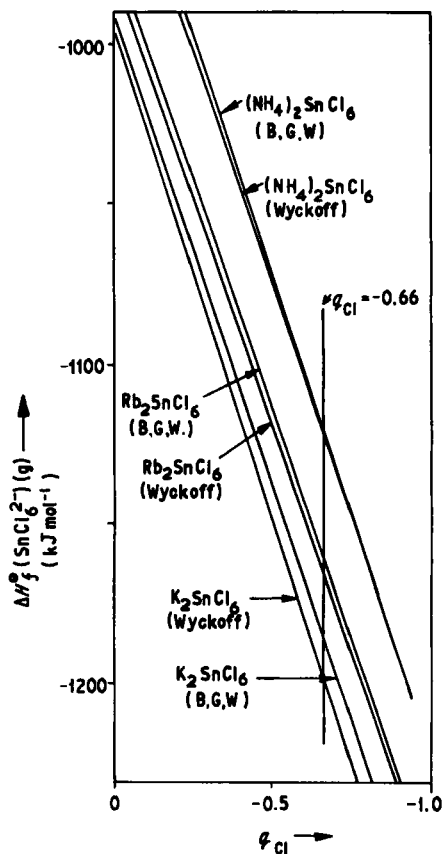


FIG. 27. Enthalpy of formation, $\Delta H_f^\theta(\text{SnCl}_6^{2-})(g)$, corresponding to a lattice potential energy minimum, as a function of the charge, q_{Cl} , on the chlorine atom.

$$\begin{aligned}\Delta H_f^\theta(\text{Rb}_2\text{SnCl}_6)(c) &= -1529 \text{ kJ mol}^{-1} (69); \\ \Delta H_f^\theta[(\text{NH}_4)_2\text{SnCl}_6](c) &= -1237 \text{ kJ mol}^{-1} (56), \\ &-1281 \pm 17 \text{ kJ mol}^{-1} (64a)^*, -1244.1 \text{ kJ mol}^{-1} (10a).\end{aligned}$$

Assigned value:

$$\Delta H_f^\theta(\text{SnCl}_6^{2-})(g) = -1156 \pm 27 \text{ kJ mol}^{-1}$$

* This value has not been used for the analysis in Fig. 27, but clearly to do so would improve the agreement.

vi. *Enthalpy of hydration of gaseous ion*

Ancillary data:

$$\Delta H_f^\theta(\text{SnCl}_6^{2-})(\text{aq}) = -970 \text{ kJ mol}^{-1} \text{ (56).}$$

Assigned value:

$\Delta H_{\text{hyd}}^\theta(\text{SnCl}_6^{2-})(\text{aq}) = -685 \pm 27 \text{ kJ mol}^{-1}$

vii. *Halide ion affinities*

Ancillary data:

$$\Delta H_f^\theta(\text{SnCl}_4)(1) = -511 \text{ kJ mol}^{-1} \text{ (56). } -520 \text{ kJ mol}^{-1} \text{ (54b)}$$

and

$$\Delta H_f^\theta(\text{SnCl}_4)(\text{g}) = -472 \text{ kJ mol}^{-1} \text{ (56),}$$

Assigned value:

$\overline{\Delta H}_{\text{Cl(l)}} = -153 \pm 27 \text{ kJ mol}^{-1}$ $\overline{\Delta H}_{\text{Cl(g)}} = -192 \pm 27 \text{ kJ mol}^{-1}$

c. *Previous Calculations.* Webster and Collins (69), Lister *et al.* (53), Welsh *et al.* (70), Gelbman and Westland (22), and Jenkins and Smith (40) have all made studies of the lattice energies of hexachlorostannate salts, the results are compared in Table I. The following thermodynamic estimates were obtained from the studies:

Webster and Collins (69):

$$\overline{\Delta H}_{\text{Cl(g)}} = -90.8 \pm 71 \text{ kJ mol}^{-1}$$

$$\Delta H_f^\theta(\text{SnCl}_6^{2-})(\text{g}) = -1070 \pm 71 \text{ kJ mol}^{-1}$$

Welsh *et al.* (70):

$$\Delta H_f^\theta(\text{SnCl}_6^{2-})(\text{g}) = -1125 \pm 84 \text{ kJ mol}^{-1}$$

$$\overline{\Delta H}_{\text{Cl(g)}} = -161 \pm 84 \text{ kJ mol}^{-1}$$

Gelbman and Westland (22):

$$U_{\text{POT}}(\text{K}_2\text{SnCl}_6) - U_{\text{POT}}(\text{K}_2\text{ZrCl}_6) \simeq 15 \text{ kJ mol}^{-1} \quad (77)$$

and following the work of Brill *et al.* (7), they obtain

$$\overline{\Delta H}_{\text{Cl(g)}} = -1547 + U_{\text{POT}}(\text{K}_2\text{SnCl}_6) \text{ kJ mol}^{-1} \quad (78)$$

which when used in conjunction with their cited lattice energies (see Section V,B,3,c) give

$$U_{\text{POT}}(\text{K}_2\text{ZrCl}_6) = 1571 \text{ kJ mol}^{-1}$$

whereupon

$$U_{\text{POT}}(\text{K}_2\text{SnCl}_6) = 1586 \text{ kJ mol}^{-1}$$

which leads to

$$\overline{\Delta H}_{\text{Cl(g)}} = +39 \text{ kJ mol}^{-1}$$

Jenkins and Smith (40)

$$\Delta H_f^\theta(\text{SnCl}_6^{2-})(\text{g}) = -1256 \text{ kJ mol}^{-1}$$

$$\overline{\Delta H}_{\text{Cl(g)}} = -278 \text{ kJ mol}^{-1}$$

5. SnBr_6^{2-} : Hexabromostannate Ion

a. Recent Studies

i. Structures

$$\text{Rb}_2\text{SnBr}_6 \ (a_0 = 10.64 \text{ \AA}, u = 0.245) \quad (74)$$

$$\text{Cs}_2\text{SnBr}_6 \ (a_0 = 10.81 \text{ \AA}, u = 0.245) \quad (74)$$

$$(\text{NH}_4)_2\text{SnBr}_6 \ (a_0 = 10.59 \text{ \AA}, u = 0.245) \quad (74)$$

ii. Charge distribution

$$q_{\text{Br}} = -0.60$$

iii. *Lattice energies*

$$\begin{aligned}
 U_{\text{POT}}(\text{Rb}_2\text{SnBr}_6) &= 1309 \text{ kJ mol}^{-1} \\
 U_{\text{POT}}(\text{Cs}_2\text{SnBr}_6) &= 1306 \text{ kJ mol}^{-1} \\
 U_{\text{POT}}[(\text{NH}_4)_2\text{SnBr}_6] &= 1319 \text{ kJ mol}^{-1}
 \end{aligned}$$

iv. “Basic” radius of ion (Fig. 26)

$$\bar{r}_{\text{SnBr}_6^{2-}} = 2.70 \text{ \AA}$$

No thermochemical data exist for these salts.

c. *Previous Calculations.* Makhija and Westland (54a) have cited the relationship:

$$\overline{\Delta H}_{\text{Br(g)}} = -1459 + U_{\text{pot}}(\text{K}_2\text{SnBr}_6) \text{ kJ mol}^{-1} \quad (79)$$

and employing their lattice energies as given in Table I they find:

$$\overline{\Delta H}_{\text{Br(g)}} = +46 \text{ kJ mol}^{-1}$$

6. SnI_6^{2-} : Hexaiodostannate Iona. *Recent Studies*i. *Structures*

$$\text{Rb}_2\text{SnI}_6 (a_0 = 11.60 \text{ \AA}, u = 0.245) \quad (74)$$

$$\text{Cs}_2\text{SnI}_6 (a_0 = 11.63 \text{ \AA}, u = 0.245) \quad (74)$$

ii. *Charge distribution*

$$q_I = -0.55$$

iii. *Lattice energies*

$$\begin{aligned}
 U_{\text{POT}}(\text{Rb}_2\text{SnI}_6) &= 1226 \text{ kJ mol}^{-1} \\
 U_{\text{POT}}(\text{Cs}_2\text{SnI}_6) &= 1243 \text{ kJ mol}^{-1}
 \end{aligned}$$

iv. "Basic" radius of ion (Fig. 26)

$$\bar{r}_{\text{SnI}_6^{2-}} = 3.07 \text{ \AA}$$

No thermochemical data exist for these salts.

7. PbCl_6^{2-} : Hexachloroplumbate Ion

a. Previous Studies

i. Structures

$$\text{Rb}_2\text{PbCl}_6 \ (a_0 = 10.197 \text{ \AA}, u = 0.2445) \ (74)$$

$$\text{Cs}_2\text{PbCl}_6 \ (a_0 = 10.415 \text{ \AA}, u = 0.24) \ (74)$$

$$(\text{NH}_4)_2\text{PbCl}_6 \ (a_0 = 10.135 \text{ \AA}, u = 0.245) \ (74)$$

ii. Charge distribution

$$q_{\text{Cl}} = -0.63$$

iii. Lattice energies

$$U_{\text{POT}}(\text{Rb}_2\text{PbCl}_6) = 1343 \text{ kJ mol}^{-1}$$

$$U_{\text{POT}}(\text{Cs}_2\text{PbCl}_6) = 1344 \text{ kJ mol}^{-1}$$

$$U_{\text{POT}}[(\text{NH}_4)_2\text{PbCl}_6] = 1355 \text{ kJ mol}^{-1}$$

iv. "Basic" radius of ion (Fig. 28)

$$\bar{r}_{\text{PbCl}_6^{2-}} = 2.48 \text{ \AA}$$

v. Enthalpy of formation of the gaseous ion

Ancillary data:

$$\Delta H_f^\theta(\text{Rb}_2\text{PbCl}_6)(\text{c}) = -1293 \text{ kJ mol}^{-1} \ (70).$$

Assigned value:

$$\Delta H_f^\theta(\text{PbCl}_6^{2-})(\text{g}) = -940 \text{ kJ mol}^{-1}$$

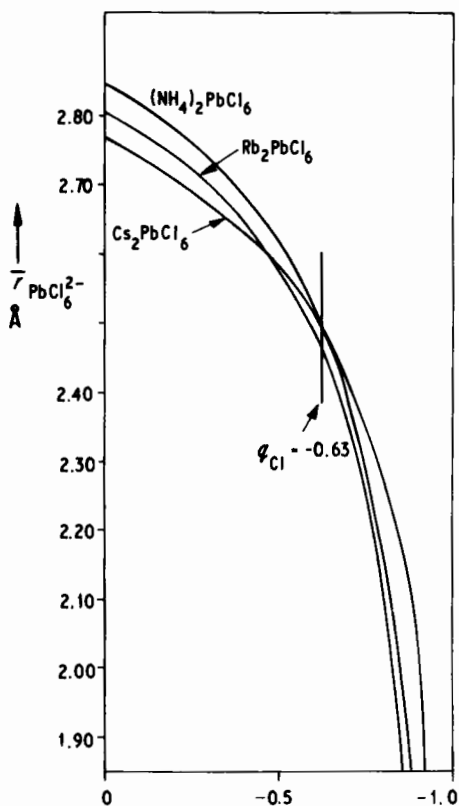


FIG. 28. Basic radius for the $PbCl_6^{2-}$ ion, corresponding to a lattice potential energy minimum, as a function of the charge distribution, q_{Cl} , on the halogen atom.

vi. *Halide ion affinities*

Ancillary data:

$$\Delta H_f^\theta(PbCl_4)(l) = -329 \text{ kJ mol}^{-1} \text{ (56),}$$

$$\Delta H_f^\theta(PbCl_4)(g) = -285 \pm 8 \text{ kJ mol}^{-1} \text{ (70).}$$

Assigned value:

$\Delta H_{Cl(l)} = -119 \text{ kJ mol}^{-1}$ $\Delta H_{Cl(g)} = -163 \pm 8 \text{ kJ mol}^{-1}$

b. Previous Calculations. Welsh *et al.* (70) have calculated the lattice energy of Rb_2PbCl_6 (Table I). The associated thermochemical data derived assigned:

$$\Delta H_f^\theta(\text{PbCl}_6^{2-})(\text{g}) = -927 \pm 92 \text{ kJ mol}^{-1}$$

$$\overline{\Delta H}_{\text{Cl}(\text{g})} = -150 \pm 92 \text{ kJ mol}^{-1}$$

H. ANTIMONY(IV) SALTS

1. SbCl_6^{2-} : Hexachloroantimonate Ion

a. Recent Calculations. No crystal structure data are available.

b. Derived Values

i. *Structure*

$$\text{Rb}_2\text{SbCl}_6 \ (a_0 = 10.14 \text{ \AA}) \ (41)$$

ii. *Prediction of lattice energy*

$$U_{\text{POT}}(\text{Rb}_2\text{SbCl}_6) = 1357 \text{ kJ mol}^{-1}$$

I. SELENIUM(IV), TELLURIUM(IV), AND POLONIUM(IV) SALTS

1. SeCl_6^{2-} : Hexachloroselenate Ion

a. Recent Studies

i. *Structures*

$$\text{Rb}_2\text{SeCl}_6 \ (a_0 = 9.978 \text{ \AA}, u = 0.24) \ (74)$$

$$\text{Cs}_2\text{SeCl}_6 \ (a_0 = 10.266 \text{ \AA}, u = 0.235) \ (74)$$

$$(\text{NH}_4)_2\text{SeCl}_6 \ (a_0 = 9.935 \text{ \AA}, u = 0.24) \ (74)$$

ii. *Charge distribution*

$$q_{\text{Cl}} = -0.56$$

iii. *Lattice energies*

$$U_{\text{POT}}(\text{Rb}_2\text{SeCl}_6) = 1409 \text{ kJ mol}^{-1}$$

$$U_{\text{POT}}(\text{Cs}_2\text{SeCl}_6) = 1397 \text{ kJ mol}^{-1}$$

$$U_{\text{POT}}[(\text{NH}_4)_2\text{SeCl}_6] = 1420 \text{ kJ mol}^{-1}$$

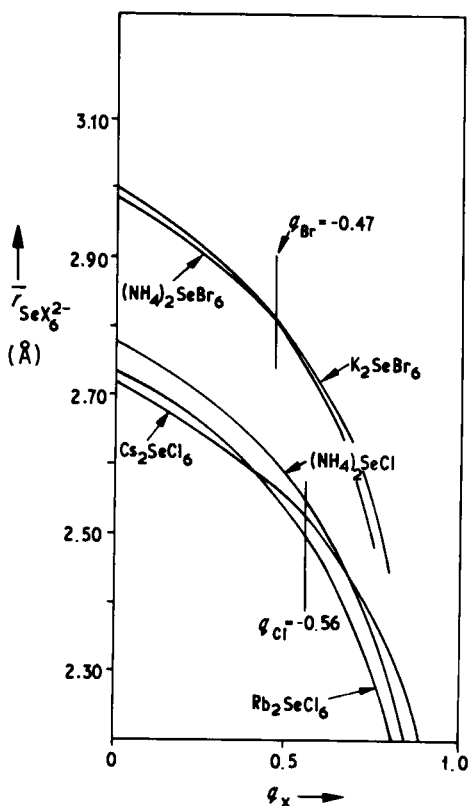


FIG. 29. Basic radius of the ions SeCl_6^{2-} and SeBr_6^{2-} , corresponding to lattice potential energy minima, as a function of the charge, q_X , on the halogen atom of the ion.

iv. "Basic" radius of ion (Fig. 29)

$$\bar{r}_{\text{SeCl}_6^{2-}} = 2.52 \text{ \AA}$$

No thermochemical data exist for these salts.

2. SeBr_6^{2-} : Hexabromoselenate Ion

a. Recent Studies

i. Structures

$$\text{K}_2\text{SeBr}_6 (a_0 = 10.363 \text{ \AA}, u = 0.245) \quad (74)$$

$$(\text{NH}_4)_2\text{SeBr}_6 (a_0 = 10.46 \text{ \AA}, u = 0.245) \quad (74)$$

ii. *Charge distribution*

$$q_{\text{Br}} = -0.47$$

iii. *Lattice energies*

$U_{\text{POT}}(\text{K}_2\text{SeBr}_6) = 1379 \text{ kJ mol}^{-1}$ $U_{\text{POT}}[(\text{NH}_4)_2\text{SeBr}_6] = 1380 \text{ kJ mol}^{-1}$
--

iv. “Basic” radius of ion (Fig. 29)

$\bar{r}_{\text{SeBr}_6^{2-}} = 2.81 \text{ \AA}$

No thermochemical data exists for these salts.

3. TeCl_6^{2-} : *Hexachlorotellurate Ion*a. *Recent Calculations*i. *Structures*

Rb_2TeCl_6 ($a_0 = 10.233 \text{ \AA}$, $u = 0.245$) (74) ($a_0 = 10.233 \text{ \AA}$, $u = 0.2468$) (69)

Cs_2TeCl_6 ($a_0 = 10.447 \text{ \AA}$, $u = 0.24$) (74)

Tl_2TeCl_6 ($a = 10.107 \text{ \AA}$, $u = 0.245$) (74)

$(\text{NH}_4)_2\text{TeCl}_6$ ($a_0 = 10.178 \text{ \AA}$, $u = 0.25$) (74) ($a_0 = 10.200 \text{ \AA}$, $u = 0.2478$) (30)

ii. *Charge distribution*

$$q_{\text{Cl}} = -0.68$$

iii. *Lattice energies*

$U_{\text{POT}}(\text{Rb}_2\text{TeCl}_6) = 1321 \text{ kJ mol}^{-1} \text{ or } 1316 \text{ kJ mol}^{-1}$ $U_{\text{POT}}(\text{Cs}_2\text{TeCl}_6) = 1323 \text{ kJ mol}^{-1}$ $U_{\text{POT}}(\text{Tl}_2\text{TeCl}_6) = 1392 \text{ kJ mol}^{-1}$ $U_{\text{POT}}[(\text{NH}_4)_2\text{TeCl}_6] = 1318 \text{ kJ mol}^{-1} \text{ or } 1320 \text{ kJ mol}^{-1}$

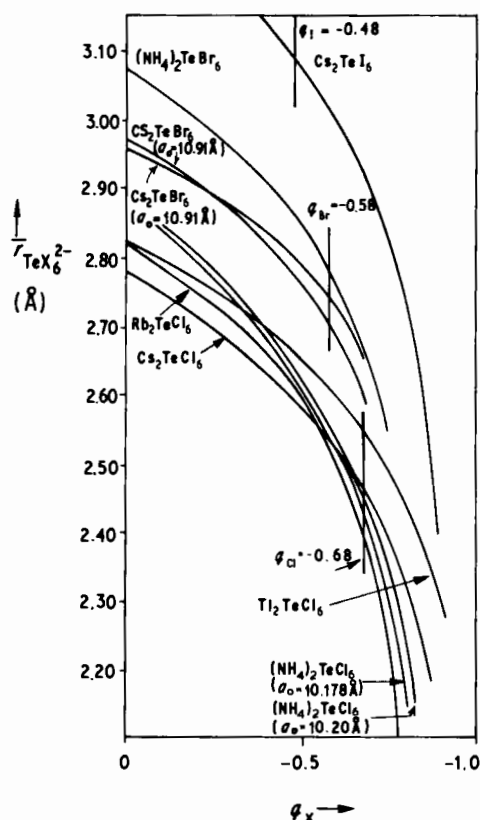


FIG. 30. Basic radii of the ions, TeCl_6^{2-} , TeBr_6^{2-} , and TeI_6^{2-} , corresponding to lattice potential energy minima, plotted as functions of the distributed charge in the ion.

iv. "Basic" radius of ion (Fig. 30)

$$\bar{r}_{\text{TeCl}_6^{2-}} = 2.41 \text{ \AA}$$

v. Enthalpy of formation of gaseous ion (Fig. 31)

Ancillary data:

$$\Delta H_f^\circ(\text{K}_2\text{TeCl}_6)(c) = -1167 \text{ kJ mol}^{-1} \text{ (25, 56),}$$

$$\Delta H_f^\circ(\text{Rb}_2\text{TeCl}_6)(c) = -1231.8 \text{ kJ mol}^{-1} \text{ (69), } -1251 \text{ kJ mol}^{-1} \text{ (25, 26).}$$

Assigned value:

$$\Delta H_f^\circ(\text{TeCl}_6^{2-})(g) = -891 \pm 24 \text{ kJ mol}^{-1}$$

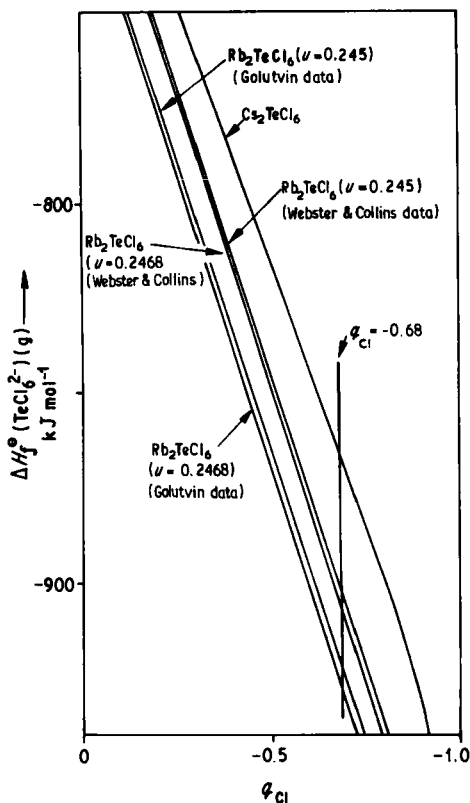


FIG. 31. Enthalpy of formation, $\Delta H_f^\circ(\text{TeCl}_6^{2-})(g)$, corresponding to a lattice potential energy minimum, as a function of charge q_{Cl} on the chlorine atom.

vi. *Halide ion affinities*

Ancillary data:

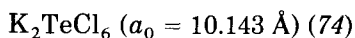
$$\Delta H_f^\circ(\text{TeCl}_4)(c) = -326 \text{ kJ mol}^{-1} \quad (56)$$

and

$$\Delta H_f^\circ(\text{TeCl}_4)(g) = -246 \text{ kJ mol}^{-1} \quad (69).$$

Assigned values:

$\overline{\Delta H}_{\text{Cl}(c)} = -73 \pm 24 \text{ kJ mol}^{-1}$ $\overline{\Delta H}_{\text{Cl}(g)} = -153 \pm 27 \text{ kJ mol}^{-1}$
--

*b. Derived Estimates**i. Structure**ii. Prediction of lattice energy*

$$U_{\text{TOT}}(K_2TeCl_6) = 1318 \text{ kJ mol}^{-1}$$

c. Previous Calculations. Webster and Collins (69) and Jenkins and Smith (40) have considered the lattice energy of Rb_2TeCl_6 . Their results are compared in Table I, and the thermodynamic estimates that they obtained are given below.

Webster and Collins (69):

$$\Delta H_f^\theta(TeCl_6^{2-})(g) = -804 \pm 71 \text{ kJ mol}^{-1}$$

$$\overline{\Delta H}_{Cl(g)} = -91 \pm 71 \text{ kJ mol}^{-1}$$

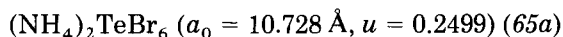
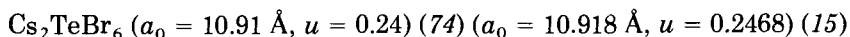
Jenkins and Smith (40).

$$\Delta H_f^\theta(TeCl_6^{2-})(g) = -1020 \text{ kJ mol}^{-1}$$

$$\overline{\Delta H}_{Cl(g)} = -304 \text{ kJ mol}^{-1}$$

Golutvin *et al.* (25, 26):

$$\Delta H_f^\theta(TeCl_6^{2-})(g) = -1130 \pm 5 \text{ kJ mol}^{-1}$$

*4. $TeBr_6^{2-}$: Hexabromotellurate Ion**a. Recent Studies**i. Structures**ii. Charge distribution*

$$q_{Br} = -0.58$$

iii. *Lattice energies*

$$U_{\text{POT}}(\text{Cs}_2\text{TeBr}_6) = 1306 \text{ kJ mol}^{-1} \quad \text{or} \quad 1292 \text{ kJ mol}^{-1}$$

$$U_{\text{POT}}[(\text{NH}_4)_2\text{TeBr}_6] = 1294 \text{ kJ mol}^{-1}$$

iv. “*Basic*” radius of ion (Fig. 30)

$$\bar{r}_{\text{TeBr}_6^{2-}} = 2.73 \text{ \AA}$$

v. *Enthalpies of formation of gaseous ion*

Ancillary data:

$$\Delta H_f^\theta(\text{K}_2\text{TeBr}_6)(\text{c}) = -972 \text{ kJ mol}^{-1} \text{ (65a)}$$

and

$$\Delta H_f^\theta(\text{Cs}_2\text{TeBr}_6)(\text{c}) = -1032 \text{ kJ mol}^{-1} \text{ (65a)}.$$

Assigned value:

$$\Delta H_f^\theta(\text{TeBr}_6^{2-})(\text{g}) = -661 \pm 40 \text{ kJ mol}^{-1}$$

vi. *Halide ion affinities*

Ancillary data:

$$\Delta H_f^\theta(\text{TeBr}_4)(\text{c}) = -190 \text{ kJ mol}^{-1} \text{ (56)}.$$

Assigned value:

$$\bar{\Delta H}_{\text{Br}(\text{c})} = 21 \pm 40 \text{ kJ mol}^{-1}$$

5. TeI_6^{2-} : Hexaiodotellurate Iona. *Recent Studies*i. *Structure*

$$\text{Cs}_2\text{TeI}_6 \text{ (} a_0 = 11.721 \text{ \AA, } u = 0.248 \text{) (74)}$$

ii. *Charge distribution*

$$q_I = -0.48$$

iii. *Lattice energies*

$$U_{\text{TOT}}(\text{Cs}_2\text{TeI}_6) = 1246 \text{ kJ mol}^{-1}$$

No thermochemical data exists for these salts.

6. PoCl_6^{2-} : *Hexachloropolonate Ion*a. *Recent Studies*i. *Structures*

$$(\text{NH}_4)_2\text{PoCl}_6 \ (a_0 = 10.35 \text{ \AA}, u = 0.23) \ (74)$$

ii. *Charge distribution*

$$q_{\text{Cl}} = -0.7$$

iii. *Lattice energies*

$$U_{\text{TOT}}(\text{NH}_4)_2\text{PoCl}_6 = 1338 \text{ kJ mol}^{-1}$$

iv. *"Basic" radius of ion* (Fig. 32)

$$\bar{r}_{\text{PoCl}_6^{2-}} = 2.60 \text{ \AA}$$

No thermochemical data exist for these salts.

7. PoBr_6^{2-} : *Hexabromopolonate Ion*a. *Recent Studies*i. *Structures*

$$\text{Cs}_2\text{PoBr}_6 \ (a_0 = 11.01 \text{ \AA}, u = 0.24) \ (74)$$

$$(\text{NH}_4)_2\text{PoBr}_6 \ (a_0 = 10.84 \text{ \AA}, u = 0.24) \ (74)$$

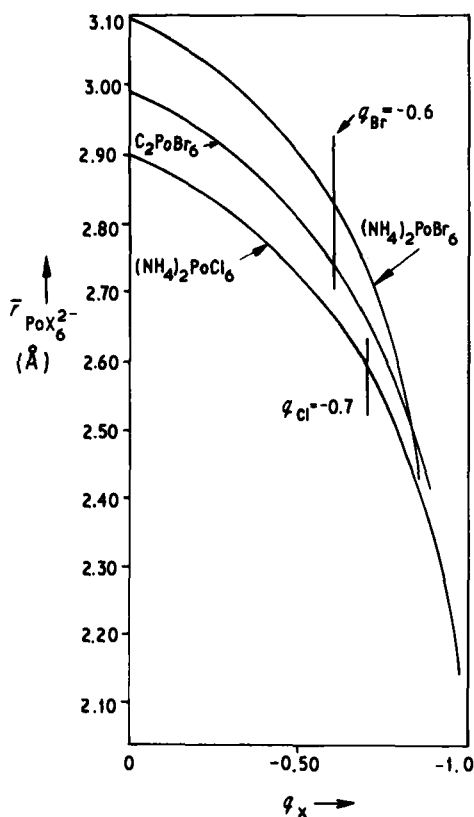


FIG. 32. Basic radii of PoCl_6^{2-} and PoBr_6^{2-} , corresponding to lattice potential energy minima, as functions of the charge q_X on the halogen atom.

ii. *Charge distribution*

$$q_{\text{Br}} \simeq -0.60$$

iii. *Lattice energies*

$$\begin{aligned} U_{\text{POT}}(\text{Cs}_2\text{PoBr}_6) &= 1286 \text{ kJ mol}^{-1} \\ U_{\text{POT}}(\text{(NH}_4)_2\text{PoBr}_6) &= 1292 \text{ kJ mol}^{-1} \end{aligned}$$

iv. “Basic” radius of ion (Fig. 31)

$$\bar{r}_{\text{PoBr}_6^{2-}} = 2.78 \text{ \AA}$$

No thermochemical data exist for these salts.

VI. Summary Tabulation of Rigorous Calculations

We give in Table III a summary of the lattice energies we have calculated rigorously; the table includes, in parentheses, occasional directly estimated values.

VII. Summary Tabulation of Derived Estimates

This section contains a number of "derived estimates" (Table IV) for the lattice energies of salts for which no full structural information is available. Equations (53)–(58) are used to derive the values from the literature a_0 values.

VIII. Discussion

A. INTRODUCTION

This article represents the first attempt to obtain lattice energies for transition metal salts A_2MX_6 on a comparative basis, and in doing this generates the possibility of commenting on donor–acceptor strengths and relative bond strengths of transition metal and main group ions of the type MX_6^{2-} .

In discussing the overall results we must establish the fact that many of the ancillary thermochemical and charge distribution data used must be regarded as *approximate* in that they both come from a multitude of sources and in that we have taken a given thermochemical value on its merit, if it was cited in the literature surveyed, although in the light of the results generated we have tried to be critical of such values. The charge distributions for the ions in question are *very tentative* in that they come from a variety of sources. The crystal structure data must also be of varying quality. In the light of these considerations we produce what we hope are qualitatively, if not *entirely* quantitatively, meaningful results, which should be strengthened by the further studies we intend. The maximum error likely in the absolute bond energy is probably of the order of $\pm 15 \text{ kJ mol}^{-1}$, which gives an indication of our notional precision.

The dispersion energies, U_{dd} and U_{qd} , in the present study are probably slightly high, resulting in a lattice energy that is also too high. This arises from the model used to calculate the dispersion terms (namely that of six X^- halide ions at the X atomic positions in the MX_6^{2-} ions).

The magnitudes used for U_{dd} , however, conform with all the studies in the literature, and so the comparison of the literature values with

the present work for $U_{\text{POT}}(\text{A}_2\text{MX}_6)$ undertaken below is unaffected by these considerations.

Calculations on TlCl , TlBr , and TlI exhibit a variation of \bar{r}_{Tl^+} from salt to salt, which makes the subsequent assignment of \bar{r}_{Tl^+} in relation to Ti_2MX_6 salts uncertain. Consequent errors for the salts Ti_2PtCl_6 and Ti_2SiF_6 will be larger than for salts with other cations.

B. CHARGE DISTRIBUTIONS

For selected ions the literature contains a host of assessments of q_{X} , the charge on the halogen atom. For example in the ion SnCl_6^{2-} , q_{Cl} is quoted as -0.498 by Brill *et al.* (8), while Kubo and Nakamura (50) cite q_{Cl} equal to -0.66 , Welsh *et al.* (70) quote -0.50 , and the Jørgensen average (42–45) (Table I) gives -0.74 . The question arises to which value we should assume in our studies and what difference such a choice makes to $U_{\text{POT}}(\text{A}_2\text{MX}_6)$. Our policy has been to take the values from the study of Brown *et al.* (9) in preference to those of Kubo and Nakamura (50), which are in turn taken in preference to the Jørgensen averages (42–45).

Taking K_2SnCl_6 as an example, using the structure of Brill *et al.* (8), we find that for a range of values of q_{Cl} from -0.498 to -0.74 , $U_{\text{POT}}(\text{K}_2\text{SnCl}_6)$ varies from 1411 to 1329 kJ mol^{-1} (a variation of about 5%) and corresponds to 70 kJ mol^{-1} difference in lattice energy. It can be shown theoretically that if we take the Eq. (51):

$$\left(\frac{\partial U_{\text{POT}}}{\partial q_{\text{X}}} \right) = \left\{ [\gamma_1 - \delta_1 \phi_2] + 2(\gamma_2 - \delta_1 \phi_3) q_{\text{X}} - \frac{(\phi_2 + 2\phi_3 q_{\text{X}})(\delta_0 + 2\phi_0 \delta_1)}{2(\phi_1 + \phi_2 q_{\text{X}} + \phi_3 q_{\text{X}}^2)^{1/2}} \right\} \quad (80)$$

and at $q_{\text{X}} = q_{\text{Cl}} = -0.50$, we have for K_2SnCl_6 :

$$\left(\frac{\partial U_{\text{POT}}}{\partial q_{\text{X}}} \right)_{q_{\text{X}} = -0.5} = [\gamma_1 - \gamma_2 - \delta_1(\phi_2 - \phi_3)] - \frac{(\phi_2 - \phi_3)(\delta_0 + 2\phi_0 \delta_1)}{2(\phi_1 - 0.5\phi_2 + 0.25\phi_3)^{1/2}} \quad (81)$$

$$= 296 \text{ kJ mol}^{-1} \text{ proton unit}^{-1} \quad (82)$$

which is the rate of variation found for $U_{\text{POT}}(\text{K}_2\text{SnCl}_6)$ in practice at $q_{\text{Cl}} = -0.50$. We see therefore that the choice of q_{X} is rather important, and hence consistent periodic trends of the type we have aimed to

select (Table I) in our choice of q_X are essential. The nonavailability of precise measures of q_X hampers the present work to some extent. The forthcoming attempts to examine salts A_2MX_6 possessing different crystal symmetry to the antiferite arrangement promises a way around this difficulty.

C. COMPARISON OF LATTICE ENERGIES GENERATED WITH LITERATURE VALUES

We shall not concern ourselves in this study with the comparison of our present results with those originating from studies whose results are obtained by using the Born-Mayer (6), Born-Lande (5) or Kapustinskii (46) equations, since these approaches are known to generate effective lattice energies, which are on the whole too high. This leaves us with the comparison of results of Welsh *et al.* (70), Webster and Collins (69), Jenkins and Smith (40), and Jenkins (36) for $U_{\text{POT}}(A_2MX_6)$, which in turn requires comparison of values for the salts K_2SnCl_6 , Rb_2SnCl_6 , Cs_2GeCl_6 , K_2PtCl_6 , Rb_2TeCl_6 , and K_2PbCl_6 (see Table V).

The agreement between the results for $U_{\text{POT}}(A_2MX_6)$ of Welsh *et al.* (70), who obtain their values using the following charge distributions: Cs_2GeCl_6 ($q_{Cl} = -0.467$), K_2SnCl_6 ($q_{Cl} = -0.50$), and Rb_2PbCl_6 ($q_{Cl} = -0.483$) is close to those of Jenkins and Pratt (who use the same structural data) in this study based on: Cs_2GeCl_6 ($q_{Cl} = -0.73$), K_2SnCl_6 ($q_{Cl} = -0.66$) and Rb_2PbCl_6 ($q_{Cl} = -0.63$). However comparison of

TABLE V
COMPARISON OF LATTICE ENERGIES AND CONSTITUENT TERMS IN OTHER
LITERATURE CALCULATIONS (kJ mol^{-1})

Salt	U_{ELEC}	q_X	U	U_R	$U_{\text{POT}}(A_2MX_6)$	Reference
Cs_2GeCl_6	1414	-0.467	166	172	1404	(70)
Cs_2GeCl_6	1305	-0.73	162	92	1375	This work
K_2SnCl_6	1394	-0.50	169	169	1370	(70)
K_2SnCl_6	1310	-0.66	113	60	1363	This work
Rb_2SnCl_6	1599	-0.3	131	143	1551	(69)
Rb_2SnCl_6	1302	-0.66	91	134	1259	(40)
Rb_2SnCl_6	1303	-0.66	129	71	1361	This work
Rb_2PbCl_6	1360	-0.483	141	161	1335	(70)
Rb_2PbCl_6	1283	-0.63	125	65	1343	This work
Rb_2TeCl_6	1578	-0.3	131	136	1533	(69)
Rb_2TeCl_6	1242	-0.68	92	136	1201	(40)
Rb_2TeCl_6	1239	-0.68	125	48	1316	This work

individual terms in Eq. (15), writing $U_{dd} + U_{qd} = U_D$, reveals notable differences (see Table V).

A recent discussion by Jenkins (36) centered on a less rigorous minimization method (but one whose results for K_2PtCl_6 ($U_{POT} = 1468 \text{ kJ mol}^{-1}$) are almost identical to those obtained during the present approach) has drawn attention to the high repulsion energies generally assigned to salts of the general type A_2MX_6 by various workers. The values of U_R obtained by Brill *et al.* (7) are sometimes almost three times those obtained in this study whereas the dispersion terms differ by much less. Hence the lower U_{ELEC} value in our study (arising from the assignment of a higher $|q_x|$ value) is compensated for by the higher U_R term in the other study, giving overall agreement for $U_{POT}(A_2MX_6)$.

Turning now to the salts Rb_2SnCl_6 and Rb_2TeCl_6 and the works of Webster and Collins and Jenkins and Smith, which we compare to the present study in Table V, we find again that repulsion energies are much lower in the present study.

D. ENTHALPIES OF FORMATION OF IONS FROM STANDARD STATES, $\Delta H_f^\theta(MX_6^{2-})(g)$

A few specific comments on our calculated results should be dealt with first.

1. In the studies on the ions $TiCl_6^{2-}$, $TiBr_6^{2-}$, and $ZrCl_6^{2-}$ we have used Korol'kov and Effimov's (48) values for the enthalpies of formation of the salts from *gaseous atoms* and have "corrected" these to standard enthalpies of formation. The question of consistency of thermodynamic data arises.

2. The $\Delta H_f^\theta(ZrCl_6^{2-})(g)$ value assigned in this study resulted from averaging the assigned values based on differing (22, 48) values for $\Delta H_f^\theta(Cs_2ZrCl_6)(c)$ in the literature. The former value being "corrected" as described in Comment 1 above.

3. In our calculations (Table III) we find that in general

$$U_{POT}(K_2MX_6) = U_{POT}[(NH_4)_2MX_6] \quad (83)$$

and in the absence of data for one salt we can estimate its lattice energy from that of the other. We have used this relation, Eq. (83), to estimate $U_{POT}(A_2MX_6)$ for $(NH_4)_2IrCl_6$ and K_2PdCl_6 .

4. The value of $\Delta H_f^\theta((NH_4)_2SiF_6)(c)$ used in Section VG comes from Technical Note 270 (56), which is an updated version of Circular 500 (61), and is some 50 kJ mol^{-1} lower; however, $\Delta H_f^\theta(K_2SiF_6)(c)$,

$\Delta H_f^\theta(\text{Rb}_2\text{SiF}_6)(c)$, and $\Delta H_f^\theta(\text{Cs}_2\text{SiF}_6)(c)$ have been *deleted* rather than revised and, moreover, show unexpected variation going from the K^+ to the Cs^+ salt (the Cs_2SiF_6 enthalpy of formation appears to be too high).

If we deal only with the ammonium salt (the only enthalpy of formation value that has been revised), we obtain

$$\begin{aligned}\Delta H_f^\theta(\text{SiF}_6^{2-})(g) &= -2275 \text{ kJ mol}^{-1} \\ \overline{\Delta H}_{F(g)} &= -119 \text{ kJ mol}^{-1} \\ \Delta H_{\text{hyd}}^\theta(\text{SiF}_6^{2-})(g) &= -985 \text{ kJ mol}^{-1}\end{aligned}$$

and we regard these values as being more reliable than the assignments based on the K^+ , Rb^+ , and Cs^+ salts, despite the operation of the point charge approximation for the NH_4^+ ion.

Turning now to a comparison of our assigned values and other literature values, Table VI gives our assigned values of $\Delta H_f^\theta(\text{MX}_6^{2-})(g)$.

Brill *et al.* (7) obtained the values

$$\begin{aligned}\Delta H_f^\theta(\text{GeCl}_6^{2-})(g) &= -956 \pm 84 \text{ kJ mol}^{-1} \\ \Delta H_f^\theta(\text{SnCl}_6^{2-})(g) &= -1125 \pm 84 \text{ kJ mol}^{-1} \\ \Delta H_f^\theta(\text{PbCl}_6^{2-})(g) &= -927 \pm 92 \text{ kJ mol}^{-1}\end{aligned}$$

in the same numerical order as our values, but some 25, 29, and 13 kJ mol^{-1} , respectively, higher. We regard this as substantial agreement.

Webster and Collins (69) obtained

$$\begin{aligned}\Delta H_f^\theta(\text{SnCl}_6^{2-})(g) &= -1070 \pm 70 \text{ kJ mol}^{-1} \\ \Delta H_f^\theta(\text{TeCl}_6^{2-})(g) &= -804 \pm 70 \text{ kJ mol}^{-1}\end{aligned}$$

and Jenkins and Smith (40) obtained

$$\begin{aligned}\Delta H_f^\theta(\text{SnCl}_6^{2-})(g) &= -1256 \text{ kJ mol}^{-1} \\ \Delta H_f^\theta(\text{TeCl}_6^{2-})(g) &= -1020 \text{ kJ mol}^{-1}\end{aligned}$$

values, which bracket our present estimates, for reasons discussed in Section III on lattice energy. The latter calculation was based on the assumption that the Lewis acid strengths of SnCl_4 and TeCl_4 toward Cl^- are very nearly the same.

TABLE VI

SUMMARY OF DERIVED THERMODYNAMIC DATA (kJ mol^{-1} UNLESS OTHERWISE STATED) INCLUDING BOND ENERGIES $E(\text{M} - \text{X})_{\text{hom}}$ AND $E(\text{M} - \text{X})_{\text{het}}$ AND TOTAL COORDINATE BOND ENERGY (c.b.e.) = $6E(\text{M} - \text{X})_{\text{het}}$ [Eq. (6)] FOR MX_6^{2-} .

Ion	$\overline{\Delta H}_{\text{X(ss)}}^{\text{a}}$ (ss) ^a	Value	$\Delta H_f^\theta(\text{MX}_6^{2-})$ (g)	$\Delta H_{\text{hyd}}^0(\text{MX}_6^{2-})$ (g)	$\bar{r}_{\text{MX}_6^{2-}}$ (Å)	$\Delta H_f^\theta(\text{MX}_6^{2-})$ (g)	$\Delta H_f^\theta(\text{MX}_6^{2-})$ (-c.b.e) (g)	$\overline{E(\text{M} - \text{X})}_{\text{hom}}$ bond energy	$\overline{E(\text{M} - \text{X})}_{\text{het}}$ Coordinate bond energy	Total coordinate bond energy (c.b.e.) for MX_6^{2-} (eV).
TiCl_6^{2-}	(l) (g)	-36 -76	-1330	—	2.48	-2530	-9252	422	1542	95.9
TiBr_6^{2-}	(c) (g)	-58 -125	-1142	—	2.61	-2281	-9148	380	1525	94.8
ZrCl_6^{2-}	(c) (g)	-54 -164	-1526	—	2.47	-2863	-8252	477	1375	85.8
HfCl_6^{2-}	(c) (g)	(-158) (-259)	(-1640)	—	—	-2985	-8015	498	1336	83.1
NbCl_6^{2-}	(c) (g)	(-78) (-171)	(-1224)	—	—	-2678	-8765	446	1461	90.8
TaCl_6^{2-}	(c) (g)	(-102) (-243)	(-1275)	—	—	-2782	-8326	464	1388	86.3
MoCl_6^{2-}	(c) (g)	-102 (-73) -192 (-163)	-1070 (-1041)	—	2.54	-2454 (-2424)	-9721 (-9691)	409 (404)	1620 (1615)	100.7 (100.4)
WCl_6^{2-}	(c) (g)	-46 -152	-985	—	2.49	-2560	-8656	427	1443	89.7
WBr_6^{2-}	(c)	-91	-705	—	2.72	-2223	-8464	371	1411	87.7

66	ReCl ₆ ²⁻	(c)	- 66	- 919	- 709	2.54	- 2416	- 8900	403	1483	92.2
	ReBr ₆ ²⁻	(c)	+ 82	- 689	—	2.81	- 2131	- 8760	355	1460	90.8
	OsCl ₆ ²⁻	(c) (g)	- 5 - 181	- 752	—	2.54	- 2269	- 8976	378	1496	93.0
	IrCl ₆ ²⁻	(g)	—	(- 785)	(- 706)	2.56	- 2179	- 8867	363	1478	91.9
	NiF ₆ ²⁻	(g)	—	- 1328	—	1.97	- 2232	- 11600	372	1933	120.2
	PdCl ₆ ²⁻	(g)	—	(- 734) (- 765)	(- 735)	2.61	(- 1856)	(- 10337)	(309)	(1723)	(107.1)
	PtCl ₆ ²⁻	(c)	- 37	- 792	- 757	2.59	- 2085	- 9461	348	1577	98.0
	PtBr ₆ ²⁻	(c)	- 18	- 645	- 703	2.85	- 1879	- 9400	313	1567	97.4
	SiF ₆ ²⁻	(g)	- 119 (- 42)	- 2275 (- 2198)	- 985 (- 1071)	1.94	- 3201 (- 3124)	- 11239 (- 11162)	534 (521)	1873 (1860)	116.5 (115.6)
	GeF ₆ ²⁻	(g)	- 240	- 1971	—	2.01	- 2822	- 10928	470	1821	113.2
	GeCl ₆ ²⁻	(1) (g)	+ 43 + 7	- 981	—	2.43	- 2085	- 10033	348	1672	104.0
	SnCl ₆ ²⁻	(1) (g)	- 153 - 192	- 1156	- 685	2.47	- 2188	- 9113	365	1519	94.5
	PbCl ₆ ²⁻	(1) (g)	- 119 - 163	- 940	—	2.48	- 1863	- 9107	311	1518	94.4
	TeCl ₆ ²⁻	(c) (g)	- 73 - 153	- 891	—	2.41	- 1814	- 9098	302	1516	94.3
	TeBr ₆ ²⁻	(c)	- 3	- 661	—	2.73	- 1529	- 8958	255	1493	92.8

^a (ss) = standard state.

DeJonge (16, 17) has calculated

$$\Delta H_f^a(\text{PtCl}_6^{2-})(g) = -2237 \text{ kJ mol}^{-1}$$

$$\Delta H_f^a(\text{PtBr}_6^{2-})(g) = -2000 \text{ kJ mol}^{-1}$$

$$\Delta H_f^a(\text{PdCl}_6^{2-})(g) = -1971 \text{ kJ mol}^{-1}$$

These values should be compared to our calculated values listed in Table VI, where the same order is preserved, but it should be noted that DeJonge's (16,17) values are derived from an extended Born-Lande (5) treatment.

E. ENTHALPIES OF HYDRATION OF IONS, $\Delta H_{\text{hyd}}^\theta(\text{MX}_6^{2-})(g)$

DeJonge (16, 17) obtains

$$\Delta H_{\text{hyd}}^\theta(\text{PtCl}_6^{2-})(g) = -602 \text{ kJ mol}^{-1}$$

$$\Delta H_{\text{hyd}}^\theta(\text{PtBr}_6^{2-})(g) = -584 \text{ kJ mol}^{-1}$$

$$\Delta H_{\text{hyd}}^\theta(\text{PtI}_6^{2-})(g) = -561 \text{ kJ mol}^{-1}$$

$$\Delta H_{\text{hyd}}^\theta(\text{PdCl}_6^{2-})(g) = -606 \text{ kJ mol}^{-1}$$

These values are similar to our values (Table VI) apart from the revised order of $\Delta H_{\text{hyd}}^\theta(\text{PdCl}_6^{2-})(g)$ and $\Delta H_{\text{hyd}}^\theta(\text{PtCl}_6^{2-})(g)$ due to the slightly larger "basic" radius we obtain for PdCl_6^{2-} (2.61 Å) compared to PtCl_6^{2-} (2.59 Å).

On the basis of our "basic" radii, we might expect the following trends of hydration enthalpies:

$$\Delta H_{\text{hyd}}^\theta(\text{TiCl}_6^{2-})(g) > \Delta H_{\text{hyd}}^\theta(\text{ZrCl}_6^{2-})(g)$$

$$\Delta H_{\text{hyd}}^\theta(\text{MoCl}_6^{2-})(g) > \Delta H_{\text{hyd}}^\theta(\text{WCl}_6^{2-})(g)$$

$$\Delta H_{\text{hyd}}^\theta(\text{TcCl}_6^{2-})(g) > \Delta H_{\text{hyd}}^\theta(\text{ReCl}_6^{2-})(g)$$

$$\Delta H_{\text{hyd}}^\theta(\text{PdCl}_6^{2-})(g) > \Delta H_{\text{hyd}}^\theta(\text{PtCl}_6^{2-})(g)$$

$$\Delta H_{\text{hyd}}^\theta(\text{GeCl}_6^{2-})(g) < \Delta H_{\text{hyd}}^\theta(\text{SnCl}_6^{2-})(g) < \Delta H_{\text{hyd}}^\theta(\text{PbCl}_6^{2-})(g)$$

$$\Delta H_{\text{hyd}}^\theta(\text{SeCl}_6^{2-})(g) > \Delta H_{\text{hyd}}^\theta(\text{TeCl}_6^{2-})(g)$$

$$\Delta H_{\text{hyd}}^\theta(\text{PtCl}_6^{2-})(g) < \Delta H_{\text{hyd}}^\theta(\text{PtBr}_6^{2-})(g)$$

Burgess and Cartwright (10a) have given single ion hydration enthalpies obtained from their thermochemical and lattice studies:

$$\Delta H_{\text{hyd}}^{\theta}(\text{ReCl}_6^{2-})(\text{g}) = -836 \text{ kJ mol}^{-1}$$

$$\Delta H_{\text{hyd}}^{\theta}(\text{ReBr}_6^{2-})(\text{g}) = -784 \text{ kJ mol}^{-1}$$

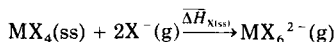
$$\Delta H_{\text{hyd}}^{\theta}(\text{IrCl}_6^{2-})(\text{g}) = -834 \text{ kJ mol}^{-1}$$

$$\Delta H_{\text{hyd}}^{\theta}(\text{PtCl}_6^{2-})(\text{g}) = -844 \text{ kJ mol}^{-1}$$

$$\Delta H_{\text{hyd}}^{\theta}(\text{PtBr}_6^{2-})(\text{g}) = -769 \text{ kJ mol}^{-1}$$

F. HALIDE ION AFFINITIES

Table VI gives the halide ion affinities for the process



using Eq. (4) to calculate $\overline{\Delta H}_{\text{X(ss)}}$.

Westland *et al.* (22, 51) have given the relationships (68), (72), (75), (76), and (78). Taking their lattice energies from Lal and Westland (51) proposed lattice energy relationships, they would obtain

$$\overline{\Delta H}_{\text{Cl(g)}} = -26 \pm 5 \text{ kJ mol}^{-1} \text{ for ZrCl}_4$$

and

$$\overline{\Delta H}_{\text{Cl(g)}} = -37 \pm 14 \text{ kJ mol}^{-1} \text{ for HfCl}_4$$

and

$$\overline{\Delta H}_{\text{Cl(g)}} = +15 \text{ kJ mol}^{-1} \text{ for NbCl}_4$$

although they further quote

$$\overline{\Delta H}_{\text{Cl(g)}} = 3 \text{ kJ mol}^{-1} \text{ for NbCl}_4$$

and

$$\overline{\Delta H}_{\text{Br(g)}} = -4 \text{ to } +17 \text{ kJ mol}^{-1} \text{ for NbBr}_4$$

and

$$\overline{\Delta H}_{\text{Cl(g)}} = -23 \text{ kJ mol}^{-1} \text{ for TaCl}_4$$

and

$$\overline{\Delta H}_{\text{Cl(g)}} = +39 \text{ kJ mol}^{-1} \text{ for SnCl}_4.$$

Westland concludes that ZrCl_4 and HfCl_4 are somewhat better acceptors of Cl^- than NbCl_4 and that ZrCl_4 and HfCl_4 are markedly better acceptors of Cl^- than SnCl_4 . TaCl_4 is found to be a better acceptor of Cl^- ion than NbCl_4 .

Westland's (22, 51) arguments are based on several assumptions given by relationships (81), (83), and (86); further, he assumes that

$$U_{\text{POT}}(\text{K}_2\text{NbCl}_6) = U_{\text{POT}}(\text{K}_2\text{TaCl}_6) = 1586 \text{ kJ mol}^{-1}$$

From our present calculations we find

$$U_{\text{POT}}(\text{K}_2\text{SnCl}_6) - U_{\text{POT}}(\text{K}_2\text{ZrCl}_6) = 24 \text{ kJ mol}^{-1} \quad (84)$$

$$U_{\text{POT}}(\text{K}_2\text{NbCl}_6) - U_{\text{POT}}(\text{K}_2\text{ZrCl}_6) = 36 \text{ kJ mol}^{-1} \quad (85)$$

$$U_{\text{POT}}(\text{K}_2\text{HfCl}_6) - U_{\text{POT}}(\text{K}_2\text{ZrCl}_6) = 16 \text{ kJ mol}^{-1} \quad (86)$$

$$U_{\text{POT}}(\text{K}_2\text{TaCl}_6) - U_{\text{POT}}(\text{K}_2\text{NbCl}_6) = 3 \text{ kJ mol}^{-1} \quad (87)$$

not too dissimilar to Westland's relationships. If we use our lattice energies in Eqs. (68), (72), (75), (76), and (80) we generate

$$\overline{\Delta H}_{\text{Cl(g)}} = -258 \text{ kJ mol}^{-1} \text{ for } \text{ZrCl}_4$$

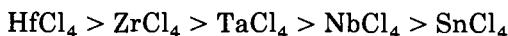
$$\overline{\Delta H}_{\text{Cl(g)}} = -266 \text{ kJ mol}^{-1} \text{ for } \text{HfCl}_4$$

$$\overline{\Delta H}_{\text{Cl(g)}} = -196 \text{ kJ mol}^{-1} \text{ for } \text{NbCl}_4$$

$$\overline{\Delta H}_{\text{Cl(g)}} = -231 \text{ kJ mol}^{-1} \text{ for } \text{TaCl}_4$$

$$\overline{\Delta H}_{\text{Cl(g)}} = -184 \text{ kJ mol}^{-1} \text{ for } \text{SnCl}_4$$

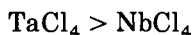
The difference arises from the fact that our lattice energies are so much lower than those of Gelbman and Westland (22). The order of the acceptor power toward Cl^- ion is preserved:



Turning to our results in Table VI for the group designated IVA in Table II, we find the chloride ion affinities of the tetrahalides are in the order

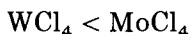


For Group VA a similar group tendency is observed:



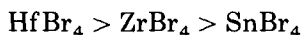
in agreement with Westland's (22) order, although the absolute order for the five tetrahalides does not agree. For group VIA, however,

the order



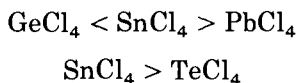
is surprisingly found.

Makhida and Westland (54a) have calculated the order:



for acceptor power toward Br^- . We cannot compare results from this study since no full crystal structure determinations for A_2HfBr_6 , A_2ZrBr_6 and A_2SnBr_6 salts are available.

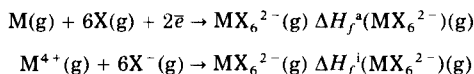
For the main group IVB we find



Few intercomparisons can be made for the tetrabromides owing to the sparseness of the data.

G. BOND STRENGTHS

The following processes give, to varying extents, a measure of the M—X bond strength:



the former involving the enthalpy of formation of the gaseous MX_6^{2-} ion from atoms; the latter, from ions.

The above thermodynamic quantities are interrelated thus:

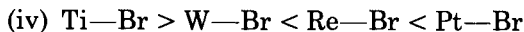
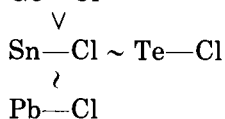
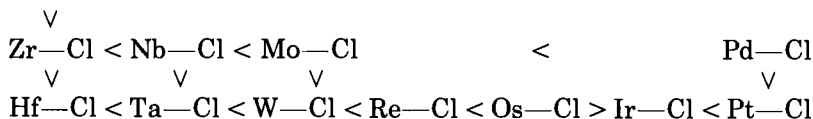
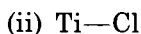
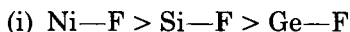
$$\Delta H_f^a(MX_6^{2-})(g) - 3D_{X_2} - \Delta H_{sub}^\theta(M)(c) = \Delta H_f^i(MX_6^{2-})(g) \quad (88)$$

$$\Delta H_f^a(MX_6^{2-})(g) - \sum_{n=1}^4 I_n - 6A_X = \Delta H_f^i(MX_6^{2-})(g) \quad (89)$$

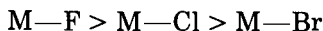
where D_{X_2} is the dissociation energy of X_2 : $X_2(ss) \rightarrow 2X(g)$; $\Delta H_{sub}^\theta(M)(c)$ is the enthalpy of the process: $M(c) \rightarrow M(g)$; $\sum_{n=1}^4 I_n$ represents the ionization potential of the process: $M(g) \rightarrow M^{4+}(g)$; A_X is the electron affinity of X: $X(g) \rightarrow X^-(g)$; I_n is the ionization potential corresponding to the process: $M^{(n-1)+}(g) \rightarrow M^{n+}(g)$.

The bond energies $\overline{E(M-X)}_{\text{het}}$ and $\overline{E(M-X)}_{\text{hom}}$ are related to the thermodynamic quantities in equations (6) and (5), respectively. We confine our comparisons of bond strengths to a discussion of the heterolytic bond energy, $\overline{E(M-X)}_{\text{het}}$, although Table VI cites the values of both.

Comparison of the bond strengths, $\overline{E(M-X)}_{\text{het}}$ obtained (Table VI) as described in Section I,B of this chapter, leads to:



In all cases:



These trends are in line with chemical prediction (38a), but are almost without exception *reversed* by consideration of $\overline{E(M-X)}_{\text{hom}}$ values.

IX. Concluding Remarks

The aim of this review has been to collect the few lattice energy calculations already in existence and blend these into the framework of our newly proposed minimization method, which has generated the vast amount of data included in this chapter. Far from concluding this study, this is rather the commencement. The reader will note that the review concentrates on the attainment of lattice energies and leaves open the discussion of the thermodynamic data obtained with a view to further examination in the light of the studies on similar A_2MX_6 salts having different crystal structures.

We repeat our plea made in the introduction for continued interest in the obtaining of crystal structure data and ancillary thermodynamic

data for such salts, and would be pleased to be informed about further studies or about studies omitted from this chapter.

ACKNOWLEDGMENTS

We wish to thank a number of people who read the first draft of this manuscript and provided minor inclusions, specifically: Norman Greenwood, Alan D. Westland, Peter G. Nelson, Ray D. Peacock and John Burgess. We are grateful to the S.R.C. for providing a studentship to one of us (K.F.P.).

Mrs. Sheila Jenkins and Mrs. Vivien Henstone are thanked for their help in checking the proofs.

REFERENCES

1. Basolo, F., and Pearson, R. G., "Mechanisms of Inorganic Reactions." Wiley, New York, 1958.
2. Beech, J. D., Wood, R. H., and Greenwood, N. N., *Inorg. Chem.* **2**, 86 (1970).
3. Bell, J. D., Hall, D., and Waters, T. N., *Acta Crystallogr.* **21**, 440 (1966).
4. Berthold, H. J., and Jakobson, G., *Angew. Chem.* **76**, 497 (1964).
5. Born, M., and Lande, A., *Ber. Preuss. Akad. Wiss., Berlin* **45**, 1048 (1918).
6. Born, M., and Mayer, J. E., *Z. Phys.* **75**, 1 (1932).
7. Brill, T. B., Gearhart, R. C., and Welsh, M. A., *J. Magn. Reson.* **13**, 27 (1974).
8. Brill, T. B., Hugus, Z., and Schreiner, A. F., *J. Phys. Chem.* **74**, 2999 (1970).
9. Brown, T. L., McDougle, W. G., and Kent, L. G., *J. Am. Chem. Soc.* **92**, 3645 (1970).
10. Burovoya, E. E., *Kristallografiya* **1**, 365 (1956).
- 10a. Burgess, J., and Cartwright, S. J., *J. Chem. Soc. Dalton.* **100** (1975).
- 10b. Busey, R. H., Gayer, K. H., Gilbert, R. A., and Bevan, R. B., *J. Phys. Chem.* **70**, 2609 (1966).
11. CATCH Tables, "Computer Analysis of Thermochemical Data." University of Sussex, 1974.
12. Cotton, F. A., and Harris, C. B. *Inorg. Chem.* **6**, 376 (1976).
13. Cotton, F. A., and Johnson, B. F. G., *Inorg. Chem.* **3**, 780 (1964).
14. Coulter, L. V., Pitzer, K. S., and Latimer, W. M., *J. Am. Chem. Soc.* **62**, 2845 (1940).
15. Das, A. K., and Brown, R. D., *Can. J. Chem.* **44**, 939 (1966).
16. DeJonge, R. M., *J. Inorg. Nucl. Chem.* **38**, 1821 (1976).
17. DeJonge, R. M., private correspondence to H. D. B. Jenkins (1977).
18. D'Orazio, L. A., and Wood, R. H., *J. Phys. Chem.* **69**, 2550 (1965).
19. Efimov, A. I., and Belorukova, L. P., *Russ. J. Inorg. Chem. (Engl. Transl.)* **12**, 792 (1967).
20. Elder, N., Ferguson, J. E., Gainsford, G. J., Hickford, J. H., and Penfold, B. R., *J. Chem. Soc. A* 1423 (1967).
- 20a. Gal'chenko, G. L., Gedakyan, D. A., and Timofeev, B. I., *Zhur. Neorg. Khim.* **13**, 307 (1968).
- 20b. Gal'chemko, G. L., Gedakyan, D. A., Timofeev, B. I., and Skivalov, S. M., *Dokl. Akad. Nauk. SSSR* **161**, 1081 (1965).
21. Gearhart, R. C., Ph.D. Thesis, University of Delaware, Newark (1972).
22. Gelbman, P., and Westland, A. D., *J. Chem. Soc., Dalton* 1598 (1974).
23. Glyshko, V. P., "Thermochemical Constants of Compounds," Vol. 7. Akad. Nauk, Moscow, (1974).
24. Goldberg, R. N., and Hepler, L. G., *Chem. Rev.* **68**, 229 (1968).

25. Golutvin, Y. M., Maslennikova, E. G., Li, A. N., Safonov, V. V., and Korshunov, B. G., *Zh. Fiz. Khim.* **48**, 2719 (1974).
26. Golutvin, Y. M., Maslennikova, E. G., Li, A. N., Safonov, V. V., and Korshunov, B. G., *Russ. J. Phys. Chem. (Engl. Transl.)* **48**, 1604 (1974).
- 26a. Gross, P., Hayman, C., and Bingham, J. T., *Trans. Faraday Soc.* **62**, 2388 (1966).
27. Grundy, H. D., and Brown, R. D., *Can. J. Chem.* **48**, 1151 (1970).
28. Hanic, F., *Chem. Zvesti* **20**, 738 (1966).
29. Hartley, F. R., *Nature (London), Phys. Sci.* **236**, 75 (1972).
30. Hazell, A. C., *Acta Chem. Scand.* **20**, 168 (1966).
31. Herzfeld, K. F., and Woolf, K. L., *Ann. Phys. (Leipzig)* [4] **78**, 35 (1928).
32. Herzig, P., Jenkins, H. D. B., and Neckel, A., *J. Phys. Chem.* **80**, 1608 (1976).
- 32a. Hopkins, K. G. G., Ph.D. Thesis, University of Hull (1970).
33. Huggins, M. L., and Mayer, J. E., *J. Chem. Phys.* **1**, 643 (1933).
34. "JANAF Thermochemical Tables" (D. A. Stull, ed.). Dow Chemical Co., Midland, Michigan, 1960-1966.
35. Jenkins, H. D. B., *J. Chem. Soc., Faraday Trans. 2* **72**, 1569 (1976).
36. Jenkins, H. D. B., *J. Phys. Chem.* **80**, 852 (1977).
37. Jenkins, H. D. B. and Morris, D. F. C., *Mol. Phys.* **32**, 231 (1976).
38. Jenkins, H. D. B., and Pratt, K. F., *J. Chem. Res. (M)* 0728 (1977).
- 38a. Jenkins, H. D. B., and Pratt, K. F., *Inorg. Chimica Acta* **32**, 25 (1979).
39. Jenkins, H. D. B., and Pratt, K. F., *Proc. Soc. London, Ser. A* **356**, 115 (1977).
40. Jenkins, H. D. B., and Smith, B. T., *J. Chem. Soc., Faraday Trans. I* **72**, 353 (1976).
- 40a. Jenkins, H. D. B., and Pratt, K. F., *Prog. Solid State Chem.* **12**, 125 (1979).
41. Jensen, A. T., and Rasmussen, S. F., *Acta Chem. Scand.* **9**, 708 (1955).
42. Jørgensen, C. K., *Adv. Chem. Phys.* **5**, 33 (1963).
43. Jørgensen, C. K., Horner, S. M., Hatfield, W. E., and Tyree, F. Y., Jr., *Int. J. Quantum Chem.* **1**, 191 (1957).
44. Jørgensen, C. K., "Oxidation Numbers and Oxidation States." Springer-Verlag, Berlin and New York, 1969.
45. Jørgensen, C. K., *Prog. Inorg. Chem.* **4**, 73 (1962).
46. Kapustinskii, A. F., *Rev., Chem. Soc.* **10**, 283 (1956).
47. Kennedy, C. D., and Peacock, R. D., *J. Chem. Soc.* 3392 (1963).
48. Korol'kov, D. V., and Efimov, A. I., *Probl. Sovrem. Khim. Koord. Soedin.* **1**, 215 (1966).
49. Korol'kov, D. V., and Kudryashava, S., *Russ. J. Inorg. Chem. (Engl. Transl.)* **15**, 1759 (1970).
50. Kubo, M., and Nakamura, D., *Adv. Inorg. Chem. Radiochem.* **8**, 257 (1966).
51. Lal, D., and Westland, A. D., *J. Chem. Soc., Dalton* 2505 (1974).
52. Lalanchette, R. A., Elliott, N., and Bernal, I., *J. Cryst. Mol. Struct.* **2**, 143 (1972).
- 52a. Lerbscher, J. A., and Trotter, J., *Acta Cryst.* **B32**, 2671 (1976).
53. Lister, M. W., Nyburg, S. C., and Poyntz, R. B., *J. Chem. Soc., Faraday Trans. 1* **70**, 685 (1974).
54. Lister, R. L., and Flengas, S. N., *Can. J. Chem.* **42**, 1102 (1964).
- 54a. Makhija, R., and Westland, A. D., *J. Chem. Soc. Dalton* 1707 (1977).
- 54b. Micklow, J., and Janitsch, A., *Monatscheft Chem.* **106**, 1307 (1975).
- 54c. Maniv, S., *J. Applied Cryst.* **9**, 245 (1976).
55. Moews, P. C., *Inorg. Chem.* **5**, 5 (1966).
56. Parker, V. B., Wagman, D. D., and Evans, W. H., *Natl. Bur. Stand. (U.S.), Tech. Note* **270** (1971).
57. Peacock, R. D., private correspondence (1976).
58. Pearson, R. G., and Mawby, R. J., *Halogen Chem.* **3**, 55 (1967).

59. Pirenne, J., and Kartheuser, E., *Physica (Utrecht)* **30**, 2005 (1964).
60. Quail, J. W., and Rivett, G. A., *Can. J. Chem.* **50**, 2447 (1972).
61. Rossini, F. D., Wagman, D. D., Evans, W. H., Levine, S., and Jaffe, I., *Natl. Bur. Stand. (U.S.), Cir.* **500** (1952).
62. Schlemper, E. O., and Hamilton, W. C., *J. Chem. Phys.* **44**, 2499 (1966).
- 62a. Shchukarev, S. A., Vasil'kova, C. V., and Korol'kov, D. V., *Russ. J. Inorg. Chem.* **9**, 980 (1964).
63. Schwochaw, K., *Z. Naturforsch., Teil B* **19**, 1237 (1964).
64. Shchukarev, S. A., Korol'kova, D. V., and Vasil'kova, I. V., *Russ. J. Inorg. Chem. (Engl. Transl.)* **9**, 980 (1964).
- 64a. Shidlovskii, A. A., *Zhur. Fiz. Khim.* **36**, 1773 (1962).
65. Shidlovskii, A. A., and Valkina, K. V., *Zh. Fiz. Khim.* **35**, 294 (1961).
- 65a. Stepin, B. D., Plyushchev, V. E., Selivanova, M. N., and Serebrennikova, G. M., *Russ. J. Phys. Chem. (Engl. Transl.)* **42**, 1233 (1968).
66. Swanson, H. E., Fuyat, R. K., and Ugrinic, G. M., *Natl. Bur. Stand. (U.S.), Monogr.* **25**, 2 and 11 (1963).
67. Swanson, H. E., Fuyat, R. K., and Ugrinic, G. M., *Natl. Bur. Stand. (U.S.), Monogr.* **25**, 1 and 6 (1962).
68. Tsintsius, V. M., and Smirnova, E. K., *Russ. J. Inorg. Chem. (Engl. Transl.)* **14**, 1729 (1969).
- 68a. Wagman, D. D., Evans, W. H., Parker, V. B., and Schumm, R. H., "Chemical Thermodynamic properties of Compounds of Sodium, Potassium and Rubidium: An Interim Tabulation of Selected Values," NBSIR 76-1034, Office of Standard Reference Data, N.B.S. Washington (1973).
69. Webster, M., and Collins, P. H., *J. Chem. Soc., Dalton* 588 (1963).
70. Welsh, W. A., Brill, T. B., Thompson, P. T., Wood, R. H., and Gearhart, R. C., *Inorg. Chem.* **13**, 1797 (1974).
71. Westland, A. D., unpublished work (1975).
72. Wood, R. H., *J. Chem. Phys.* **32**, 1690 (1960).
73. Wood, R. H., and D'Orazio, D. A., *Inorg. Chem.* **5**, 682 (1966).
74. Wyckoff, R. W. G., "Crystal Structures," 2nd ed. Vol. III. Wiley (Interscience), New York, 1965.

X. Appendix

Since this chapter was written, a number of additional studies have been undertaken by the author. In order of likely appearance in print these are:

(i) A study and fuller discussion of the bond strengths and double halide ion affinities derived from the present study (Section VIII, F and G) with some estimates for metal-bromide bond strengths (A1).

(ii) Following some measurements by Makhija and Westland (A2) of:

$$\Delta H_f^\theta(K_2SeCl_6)(c) = -1076 \pm 2 \text{ kJ mol}^{-1}$$

$$\Delta H_f^\theta(Rb_2SeCl_6)(c) = -1103 \pm 2 \text{ kJ mol}^{-1}$$

$$\Delta H_f^\theta(K_2SeBr_6)(c) = -876 \pm 2 \text{ kJ mol}^{-1}$$

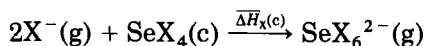
$$\Delta H_f^\theta(Rb_2SeBr_6)(c) = -907 \pm 2 \text{ kJ mol}^{-1}$$

the lattice energies of Rb_2SeCl_6 (Section V,I,1,a,iii) and K_2SeBr_6 (Section V,I,2,a,iii) are used to generate:

$$\Delta H_f^\theta(\text{SeCl}_6^{2-})(g) = -684 \text{ kJ mol}^{-1}$$

$$\Delta H_f^\theta(\text{SeBr}_6^{2-})(g) = -525 \text{ kJ mol}^{-1}$$

which in turn lead to halide ion affinity values, corresponding to the process:



of

$$\Delta \bar{H}_{\text{Cl}(c)} = -13 \text{ kJ mol}^{-1}$$

$$\Delta \bar{H}_{\text{Br}(c)} = +18 \text{ kJ mol}^{-1}$$

which can be compared to the Te values in Table VI. See Jenkins *et al.* (A3).

(iii) A further theoretical development (A4) made has enabled us to make a complete study of the salts A_2MX_6 having noncubic lattices (A5). Careful discussion and consideration of the literature crystal structure data for these salts is made and calculations are carried out for: $\text{M}=\text{Ti, Zr, Hf, Mo, Mn, Re, Rh, Pt, Si, Ge, X}=\text{F}$; $\text{M}=\text{Ce, Th, U, Pu, Bk, X}=\text{Cl}$; and $\text{M}=\text{Te, X}=\text{Br}$. These calculations enable us to predict enthalpies of formation for the ions:

$$\Delta H_f^\theta(\text{TiF}_6^{2-})(g) = -2321 \text{ kJ mol}^{-1}$$

$$\Delta H_f^\theta(\text{SiF}_6^{2-})(g) = -2295 \text{ kJ mol}^{-1}$$

$$\Delta H_f^\theta(\text{GeF}_6^{2-})(g) = -1973 \text{ kJ mol}^{-1}$$

$$\Delta H_f^\theta(\text{TeBr}_6^{2-})(g) = -682 \text{ kJ mol}^{-1}$$

$$\Delta H_f^\theta(\text{ThCl}_6^{2-})(g) = -1718 \text{ kJ mol}^{-1}$$

$$\Delta H_f^\theta(UCl_6^{2-})(g) = -1546 \text{ kJ mol}^{-1}$$

$$\Delta H_f^\theta(PuCl_6^{2-})(g) = -1527 \text{ kJ mol}^{-1}$$

halide ion affinities for:

TiF_4 :

$$\overline{\Delta H}_{F(c)} = -130 \text{ kJ mol}^{-1}$$

$$\overline{\Delta H}_{F(g)} = -228 \text{ kJ mol}^{-1}$$

SiF_4 :

$$\overline{\Delta H}_{F(g)} = -138 \text{ kJ mol}^{-1}$$

GeF_4 :

$$\overline{\Delta H}_{F(g)} = -242 \text{ kJ mol}^{-1}$$

$TeBr_4$:

$$\overline{\Delta H}_{Br(c)} = -24 \text{ kJ mol}^{-1}$$

$ThCl_4$:

$$\overline{\Delta H}_{Cl(c)} = -34 \text{ kJ mol}^{-1}$$

UCl_4 :

$$\overline{\Delta H}_{Cl(c)} = -3 \text{ kJ mol}^{-1}$$

$PuCl_4$:

$$\overline{\Delta H}_{Cl(c)} = -115 \text{ kJ mol}^{-1}$$

and enthalpy of hydration of SiF_6^{2-} :

$$\Delta H_{\text{hyd}}^{\theta}(\text{SiF}_6^{2-})(\text{g}) = -965 \text{ kJ mol}^{-1}$$

and heterolytic and homolytic bond strengths. Agreement, where comparison with cubic salt calculations is possible (SiF_6^{2-} , GeF_6^{2-} and TeBr_6^{2-}), is impressive in view of the fact that noncubic calculations do not require estimates of the charge distribution in the ion.

(iv) In a study of the hydrolysis of alkali metal hexachloro and hexabromo tungstates (IV) and rhenates (IV), Burgess *et al.* (46) have obtained a value, $\Delta H_f^{\theta}(\text{WBr}_4)(\text{c}) = -300 \text{ kJ mol}^{-1}$, at variance with currently accepted literature value cited in this chapter (11, 56). This value and others determined in this recent study lead us to two halide ion affinities for WCl_4 :

$$\Delta H_{\text{Cl}(\text{c})} = -70 \text{ kJ mol}^{-1}$$

$$\Delta H_{\text{Cl}(\text{g})} = -176 \text{ kJ mol}^{-1}$$

(previous values in Section V,D,3,vi contain the above values within their stated ranges).

For WBr_4 :

$$\overline{\Delta H}_{\text{Br}(\text{c})} = -50 \text{ kJ mol}^{-1}$$

(this value supersedes the value of Section V,D,4,vi).

For ReCl_4 :

$$\overline{\Delta H}_{\text{Cl}(\text{c})} = -90 \text{ kJ mol}^{-1}$$

(previous value in Section V,E,4,vii contains the above within stated range).

For ReBr_4 :

$$\overline{\Delta H}_{\text{Br}(\text{c})} = -80 \text{ kJ mol}^{-1}$$

(very close to value quoted in this chapter, Section V,E,5,vi).

The hydration studies lead us to a value:

$$\Delta H_{\text{hyd}}^{\theta}(\text{ReCl}_6^{2-})(\text{g}) = -740 \text{ kJ mol}^{-1}$$

not previously assigned.

(v) The fifth and most recent study (A7) contains some measurements of the enthalpies of solution of some hexafluorosilicates ($\text{Na}^+ = +30.8 \pm 1.1 \text{ kJ mol}^{-1}$; $\text{K}^+ = +73.0 \pm 2.0 \text{ kJ mol}^{-1}$; $\text{Rb}^+ = +86.1 \pm 3.3 \text{ kJ mol}^{-1}$; $\text{Cs}^+ = +131.7 \pm 0.9 \text{ kJ mol}^{-1}$; $\text{NH}_4^+ = +33.8 \pm 0.9 \text{ kJ mol}^{-1}$ and $\text{Ba}^{2+} = +40.5 \pm 0.3 \text{ kJ mol}^{-1}$); hexafluorotitanates ($\text{K}^+ = +74.0 \pm 1.8 \text{ kJ mol}^{-1}$ and $\text{Cs}^+ = +125.8 \pm 2.8 \text{ kJ mol}^{-1}$); hexafluoromanganates ($\text{K}^+ = +61.1 \pm 1.1 \text{ kJ mol}^{-1}$); hexafluororhenates ($\text{Na}^+ = +32.9 \pm 1.5 \text{ kJ mol}^{-1}$, $\text{K}^+ = +63.0 \pm 0.3 \text{ kJ mol}^{-1}$; $\text{Cs}^+ = +112.9 \pm 0.2 \text{ kJ mol}^{-1}$ and $\text{Ba}^{2+} = +35.4 \pm 1.2 \text{ kJ mol}^{-1}$) and hexafluoruthenates ($\text{K}^+ = +59.4 \pm 1.5 \text{ kJ mol}^{-1}$). From these studies and the associated lattice energies we assign:

$\Delta H_{\text{hyd}}^{\theta}(\text{SiF}_6^{2-})(\text{g}) = -971 \text{ kJ mol}^{-1}$
$\Delta H_{\text{hyd}}^{\theta}(\text{TiF}_6^{2-})(\text{g}) = -881 \text{ kJ mol}^{-1}$
$\Delta H_f^{\theta}(\text{MnF}_6^{2-})(\text{g}) = -1823 \text{ kJ mol}^{-1}$
$\Delta H_{\text{hyd}}^{\theta}(\text{MnF}_6^{2-})(\text{g}) = -912 \text{ kJ mol}^{-1}$
$\Delta H_{\text{hyd}}^{\theta}(\text{ReF}_6^{2-})(\text{g}) = -903 \text{ kJ mol}^{-1}$
$\Delta H_f^{\theta}(\text{ReF}_6^{2-})(\text{g}) = -1961 \text{ kJ mol}^{-1}$

Such studies are continuing.

REFERENCES

- A1. Jenkins, H. D. B., and Pratt, K. F., *Inorganic Chim Acta*, **32**, 25 (1979).
- A2. Westland, A.D., and Makhija, R., *Canad. J. Chem.*, **56**, 1586 (1978).
- A3. Jenkins, H. D. B., Westland A. D., and Makhija, R., *J. Chem. Res.*, accepted for publication (1979).
- A4. Jenkins, H. D. B., and Pratt, K. F., *J. Chem. Soc. Faraday II*, **74**, 968 (1978).
- A5. Jenkins, H. D. B., and Pratt, K. F. *Prog. Solid State Chem.* **12**, 125 (1979).
- A6. Burgess, J., Cartwright, S. J., Haigh, I. Peacock, R. D., Jenkins, H. D. B., and Pratt, K. F., *J. Chem. Soc. Dalton*, in press (1979).
- A7. Blandamer, M. J., Burgess, J., Hamshire, S. J., Peacock, R. D., Rogers, J. H., and Jenkins, H. D. B., *J. Chem. Soc. Dalton*, to be submitted (1979).

REACTION MECHANISMS OF INORGANIC NITROGEN COMPOUNDS

G. STEDMAN

Department of Chemistry, University College of Swansea, Singleton Park, Swansea, England

I. Introduction	114
II. Sulfamic Acid	115
A. Hydrolysis Reactions	115
B. Oxidation by Nitric Acid	115
III. Nitrogen Trihalides	116
A. Nitrogen Trichloride	116
B. Nitrogen Tribromide	117
IV. Hydrazine	118
A. Protonation of Hydrazine	118
B. Reaction of Hydrazine with Oxidizing Agents	118
V. Diimide and Tetrazene	121
A. Diimide	121
B. Tetrazene	121
VI. Hydroxylamine	122
A. Decomposition of Hydroxylamine in Alkaline Solution	122
B. Photolysis and Radiolysis of Hydroxylamine Solutions	123
C. Reaction of Hydroxylamine with Oxidizing Agents	124
D. Reaction of Hydroxylamine with Reducing Agents	128
VII. The Sulfonic Acids of Hydroxylamine and Derived Species	128
A. Hydroxylamine- <i>O</i> -Sulfonic Acid	128
B. Hydroxylamine- <i>N</i> -Monosulfonic Acid	129
C. Nitrosyldisulfonic Acid	129
D. <i>N</i> -Nitrosohydroxylamine <i>N</i> -Sulfonate	130
VIII. Hydrazoic Acid	131
A. Oxidation of Azide by Metal Ions or Metal Complexes	131
B. Oxidation of Hydrazoic Acid by Nonmetallic Species	132
C. Reactions of the Coordinated Azide Ion	133
IX. Hyponitrous Acid and Nitroxyl	135
A. Hyponitrous Acid	135
B. Nitroxyl	138
X. Nitramide	138
XI. Nitric Oxide	139
XII. Trioxodinitrate (II)	141
XIII. Nitrous Acid	143
A. Species Present in Solutions of Nitrous Acid	143
B. Electrophilic Nitrosations	144
C. Oxidation of Nitrite by Metal Ions and Metal Complexes	152

D. Oxidation of Nitrous Acid by the Halogens	154
E. Reduction of Nitrous Acid by Metal Ions and Metal Complexes	155
XIV. Dinitrogen Tetroxide and Nitrogen Dioxide	156
XV. Nitric Acid	160
A. Radiolysis and Photolysis	160
B. Reactions of Nitric Acid as an Oxidizing Agent	161
References	165

I. Introduction

Any reviewer of aspects of the chemistry of inorganic compounds of nitrogen faces a problem because of the amount and the variety of material available. Many common ligands contain nitrogen, and complexes containing such ligands could be held to fall within the scope of the title of this chapter. Attention has been focused upon the "simple" compounds of nitrogen, and upon a few reactions of coordinated ligands containing nitrogen, but the bulk of coordination chemistry has been deliberately excluded. The chemistry of nitrogen is one of those areas where the border between inorganic and organic chemistry is difficult to define, and some readers may feel that some of our excursions stray into the province of physical-organic chemistry. Such raiding parties may return with valuable plunder, and this type of foray into neighboring territory should be encouraged. Most of the papers cited deal with aspects of solution chemistry, and gas-phase reactions are only occasionally included. A new field of inorganic work, bioinorganic chemistry has also been mentioned only in passing. The last readily accessible and substantial review of the reaction mechanisms of nitrogen compounds was published in 1974 (92), and includes material up to late 1972. In this review particular attention has been paid to material published since that date, but many earlier papers have also been included. Literature coverage goes to about the end of 1977. Interested readers will find a great deal of information about recent work in the various sections of the Chemical Society Specialist Reports devoted to Inorganic Reaction Mechanisms. Developments in the inorganic chemistry of nitrogen have been reviewed in volumes edited by Colburn (47), and a good deal of kinetic material is to be found in volume 6 of the series on Comprehensive Chemical Kinetics edited by Bamford and Tipper (13). A recent book, "Mechanism of Oxidation by Metal Ions" by Benson, includes mention of many papers dealing with the oxidation of inorganic nitrogen compounds (23).

The types of reaction examined are so varied that it seems best to classify material by the compound studied, ordering the material in the

sequence of the average formal oxidation state of nitrogen, and then dealing in turn with different types of mechanism. Many systems could be classified under more than one heading, and the arrangement of material has necessarily been somewhat arbitrary at times.

II. Sulfamic Acid

A. HYDROLYSIS REACTIONS

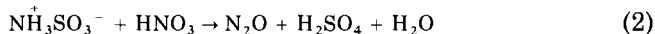
The kinetics of the acid-catalyzed hydrolysis of sulfamic acid have been followed in solutions containing up to 10 *M* perchloric acid (93), a much higher acidity than was used in previous studies. In earlier work the rate had been found to increase with acidity, leveling off around 2 *M* acid. The new measurements show that a rate maximum is observed, with a slow decrease in rate with increase of acidity beyond 2 *M* perchloric acid. Candlin and Wilkins (41) had previously proposed an A-1 mechanism for the hydrolysis of sulfamic acid ($\text{NH}_3^+\text{SO}_3^-$) at lower acidities, and the new results are interpreted as an additional A-2 pathway (in an A-1 mechanism a water molecule is not involved as a nucleophile in the transition state, whereas in an A-2 process it is involved).

$$\text{Rate} = k[\text{H}^+][\text{NH}_3^+\text{SO}_3^-]a_w \quad (1)$$

An A-2 mechanism is also postulated for *N*-phenylsulfamic acid hydrolysis (180). The kinetics of hydrolysis of the sulfamate anion in aqueous alkali at high temperatures have also been measured (156).

B. OXIDATION BY NITRIC ACID

Sulfamic acid is commonly used as a scavenger for nitrous acid in solutions of nitric acid, but if the concentration of the latter is sufficiently great, another reaction is observed:



At low temperatures nitramide can be isolated from the reaction mixture (195); as nitramide readily decomposes to nitrous oxide and water, this suggests that it might be an intermediate. A brief kinetic study gave a rate equation first order in sulfamic acid and in nitric acid, and this was interpreted (9) as an electrophilic displacement of SO_3H^+ by NO_2^+ to form nitramide. However, this mechanism apparently needs modification. A more extensive study (94, 107) shows that

reaction involves three consecutive stages, with relative rates $v_1 > v_2 \geq v_3$. The kinetics of the last of these stages, v_3 , are identical with those reported in (9). However the details of the mechanism are not yet clear, and at this stage it is not possible to postulate equations for the three stages with any degree of confidence.

III. Nitrogen Trihalides

A. NITROGEN TRICHLORIDE

Nitrogen trichloride is best known as a notoriously explosive compound, but there is a great deal of interest in the chemistry of its reactions in aqueous solution. It can be formed during the treatment of water, by chlorination of traces of ammonia. It gives an unpleasant taste and odor to drinking water, and it irritates mucus membranes with which it has contact. Aspects of its chemistry in aqueous solution have been discussed by Saguinsin and Morris (164). The chlorination of ammonia by hypochlorous acid involves a slow formation of chloramine, which is followed by faster processes to give dichloramine and nitrogen trichloride. It has proved possible to examine the kinetics of the final stage, and rate equation (3) has been deduced.

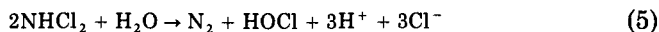
$$(d[\text{NCl}_3]/dt)_0 = (k_1 + k_2[\text{H}^+][\text{Cl}^-])[\text{HOCl}][\text{NH}_2\text{Cl}]_0 \quad (3)$$

This corresponds to chlorination by hypochlorous acid and chlorine. The chlorination of ammonia by Me_3CCOCl in *cyclo*-hexane solution containing 0.2 *M* *t*-butanol has also been investigated. Chloramine, dichloramine, and nitrogen trichloride were found to be formed successively (19).

The decomposition reaction of nitrogen trichloride in aqueous media has also been studied. The rate increases in alkaline solution, and follows Eq. (4).

$$-(d[\text{NCl}_3]/dt)_0 = (k_3 + k_4[\text{OH}^-])[\text{NCl}_3] \quad (4)$$

Reaction is thought to involve formation of dichloramine, followed by a complex disproportionation of this species



There has been a study of the thermal decomposition of nitrogen trichloride in carbon tetrachloride solution (158). The presence of aromatic compounds such as benzene, toluene, etc., increases the rate

of decomposition, due to π complex formation; thus in the presence of toluene the activation energy drops by ca. 10 kcal mol⁻¹. In the presence of mesitylene an autocatalytic reaction is observed.

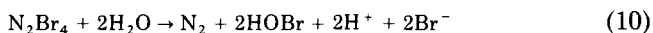
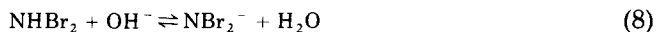
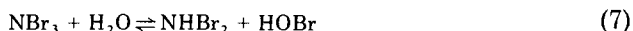
The reactions of one of the above intermediates, chloramine, were investigated by Anbar and Yagil (6) some years ago. In sufficiently alkaline solution chloramine hydrolyzes to give hydroxylamine as a primary product, probably by a bimolecular nucleophilic substitution by hydroxide ion. The same authors examined the formation of hydrazine from chloramine and ammonia (5), and concluded that reaction involved nucleophilic attack by ammonia on chloramine or its conjugate base.

B. NITROGEN TRIBROMIDE

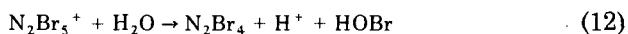
A detailed picture has emerged of the decomposition of a closely related compound, nitrogen tribromide, in aqueous media in the pH range 6 to 8 (112, 127). The tribromide is generated by treating an aqueous solution of ammonia with hypobromous acid or bromine, the bromamines being formed much more rapidly than the corresponding chloramines. In the decomposition of nitrogen tribromide the ammonia is oxidized to dinitrogen, and a two-term rate law [Eq. (6)] is observed.

$$-d[\text{NBr}_3]/dt = k_5[\text{NBr}_3]^2[\text{OH}^-][\text{HOBr}]^{-1} + k_6[\text{NBr}_3]^2 \quad (6)$$

The pathway proposed to account for the first term is (7)–(10), with (9) as the slow step



The rate-determining step corresponding to the second term in equation (6) is suggested to be reaction (11), followed by fast steps (12) and (10)



A related species (NCl_2^-), a chloronitrene (NCl) and dichlorodiimide ($\text{ClN}=\text{NCl}$) have been postulated (218) as intermediates in the reaction of *N,N*-dichloroamides with alkoxides.

IV. Hydrazine

A. PROTONATION OF HYDRAZINE

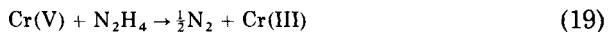
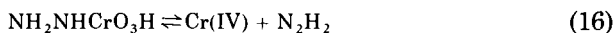
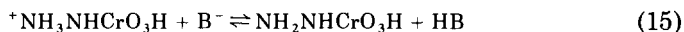
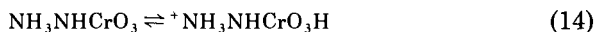
Hydrazine normally exists in aqueous solution as the free base or the monoprotonated conjugate acid N_2H_5^+ , and both of these species are frequently postulated as the active species in kinetic studies of reactions of hydrazine. The doubly protonated form $\text{N}_2\text{H}_6^{2+}$ is known in the solid state, and there are reports of its existence in aqueous solution. A $\text{p}K_a$ of -0.88 has been reported (166). If this is correct, it would be expected that a significant proportion of hydrazine would exist in this form in solutions containing several moles per liter of strong mineral acids, and this should show up in the dependence of rate reaction upon acidity. Attempts to observe this effect in the nitrosation of hydrazine have been unsuccessful (154). A search for PMR evidence for a second protonation of methylhydrazine was also unsuccessful. Spectrophotometric studies of the arylhydrazines in concentrated mineral acids indicate $\text{p}K_a$ values for the doubly protonated species in the range -5 to -6 (116). Mechanistic studies of the oxidation of hydrazine often use a comparison of the reactivity of the alkylhydrazines with hydrazine as a criterion of mechanism, and it has always been assumed that protonation is almost 100% on the alkylated nitrogen. A study has been made by Condon and co-workers of the basicity; thus for protonated methylhydrazine it is calculated that there is 70% $\text{CH}_3\text{NH}_2^+\text{NH}_2$ and 30% $\text{CH}_3\text{NHNH}_3^+$ (50). This result is in close agreement with proportions of products observed in the electrophilic nitrosation of methylhydrazine, which appear to be derived from the two tautomers (152). Thus it seems desirable to consider the two different conjugate acid species when interpreting the results of mechanistic studies of the reactions of alkylhydrazines in acid solution.

B. REACTION OF HYDRAZINE WITH OXIDIZING AGENTS

Hydrazine has long been a favorite substrate for mechanistic studies with oxidizing agents because of the relationship between stoichiometry and mechanism. One equivalent reagents produce nitrogen and

ammonia as products and may involve N_2H_3 (and N_4H_6) as intermediates, whereas two equivalent reagents form diimide, N_2H_2 , and this gives exclusively nitrogen. At high acidities, and with two equivalent reagents, hydrazoic acid may be a product (89). Earlier work has been summarized by Sykes (192) and by Bottomley (29). Evidence for these species has recently come from a number of sources. Diimide and tetrazene have been obtained as pure species, and their decomposition reactions were investigated (Section V). The species N_2H_3 has been observed in pulse-radiolysis studies of the oxidation of hydrazine by the hydroxyl radical (88), and the conjugate acid $N_2H_4^+$ has been observed as an intermediate in the oxidation of hydrazine by cerium(IV) using electron spin resonance (ESR) methods (140).

The system that has been most intensively studied recently is the oxidation by chromium(VI). Haight *et al.* (86) have extended kinetic measurements up to 2 *M* acid. At lower acidities, pH 1.6–3.0, they find evidence for general acid catalysis. The mechanism proposed involves $^+NH_3NH_2CrO_3^-$ and related conjugate acid and base species, and complex formation occurs to a sufficient extent to allow the estimation of a formation constant.



It is concluded that chromium(V) is formed by reaction (18), not by trapping with chromium(VI). Three other studies of the reaction have been reported (16, 83, 159). In the third of these papers (159), the formation of chromium(V) is explained as due to a reaction between chromium(IV) and chromium(VI), and the authors also suggest a direct reduction of chromium(V) to chromium(III) by diimide.

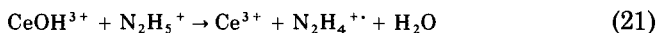
A number of other oxidizing agents have been studied. Thallium(III) oxidizes hydrazine, forming thallium(I) and nitrogen. The rate law is

given in Eq. (20), and it is suggested that the inverse dependence upon $[H^+]$ indicates complexing between N_2H_4 and thallium(III) (198).

$$-d[Tl(III)]/dt = k[Tl(III)][N_2H_5^+][H^+]^{-1} \quad (20)$$

The oxidation of hydrazine by thallium(III) acetate complexes has been reported (84).

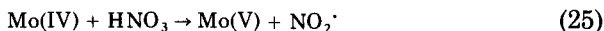
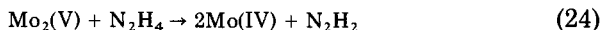
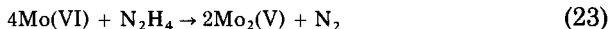
In the oxidation of hydrazine by $[Co(NTA)(OH_2)_2]$, reaction is thought to occur between the conjugate base of the complex and $N_2H_5^+$ (NTA = nitrilotriacetate) (197). Similarly the oxidation of hydrazine by cerium(IV) is thought (144) to involve the hydrazinium ion in the rate-determining stage



The protonated hydrazyl radical has been identified by flow ESR techniques (140). The oxidation of methylhydrazine by cerium(IV) in acid solution has also been investigated (118). Another powerful one-equivalent oxidizing agent, manganese(III), also reacts with the hydrazinium ion by pathways involving Mn^{3+} and $MnOH^{2+}$ (55). Two studies of oxidation reactions of hydrazine involving copper(II) have been published. The copper(II)-catalyzed oxidation of hydrazine by hydrogen peroxide obeys a rate law that is interpreted as showing the formation of a substantial amount of a copper(II)-hydrazine complex (213).

$$d[N_2]/dt = k[N_2H_4][H_2O_2][Cu(II)](1 + K[N_2H_4])^{-1} \quad (22)$$

The other study concerns the oxidation of 1,1-dimethylhydrazine by copper(II) chloride in hydrochloric acid (25). Outer sphere mechanisms have been proposed (128) for the oxidation of hydrazine by $Mo(CN)_8^{3-}$ and $W(CN)_8^{3-}$. A rather complex mechanism, again involving a molybdenum(V) species, has been proposed for the molybdenum(VI)-catalyzed oxidation of hydrazine by nitric acid (122).



The oxidation of hydrazine by vanadium(V) has been studied (20), and so has the oxidation by $PtCl_6^{2-}$ (173). Finally, we note studies of the reaction of $trans-Coen_2Cl_2^+$ with hydrazine, with methylhydrazine

and with 1,1-dimethylhydrazine (42), and of the reaction of methylhydrazine with $\text{PtCl}_2(\text{CNAr})_2$ in dichloromethane (44).

V. Diimide and Tetrazene

A. DIIMIDE

Diimide (N_2H_2) also known as diimine or diazene, has long been proposed as an active intermediate, particularly in the oxidation of hydrazine. It can be made by passing hydrazine vapor through a microwave discharge and can be frozen out. Rapid warming of the frozen material enables diimide to be obtained in the gas phase (together with ammonia) (225). It can also be obtained by the thermal decomposition of alkali metal tosyl hydrazides (Li, Na, K) at very low pressures (219). Infrared spectra enable the *cis* and the *trans* isomers to be identified (220). With the cesium salt a different product is obtained: $\text{NH}_2=\text{N}$. Diimide is a moderately stable substance in the gas phase with a half-life typically of the order of minutes (225, 227). The kinetics of decomposition are complex, and first-order, second-order, or mixed-order behavior may be observed. The decomposition in liquid ammonia (-65° to -38°C) follows a somewhat complex path. In the early stages there is a rapid reaction with a kinetic order greater than one, while in the later stages a simple first-order decay is observed with $k_1 = 1.9 \times 10^3 \exp(-3300/T) \text{ sec}^{-1}$. The authors speculate that the rapid initial process may involve the *cis* isomer while the slower first-order reaction may be a *trans* to *cis* isomerization (225). The activation energy is very much less than that calculated for the gas-phase isomerization (see below), and further work on this system would be of interest. Diimide is, of course, a good reagent for stereospecific hydrogenation, and the mechanism of reaction with a series of unsaturated compounds in the gas phase has been examined (226).

Diimide is a compound for which theoretical calculations can be useful in helping us to understand its properties. Winter and Pitzer (230) calculate that the *trans*-isomer is $6.6 \text{ kcal mol}^{-1}$ more stable than the *cis* form, and the lowest energy pathway for isomerization should involve inversion at one nitrogen, with $E_a = 47 \text{ kcal mol}^{-1}$. Calculations of the activation energy for *cis*- to *trans*-isomerization in XNNX by this mechanism are in the sequence $\text{F} > \text{H} > \text{Me} > \text{CN}$ (1931).

B. TETRAZENE

Another frequently postulated intermediate is *trans*-2-tetrazene, NH_2NNNH_2 , and this has now been isolated as a product of the

reaction of tetrakis (trimethylsilyl) tetrazene with trifluoroacetic acid in methylene chloride at -78°C . It is unexpectedly stable; the solid begins to thermolyse at 0°C , and the gaseous substance is metastable at room temperature. On thermolysis of the pure compound a yield of 75% $\text{N}_2 + \text{N}_2\text{H}_4$ and 25% of $\text{NH}_4^+ \text{N}_3^-$ was obtained. In methanol solution the corresponding yields were 40% and 60%, respectively (221). Other studies indicate that the thermal decomposition of tetrazene, which may be explosive, has a high activation energy (123, 149).

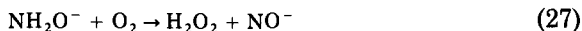
VI. Hydroxylamine

A. DECOMPOSITION OF HYDROXYLAMINE IN ALKALINE SOLUTION

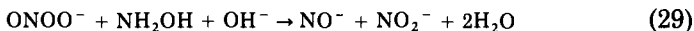
Hydroxylamine is normally thought of as a moderately basic substance (in water NH_3OH^+ has a $\text{p}K_a$ of 5.9), but it can also function as an acid. A value of 13.7 has been obtained for the $\text{p}K_a$ of free hydroxylamine in aqueous solution at 25° (97).



In the absence of oxygen such solutions are stable, but in the presence of oxygen reaction occurs by attack upon the conjugate base, with the formation of the nitroxyl anion. This in turn reacts with oxygen to form the peroxonitrite anion (95).



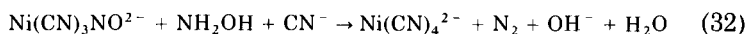
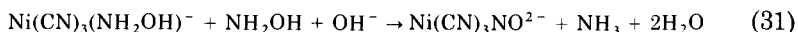
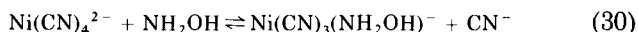
In the presence of copper(II) peroxonitrite then reacts with hydroxylamine, regenerating the nitroxyl anion, which in turn can form more peroxonitrite (96).



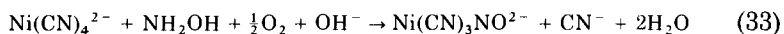
Thus, in the presence of oxygen, alkaline solutions of hydroxylamine are effectively oxidized to nitrite.

Veprek-Siska and Lunak have examined the decomposition of hydroxylamine in the presence of $\text{Ni}(\text{CN})_4^{2-}$, a complex that is known to act as a trap for NO^- . In alkaline media decomposition of hydroxyl-

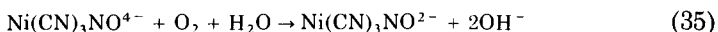
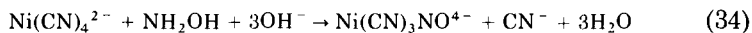
amine is reported to follow a rate law that is first order in hydroxylamine, and third order in hydroxide ion (132). Reaction is catalyzed by a range of cations, and when these are completely complexed decomposition does not occur. In the presence of Ni(CN)_4^{2-} in an inert atmosphere, the pathway below is suggested. The absence of N_2O among the products is held to argue against nitroxyl as an intermediate (209).



In the presence of oxygen, a different stoichiometry is found



The rate is increased by metal ions, and is decreased by added cyanide ion, and the mechanism (34) to (35) is postulated: (210).



B. PHOTOLYSIS AND RADIOLYSIS OF HYDROXYLAMINE SOLUTIONS

Photolysis of hydroxylamine is thought to involve the formation of amino and hydroxyl radicals in the primary stage, and these may attack hydroxylamine with the abstraction of hydrogen to form NHOH^\cdot (18), which can then disproportionate.



Pulse radiolysis studies also lead to the conclusion that NHOH^\cdot radicals are produced in the oxidation of hydroxylamine by hydroxyl (178). This radical can form a conjugate acid ($\text{NH}_2\text{OH}^{+\cdot}$), with a $\text{p}K_a$ of 4.2. In more acidic media the radical $\text{NH}_2\text{O}^\cdot$ is often considered to be involved in the oxidation of hydroxylamine by metal ions, and this is a tautomer of NHOH^\cdot . The amino radical also acts as a base, and a $\text{p}K_a$ of 6.7 has been suggested for $\text{NH}_3^{+\cdot}$.

C. REACTION OF HYDROXYLAMINE WITH OXIDIZING AGENTS

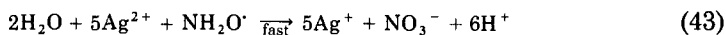
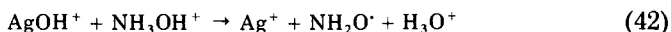
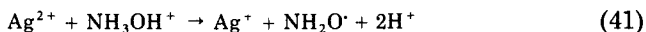
Hydroxylamine is oxidized by a wide variety of reagents and the stoichiometry is often a function of concentration. In many cases the postulated reaction mechanism involves oxidation to $\text{NH}_2\text{O}^\cdot$, which can decompose to nitrogen



In the presence of a suitable oxidizing agent, further oxidation to nitroxyl may occur, as in the oxidation of hydroxylamine by cerium(IV) (211)

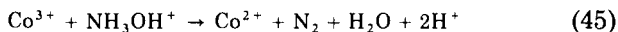
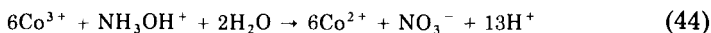


In the oxidation of hydroxylamine by plutonium(IV), dinitrogen and nitrous oxide are products formed by this type of mechanism (15). The effect of ferric ion catalysis on the plutonium(IV)-hydroxylamine reaction has also been reported (14). In some cases further oxidation occurs to nitrous or nitric acids. This can sometimes be detected by changes in rate or stoichiometry when a nitrite trap, such as urea or sulfamic acid, is added to the reacting system as in the oxidation of hydroxylamine by thallium(III) (199). Here the stoichiometry varies with the ratio in which the reactants are used; with a sufficient excess of the oxidizing agent either nitrate or nitrate may be obtained; addition of urea (a nitrite scavenger) reduces the stoichiometry from $\text{Tl(III)}:\text{NH}_2\text{OH}::3:1$ to $2:1$. In many cases these later stages in the oxidation are rapid, and only the initial oxidation to $\text{NH}_2\text{O}^\cdot$ can be detected kinetically, as in the oxidation of hydroxylamine to nitric acid by manganese(III) (54) or silver(II) (90).

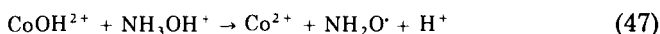
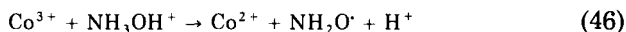


The oxidation of hydroxylamine by cobalt(III) shows the complications that can arise. With a large enough excess of cobalt(III) the stoichi-

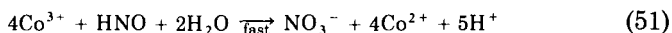
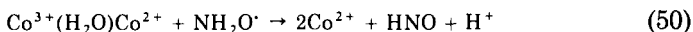
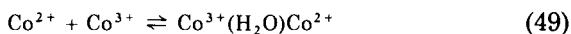
ometry is given by (44), but when hydroxylamine is in large excess a different reaction (45) is observed.



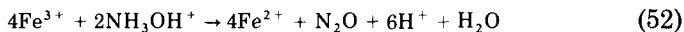
In the latter case the pathway is (31) to (33).



In excess oxidizing agent, the NH_2O^+ is further oxidized, the active species being a cobalt(III)–cobalt(II) dimer (181).



Many of the reactions in which hydroxylamine is oxidized by metal ions involve the formation of hydroxylamine complexes. The analytically useful reaction between hydroxylamine and ferric ion has been examined (21) kinetically by Bengtsson. In the absence of copper(II) as a catalyst, rate law (53) is observed in 0.1 *M* acid.



$$\text{Rate} = \frac{k[\text{Fe(III)}]^2[\text{NH}_2\text{OH}]^2}{([\text{NH}_2\text{OH}] + k_2[\text{Fe(II)}])} \quad (53)$$

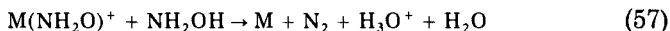
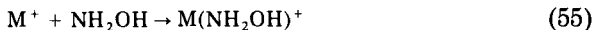
In the presence of copper(II) a more complex rate law is observed.

$$\text{Rate} = \frac{k_3[\text{Fe(II)}][\text{Cu(II)}][\text{NH}_2\text{OH}]}{([\text{Fe(II)}][\text{NH}_2\text{OH}] + k_4[\text{Cu(II)}][\text{NH}_2\text{OH}] + k_5[\text{Fe(II)}])} \quad (54)$$

[The concentration terms here refer to stoichiometric concentrations.] Bengtsson suggests that the mechanism involves binuclear intermediates containing two hydroxylamine bridges. He has also examined

the oxidation of hydroxylamine by vanadium(V), and proposes a mechanism with two parallel pathways involving complexes of vanadium(V) with one or two hydroxylamine ligands, respectively (22).

The oxidation of hydroxylamine by hexacyanoferrate(III) is markedly affected by traces of iron(II) or copper(II) present in the reagents used. Addition of EDTA eliminates catalysis by copper(II), but introduces a new pathway involving the iron(III)-EDTA complex as a reactant, with a rate law first order in hydroxylamine and the total concentration of iron-EDTA complexes. The mechanism proposed (31) again involves formation of a hydroxylamine complex and is shown below, (55)–(58), where M^+ and M represent the oxidized and reduced forms of the catalytic species, i.e., $M^+ = \text{Fe(III) EDTA}^-$.



If the forward reaction in (55) is rate limiting, the kinetics are accounted for satisfactorily. For the copper(II)-catalyzed reaction (in the absence of EDTA), the rate law is accounted for if (56) is rate determining ($M^+ = \text{Cu}^{2+}$). Copper(II) is also a catalyst in the oxidation of hydroxylamine by peroxodisulfate to nitrous oxide (190). The oxidation of hydroxylamine by copper(II) in the presence of a reagent to scavenge the copper(I) formed has also been examined (111).

Another oxidation of hydroxylamine in which complex formation with a metal ion is assumed, and that has aroused a good deal of interest, is the copper(II)-catalyzed reaction with hydrogen peroxide. The mechanism suggested (69) involves an active species in which both hydroxylamine and hydrogen peroxide are coordinated to the metal, and it has been proposed that this system models some features of the peroxidases. A study of oxidation of $[\text{Coen}_2\text{Cl}(\text{NH}_2\text{OH})]^{2+}$ by hydrogen peroxide has recently been carried out, as in this case the hydroxylamine starts out coordinated to the metal ion. The dependence of rate upon acidity is not simple, but for solutions with a pH less than 3.9 the rate of reaction is first order with respect to the concentration of complex and hydrogen ion, and zero order with respect to that of hydrogen peroxide. A rate-determining loss of chloride ion, followed by a rapid entry of peroxide into the coordination sphere is postulated (177).

Another reaction of the same complex that has been studied involves nitrous acid, and has proved to be a complicated system. At sufficiently high acidities, the rate law has the form (59), while at low acidities Eq. (60) appears to hold.

$$\text{Rate} = k[\text{H}^+][\text{HNO}_2][\text{complex}] \quad (59)$$

$$\text{Rate} = k'[\text{H}^+]^{-1}[\text{HNO}_2][\text{complex}] \quad (60)$$

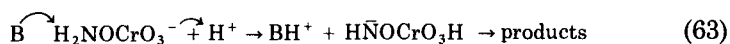
When the *O*-methylhydroxylamine complex is used, no reaction occurs. In acidic media, $\text{pH} < 2$, Eq. (59) is strictly analogous to the law observed (98) for reaction between hydroxylamine and nitrite, except that the coordinated hydroxylamine is roughly one-tenth as reactive as the free hydroxylammonium ion. An electrophilic nitrosation on the oxygen to form a species $\text{Co}-\text{NH}_2-\text{O}-\text{NO}$ is proposed (177), and this seems very likely (the effect of *O*-methylation exactly parallels what is observed with the nitrosation of free hydroxylamine) (99). Interpretation of (60) is much more difficult. Reaction does not appear to involve substitution by nitrite ion at the complex because the direct displacement reaction leads to products different to those observed under the conditions where (60) holds. A reaction between nitrosonium ion and a doubly deprotonated complex would be consistent with the kinetic form, but one must ask whether the concentration of the doubly deprotonated complex could be great enough to account for the observed rate. This is an interesting but very difficult system.

The oxidation of hydroxylamine by chromium(VI) is also a complex system and has been studied in some detail by Haight *et al.* (167), and by Sen Gupta *et al.* (174). The stoichiometry varies with the pH, and with the initial composition of the reaction mixture. In acetate buffer the rate law reported is (61):

$$\begin{aligned} -d[\text{Cr(VI)}]/dt = & \{[\text{Cr(VI)}][\text{NH}_3\text{OH}^+](k_A[\text{H}^+] + k_B[\text{HOAc}] + k_C \\ & + k_D K_f K_{An} [\text{H}^+]^{-1} + k_E K_f K_{An} [\text{OAc}^-] K_a^{-1})\} \\ & \times \{1 + [\text{H}^+] K_{Ac}^{-1} + K_f [\text{HOAc}]\} \\ & + K_f K_{An} [\text{NH}_3\text{OH}^+][\text{H}^+]^{-1} \}^{-1} \end{aligned} \quad (61)$$

Reaction is thought to proceed through the formation of an *O*-bonded ester (in *O*-methylhydroxylamine reaction is greatly inhibited), and the ester $\text{NH}_3^+ \text{OCrO}_3^-$ and its conjugate base are thought to undergo acid- and base-assisted internal redox reactions.





Sen Gupta and co-workers have also examined the oxidation of hydroxylamine by platinum(IV) in acetate buffers (172). The kinetics of oxidation of hydroxylamine by aqueous solutions of bromine have also been reported (125).

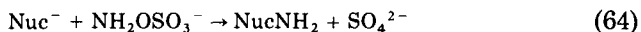
D. REACTION OF HYDROXYLAMINE WITH REDUCING AGENTS

Hydroxylamine also acts as an oxidizing agent. Tertiary phosphines are converted to phosphine oxides, with reduction of hydroxylamine to ammonia, and different pathways are proposed when the hydroxylamine is in the acidic and basic forms (183). The reduction of hydroxylamine by vanadium(III) (204) and by titanium(III) (205) has also been reported. It is postulated that NH_2^{\cdot} radicals are intermediates, as suggested by earlier ESR measurements (60). The titanium(III) reaction has also been investigated by another group, who also propose an NH_2^{\cdot} radical intermediate (155).

VII. The Sulfonic Acids of Hydroxylamine and Derived Species

A. HYDROXYLAMINE-O-SULFONIC ACID

The sulfonic acids derived from hydroxylamine, and some of the derivatives of these compounds, are treated as a group for the sake of convenience. Some earlier work has been summarized by Becke-Goehring and Flück (17). The reactions of hydroxylamine *O*-sulfonate with a variety of nucleophiles have led to the establishment of a reactivity sequence similar to that observed with substitution at methyl iodide, at *trans*-dipyridinedichloroplatinum(II) and at hydrogen peroxide.



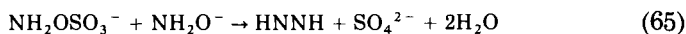
The polarizability of the nucleophile seems to be important in determining the reactivity, and its basicity is of only minor importance (124). There seems to be a general similarity in the reactivity spread observed for nucleophilic substitution at sp^3 carbon and at sp^3 nitrogen. In some of these substitutions the rate law contains an acid-catalyzed term. Kinetic data are given in Table I.

The alkaline hydrolysis of hydroxylamine *O*-sulfonate is catalyzed by trace metal ions. This effect can be eliminated by the addition of

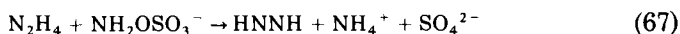
TABLE I
RELATIVE REACTIVITIES OF NUCLEOPHILES TOWARD $\text{NH}_2\text{OSO}_3^-$ AT 20° (124)

$\text{C}_2\text{H}_5\text{S}^-$	Ph_3P	$(\text{NH}_2)_2\text{CS}$	$\text{S}_2\text{O}_3^{2-}$	I^-	$(\text{C}_2\text{H}_5)_3\text{N}$	HONH_2	OH^-
460	> 28	24	8	1.00	0.32	0.020	0.0003

EDTA as a complexing agent, although the advantages are somewhat offset by the introduction of a new reaction pathway involving EDTA (189). In the presence of hydrazine and hydroxylamine new pathways are observed involving N_2H_4 and NH_2O^- as nucleophiles. In the latter case diimide is postulated as a reaction intermediate.



A kinetic analysis of the variation of rate with pH leads to a $\text{p}K_a$ of 13.7 for hydroxylamine, in agreement with other values (see Section VI, A). The disproportionation of diimide can yield hydrazine, and this can lead to kinetic complications. These can be minimized by scavenging the diimide with fumarate ions.



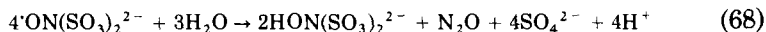
When thiourea is the nucleophile, the interesting new species $(\text{NH}_2)_2\text{CSNH}_2^+$ is formed.

B. HYDROXYLAMINE-*N*-MONOSULFONIC ACID

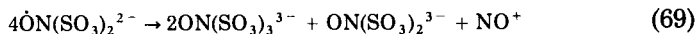
This species undergoes alkaline hydrolysis through the conjugate base ONHSO_3^{2-} , as the active form (168).

C. NITROSYLDISULFONIC ACID

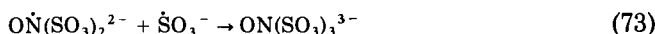
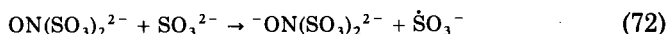
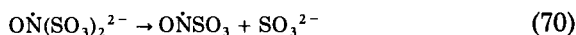
The nitrosyldisulfonate radical anion, $^-\text{ON}(\text{SO}_3)_2^{2-}$ (Fremy's salt) is a moderately stable substance. It has been used as an ESR standard, and as a selective oxidizing agent. It decomposes in aqueous solution by a first-order process, accompanied by a rapid chain reaction propagated by nitrous acid (a product of the first-order pathway). The stoichiometry of the chain process is probably given by (68).



Nitrous acid has been found to be an intermediate, on the basis of spectrophotometric measurements (228). Addition of sulfamic acid as a nitrite trap eliminates the chain process and enables the first-order reaction to be studied in isolation. The stoichiometry is quite different in the presence of a nitrite scavenger.



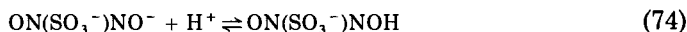
The likely mechanism is set out below, with (70) as the rate-determining stage:



Wilson has also examined the decomposition of the nitrosodisulfonate radical anion in strongly alkaline solutions (229) and concludes that nucleophilic attack by hydroxide ion results in displacement of the sulfite ion.

D. *N*-NITROSOHYDROXYLAMINE *N*-SULFONATE

The decomposition of *N*-nitrosohydroxylamine *N*-sulfonate, $\text{ON}(\text{SO}_3^-)(\text{NO}^-)$, can occur by an acid-catalyzed route, in which *cis*-hyponitrite has been suggested as an intermediate (191)



The intermediacy of *cis*-hyponitrite was postulated on the basis of nitrogen-15 labeling studies that showed that the two nitrogens became equivalent (46). No direct evidence for its formation was found. In the presence of boric acid another term appears in the rate law,

and coordination of one of the oxygens of the SO_3^- group to boron is suggested

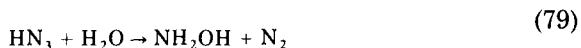
$$\text{Rate} = k[\text{ON}(\text{SO}_3^-)\text{NO}^-][\text{B}(\text{OH})_3] \quad (77)$$

VIII. Hydrazoic Acid

Hydrazoic acid is a weak acid, $\text{p}K_a = 4.7$, but in sufficiently concentrated mineral acids it can act as a base, and a $\text{p}K_a$ of -6.2 for H_2N_3^+ has been obtained (12) together with evidence that may indicate the formation of $\text{H}_3\text{N}_3^{2+}$. In aqueous solution hydrazoic acid is quite stable, though losses may occur because of its volatility. Values of the Henry's law constant are available (196). Photolysis results in the formation of a nitrene, and in the gas phase ΔH is 33 kcal mol^{-1} for forming NH in the lowest singlet state (47).



In aqueous media photolysis of hydrazoic acid produces a quantitative yield of hydroxylamine, and a nitrene intermediate is involved (175).



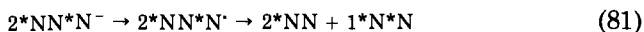
A. OXIDATION OF AZIDE BY METAL IONS OR METAL COMPLEXES

Many studies are available in which hydrazoic acid acts as a reducing agent. A common product is dinitrogen, but multiequivalent reagents often produce in addition nitrogen compounds in a higher oxidation state (235). Oxidation by cobalt(III) gives rate law (80), and this is consistent with either a rate-determining breakdown of $\text{Co}(\text{H}_2\text{O})_5\text{N}_3^{2+}$ (or a species in tautomeric equilibrium, such as $\text{Co}(\text{H}_2\text{O})_4(\text{OH})(\text{HN}_3)^{2+}$) (145).

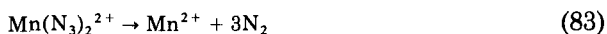
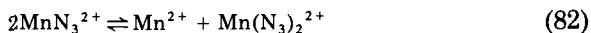
$$\text{Rate} = k[\text{Co(III)}][\text{HN}_3][\text{H}^+]^{-1} \quad (80)$$

A different rate law has been reported by another group of workers (214), but this has been disputed (203). The likely mechanism involves oxidation to N_3^\cdot radicals, which then react in a bimolecular step, possibly to form an adduct that breaks down to dinitrogen. Isotopic

tracer experiments are consistent with this picture (a 6-membered ring would also fit the isotopic data).



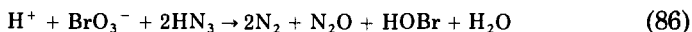
Manganese(III) also oxidizes azide to dinitrogen, and the mechanism set out in (82) to (85) has been proposed (52).



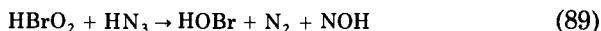
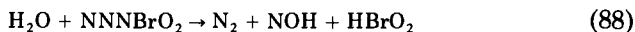
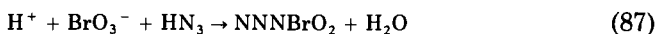
The same reaction has been studied by another group of workers, but with rather different results (215). It is claimed that the reaction is first order in [Mn(III)] rather than second order, and that there is no inhibition by Mn^{2+} . The oxidation of hydrazoic acid by cerium(IV) has also been studied (216), as has the oxidation by uranium(III) (1).

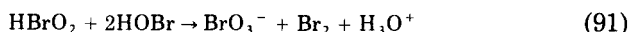
B. OXIDATION OF HYDRAZOIC ACID BY NONMETALLIC SPECIES

The oxidation of hydrazoic acid by bromate has been investigated by Thompson (201), who has shown that nitrous oxide is a product as well as dinitrogen. In the presence of an excess of azide the stoichiometry is given by (86).



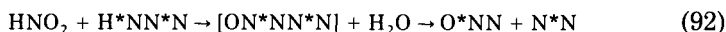
In addition, some bromine is produced. Tracer experiments with azide ion labeled with nitrogen-15 in the terminal positions gave nitrogen containing 50% of the label, and nitrous oxide with *both* nitrogen atoms labeled. The rate law was first order in $[H^+]$, $[BrO_3^-]$, and $[HN_3]$, and the proposed mechanism is set out in reactions (87)–(91)





This last reaction allows for the formation of bromine as a product. The rate equation can be rewritten in a form equivalent to $[\text{H}^+][\text{HBrO}_3][\text{N}_3^-]$, which fits attack by N_3^- upon BrO_2^+ , the latter being a species often postulated in reactions of bromic acid. For reaction with an excess of bromate over azide, a complex stoichiometry is observed with higher oxidation states of nitrogen being formed, and these have been attributed to the oxidation of nitroxyl.

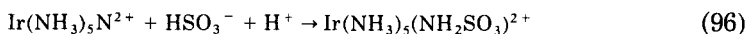
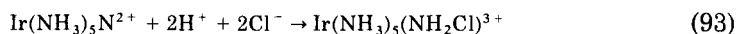
Another reaction that has been studied in detail is the oxidation of azide by nitrous acid. This work is relevant to some of the studies on coordinated azide mentioned below. Isotopic labeling experiments with nitrogen-15 indicate (45) that nitrosyl azide may be an intermediate, and this species can be isolated at low temperatures (131).



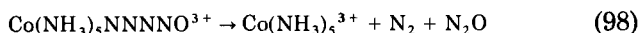
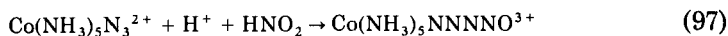
There are several kinetic investigations of the reaction of azide ion or hydrazoic acid with electrophilic nitrosating agents (38, 168, 184). The oxidation of hydrazoic acid by nitric acid has been briefly studied polarographically (137).

C. REACTIONS OF THE COORDINATED AZIDE ION

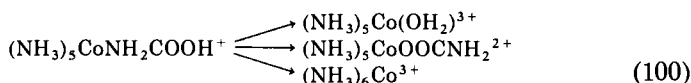
Some of the most interesting aspects of azide chemistry investigated in recent years deal with the reactions of coordinated azide ion. In acidic solution hydrolysis may occur by an acid-catalyzed mechanism, as is common for basic ligands. In other cases, however, a coordinated nitrene may be produced, as in the case of ruthenium(III) complexes (115), and iridium(III) complexes (126). These species can also be produced photochemically (160, 161). The reactions of the nitrene complex $\text{Ir}(\text{NH}_3)_5\text{N}^{2+}$ illustrate the interesting variety of behavior that can be observed (71, 212).



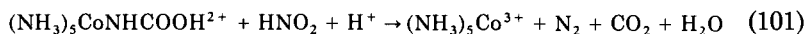
Another interesting class of reactions of coordinated azide are these occurring with nitrous acid. Haim and Taube used the reaction with $\text{Co}(\text{NH}_3)_5\text{N}_3^{2+}$ to generate the five-coordinate species $\text{Co}(\text{NH}_3)_5^{3+}$, taking advantage of the instability of nitrosyl azide (87).



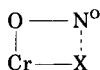
The same five coordinate intermediate has been generated again, using reactions of a coordinated cyanate ion (34).



In the presence of nitrous acid the deprotonated complex $(\text{NH}_3)_5\text{CoNHCOOH}^{2+}$ is nitrosated, and the product decomposes to liberate $(\text{NH}_3)_5\text{Co}^{3+}$



A number of other systems in which coordinated azide reacts with nitrous acid have been studied. However, in examining reactions of this sort it is important to consider other possibilities, apart from the obvious mechanism. Thus Moore and his co-workers (138, 139) have shown that nitrous acid can accelerate the aquation of $\text{Cr}(\text{H}_2\text{O})_5\text{X}^{2+}$, but not that of $\text{Cr}(\text{NH}_3)_5\text{X}^{2+}$, where $\text{X}^- = \text{Cl}^-$ or Br^- . The same acceleration is observed with *cis*- $\text{Cr}(\text{NH}_3)_4(\text{H}_2\text{O})\text{Cl}^{2+}$, but not with *trans*- $\text{Cr}(\text{NH}_3)_4(\text{H}_2\text{O})\text{Cl}^{2+}$. The effect is due to O-nitrosation in a position *cis* to the leaving group, with the possibility of neighboring group assistance because of an interaction between NO^+ and X^- . A similar effect can be seen in the hydrolysis of *cis*- $\text{Cr}(\text{NH}_3)_4(\text{ONO})(\text{NCS})^+$.

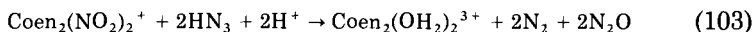


A distinction can be drawn upon kinetic grounds. In the reaction between $\text{Cr}(\text{H}_2\text{O})_5\text{N}_3^{2+}$ and nitrous acid, the rate law characteristic of electrophilic nitrosations was observed (202), [Eq (102)], whereas in

the systems studied by Moore a different dependence upon acidity is found:

$$\text{Rate} = k[\text{complex}][\text{HNO}_2](1 + K[\text{H}^+])^{-1} \quad (102)$$

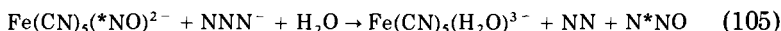
In addition to studying the attack of nitrite on coordinated azide, one can examine the attack of azide upon coordinated nitrosyl, nitrito, or nitro groups. Seel and Meyer have examined (171) the reaction of *cis*- and *trans*-Coen₂(NO₂)₂⁺ with hydrazoic acid.



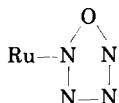
The rate law, (104), is consistent with the attack of azide ion upon a protonated NO₂⁻ ligand.

$$\text{Rate} = k[\text{Coen}_2(\text{NO}_2)_2^+][\text{HN}_3] \quad (104)$$

Swinehart *et al.*, (231) have examined the reaction of nitroprusside with azide ion at pH 6 by a tracer method, and the results are consistent with intermediacy of a nitrosyl azide species.



Not all systems react in this fashion. Feltham and Douglas (61) have examined the reaction of *trans*-RuCl(NO)(das)₂²⁺ with azide [das = *o*-phenylenebis(dimethylarsine)] using a nitrosyl group labeled with ¹⁵N. Approximately equal amounts of ¹⁴N¹⁴NO and ¹⁴N¹⁵NO were found, suggesting a cyclic intermediate:



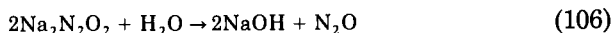
It is suggested that the N₄O unit is lost into the solution before it breaks down to N₂ + N₂O. This structure is reminiscent of the cyclic pentazoles observed in the reaction of azide ions with diazonium ions (236).

IX. Hyponitrous Acid and Nitroxyl

A. HYPONITROUS ACID

A detailed account of the chemistry of the hyponitrites can be found in a review by Hughes (101). Although there is evidence that the *cis*

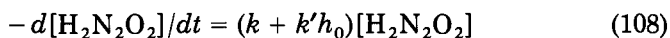
isomer of sodium hyponitrite can exist as a solid, instantaneous decomposition occurs on addition to water.



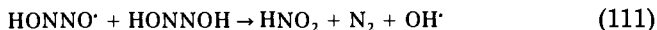
Tracer experiments on the distribution of ^{15}N between the two nitrogen atoms of nitrous oxide indicate that a symmetrical intermediate may be formed in the decomposition of $\text{ON}(\text{SO}_3^-)(\text{NO}^-)$ (see Section VII, C), and in the reaction between sodium nitrite and hydroxylamine hydrochloride at pH 7 *cis*-hyponitrous acid may be involved. The only stable species known in aqueous solution are derived from the *trans* isomer. The three conjugate acid-base species $\text{H}_2\text{N}_2\text{O}_2$, HN_2O_2^- , and $\text{N}_2\text{O}_2^{2-}$, are all known, the $\text{p}K_a$ values of hyponitrous acid being 7.2 and 11.5. Under normal conditions, pH 1–12, 25°C, decomposition occurs almost exclusively by the breakdown of the mono-anion.



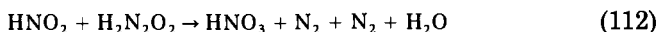
A plot of the rate of decomposition against pH shows a typical bell-shaped profile, with a flat maximum from pH 8 to 10, the variation of rate with pH being controlled by the acid-base equilibria between the three hyponitrite species (7, 32, 102, 157). In acidic solutions, pH 1, and at sufficiently high temperatures, two other pathways can be distinguished involving the dehydration of $\text{H}_2\text{N}_2\text{O}_2$ (32, 103).



Under some conditions erratic kinetics can be observed, due to the incursion of free-radical processes, which can be suppressed by the addition of ethanol. A variety of metal cations can cause oxidation of $\text{H}_2\text{N}_2\text{O}_2$ to $\text{HN}_2\text{O}_2^\cdot$ which cleaves to $\text{N}_2\text{O} + \text{OH}^\cdot$. A possible series of reactions that has been suggested is set out below:



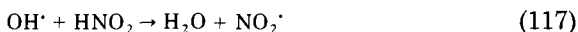
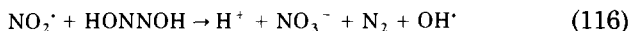
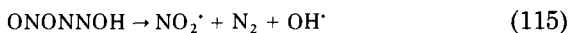
One of the products of the above scheme, nitrous acid, itself reacts further with hyponitrous acid, and shows a number of interesting features.



The reaction obeys a simple second-order rate law, which can readily be rearranged into the form characteristic of electrophilic attack by NO^+ upon the mono-anion HN_2O_2^- .

$$\text{Rate} = k_2[\text{HNO}_2][\text{H}_2\text{N}_2\text{O}_2] = (k_2/K_1)[\text{H}^+][\text{HNO}_2][\text{HN}_2\text{O}_2^-] \quad (113)$$

K_1 is the first dissociation constant of hyponitrous acid. This interpretation would suggest that nitrosyl hyponitrite, $\text{O}=\text{N}-\text{O}-\text{N}=\text{N}-\text{OH}$, is an intermediate from which the breakdown to $\text{NO}_2^+ + \text{N}_2 + \text{OH}^-$ could readily be envisaged. However, the value of k_2/K_1 is about 400 times greater than the expected rate of encounter between NO^+ and a singly charged anion (see Section XIII,B). It has been suggested (33) that a radical chain process is involved. The addition of 1.4% ethanol, a known hydroxyl radical trap, produces a decrease rate of a factor of 4.5. The likely mechanism is set out below, following Buchholz and Powell's original suggestion:



Powell and Buchholz suggest a minimum chain length of ca. 8, but in view of the factor of 400 mentioned above it seems likely that the chain length is much longer.

Measurements on this reaction have been extended to higher acidities, with interesting results. The rate increases with increasing perchloric acid concentration, reaches a maximum in 7 *M* acid, and then decreases sharply in those solutions where there is substantial conversion of molecular nitrous acid to the nitrosonium ion. When a correction for this last factor is introduced, the results fit Eq. (119).

$$-d[\text{H}_2\text{N}_2\text{O}_2]/dt = (k_2 + k_3h_0a_w)[\text{HNO}_2][\text{H}_2\text{N}_2\text{O}_2] \quad (119)$$

It thus appears that the nitrosonium ion is not the active species. Hughes and Wimbleton (104) suggest that the mechanism may involve nitric oxide in a radical pathway, and Buchholz and Powell earlier noted that nitric oxide is rapidly absorbed by a solution of hyponitrous acid in 1 *M* mineral acid.

B. NITROXYL

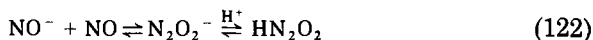
Nitroxyl is a species that is quite often postulated as an intermediate in reactions in which nitrous oxide is formed. It is sometimes written as the O-protonated species, and sometimes as the N-protonated form.



Sometimes hyponitrous acid is postulated as an additional intermediate (presumably the *cis* species). Angeli's Salt, $\text{Na}_2\text{N}_2\text{O}_3$ (see Section XIII), is a good source of nitroxyl, the kinetics of decomposition being well understood (28, 106).



Nitroxyl has been directly observed in pulse-radiolysis studies (79), when nitric oxide reacts with the solvated electron to produce NO^- , or with the hydrogen atom to form HNO; a $\text{p}K_a$ of 4.7 for HNO was reported. A variety of other species have been identified, resulting from further reactions of NO^- , and $\text{p}K_a$ values, equilibrium constants and rate constants have been evaluated.



In the presence of oxygen, the anion NO^- reacts readily to form peroxonitrite, which in acidic solution isomerizes to nitric acid (96, 143, 234).



A characteristic reaction, which can be used to show the formation of nitroxyl in solution, is the reaction with $\text{Ni}(\text{CN})_4^{2-}$ to form the violet complex $\text{Ni}(\text{CN})_3\text{NO}^{2-}$. Electrochemical studies of the cathodic reduction of nitrous acid in moderately concentrated perchloric acid indicate a rapid reaction between nitroxyl and nitrous acid to form nitric oxide and water (88a).

X. Nitramide

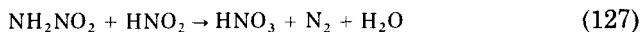
Nitramide, NH_2NO_2 , also known as nitroamine, is an isomer of hyponitrous acid, and it can also decompose to give nitrous oxide.

This reaction is one of the classic examples of general base catalysis, and there has been a recent investigation of the solvent isotope effect for the phenolate anion catalyzed decomposition (113). The isotope effect shows a maximum in the region $\Delta pK = 0$. The decomposition in acid media has not been studied so intensively, but previous work has now been extended up to 8.27 *M* perchloric acid. The results show a mild degree of acid catalysis.

$$\text{Rate} = k[\text{NH}_2\text{NO}_2] + k'[\text{NH}_2\text{NO}_2] h_0^{0.34} \quad (126)$$

This somewhat low dependence upon H_0 is interesting, and on the basis of Bunnett's w and w^* values it would appear that water may act as a nucleophile, though this does not fit in well with the value of ΔS^\ddagger . At this stage the details of the mechanism are not at all clear (133).

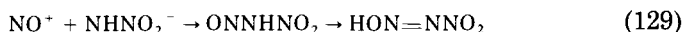
It is convenient at this point to consider another reaction of nitramide, that occurring with nitrous acid. The stoichiometry is similar to that of the analogous reaction (112) with isomeric hyponitrous acid.



The rate law is shown in Eq. (128).

$$\text{Rate} = (k_3 + k_4[\text{H}^+])[\text{NH}_2\text{NO}_2][\text{HNO}_2] \quad (128)$$

This is interpreted (108) as being due to parallel reaction pathways involving electrophilic nitrosation of nitramide (k_4) and its conjugate base (k_3).



Further fast steps are postulated to lead to the final products. It is interesting to note that the conjugate base species NHNO_2^- is a much stronger nucleophile toward the nitrosonium ion than is the iso-electronic nitrate ion, presumably because of the more nucleophilic nitrogen of the imide group. Evidence for reaction between nitrosyl thiocyanate and the conjugate base of nitramide has recently been obtained (104).

XI. Nitric Oxide

Nitric oxide is normally described as a neutral oxide, and it shows no exchange of oxygen atoms with ^{18}O -enriched water under acid or

alkaline conditions. Angeli's salt, $\text{Na}_2\text{N}_2\text{O}_3$, decomposes in acidic solution to liberate nitric oxide, and has been described (148) sometimes as the salt of an oxyacid of nitric oxide (see Section XII). Pulse radiolysis studies have shown that the nitrite ion reacts with the solvated electron to form NO_2^{2-} (79). In acid solutions HNO_2^- and H_2NO_2 are formed with $\text{p}K_a$ values of 7.7 and 5.7, respectively, and these species can decompose to liberate nitric oxide.



If one is to regard nitric oxide as an acid anhydride, H_2NO_2 rather than $\text{H}_2\text{N}_2\text{O}_3$ is to be looked on as the corresponding oxyacid.

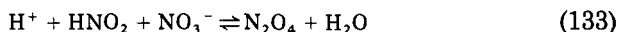
In the presence of nitrous acid, oxygen exchange between nitric oxide and water does occur. Bonner and Jordan have studied the isotope exchange reactions between ^{15}NO and potassium nitrite in H_2^{18}O , following the isotopic composition of the nitric oxide (26). Nitrogen exchange seems to occur by a single mechanism with rate law (131).

$$\text{Rate} = k[\text{HNO}_2][\text{NO}] \quad (131)$$

Thus in a solution of sodium nitrite the small amount of nitrous acid produced by hydrolysis is essential for exchange to occur. Although mechanisms that can be postulated to account for nitrogen exchange should also lead to oxygen exchange, the rate of oxygen exchange is *less* than that of nitrogen exchange at the higher pH values studied. This is a complex system because oxygen exchange between nitrite and water is very dependent upon pH; however, Bonner *et al.* find that the rates of oxygen exchange that they observe are much *greater* than is predicted from experiments on the exchange between nitrous acid and water. The authors tentatively propose a rate law (132) for oxygen exchange, but further work on this most interesting system seems desirable, in particular experiments using a nitrite-water system labeled with ^{18}O , and in isotopic equilibrium.

$$\text{Rate} = k[\text{H}^+][\text{HNO}_2][\text{NO}] \quad (132)$$

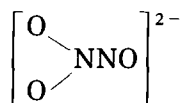
Bonner and Jordan (27) have also examined the exchange of ^{15}N and ^{18}O tracer between nitric oxide and dilute nitric acid (0.05–0.94 *M*). Nitrogen exchange appears to be controlled by the formation and hydrolysis of dinitrogen tetroxide.



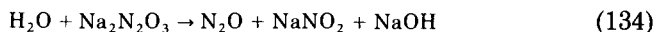
The exchange processes between NO , NO_2 , N_2O_3 , and N_2O_4 are known to be quite rapid (Section XIV). Other studies of related systems have been reported (10, 11).

XII. Trioxodinitrate(II)

Sodium trioxodinitrate(II), $\text{Na}_2\text{N}_2\text{O}_3$, also known as sodium oxyhyponitrite, sodium nitrohydroxylamate, sodium hyponitrate, or Angeli's salt is something of a chemical curiosity. It has the structure



with a nitrogen to nitrogen bond length of 0.1264 nm, suggesting a fair degree of double-bond character. In alkaline solution its decomposition yields the products shown in (134), whereas in acid media it decomposes to nitric oxide.



The changeover from one stoichiometry to the other seems to occur about pH 5. The $\text{p}K_a$ values for H_2NO_3 have been measured by potentiometric titration and are ca. 2.4 and 9.4. It is of interest as a source of nitroxyl and has been postulated as an intermediate in the nitrogen cycle. It is an awkward compound to work with, and it can be difficult to prepare really pure samples. In the presence of oxygen, oxidation to nitrite occurs, and samples can easily be contaminated with nitrite.

The chemistry has been much clarified by two independent kinetic studies by Bonner and Ravid (28) and by Hughes and Wimbledon (106). At pH values greater than 5, the two sets of results are in agreement, the reaction involving the monoanion as reactant, with fission of the nitrogen to nitrogen bond.

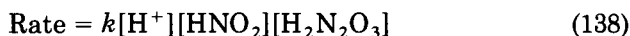


The doubly charged anion seems to be quite stable. In more acid media the behavior is complex, and there is some disagreement between the two investigations. The account below follows the work of Hughes and Wimbledon, which appears to be more extensive than that of Bonner and Ravid. Individual kinetic runs still give good first-order kinetics in Angeli's salt (k_1), and the rate increases sharply with increasing

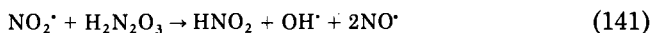
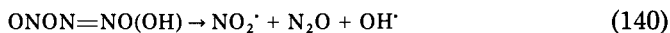
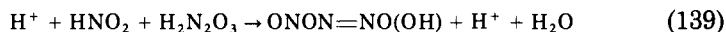
acidity below pH 3. However, the pseudo first-order rate constant increases markedly with increase in the initial concentration of Angeli's salt. This is attributed to the presence of an impurity that catalyzes the decomposition, and the most likely culprit is sodium nitrite. Added sodium nitrite certainly causes a marked acceleration in the rate of decomposition at low pH values. By extrapolating plots of k_1 against initial concentration of Angeli's salt to $[\text{Na}_2\text{N}_2\text{O}_3]_0 = 0$ it is possible to obtain limiting values of k_1 , free from the effects of the impurity. These limiting rate constants actually *decrease* with increasing acidity, in marked contrast to the raw k_1 values. Analysis of the data shows that the decrease in rate is due to protonation of HN_2O_3^- to H_2NO_3 , and yields a first $\text{p}K_a$ value of 3.0 for the latter species. This may be more accurate than values obtained by the more direct method of carrying out a pH titration of a solution of Angeli's salt with standard acid.

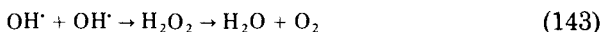
Experiments on the effect of added nitrite (the suspected catalytic impurity) reveal a complex pattern of behavior. At higher pH values, around 5, added nitrite stabilises Angeli's salt, and k_1 *decreases* to a limiting value at around $[\text{NO}_2^-] = 0.005\text{--}0.01\text{ M}$. This is presumably due to the reversal of the breakdown of HN_2O_3^- to NOH and NO_2^- . The fact that the kinetics remain first order with respect to Angeli's salt implies either that the formation of nitrous oxide is first order in nitroxyl concentration (possibly involving some reaction with water?) or that there is some molecular mechanism for the breakdown of HN_2O_3^- to $\frac{1}{2}\text{N}_2\text{O} + \text{NO}_2^-$. Further work is needed on this point (105).

In sufficiently acidic media, where the decomposition products are 100% nitric oxide, the rate law is given by (138).

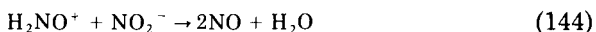


Although this equation has the characteristic kinetic form for an electrophilic nitrosation reaction, the magnitude of the rate constant is much greater than the normal limiting value for such processes (the encounter limit). Reaction is inhibited by added ethanol, a known trap for hydroxyl radicals, and Hughes and Wimbledon suggest a chain mechanism for the decomposition.





A different mechanism for the decomposition to nitric oxide in acidic media has been proposed by Bonner (28). He suggests that there may be a rapid decomposition reaction of $\text{H}_2\text{N}_2\text{O}_3$, followed by another rapid redox reaction such as (144), where H_2NO^+ is protonated nitroxyl.



Attempts to distinguish between this proposal, and that of Hughes and Wimbeldon by using ^{15}N enriched nitrite have not yielded any firm conclusion, partly because of complications due to the formation of nitric oxide by the spontaneous decomposition of nitrous acid. It is clear, however, that although the decomposition of Angeli's salt in acidic solutions yields nitric oxide, the reaction is *not* a dehydration of $\text{H}_2\text{N}_2\text{O}_3$.

XIII. Nitrous Acid

The chemistry of nitrous acid is one of those areas where there has been a particularly fruitful interaction between physical-organic and physical-inorganic chemistry. Most of the common electrophilic nitrosating agents are inorganic species, and the mechanisms by which they are formed in aqueous solutions were largely worked out from studies of diazotization and deamination. Ideas from these studies have proved applicable to many inorganic systems, and a few of the main features are outlined below. Diazotization and deamination have been reviewed by Ridd (162), and Turney and Wright (207) have reviewed nitrosation reactions.

A. SPECIES PRESENT IN SOLUTIONS OF NITROUS ACID

It is useful to consider first the species present in aqueous solutions of "nitrous acid". It is a weak acid, $\text{p}K_a = 3.3$ at 25° , and in sufficiently concentrated solutions (ca. 0.05 – $0.1\text{ }M$) in moderately concentrated mineral acid ($4\text{ }M$) will dehydrate to the anhydride dinitrogen trioxide.

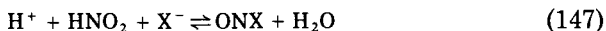


This is a blue species with a maximum at 625 nm, and from measurements of the absorbance at this wavelength an approximate equilibrium constant $[\text{N}_2\text{O}_3]/[\text{HNO}_2]^2 = 0.2 \text{ M}^{-1}$ at 20° has been estimated (37). Other spectrophotometric and distribution measurements lead to similar results, and Turney (206) has proposed a mean value of 0.2 M^{-1} . Schmid and Krenmayr (165) propose a slightly lower value of 0.16 M^{-1} . Another approach to estimating this equilibrium constant is to combine a value of 530 sec^{-1} for the first-order rate constant for the hydrolysis of N_2O_3 at 20° (80) with a value for the rate of formation of N_2O_3 from 2HNO_2 of $4 \text{ M}^{-1} \text{ sec}^{-1}$ at 20° , giving $[\text{N}_2\text{O}_3]/[\text{HNO}_2]^2 = 7.5 \times 10^{-3} \text{ M}^{-1}$. The source of the somewhat large discrepancy between these two values is not clear. The extinction coefficient for N_2O_3 used in the original publication (37) is some 5 to 10 times lower than values measured recently for solutions of dinitrogen trioxide in a range of organic solvents (176), but the distribution experiments also gave results close to 0.2. Calculations based on a thermodynamic cycle gave a value 0.0089 M^{-1} for 25° (208).

At higher concentrations of mineral acid, ionization to the nitrosonium ion occurs, and this can be quantitative in sufficiently acidic solutions.



The equilibrium has been studied spectrophotometrically and has been shown to follow the H_{R} acidity function (59) over at least a limited range of acidity. A range of values for the $\text{p}K_{\text{a}}$ have been reported from -6.5 to -8.5 (182). A great deal of effort has been devoted to looking for evidence for the nitrous-acidium ion, H_2NO_2^+ , but so far no firm evidence for the existence of sizable concentrations of this species has been found. In the presence of other anions the corresponding nitrosyl compounds may be formed



These often have characteristic colors, and the equilibrium constants have been measured spectrophotometrically.

B. ELECTROPHILIC NITROSATIONS

Many reactions of nitrous acid involve an electrophilic nitrosation in the initial stages, and the common nitrosating agents in order of

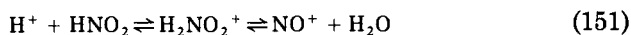
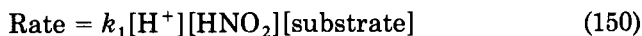
$$d[\text{ONX}]/dt = k[\text{H}^+][\text{HNO}_2][\text{X}^-] \quad (148)$$
$$\text{ONX} + \text{ArNH}_2 \rightarrow \text{ArNH}_2\text{NO}^+ + \text{X}^- \quad (149)$$

$X^- =$	Cl^-	Br^-	I^-	SCN^-	NO_2^-	CH_3COO^-	N_3^-	NO_3^-	$NH_2SO_3^-$
k	975	1170	1370	1460	1893	2000	2340	0.0018	170
$10^4 K$	5.5	220	—	46000	570	—	—	0.000026	—

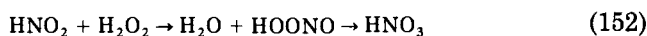
$d[XNO]/dt = k[H^+][HNO_2][X^-]$; $K = [ONX]x_w/[H^+][HNO_2][X^-]$

These bimolecular rate constants are found to be greater than $10^9 M^{-1} \text{ sec}^{-1}$, indicating an encounter-controlled process. It seems certain that the reason for the narrow spread in reactivities among the anions, and among the neutral nucleophiles, is that in each case we are observing an encounter-controlled reaction. The somewhat greater reactivity of the anions than the neutral species reflects the effect of coulombic attraction on the encounter rate. Less reactive nitrosating agents, such as ONSCN , ONNO_2 , do not in general react at the encounter rate.

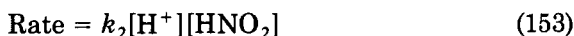
For many years there was a dispute in the literature as to whether the active nitrosating species in dilute aqueous solutions of nitrous acid, and responsible for Eq. (150), was the nitrous-acidium ion or an equilibrium concentration of the nitrosonium ion NO^+ .



Provided that the equilibria were established rapidly, either reagent could give rise to Eq. (150). Anbar and Taube (3) produced evidence that the nitrosonium ion was the active species by a kinetic and isotopic study of the reaction with hydrogen peroxide.



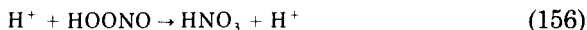
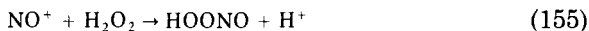
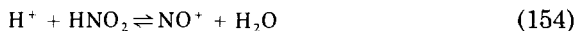
At high concentrations of hydrogen peroxide they claimed to observe a rate law of form (153), corresponding to a rate-determining formation of the nitrosonium ion.



Similar rate laws have been observed in the reaction of azide with nitrite (169) and sulfite with nitrite (170). Their case was strengthened by an ^{18}O tracer study, which indicated that at high concentrations of hydrogen peroxide exchange of the tracer into nitrous acid was inhibited, presumably because of competition between hydrogen peroxide and water for the same electrophile. This view was vigorously disputed (91), but a recent study of the reaction by the stopped-flow method by Moore and Benton (143) provides strong support for Anbar and Taube's original interpretation.

Benton and Moore worked in perchloric acid solution, and so avoided possible complications due to nucleophilic buffer anions, and they

followed the formation of the initial product, pernitrous acid, over the concentration range in which a switch in rate-determining stage took place from (155) to the forward reaction of (154)



Their rate law is shown in (157), and has the required kinetic form.

$$d[\text{HOONO}]/dt = k_3[\text{H}^+][\text{HNO}_2][\text{H}_2\text{O}_2](1 + k_4[\text{H}_2\text{O}_2])^{-1} \quad (157)$$

The limiting rate for high concentrations of hydrogen peroxide agreed with Anbar and Taube's value. At 0°C it is given in (158).

$$\text{Rate} = 637[\text{H}^+][\text{HNO}_2] \text{ } M \text{ sec}^{-1} \quad (158)$$

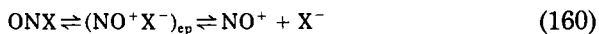
One problem with this result is that the rate is about 3-fold faster than the measured rate of oxygen exchange between nitrous acid and water at 0°, which has the same kinetic dependence (37) upon $[\text{H}^+]$ and $[\text{HNO}_2]$. Ridd has pointed out (163) that the average lifetime of a nitrosonium ion in water must be very short, ($t_{1/2} \approx 3 \times 10^{-10}$ sec) and that such a short-lived species might stand a good chance of reacting with the same water molecule on rehydration that it lost in the dehydration stage. This is an interesting idea, because it has been always assumed that the water exchange rate gives a good value for the rate of dehydration of the oxyacid. In aromatic nitration it has been shown that the rate of oxygen exchange between nitric acid and water is equal to the rate of the zero-order nitration of reactive aromatic substrates in aqueous nitric acid, and this has been used as evidence that the nitrating agent in such media is NO_2^+ , not H_2NO_3^+ . However, the average half-lifetime for the nitronium ion in 68% w/w H_2SO_4 is ca 10^{-6} sec, so long that the water molecule lost from H_2NO_3^+ upon dehydration will be "lost" in the solvent. Hence the oxygen exchange rate should be a good measure of the rate of formation and rehydration of the nitronium ion. However, for much shorter-lived electrophiles such as NO^+ , it appears that this may not be true. To round off this argument, we may note that if the $\text{p}K_a$ for (154) is taken to be -6.5 , then taking the experimentally determined rate constants for (148), it is found (163)

that the bimolecular rate constant for (159) are ca. $7 \times 10^9 M^{-1} \text{sec}^{-1}$ at 0° , very close to the encounter rate.

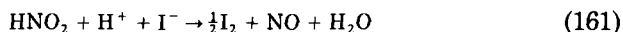


This topic has been discussed at some length partly because of its intrinsic interest, partly because it represents an interesting interface between physical organic and physical inorganic chemistry, and also partly because reactions of nitrous acid with a variety of other nitrogen-containing substrates involve similar processes.

We may also note that if the nitrosyl compounds ONX are formed by a reaction between NO^+ and X^- , then the principle of microscopic reversibility requires that the hydrolysis should proceed by dissociation to $\text{NO}^+ + \text{X}^-$, followed by reaction with water. Because in many cases the anion X^- will be a much better nucleophile than a water molecule, it is likely that the hydrolysis of nitrosyl halides involve the formation of an encounter pair, $(\text{NO}^+ \text{X}^-)_{\text{ep}}$, in a solvent cage, which usually recombines to form ONX, but undergoes hydrolysis following the diffusion apart of its constituents.

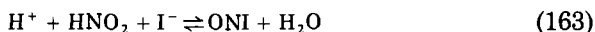


We will now consider the reactions of nitrous acid with a variety of inorganic species. These all appear to involve the initial formation of a nitrosyl compound, although the fate that this species undergoes varies widely. Starting with simple nucleophiles, we will consider the oxidation of iodide to iodine.



The rate equation has been established by Indelli and his co-workers (72) to be (162), and the interpretation is set out in reactions (163) and (164):

$$\text{Rate} = k_5[\text{H}^+]^2[\text{HNO}_2]^2[\text{I}^-]^2 \quad (162)$$



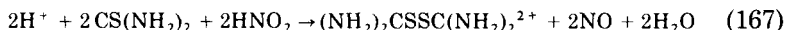
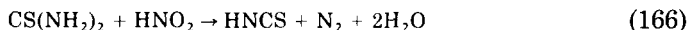
This is the reverse of the familiar mechanism for the termolecular reaction in the gas phase between nitric oxide and chlorine or bromine

to form the nitrosyl halide. Beck and his co-workers report in the rate law an additional term which is ascribed to reaction (165), followed by a rapid oxidation of I_2^- (62).

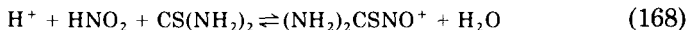


The oxidation of thiocyanate by nitrous acid to nitric oxide, sulfuric acid, and hydrogen cyanide probably involves nitrosyl thiocyanate as an intermediate. This is readily detected in solutions by its red color, and decomposition to nitric oxide and thiocyanogen could occur by a mechanism(s) similar to that for nitrosyl iodide. The hydrolysis of thiocyanogen is known to form sulfuric acid and hydrogen cyanide. However, a mechanistic study has not been reported yet. The reaction between azide ion and nitrous acid, which fits the same general pattern, was discussed in Section VIII,B. A preliminary account of the thermal decomposition of nitrosyl cyanide has appeared (110).

Some work that has analogies to the nitrous acid-iodide system is a recent kinetic study of the reaction between nitrous acid and thiourea. This system was originally examined by Werner (217), who showed that there were two reactions (166) and (167), the former favored by low acidities, and the latter by high acidities.



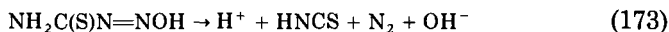
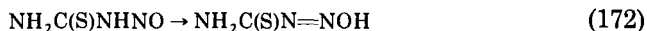
Werner also reported a transient red color in his reaction mixtures, and this has recently been identified (2) as due to $(NH_2)_2CSNO^+$. This is formed by an encounter-controlled electrophilic nitrosation of the type described above, with the usual rate law. Values for the equilibrium constant, and the rate constants for the forward and back reactions have been obtained, together with extinction coefficients for the visible and UV maxima for the S-nitroso compound.



A kinetic study of (166) shows the rate law to be given by (169).

$$d[HNCS]/dt = k_6[HNO_2][CS(NH_2)_2] \quad (169)$$

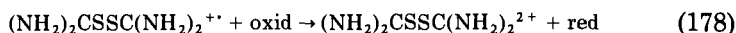
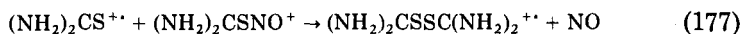
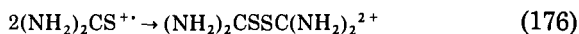
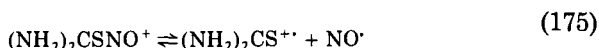
This is interpreted as a rate-determining nitrosyl migration from sulfur to nitrogen in the conjugate base of the S-nitroso compound.



Steps (172) and (173) are very similar to those postulated in the deamination of organic primary amino compounds.

The other reaction that Werner observed has been examined in oxygen free solutions, with a large excess of thiourea over nitrite, under conditions such that virtually all the nitrite is converted to $(\text{NH}_2)_2\text{CSNO}^+$. Reaction was followed by the fading of the yellow color, and individual runs gave reasonable pseudo-second-order plots, suggesting a mechanism analogous to (164). However, a comparison of initial rates of reaction yielded a quite different rate law, and a radical cation mechanism may be operative (48)

$$\text{Rate} = [(\text{NH}_2)_2\text{CSNO}^+](k + k'[(\text{CS}(\text{NH}_2)_2)_2]) \quad (174)$$



Similar studies on the formation of sulfur S-nitroso compounds of the alkylthioureas have appeared (49). Further work on these compounds is desirable in view of the possible biological significance of sulfur-nitroso compounds (141). Werner's intermediate, $(\text{NH}_2)_2\text{CSNO}^+$, can also act as an electrophilic nitrosating agent, and Williams has shown (222) that its behavior is very similar to that of another sulfur-nitroso compound, ONSCN .

Another sulfur nucleophile, the thiosulfate anion, reacts with nitrous acid to form a yellow species, which appears to be O_3SSNO^- . A preliminary study of the thiosulfate-nitrite reaction was published many years ago by Edwards, who reported (68) a rate equation that was almost zero order in thiosulfate (179):

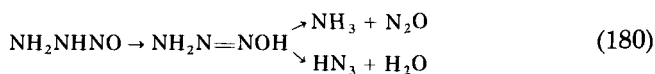
$$\text{Rate} = k[\text{H}^+]^2[\text{NO}_2^-][\text{S}_2\text{O}_3^{2-}]^{0.2} \quad (179)$$

a form that is very similar to that observed by Anbar and Taube, and by Moore and Benton. A stopped-flow study of the formation of the yellow species also shows (74) the existence of a term that is second order in nitrite and zero order in thiosulfate, indicating that the yellow species may also be formed from $\text{S}_2\text{O}_3^{2-}$ and N_2O_3 .

Interest in the chemistry of nitrous acid often arises from the need to remove the last traces from a particular system because it catalyzes some undesirable process [e.g., in nuclear fuel reprocessing where there can be autocatalytic reoxidation of plutonium(III) to plutonium(IV) in the presence of traces of nitrite (65)]. There have been studies of the efficiency of various inorganic scavengers of nitrous acid in moderately concentrated solutions of mineral acid (24, 154).

Williams has determined (224) the relative reactivities of sulfamic acid, hydrazine, hydroxylamine, hydrazoic acid, and urea by a kinetic and product study of the Fischer-Hepp rearrangement of *N*-nitroso-*N*-alkylanilines in the presence of nitrite traps (224). The interpretation of such experiments requires caution, because the dependence of rate upon acidity varies widely from one scavenging agent to another, and unless comparisons are made at the same acidity erroneous conclusions may be drawn (154). Another complication is the possible catalytic effect of nucleophilic anions. When allowance is made for these factors there is good agreement between the relative reactivities determined from the Fischer-Hepp studies and those determined directly. Williams has also used his method to determine the reactivities of nitrosyl chloride and nitrosyl thiocyanate as electrophilic nitrosating agents (223).

A detailed study of the reaction of the scavenger hydrazine with nitrous acid has been published (153). This again involves an initial encounter-controlled nitrosation of the hydrazinium ion, and parallel pathways to form hydrazoic acid + water, or ammonia + nitrous oxide are proposed, which are represented in a simplified form in (180).



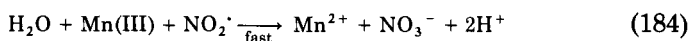
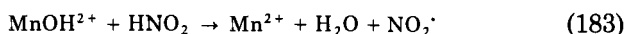
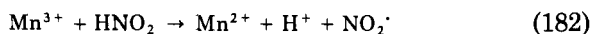
At high acidities the products are 100% hydrazoic acid, while at low acidities a limiting yield of 40% of azide is obtained. This mechanism has many analogies to the processes thought to occur in the reactions of nitrosating agents with organic amino compounds. It is very different to the mechanisms usually put forward for oxidation of hydrazine by inorganic reagents, in which diimide and tetrazene intermediates feature. One such mechanism has been proposed, largely on the basis of a reported stoichiometry (12) shown in equation (181).



However, it has been argued that reaction is so fast that mixing effects and complications due to secondary reactions of the primary product (153), were responsible for the unusual stoichiometries reported. Application of a new fast reaction method indicates the formation of a transient species absorbing at 370 nm under some conditions, but no structure or mechanism has yet been proposed (117). Measurements have also been made of the kinetics of nitrosation of some alkyl and arylhydrazines (152, 186).

C. OXIDATION OF NITRITE BY METAL IONS AND METAL COMPLEXES

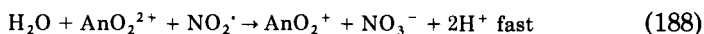
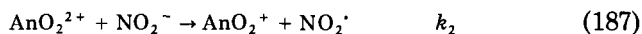
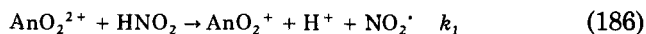
The reactions discussed above all appear to involve an electrophilic nitrosation as the first stage. Other pathways are also possible. Thus the oxidation of nitrous acid by manganese(III) involves the oxidation to nitrogen dioxide (54)



Similar behavior was found for the oxidation of nitrous acid by cobalt(III) (53). Hexacyanoferrate(III) reacts in a similar way to (182) (187). Interest in the redox reactions of the actinides with nitric and nitrous acids continues. The rate law observed for neptunium(VI) and americium(VI) is shown in (185), where An = Actinide.

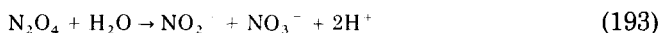
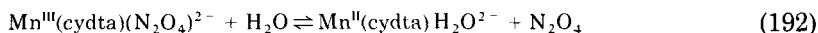
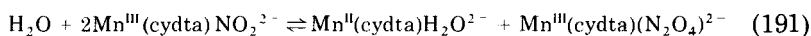
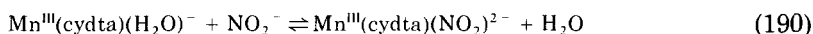
$$\text{Rate} = [\text{AnO}_2^{+}][\text{HNO}_2](k_1 + k_2[\text{H}^+]^{-1}) \quad (185)$$

Again a rate law with a term containing a dependence upon $[\text{H}^+]^{-1}$ is observed, as for manganese(III) and cobalt(III). This is interpreted as a pathway involving the nitrite ion as a reducing agent (232).



The oxidation of nitrite ion by 1,2-diaminocyclohexanetetraacetato-manganate(III), $[\text{Mn(III)(cydta)}]^-$, gives a rate law with a second-order dependence upon nitrite concentration in the pH range where nitrite ion is the bulk component (pH 4.5–7.5). The mechanism proposed (114) is set out in (189)–(193).

$$-d[\text{Mn}^{\text{III}}(\text{cydta})^-]/dt = k_3[\text{Mn}^{\text{III}}(\text{cydta})^-]^2[\text{NO}_2^-]^2(k_4[\text{Mn}^{\text{II}}(\text{cydta})^{2-}]^2 + [\text{Mn}^{\text{III}}(\text{cydta})^{2-}]^{-1} \quad (189)$$



Oxidation of nitrite by another powerful oxidizing agent, thallium(III), has been studied by Gupta (200). He suggests the formation of complexes of the form TlNO_2^{2+} , $\text{Tl}(\text{NO}_2)_2^+$, and $\text{Tl}(\text{NO}_2)_3$, and reaction occurring by an internal redox reaction in the dinitro species.

The mechanism of oxidation of nitrous acid by another familiar reagent, potassium permanganate, has been studied by two groups of workers. Beck and Dòzsa originally postulated (63) a rate law containing terms that were first order, second order, and third order in nitrous acid, but a reinvestigation with the aid of stopped-flow techniques has led to a modified rate equation (64).

$$-d[\text{MnO}_4^-]/dt = k_5[\text{HNO}_2] + k_6k_7[\text{HNO}_2]^2[\text{Mn(VII)}](k_7[\text{Mn(VII)}] + k_6K[\text{H}^+][\text{HNO}_2])^{-1} \quad (194)$$

Beck suggests that there is a sizable amount of nitrosyl permanganate species formed, O_3MnONO , and he obtains a value for the equilibrium constant $K = [\text{O}_3\text{MnONO}]/[\text{H}^+][\text{HNO}_2][\text{MnO}_4^-]$ by means of an analysis of his kinetic data. This species is thought to be *inert* to redox reaction, and thus reduces the active concentration of nitrous acid and permanganate. It would be desirable to obtain direct spectrophotometric evidence for this species.

An independent investigation by Hughes and Shrimanker (177) also using stopped-flow spectrophotometry is generally consistent with (194) although the kinetics are expressed in a less explicit form (195):

$$-d[\text{MnO}_4^-]/dt = k_8[\text{HNO}_2]^{1.6} \quad (195)$$

On decreasing the permanganate concentration the order in $[\text{MnO}_4^-]$ increases from 0 to ca. 0.5. Both groups of authors propose a mechanism that involves a rate-determining formation of dinitrogen trioxide, which is rapidly trapped by some permanganate species. This seems very plausible, but unfortunately does not give information about the details of the mechanism. We have, in fact, returned to a mechanism where the initial stage is an electrophilic nitrosation process. These studies have been made by following the decrease in absorbance due to the permanganate ion. Although the normal reduction product of the oxidizing agent is manganese(II), Beck states that manganese(IV) accumulates in the reaction solution. However, the stoichiometry for reaction in acetate buffers at pH 3.5 (177) is definitely the expected value $\text{NaNO}_2:\text{KMnO}_4::5:2$. A complex rate law is also found for the oxidation of nitrous acid by chromium(VI). Nitrite esters of chromic acid are proposed as intermediates (66).

D. OXIDATION OF NITROUS ACID BY THE HALOGENS

The kinetics of oxidation of nitrite to nitrate by halogens or related species follow reasonably simple kinetics in alkaline media. In a study of hypochlorite oxidation, the results fit Eq. (196), and a mechanism involving nitryl chloride is proposed (40).

$$-d[\text{ClO}^-]/dt = (k_1 + k_2[\text{NO}_2^-])[\text{ClO}^-][\text{NO}_2^-][\text{OH}^-] \quad (196)$$

In more acid media some very complex rate laws can be obtained, as is shown below (151).

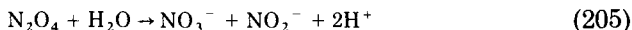
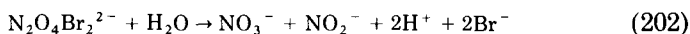
$$-d[\text{Cl}_2]/dt = (k_3 + k_4[\text{HNO}_2])[\text{Cl}_2][\text{NO}_2^-][\text{Cl}^-]^{-2} \quad \text{pH } 0-1 \quad (197)$$

$$-d[\text{Br}_2]/dt = (k_5 + k_6[\text{Br}^-]^{-1})[\text{Br}_2][\text{NO}_2^-]^2 \quad \text{pH } 4.2-5.8 \quad (198)$$

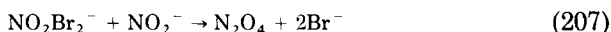
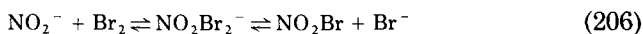
$$\begin{aligned} -d[\text{Br}_2]/dt = & [\text{Br}_2][\text{HNO}_2]^2(k_7 + k_8[\text{Br}^-]^{-1}) \\ & \times (1 + k_9[\text{H}^+][\text{Br}_2])^{-1} \quad \text{pH } 0.8-2.5 \end{aligned} \quad (199)$$

Several unusual intermediates have been postulated. For the reaction with bromine, pH 4.2–5.8, (200)–(202) is proposed as a mechanism for the first term (k_5) while (203)–(205) is suggested for the second (k_6).





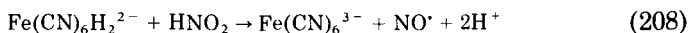
An alternative explanation of the k_5 term in (198) is an attack by NO_2^- on a species NO_2Br_2^- .



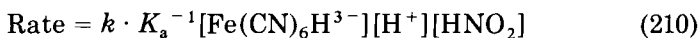
This is rejected on the grounds that at lower pH values a mechanism involving a double nitrite species, possibly N_2O_3 , is involved. This does not seem a conclusive argument; to the writer, (206)–(207) seems preferable to (200)–(202). The authors also discuss earlier studies on the oxidation of nitrite by iodine (67).

E. REDUCTION OF NITROUS ACID BY METAL IONS AND METAL COMPLEXES

Only a few of these reactions have been studied. The reduction by hexacyanoferrate(II) gives simple second-order kinetics, independent of acidity.



Such a rate law can be rearranged to a form consistent with nucleophilic attack upon the nitrosonium ion, substituting from the ionization constant $K_a = [\text{H}^+][\text{Fe}(\text{CN})_6\text{H}^{3-}]/[\text{Fe}(\text{CN})_6\text{H}_2^{2-}]$.

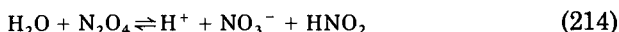


The value of $k \cdot K_a^{-1}$ at 25° and 1 *M* ionic strength is 55,000 $M^{-2} \text{sec}^{-1}$, close to the figure expected for an encounter-controlled reaction between NO^+ and $\text{Fe}(\text{CN})_6\text{H}^{3-}$ (187). Two other systems of interest,

the reduction of nitrous acid by chromium(II) and by molybdenum(V), are discussed in Section XV together with the corresponding reactions of nitric acid. The cathodic reduction of HNO_2 has been studied (88a).

XIV. Dinitrogen Tetroxide and Nitrogen Dioxide

Dinitrogen tetroxide is the mixed anhydride of nitric and nitrous acid, and it plays a vital role in a range of reactions in which nitric acid acts as an oxidizing agent. It is convenient at this point to summarize the main facts in its aqueous chemistry. The foundation for a great deal of the chemistry of the nitric acid/nitrous acid system is to be found in the classic studies of the formation and decomposition reactions of nitrous acid carried out by Abel and his co-workers. These have been summarized by Bray (30).



The rate-determining step is stage (214), and Abel obtained rate constants for the formation of dinitrogen tetroxide.

$$d[\text{N}_2\text{O}_4]/dt = k[\text{H}^+][\text{HNO}_2][\text{NO}_3^-] \quad (215)$$

Although this is the same form of rate law as that observed for the formation of other nitrosyl compounds, the reactivity of the nitrate ion is many orders of magnitude *less* than that of azide, nitrite, chloride ion, etc. Abel's value for k is consistent with other values for the same reaction, such as that obtained from the nitrite-catalyzed exchange of oxygen atoms between nitric acid and water (35), and of the nitrite-catalyzed oxidation of thiocyanic acid by nitric acid (100). Both these studies involve a rate-determining formation of dinitrogen tetroxide, as in (214). More recently rate constants have become available for the forward and back reactions of all stages; the data are set out in Table III. Many of these data are due to pulse-radiolysis studies (80, 81). It should be noted that there are quite different values in the literature for some of these quantities, e.g., for the recombination of nitrogen

TABLE III
 RATE CONSTANTS FOR THE STEPS IN DECOMPOSITION OF NITROUS ACID AT 20°

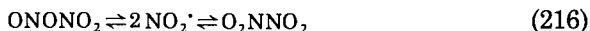
Reaction	Rate/ $M \text{ sec}^{-1}$	References
$2\text{HNO}_2 \rightarrow \text{N}_2\text{O}_3 + \text{H}_2\text{O}$	$4 [\text{HNO}_2]^{2a}$	(36, 163)
$\text{H}_2\text{O} + \text{N}_2\text{O}_3 \rightarrow 2\text{HNO}_2$	$5.3 \times 10^2 [\text{N}_2\text{O}_3]^a$	(80)
$\text{N}_2\text{O}_3 \rightarrow \text{NO} + \text{NO}_2$	$8 \times 10^4 [\text{N}_2\text{O}_3]^a$	(80)
$\text{NO} + \text{NO}_2 \rightarrow \text{N}_2\text{O}_3$	$1.1 \times 10^9 [\text{NO}][\text{NO}_2]^a$	(80)
$\text{N}_2\text{O}_4 \rightarrow 2\text{NO}_2$	$6.9 \times 10^3 [\text{N}_2\text{O}_4]^a$	(81)
$\text{NO}_2 + \text{NO}_2 \rightarrow \text{N}_2\text{O}_4$	$9 \times 10^8 [\text{NO}_2]^{2a}$	(81)
$\text{H}^+ + \text{HNO}_2 + \text{NO}_3^- \rightarrow \text{N}_2\text{O}_4 + \text{H}_2\text{O}$	$1.7 \times 10^{-2} [\text{H}^+][\text{HNO}_2][\text{NO}_3^-]^b$	(30)
$\text{H}_2\text{O} + \text{N}_2\text{O}_4 \rightarrow \text{H}^+ + \text{HNO}_2 + \text{NO}_3^-$	$1 \times 10^3 [\text{N}_2\text{O}_4]^b$	(81)

^a Using E_a of 13 kcal mol⁻¹.^b Using E_a of 17.2 kcal mol⁻¹.

dioxide to dinitrogen tetroxide (51, 147). The equilibrium constant for reaction (4), $[\text{N}_2\text{O}_4]/[\text{H}^+][\text{HNO}_2][\text{NO}_3^-]$, can be calculated from the rate constant for the back reaction obtained by Abel, and that for the forward reaction obtained by Henglein (81). At 20° this is $1.66 \times 10^{-5} M^{-2}$, in good agreement with a figure of $2.6 \times 10^{-5} M^{-2}$ obtained by Maschka (136) by spectrophotometric methods. Other spectrophotometric measurements of the percentage conversion of nitrite to dinitrogen tetroxide in concentrated nitric acid solution have been reported (130), and are consistent with this picture. It is of interest to calculate what degree of dissociation one might expect under typical conditions. If one takes a solution of 0.001 M total nitrite in 8.6 M nitric acid (for which spectrophotometric results suggest a lower limit of about 10% conversion of nitrite to $\text{N}_2\text{O}_4 + 2\text{NO}_2^*$), then a simple calculation suggests that it might contain $8.2 \times 10^{-5} M$ of N_2O_4 and $3.54 \times 10^{-5} M$ of NO_2^* . Clearly the dissociation may be greater at lower concentrations of nitrite and nitric acid, and vice versa. It might have been thought that with degrees of dissociation as large as these, deviations might be observed in the Beer-Lambert law plots of absorbance against [nitrite] at wavelengths in the range 350–400 nm (where HNO_2 , NO_2^* , and N_2O_4 all absorb). However, such plots have been found to be linear (37).

The discussion so far has ignored the problem of the mechanism of the hydrolysis reaction. Dinitrogen tetroxide has the symmetrical structure O_2NNO_2 (82), the rate law for its formation (215) leads one to expect that ONONO_2 will be formed from NO^+ and NO_3^- and the principle of microscopic reversibility requires that the hydrolysis reactions involve the same species. It has long been recognized that

liquid dinitrogen tetroxide reacts as NO^+NO_3^- . The symmetrical form might be obtained from the unsymmetrical species by homolytic dissociation and recombination.



The low rate of formation of dinitrogen tetroxide may be due to low nucleophilic reactivity of the nitrate ion, or to the fact that ONONO_2 dissociates heterolytically much more readily than it does homolytically.

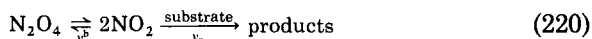
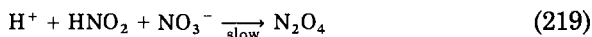
Anbar and Taube (4) attempted to examine the problem directly by allowing dinitrogen tetroxide + nitrogen dioxide vapor to bubble through alkaline ^{18}O enriched water. This sort of experiment is very difficult, because of the possibility of adventitious exchange due to high local concentrations of acid, nitrite, etc. At low nitrogen oxide concentrations the results indicated that all three oxygens in the nitrite were derived from the dinitrogen tetroxide as required for reaction of NO^+ with NO_3^- . However, in many other experiments they obtained results indicating that only two of the oxygens were so derived; this would appear to suggest a reaction of $\text{NO}_2^{\delta+}\text{NO}_2^{\delta-}$.

A distinction between mechanisms involving N_2O_4 as active species, and those involving NO_2 is readily made upon kinetic grounds. For a rate-determining attack by N_2O_4 on a substrate the rate law should take the form of (217), whereas for attack by NO_2 Eq. (218) would be expected.

$$\text{Rate} = k[\text{H}^+][\text{HNO}_2][\text{NO}_3^-][\text{substrate}] \quad (217)$$

$$\text{Rate} = k[\text{H}^+]^{1/2}[\text{HNO}_2]^{1/2}[\text{NO}_3^-]^{1/2}[\text{substrate}] \quad (218)$$

The distinction between the two cases when there is a rate-determining formation of dinitrogen tetroxide is not so clear cut, because the possibility of rapid dissociation to NO_2^* and capture by the substrate (i.e., $v_a \gg v_b$) would also yield (215)



Thus in the oxidation of thiocyanic acid by nitric and nitrous acids, the active species is established (100) as N_2O_4 by observing (221) at high values of $[\text{H}^+][\text{SCN}^-]$, and (222) at low $[\text{H}^+][\text{SCN}^-]$.

$$\text{Rate} = k[\text{H}^+][\text{HNO}_2][\text{NO}_3^-] \quad (221)$$

$$\text{Rate} = k[\text{H}^+]^2[\text{HNO}_2][\text{NO}_3^-][\text{SCN}^-] \quad (222)$$

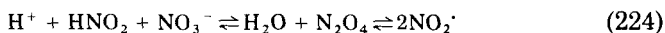
Sometimes conflicting evidence is obtained, as in the technologically important oxidation of plutonium(III) to plutonium(IV). Dukes has produced (65) a rate law implicating N_2O_4 as the species reacting with plutonium(III), whereas Koltunov and Marchenko find nitrogen dioxide as the active species (119). Koltunov has also suggested a similar interpretation for the kinetics of oxidation of uranium(IV) and neptunium(V) by nitric and nitrous acids. The existence of good values for the rate constants for the forward and back reactions of (213) should be valuable when considering the mechanism of the process involving nitrogen(IV) oxides as catalysts.

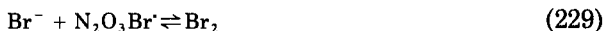
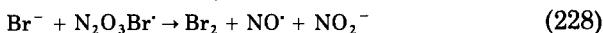
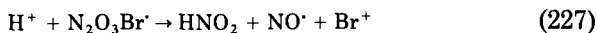
The usual role of nitrogen dioxide involves the reduction to nitrite ion, as postulated above by Koltunov. A more unusual mode of action has been observed in the reaction of hexacyanoferrate(III) with nitric and nitrous acids. The product appears to be a dimer $[(\text{NC})_5\text{Fe(II)}\mu(\text{NO})\text{Fe(II)}(\text{CN})_4\text{NO}]^{3-}$, and the nitrogen dioxide reduces iron(III) to iron(II), oxidizes a cyanide ligand to cyanate (which in aqueous solution gives carbon dioxide and water), and introduces the NO^+ ligand (56). This is not a reaction peculiar to ferricyanide; similar behavior has been observed for $\text{Fe}_2(\text{CN})_{10}^{4-}$, $\text{Fe}(\text{bipy})(\text{CN})_4^-$, and $\text{Fe}(\text{phen})(\text{CN})_4^-$ (48), and there is evidence that a similar reaction occurs with $\text{Ru}(\text{CN})_6^{3-}$ (57).

Nitrogen dioxide is also thought to be the active species in the nitrous acid-catalyzed oxidation of hydrobromic acid to bromine. The rate law is shown in (223).

$$\text{Rate} = k[\text{HNO}_2]^{1.5}[\text{Br}^-]^x[\text{H}^+]^y \quad (223)$$

At low acidities, $[\text{H}^+] \leq 0.5 \text{ M}$, x and y are close to 2, but at high acidities y rises to ca. 6 and x can fall to ca. 1. The results (70) are generally consistent with an earlier study (129), in which a similar intermediate $\text{N}_2\text{O}_3\text{BrH}^+$ was postulated





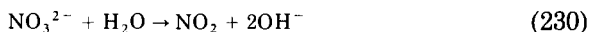
XV. Nitric Acid

Nitric acid is only a moderately strong mineral acid, and solutions containing several moles per liter contain an appreciable amount of the nonionized HNO_3 . A very useful paper by Davis and de Bruin (58) tabulates the degree of dissociation, the activity coefficients of the species involved, and the activity of water over a wide concentration range. This information can be valuable when interpreting kinetic data obtained for moderately concentrated solutions of nitric acid. Measurements of the acidity of nitric acid solutions, expressed as H_0 values, have been reported by Wyatt and Dawber (233). In sufficiently concentrated solutions of nitric acid, the nitronium ion is detectable by Raman spectroscopy. Measurements of the kinetics of ^{18}O exchange between nitric acid and water at 0° have established the nitronium ion as an active species down to 40 mol % HNO_3 in both isotope exchange and aromatic nitration (35). Stopped-flow methods have been used to measure the rate of nitronium ion formation in solutions of nitric acid in 74–82% w/w sulfuric acid (43). Other workers have somewhat different values for the rate of nitronium ion formation (142). Many reactions of nitric acid in solutions of high acidity are catalyzed by traces of nitrous acid, and in order to eliminate such effects it is often necessary to add a scavenger to remove the last traces of nitrite. When this is done, the residual rate, due to nitrogen(V) species alone, may be observed. A study of the oxidation of thiocyanic acid in the presence of nitrite scavengers has been reported (188). In some cases the substrate itself may be a nitrite trap, as is the case in the nitric acid oxidation of hydrazine. Here it has been suggested that the active oxidizing agent is the nitronium ion itself (120).

A. RADIOLYSIS AND PHOTOLYSIS

There have been many studies of the radiolysis of nitric acid and of nitrate solutions, partly because of the use of nitric acid as a medium in the processing of nuclear fuels. One pulse radiolytic study that is of interest is that by Gratzel, Henglein, and Taniguchi, in which it was shown that NO_3^{2-} , HNO_3^- , and H_2NO_3 could be formed. The last

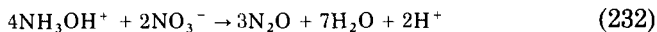
of these three is the oxyacid of which the familiar nitrogen dioxide is the anhydride. pK_a values were reported to be 4.8 and 7.5, and the decomposition reactions to form nitrogen dioxide were observed at 20° (78).



Under other conditions, pulse radiolysis of concentrated sodium nitrate solutions is reported to form NO_3 , and these combine in a bimolecular step to form N_2O_6 , with $k = 6.8 \times 10^7$ (51). The photolysis of nitrate solutions has been suggested (11) to involve the formation of excited pyramidal NO_3^- in the $^3\pi\pi$ state, followed by intramolecular rearrangement to the peroxonitrite, i.e., ONOO^- . In acid media peroxonitrite isomerizes to nitric acid, and the kinetics of this reaction have been reported (78, 143).

B. REACTIONS OF NITRIC ACID AS AN OXIDIZING AGENT

A feature of the nitrous acid-catalyzed oxidation reactions of nitric acid is that they commonly involve reduction of nitrate to nitrous acid or some equivalent species. The reaction is thus autocatalytic, and there are many examples in the literature (65, 100, 130). An example of this effect under current investigation (150) can be observed in the oxidation of hydroxylamine by nitric acid; the stoichiometry varies with the reactant concentrations, but at higher hydroxylamine concentrations approximates to (232)



Hydroxylamine is only a relatively poor scavenger for nitrite, and thus the reaction shows autocatalytic behavior as nitrous acid (an intermediate species) builds up. This is in contrast to the oxidation of hydrazine by nitric acid [see Koltunov *et al.* (120)].

An oxidation reaction of some technological interest is that in which iodine reacts with concentrated nitric acid (16–21 *M*). Reaction occurs by a two-stage process.

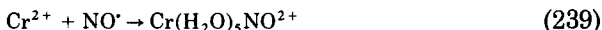
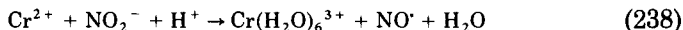
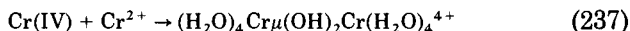
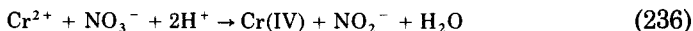


(The charges on the cationic iodine species merely represent formal oxidation states.) The kinetics of the forward process are first order with respect to I_2 and I^+ , respectively. Equilibrium constants have been obtained, but no detailed mechanism has been postulated (134, 135). It would be surprising if the mechanism did not involve NO_2^+ or N_2O_4 . Indeed although the stoichiometric equations quote HNO_2 as the product, in 16–21 *M* nitric acid, this would be almost completely converted to $N_2O_4 + NO_2^+$. An unusual species postulated (39) for reactions of aromatic iodo compounds with concentrated nitric acid is HNO_2I^+ .

Turning now to the reduction of nitrate by metal complexes, there is a complicated reaction with chromium(II). The products depend upon the initial proportions of the reactants, but with an excess of nitric acid three main species are formed, $Cr(H_2O)_5NO^{2+}$, $Cr(H_2O)_6^{3+}$, and $(H_2O)_4Cr\mu(OH)_2Cr(H_2O)_4^{4+}$. The rate law takes the form (235), and parallel reaction pathways involving the nitrate ion and nitric acid are postulated (146)

$$\text{Rate} = (k + k^1[H^+])(1 + K[H^+])^{-1}[Cr^{2+}][NO_3^-] \quad (235)$$

The proposed mechanism is summarized below.

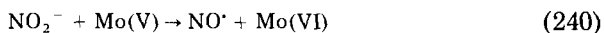


The authors have also examined the reaction of nitrous acid with Cr^{2+} , and found a rate law with a simple first-order dependence upon each component. As, under these conditions, nitrous acid was only slightly ionized, the result does not exclude a reaction between nitrite ion and Cr^{2+} . Armour and Buchbinder (8) have found that, when there is an excess of nitric acid over Cr^{2+} , complications ensue because of reactions between Cr^{2+} and $Cr(H_2O)_5NO^{2+}$.

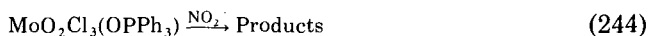
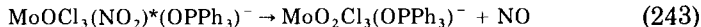
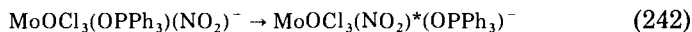
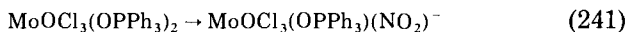
A very interesting study on the reduction of nitrate ion by a molybdenum(V) complex, $[MoOCl_3(OPPh_3)_2]$, in dichloromethane solution has been reported (76), together with an associated paper on the reduction of nitrite (109). The interest in this system is stimulated by the fact that interaction between a molybdenum(V) center and a

nitrate ion has been proposed to be involved in the reduction path of *nitrate reductase* enzymes.

It is convenient to consider the paper on nitrite reduction first. The overall stoichiometry appears to be of type (240):



but the nature of the Mo(VI) product depends upon the initial proportions of the reactants. With a 1:1 ratio the products consist of of equimolar amounts of $\text{MoO}_2\text{Cl}_4^{2-}$ and $\text{MoO}_2\text{Cl}_2(\text{OPPh}_3)_2$, but as the amount of nitrite (used as the tetraethylammonium salt) is increased above that of Mo(V) there is a reduction in the amount of $\text{MoO}_2\text{Cl}_4^{2-}$ formed (and possibly also of $\text{MoO}_2\text{Cl}_2(\text{OPPh}_3)_2$). In the presence of at least a 6-fold excess of nitrite a solid product $[\text{Et}_4\text{N}]_4[\text{Mo}_8\text{O}_{26}]$ can be isolated in essentially quantitative yield. Kinetic studies showed the presence of three consecutive reactions:



Stage (242) may be an isomerization from an *N*-bonded to an *O*-bonded nitrite group, and stage (243) is postulated as a rapid process. The details of the final stages are not fully worked out, rate law (245) being postulated:

$$\begin{aligned} \text{Rate} = & [\text{MoO}_2\text{Cl}_3(\text{OPPh}_3)^-](a + b[\text{OPPh}_3]^{-1}) \\ & \times [(\text{Et})_4\text{NNO}_2](1 + c[\text{Et}_4\text{NNO}_2])^{-1} \end{aligned} \quad (245)$$

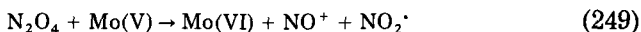
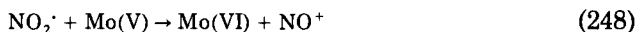
A rather similar pattern of behavior is found when the oxidant is the nitrate ion (76). Once again the products depend upon the initial ratio of the reactants, and the mechanism proposed involves an initial dissociation of a triphenylphosphineoxide ligand, complexation with a nitrate ion, and nitrogen-oxygen bond fission in a redox step to form an oxo complex and nitrogen dioxide.

For reactions with at least a 2-fold initial excess of Mo(V) over nitrate, a slower reaction may occur in which the nitrogen dioxide in turn oxidizes Mo(V) to Mo(VI). This process has been separately

studied, using $\text{MoOCl}_3(\text{OPPh}_3)_2$ and nitrogen(IV) oxide in methylene chloride as initial reactants. Parallel pathways involving NO_2^\cdot and N_2O_4 are found to occur (75).

$$-d[\text{Mo(V)}]/dt = k[\text{NO}_2^\cdot][\text{Mo(VO)}] + k'[\text{NO}_2^\cdot]^2[\text{Mo(V)}] \quad (246)$$

The mechanism proposed is shown in (247) to (249).



One problem with reactions involving the nitrogen dioxide–dinitrogen tetraoxide system is that the kinetic order depends upon the position of equilibrium (247). A reaction involving NO_2^\cdot as active species is first order with respect to $[\text{N(IV)}]$ if the equilibrium lies largely in favor of NO_2^\cdot , whereas it is half order if the equilibrium strongly favors N_2O_4 . With the concentrations quoted in this investigation, $1.2\text{--}27.5 \times 10^{-3} \text{ M}$, one would expect the bulk component of the N(IV) species to be N_2O_4 based upon reported (82) values for K_1 in solvents similar to CH_2Cl_2 . Thus a term that is first order in $[\text{N(IV)}]$ should correspond to N_2O_4 as reactant, and a term that is second order would appear to require *two* molecules of N_2O_4 . Many of the data for K_1 are rather old, but even so it seems unlikely that, at concentrations of around 10^{-3} M nitrogen(IV) oxide should be largely dissociated to NO_2^\cdot . Another investigation of the reduction of nitrate by molybdenum(V) complexes involves the reaction of $(\text{NH}_4)_2\text{MoOCl}_5$ in DMF (194). The mechanistic interpretation of the results has been the subject of some discussion (77, 179).

These results are in marked contrast to earlier studies (85) on the reduction of nitrate by molybdenum(V) in aqueous media, where the main reduction product was nitric oxide, and kinetics that were half-order with respect to molybdenum were ascribed to a monomer–dimer equilibrium in the reducing agent. The reduction of nitrite to nitric oxide by molybdenum(V) also follows a quite different path in aqueous media (73).

ACKNOWLEDGMENTS

The author gladly acknowledges his indebtedness to Professor J. H. Ridd and to Dr. M. N. Hughes for many helpful discussions of various aspects of the reaction mechanisms of nitrogen compounds and for permission to quote unpublished results.

REFERENCES

1. Adamcikova, L., and Treindl, L., *Chem. Zvesti* **30**, 593 (1976).
2. Al-Mallah, K. Y., Collings, P., and Stedman, G., *J. Chem. Soc., Dalton Trans.* p. 2469 (1974).
3. Anbar, M., and Taube, H., *J. Am. Chem. Soc.* **76**, 6243 (1954).
4. Anbar, M., and Taube, H., *J. Am. Chem. Soc.* **77**, 2993 (1955).
5. Anbar, M., and Yagil, G., *J. Am. Chem. Soc.* **84**, 1797 (1962).
6. Anbar, M., and Yagil, G., *J. Am. Chem. Soc.* **84**, 1790 (1962).
7. Anderson, J. H., *Analyst* **88**, 4941 (1963).
8. Armour, J. N., and Buchbinder, M., *Inorg. Chem.* **12**, 1086 (1973).
9. Attwood, D., and Stedman, G., *J. Chem. Soc., Dalton Trans.* p. 508 (1976).
10. Axente, D., Lacoste, G., and Mahenc, J., *J. Inorg. Nucl. Chem.* **36**, 1693 (1973).
11. Axente, D., Piringer, O., Abrudean, M., Baloca, A., and Palibroda, N., *J. Radioanal. Chem.* **30**, 233 (1976).
12. Bak, T. E., and Praestgaard, E. L., *Acta Chem. Scand.* **11**, 901 (1957).
13. Bamford, C. F., and Tipper, C. F. H., eds., "Comprehensive Chemical Kinetics," Vol. 6. Elsevier, Amsterdam, 1972.
14. Barney, G. S., *U.S. At. Energy Comm. ARH-1920* (1971).
15. Barney, G. S., *J. Inorg. Nucl. Chem.* **38**, 1677 (1976).
16. Beck, M. T., Durham, D., and Rabai, G., *Inorg. Chim. Acta* **18**, L17 (1976).
17. Becke-Geohring, M., and Flück, E., in "Developments in Inorganic Chemistry" (C. B. Colburn, ed.), Vol. I, p. 227. Elsevier, Amsterdam, 1966.
18. Behar, D., Shapira, D., and Treinin, A., *J. Phys. Chem.* **76**, 180 (1972).
19. Bekiaroglou, P., Drusas, A., and Schwab, G. M., *Z. Phys. Chem. (Frankfurt am Main)* **77**, 43 (1972).
20. Bengtsson, G., *Acta Chem. Scand.* **25**, 2989 (1971).
21. Bengtsson, G., *Acta Chem. Scand.* **27**, 1717 (1973).
22. Bengtsson, G., *Acta Chem. Scand.* **27**, 3053 (1973); **26**, 2492 (1972).
23. Benson, D., "Mechanism of Oxidation by Metal Ions." Elsevier, Amsterdam, 1976.
24. Biddle, P., and Miles, J. H., *J. Inorg. Nucl. Chem.* **30**, 1929 (1968).
25. Boehm, J. R., Balch, A. L., Bizol, K. F., and Enemerck, J. H., *J. Am. Chem. Soc.* **97**, 501 (1975).
26. Bonner, F. T., and Jordan, S., *Inorg. Chem.* **12**, 1363 (1973).
27. Bonner, F. T., and Jordan, S., *Inorg. Chem.* **12**, 1369 (1973).
28. Bonner, F. T., and Ravid, B., *Inorg. Chem.* **14**, 558 (1975).
29. Bottomley, F., *Q. Rev., Chem. Soc.* **24**, 617 (1970).
30. Bray, W. C., *Chem. Rev.* **10**, 161 (1932).
31. Bridgart, G. J., Waters, W. A., and Wilson, I. R., *J. Chem. Soc., Dalton Trans.* p. 1582 (1973).
32. Buchholz, J. R., and Powell, R. E., *J. Am. Chem. Soc.* **85**, 509 (1963).
33. Buchholz, J. R., and Powell, R. E., *J. Am. Chem. Soc.* **87**, 2350 (1965).
34. Buckingham, D. A., Francis, D. J., and Sargeson, A. M., *Inorg. Chem.* **13**, 2630 (1974); Buckingham, D. A., Marty, W., and Sargeson, A. M., *ibid.* p. 2165.
35. Bunton, C. A., Llewellyn, D. R., and Halevi, E. A., *J. Chem. Soc.* p. 4913 (1952); Bunton, C. A., and Stedman, G., *ibid.* p. 2420 (1958).
36. Bunton, C. A., Llewellyn, D. R., and Stedman, G., *J. Chem. Soc.* p. 568 (1959).
37. Bunton, C. A., and Stedman, G., *J. Chem. Soc.* p. 240 (1958).
38. Bunton, C. A., and Stedman, G., *J. Chem. Soc.* p. 3467 (1959).
39. Butler, A. R., and Sanderson, A. P., *J. Chem. Soc., Perkin Trans. 2* p. 989 (1972); *ibid.* p. 1784 (1974).

40. Cachaza, J., Casado, J., Castro, M., and Lopez-Quintela, M. A., *Can. J. Chem.* **54**, 3401 (1976).
41. Candlin, J. P., and Wilkins, J. H., *J. Chem. Soc.* p. 4236 (1960).
42. Chan, S. C., and Lee, C. K., *Aust. J. Chem.* **26**, 1923 (1973).
43. Chapman, J. W., and Strachan, A. N., *Chem. Commun.* p. 293 (1974).
44. Chatecontzis, D. H., and Miller, J. D., *J. Chem. Res. (S)* p. 137 (1977).
45. Clusius, K., and Effenberger, E., *Helv. Chim. Acta* **38**, 1843 (1955).
46. Clusius K., and Schumacher, H., *Helv. Chim. Acta* **40**, 1137 (1957).
47. Colburn, C. B., ed., "Developments in Inorganic Nitrogen Chemistry," Vols. I and II. Amsterdam, 1966 and 1973, resp.
48. Collings, P., and Stedman, G., unpublished work.
49. Collings, P., and Stedman, G., *J. Chem. Soc., Perkin Trans. 2* p. 1734 (1975).
50. Condon, F. E., Reece, R. T., Shapir, D. G., Thakker, D. C., and Goldstein, T. B., *J. Chem. Soc., Perkin Trans. 2* p. 112 (1974).
51. Daniels, M., *J. Phys. Chem.* **73**, 3710 (1969).
52. Davies, G., Kirschenbaum, L., and Kustin, K., *Inorg. Chem.* **8**, 663 (1969).
53. Davies, G., and Watkins, K. D., *J. Phys. Chem.* **74**, 3488 (1970).
54. Davies, G., and Kustin, K., *Inorg. Chem.* **8**, 484 (1969).
55. Davies, G., and Kustin, K., *J. Phys. Chem.* **73**, 2248 (1969).
55. Davies, G., and Kustin, K., *J. Phys. Chem.* **73**, 2248 (1969).
56. Davies, K. M., and Stedman, G., *J. Chem. Soc., Dalton Trans.* p. 2176 (1974); Davies, K. M., Bates, J. C., and Stedman G., *ibid.* p. 2182.
57. Dakies, K. M., private communication.
58. Davis, W., and de Bruin, H. J., *J. Inorg. Nucl. Chem.* **26**, 1069 (1964)[†]
59. Deno, N. C., Berkheimer, H. E., Evans, W. L., and Peterson, H. J., *J. Am. Chem. Soc.* **81**, 2344 (1959).
60. Dewing, J., Longster, G. F., Myatt, J., and Todd, P. F., *Chem. Commun.* p. 391 (1965).
61. Douglas, P. G., and Feltham, R. D., *J. Am. Chem. Soc.* **94**, 5254 (1972).
62. Dozsa, L., Szilassy, I., and Beck, M. T., *Inorg. Chim. Acta* **17**, 147 (1976).
63. Dozsa, L., and Beck, M. T., *Inorg. Chim. Acta* **4**, 219 (1970).
64. Dozsa, L., Szilassy, I., and Beck, M. T., *Inorg. Chim. Acta* **23**, 29 (1977).
65. Dukes, E. K., *J. Am. Chem. Soc.* **82**, 9 (1960)[†]
66. Durham, D. A., Dozsa, L., and Beck, M. T., *J. Inorg. Nucl. Chem.* **33**, 2971 (1971).
67. Durrant, G. G., Griffith, R. O., and McKeown, A., *Trans. Faraday Soc.* **32**, 999 (1936).
68. Edwards, J. O., *Science* **113**, 392 (1951)[†]
69. Erlenmeyer, H., Flierl, C., and Sigel, H., *J. Am. Chem. Soc.* **91**, 1065 (1969).
70. Feilchenfeld, H., Manor, S., and Epstein, J. A., *J. Chem. Soc., Dalton Trans.* p. 2675 (1972).
71. Ferraudi, G., and Endicott, J. F., *Inorg. Chem.* **12**, 2389 (1973).
72. Ferranti, F., Indelli, A., Secco, F., and Lucarelli, M. G., *Gazz. Chim. Ital.* **102**, 125 (1972).
73. Frank, J. A., and Spence, J. T., *J. Phys. Chem.* **68**, 2131 (1964).
74. Garley, M. F., and Stedman, G., unpublished work.
75. Garner, C. D., Hyde, M. R., and Mabbs, F. E., *Inorg. Chem.* **16**, 2122 (1977).
76. Garner, C. D., Hyde, M. R., Mabbs, F. E., and Routledge, V. I., *J. Chem. Soc., Dalton Trans.* p. 1180 (1975).
77. Garner, C. D., Hyde, M. R., and Mabbs, F. E., *Inorg. Chem.* **15**, 2328 (1976).
78. Gratzel, M., Henglein, A., and Taniguchi, S., *Ber. Bunsenges. Phys. Chem.* **74**, 292 (1970).
79. Gratzel, M., Taniguchi, S., and Henglein, A., *Ber. Bunsenges. Phys. Chem.* **74**, 1003 (1970).

80. Gratzel, M., Taniguchi, S., and Henglein, A., A., *Ber. Bunsenges. Phys. Chem.* **74**, 488 (1970).
81. Gratzel, M., Henglein, A., Lilie, J., and Beck, G., *Ber. Bunsenges. Phys. Chem.* **73**, 646 (1969).
82. Gray, P., and Yoffe, A. D., *Chem. Rev.* **55**, 1069 (1955).
83. Gupta, K. K. Sen, Sen Gupta, S., and Chatterjee, H. R., *J. Inorg. Nucl. Chem.* **38**, 549 (1976).
84. Gupta, K. S., *J. Inorg. Nucl. Chem.* **39**, 2093 (1977).
85. Guymon, E. P., and Spence, J. T., *J. Phys. Chem.* **70**, 1964 (1966).
86. Haight, G. P., Huang, T. J., and Platt, H., *J. Am. Chem. Soc.* **96**, 3137 (1974).
87. Haim, A., and Taube, H., *Inorg. Chem.* **2**, 1199 (1963).
88. Hayon, E., and Simic, M., *J. Am. Chem. Soc.* **94**, 42 (1972).
- 88a. Heckner, H. N., *J. Electroanal. Chem.* **83**, 51 (1977).
89. Higginson, W. C. E., *Spec. Publ. Chem. Soc.* **10**, 95 (1975).
90. Honig, D. S., Kustin, K., and Martin, J. F., *Inorg. Chem.* **11**, 1895 (1972).
91. Hughes, E. D., Ingold, C. K., and Ridd, J. H., *J. Chem. Soc.* p. 88 (1958).
92. Hughes, M. N., *Int. Rev. Sci., Inorg. Chem., Ser. Two* **9**, 21 (1974).
93. Hughes, M. N., and Lusty, J. R., *J. Chem. Soc., Dalton Trans.* p. 509 (1977).
94. Hughes, M. N., private communication.
95. Hughes, M. N., and Nicklin, H. G., *J. Chem. Soc. A* p. 164 (1971).
96. Hughes, M. N., and Nicklin, H. G., *J. Chem. Soc. A* p. 925 (1970).
97. Hughes, M. N., Nicklin, H. G., and Shrimanker, K., *J. Chem. Soc. A* p. 3485 (1971).
98. Hughes, M. N., and Stedman, G., *J. Chem. Soc.* p. 2824 (1963).
99. Hughes, M. N., Morgan, T. D. B., and Stedman, G., *J. Chem. Soc. B* p. 344 (1968).
100. Hughes, M. N., Phillips, E. D., Stedman, G., and Whincup, P. A. E., *J. Chem. Soc. A* p. 1148 (1969).
101. Hughes, M. N., *Q. Rev., Chem. Soc.* **22**, 1 (1968).
102. Hughes, M. N., and Stedman, G., *J. Chem. Soc.* p. 1239 (1964).
103. Hughes, M. N., and Stedman, G., *J. Chem. Soc.* p. 163 (1964).
104. Hughes, M. N., and Wimbledon, P. E., unpublished work.
105. Hughes, M. N., and Wimbledon, P. E., *J. Chem. Soc., Dalton Trans.* p. 1650 (1977).
106. Hughes, M. N., and Wimbledon, P. E., *J. Chem. Soc., Dalton Trans.* p. 703 (1976).
107. Hughes, M. N., and Lusty, J. R., *Inorg. Nucl. Chem. Lett.* **13**, 37 (1977).
108. Hughes, M. N., and Lusty, J. R., *J. Chem. Soc., Dalton Trans.* p. 1175 (1976).
109. Hyde, M. R., and Garner, C. D., *J. Chem. Soc., Dalton Trans.* p. 1186 (1975).
110. Illige, J. D., and Jolly, W. L., *Inorg. Chem.* **16**, 2637 (1977).
111. Imamura, T., and Fujimoto, M., *Bull. Chem. Soc. Jpn.* **48**, 2971 (1975).
112. Inman, G. W., Lapointe, T. F., and Johnson, I. D., *Inorg. Chem.* **15**, 3037 (1976).
113. Jones, J. R., and Rumney, T. G., *Chem. Commun.* p. 995 (1975).
114. Jones, T. E., and Hamm, R. E., *Inorg. Chem.* **14**, 1027 (1975).
115. Kane-Maguire, L. A. P., Sheridan, P. S., Basolo, F., and Pearson, R. G., *J. Am. Chem. Soc.* **92**, 5865 (1970).
116. Katritzky, A. R., Brignall, P. J., Johnson, C. D., Shakir, N., Tarkon, H. D., and Walker, G., *J. Chem. Soc. B* p. 1233 (1967).
117. Kelmers, A. D., private communication.
118. Knoblowitz, M., Miller, L., Morrow, J. I., Rich, S., and Schainbart, T., *Inorg. Chem.* **11**, 2487 (1970).
119. Koltunov, V. S., and Marchenko, V. I., *Radiokhimiya* **15**, 777 (1973).
120. Koltunov, V. S., Nikolskii, V. A., and Agureev, Yu. P., *Kinet. Katal.* **3**, 877 (1962).
121. Koltunov, V. S., and Marchenko, V. I., *Kinet. Katal.* **7**, 224 (1966).

122. Koltunov, V. S., Tikhonov, M. F., and Kuperman, A. Ya., *Russ. J. Phys. Chem. (Engl. Transl.)* **50**, 1521 (1976).
123. Krein, G., *Symp. Chem. Probl. Connected Stab. Explos. [Proc.]* **4**, 371 (1977).
124. Krueger, J. H., Sudbury, B. A., and Blanchett, P. F., *J. Am. Chem. Soc.* **96**, 5733 (1974).
125. Kudesia, V. P., *Acta. Cienc. Indica* **2**, 237 (1976); *Chem. Abstr.* **87**, 107195 (1977).
126. Lane, B. C., McDonald, J. W., Basolo, F., and Pearson, R. G., *J. Am. Chem. Soc.* **94**, 3786 (1972).
127. LaPointe, T. F., Inman, G., and Johnson, J. D., in "Disinfection; Water and Waste Water" (J. D. Johnson, ed.), Chapter 15, p. 301. Ann Arbor Sci. Publ. Ann Arbor. Michigan, 1975.
128. Leipoldt, J. G., Bok, L. D. C., Van Wyk, A. J., and Dennis, C. R., *React. Kinet. Catal. Lett.* **6**, 467 (1977).
129. Longstaff, J. V. L., *J. Chem. Soc.* p. 3488 (1957).
130. Longstaff, J. V. L., and Singer, K., *J. Chem. Soc.* p. 2610 (1954).
131. Lucien, H. W., *J. Am. Chem. Soc.* **80**, 4458 (1958).
132. Lunak, S., and Veprek-Siska, J., *Collect. Czech. Chem. Commun.* **39**, 391 (1974).
133. Lusty, J. R., and Hughes, M. N., unpublished work.
134. Mailen, J. C., and Tiffany, T. O., *J. Inorg. Nucl. Chem.* **37**, 127 (1975).
135. Mailen, J. C., *J. Inorg. Nucl. Chem.* **37**, 1019 (1975).
136. Maschka, A., *Monatsh. Chem.* **84**, 872 (1953).
137. Masek, J., *Nature (London)* **191**, 167 (1961); *Collect. Czech. Chem. Commun.* **27**, 667 (1962).
138. Matts, T. C., and Moore, P., *J. Chem. Soc. A* p. 1632 (1971).
139. Matts, T. C., Moore, P., Ogilvie, D. M. W., and Winterton, N., *J. Chem. Soc. Dalton Trans.* p. 992 (1973).
140. McAuley, A., private communication.
141. McWeeny, D. J., Gilbert, J., and Knowles, M. E., *J. Sci. Food Agric.* **26**, 1785 (1975).
142. Moodie, R. B., private communication.
143. Moore, P., and Benton, D. J., *J. Chem. Soc. A* p. 3179 (1970).
144. Morrow, J. I., and Sheeres, G. W., *Inorg. Chem.* **11**, 2606 (1972).
145. Murmann, R. K., Sullivan, J. C., and Thompson, R. C., *Inorg. Chem.* **7**, 1876 (1968).
146. Ogino, H., Tsukahara, K., and Tanaka, N., *Bull. Chem. Soc. Jpn.* **47**, 308 (1974).
147. Ottolenghi, M., and Rabani, J., *J. Phys. Chem.* **72**, 593 (1968).
148. Partingdon, J. R., "A Textbook of Inorganic Chemistry," 2nd ed., p. 561. Macmillan, New York, 1927.
149. Patel, R. G., and Chaudhri, M. M., *Symp. Chem. Probl. Connected Stab. Explos. [Proc.]* **4**, 347 (1977).
150. Pembridge, J. R., and Stedman, G., unpublished work.
151. Pendlebury, J. N., and Smith, R. H., *Aus. J. Chem.* **26**, 1847 and 1857 (1973).
152. Perrott, J. R., Stedman, G., and Uysal, N., *J. Chem. Soc. Perkin Trans. 2* p. 274 (1977).
153. Perrott, J. R., Stedman, G., and Uysal, N., *J. Chem. Soc. Trans. Dalton* p. 2058 (1976).
154. Perrott, J. R., and Stedman, G., *J. Inorg. Nucl. Chem.* **39**, 325 (1977).
155. Petek, M., Neal, T. E., McNeely, R. L., and Murray, R. W., *Anal. Chem.* **45**, 32 (1973).
156. Plakhotnik, V. N., and Drabkina, A. Kh., *Kinet. Katal.* **13**, 60 (1975); *Chem. Abstr.* **83**, 181147 (1975).
157. Polydoropoulos, C. N., and Pipinis, M., *Z. Phys. Chem. (Frankfurt am Main)* **40**, 322 (1964).

158. Radbil, B., *Kinet. Katal.* **16**, 360 (1975); *Chem. Abstr.* **83**, 85541 (1975).
159. Ramanujam, W. M. S., Sundaram, S., and Venkatsubramaniam, N., *Inorg. Chim. Acta* **13**, 133 (1975).
160. Reed, J. L., Gafney, H. D., and Basolo, F., *J. Am. Chem. Soc.* **96**, 1363 (1974).
161. Reed, J. L., Wang, F., and Basolo, F., *J. Am. Chem. Soc.* **94**, 7173 (1972).
162. Ridd, J. H., *Q. Chem. Soc. Rev.*, **15**, 418 (1961).
163. Ridd, J. H., *Recent Adv. Phys. Org. Chem.* Submitted for publication (1979).
164. Saguinsin, J. L. S., and Morris, J. C., in "Disinfection; Water and Waste Water" (J. D. Johnson, ed.), Chapter 14, p. 227. Ann Arbor Sci. Publ., Ann Arbor, Michigan, 1975.
165. Schmid, M., and Krenmayr, P., *Monatsh. Chem.* **98**, 417 (1967).
166. Schwarzenbach, G., *Helv. Chim. Acta* **19**, 178 (1936).
167. Scott, R. A., Haight, G. P., and Cooper, J. N., *J. Am. Chem. Soc.* **96**, 4136 (1974).
168. Seel, F., and Kaschuba, J., *Z. Phys. Chem. (Frankfurt am Main)* **92**, 235 (1974).
169. Seel, F., and Schwaebel, R., *Z. Anorg. Allg. Chem.* **274**, 169 (1953).
170. Seel, F., and Degener, E., and *Z. Anorg. Allg. Chem.* **284**, 101 (1956).
171. Seel, F., and Meyer, D., *Z. Anorg. Allg. Chem.* **408**, 283 (1974).
172. Sen Gupta, K. K., and Sen, P. K., *J. Inorg. Nucl. Chem.* **39**, 1651 (1977).
173. Sen Gupta, K. K., Sen, P. K., and Sen Gupta, S., *Inorg. Chem.* **16**, 1397 (1977).
174. Sen Gupta, K. K., Sen Gupta, S., Sen, P. K., and Chatterjee, H. R., *Indian J. Chem., Sect. A* **15**, 506 (1977).
175. Shapira, D., and Treinin, A., *J. Phys. Chem.* **77**, 1195 (1973).
176. Shaw, A. W., and Vosper, A. J., *J. Chem. Soc. Dalton Trans.* p. 961 (1972).
177. Shrimanker, K., and Hughes, M. N., unpublished work.
178. Simic, M., and Hayon, E., *J. Am. Chem. Soc.* **93**, 5982 (1971).
179. Spence, J. T., and Taylor, R. D., *Inorg. Chem.* **16**, 1256 (1977).
180. Spillane, W. J., Goggin, C. B., Regan, N., and Scott, F. L., *Int. J. Sulfur Chem.* **8**, 565 (1976).
181. Sramkova, B., Sramek, J., and Zyka, J., *Anal. Chim. Acta* **62**, 113 (1972).
182. "Stability Constants," *Chem. Soc., Spec. Publ.* **17**, 164 (1964).
183. Stec, W. J., and Okruszek, A., *J. Chem. Res. (S)* p. 142 (1977).
184. Stedman, G., *J. Chem. Soc.* pp. 2943 and 2949 (1959).
185. Stedman, G., *J. Chem. Soc.* p. 1702 (1960).
186. Stedman, G., and Uysal, N., *J. Chem. Soc., Perkin Trans. 2* p. 667 (1977).
187. Stedman, G., unpublished work.
188. Stedman, G., and Thomas, N. B., *J. Inorg. Nucl. Chem.* **39**, 1015 (1977).
189. Steinmetz, W. E., Robinson, D. H., and Ackermann, M. N., *Inorg. Chem.* **14**, 421 (1975).
190. Swaroop, R., and Gupta, Y. K., *J. Inorg. Nucl. Chem.* **36**, 169 (1974).
191. Switkes, E. G., Dasch, G. A., and Ackermann, M. N., *Inorg. Chem.* **12**, 1120 (1973).
192. Sykes, A. G., *Adv. Inorg. Chem. Radiochem.* **10**, 153 (1967).
193. Talaty, E. R., Schwarz, A. K., and Simons, G., *J. Am. Chem. Soc.* **97**, 972 (1975).
194. Taylor, R. D., and Spence, J. T., *Inorg. Chem.* **14**, 2815 (1975).
195. Tellier-Pollon, S., and Heubal, J., *Rev. Chim. Miner.* **4**, 413 (1967).
196. Templeton, J. C., and King, E. L., *J. Am. Chem. Soc.* **93**, 7160 (1971).
197. Thacker, M. A., and Higginson, W. C. E., *J. Chem. Soc. Dalton Trans.* p. 704 (1975).
198. Thakuria, B. M., and Gupta, Y. K., *J. Chem. Soc. Dalton Trans.* p. 2541 (1975).
199. Thakuria, B. M., and Gupta, Y. K., *J. Chem. Soc. Dalton Trans.* p. 77 (1975).
200. Thakuria, B. M., and Gupta, Y. K., *Inorg. Chem.* **16**, 1399 (1977).
201. Thompson, R. C., *Inorg. Chem.* **8**, 1895 (1969).
202. Thompson, R. C., and Kaufmann, E. J., *J. Am. Chem. Soc.* **92**, 1540 (1970).

203. Thompson, R. C., and Sullivan, J. C., *Inorg. Chem.* **9**, 1590 (1970).
204. Tomat, R., and Rigo, A., *J. Inorg. Nucl. Chem.* **36**, 611 (1974).
205. Tomat, R., and Rigo, A., *J. Electroanal. Chem. Interfacial Electrochem.* **35**, 21 (1972).
206. Turney, T. A., *J. Chem. Soc.* p. 4263 (1960).
207. Turney, T. A., and Wright, G. A., *Chem. Rev.* **59**, 497 (1959).
208. Turney, T. A., and Wright, G. A., *J. Chem. Soc.* p. 2415 (1958).
209. Veprek-Siska, J., and Lunak, S., *Collect. Czech. Chem. Commun.* **39**, 41 (1974).
210. Veprek-Siska, J., and Lunak, S., *Collect. Czech. Chem. Commun.* **37**, 3846 (1972).
211. Waters, W. A., and Wilson, I. R., *J. Chem. Soc. A* p. 534 (1966).
212. Weaver, R. T., and Basolo, F., *Inorg. Chem.* **13**, 1535 (1974).
213. Wellman, C. R., Ward, J. R., and Kuhn, L. P., *J. Am. Chem. Soc.* **98**, 1683 (1976).
214. Wells, C. F., and Mays, D., *J. Chem. Soc. A* p. 2175 (1969).
215. Wells, C. F., and Mays, D., *J. Chem. Soc.* p. 1622 (1968).
216. Wells, C. F., and Husain, M., *J. Chem. Soc. A* p. 2981 (1968).
217. Werner, A. E., *J. Chem. Soc.* **101**, 2180 (1912).
218. White, R. E., and Kovacic, P., P., *J. Am. Chem. Soc.* **97**, 1180 (1975).
219. Wiberg, N., Fischer, G., and Bachhuber, H., *Chem. Ber.* **107**, 1456 (1974).
220. Wiberg, N., Fischer, G., and Bachhuber, H., *Angew. Chem. Int. Ed. Engl.* **16**, 780 (1977).
221. Wiberg, N., Bayer, H., and Bachhuber, H., *Angew. Chem. Int. Ed. Engl.* **14**, 177 (1975).
222. Williams, D. L. H., *J. Chem. Soc., Perkin Trans. 2* p. 128 (1977).
223. Williams, D. L. H., *J. Chem. Soc., Perkin Trans. 2* p. 502 (1977).
224. Williams, D. L. H., *J. Chem. Soc., Perkin Trans. 2* p. 655 (1975).
225. Willis, C., and Back, R. A., *Can. J. Chem.* **51**, 3605 (1973); **52**, 2513 (1974).
226. Willis, C., Back, R. A., Parsons, J. M., and Burdon, J. G., *J. Am. Chem. Soc.* **99**, 4451 (1977).
227. Willis, C., Beck, R. A., and Purdon, J. G., *Int. J. Chem. Kinet.* **9**, 787 (1977).
228. Wilson, B. J., Hayes, J. M., and Durbin, J. A., *Inorg. Chem.* **15**, 1702 (1976).
229. Wilson, B. J., and Fillmore, D. L., *Inorg. Chem.* **16**, 1404 (1977).
230. Winter, N., and Pitzer, R. M., *J. Chem. Phys.* **62**, 1269 (1975).
231. Wolfe, S. K., Andrade, C., and Swinehart, J. H., *Inorg. Chem.* **13**, 2567 (1974).
232. Woods, M., Montag, T. A., and Sullivan, J. C., *J. Inorg. Nucl. Chem.* **38**, 2059 (1976).
233. Wyatt, P. A. H., and Dawber, J. G., *J. Chem. Soc.* p. 3589 (1960).
234. Yagil, G., and Anbar, M., *J. Inorg. Nucl. Chem.* **26**, 453 (1964).
235. Yost, D. M., Russell, H., Jr., "Systematic Inorganic Chemistry," p. 129. Prentice-Hall, Englewood Cliffs, New Jersey, 1946.
236. Zollinger, H., "Azo and Diazo Chemistry," p. 147. Wiley (Interscience), New York, 1961.

THIO-, SELENO-, AND TELLUROHALIDES OF THE TRANSITION METALS

M. J. ATHERTON* AND J. H. HOLLOWAY

Department of Chemistry, The University, Leicester, England

I. Introduction	171
II. Group IIIA	174
A. Yttrium	174
B. Lanthanum	176
III. Group IVA	176
Titanium	176
IV. Group VA	177
A. Vanadium	177
B. Niobium	177
C. Tantalum	179
V. Group VIA	180
A. Chromium	180
B. Molybdenum	180
C. Tungsten	186
VI. Group VIIA	192
A. Manganese	192
B. Rhenium	192
VII. Group VIII	193
Platinum	193
VIII. Group IB	193
A. Copper	193
B. Silver	194
C. Gold	194
References	195
Note Added in Proof	198

I. Introduction

Thio-, seleno-, and tellurohalides are classes of compounds with only sparse coverage in the chemical literature. Over the past 20 years, however, there has been a gradual increase in activity in these areas of chemistry, although the papers published so far have been the almost exclusive preserve of a small number of research groups.

* Present address: Springfields, British Nuclear Fuels Limited, Salwick, Preston PR4 OXN, Lancashire, England.

This review summarizes the preparation and chemistry of known thio-, seleno-, and tellurohalides of the transition-metal elements, the compounds being dealt with element by element and group by group. For the purposes of the review we have adopted the definition of transition elements as those which, as elements, have partly filled *d* or *f* shells in any of their commonly occurring oxidation states. This means that copper, silver, and gold are included. However, whereas the Group I elements may lose one or two *d* electrons to give ions or complexes in the II and III oxidation states, this is no longer possible for Group II, and zinc, cadmium, and mercury compounds have been omitted. Tables I, II, and III list the compounds considered. No thio-, seleno-, or tellurohalides have yet been prepared for scandium, zirconium, hafnium, technetium, iron, ruthenium, osmium, cobalt, rhodium, iridium, nickel, or palladium. For the remaining elements

TABLE I
KNOWN TRANSITION-METAL THIOHALIDES^a

Group IIIA	Group IVA	Group VA	Group VIA	Group VIIA	Group VIII
	TiSCl ₂	VSCl	CrSBr	MnSCl ₂	
YSHal	TiSCl	(VSBBr)?	CrSI _{0.83}		
		NbSCl ₃	MoSCl ₃		
		NbSBr ₃	MoSBr ₃		
		NbSCl ₂	MoSCl ₂		
		NbS ₂ X ₂	MoS ₂ Cl ₃		
		Nb ₃ S ₃ Cl ₈	MoS ₂ Cl ₂		
			MoS ₂ Br ₂		
			MoSX		
			Mo ₂ S ₄ Cl ₅		
			Mo ₂ S ₅ X ₃		
			Mo ₃ S ₇ Cl ₄		
			Mo ₃ S ₇ Br ₄		
			Mo ₆ SBr ₁₀		
			Mo ₆ S ₁₄ I ₈		
LaSHal		TaSCl ₃	WSF ₄	ReSCl ₄	PtS _n Cl _m
MSBr		TaSBr ₃	WSCl ₄	ReSCl ₃	PtS _n Br _m
		TaSCl ₂	WSBr ₄	ReSCl ₂	
		TaS ₂ Cl ₂	WSCl ₃	ReSBr ₂	
			WSCl ₂	ReS ₂ Br	
			WS ₂ Cl ₂	ReS ₃ Cl	
			WOSCl ₂	Re ₂ S ₃ Cl ₄	
			WSSeCl ₂		

^a M = La, Ce, Pr, Sm, Gd, Tb, Dy, Ho, Er, Yb, Lu; Hal = F, Cl, Br, I; X = Cl, Br, I; *m* and *n* = integers that depend on the ratio of reactants and temperature.

TABLE II
 KNOWN TRANSITION-METAL SELENOHALIDES^a

Group IIIA	Group IVA	Group VA	Group VIA	Group VIIA	Group VIII	Group IB
			CrSeI Cr ₂ CuSe ₃ Br	MnSeBr ₂ MnSeI ₂ MnSeCl MnSe ₂ Cl ₂ Mn ₂ SeBr ₂		CuSe ₂ Cl CuSe ₃ Br CuSe ₃ I CuCr ₂ Se ₃ Br
YSeF		NbSeCl ₃ NbSeBr ₃ NbSe ₂ X ₂	MoSeCl ₃ MoSeCl ₂ Mo ₃ Se ₇ Cl ₄ Mo ₃ Se ₇ Br ₄ Mo ₆ SeBr ₁₀ Mo ₆ SeI ₁₀ Mo ₆ Se ₁₄ I ₈			
LaSeF		TaSeBr ₃	WSeF ₄ WSeCl ₄ WSeBr ₄ WSeBr ₃ WSeBr ₂ WSeCl ₂ WSSeCl ₂	ReSeCl ₂ ReSeBr ₂ Re ₃ Se ₂ Cl ₅		AuSeCl AuSeBr

^a X = Cl, Br, I.
 TABLE III
 KNOWN TRANSITION-METAL TELLUROHALIDES^a

Group IIIA	Group IVA	Group VA	Group VIA	Group VIIA	Group VIII	Group IB
			CrTe _{0.73} I			CuTeX CuTe ₂ X Ag ₃ TeBr Ag ₅ Te ₂ Cl AuTeI AuTe ₂ X

^a X = Cl, Br, I.

the most usual preparative routes for thio and seleno derivatives are:

1. Direct combination of the elements (a method often used to prepare chalcogenide halides of the main group elements)
2. The halogenation of a metal sulfide or selenide
3. The reaction of a metal halide with sulfur, selenium, a sulfide or a selenide (such methods being mainly employed for the early transition elements)

4. Hydrothermal synthesis at high temperature and pressure in an autoclave (this route has been employed exclusively for the later transition elements).

At present the number of tellurohalides known is limited, and it is perhaps too soon to list "general" methods for their preparation.

II. Group IIIA

A. YTTRIUM

The series of yttrium thiohalides YSX ($X = F, Cl, Br, I$) have been synthesized, and X-ray crystallographic studies have yielded comprehensive data on their space groups and unit cell parameters (29). Yttrium thiofluoride, prepared by the reaction of Y_2S_3 with YF_3 (at 900° – $1200^\circ C$) (29) or other fluorinating agents (52), has both α - and β -forms, which are tetragonal and hexagonal, respectively (27, 29, 75). The β -form has been studied by three-dimensional X-ray diffraction and shown to consist of compact layers of (YS_2) and (YF_2) units parallel to the (001) plane (Fig. 1) (75).

Yttrium selenofluoride may be prepared using YF_3 and Y_2Se_3 (25, 26) and is known to exist in at least three forms: orthorhombic (33), monoclinic (34) and one that is either hexagonal or rhombohedral (26). The orthorhombic polytype has selenium atoms at the vertices of a slightly distorted octahedron. Each selenium has 4-fold coordination, and the three-coordinate fluorines are each at the center of a yttrium

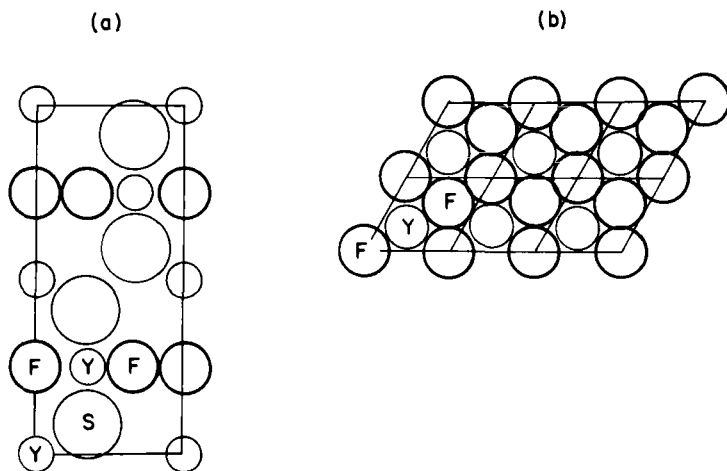


FIG. 1. Crystal structure of β -YSF (75). (a) View of the structure in the diagonal plane (110). (b) Planar layer of YF_2 at $z = \frac{1}{4}$. Reproduced with permission.

isosceles triangle. The yttrium atoms have 7-fold coordination. The main feature of the structure is the planar Y-F groups along two diagonals of the projected selenium hexagons (33). Comparison of this two-layer orthorhombic polytype with the four-layer monoclinic polytype (Fig. 2) has been made (34). More recently, structures of other

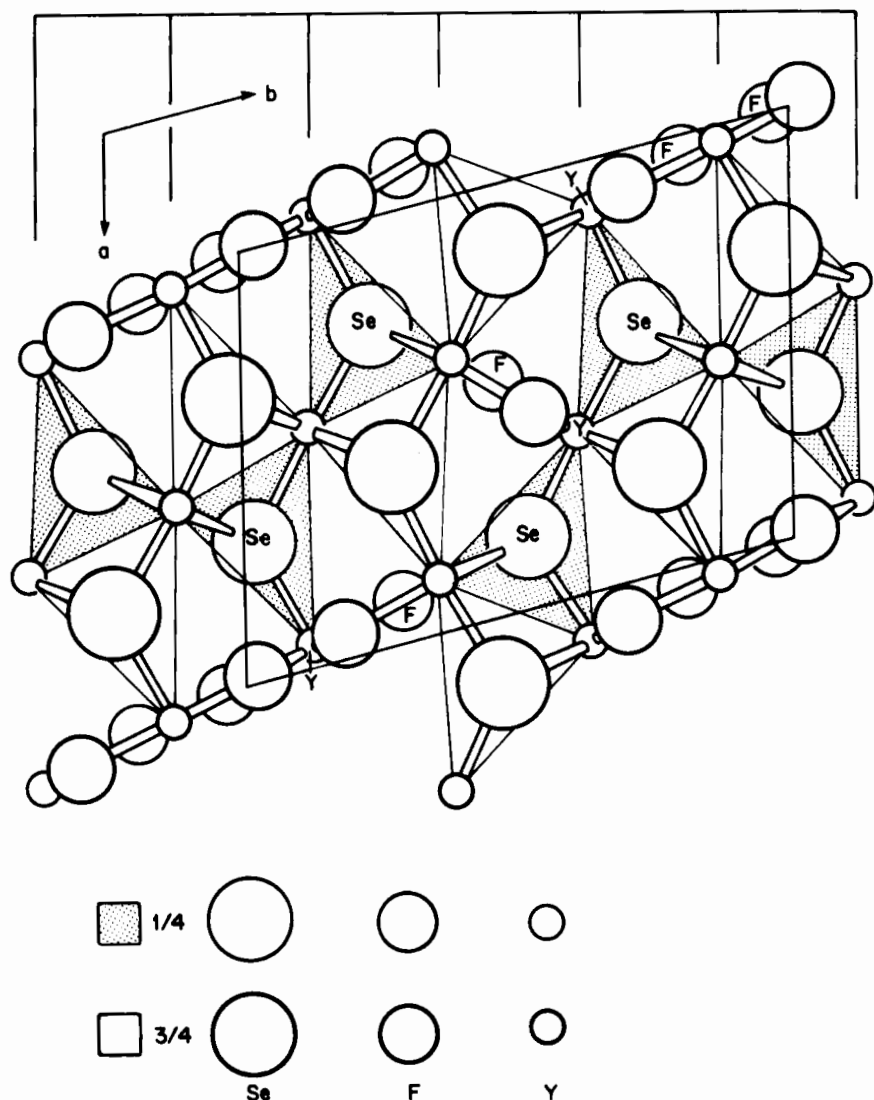


FIG. 2. Projection on the x_0y plane of the structure of four-layer monoclinic polytype of YSeF (34). Reproduced with permission.

polytypes have been studied by lattice imaging using electron microscopy (88).

B. LANTHANUM

The series of compounds LaSX ($X = \text{Cl}, \text{Br}, \text{I}$), each of which is orthorhombic (23, 27), may be made by the reaction of metallic lanthanum with sulfur and the appropriate halogen at 500°C (27). Lanthanum thiofluoride (LaSF), however, has only been prepared by reaction of LaF_3 with La_2S_3 (5, 29, 44, 89) or La_3S_4 and sulfur at high temperature (78). This gray-white solid, which melts at 1810°C (89), possesses a tetragonal structure of the PbClF type (27, 44, 78). The infrared spectrum has been compared with those of CeSF , PrSF , and NdSF (5). The thioclauride and thioiodide of lanthanum are of unknown structure whereas LaSBr has three structures, all of which are characterized by alternate layers of bromine ions and La_4S tetrahedra (28). A number of other analogous lanthanide and actinide thiobromides have also been reported (Table I) (28).

Light gray LaSeF has been prepared by routes analogous to those used to prepare LaSF (24, 78) and has been identified in three forms, tetragonal (24), hexagonal (32), and orthorhombic (78). The tetragonal structure is of the PbClF type and contains layers of $(\text{LaF})_n$ and Se (24). The hexagonal form consists of layers of selenium anions and planes of lanthanum and fluoride ions. Each lanthanum and fluorine occupies the center of an equilateral triangle formed by the other ions. The selenium and fluorine anions together form a rhombohedral stacking sequence (32). The corresponding chloride, bromide, and iodide are not known.

III. Group IVA

TITANIUM

Low yields of TiSCl_2 were obtained by bubbling hydrogen sulfide through solutions of titanium tetrachloride in CS_2 at $20^\circ\text{--}65^\circ\text{C}$ (35). The product was reported to be oxygen and moisture sensitive and to decompose into TiS_2 and TiCl_4 at temperatures above 400°C . This work has been repeated by Riera and Uson (74), and no evidence for TiSCl_2 was obtained, although very small yields of insoluble, air- and water-sensitive TiSCl were produced. This had infrared peaks at 550 cm^{-1} and 370 cm^{-1} , which were assigned to Ti-S and Ti-Cl stretching frequencies, respectively. Attempts to prepare TiSCl by reaction of TiCl_4 with As_2S_3 , Sb_2S_3 , or MoS_2 also proved to be unsuccessful (74). Mixtures of TiSCl and TiSCl_2 appear to be produced

from reaction of TiCl_3 with sulfur in benzene in an autoclave. The brown product can be used as a catalyst in the production of crystalline polypropylene (85).

IV. Group VA

A. VANADIUM

The vanadium thiochloride (VSCl) has been prepared by the reaction of vanadium trichloride with antimony trisulfide at $380^\circ\text{--}390^\circ\text{C}$. The thermal conditions for the reaction require careful control. The infrared spectrum and magnetic susceptibility have been obtained (3). An attempt to prepare the analogous thiobromide has been less successful, the product always containing less than the theoretical amount of bromine (3).

B. NIOBIUM

Reaction of niobium pentachloride with both antimony trisulfide and sulfur has been used to prepare a complex series of species that includes predominantly $\text{Nb}_3\text{S}_3\text{Cl}_8$, a red-brown solid believed to be a cluster compound (38). These materials appear to originate from the disproportionation of NbSCl_3 , formed as an intermediate in the reaction. Niobium thiotrichloride, NbSCl_3 , has been isolated as golden-yellow, air-sensitive crystals from the reaction of NbCl_5 with Sb_2S_3 at room temperature in carbon disulfide (38, 39), and the analogous compounds NbSBr_3 , NbSeCl_3 , and NbSeBr_3 have been prepared by the same method (39). NbSCl_3 has also been prepared by the reaction of NbCl_5 with B_2S_3 (4). The infrared spectra of the thiohalides exhibit metal-sulfur stretches in the region of 550 cm^{-1} (Table IV) (4).

TABLE IV
METAL-SULFUR STRETCHING
FREQUENCIES (IN CM^{-1}) FOR
NIOBIUM AND TANTALUM
THIOHALIDES MSX_3
($\text{M} = \text{Nb, Ta}$; $\text{X} = \text{Cl, Br}$)
(39)

Compound	$\nu(\text{M} = \text{S})$
NbSCl_3	552
TaSCl_3	463
NbSBr_3	542
TaSBr_3	448

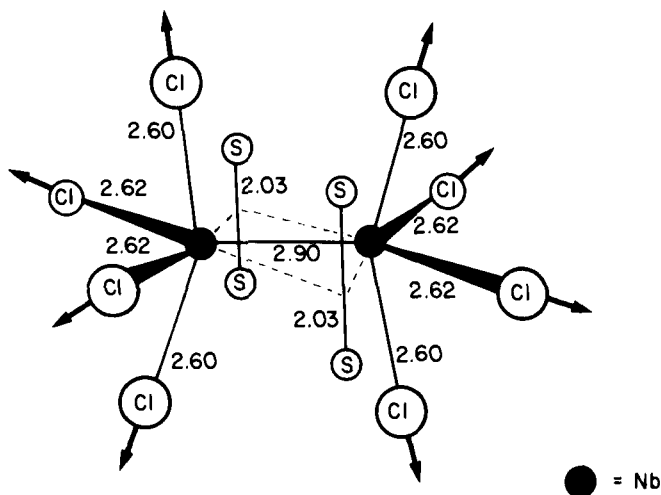


FIG. 3. Coordination polyhedron of an Nb_2 pair in the NbS_2Cl_2 structure (79). Reproduced with permission.

A series of compounds, NbX_2Y_2 ($\text{X} = \text{S}, \text{Se}$; $\text{Y} = \text{Cl}, \text{Br}, \text{I}$), has been prepared (76, 77, 79) by reaction of the elements at $\sim 500^\circ\text{C}$. Niobium dithiodichloride has also been made by heating a 1:1 mixture of niobium metal and S_2Cl_2 (76). These niobium dithiodihalides contain bridging S_2 groups, and the structure of single crystals of NbS_2Cl_2 has been determined (79) and can be described in terms of $\text{Nb}_2(\text{S}_2)_2$ groups linked to one another via chlorine atoms (Fig. 3).

Vibrational studies of the octahedral cages $[\text{Nb}-(\text{S}_2)_2-\text{Nb}]$ in the thiohalides NbS_2X_2 ($\text{X} = \text{Cl}, \text{Br}, \text{I}$) show metal— (S_2) bridging vibrations at $<400\text{ cm}^{-1}$ and sulfur—sulfur stretches that are both infrared and Raman active at $500\text{--}600\text{ cm}^{-1}$ (61, 63). This high S—S stretching frequency has been accounted for in later theoretical studies (60). The frequencies associated with S—S, Nb—S, and Nb—X are listed in Table V.

Niobium thiodichloride, NbSCl_2 , is the product of the reaction of NbCl_4 with M_2S_3 ($\text{M} = \text{As}, \text{Sb}$) at 250°C under an atmosphere of argon (54) and the reaction of NbCl_5 with sulfur in benzene (83). In the latter study a series of compounds $\text{Nb}(\text{S}_2)_m\text{Cl}_n$ ($m = 1\text{--}3$, $n = 1\text{--}4$) were also produced by interaction of Nb(V) chloride with elemental sulfur in melts at $240\text{--}300^\circ\text{C}$ in a vacuum and the products were examined by infrared spectroscopy. Intense absorptions at 535 cm^{-1} were attributed to stretching vibrations of S—S bonds coordinated to the metal. All the products from the melts are unstable hydrolytically, insoluble in

TABLE V
FREQUENCIES (IN cm^{-1}) OF INFRARED AND RAMAN VIBRATIONS OF
NIOBIUM THIOHALIDES NbS_2X_2 ($\text{X} = \text{Cl}, \text{Br}, \text{I}$) (61, 63)

Assignments	Compound				
	NbS_2Cl_2		NbS_2Br_2		NbS_2I_2
	IR	Raman	IR	Raman	IR
S—S	558s	592vs	585s	585vs	575s
	582sh		580sh		570sh
Nb—S	377m		370m		358m
	362vs		358vs		348vs
		336s		328s	
	323vs		320s		315s
		317m		310m	
		252m		243s	
		188m		183w	
	166s		174s		169s
Nb—X	295vs		205vs		148s
		285m		170w	
	255sh				
	250vs		190vs		131s
	245sh				
			143sh		
	218w		140m		

the usual organic solvents, decomposed by mineral acids, and dissolve in a mixture of potassium hydroxide and hydrogen peroxide with separation of elemental sulfur (83).

C. TANTALUM

The first identification of a tantalum thiohalide was made by Boehland and Schneider, who studied the reaction of TaCl_5 with PhNCS in hexane and heptane (10). These reactions yielded $\text{TaCl}_5 \cdot \text{PhNCS}$, which was totally converted to $\text{TaSCl}_3 \cdot \text{PhNCCl}_2$ on refluxing. Heating a mixture of TaCl_5 with Sb_2S_3 to 120°C produces a material of empirical formula TaSCl_3 (38, 39). This has been separated into a black residue and white and yellow sublimates by heating to 140°C for 14 days. Yellow TaSCl_3 produced by the reaction of TaCl_5 with Sb_2S_3 in dry CS_2 (38) or by direct reaction of stoichiometric amounts of TaCl_5 and B_2S_3 at 80°C (4) has also been shown to be thermally unstable and, on heating, decomposes producing a white sublimate, TaCl_5 , and a black residue of TaSCl_2 . The metal-sulfur stretching frequency in

TaSCl_3 , 463 cm^{-1} , is similar to the Nb—S frequencies of analogous niobium compounds (Table IV) (39). Both TaSBr_3 and TaSeBr_3 have been synthesized by reaction of the appropriate antimony chalcogenide with TaBr_5 in CS_2 (39). The dithiodichloride, TaS_2Cl_2 , has been reported as the product from the reaction of TaCl_5 and sulfur in benzene (83).

V. Group VIA

A. CHROMIUM

There have only been two reports of chromium thio-, seleno- and tellurohalides (46, 71). Black CrSBr may be prepared from Cr_2S_3 and CrBr_3 in a sealed ampoule at 870°C , and $\text{CrSI}_{0.83}$ and CrSeI and $\text{CrTe}_{0.73}\text{I}$ are the products from the reaction of iodine and the respective metal chalcogenide at 400°C (46). All are hexagonal, and all three compounds are readily hydrolyzed. The preparation of single crystals of $\text{CuCr}_2\text{Se}_3\text{Br}$ has been reported (71).

B. MOLYBDENUM

The variety of, and number of publications concerning, molybdenum thio-, and selenohalides is surpassed only by those on the corresponding tungsten species. Compounds with molybdenum in the oxidation states 3, 4, 5, and 6 have been successfully synthesized.

The series of molybdenum(III) thiohalides, MoSX ($\text{X} = \text{Cl}, \text{Br}, \text{I}$), has recently been reported (58, 59). Each is prepared by heating a mixture of sulfur, powdered molybdenum metal, and the appropriate molybdenum dihalide. All are cubic with tetrahedral Mo_4 clusters, which are bridged together by the halogen atoms. The thiobromide structure has been studied in detail (Fig. 4) (59).

Black molybdenum thiodichloride, MoSCl_2 , may be prepared in three ways, by the reaction of antimony trisulfide with MoCl_4 at 140°C for 7 days (15), from the disproportionation of MoSCl_3 (15) or by the direct chlorination of MoS_2 in a flow system (40, 70). Of these three routes the first has been reported to give the best yields.

Involatile, dark green, MoSCl_3 may be prepared by the reaction of MoCl_5 with sulfur at 140°C for 3 weeks (15) or in carbon disulfide at room temperature (73). Alternatively, it can be made by reaction of MoCl_5 and sulfur with antimony trisulfide at 170°C for 7 days (14, 15) or in CS_2 at 25°C for 3 days (73). Another method is the reaction of stoichiometric quantities of MoCl_5 with B_2S_3 at 190°C (4). It has also

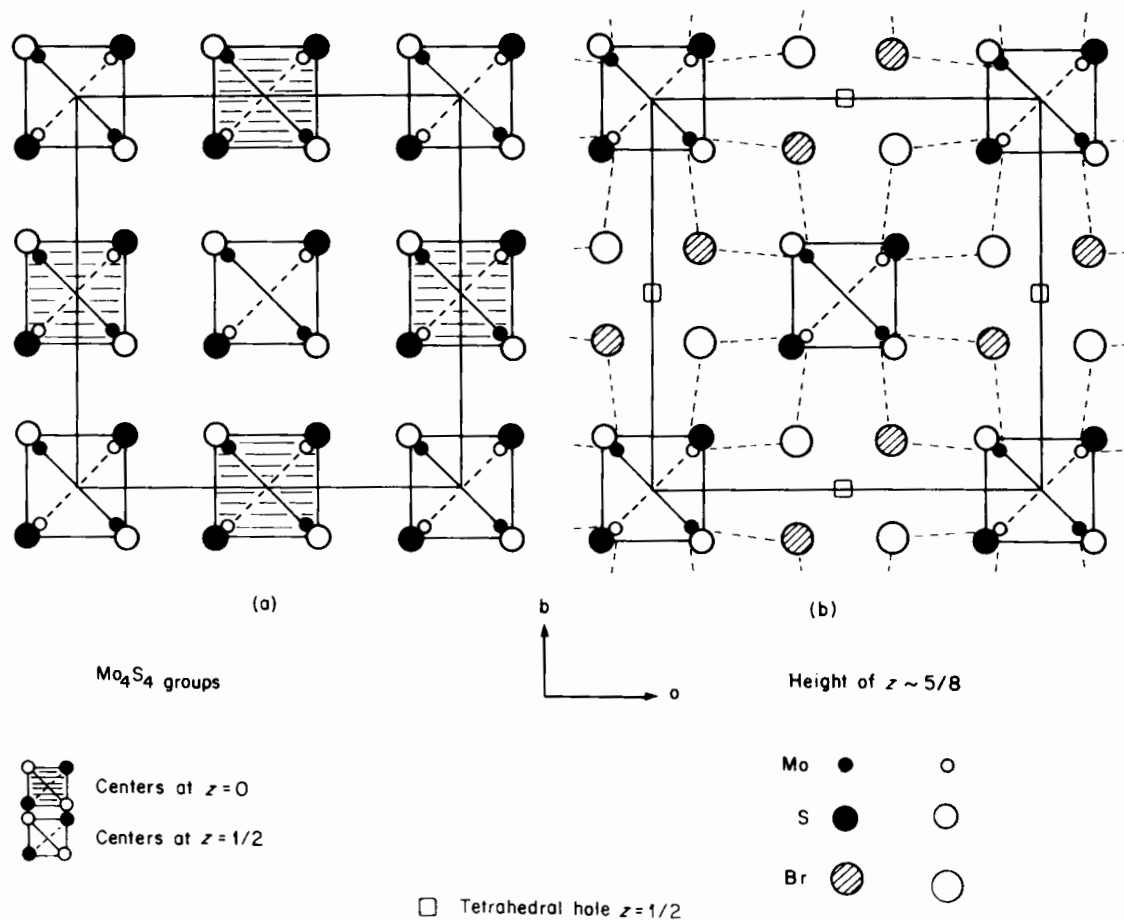


FIG. 4. Crystal structure of MoSBr (59). (a) Disposition of Mo_4S_4 group in the lattice. (b) Projection of the atoms lying between $z = \frac{1}{4}$ and $\frac{3}{4}$ on the (001) plane. Reproduced with permission.

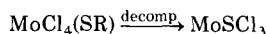
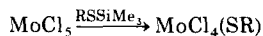
TABLE VI
MAGNETIC MOMENTS (B.M.) AND FREQUENCIES OF INFRARED VIBRATIONS (cm^{-1}) OF MOLYBDENUM AND TUNGSTEN THIOHALIDES AND MOLYBDENUM THIOCHLORIDE COMPLEXES (14, 16)

	MoSCl ₃	MoSCl ₃ ·MeCN	MoSCl ₃ ·2MeCN	MoSCl ₃ ·2diox	MoSCl ₃ ·bme	MoSCl ₃ ·3py	[Hpy][MoSCl ₄ ·py]	MoSCl ₂ ·phen	WScCl ₃	WScCl ₄	WSBr ₄
μ (B.M.)	0.75	1.07	1.85	1.71	1.68	2.01	1.74	1.99	0.54		
ν (M = S) ^a (cm^{-1})			480	475	470	475	490	460		569s	555s
Infrared	383(sh)	340s ^b	320s,br ^b	320s,br ^b	315s,br ^b	320s ^b	340s ^b	335s ^b	373s	392(sh)	395w
spectra,	364m	285m	285(sh)	285s		300s	322s	330s	334s	355s	346w
other	320m	270m	245w			280(sh)	255	295s	298w	306s	250m
bands	271w							235w		284w	

^a M = Mo, W.

^b Designated as probable Mo—Cl bands [see Britnell *et al.* (16)].

been found as the ultimate product in the decomposition of alkylthiolates prepared using the reagents RSSiMe_3 ($\text{R} = \text{Me}, \text{Et}, t\text{-Bu}$) as follows:



where rate $t\text{-Bu} > \text{Et} > \text{Me}$ (11). The infrared spectrum of MoSCl_3 (14) is devoid of bands above 383 cm^{-1} (Table VI), which indicates a polymeric structure containing $\text{Mo}-\text{S}-\text{Mo}$ bridges. The compound is paramagnetic, and this has been attributed to the interactions between electrons on adjacent metal atoms through nonlinear bridging systems. X-Ray powder photographs show MoSCl_3 to be isomorphous with MoOCl_3 and NbOCl_3 , which have six-coordinate metal atoms bridged by both chlorine and oxygen atoms (16).

On prolonged reaction with neat donor solvents (16), acetonitrile and pyridine, the adducts $\text{MoSCl}_3 \cdot n\text{MeCN}$ ($n = 1$ or 2) and $\text{MoSCl}_3 \cdot 3\text{py}$ are formed. The $\text{MoSCl}_3 \cdot n\text{MeCN}$ adducts contain $\text{Mo}-\text{S}-\text{Mo}$ bridges and terminal $\text{Mo}=\text{S}$ bonds. On the basis of magnetic measurements and infrared spectra (Table VI), each adduct appears to have a monomeric structure based on six-coordinate molybdenum atoms. The complex $\text{MoSCl}_3 \cdot 2\text{MeCN}$ will react with other ligands, 1,4-dioxane and 1,2-bis(methoxy)ethane, to form $\text{MoSCl}_3 \cdot 2\text{diox}$ and $\text{MoSCl}_3 \cdot \text{bme}$. With pyridine the pyridinium salt, $[\text{Hpy}]^+[\text{MoSCl}_4\text{py}]^-$, is formed, and 1,10-phenanthroline has been found to reduce molybdenum(V) to molybdenum(IV) forming $\text{MoSCl}_2 \cdot \text{phen}$. Reactions of MoSCl_3 alone with these ligands did not proceed, and it appears that $\text{Mo}-\text{S}-\text{Mo}$ bridges are more resistant to attack by donor ligands than $\text{Mo}-\text{O}-\text{Mo}$ bridges.

In 1967 MoS_2Cl_2 was reported (72) as the product when S_2Cl_2 was passed over molybdenum metal heated to 500°C . Sharma *et al.*, (81) in an attempt to prepare MoOS_2 , bubbled H_2S through a solution of MoOCl_4 in dry benzene. The brown precipitate they obtained was also tentatively identified as MoS_2Cl_2 . Later, by passing H_2S through MoCl_4 in CS_2 , Britnell *et al.* (15) obtained the same compound. In spite of the fact that this compound has been reported three times, it has still not been conclusively characterized.

If a large excess of S_2Cl_2 is heated with molybdenum pentachloride at 250°C low yields of MoS_2Cl_3 are produced (36), Marcoll *et al.* (51) have solved the structure of this compound, which contains (S_2) bridging groups (Fig. 5). It is clearly related to that of NbS_2Cl_2 (Fig. 3).

After volatiles were removed from mixtures of MoCl_3 and sulfur which had been heated to 450°C for 24 hours the residue was found to

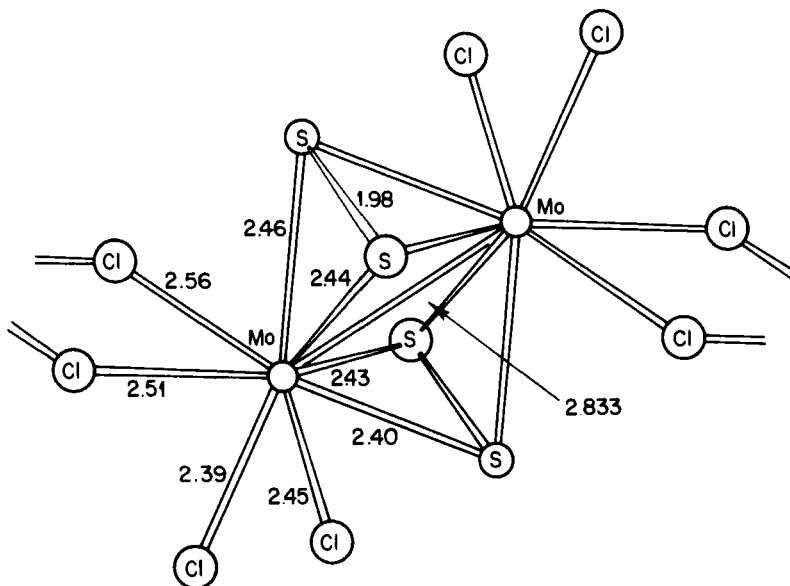


FIG. 5. Crystal structure of MoS_2Cl_3 (51). Reproduced with permission.

be a single compound which decomposed at 530°C evolving sulfur chlorides and forming MoS_2 (55). The compound, $\text{Mo}_3\text{S}_7\text{Cl}_4$, has been studied crystallographically and contains not only bridging (S_2) groups, but also a sulfur atom in the center of a triangle of molybdenum atoms (Fig. 6) (51).

$\text{Mo}_3\text{S}_7\text{Br}_4$, a brown, air-stable, amorphous powder, has been prepared by heating MoBr_2 with sulfur at 300°C (57). Its infrared spectrum has been recorded but not interpreted.

$\text{Mo}_2\text{S}_4\text{Cl}_5$, a brown microcrystalline solid, results when MoS_3 is treated with S_2Cl_2 at 350°C . The same reaction at 450°C produces red $\text{Mo}_2\text{S}_5\text{Cl}_3$, which may also be prepared by the reaction of molybdenum metal with excess S_2Cl_2 at 450°C (72). Both compounds are air-stable and are oxidized to MoO_3 at 250°C . The analogous bromine-containing compound, $\text{Mo}_2\text{S}_5\text{Br}_3$, may be prepared in a similar fashion from S_2Br_2 . Both this and $\text{Mo}_2\text{S}_5\text{Cl}_3$ have been shown to contain $\text{Mo}-\text{S}-\text{Mo}$ bridges and (S_2) groups by infrared spectroscopy (Table VII) (61, 63). The reaction of $[\text{Mo}_6\text{Cl}_8]\text{Cl}_4$ and dimeric MoCl_2 with sulfur at 380°C – 400°C gives $\text{Mo}_3\text{S}_7\text{Cl}_4$ (53).

The compound $\text{Mo}_6\text{SBr}_{10}$ is formed when molybdenum powder, MoBr_3 , and sulfur are heated to 1100°C (62), and $[\text{Mo}_6\text{I}_8]\text{S}_{14}$ results from the reaction of MoI_3 or MoI_2 with sulfur (47).

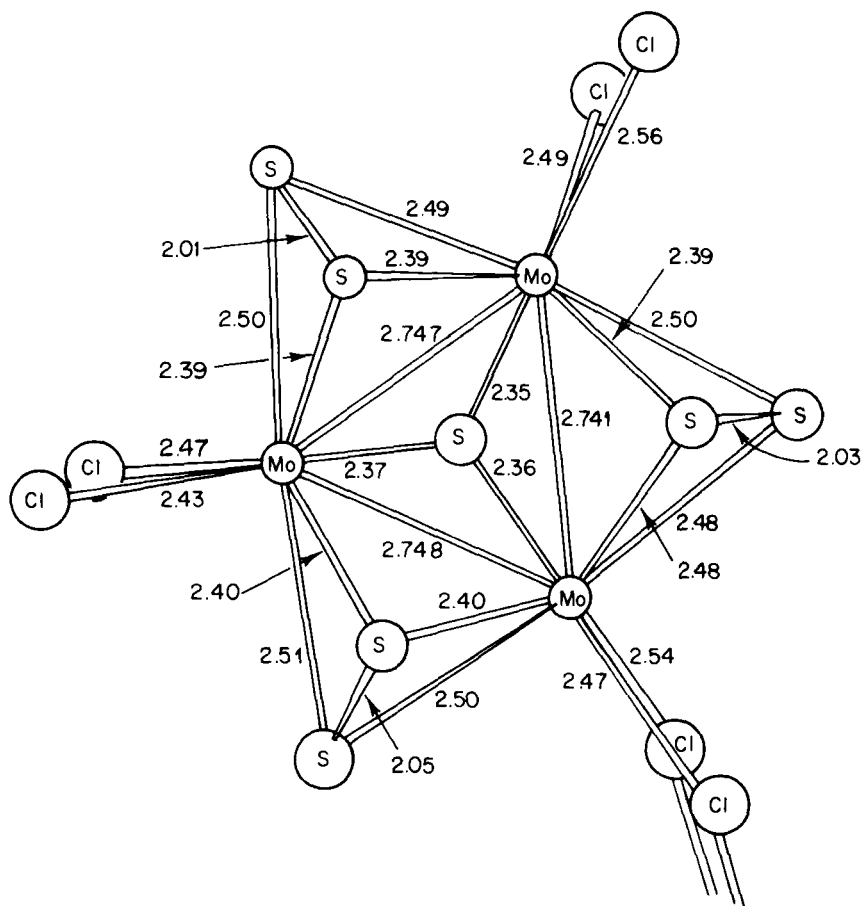


FIG. 6. Crystal structure of $\text{Mo}_3\text{S}_7\text{Cl}_4$ (51). Reproduced with permission.

Selenohalide chemistry of molybdenum is not as extensive as that of the thiohalides. Black MoSeCl_2 is produced during the disproportionation of MoSeCl_3 or by the action of Sb_2Se_3 on MoCl_4 (15). Attempts to prepare MoSeBr_2 from MoSe_2 and bromine result only in the formation of molybdenum tribromide and selenium tetrabromide (56). Molybdenum selenotrichloride (MoSeCl_3) is a maroon solid prepared by treating MoCl_5 with Sb_2Se_3 (15). Attempts to prepare complexes with py, phen, diox, and bme have failed (16). Both $\text{Mo}_3\text{Se}_7\text{Cl}_4$ and $\text{Mo}_3\text{Se}_7\text{Br}_4$ have been prepared, the former from MoCl_3 (55) or

TABLE VII
FREQUENCIES (IN CM^{-1}) OF INFRARED AND RAMAN VIBRATIONS OF
MOLYBDENUM THIOHALIDES $\text{Mo}_2\text{S}_5\text{X}_3$ ($\text{X} = \text{Cl, Br, I}$) (61, 63)

Assignments	Compound				
	$\text{Mo}_2\text{S}_5\text{Cl}_3$		$\text{Mo}_2\text{S}_5\text{Br}_3$		$\text{Mo}_2\text{S}_5\text{I}_3$
	IR	Raman	IR	Raman	IR
S—S			560(sh)	565vs	550(sh)
	560vs	570vs	555vs	555(sh)	545vs
Mo—S	397w	420m	395w	395w	390w
	368w	368m	360w	366m	362w
	335w	332m	335m	320m	335w
	315vs		315vw		305s
	295(sh)				295(sh)
	280(sh)	288s	278m	280s	272w
			250(sh)		250vw
	192w	176m	185w	180m	180w
	168m		165s		165m
Mo—X	405w	417w	335m	341w	215m
	340vs	343vw	253vs	257m	140vs
	305vs	306(sh)	227vs	224w	118vs
	257vs	245s	170s	165w	
	240m	235(sh)	150w	155w	

$[\text{Mo}_6\text{Cl}_8]\text{Cl}_4$ (53) and selenium and the latter from MoBr_3 and selenium (57). A compound $[\text{Mo}_6\text{I}_8]\text{Se}_{14}$ results from the reaction of MoI_3 or MoI_2 with selenium (47), and $\text{Mo}_6\text{SeBr}_{10}$ and $\text{Mo}_6\text{SeI}_{10}$ are formed when molybdenum powder, the appropriate metal halide, and selenium are heated to 1100°C (62).

All attempts to prepare molybdenum tellurohalides have failed (15).

C. TUNGSTEN

More work has been published on the thio- and selenohalides of tungsten than on any other transition element.

The first reported preparation of a tungsten thiochloride was by Smith and Oberholtzer (84), who obtained it from the reaction of red-hot tungsten metal with sulfur monochloride. Brown WScI_2 has been reported as being formed when WScI_3 disproportionates at 275°C . WSBr_2 has been prepared from the reaction of WBr_5 with Sb_2S_3 (15). Tungsten thiotrichloride itself has been synthesized by heating finely divided, intimately mixed WCl_5 and Sb_2S_3 at $120^\circ\text{--}150^\circ\text{C}$ for 7 days

(14, 15). Tungsten thiotrichloride, WScCl_3 , is a black involatile solid which appears, from its infrared spectrum, to contain W—S—W bridges (14) (see Table VI). WScCl_3 does not form complexes with py, phen, diox, or bme (16).

Red, air-sensitive, WScCl_4 is the most studied transition-metal thiohalide; it can be prepared by many methods, such as the action of chlorine on WS_2 or WS_3 in a flow system (15), by treating WCl_6 with Sb_2S_3 (14, 15) or sulfur (14, 15, 37, 86), by heating a mixture of WCl_5 and sulfur (15), or by the reaction of WCl_5 with RSSiMe_3 ($\text{R} = \text{Me}$, Et , $t\text{-Bu}$) and the subsequent decomposition of the product $\text{WCl}_5(\text{SR})$ (11). The rate of decomposition of the alkylthiolates is in the order $t\text{-Bu} > \text{Et} > \text{Me}$ (11).

WScCl_4 is a diamagnetic compound that readily sublimes under vacuum to form triclinic crystals. The crystal structure has been studied (30). Each tungsten atom is strongly bonded to a sulfur atom and four chlorine atoms in a square-based pyramidal arrangement with the sulfur apical. Two of these WScCl_4 units form a dimer with two weak W—Cl bridges trans to the tungsten—sulfur bonds (Fig. 7).

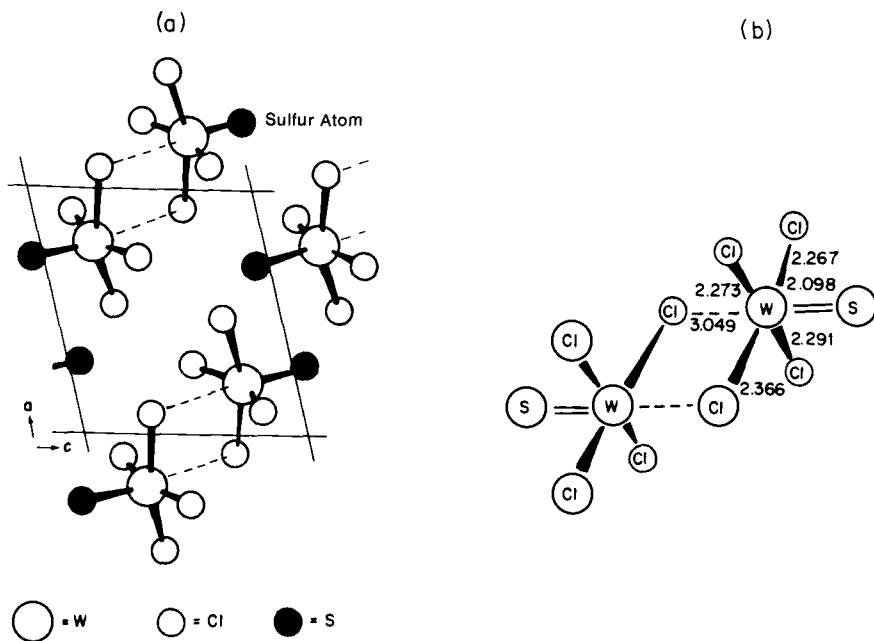


FIG. 7. Crystal structure of WScCl_4 (30). (a) The contents of the unit cell in the b projection. (b) The $(\text{WScCl}_4)_2$ dimer, showing bond lengths. Reproduced with permission.

The mass spectrum of WScI_4 (82) comprises a fragmentation pattern, similar to those of MoOCl_4 , WOCl_4 , and WOBr_4 , in which the parent ion, WScI_4^+ , is only 1% abundant and the most abundant ion is WScI_3^+ . As WScI_3 is involatile, the WScI_3^+ ion could only have been formed by the fragmentation and ionization of WScI_4 . The infrared spectrum of tungsten thiotetrachloride has been reported (14), the main features being strong bands at 569 cm^{-1} and 355 cm^{-1} assigned to $\text{W}=\text{S}$ and $\text{W}-\text{Cl}$ stretching modes respectively (Table VI).

Tungsten thiotetrabromide, WSBr_4 , may be prepared from the reaction of antimony trisulphide with WBr_6 (14, 15) or WBr_5 (15), along with WSBr_2 , and from the reaction of WBr_6 with elemental sulphur (15). It dissolves and forms adducts in donor solvents and its infrared spectrum (14) has a strong band at 555 cm^{-1} assigned to a $\nu(\text{W}=\text{S})$ (Table VI).

WS_2Cl_2 , a blue-black amorphous solid, first reported as the final product when H_2S was bubbled through WOCl_4 in dry benzene (81), has since been prepared by bubbling H_2S through WCl_6 in CS_2 at 18°C (15) and by the reaction of WScI_4 with Sb_2S_3 in CS_2 at room temperature (39, 73). The last reaction, WYCl_4 ($\text{Y} = \text{O}, \text{S}, \text{Se}$) with $\text{Sb}_2\text{Y}'_3$ ($\text{Y}' = \text{O}, \text{S}, \text{Se}$) in CS_2 , has also been employed to prepare WOSCl_2 , WOSeCl_2 , and WSSeCl_2 (39, 73). Best yields are obtained when Y' is lower in the group than Y .

The selenohalides of tungsten are less well known than the thiohalides. Attempts to prepare WSeBr_2 by brominating WSe_2 only resulted in the formation of WBr_6 and SeBr_4 (56), and, so far, WSeBr_2 has been prepared only during the disproportionation of WSeBr_3 (15). Tungsten selenotribromide may be prepared when WBr_5 is heated with Sb_2Se_3 . The analogous reaction employing WCl_5 results in the formation of WSeCl_3 (15). Both WSeCl_4 and WSeBr_4 are known and may be synthesized by heating a mixture of the appropriate tungsten hexahalide and Sb_2Se_3 (15). The infrared spectra of both compounds have been recorded (15), and that of WSeCl_4 has a strong band at 396 cm^{-1} assigned to $\text{W}=\text{Se}$ while the equivalent feature is absent from the WSeBr_4 spectrum.

The compounds WXY_4 ($\text{X} = \text{S}, \text{Se}$; $\text{Y} = \text{Cl}, \text{Br}$) react with a number of ligands, containing nitrogen, oxygen, phosphorus, and sulfur donor atoms, to form the six-coordinate adducts $\text{WXY}_4\cdot\text{L}$ and $2\text{WXY}_4\cdot\text{L}'$ ($\text{L} = \text{unidentate}$; $\text{L}' = \text{bidentate}$) in which the terminal $\text{W} = \text{X}$ is retained (17). With tetrahydrofuran, 1,4-dioxane and acetonitrile all four compounds form 1:1 adducts. With pyridine and 1,4-oxathian, 1:1 adducts are formed by the chlorides only, the bromides forming 1:2 complexes, $\text{WXBr}_4\cdot 2\text{py}$, with pyridine. The reactions of all four com-

pounds with 2,2'-bipyridyl result in nonstoichiometric products that were not characterized. With 1,2-bis(methylthio)ethane WSY_4 reacts to form both $WSY_4 \cdot mte$ and $2WSY_4 \cdot mte$. When $WSeCl_4$ was allowed to react with a large excess of acetonitrile evidence was obtained for the adduct $WCl_4 \cdot NCMe \cdot NCSeMe$, in which the selenium atom was incorporated into an acetonitrile molecule. The adduct, however, was not isolable. Under severe conditions, such as high temperature or a large excess of ligand, reduction to tungsten(V) or even tungsten(IV) took place. With excess 1,2-bis(methylthio)ethane $WSeCl_4$ formed $WSeCl_3 \cdot mte$ which has a band at 535 cm^{-1} in its IR spectrum assigned to $\nu(W=S)$. Such a band does not occur in the IR spectrum of $WSeCl_3$, which is thought to contain $W-S-W$ bridges (Table VI). Excess 2,2'-bipyridyl also reduces W(VI) to W(V) forming $WSeCl_3 \cdot bipy$ from $WSeCl_4$. At high temperatures triphenylphosphine reduces WXY_4 to W(IV) by abstracting the chalcogen atom and incorporating it in a PPh_3 molecule forming $WX_4 \cdot PPh_3 \cdot P(Y)Ph_3$.

The reaction between $WSeCl_4$ and 1,2-bis(methoxy)ethane results in oxygen abstraction and the resultant formation of $WSeCl_4 \cdot WOSCl_2 \cdot bme$, which has been investigated by X-ray crystallography (12). The $WSeCl_4$ and $WOSCl_2$ units are linked through the oxygen atom, both tungsten atoms having a distorted octahedral environment (Fig. 8).

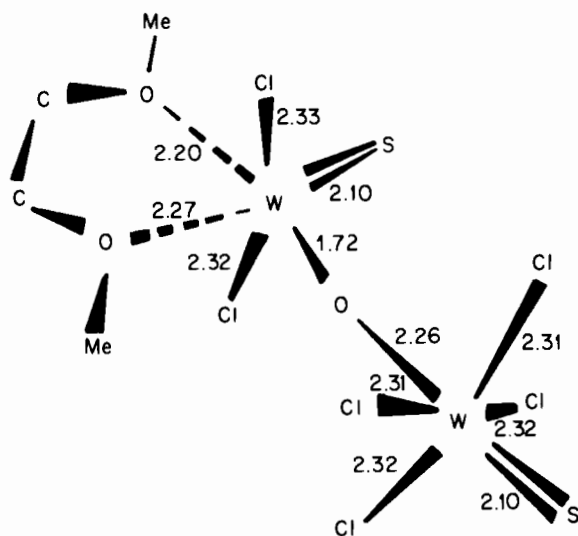


FIG. 8. Crystal structure of $WSeCl_4 \cdot WOSCl_2 \cdot dme$ (12). Reproduced with permission.

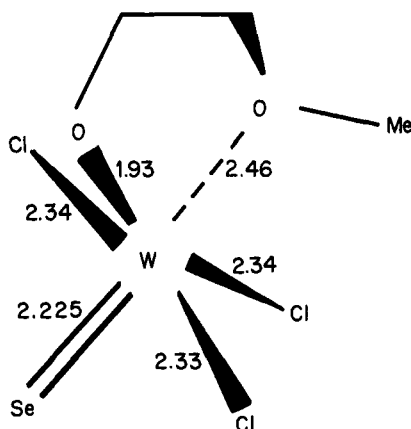


FIG. 9. Crystal structure of $C_3H_7Cl_3O_2SeW$ (13). Reproduced with permission.

The analogous reaction with $WSeCl_4$ results in selective demethylation and the formation of selenotrichlorotungsten(VI)-(2-methoxy) ethoxide (Fig. 9) (13).

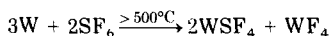
Excepting yttrium and lanthanum, which are usually classed as lanthanides, not transition metals, tungsten is the only transition element for which thiofluoride species have been reported (1, 18, 45, 48–50). Gaseous SF_6 , when admitted to a tungsten effusion cell at 1600 K, reaches an equilibrium. The equilibrium mixture was investigated by mass spectrometry, and among those species identified were WSF_3^+ , WSF_4^+ , $WS_2F_2^+$, and $WOSF_2^+$ (45). ^{19}F NMR studies of the reaction of $WSeCl_4$ in acetonitrile with HF have revealed the existence of WSF_4 , $WSFCl_4^-$, $WSF_2Cl_3^-$, $WSF_3Cl_2^-$, WSF_4Cl^- , WSF_5^- , and $W_2S_2F_9^-$ (1, 18); and with XeF_2 , WSF_4 , WSF_3Cl , WSF_2Cl_2 , and $WSFCl_3$ are formed (1). These species are all extremely unstable and readily form oxyfluorotungsten anions.

The reactions of inorganic sulfides with WF_6 in acetonitrile have been studied by ^{19}F NMR (48). It was found that short-lived monothiofluoride species were formed when sulfur replaced two fluorines on the tungsten atom. The greatest yields were obtained using H_2S , and the species were also formed when K_2S , Na_2S , Bu_2S , Ph_2S , Me_2S_2 , and thiourea were used. Attempts to prepare WSF_4 by passing H_2S through WOF_4 in MeCN and through $K_2WO_2F_4$ in DMSO yielded no product.

In spite of the observations of WSF_4^+ and $WS_2F_2^+$ (45) mass spectrometrically and of $WSeCl_xF_y^-$ ($x + y = 5$) by ^{19}F NMR (18), only recently has any thiofluoride been isolated as a solid compound (1). Thus yellow

WSF_4 is the main product of the reaction of WF_6 with Sb_2S_3 at 300°C ($3\text{WF}_6 + \text{Sb}_2\text{S}_3 \rightarrow 3\text{WSF}_4 + 2\text{SbF}_3$). Crystals of WSF_4 melt at $\sim 90^\circ\text{C}$ and, on exposure to the atmosphere, HF and H_2S are rapidly evolved. The main features of the infrared spectrum of the solid include strong peaks at 699, 673, and 643 cm^{-1} which can be attributed to $\nu(\text{W}-\text{F})$ for three terminal fluorines. The $\text{W}=\text{S}$ bond is evidenced by an intense peak at 577 cm^{-1} in the IR and at 580 cm^{-1} in the Raman, which are close to that for $\nu(\text{W}=\text{S})$ in WScI_4 . Observation of peaks at 534 and 514 cm^{-1} in the infrared, which can be assigned to $\text{W}-\text{F}-\text{W}$ bridge vibrations, suggest that the structure is polymeric, and it has been suggested that it may be the same as that of WOF_4 (1). ^{19}F NMR spectra of WSF_4 in MeCN show the characteristic singlet at τ , -85.1 ppm. Solutions of WSF_4 in MeCN decompose slowly over several weeks to give WF_6 and WS_3 (1).

WSF_4 has also been recently obtained by condensation of the product formed by the reaction of a tungsten filament with SF_6 at 200 torr (20):



The WSF_4 was identified by its ^{19}F NMR spectrum.

The adduct $\text{WSF}_4 \cdot \text{MeCN}$ was prepared when the reaction between H_2S and WF_6 in MeCN was recently reexamined (50). It has also been observed in the products of reaction of WSF_4 with BuNH_2 or H_2O in MeCN (19). The complex melted at 106°C with partial decomposition, and H_2S was evolved on exposure to air (50). $\text{WS}_2\text{F}_2 \cdot 2\text{MeCN}$ was also isolated when H_2S was passed through a solution of $\text{WSF}_4 \cdot \text{MeCN}$ in acetonitrile for a prolonged period. The replacement of the acetonitrile molecule of the complex by ethanol, phenol, 1,2-ethanediol, acetylacetone, diethylamine, and BuSH has been examined by ^{19}F NMR (49). It was found that the new complexes were formed less readily than their oxyfluoride counterparts. The adduct $\text{WSF}_4 \cdot \text{H}_2\text{O}$ has been observed as a product of the reaction of WSF_4 with H_2O in MeCN (19).

The first transition-metal selenofluoride, WSeF_4 , has recently been prepared by the reaction of stoichiometric quantities of WF_6 and Sb_2Se_3 at 350°C (2). The amber solid quickly decomposes in the atmosphere, liberating HF and H_2Se . The infrared spectrum is very similar to that of WSF_4 , with strong peaks at 690, 661, and 629 cm^{-1} [$\nu(\text{W}-\text{F})$], 366 cm^{-1} [$\nu(\text{W}=\text{Se})$] and 540 and 517 cm^{-1} [$\text{W}-\text{F}$ bridging modes]. ^{19}F NMR spectra in CH_3CN gave rise to a singlet at $\tau = -87.9$ ppm ($\tau = 0$ ppm. for CFCI_3), $J_{\text{W}-\text{F}} = 36 \pm 1\text{ Hz}$, which was assigned to WSeF_4 (2).

As with molybdenum, all attempts to prepare tungsten tellurohalides have been unsuccessful (15).

VI. Group VIIA

A. MANGANESE

Manganese selenochloride, MnSeCl , a green crystalline solid, has been prepared by the direct chlorination of MnSe (6). It decomposes in air and water, and upon heating to 90°C *in vacuo* gray MnSe_2Cl_2 is formed.

Manganese thiodichloride, MnSCl_2 , can be made by heating MnS and chlorine in a bomb for 35 hours. It is reported to be slightly soluble in water (7). Brown MnSeBr_2 , prepared by heating MnSe and bromine in a bomb, is readily hydrolyzed on exposure to air and is thermally unstable. At 70°C *in vacuo* Mn_2SeBr_2 is formed. This yellow-gray material is reported to turn brown at 100°C , but its empirical composition remains unchanged (6). Manganese selenodiodide (MnSeI_2), prepared by heating a mixture of MnSe and iodine to 160°C for 20 hours, has also been obtained (6).

B. RHENIUM

Direct chlorination of ReS_2 results in the formation of a small amount of nonvolatile, brown, ReSCl_2 as a minor product (87). The compounds ReSCl_2 and ReSBr_2 have also been observed in DTA studies of the reaction of the appropriate trihalide with sulfur. The related ReS_2Br has also been detected in the reaction of ReBr_3 with sulfur (80). Rhenium thiodichloride, along with $\text{Re}_2\text{S}_3\text{Cl}_4$, has been isolated following the direct chlorination of Re_2S_7 in a flow system (42) and from the rhenium-sulfur-chlorine system (31). The thiochlorides, ReS_3Cl and ReSCl_4 (m.p. $80 \pm 2^\circ\text{C}$), have been isolated from $\text{ReS}_2\text{-S}_2\text{Cl}_2$ and the $\text{ReCl}_3\text{-S}_2\text{Cl}_2$ systems (31). Rhenium thiotrichloride, ReSCl_3 , prepared from the reaction of ReCl_5 with Sb_2S_3 in carbon disulfide at low temperatures, has also recently been isolated (39).

The reactions of ReSCl_2 with hydrogen and steam at 350°C have been studied. With hydrogen, hydrogen chloride is formed leaving ReS and with steam, HCl is again formed while amorphous ReOS remains (41).

Three rhenium selenohalides have been reported. Brown ReSeCl_2 is formed when ReSe_2 is heated, under chlorine, in a sealed quartz ampoule (56), or when ReCl_3 and Se combine (80). The related bromide, ReSeBr_2 , has also been observed in DTA studies (80). Brown, $\text{Re}_3\text{Se}_2\text{Cl}_5$ is the product when a mixture of ReSe_2 and Re_3Cl_9 is heated to 700°C (56), and air-stable, dark violet $\text{Re}_3\text{Se}_2\text{Br}_5$, is produced by the analo-

gous reaction using ReBr_3 or by heating ReSe_2 to 600°C under an atmosphere of bromine (56).

VII. Group VIII

PLATINUM

There has been only one report of a thiohalide of platinum (8). Heating a mixture of PtX_2 ($\text{X} = \text{Cl}, \text{Br}$), and sulfur produces a series of compounds PtX_mS_n , where m and n depend upon the ratio of reactants and the reaction temperature.

VIII. Group IB

A. COPPER

Copper seleno- and tellurohalides may be prepared in polycrystalline form by the reaction of stoichiometric amounts of copper(I) halide with selenium or tellurium in a sealed ampoule at $300\text{--}350^\circ\text{C}$. However, separation from other phases often causes difficulties. Many can be obtained as single crystals by the reaction of the respective elements, binary compounds, or both with the appropriate hydrogen halide acid under hydrothermal conditions (65, 66, 68), or by chemical transport during the reaction of the appropriate copper(I) halide with selenium or tellurium in a temperature gradient (22). The compounds that have been prepared are listed in Table VIII with X-ray photographic and

TABLE VIII
X-RAY CRYSTALLOGRAPHIC AND SPECTRAL REFLECTION DATA FOR COPPER
CHALCOGENIDE HALIDES (22, 64, 65)

Compound	Symmetry	Unit cell dimensions				Z	Optical band gaps (eV)
		a (Å)	b (Å)	c (Å)	β°		
CuSe_2Cl	Monoclinic	7.62	4.68	30.73	91.6	12	1.6
CuSe_3Br	Orthorhombic	7.64	4.49	14.23		4	~2.0
CuSe_3I	Rhombohedral ^a	14.083		14.187		18	
CuTeCl	Tetragonal	15.53		4.78		16	1.4
CuTeBr		16.417		4.711			
CuTeI		17.07		4.83			
CuTe_2Cl	Monoclinic	8.168	4.195	15.187	134.9	4	1.2
CuTe_2Br		8.358	4.951	15.704	135.1		
CuTe_2I		8.672	4.881	16.493	135.0		

^a Referred to a hexagonal cell.

optical band gap data. All the compounds are air-stable and exhibit temperature-independent diamagnetism, which implies that copper is present as Cu(I). The tellurium compounds are stable in alkali but decompose in concentrated HNO_3 and H_2SO_4 . The selenium compounds are readily decomposed by alkali.

A recent single-crystal determination on CuTeBr (21) has shown that the structure consists of infinite spirals of tellurium atoms with bromine tetrahedra interspersed. Two basic types of disordered copper atoms occur: one where the copper atom is at the center of the bromine tetrahedron, the other where the copper lies in two possible sites in a distorted tetrahedral environment with tellurium and two bromine atoms as nearest neighbors.

B. SILVER

Differential thermal analytical investigations of the $\text{AgCl-Ag}_2\text{Se}$, $\text{AgCl-Ag}_2\text{Te}$, $\text{AgBr-Ag}_2\text{Se}$, and $\text{AgBr-Ag}_2\text{Te}$ systems have led to the discovery of two peritectic compounds, Ag_3TeBr and $\text{Ag}_5\text{Te}_2\text{Cl}$ (9).

C. GOLD

Both AuSeCl and AuSeBr are known; the former is produced when a gold selenium mixture is heated to 200°C under an atmosphere of chlorine, and the latter when AuSe is heated under bromine (70). Each compound crystallizes in the orthorhombic system.

Hydrothermal synthetic methods analogous to those used in the preparation of copper chalcogenides have been used to prepare gold halide tellurides (65, 67, 69). The compounds are listed and preparative conditions are summarized in Table IX. All are insoluble in dilute acid and alkali and decompose in concentrated HNO_3 and H_2SO_4 .

Earlier X-ray diffraction data for AuTe_2X ($\text{X} = \text{Cl}, \text{Br}, \text{I}$) from powders has been more recently refined by single-crystal studies on AuTe_2Cl and AuTe_2I . The compound AuTe_2Cl is orthorhombic, space group Cmcm , with $a = 4.020$, $b = 11.867$, $c = 8.773 \text{ \AA}$, $z = 4$; and AuTe_2I is orthorhombic, space group Pmmb , with $a = 4.056$, $b = 12.579$, $c = 4.741 \text{ \AA}$, $z = 2$. The structures consist essentially of corrugated two-dimensional nets of Au and Te atoms with interleaved halogens. This explains their metallic conductivity. The Te atoms form pairs coordinated to four Au atoms, and each Au is coordinated to four Te atoms (43). The iodine, AuTeI is monoclinic, with $a = 7.245$, $b = 7.622$, $c = 7.313 \text{ \AA}$ and $\beta = 106.3^\circ$ (65).

TABLE IX
 PREPARATIVE CONDITIONS FOR GOLD HALIDE TELLURIDES (65)

Compound	Starting materials (grams)	Solvent	Temperature (°C)	Time (days)
AuTe ₂ Cl	5.9 Au 1.9 Te 1.0 Cl	HCl	100–400	10
AuTe ₂ Br	13.9 Au 5.1 Te 5.7 Br	HBr	150–350	10
AuTe ₂ I	6.2 Au 4.0 Te	HI	150–450	10
AuTeI ^a	6.2 Au 4.0 Te 8.0 I	HI		

^a The corresponding AuTeCl and AuTeBr were not obtained.

REFERENCES

1. Atherton, M. J., and Holloway, J. H., *J. Chem. Soc., Chem. Commun.* p. 424 (1977).
2. Atherton, M. J., and Holloway, J. H., *Inorg. Nucl. Chem. Lett.* **14**, 121 (1978).
3. Baghlaf, A. O., M. Sc. Thesis, University of Manchester, England (1972).
4. Baghlaf, A. O., and Thomson, A., *J. Less-Common Metals* **53**, 291 (1971).
5. Batsanov, S. S., Filatkina, V. S., and Kustova, G. N., *Izv. Akad. Nauk SSSR, Ser. Khim.* p. 1190 (1971).
6. Batsanov, S. S., and Gorogotskaya, L. I., *Izv. Sib. Otd. Akad. Nauk SSSR, Ser. Khim. Nauk* p. 42 (1959).
7. Batsanov, S. S., and Gorogotskaya, L. I., *Zh. Neorg. Khim.* **4**, 62 (1959).
8. Batsanov, S. S., Ruchkin, E. D., and Khripin, L. A., *Izv. Akad. Nauk SSSR, Neorg. Mater.* **2**, 105 (1966).
9. Blachnik, R., and Kudermann, G., *Z. Naturforsch., Teil B* **28**, 1 (1973).
10. Boehland, H., and Schneider, F. M., *Z. Chem.* **12**, 28 (1972).
11. Boorman, P. M., Chivers, T., Mahadev, K. N., and O'Dell, B. D., *Inorg. Chim. Acta* **19**, L35 (1976).
12. Britnell, D., Drew, M. G. B., Fowles, G. W. A., and Rice, D. A., *J. Chem. Soc., Chem. Commun.* p. 462 (1972).
13. Britnell, D., Drew, M. G. B., Fowles, G. W. A., and Rice, D. A., *Inorg. Nucl. Chem. Lett.* **9**, 415 (1973).
14. Britnell, D., Fowles, G. W. A., and Mandyczewsky, R., *J. Chem. Soc., Chem. Commun.* p. 608 (1970).
15. Britnell, D., Fowles, G. W. A., and Rice, D. A., *J. Chem. Soc., Dalton Trans.* p. 2191 (1974).
16. Britnell, D., Fowles, G. W. A., and Rice, D. A., *J. Chem. Soc., Dalton Trans.* p. 28 (1975).
17. Britnell, D., Fowles, G. W. A., and Rice, D. A., *J. Chem. Soc., Dalton Trans.* p. 213 (1975).

18. Buslaev, Y. A., Kokunov, Y. V., and Chubar, Y. D., *Dokl. Akad. Nauk SSSR* **213**, 912 (1973).
19. Buslaev, Y. A., Kokunov, Y. V., Gustyakova, M. P., Chubar, Y. D., and Moiseev, I. I., *Dokl. Akad. Nauk. SSSR* **233**, 357 (1977).
20. Butskii, V. D., and Perov, V. S., *Russ. J. Inorg. Chem. (Engl. Transl.)* **22**, 6 (1977).
21. Carkner, P. M., and Haendler, H. M., *J. Solid State Chem.* **18**, 183 (1976).
22. Carkner, P. M., and Haendler, H. M., *J. Cryst. Growth* **33**, 196 (1976).
23. Dragon, C., *C. R. Hebd. Seances Acad. Sci., Ser. C* **262**, 1575 (1966).
24. Dragon, C., *C. R. Hebd. Seances Acad. Sci., Ser. C* **273**, 352 (1971).
25. Dragon, C., *C. R. Hebd. Seances Acad. Sci., Ser. C* **275**, 817 (1972).
26. Dragon, C., *C. R. Hebd. Seances Acad. Sci., Ser. C* **283**, 743 (1976).
27. Dragon, C., and Thévet, F., *C. R. Hebd. Seances Acad. Sci., Ser. C* **268**, 1867 (1969).
28. Dragon, C., and Thévet, F., *C. R. Hebd. Seances Acad. Sci., Ser. C* **271**, 677 (1971).
29. Dragon, C., and Thévet, F., *Ann. Chim. (Paris)* [14] **6**, 67 (1971).
30. Drew, M. G. B., and Mandyczewsky, R., *J. Chem. Soc. A* p. 2815 (1970).
31. Drobot, D. V., Korshunov, B. G., and Kovacheva, S. L., *Russ. J. Inorg. Chem. (Engl. Transl.)* **17**, 139 (1972).
32. Dung, N. H., *Bull. Soc. Chim. Fr. Mineral Cristallogr.* **96**, 41 (1973).
33. Dung, N. H., *Acta Crystallogr., Sect. B* **29**, 2095 (1973).
34. Dung, N. H., Dragon, C., and Laruelle, P., *Acta Crystallogr., Sect. B* **31**, 519 (1975).
35. Ehrlich, P., and Siebert, W., *Z. Anorg. Allg. Chem.* **301**, 288 (1959).
36. Fortunatov, N. S., and Timoshchenko, N. I., *Uk. Khim. Zh.* **31**, 1078 (1965).
37. Fortunatov, N. S., and Timoshchenko, N. I., *Uk. Khim. Zh.* **35**, 1207 (1969).
38. Fowles, G. W. A., Hobson, R. J., Ibrahim, B. B., and Rice, D. A., *Abstr. Chem. Soc., Autumn Meet.* p. B6 (1975).
39. Fowles, G. W. A., Hobson, R. J., Rice, D. A., and Shanton, K. J., *J. Chem. Soc., Chem. Commun.* p. 552 (1976).
40. Glukhov, I. A., *Izv. Otd. Estestv. Nauk, Akad. Nauk Tadzh. SSR* p. 21 (1957).
41. Glukhov, I. A., Davidyants, S. B., El'manova, N. A., and Yunusov, M. A., *Russ. J. Inorg. Chem. (Engl. Transl.)* **8**, 47 (1963).
42. Glukhov, I. A., Davidyants, S. B., Yunusov, M. A., and El'manova, N. A., *Russ. J. Inorg. Chem. (Engl. Transl.)* **6**, 649 (1961).
43. Haendler, H. M., Mootz, D., Rabenau, A., and Rosenstein, G., *J. Solid State Chem.* **10**, 175 (1974).
44. Hahn, H., and Schmid, R., *Naturwissenschaften* **52**, 475 (1965).
45. Hildenbrand, D. L., *U.S. Navy Tech. Inf. Serv. AD Rep No. 757231* (1972).
46. Katscher, H., and Hahn, H., *Naturwissenschaften* **53**, 361 (1966).
47. Kirillovich, E. V., *Mater. Vses. Nauchn. Stud. Konf. Khim., 13th, 1975* p. 27 (1975).
48. Kokunov, Y. V., Chubar, Y. D., Bochkareva, V. A., and Buslaev, Y. A., *Koord. Khim.* **1**, 1100 (1975).
49. Kokunov, Y. V., Chubar, Y. D., and Buslaev, Y. A., *Koord. Khim.* **2**, 1227 (1976).
50. Kokunov, Y. V., Chubar, Y. D., Kopytin, A. V., and Buslaev, Y. A., *Koord. Khim.* **2**, 796 (1976).
51. Marcoll, J., Rabenau, A., Mootz, D., and Wunderlich, H., *Rev. Chim. Miner.* **11**, 607 (1975).
52. Markovskii, L. Y., Lantratov, V. M., and Pesina, E. Y., *Otkrytiya, Izobret., Prom. Obraztsy, Tovarnye Znaki* **52**, 51 (1975).
53. Mazhara, A. P., Opalovskii, A. A., Fedorov, V. E., and Kirk, S. D., *Zh. Neorg. Khim.* **22**, 1827 (1977).
54. Morozov, I. S., and Dergacheva, N. P., *Otkrytiya Izobret., Prom. Obraztsy, Tovarnye Znaki* **51**, 64 (1974).

55. Opalovskii, A. A., Fedorov, V. E., and Khaldoyanidi, K. A., *Dokl. Akad. Nauk SSSR* **182**, 907 (1968).
56. Opalovskii, A. A., Fedorov, V. E., Lobkov, E. U., and Erenburg, B. G., *Russ. J. Inorg. Chem. (Engl. Transl.)* **16**, 1685 (1971).
57. Opalovskii, A. A., Fedorov, V. E., Mazhara, A. P., and Cheremisina, I. M., *Russ. J. Inorg. Chem. (Engl. Transl.)* **17**, 1510 (1972).
58. Perrin, C., Chevrel, R., and Sergent, M., *C. R. Hebd. Seances Acad. Sci., Ser. C* **280**, 949 (1975).
59. Perrin, C., Chevrel, R., and Sergent, M., *C. R. Hebd. Seances Acad. Sci., Ser. C* **281**, 23 (1975).
60. Perrin, C., Perrin, A., and Caillet, P., *J. Chim. Phys. Phys.-Chim. Biol.* **70**, 101 (1973).
61. Perrin, C., Perrin, A., and Prigent, J., *Bull. Soc. Chim. Fr.* p. 3087 (1972).
62. Perrin, C., Sergent, M., and Prigent, J., *C. R. Hebd. Seances Acad. Sci., Ser. C* **277**, 465 (1973).
63. Perrin-Billot, C., Perrin A., and Prigent, J., *J. Chem. Soc., Chem. Commun.* p. 676 (1970).
64. Rabenau, A., and Rau, H., *Solid State Commun.* **7**, 1281 (1969).
65. Rabenau, A., and Rau, H., *Inorg. Synth.* **14**, 160 (1973).
66. Rabenau, A., Rau, H., and Rosenstein, G., *Naturwissenschaften* **56**, 137 (1969).
67. Rabenau, A., Rau, H., and Rosenstein, G., *Angew. Chem., Int. Ed. Engl.* **8**, 145 (1969).
68. Rabenau, A., Rau, H., and Rosenstein, G., *Z. Anorg. Allg. Chem.* **374**, 43 (1970).
69. Rabenau, A., Rau, H., and Rosenstein, G., *J. Less-Common Metals* **21**, 395 (1970).
70. Rabenau, A., Rau, H., and Rosenstein, G., *Monatsh. Chem.* **102**, 1425 (1971).
71. Radautan, S. I., Molodyan, I. P., Kovel, L. S., and Kus'menko, G. S., *Fiz.-Khim. Slozhnykh Poluprovodn.* p. 158 (1975).
72. Rannou, J. P. and Sergent, M., *C. R. Hebd. Seances Acad. Sci., Ser. C* **265**, 734 (1967).
73. Rice, D. A., *Abstr. Chem. Soc., Autumn Meet.* B5 (1975).
74. Riera, V., and Uson, R., *Rev. Acad. Cienc. Exactas, Fis-Quim. Natr. Zaragoza* **24**, 115 (1969).
75. Rysanek, N., and Loye, O., *Acta Crystallogr., Sect. B* **29**, 1567 (1973).
76. Schäfer, H., Bauer, D., Beckmann, W., Gerken, R., Nieder-Vahrenholz, H. G., Niehues, K. J., and Scholz, H., *Naturwissenschaften* **51**, 241 (1964).
77. Schäfer, H., and Beckmann, W., *Z. Anorg. Allg. Chem.* **347**, 225 (1966).
78. Schmid, R., and Hahn, H., *Z. Anorg. Allg. Chem.* **373**, 168 (1970).
79. Schnering, H. G. von, and Beckmann, W., *Z. Anorg. Allg. Chem.* **347**, 231 (1966).
80. Sergeevna, G. E., *Mater. Vses. Nauchn. Stud. Knof. Khim., 13th*, 1975 p. 26 (1975).
81. Sharma, K. M., Anand, S. K., Multani, R. K., and Jain, B. D., *Chem. Ind. (London)* p. 1556 (1969).
82. Singleton, D. L., and Stafford, F. E., *Inorg. Chem.* **11**, 1208 (1972).
83. Sinitsyna, S. M., Khlebodarov, V. G., and Bukhtereva, N. A., *Russ. J. Inorg. Chem. (Engl. Transl.)* **20**, 1267 (1975).
84. Smith, E. F., and Oberholtzer, V., *Z. Anorg. Allg. Chem.* **5**, 68 (1894).
85. Solvay and Cie, *Neth. Patent* 288, 255 (1964).
86. Timoshchenko, N. I., *U.S.S.R. Patent* 220,974 (1969).
87. Tronev, V. G., Bekhtle, G. A., and Davidyants, S. B., *Tr. Inst. Khim. Nauk, Akad. Nauk Kaz. SSR* **84**, 105 (1958).
88. Van Dyck, D., Van Landuyt, J., Amelinckx, S., Dung, N. H., and Dragon C., *J. Solid State Chem.* **19**, 179 (1976).
89. Verkhovets, M. N., Kamarazin, A. A., and Sokolov, V. V., *Izv. Sib. Otd. Akad. Nauk SSSR Ser. Khim. Nauk* p. 125 (1973).

NOTE ADDED IN PROOF

Preparative routes to, and the properties of, transition metal thio-, seleno-, and tellurohalides are the subject of an informative article by Rice (1) which serves as a useful complement to this review.

The series of thiochlorides $\text{Mo}_6\text{YCl}_{10}$ ($\text{Y} = \text{S}, \text{Se}, \text{Te}$) has recently been prepared (2) from the reaction between molybdenum dichloride, molybdenum metal and the elemental chalcogen at 1000°C in a silica reactor for about 24 hours. The compounds produced are isostructural with Nb_6I_{11} being of space group Pccn. with $z = 4$. The X-ray structure of octahedral crystals of dark red $\text{Mo}_6\text{SeCl}_{10}$ has been determined, this reveals a central $(\text{Mo}_6\text{X}'_8)$ unit in which the selenium atom is statistically distributed among the eight X' positions.

REFERENCES

1. D. A. Rice, *Coord. Chem. Rev.*, **25**, 199 (1978).
2. C. Perrin, M. Sergent, F. Le Traon and A. Le Traon, *J. Solid State Chem.* **25**, 197 (1978).

CORRELATIONS IN NUCLEAR MAGNETIC SHIELDING, PART II

JOAN MASON

Open University, Milton Keynes, Buckinghamshire, England

I. Introduction	199
II. Diamagnetic and Paramagnetic Currents	199
III. Shielding Terms	201
A. The Ramsey Theory	201
B. The "Atom in a Molecule" Approximation	204
C. The Diamagnetic Term and Xpes Connection	207
D. Other Restricted Term Approximations	210
E. Finite Perturbation Theory	211
IV. Patterns of Shielding in Inorganic Molecules	212
A. Excitation Energies	213
B. The Radial Factor and the Electric Field Gradient; the NQCC and Mössbauer Connection	214
C. Local Symmetry, Substituent Effects, and the Shielding Tensor	218
V. Main Group Elements	221
VI. Transition Metals	225
VII. Correlations with Spectroscopic and Other Properties	230
References	231
Note Added in Proof	236

I. Introduction

Nuclear magnetic shielding in molecules depends on the currents induced by the magnetic field in the conductor formed by the molecular electronic atmosphere. This is no simple matter, and in suitably chosen compounds the chemical shifts may correlate with a variety of other physical, spectroscopic, and chemical properties of the molecule (which here includes ions and extended structures). Such correlations form the subject of this article, which, like Part I (*111a*), aims to describe physical models and chemical and spectroscopic relationships of interest to the inorganic chemist.

II. Diamagnetic and Paramagnetic Currents

A first approximation in nuclear magnetic shielding is to quasi-spherical symmetry, such that the molecular electrons circulate in the

applied field in their ground-state atomic or molecular orbitals, without constraint by the other nuclei (a ring current in an aromatic molecule is of this type). Such a shielding term gives a poor approximation to the observed shielding of a nucleus in a molecule. It is known as the molecular *diamagnetic shielding term* $\sigma_d(A)$, so called because the field induced by the free precession opposes the applied field. Its use is to enable us to separate the more complex *paramagnetic term* $\sigma_p(A)$, which arises from the asymmetry of the charge, due to the presence of the other nuclei.

We are concerned only with diamagnetic molecules (to exclude the larger effects of the spin of unpaired electrons). In these, the electrostatic field of the neighboring nuclei quenches the orbital angular momentum about the observed nucleus (by lifting orbital degeneracies present in the free atom) so that there is no net circulation of electrons, in zero magnetic field. But the stationary waves are equivalent to superposed running waves, with the appropriate directionality and phase. Thus a p_x and a p_y electron together form two countercurrents ($m = \pm 1$, i.e., with moments of ± 1 Bohr magneton) circulating the z axis (29). If we apply a magnetic field in the z direction one sense of rotation is favored, and there is a net magnetic moment. This now augments the applied field, i.e., the current is "paramagnetic." The instantaneous fields due to the orbital motion, which normally cancel, are very large, and a slight polarization gives us the nuclear magnetic shielding we observe.

In Section VI, we shall be concerned with low-spin transition-metal complexes, in which (as is well known) the quenching of the orbital angular momentum by the ligand field leads to an energy difference Δ (the ligand field splitting) between the π - or nonbonding orbitals, which point between the ligands, and the σ^* orbitals, which point toward them. If the σ^* orbitals are unoccupied, a magnetic field can induce $\pi \rightarrow \sigma^*$ currents of the d electrons. These are usefully imagined as virtual excitations, with energy Δ . On molecular orbital (MO) theory, the orbitals distort in the applied field to allow the circulation, by the mixing in of excited states. The smaller the excitation energy, the larger the current and the deshielding of the metal, other things being equal. We may then expect to find correlations of the NMR shift with the spectrochemical series of the ligands, and these can be observed in cobalt(III) complexes.

The deshielding is greater, the smaller the radius of the circulating electrons. Therefore in complexes in which covalent bonding is important, and the d electrons are delocalized on the ligands (and for smaller variations in excitation energies), we may look for correlations

of the NMR shifts with the nephelauxetic (electron-cloud expanding) series of the ligands. This is found, for example, in platinum complexes. These correlations are discussed in Section VI.

The inorganic chemist is accustomed to think of orbital angular momentum as a property of an electron, if rotation about some axis transforms its orbital into another of the same energy and shape (and if both orbitals do not contain equal numbers of electrons of the same spin). In a magnetic field, however, paramagnetic currents can circulate between *any* p , d , f ... orbitals, if they are appropriately oriented, incompletely filled, and not too far apart in energy. Since the mixing of orbitals and the electron current is the greater the smaller the energy separation ΔE , the largest deshielding is caused by non-bonding (n) or loosely held (π , sometimes σ) electrons, circulating in low-lying orbitals, as close as possible to the resonant nucleus.

Such "paramagnetic" currents located on other groups can have a shielding or a deshielding effect at a nucleus A, depending on the orientation (as in the familiar "neighbor anisotropy" approximation) (142). In proton shielding, neighboring currents may well overwhelm the tiny current of the proton's own electrons. A dramatic example is the high shielding observed for many or most transition metal hydrides, in which paramagnetic circulations of d electrons which deshield the metal, shield a proton attached to it (Section VI).

III. Shielding Terms

A. THE RAMSEY THEORY

The shielding of a nucleus (A) was described by Ramsey (143, 144) as the sum of two molecular terms, derived, respectively, by first-order and second-order perturbation theory. [Analogous results have been obtained by valence bond theory (63, 151) by variation methods (33), or by the finite perturbation theory discussed below.] The Ramsey equations (in SI units) for the averaged shielding are

$$\sigma(A) = \sigma_d(A) + \sigma_p(A) \quad (1)$$

$$\sigma_b(A) = \frac{\mu_0}{4\pi} \frac{e^2}{3m} \left\langle 0 \left| \sum_j r_j^{-1} \right| 0 \right\rangle \quad (2)$$

$$\sigma_p(A) = \frac{-\mu_0}{4\pi} \frac{e^2}{3m^2} \sum_j \left[\frac{\left\langle 0 \left| \sum_j \mathbf{L}_j \right| n \right\rangle \left\langle n \left| \sum_j (L_j r_j^{-3}) \right| 0 \right\rangle + \text{c.c.}}{(E_n - E_0)} \right] \quad (3)$$

where μ_0 is the permeability of free space, e and m are the electronic charge and mass, and E_n is the energy of the n th excited state, sums being taken over all electrons j and states n except the ground state $n = 0$. \mathbf{L} and \mathbf{r} are the angular momentum and position vectors of the j th electron, and $\mathbf{L} = \mathbf{r} \times (\hbar/i)\nabla$, the gradient operator ∇ being equal to $\partial/(\partial x)$ for rotation about the x axis; c.c. stands for complex conjugate. Expressions for the tensor elements are given by Raynes (146).

Since we are interested in the chemical phenomena, and their physical basis, we take the gauge origin at the observed nucleus A. In MO calculations the paramagnetic term, and the errors therein, may be reduced by taking the molecular electronic centroid as the origin of coordinates [25; (cf. also Sadlej (150)). Change of axes gives rise to equal and opposite changes in σ_d and σ_p , in principle, but gauge invariance in MO calculations is achieved only in the limit of a complete basis set.

The diamagnetic term is straightforward to calculate. Semiempirical methods give reasonably good results, as also does the Ramsey–Flygare or extended Flygare approximation, discussed in Section III,C.

In Eq. (3) each $\langle 0|L|n\rangle/(E_n - E_0)$ term corresponds to a paramagnetic current at a distance r from A, and the related $\langle n|L(r^{-3})|0\rangle$ term represents the translation of the magnetic field due to this current to the nucleus A. Net shielding terms vanish for electrons tightly bound to "distant" nuclei, and the paramagnetic term vanishes for electrons in closed shells on the atom A, so errors may be reduced by confining the summation to valence electrons (143). All the same, we cannot sum accurately over the excited states, because of lack of knowledge of the wave functions and energies. This general problem of second-order perturbation theory is commonly evaded by recourse to the closure approximation: the series of excitation energies ($E_n - E_0$) is replaced by an effective excitation energy ΔE , so that the sum in Eq. (3) may be replaced by a ground-state expectation value, using the law of matrix multiplication (143).

$$\sigma_p = \frac{-\mu_0\mu_B^2}{3\pi(\Delta E)} \langle 0|L_j \cdot L_k(r_k^{-3})|0\rangle \quad (4)$$

where $\mu_B = (e\hbar)/(2m)$ is the Bohr magneton.

This expression does not give accurate results: it depends on the second derivative of the wave function, and is very sensitive to errors in it. Another general problem (102) is that contributions from all the excited states do not necessarily have the same sign [this problem arises in spin–spin coupling calculations also (72)]. Particular care is

needed with delocalized systems. The deshielding contributions usually dominate, but sometimes they do not, as in ClF, shown by Cornwell (28) and Santry (152a) to have a positive value of $\sigma_p(A)$. [The term "Cornwell effect" was suggested in Part I for positive "paramagnetic" contributions; or confusion may be avoided by calling the paramagnetic term the high-frequency term (33), following Van Vleck (169).]

The theory of nuclear magnetic shielding has been based on that of diamagnetic susceptibility, since this depends on the same paramagnetic and diamagnetic currents and has been known much longer. Just as Van Vleck added a high-frequency term χ_p , the "temperature-independent paramagnetism," to the Langevin term for the diamagnetic susceptibility (169), so Ramsey added the paramagnetic term σ_p to the Lamb term σ_d for the nuclear magnetic shielding (143). The significant difference between χ_p and σ_p is in the radial factor $\langle r^{-3} \rangle$, which appears only in the shielding, since the nucleus samples the magnetic field from its vantage point:

$$\chi = \chi_d + \chi_p \quad (5)$$

$$\chi_d = (-N\mu_0/4\pi)(2e^2\langle r^2 \rangle/3m)$$

$$\chi_p = \frac{N\mu_0}{4\pi} \frac{2\mu_B^2}{3} \sum \left[\frac{\langle 0|L|n \rangle \langle n|L|0 \rangle}{E_n - E_0} \right] \quad (6)$$

so that, approximately

$$\sigma_d = -2\langle r^{-3} \rangle \chi_d / N$$

and

$$\sigma_p = -2\langle r^{-3} \rangle \chi_p / N \quad (7)$$

where N is the Avogadro constant. (The susceptibility is the ratio of the induced field to the applied field, and so is negative for diamagnetic currents. These usually dominate the molecular susceptibility, because of the importance of distant currents, with large r). Some diamagnetic compounds, however, show a weak paramagnetism because of very low excitation energies [examples are MnO_4^- (169) and $(\text{NO})_2$ (107)] and this should correlate with resonance at very low field.

A practical though approximate method of evaluating the sum over excited states in nuclear magnetic shielding is to use susceptibility measurements, as in the atomic approximation described below. In the familiar neighbor anisotropy approximation, the shielding effect of a

neighboring group is estimated from the anisotropy of the diamagnetic susceptibility (142).

Ramsey pointed out also the connection between nuclear magnetic shielding in an applied magnetic field, and the spin-rotation interaction of the nuclear spin with the magnetic field generated by the rotation of the molecule (144). (The effects of the positive and negative charges do not cancel, since the electrons slip relative to the nuclei, except for the valence electrons, which are shared between atoms.) Observation of this interaction in molecular beam or microwave experiments on small molecules allows direct measurement of the molecular paramagnetic term σ_p , which is particularly useful in establishing absolute scales for nuclear magnetic shielding, as discussed in Part I (40, 144). Thus a scale for chlorine can now be based on the molecular beam measurements on HCl (35, 69) together with a calculated diamagnetic term (22, 103) and an accurate measurement of the chemical shift in HCl gas (89).

The magnetic moment of a molecule that arises from its rotation is described by the molecular g value tensor, which is related to the magnetic susceptibility tensor, as well as to other electrical and magnetic properties of the molecule, such as the electric dipole and quadrupole moments. In recent years the molecular Zeeman effect in diamagnetic molecules has been investigated by microwave spectroscopy, notably by Flygare (40) and co-workers, and their measurements and correlations (some of which we return to below) have greatly extended our understanding of magnetic interactions in diamagnetic molecules.

B. THE "ATOM IN A MOLECULE" APPROXIMATION

Ramsey's shielding terms, like Van Vleck's susceptibilities, were summed over the whole molecule, but subsequent workers, beginning with Saika and Slichter (151), have found it more convenient to use local (atomic) shielding terms. These are more readily compared, for a particular nucleus in different molecules, as Saika and Slichter compared fluorides (Section IV). They are also much simpler to calculate; LCAO-MO theory is based on atomic orbitals; and magnetic susceptibility tensor elements can be obtained as a sum of atomic terms (40, 49).

In the Pople LCAO-MO theory of diamagnetism of the early 1960s (138, 139) the susceptibility tensor was calculated as a sum of atomic contributions χ^A , each the sum of a diamagnetic and a paramagnetic term, χ_d and χ_p . These are related in rather complex fashion to the

Pascal constants, which give the molar susceptibility as a sum of atomic and constitutive terms (40, 157). The atomic shielding terms σ_d^A and σ_p^A were derived from χ_d^A and χ_p^A as in Eq. (7) above: for the second-row elements with which the theory was concerned, the radial term $\langle r^{-3} \rangle$ is the expectation value for the $2p$ electrons. Such atomic terms can be expressed by the Ramsey Eqs. (2) and (3), but with the summations restricted to the electrons on the atom A. Additional terms σ^{AB} represent the shielding at A due to the currents on the other atoms B (strictly σ_d^A , σ_p^A , should be σ_d^{AA} , σ_p^{AA}). Ring currents need a further term but are unimportant in the shielding of nuclei other than hydrogen. Thus

$$\sigma(A) = \sigma_d^A + \sigma_p^A + \sum \sigma^{AB} \quad (8)$$

The so-called gauge-invariant atomic orbitals (GIAO) of London (93) were used to avoid large and canceling shielding terms (57, 139). (These orbitals are in fact gauge dependent, since the phase of the wave functions is so chosen that the origin of vector potential for each atom is at its own nucleus.) In the paramagnetic term the sum over excited states may be retained, or it may be avoided by the use of an effective energy ΔE , as in the Karplus-Pople expression for second-row elements (73)

$$\sigma_p^A = \frac{-\mu_0 \mu_B^2}{2\pi(\Delta E)} \langle r^{-3} \rangle \sum Q \quad (9)$$

The Q terms express the imbalance of charge in the valence shell and are obtained from the charge densities and bond orders.

Jameson and Gutowsky have given a more general expression (63):

$$\sigma_p^A = \frac{-2\mu_0 \mu_B^2}{\pi(\Delta E)} [\langle r^{-3} \rangle_{np} P_u + \langle r^{-3} \rangle_{nd} D_u] \quad (10)$$

where P_u and D_u represent the imbalance of the valence electrons in p and d orbitals on the atom A. P_u has a maximum value of 2, when two p orbitals are filled and one is not (or vice versa). The maximum achieved, however, depends on the element. For fluorine, with only one bonding (p) orbital, the highest value is 1, and for carbon it is 3/2. In d orbitals the maximum D_u is 12, in low-spin d^6 octahedral or d^4 tetrahedral complexes, with the t_{2g} orbitals filled and the e_g unfilled, or vice versa (in principle). Equation (10) gives the same results as the Griffith and Orgel expression (Section VI).

In this approximation, the diamagnetic term is an extension of the Lamb term for the free atom (85). The "atom in a molecule" is considered to have spherical symmetry, but to be acted upon by the inductive effects of the ligands (138):

$$\sigma_d^A = \frac{\mu_0}{4\pi} \frac{e^2}{3m} \sum_{\lambda}^A P_{\lambda\lambda}(r^{-1}) \quad (11)$$

where the $P_{\lambda\lambda}$ terms are the electron populations of the atomic orbitals λ on the atom A, and r is the average electron distance from the nucleus. Electronegative ligands reduce the valence-shell electron population, but by increasing the effective nuclear charge of the atom A, they reduce r also. The net result is that the atomic diamagnetic term changes rather little for a given atom in different molecules: how much it changes can be estimated by X-ray photoelectron spectroscopy, as discussed in the next section. The result is that variation in σ_d^A is usually neglected in comparison with the much larger variation (and uncertainty) in σ_p^A .

The neighbor contributions σ^{AB} are estimated by the neighbor anisotropy approximation (142), from which they appear to be small: so these, too, are commonly neglected. The net result is that variations in chemical shift are taken as variations in σ_p^A , or as so often in the literature, as variations in "the" paramagnetic term. In truth "the" paramagnetic term is the molecular term, as measured in the spin-rotation interaction. The atomic paramagnetic term σ_p^A cannot be observed without neighbor contributions that are difficult to quantify. It is true that distant paramagnetic and diamagnetic contributions to the shielding cancel, but those from the nearest neighbors in general do not, and these are worst served by the neighbor anisotropy approximation, which assumes point dipoles [or by extensions of this to finite dipoles (7)]. The atomic approximation clearly breaks down when there are heavy-atom substituents, for which the diamagnetic and paramagnetic contributions to the shielding of the atom A are large and noncanceling, as discussed in later sections (cf. 120a).

Generally speaking, however, the "atom in a molecule" model has the advantage of ease of application, with concomitant loss of accuracy. The approximate equations for σ_p^A , such as Eqs. (9) and (10), are particularly valuable when one low-lying excitation dominates the shielding, as in transition-metal complexes when there are strong paramagnetic currents of the d electrons. The equations are also readily modified to take some account of important influences of the ligands that are neglected in the simple theory (Section VI). More

generally, they are important in demonstrating physical characteristics of the shielding, such as the dependence on excitation energies and on the radial term, on which our qualitative understanding of chemical shifts is based. Useful results can also be obtained by the use of ΔE as a semiempirical parameter, in appropriate series of molecules.

C. THE DIAMAGNETIC TERM AND THE XPES CONNECTION

Someone has remarked that X-ray photoelectron spectroscopy (Xpes, ESCA) will correlate with every chemist's favorite property. This is not very surprising since the core-binding energy reflects the atomic charge. Only a partial correlation is possible with NMR, since the paramagnetic term depends on other factors as well; but a direct connection can be made with the local diamagnetic term σ_d^A (10, 154). In its original formulation this was a purely theoretical construct, as mentioned in Section III,B, an extension of Lamb's term for the free atom. Lamb pointed out that σ_d^A depends directly on the electrostatic potential $V(O)$ produced at the nucleus by the atomic electrons (85):

$$\sigma_d^A = \frac{\mu_0}{4\pi} \frac{e^2}{3m} V(O) \quad (12)$$

In Xpes, the energy to remove the core electron depends on its electrostatic potential energy within the atom (V'), and at the atomic site (V'') arising from the surrounding charges in the molecule or lattice. The observed core binding energy E_b depends also on the relaxation of the other electrons, which speeds the parting electron; but for broad correlations, we may assume Koopmans' theorem (frozen orbitals).

Measured core-binding energies, it is found, can be fitted to an equation of the type (65, 160)

$$E_b = kQ_A + V'' + l \quad (13)$$

where k and l are empirical constants, Q^A is the (calculated) net atomic charge of the ionizing atom A, and V'' is the (calculated) molecular or Madelung potential $\sum_B (Q_B/r_{AB})$ due to the surrounding charges Q_B at distance r_{AB} from A. Since kQ_A represents the atomic potential V' , k is an (r^{-1}) term; l depends on the reference level. The connection can then be made with the extended Ramsey-Flygare

equation for the molecular diamagnetic term (41, 49)

$$\sigma_d(A) = \sigma_d^A + \frac{\mu_0}{4\pi} \frac{e^2}{3m} \sum_B (Z_B/r_{AB}) \quad (14)$$

As an approximation for σ_d^A , Flygare suggested the use of the Lamb term for the free atom, for which tabulated (Hartree-Fock) values are available (104). In the "extended Flygare method," σ_d^A is obtained by interpolation of the Hartree-Fock values of σ_d for free atoms and \pm ions, using atomic charges calculated by semiempirical methods. The second term is related to V'' and is a molecular or Madelung potential term, in which the sum runs over all the other nuclei, with atomic number Z , and at a distance r_{AB} from A. This "distant contribution" figures in the molecular diamagnetic term, but not in the atomic term, since it roughly cancels with a similar contribution (σ_{nuc}) in the molecular paramagnetic term.

There should be a direct correlation therefore between chemical shifts in the core-binding energy (ΔE_b) and in the atomic diamagnetic term ($\Delta\sigma_A$), since both depend directly on the potential inside the valence shell, imagined as a hollow charged sphere (159); this potential depending on Q/r , as in Eq. (11) for σ_d^A . (The summation over electrons in σ_d^A includes the core electrons, but their contribution to the potential at the nucleus does not change with the chemical environment.) Thus ΔE_b and $\Delta\sigma_d^A$ both depend on the changes in the valence shell, induced by the ligands. For any atom A,

$$\Delta\sigma_d^A/\text{ppm} = (-17.75/27.21)E_b/\text{eV} \quad (15)$$

As mentioned above, diamagnetic terms are not difficult to calculate. The tabulated values for free atoms and ions (104) afford an estimate of the range of σ_d^A for a given element: thus for nitrogen, σ_d^A varies by 18 ppm from N^+ to N^- , compared with 12 ppm for phosphorus from P^+ to P^- , or 9 ppm for fluorine from F to F^- . In the periodic table the range decreases down the group and seems to be largest for nitrogen. The value of the Xpes correlation is to connect calculated σ_d^A values with physical measurements on atoms in molecules, or ions in lattices. For carbon (112), the range of variation of σ_d^A is about 7–8 ppm from C_2H_2 to CF_4 , or 10 ppm if one includes negative ions, such as CN^- (Interestingly, carbon is more positively charged in CF_4 than in Me_3C^+ .) For nitrogen, the range is about 13 ppm from ONF_3 to negative ions, such as CN^- (113). For covalent fluorine the range is only 2–3 ppm, increasing perhaps to 10 ppm if ionic solids are included. As yet

the observed core binding energies are not directly comparable for gases and solids, because of uncertainties in work function, charging, and surface effects in solid samples. For comparable compounds, however, a calibration of free atom/ion values for σ_d^A can perhaps be obtained from empirical values of the coefficient k in Eq. (13), since this expresses the decrease in core electron-binding energy for the gain of one valence electron ($Q_A = 1$). For a suitable set of related compounds, such as the xenon fluorides, experimental values can be obtained for k and the atomic charges from simultaneous Eqs. (13) for the core-binding energies of the different atoms (24). Experimental values of k for atoms in molecules are larger than the free atom or ion values, which may be interpreted by contraction of the orbitals on compound formation (137). Thus the ranges for σ_d^A given above may be underestimated.

In detailed comparisons of ΔE_b and σ_d^A it may be necessary to correct for relaxation processes. This was found to improve the correlation for nitrogen compounds (113), but to be less important for carbon (112). (Chemical shifts in the relaxation energy can dominate the variation of E_b for progressive substitution by heavier ligands; thus in the series NH_4^+ to Me_4N^+ , $E_b(\text{N} - 1s)$ reflects the relaxation process, rather than inductive effects, which are small.)

As mentioned above, there is no general δ/E_b correlation, of NMR and core binding energy shifts. Thus core-binding energies correlate well with electronegativities, and NMR shifts do not. Several workers (14, 26, 116, 177) have tried to demonstrate linear correlations for groups of closely related molecules. Of these, the correlation of ^{13}C and $E_b(\text{C} - 1s)$ shifts in certain halomethanes was found to break down when a fuller range was compared, by Gelius and co-workers (45, 46), who have also compared large numbers of NMR and Xps shifts for boron and fluorine. They pointed out that correlation is only to be expected if the NMR shift reflects the local charge density, as in aromatic systems. It occurs only to a limited degree for the substituted methanes.

Gelius has pointed out that there is a good correlation between nuclear magnetic shielding, the E_b chemical shift, and the spin-rotation constant (45). The E_b/σ_d^A correlation does not extend to the *molecular* diamagnetic term (or the atom-plus-ligand term discussed in Section III,D) because this includes the "distant" contribution, given in the Ramsey-Flygare Eq. (14) by the summation over Z/r . However, a (roughly) equal and opposite term σ_{nuc} (arising from the motion of the other nuclei) balances the molecular paramagnetic term (arising from the motion of the electrons) in the spin-rotation interaction

(between the nuclear spin and the magnetic field due to the rotation of the molecule):

$$\sigma_{\text{sr}}(\text{A}) = \sigma_{\text{p}}(\text{A}) - \sigma_{\text{nuc}} \quad (16)$$

Combination of this equation with the extended Flygare equation and the Ramsey Eq. (1) gives

$$\sigma = \sigma_{\text{d}}^{\text{A}} + \sigma_{\text{sr}} \quad (17)$$

Thus spin-rotation constants can be deduced from E_{b} and the observed shielding.

D. OTHER RESTRICTED TERM APPROXIMATIONS

The "atom in a molecule" approximation has found extensive use in inorganic chemistry, as shown in later sections. It does not, however, give good results in comparisons of molecules having ligand atoms from different rows of the Periodic Table, or differing numbers of such ligands, particularly when the observed nucleus is from the second row. Unexplained high-field shifts appear for multiple substitution by heavier ligand atoms, as shown in the familiar U-shaped or "sagging" curves (Section IV,C). Thus Cl_4 is red, and $\Delta E(\sigma \rightarrow \sigma^*)$ is likely to be low, as is the radial term $\langle r^{-3} \rangle_{2p}$, but all the same the ^{13}C line is 280 ppm upfield of methane. Similar high shielding of the central atom is found in other iodides (BI_4^- , AlI_4^- , SiI_4 , GeI_4 , SnI_4 , PbI_4 , and transition-metal complexes).

Such heavy ligand atom effects can be traced, at least in part, to neglect of the ligand contributions to the nuclear magnetic shielding. This neglect is in a sense an artifact of the "atom in a molecule" approximation. In this the variation in the local diamagnetic term $\sigma_{\text{d}}^{\text{A}}$, as defined, is small, and so are values of the neighbor contributions as given by the dipole approximation. This means that variations in the chemical shift have to be accounted for by the local paramagnetic term, and in the event it fails to do so, for many substituent effects are much larger than the theory predicts [even for less heavy ligand atoms, as shown by the ^{13}C alkyl substituent parameters (110)].

A less severe approximation is to include the ligand atoms L in the diamagnetic and paramagnetic shielding terms, as in the "atom-plus-ligand" (AL) approximation (Part I). Like the atomic terms, the AL terms have the advantage over the Ramsey (molecular) terms of being easier to estimate, and directly comparable in related compounds, since the "distant" contributions cancel: but the more distant contri-

butions can now more safely be neglected. As described in Part I, the AL diamagnetic term is readily calculated by the Ramsey–Flygare approximation (or its extended form, which takes account of inductive effects on the atom A). The AL paramagnetic term can be calculated, or obtained by difference from the absolute shielding, given by the observed shift referred to an absolute scale based on spin rotation or other measurement of the (molecular) paramagnetic term.

A useful approach is to regard the AL diamagnetic term as a simple physical correction that allows us to identify significant chemical relationships of the paramagnetic term. Thus the molecular paramagnetic term was found to vary periodically with the atomic number of the ligand, in proton (108) and fluorine (109) resonance. This periodicity is shown clearly by the AL term also, but not by the chemical shift, nor by the local paramagnetic term, which varies as the chemical shift.

Effects of multiple substitution, which are often additive, emerge clearly only after separation of the diamagnetic and paramagnetic terms, since substituents contribute to both in different ways. Thus in the substituted methanes CX_4 , the ^{13}C shielding increases in the order $F < Cl < OR < Me < Br < I$. With separation of the diamagnetic and paramagnetic terms, both are seen to increase (numerically) in the order $Me < OR < F < Cl < Br (< I \text{ for the diamagnetic term, but } Br \lesssim I \text{ for the paramagnetic term, showing the emergence of some other heavy-atom substituent effect})$. This order for the paramagnetic term is in better accord with expectation based on the relative excitation energies.

The AL (or Ramsey) diamagnetic correction changes the sequence drastically in comparisons of ligands from different rows of the Periodic Table, in comparisons involving progressive substitution by a heavier ligand, and in comparisons of different coordination numbers. High coordination numbers may correlate with higher shielding not only because of the higher symmetry [reducing $\sigma_p(A)$], but because of the increase in the number of ligands (increasing $\sigma_d(A)$). In such comparisons, therefore, the “chemical” correlations (with ΔE , with the radial factor, or with other factors), or spectroscopic correlations, are obscured in the observed shifts, and revealed by a diamagnetic correction.

E. FINITE PERTURBATION THEORY

A powerful method that can be used to avoid the difficult summation over excited states, or an arbitrary choice of excitation energy, is to allow the magnetic field to perturb the Roothaan–Hartree–Fock equations, modifying the orbital coefficients. As Lipscomb has shown (92,

166), expressions so obtained for the diamagnetic susceptibility or the nuclear magnetic shielding correspond to those obtained by Ramsey using Rayleigh-Schrödinger perturbation theory. Pople's finite perturbation method (38, 141) gives similar equations and has made the method more accessible. The equations can be used to obtain molecular shielding terms, or local terms, and can be used at any level of approximation (37, 44, 83, 84). Better results are obtained with gauge-dependent atomic orbitals, as in Ditchfield's *ab initio* calculations (37). Reparameterization is advisable for best results with semiempirical methods, such as INDO (44). With Eqs. (1) and (2) as before,

$$\sigma_p(A) = \frac{-\mu_0\mu_B}{3\pi} \sum_{\mu,\nu} \left(\frac{\partial P_{\mu\nu}(H_\alpha)}{\partial H_\alpha} \right)_{H=0} \langle \phi_\mu | Lr^{-3} | \phi_\nu \rangle \quad (18)$$

for orbitals ϕ_μ and ϕ_ν . The $P_{\mu\nu}(H_\alpha)$ terms are elements of the density matrix with the perturbation due to the magnetic field. They are obtained by solving the Roothaan equation with the perturbed Fock matrix $F_{\mu\nu}(H_\alpha)$, which contains the additional (perturbation) term $-\mu_B \sum_\alpha H_\alpha \langle \phi_\mu | L | \phi_\nu \rangle$, generating paramagnetic currents. The differential coefficients $\{[\partial P(H_\alpha)]/\partial H_\alpha\}_{H=0}$ can be replaced numerically by $\text{Im}[P_{\mu\nu}(H_\alpha)]/H_\alpha$, where $\text{Im}[P_{\mu\nu}(H_\alpha)]$ is the imaginary part of the density matrix H_α .

The results can be interpreted in terms of excitation energies, as for the Ramsey theory. In the finite perturbation method, the bond parameter β (the matrix element corresponding to the resonance integral of Hückel theory) may be reduced (becoming less negative), allowing some recovery of orbital angular momentum quenched by the molecular field (83). This amounts to destabilization of the occupied MOs, and decrease in excitation energies, facilitating paramagnetic currents.

The finite perturbation method is well suited also to calculation of neighbor contributions to nuclear magnetic shielding, as in recent work by Kondo and co-workers on the effects on proton shielding of paramagnetic currents on neighboring carbon (84). Their results are relevant to the study of proton shielding in inorganic hydrides, including the transition-metal hydrides discussed in Section VI.

IV. Patterns of Shielding in Inorganic Molecules

The interplay of the factors that determine chemical shifts can be observed in the fluorine molecule, for which the strong deshielding, compared with fluorine in HF, or fluoride ion, was interpreted by Saika and Slichter, early in the history of NMR. A $2p_x$ electron is

considered to be missing at a given instant from the valence shell on each fluorine (with the x axis along the bond). A magnetic field applied in the z direction may then unquench angular momentum between the (filled) $2p_y$ and (half-filled) $2p_x$ orbital, to bring up the $\sigma^*(^1\pi_g)$ state, and a degree of paramagnetism (151).

The fluorine shielding is observed to increase in the order $F_2 < HF < F^-$. For the fluoride ion there is a closed shell, so that (weak) paramagnetic currents arise only by interaction with the solvent. In gaseous HF the ionic character ($i \approx 0.43$) reduces the deshielding compared with F_2 by a factor $(1 - i)$, since i equal to 1 corresponds to a closed shell. The fluorine chemical shift was thus expected (151) to correlate with the ionic character of the E—F bond, and this is true to a degree (28); however, effects of covalency, including π bonding, are important also (63).

In the fluorine molecule the virtual excitation is from the highest occupied orbital [π^* , formed from nonbonding (n) orbitals], to the lowest unoccupied orbital, i.e., $\pi^* \rightarrow \sigma^*$. HF, however, has no π orbitals, and the lowest excitation ($n \rightarrow \sigma^*$) has a higher energy. The effect of the radial term is rather small; an estimate using Slater orbitals shows an increase of 4.5% in $\langle r^{-3} \rangle_{2p}$ from HF to F_2 , equivalent to about 30 ppm in NMR shift.

Patterns of nuclear magnetic shielding are thus determined by the relative importance, in the compounds considered, of the effective excitation energy ΔE , the local symmetry, and the radial term (r^{-3}). These factors are not independent, as we have seen in the simple example of F_2 compared with HF, but frequently one can be seen to dominate. A further factor may be variation in the diamagnetic term, notably for heavier ligands, for multiple substitution, or for both of these.

A. EXCITATION ENERGIES

Relatively high-field ^{13}C and ^1H resonances are observed for the alkanes, which have no loosely held electrons or low-lying excited states, and similarly for the other second-row atoms in BH_4^- , NH_4^+ , NH_3 , H_2O , and HF. Bonds to hydrogen are particularly strong for the nonmetals, and this may account for the high shielding observed for the heavy atom in PH_3 , AsH_3 , H_2S , H_2Se , HCl , etc.

Low-field resonances are observed when ΔE is small, and linear δ/λ correlations are observed between the chemical shifts δ and the wavelength λ of the lowest energy electronic absorption band, in appropriate compounds. They are well known for groupings with $n \rightarrow \pi^*$ transitions, as in nitrosyl or azo (3, 114) or keto groups (since the bands lie at longer

wavelengths than for excitations of bonding electrons). They are better known for nitrogen than for oxygen since $n_N \rightarrow \pi^*$ excitations have components that are magnetic and electric dipole allowed, so the bands are of reasonable intensity. (In bent $R-N=X$ compounds the lone pair is usually sp^2 hybridized; the $s \rightarrow p\pi^*$ part of the $n \rightarrow \pi^*$ excitation is optically allowed and magnetically inactive, and the reverse is true for the $p \rightarrow p\pi^*$ part. The lowest $n_O \rightarrow \pi^*$ excitation in $X_2C=O$ compounds is however from a pure p orbital.) If charge rotates without translation the excitation is electric dipole forbidden, and so may be difficult to locate in the electronic spectrum, as, for example, the $\sigma \leftrightarrow \pi$ excitations in the ethene spectrum in the presence of the strong but magnetically inactive $\pi \rightarrow \pi^*$ band. The problem is not made any easier by the bands appearing in the vacuum ultraviolet region. In ethene, however, the most important excitation is $\pi \rightarrow \sigma^*$, and a measure of the excitation energy in ethene and substituted ethenes can be obtained from the photoelectron spectrum in the form of the first ionization energy $I_1(\pi)$ (113a). Other correlations involving excitation energies are discussed in later sections (correlations of transition-metal chemical shifts with $d \rightarrow d$ wavelengths in Section VI).

B. THE RADIAL FACTOR, AND THE ELECTRIC FIELD GRADIENT; THE NQCC AND MÖSSBAUER CONNECTION

Since we are dealing with a dipolar field, the paramagnetic term falls off as (r^{-3}) , that is, fairly steeply. The periodicity of the radial factor $\langle r^{-3} \rangle_{np}$ for the valence p electrons (9a), which arises from its dependence on the effective nuclear charge, is reflected in the ranges of chemical shifts of the elements (63). As the resonant atom moves across the row of the periodic table the range increases with increase in $\langle r^{-3} \rangle_{np}$, and also in the number of nonbonding electrons, which reduce ΔE and may reduce the local symmetry. Down the group also the range increases with increase in $\langle r^{-3} \rangle_{np}$, and also with decrease in ΔE as bond lengths increase and orbitals proliferate.

Parallelisms of chemical shifts can be found for neighboring elements in the periodic table, if similarly bonded, with the shifts in the ratio of the radial factors: thus the ^{77}Se and ^{125}Te shifts in analogous compounds are closely related by a line of this slope (98a), and similarly (though more approximately) for ^{14}N and ^{17}O (2a) or ^{13}C and ^{17}O (113a) in the same chromophore. For cadmium and mercury, however, or tin and lead (77a), the shifts for the heavier atom are larger than can be accounted for by the increase in radial factor, suggesting perhaps that more orbitals come into play for these heavier elements.

Because of the (r^{-3}) fall-off, correlations may be found with bond lengths to the ligands—for example, in proton resonance, in which neighbor effects are important; particularly in transition-metal hydrides, in which the neighbor effects are large (7a, 19).

Electronegative ligands increase the radial term, and thus the paramagnetic term, by increasing the effective nuclear charge of the atom A, pulling in the electrons involved in the paramagnetic circulation (31). For carbon, the radial term nearly doubles from C^- to C^+ , and for nitrogen it increases by a factor of 1.7 from N^- to N^+ . Thus the radial factor tends to increase as the neighbor atom moves to the right in the Periodic Table: and this applies also if the resonant nucleus is a ligand atom (H, C, F, etc.) and the neighbor moves across the row of the transition metals, for comparable compounds.

When ligands from different rows of the Periodic Table are being compared, an important effect may be the greater availability in the larger ligands of d orbitals, in which electrons from the resonant atom may be delocalized. This, with the greater bond length, acts to reduce the effectiveness of paramagnetic currents. The decrease in the radial factor as the ligand or neighbor moves down the group of the Periodic Table must contribute to the high-field shifts observed with heavy-atom substituents. The radial factor is decreased also by π -delocalization onto ligands such as CO, CN^- , or PR_3 , although an important part is played also by the σ -donation, and the concomitant increases in ΔE . Radial factors are frequently overwhelmed by larger changes in excitation energies.

A correlation that will become increasingly fruitful as more measurements are made is that of NMR shifts with the ground-state electronic charge distribution, as revealed by interaction with a quadrupolar nucleus and as studied by microwave, NQR, or Mössbauer spectroscopy. Thus for nuclei such as ^{14}N , ^{35}Cl , ^{55}Mn , or ^{59}Co the paramagnetic shielding tensor can be related to the nuclear quadrupole coupling constant (nqcc) e^2qQ/h , since the electric field gradient (efg) tensor represented by q has a similar (r^{-3})-dependence on the p or d electron charge distribution. In appropriate molecules we may find σ_p proportional to the nqcc if ΔE is sufficiently constant, or proportional to the ratio nqcc/ ΔE if ΔE varies, and if an effective excitation energy can be identified. In studies of inorganic (64, 115) and organic (152) chlorides, δ /nqcc comparisons were limited by the difficulty of estimating appropriate excitation energies; for the covalent inorganic chlorides, including some of transition metals, ΔE was estimated from the nqcc/ δ ratio (64). In nitroso or nitrosyl compounds XNO , however, the nitrogen shift (or σ_p^{AL}) correlates well with the nitroso ($n \rightarrow \pi^*$) excitation energy, which can be used for ΔE (3), and nqcc data are available

from microwave measurements for $X = \text{hal, Me, NMe}_2, \text{OMe, etc.}$ A linear correlation is observed of δ or σ_p^{AL} with the $\text{nqcc}/\Delta E$ ratio, and a poor correlation with the nqcc alone. There is also a reasonably linear correlation with $\eta/\Delta E$, where η is the ^{14}N asymmetry parameter (111).

Such correlations are particularly useful when components of the shielding tensor and of the efg tensor can be compared, and effects of the different paramagnetic circulations isolated, as in combined NMR/NQR measurements of crystalline solids. Important studies of this type include those of complexes of manganese (8, 119, 120, 161, 165), rhenium (120), and cobalt (18, 86, 118, 119, 163, 164).

In Mössbauer spectroscopy the quadrupole splitting arises from the interaction of the nuclear quadrupole with the electric field gradient [the isomer shift being related to the electron density at the nucleus (126)]. As yet there has been little direct correlation with nuclear magnetic shielding. For ^{57}Fe , the most useful Mössbauer nucleus, NMR studies are in their infancy (155); nuclei such as ^{119}Sn may be more promising (75, 162) but the Mössbauer sensitivity is low (131). Many general conclusions, however, are of interest, together with those from NQR studies, and can provide useful insights into NMR shielding, for example, on questions of ionic versus covalent bonding, on the Townes–Dailey model (18, 115).

An important consideration for NMR shielding in metal complexes is that of additivity (or otherwise) of ligand effects. We have on the one hand the spectroscopic evidence as to excitation energies, and now, from NQR and Mössbauer studies, the concept of partial field gradients (pfg) with which we can quantify the crystal field and observe direct effects of changes in σ and π orbital populations. ^{57}Fe and ^{119}Sn Mössbauer splittings, it is found, can be interpreted in terms of a (tensor) sum of pfg parameters characteristic of individual ligands (131), and this model has been applied to ^{55}Mn and ^{59}Co , for both of which NQR and NMR data can be compared. Thus in low-spin d^6 octahedral complexes, the cobalt nqcc is little changed from the mono-substituted $[\text{CoA}_5\text{X}]$ to the *cis*- $[\text{CoA}_4\text{X}_2]$ complex, but it is doubled in *trans*- $[\text{CoA}_4\text{X}_2]$, where $\text{A} = \text{amine}$ and $\text{X} = \text{Cl}$ (18). Deviations from additivity are likely to arise, however, if there is direct interaction between ligands, asymmetry of the ligand about the M-L axis, etc.

Additivity of ligand pfg contributions has been tested also in the cobaloximes (86), which are model compounds for vitamin B_{12} . The field gradient tensor can be defined in terms of two pfg parameters, N , for the four nitrogens in the plane, and X , the average for the two axial ligands. In this system the N and X parameters are not independent, since the sum is roughly constant, although the individual contributions vary quite widely over the range of ligand atoms (C, N, S, P, As,

Br, Cl). A reasonably linear δ/efg correlation was then found, the cobalt resonance moving upfield (over a range of 3600 ppm), with decrease in N/X , that is, with increase in the ligand field of the axial ligands, since the equatorial ligands are constant.

Cobalt NQR measurements have also been used to obtain information on σ - π donor-acceptor properties of the ligands, with which to compare the NMR shifts. In trigonal bipyramidal cobalt(I) complexes such as $\{\text{Co}[\text{P}(\text{OMe})_3]_5\}^+$ the field gradient, which depends largely on the $3d$ orbital populations, can be correlated with that in the isostructural iron complex $[\text{Fe}(\text{CO})_5]$, from Mössbauer spectra, and $[\text{Mn}(\text{CO})_5]^-$, from manganese NQR, to provide information on the parent compound $[\text{Co}(\text{CO})_5]^+$ (18). The substituted carbonyls $[\text{Co}(\text{CO})_4\text{L}]$ were then compared for a range of ligand atoms (Si, Ge, Sn, Pb, Hg) with organo- and halosubstituents. Larger quadrupole coupling constants are observed for ligands that are relatively poor σ -donors and/or strong π -acceptors (such as SnCl_3), and vice versa (e.g., SnMe_3). This can be explained on the assumption that the d_{xy} and $d_{x^2-y^2}$ orbitals are more highly populated than the d_{z^2} and d_{xz} , d_{yz} ; a strong π -acceptor reduces the d_{xz} , d_{yz} population, increasing q_{zz} (whereas a strong σ -donor would increase the d_{z^2} population, restoring the balance). It is of course difficult to separate the σ and π effects. NMR studies of single crystals (164) showed the z component of the cobalt shielding to be constant within the $[\text{Co}(\text{CO})_4(\text{MX}_3)]$ series, as expected, and showed the variation of the x and y components with the ligands: the results suggesting that among the group IV ligands, π -bonding effects are strongest for the cobalt-tin bond (164, 174). The NQR/NMR correlation was particularly valuable here since the $d \rightarrow d$ bands could not be observed, being obscured in the electronic spectrum by strong ligand transitions. Correlations are found also of the nqcc with the highest frequency CO stretching mode (18).

Similarly detailed work has been done on the corresponding manganese complexes (9). The manganese shielding increases with increase in σ -donor ability of the ligand, correlating also with Graham's σ parameter (51).

Yet another correlation that emerges in studies of quadrupolar nuclei is between the chemical shift and $\sqrt{\Delta B}$, where ΔB is the line width in units of magnetic field (8, 23, 64, 126, 174). Quadrupolar relaxation dominates the spin-lattice relaxation time T_1 , which in the extreme narrowing case is given by

$$1/T_1 = \frac{3}{40} \frac{(2I + 3)}{I^2(2I - 1)} (1 + \eta^2/3) (e^2 q Q / \hbar)^2 \tau_q$$

where I is the nuclear spin quantum number and τ_q the correlation time for molecular reorientation (1). As we have seen, the paramagnetic shielding term is proportional to the nqcc, if excitation energies do not change overmuch.

C. LOCAL SYMMETRY, SUBSTITUENT EFFECTS, AND THE SHIELDING TENSOR

Since paramagnetic currents require an imbalance of charge in the valence shell, correlations arise of increased shielding with increase in local symmetry, although it is often difficult to disentangle the operative factors.

Among the lighter elements, low-field resonance is observed for planar molecules, because of deshielding by $\sigma \leftrightarrow \pi$ circulations. Carbon is most strongly deshielded in carbocations R_3C^+ and in carbene ligands in metal complexes (15, 27), and boron in BMe_3 and BH_3 (123), in which charge can circulate from σ bonds into the underoccupied π orbital; the shielding increases with π -donor ligands (15, 30) (Section V). Boron is more highly shielded when 4-coordinate, and in apical positions in boranes, such as pentaborane. Similarly, in ethene and perhaps in NO_3^- , carbon and nitrogen are deshielded by circulations of π electrons in σ^* orbitals, and deshielding is stronger still for $n \rightarrow \pi^*$ circulations, as in NO_2^- or ozone.

In linear molecules, however, resonance may be at relatively high field, since there is no paramagnetic circulation about the C_∞ or D_∞ axis (as in the free atom), the classic example being acetylenic carbon. But resonance may be at low field when the perpendicular circulations are particularly effective, as in F_2 , or PN in phosphorus shielding [studied by molecular-beam electric resonance (6, 145)].

Among the medium-to-heavy main-group elements (discussed in Section V), higher shielding is observed for higher local symmetry (for comparable ligands), that is planar < tetrahedral < octahedral. There is a pleasing sequence in chlorophosphorus compounds, in which the phosphorus shielding increases $PCl_3 < PCl_4^+ < PCl_5 < PCl_6^-$ (54). Theoretical analysis of ^{31}P shifts in a wide range of compounds showed their sensitivity to asymmetric electronic loading of phosphorus (91).

In transition-metal complexes, however, the metal may be more shielded in a less symmetrical ligand field, because of the smaller ligand field splitting. Examples are rhodium and platinum, which are more highly shielded in square-planar than in octahedral complexes (17, 39, 62, 78, 98, 176).

The question of substituent effects is a complicated one (and will not be considered in detail). Heavy-ligand-atom effects are not well under-

stood. In proton shielding, a plot of the molecular diamagnetic and paramagnetic terms against the atomic number of the ligand in the binary hydrides shows that $\sigma_d(\text{H})$ and $\sigma_p(\text{H})$ both increase fairly symmetrically, and in periodic fashion, but for heavier ligands the diamagnetic term increases slightly faster (108). The rationale may be along familiar lines, or there may be special effects, e.g., of spin-orbit coupling (143), as suggested in ^{13}C studies of CH_3I (120a); there has been little investigation of this.

There have been many studies of multiple substitution, and this again is a complicated question, since the diamagnetic and paramagnetic effects of the substituent are usually opposed, and within the paramagnetic term, ΔE and radial (and charge density) factors may be opposed. Characteristic U-shaped or "sagging" curves are often observed for the shielding of the central atom with progressive substitution, e.g., of hydrogen or methyl by halogen, NMe_2 , OR, or other groups, as shown originally by Lauterbur for carbon in substituted methanes (88), and now demonstrated for aluminum (79), silicon (153), tin (59, 162), phosphorus (90), and others. Frequently the shielding decreases with the first, and perhaps the second, substituent, then increases with further substitution. For carbon in the methanes it was shown (in the AL approximation) that the sagging results largely from the opposition of the diamagnetic and paramagnetic terms. Each term separately gives a monotonic curve, but only the diamagnetic term is linearly additive, and this increases faster than the paramagnetic term for multiple substitution by a heavier ligand, giving the upfield turn to the U-shaped curve (Part I). With heavier atoms particularly, there is a pronounced sagging in the plot of the paramagnetic term, and we then have to explain the larger paramagnetic contribution for the partially substituted molecules.

For substituents differing in electronegativity, the overall variation of the paramagnetic term is strongly influenced by the changes with substitution in the radial term and in the valence p orbital population on the central atom (75). But in addition to this, the excitation energies themselves form a U- (or W-) shaped curve, since the energy levels which are degenerate in the unsubstituted AX_4 and AY_4 molecules are split in the less symmetrical AX_3Y , AX_2Y_2 , and AXY_3 molecules, and this splitting introduces some lower energy excitations. Lyubimov and Ionov (96a) have relaxed the severity of the Karplus-Pople average energy approximation, following Cornwell (28), to take account of the additional magnetically allowed excitations in the C_{3v} and C_{2v} molecules (for $\text{A} = \text{Al}, \text{Si}, \text{Sn}$; $\text{X/Y} = \text{F/Cl}, \text{F/Br}, \text{Cl/Br}, \text{Cl/I}, \text{H/OH}$). The calculations are difficult because of the many uncertainties, but they achieve some qualitative agreement with observed deviations from

additivity. Again, it seems that lower symmetry correlates with lower shielding. This approach is applicable also to other symmetries (octahedral, trigonal, etc.); and to π -bonding or electron delocalization among the ligands, as in polyfluoro compounds in which the lone pairs interact at close approach, or polybromo or iodo compounds in which there are steric interactions.

The information from experiment that we need in order to understand these relationships is increasingly becoming available now from various sources, in the form of individual elements of the shielding tensor, or anisotropies. Cross-correlation of NMR and NQR results has already been mentioned, and molecular beam and microwave methods that give the elements of the paramagnetic shielding tensor were referred to in Part I. Many studies have used liquid crystals (95). Recent years have seen important advances in techniques for high-resolution NMR spectroscopy with solid (preferably single crystal) samples, removing the dipolar interactions that broaden the resonance lines, sometimes by several kilohertz (105). An early technique to impose motional narrowing, which also removes quadrupolar broadening, is to rotate the solid at the magic angle (α) at which the dipolar interaction $\frac{1}{2}(3\cos^2\alpha - 1)$ is zero (5); but the shielding tensor elements are then averaged to the isotropic value. A powerful method for obtaining the full shielding tensor in a high-resolution spectrum is to hold the single crystal still, and rotate the nuclear spin system by a special sequence of 90° pulses, with Fourier transform of the free induction decay. The WAHUA sequence of Waugh, Huber, and Haeberlen (171) magnetizes the sample for equal periods of time along each of the axes in the rotating reference frame in alternation. This removes interactions between like nuclei, but not between unlike nuclei, for which multiple resonance (or magic axis rotation) can be used. The phosphorus shielding tensors in α - $\text{Ca}_2\text{P}_2\text{O}_7$ have been measured in this way (81), and proton shielding tensors (with and without hydrogen bonding) (87), for example.

An important extension of the multipulse technique enables "rare" spins (which may be chemically or isotopically dilute), such as ^{13}C , ^{15}N , or ^{17}O , to be studied in the presence of an abundant spin such as ^1H or ^{19}F . This is used to cross-polarize the rare spin (61), as in Waugh's proton-enhanced nuclear induction (alias NMR) spectroscopy (48, 134, 135). The shielding tensor has been obtained in this way for ^{13}C in $\text{K}_2\text{Pt}(\text{CN})_4\text{Br}_{0.3}\cdot 3\text{H}_2\text{O}$ (which is a one-dimensional conductor) (167), in calcium formate (168), and in several organic molecules; for ^{15}N in NH_4NO_3 (47), etc; and for ^{29}Si in some organosilicon compounds (48). This technique has now been extended so that nuclei such as ^{25}Mg and

^{43}Ca of low gyromagnetic ratio, as well as low natural abundance (13), can be studied under high resolution in solid samples.

Such methods are in their infancy (and are expensive). Their potential for inorganic chemistry is enormous. Degrees of ionicity can be quantified (since σ_p is zero for a free ion), as in ^{19}F studies of the group II difluorides (170), which can be compared with results obtained for the alkali metals in their halides (156). Suggestions of π bonding can be tested, by reference to observed anisotropies about the bonds in question; and so on.

Information on magnetic shielding and susceptibility anisotropies has been assembled by Appleman and Dailey (6), and the experimental shielding tensor components were compared with (*ab initio*) calculated values, for second-row atoms. Their review contains much of interest to the inorganic chemist; for example, ^{19}F shielding anisotropies in inorganic fluorides (of opposite sign in PtF_6 compared to MoF_6 , WF_6 , and UF_6); and the small phosphorus anisotropy in PH_3 (as for nitrogen in NH_3), compared with large anisotropies in PN , N_2 , and ClCN .

V. Main Group Elements

Like chemical bonding, nuclear magnetic shielding depends on electrons, and there are characteristic variations across the row and down the group of the periodic table. Thus the chemical shifts of boron, carbon, and nitrogen vary in parallel for isoelectronic compounds, such as BR_3 and R_3C^+ , or R_3BNH_3 and R_3CCH_3 (123); and the resonance of the central atom in borate, carbonate, or nitrate ion appears at relatively low field.

In the comparisons that follow, in which an attempt is made to pick out important factors determining chemical shifts, it is usually difficult to ensure constancy of other factors. This general caveat applies particularly to the heavy substituent effect; thus many or most generalizations have the exception that the iodides (and perhaps bromides, selenides, etc.) appear too far upfield.

In boron resonance the planar alkyl boranes BR_3 , with only 6 electrons (formally) in the boron valence shell, appear at lowest field, and the BX_3 line moves upfield over a range of nearly 100 ppm for $\text{X} = \text{R} < \text{H} < \text{SMe} < \text{Cl} < \text{Br} < \text{NMe}_2 < \text{OMe} < \text{F} < \text{I}$ (30, 101, 122–124). This sequence is roughly as expected for increasing population of the boron $p\pi$ orbital (except for the heavy ligand effect). In support of this rationale, the deshielding of boron in BMe_3 relative to BMe_4^- (or BH_3 relative to BH_4^-) is very large, about 100 ppm, but the difference is only 14 ppm for BF_3 relative to BF_4^- ; and a different sequence is

observed in the BX_4^- compounds, $\text{Cl} \lesssim \text{OH} \lesssim \text{NHMe} \approx \text{F} < \text{Me} < \text{Br} < \text{H} < \text{I}$. The BX_3 and BX_4^- sequences overlap, the resonance of BF_3 at medium field being close to those for B_2H_6 and BCl_4^- . (As previously mentioned, relatively high shielding is observed for apical boron in the pentaboranes.) Effects of multiple substitution are evident, since the sequence differs in the Me_2BX compounds, for which the boron shielding increases as $\text{X} = \text{Me} \approx \text{H} < \text{Br} < \text{Cl} < \text{F} < \text{OMe} < \text{NMe}_2$.

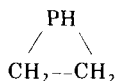
In nitrogen resonance the range is extended to low field by the presence of lone pairs on nitrogen, with strong deshielding from $n_{\text{N}} \rightarrow \pi^*$ circulations as in $\text{XN}=\text{NX}$ (114) or $\text{NX}=\text{O}$ compounds (3). In ammonia and the amines, however, relatively little deshielding of nitrogen can be attributed to the presence of the lone pair, and a similar pattern is observed for the other nonmetal hydrides (as already mentioned), related to high excitation energies, and small p character of the lone pair electrons.

In aluminum resonance (2, 79, 127), alkyl compounds, such as $\text{Al}^i\text{Bu}_3-\text{Al}_2^i\text{Bu}_6$ appear at lowest field. Then follow overlapping sequences of Al_2X_6 and AlX_4^- compounds, in which the aluminum shielding increases, for Al_2X_6 as $\text{X} = \text{R} < \text{Cl} < \text{Br} < \text{I}$, and for AlX_4^- as $\text{X} = \text{Cl} < \text{H} < \text{OH} < \text{Br} < \text{F} < \text{I}$. At highest field are the octahedral complexes $[\text{Al}(\text{acac})_3] \sim [\text{Al}(\text{H}_2\text{O})_6]^{3+} < [\text{Al}(\text{NCMe})_6]^{3+}$ (with AlI_4^- among them) (58). These relationships, with AlH_4^- at medium field, suggest that $p\sigma \rightarrow d\pi$ circulations may be significant in the shielding. Gallium is a more difficult nucleus to measure: of the compounds studied, GaH_4^- appears at low field and GaI_4^- at high field (2). 6-Coordinate gallium(III) (with water or DMF as ligands) is now in the middle of the range, since the highest shielding is observed for Ga^+ in Ga_2Br_4 and Ga_2Cl_4 , which are gallium gallates $\text{Ga}^+\text{GaX}_4^-$.

The group IV elements are well studied by NMR, since all except germanium have spin- $\frac{1}{2}$ nuclei in adequate abundance, and the nuclear quadrupole moment for germanium is not very large. Silicon resonance (153a) resembles that of aluminum in that 6-coordinate silicon $[\text{Si}(\text{acac})_3, \text{SiF}_6^{2-}]$ is upfield of 4-coordinate silicon (although SiI_4 appears at highest field). In the SiX_4 compounds, there is some indication of increased shielding with increasing π -donor ability of the ligand, as for BX_3 , with the silicon shielding increasing in the order $\text{Me} < \text{Cl} < \text{NMe}_2 < \text{OMe} < \text{Br} < \text{F} (< \text{I})$. The order for Me_3SiX compounds is $\text{F} < \text{Cl} < \text{Br} < \text{OMe} < \text{I} < \text{NMe}_2 < \text{Me} < \text{Cl} < \text{H}$. At very low field is the silicon resonance in $\text{Hg}(\text{SiMe}_3)_2$, and this may be related to Orgel's description (given below) of d orbital contributions to deshielding for posttransition metals in $d^{10}s^2$ configurations.

The germanium compounds measured in germanium resonance (74, 80) roughly follow the SiX_4 pattern, and similarly for SnX_4 . A wide range of compounds has been measured in tin resonance (21, 32, 59, 75, 162). At high field (apart from SnI_4) are the highly symmetrical ions Sn^{2+} , SiF_6^{2-} , $\text{Sn}(\text{OH})_6^{2-}$, and also $[\text{MeSnBr}_5]^-$; at low field, $\text{Sn}(\text{SMe})_4$.

At high field in phosphorus resonance (158) are the hydride species, in which the phosphorus shielding increases with decreasing symmetry, $\text{PH}_4^+ < \text{PH}_3 < \text{PH}_2^-$ (the series is isoelectronic, and excitation energies are high). Unexpectedly high phosphorus shielding is observed in P_4 and in phosphirane



(170a). The tetrahedral species (PO_4^{3-} , etc.) are at medium field, and at lowest field, PX_3 with $\text{X} = \text{Br} < \text{Cl} < \text{I} < \text{OMe} < \text{NMe}_2 < \text{F}$ (90, 117). The small number of arsenic compounds that have been measured follow the phosphorus pattern (8). Sulfur has been rather little studied because the magnetic nucleus ^{33}S has a low natural abundance (1%) and sensitivity. Shielding increases in the order $\text{SO}_4^{2-} < \text{Me}_2\text{SO} < \text{thiophene} < \text{CS}_2 < \text{Et}_2\text{S} < \text{S}^{2-}$ (149). Spin-rotation constants have been measured for $^{16}\text{O}^{12}\text{C}^{33}\text{S}$, so the absolute shielding can be determined (148). Selenium is somewhat less difficult. In the oxyacids and anions the shielding increases as the symmetry increases, $\text{HSeO}_3^- < \text{H}_2\text{SeO}_3 < \text{SeO}_3^{2-} < \text{Se}(\text{OH})_3^+ < \text{H}_2\text{SeO}_4$ (82). Of the compounds that have been studied, H_2Se is at highest field, SeF_6 at medium field, and then the tetrahedral compounds SeO_4^{2-} , SeF_4 , and SeCl_4 ; and the planar SeOCl_2 and SeOBr_2 molecules at lowest field (12).

Fluorine chemical shifts are well known, with the more ionic fluorides (and gaseous HF , LiF , NaF) at high field [and ClF at unexpectedly high field (28, 152a)]. In the xenon fluorides (50) the decrease in fluorine shielding $\text{XeF}^+ > \text{XeF}_2 > \text{XeF}_4 > \text{XeF}_3^+ > (\text{XeF}_6)_4 > \text{XeF}_5^+$ follows the decrease in ionicity of the $\text{Xe}-\text{F}$ bond, and is accompanied by decrease in the $\text{Xe}-\text{F}$ coupling constant. The periodicity of the fluorine shift with the atomic number of the ligand (109) was discussed in Part I. The fluorine resonance is at very low field in UF_6 in which fluorine non-bonding electrons may circulate in d (or f) orbitals. It is likely that this can happen even when fluorine is a β -substituent on a transition metal, since fluorine in fluorocarbon ligands is deshielded when bonded through carbon to manganese, rhenium, iron, or cobalt in low-spin d^6 complexes, though not when bonded (through carbon) to a main-group element, such as tin or phosphorus. This has been explained in terms of

circulation of fluorine lone-pair electrons ($2p_y$) using the metal $nd_{z^2}(\sigma^*)$ orbital (136).

For the other halogens, the nuclei are quadrupolar, and the quadrupole moments are large for bromine and iodine. Chlorine is reasonably amenable to NMR study, although sensitivity is low (64, 152). Of the compounds studied in chlorine resonance, Cl^- , HCl , and CH_3Cl are at highest field, and ClO_3^- at lowest. Then follow chlorides and oxychlorides, for which the chlorine shielding increases $\text{ClO}_4^- < \text{TiCl}_4 < \text{VOCl}_3 < \text{SO}_2\text{Cl}_2 < \text{SOCl}_2 < \text{CrO}_2\text{Cl}_2 < \text{PSCl}_3 < \text{CCl}_4 < \text{S}_2\text{Cl}_2 < \text{POCl}_3 < \text{PCl}_3$; then Cl_2 ; and at fairly high field $\text{SiCl}_4 \approx \text{GeCl}_4 < \text{AsCl}_3 < \text{SnCl}_4$. There is a very rough correlation of the chemical shift with the nqcc if the compounds of the transition metals are ignored; for these the further deshielding can be explained by low-lying d orbitals on the metal (64).

Orgel (129) has accounted for the shielding of posttransition metals in $d^{10}s^2$ configurations in terms of $p_x \rightarrow p_y$ circulations; this applies to Ga(I) to Tl(I), Ge(II) to Pb(II), and As(III) to Bi(III). For the ions in the $d^{10}s^2$ ground state, there are no paramagnetic currents, and Ga^+ (as mentioned) resonates at high field. In environments lacking a center of symmetry there is stabilization by sp hybridization, and this accounts for the low coordination numbers that are observed in compounds of Pb(II), Sb(III), and Bi(III). The so-called inert pair occupies an orbital with varying proportions of s and p character, and provides the main contribution to paramagnetic currents—the more, the greater the p character. Thus in (solid) red (tetragonal) PbO the lead resonates 3000 ppm downfield of Pb^{2+} , and in the same region as PbMe_4 . In yellow (rhombic) PbO , however, the lead resonates about 4000 ppm farther downfield. In the tetragonal form the lead is at the apex of a rather flat square pyramid, so that it has four oxygens to one side and the “inert pair” to the other (172). The orthorhombic structure contains chains of alternating lead and oxygen, weakly bonded into layers, so that there are two nearer and two more distant oxygen neighbors (172) (and presumably more p character in the nonbonding electrons on lead). A variety of covalent lead compounds has now been studied (77, 77a, 97, 133).

Metals in d^{10} configurations, Cu(I) to Au(I), Hg(II), or Tl(I), can be deshielded by currents of p or d electrons. The bonding in linear ML_2 groupings has been described by Orgel (128) in terms of sd hybridization, since the $d-s$ splitting is small. This allows circulations via d^9s excited states to deshield the metal. Schneider and Buckingham (153) have compared the heavy-metal shielding in HgMe_2 , TlMe_3 , and PbMe_4 in terms of sp , sp^2 , and sp^3 valence states, respectively, with a

large deshielding for incomplete p and d shells. Thus mercury is strongly deshielded in HgMe_2 , compared with the aqueous Hg^{2+} ion at high field (76). Thallium in TlMe_3 is deshielded compared with aqueous Tl^+ at high field; with aqueous Tl^{3+} in between, since this ion has a degree of covalent bonding to water, as $[\text{Tl}(\text{H}_2\text{O})_4]^{3+}$, with an sp^3 valence state (97, 153).

VI. Transition Metals

The approximate (crystal field) theory for transition-metal complexes with incomplete d shells is simple. For diamagnetic compounds we are restricted to a limited number of d -electron configurations, mainly d^6 (octahedral), d^8 (square planar or trigonal bipyramidal), some d^4 (e.g., h^5 -cyclopentadienyl), and a few d^2 (cubic) (96). Only one-electron terms and singlet states are involved. Complications then arise, with more detailed considerations of ligand electronegativity, σ and π bonding, asymmetric substitution, and so on (some of these have been considered to some extent in Section IV,C). There are technical limitations to the NMR studies, in that rather few transition metals have abundant isotopes of suitable spin. Most work has been done with cobalt, platinum, tungsten, rhodium, or manganese, but the range is fast increasing as multiple resonance and Fourier-transform techniques are reducing the obstacles. For the quadrupolar nuclei, ^{51}V , ^{55}Mn , and ^{59}Co , there are problems of rapid relaxation (in asymmetric environments), but these are perhaps offset by the availability of NQR techniques as well, as already discussed.

Griffith and Orgel (54, 55) applied crystal field theory to the Ramsey shielding theory, in the local term approximation of Saika and Slichter. Their subject was d^6 (low spin) complexes of cobalt(III), but the method is a general one. Neglecting variation in the diamagnetic term, they derived the expression for the paramagnetic term:

$$\sigma = \frac{-\mu_0}{4\pi} \frac{4\mu_B^2 \langle r^{-3} \rangle_{3d}}{3\Delta_0} \langle 0 | L^2 | 0 \rangle \quad (19)$$

for a sum over six d electrons in a strong octahedral field, $\langle r^{-3} \rangle_{3d}$ being the average over a single d orbital, and Δ_0 the splitting in the octahedral crystal field. Thus the metal nucleus is deshielded by circulation of the t_{2g} (d_{xy} , d_{yz} , d_{xz}) electrons, via e_g orbitals ($d_{x^2-y^2}$, d_{z^2}) unoccupied in the ground state. The theory thus predicts linear δ/Δ^{-1} or δ/λ relationships between the chemical shift and the wavelength of the $d \rightarrow d$ (${}^1A_1 \rightarrow {}^1T_{1g}$) absorption. A close correlation was in fact

found by Freeman, Murray, and Richards, between the cobalt resonance frequencies and the spectrochemical series of the ligands, for fourteen complexes of cobalt(III) (42).

The theory also predicts a small decrease in shielding with increasing temperature, since the increasing population of higher vibrational modes, particularly the bending modes, tends to reduce Δ_0 . This has been confirmed for cobalt (42), platinum (98), and rhodium (62); it is not observed for closed d shells. The effect of spin-orbit coupling was considered to be negligible. Griffith and Orgel pointed out that neglect of covalent bonding between metal and ligand overestimates the orbital angular momentum, since electron delocalization is underestimated: but that neglect of configuration interaction tends to compensate for this. Betteridge and Golding have made semiquantitative estimates of these effects for cobalt(III) (11). As to spin-orbit interaction, mixing in of the 3T_1 excited state contributes rather little to σ_p , about 0.3%. Configurational mixing is rather more important, since the effect of mixing the possible configurations of the 1A_1 , 3T_1 , and 1T_1 states over the crystal range of interest is to lower the shielding term by about 3%. Distortion effects are relatively small and can be allowed for by an orbital reduction term. The largest effect is that of covalent bonding, with a large quenching of the orbital angular momentum, because of transfer of spin to the ligands. We return to this subject below.

Buckingham and Stephens extended the theory of the d^6 octahedral complexes to examine the effect of the d electron currents on a proton attached to the transition metal (19). They calculated the d -electron contribution to the proton shielding, using the Ramsey–Orgel theory, assuming $\delta \simeq 5$ ppm for the other contributions to the proton shielding; and give diagrams showing the variation of the shielding tensor elements with distance R for various values of the Slater orbital exponent k and the principal quantum number n . They show that the σ_{xx}^p and σ_{yy}^p tensor elements are positive for circulations about axes perpendicular to the M—H bond axis, at a normal proton distance (68) ($R \simeq 3$ a.u.) and for likely values of k (between 3 and 4). These tensor elements are negative for lower values of k , and the paramagnetic term σ_{zz}^p for circulation about the M—H bond axis is always negative. Thus the average value of the paramagnetic term is positive at the proton, accounting for the high-field resonance observed. The theory predicts a very high anisotropy in the proton shielding ($\sigma_{xx}^p - \sigma_{zz}^p = -500$ ppm); and predicts also that the paramagnetic term is not very sensitive to the ligand field splitting. For $R = 0$, the expressions for σ_p reduce to Griffith and Orgel's Eq. (19). Only in the limit of an infinite orbital exponent k , i.e., when the metal orbitals are contracted to a

point at the nucleus, do the equations give the same (zero) shielding as the neighbor anisotropy approximation for an isotropic near neighbor; that is, a point dipole approximation does little justice to a metal atom at the normal M—H distance.

Buckingham and Stephens extended the theory also to d^8 square-planar complexes, using platinum(II) as example (with diagrams to show the variation of the shielding terms with R and k) (20). The paramagnetic circulations of d_{xy} , d_{yz} , and d_{xz} electrons now use the $d_{x^2-y^2} \sigma^*$ orbital, unoccupied in the ground state. The excitation energies are ΔE_A (i.e., $^1A_1 \rightarrow ^1A_2$) for the d_{xy} electrons, and ΔE_E (i.e., $^1A_1 \rightarrow ^1E$) for the d_{yz} and d_{xz} electrons, with $\Delta E_A < \Delta E_E$. Once again the paramagnetic term is positive for circulations about the axes perpendicular to the M—H bond axis (with excitation energy ΔE_E) and negative for circulation about the M—H bond axis (with excitation energy ΔE_A) for $R \simeq 3$ a.u. and k between 3 and 4. The resultant effect is again to shield the proton, although less in general than in the octahedral case. There is the further prediction that protons above the plane should be strongly deshielded.

As before, the equations reduce in the limit of $R = 0$ to those for the d electron contribution to the shielding of the metal nucleus, in d^8 square-planar complexes, that is:

$$\sigma_{xx}^p = \sigma_{yy}^p = \frac{-\mu_0}{4\pi} \frac{8\mu_B^2 \langle r^{-3} \rangle_d}{\Delta E_E} = \frac{-\mu_0}{4\pi} \frac{4\mu_B^2 k^3}{21 \Delta E_E}$$

$$\sigma_{zz}^p = \frac{-\mu_0}{4\pi} \frac{32\mu_B^2 \langle r^{-3} \rangle_d}{\Delta E_A}$$

The shielding reduces in the limit of $k \rightarrow \infty$ to the value given by the neighbor anisotropy approximation, with the same wave functions; but this now predicts the sign (though not the magnitude) of the metal contribution to the proton shielding correctly, since the paramagnetic susceptibility due to $d \rightarrow d$ excitations is greater (in fact 4 times greater) perpendicular to the plane than in the plane. A pleasing sequel is the near-linear correlation, with negative slope, found by Dean and Green (34) between the shielding of the platinum and of the attached proton, in a series of square-planar complexes, *trans*-[PtHL(PEt₃)₂], with a variety of anionic ligands L.

The subject of coordination shifts is a large one, and will not be considered in detail here. The deshielding observed for fluorine in CF₂ or CF₃ ligands on a d^6 metal has been mentioned (136): the excitation energy for the $2p_y \rightarrow nd_{z^2}$ circulations (about the axes perpendicular

to the M—F axis) being given by the difference between the fluoride ionization energy and the ionization energy of the metal in the ligand field, plus the ligand field splitting.

In cobalt shielding, the (δ/Δ_0^{-1}) correlation with the spectrochemical series of the ligands was found to be successful for cobalt(III) complexes with second-row ligand atoms (C, N, O) (36, 147, 175). Subsequent work showed increased shielding for heavier ligand atoms (S, Se, As, etc.) (11, 43, 71, 106), and in appropriate complexes, different correlation lines can be drawn for ligands from different rows of the Periodic Table. Similarly in organo-cobalt complexes, and low oxidation states of cobalt, the crystal field model was found to be inadequate (118, 119, 164, 165). Lucken, Noack, and Williams used a ligand field extension of the theory, to account for the shielding in cobalticinium ion, and in cobalt complexes with carbonyl, nitrosyl, hydride, and phosphine ligands. Effective excitation energies were taken from MO correlation diagrams. In the cobalticinium ion, cobalt is deshielded by $\pi \rightarrow \sigma^*$ circulations of d_z^2 , and d_{xy} , $d_{x^2-y^2}$ electrons into d_{xz} , d_{yz} orbitals. In the carbonyl and phosphine compounds cobalt is relatively highly shielded as the d shell is (formally) closed, and the relative shielding was accounted for in terms of circulations of d electrons in $4p(\pi^*)$ orbitals (94).

A useful approach is to introduce some allowance for covalency into the simple crystal field model, in which the e_g and t_{2g} orbitals are taken to be pure d orbitals. Freeman, Murray, and Richards gave the shielding, following the Orgel theory, as $\sigma = A - B/\Delta$, with A and B effectively constant among their octahedral complexes. A is the diamagnetic term σ_d , and

$$\sigma_p = -B_0/\Delta_0 = \frac{-32\mu_B^2 \langle r^{-3} \rangle_{3d}}{\Delta_0}$$

Effects of covalent bonding may be simulated by an orbital reduction factor $k_{\sigma\pi}$ between the t_{2g} and e_g orbitals (11, 43, 54, 70, 106, 130):

$$\sigma_p = \frac{-32\mu_B^2 k_{\sigma\pi}^2 \langle r^{-3} \rangle_{nd}}{\Delta_0}$$

The problem is then to find separate estimates of $k_{\sigma\pi}$ and $\langle r^{-3} \rangle_{nd}$, since the discussion becomes circular when these, or their products, are deduced from the observed shifts. An argument for taking the $\langle r^{-3} \rangle_{nd}$ factor as effectively constant is that its relative importance is greatest near the nucleus, where it is least affected by the ligands. Betteridge and Golding have calculated values of the orbital reduction factor k

(from the chemical shift and Δ_0) for cobalt(III) complexes as 0.85 for first-row ligands (C, N, O), decreasing to 0.72 for second-row ligands (Si, P, S, Cl), and 0.67 for third row (As, Se); the corresponding values of the percentage spin transferred to the ligands being 2.86, 5.35, and 6.31. A problem in this approach is that near-constancy of the $\langle r^{-3} \rangle$ and the $k^2 \langle r^{-3} \rangle$ factors, e.g., for C, N, and O ligand atoms implies that k has similar values for π -acceptor ligands such as CN, and for π -donor ligand atoms nitrogen and oxygen, as the k^2 and $\langle r^{-3} \rangle$ factors would not be expected to vary inversely. Some comparisons were made (11) with independent estimates of k from ESR studies (56).

An alternative formulation, in adapting the crystal field theory to allow for covalency, is to insert a C_M^2 factor into the expression for the paramagnetic term, where C_M is the coefficient of the metal orbital in the molecular orbital, as defined (52) by Gray and Ballhausen. Platinum shifts have been discussed in this way, and correlated with other measures of covalency, as discussed below (34, 132); and similarly for vanadium and manganese in octahedral complexes (121a).

Effects of the radial factor ($k^2 \langle r^{-3} \rangle_{nd}$, $C_M^2 \langle r^{-3} \rangle_{nd}$, etc.) can usefully be considered in general terms. In general, increase in d electron radius, as by π -delocalization on the ligands, may be expressed as an increase in nephelauxetic (electron cloud-expanding) (66, 67) effect, which corresponds to a reduced paramagnetic term, since the electron circulation is farther away from the metal nucleus. Values of $k^2 \langle r^{-3} \rangle_{3d}$ in cobalt complexes, as determined from the chemical shifts and ligand field splittings, were found to be 35–55% smaller than in the free ion, and this was interpreted by radial expansion of the e_g orbitals, as a consequence of covalent bonding. Smaller radial factors are found for heavier ligand atoms (43).

In square-planar complexes of platinum(II) (d^8), with a smaller variation in the ligand field splitting, it is possible to trace correlations with the nephelauxetic series of the ligands, in particular series of compounds, as well as with the spectrochemical series. The Δ_s term is taken as a linear combination of the $^1A_{2g}$ and the 1E_g energies. In $[\text{PtX}_2\text{L}_2]$ complexes, where X is halogen and L a ligand bonded through nitrogen, oxygen, phosphorus, arsenic, etc., Pidcock, Richards, and Venanzi (132) found that the platinum shifts follow the spectrochemical series of the ligands L if the halogen is the same. For changes in the halogen, however, the radial factor $C_M^2 \langle r^{-3} \rangle_{5d}$ dominates, the shielding increasing $\text{Cl} < \text{Br} < \text{I}$ (although the ligand field splitting decreases $\text{Cl} > \text{Br} > \text{I}$). The nephelauxetic series was followed also in a series of square-planar platinum hydride complexes with *trans*-phosphine ligands and a fourth anionic ligand $\text{L} = \text{halide}, \text{NO}_2^-$,

NO_3^- , etc. (34). The order of increasing platinum shielding is $L = \text{RCOO}^- < \text{NO}_3^- < \text{NO}_2^- < \text{Cl}^- < \text{SCN}^- < \text{Br}^- < \text{CN}^- < \text{I}^-$, which differs from the nephelauxetic order only in the placement of CN^- , and is quite different from the spectrochemical order, in which the shielding increases $\text{I} < \text{Br} < \text{Cl}$. The conclusion is that the more polarizable ligands reduce the deshielding by reducing the coefficient C_M (subsuming the radial term $\langle r^{-3} \rangle_{5d}$). This conclusion is confirmed in more recent work, on platinum shielding in square-planar complexes (51a, 78): a plot of the shielding against λ_{av} gives different lines for chlorides, bromides, and iodides, with the polarizable ligands (Sb, Te) below the lines (this corresponds to increased shielding) and the less polarizable ones (N, C) above. Some correspondence is observed also between the chemical shifts and other measures of ligand covalency, such as ligand dissociation equilibrium constants, and the $\text{p}K_a$ of the acid HL. The high covalency attributed to the Pt—I bond is in keeping with other spectroscopic observations, such as low infrared intensity and high Raman intensity of the bands for Pt—I stretching vibrations.

Broad correlations are possible, therefore, for compounds with a given d electron configuration, and between the different configurations; despite the complications of opposing factors, such as increasing covalency (σ or $\sigma + \pi$) increasing the excitation energies as well as decreasing the radial factor. In general the spectrochemical series correlation is likely to be observed for less polarizable (hard, class A) ligands, and higher oxidation states of the metal, whereas the nephelauxetic pattern is observed in complexes of polarizable or ($\sigma + \pi$)-bonding ligands, with metals in low oxidation states. Relevant studies (including many already referred to) are those of vanadium (121a, 146a), manganese (9, 23, 121a, 125, 126), molybdenum (96), tungsten (53, 99, 100), rhodium (17, 62), and platinum (78, 98, 176), and reviews of heavy-atom shielding (97, 173).

VII. Correlations with Spectroscopic and Other Properties

As we have seen, linear δ/λ or δ/IE (ionization energy) correlations (113a) can be observed in appropriate series of compounds. Near-linear δ/J (spin-spin coupling constant) correlations have been reported also, in fluorides of carbon (121), boron (60), xenon (50), etc. and in hydride complexes of platinum (7a), for example. In the xenon fluorides and oxyfluorides and their cations (50) the relation between $\delta(\text{F})$ and $J(\text{XeF})$ was attributed to the importance of a mean excitation energy ΔE in the paramagnetic shielding term and in the Fermi contact contribution, which is assumed to be dominant in the Xe—F spin-spin

coupling. The excitations are different in the paramagnetic term and in the Fermi contact term, since the latter is concerned with s orbitals and triplet states (140); but all the same, the energies may vary in parallel. In the platinum hydride complexes (7a) *trans*-[PtHL(PEt₃)₂], with 26 different carboxylate ligands L, the different factors contributing to the Fermi contact term were examined. This term depends directly on the amount of platinum 6s orbital involved in the Pt—H bond, the magnitude of this orbital at the nucleus, and the mean triplet excitation energy ${}^3\Delta E$. Since changes in the carboxylate ligands produced negligible changes in the electronic spectrum, it was concluded that the variation in J_{PtH} was unlikely to be with ${}^3\Delta E$, and more likely to be with the increase in s -character of the bond. This is accomplished by a shortening of the bond, which should increase the proton shielding, in the theory of Buckingham and Stephens (Section VI). In other square-planar platinum complexes the chemical shifts are found to correlate more with covalency of the bonds to the ligands, and with the nephelauxetic series, than with the spectrochemical series. However, in a series of platinum hydride complexes with inorganic acido-ligands ($L = \text{hal}^-$, NO_3^- , etc.) the spin-spin coupling constant was found to follow the order of the spectrochemical series for the *trans*-ligand (7a).

In the platinum hydride carboxylate complexes linear correlations were found also between the chemical shift of the hydride ligand and the Pt—H stretching frequency, and the $\text{p}K_a$ of the parent carboxylic acid (7a). δ/ν (vibration frequency) correlations are not uncommon. Correlations are found also with bond energies, as in a study of ${}^{13}\text{C}$ shifts in methyl- and phenylmercury(II) compounds, in which the effective excitation energy is $\sigma \rightarrow \sigma^*$, so that deshielding correlates with a decrease in the C—Hg bond dissociation energy (16). In the range of Xe-F compounds mentioned above, the Xe—F bond length correlates inversely with J , ν , and with the nuclear magnetic shielding (50).

Since nuclear magnetic shielding depends on the number of electrons, chemical shifts may correlate with charge densities, with Hammett substituent parameters, or with $\text{p}K_a$ or $\text{p}K_b$ values, if other factors involved in the shielding remain sufficiently constant.

REFERENCES

1. Abragam, A., "The Principles of Nuclear Magnetism." Oxford Univ. Press (Clarendon), London and New York, 1961.
2. Akitt, J. W., *Annu. Rep. NMR Spectrosc.* **5A**, 465 (1972).
- 2a. Andersson, L.-O., and Mason, J., *J. Chem. Soc., Dalton Trans.* p. 202 (1974).

3. Andersson, L.-O., Mason, J., and van Bronswijk, W., *J. Chem. Soc. A* p. 296 (1970).
4. Andrew, E. R., *Int. Rev. Sci.: Phys. Chem., Ser. Two*, **4**, 173 (1975).
5. Andrew, E. R., *Prog. NMR Spectrosc.* **8**, 1 (1971).
6. Appleman, B. R., and Dailey, B. P. *Adv. Magn. Reson.* **7**, 231 (1974).
7. apSimon, J. W., Graig, W. G., Demarco, P. V., Matheson, D. W., Saunders, L., and Whalley, W. B., *Tetrahedron* **23**, 2339 and 2357 (1967).
- 7a. Atkins, P. W., Green, J. C., and Green, M. L. H., *J. Chem. Soc. A* p. 2275 (1968).
8. Baliman, G., and Pregosin, P. S., *J. Magn. Reson.* **26**, 283 (1977).
9. Bancroft, G. M., Clark, H. C., Kidd, R. G., Rake, A. T., and Spinney, H. C., *Inorg. Chem.* **12**, 728 (1973).
- 9a. Barnes, R. G., and Smith, W. V., *Phys. Rev. [2]* **93**, 95 (1954).
10. Basch, H., *Chem. Phys. Lett.* **5**, 337 (1970).
11. Betteridge, G. P., and Golding, R. M., *J. Chem. Phys.* **51**, 2497 (1969).
12. Birchall, T., Gillespie, R. J., and Vekris, S. L., *Can. J. Chem.* **43**, 1672 (1965).
13. Bleich, H. E., and Redfield, A. G., *J. Chem. Phys.* **67**, 5040 (1977).
14. Block, R. E., *J. Magn. Reson.* **5**, 155 (1971).
15. Bodner, G. M., Kahl, S. B., Bork, K., Storhoff, B. N., Waller, J. E., and Todd, L. J., *Inorg. Chem.* **12**, 1071 (1973).
16. Brown, A. J., Howarth, O. W., and Moore, P., *J. Chem. Soc., Dalton Trans.* p. 1589 (1976).
17. Brown, T. H., and Green, P. J., *J. Am. Chem. Soc.* **92**, 2359 (1970).
18. Brown, T. L., *Acc. Chem. Res.* **7**, 408 (1974).
19. Buckingham, A. D., and Stephens, P. J., *J. Chem. Soc., London* p. 2747 (1964).
20. Buckingham, A. D., and Stephens, P. J., *J. Chem. Soc., London* p. 4583 (1964).
- 20a. Buckingham, A. D., and Urland, W., *Mol. Phys.* **26**, 1571 (1973).
21. Burke, J. J., and Lauterbur, P. C., *J. Am. Chem. Soc.* **83**, 326 (1961).
22. Cade, P. E., and Huo, W. M., *J. Chem. Phys.* **47**, 649 (1967).
23. Calderazzo, F., Lucken, E. A. C., and Williams, D. F., *J. Chem. Soc. A* p. 154 (1967).
24. Carroll, T. X., Shaw, R. W., Thomas, T. D., Kindle, C., and Bartlett, N., *J. Am. Chem. Soc.* **96**, 1989 (1974).
25. Chan, S. I., and Das, T. P., *J. Chem. Phys.* **37**, 1527 (1962).
26. Clark, D. T., and Kilcast, D., *J. Chem. Soc. A* p. 3286 (1971).
27. Connor, J. A., Jones, E. D., Randall, E. W., and Rosenberg, E., *J. Chem. Soc., Dalton Trans.* p. 2419 (1972).
28. Cornwell, C. D., *J. Chem. Phys.*, **44**, 874 (1966). *Abstr. Columbus Symp. Molec. Spectrosc.*, p. 40 (1964).
29. Coulson, C. A., "Valence," p. 44. Oxford Univ. Press, London and New York, 1961.
30. Coyle, T. D., Stafford, S. L., and Stone, F. G. A., *J. Chem. Soc., London* p. 3103 (1961).
31. Craig, D. P., and Magnusson, E. A., *J. Chem. Soc., London* p. 4895 (1956).
32. Davies, A. G., Harrison, P. G., Kennedy, J. D., Mitchell, T. N., Puddephatt, R. J., and McFarlane, W., *J. Chem. Soc. C* p. 1136 (1969).
33. Davies, D. W., "The Theory of the Electric and Magnetic Properties of Molecules." Wiley, New York, 1967.
34. Dean, R. R., and Green, J. C., *J. Chem. Soc. A* p. 3047 (1968).
35. De Leeuw, F. H., and Dymanus, A. *J. Mol. Spectrosc.* **48**, 427 (1973).
36. Dharmatti, S. S., and Kanekar, C. R., *J. Chem. Phys.* **31**, 1436 (1959).
37. Ditchfield, R., *Mol. Phys.* **27**, 789 (1974).
38. Ditchfield, R., Miller, D. P., and Pople, J. A., *J. Chem. Phys.* **53**, 613 (1970); **54**, 4186 (1971).
39. Drain, L. E., *J. Phys. Chem. Solids* **24**, 379 (1963).

40. Flygare, W. H., *Chem. Rev.* **74**, 653 (1974).
41. Flygare, W. H., and Goodisman, J., *J. Chem. Phys.* **49**, 3122 (1968).
42. Freeman, R., Murray, G. R., and Richards, R. E., *Proc. R. Soc. London, Ser. A* **242**, 455 (1957).
43. Fujiwara, A., Yajima, F., and Yamasaki, A., *J. Magn. Reson.* **1**, 203 (1969).
44. Fukui, H., *Bull. Chem. Soc. Jpn.* **47**, 751 (1974).
45. Gelius, U., *Phys. Scr.* **9**, 133 (1974).
46. Gelius, U., Johanssen, G., Siegbahn, H., Allan, C. J., Allison, D. A., Allison, J., and Siegbahn, K., *J. Electron Spectrosc.* **1**, 285 (1972/3).
47. Gibby, M. G., Griffin, R. G., Pines, A., and Waugh, J. S., *Chem. Phys. Lett.* **17**, 80 (1972).
48. Gibby, M. G., Pines, A., and Waugh, J. S., *J. Am. Chem. Soc.* **94**, 6231 (1972).
49. Gierke, T. D., and Flygare, W. H., *J. Am. Chem. Soc.* **94**, 7277 (1972).
50. Gillespie, R. J., and Schrobilgen, G. J., *Inorg. Chem.* **13**, 765, 1455, and 2370 (1974).
- 50a. Goggin, P. L., Goodfellow, R. J., Haddock, S. R., Taylor, B. F., and Marshall, I. R. H., *J. Chem. Soc., Dalton Trans.* p. 459 (1976).
51. Graham, W. A. G., *Inorg. Chem.* **7**, 315 (1968).
52. Gray, H. B., and Ballhausen, C. J., *J. Am. Chem. Soc.* **85**, 260 (1963).
53. Green, P. J., and Brown, T. H., *Inorg. Chem.* **10**, 206 (1971).
54. Griffith, J. S., "The Theory of Transition Metal Ions," p. 374. Cambridge Univ. Press, London and New York, 1961.
55. Griffith, J. S., and Orgel, L. E., *Trans. Faraday Soc.* **53**, 601 (1957).
56. Hall, T. P. P., Hayes, W., Stevenson, R. W. H., and Wilkens, J., *J. Chem. Phys.* **39**, 35 (1963).
57. Hameka, H. F., *Rev. Mod. Phys.* **34**, 87 (1962).
58. Haraguchi, H., and Fujiwara, S., *J. Phys. Chem.* **73**, 3467 (1969).
59. Harris, D. H., Lappert, M. F., Poland, J. S., and McFarlane, W., *J. Chem. Soc., Dalton Trans.* p. 311 (1975).
60. Hartman, J. S., and Schrobilgen, G. J., *Inorg. Chem.* **11**, 940 (1972).
61. Hartmann, S. R., and Hahn, E. L., *Phys. Rev.*, **128**, 2042 (1962).
62. Hyde, E. M., Kennedy, J. D., Shaw, B. L., and McFarlane, W., *J. Chem. Soc., Dalton Trans.* p. 1571 (1977).
63. Jameson, C. J., and Gutowsky, H. S., *J. Chem. Phys.* **40**, 1714 (1964).
64. Johnson, K. J., Hunt, J. P., and Dodgen, H. W., *J. Chem. Phys.* **51**, 4493 (1969).
65. Jolly, W. L., *Coord. Chem. Rev.* **13**, 47 (1974).
66. Jørgensen, C. K., "Absorption Spectra and Chemical Bonding," Chapter 8, Pergamon, Oxford, 1962.
67. Jørgensen, C. K., "Oxidation Numbers and Oxidation States." Springer-Verlag, Berlin and New York, 1969.
68. Kaesz, H. D., and Saillant, R. B., *Chem. Rev.* **72**, 231 (1972).
69. Kaiser, E. W., *J. Chem. Phys.* **53**, 1686 (1970).
70. Kamimura, H., *J. Phys. Soc. Jpn.* **21**, 484 (1966).
71. Kanekar, C. R., Dhingra, M. M., Marathe, V. R., and Nagarajan, R., *J. Chem. Phys.* **46**, 2009 (1967).
72. Karplus, M., *J. Chem. Phys.* **33**, 941 (1961).
73. Karplus, M., and Pople, J. A., *J. Chem. Phys.* **38**, 2803 (1963).
74. Kaufmann, J., Sahm, W., and Schwenk, A., *Z. Naturforsch., Teil A* **26**, 1384 (1971).
75. Kennedy, J. D., and McFarlane, W., *Rev. Silicon, Germanium, Tin and Lead Comp.* **1**, 235 (1974).
76. Kennedy, J. D., and McFarlane, W., *J. Chem. Soc., Faraday Trans.* **272**, 1653 (1976).
77. Kennedy, J. D., McFarlane, W., and Wrackmeyer, B., *Inorg. Chem.* **15**, 1299 (1976).

- 77a. Kennedy, J. D., McFarlane, W., and Pyne, G. S., *J. Chem. Soc., Dalton Trans.* p. 2332 (1977).
78. Kennedy, J. D., McFarlane, W., Puddephatt, R. J., and Thompson, P. J., *J. Chem. Soc., Dalton Trans.* p. 875 (1976).
79. Kidd, R. G., and Truax, D. R., *J. Am. Chem. Soc.* **90**, 6867 (1968).
80. Kidd, R. G., and Spinney, H. G., *J. Am. Chem. Soc.* **95**, 88 (1973).
81. Kohler, S. J., Ellett, J. D., and Klein, M. P., *J. Chem. Phys.* **64**, 4451; **65**, 2922 (1976).
82. Kolshorn, H., and Meier, H., *J. Chem. Res. (S)* p. 338 (1977).
83. Kondo, M., Ando, I., Chûjô, R., and Nishioka, A., *J. Magn. Reson.* **24**, 315 (1976).
84. Kondo, M., Ando, I., Chûjô, R., and Nishioka, A., *Mol. Phys.* **33**, 463 (1977).
85. Lamb, W. E., *Phys. Rev.* [2] **60**, 817 (1941).
86. LaRossa, R. A., and Brown, T. L., *J. Am. Chem. Soc.* **96**, 2072 (1974).
87. Lau, K. F., and Vaughan, R. W., *Chem. Phys. Lett.* **33**, 550 (1975).
88. Lauterbur, P. C., *Ann. N.Y. Acad. Sci.* **70**, 840 (1958).
89. Lee, C. Y., and Cornwell, C. D., *Magn. Reson. Relat. Phenom., Proc. Congr. AMP-ERE 19th*, p. 261 (1976).
90. Letcher, J. H., and Van Wazer, J. R., "Topics in Phosphorus Chemistry," Vol. 4. Wiley (Interscience), New York, 1966.
91. Letcher, J. H., and Van Wazer, J. R., *J. Chem. Phys.* **44**, 815 and **45**, 2916 and 2921 (1966).
92. Lipscomb, W. N., *Adv. Magn. Reson.* **2**, 137 (1966).
93. London, F., *J. Phys. Radium* **8**, 397 (1937).
94. Lucken, E. A. C., Noack, K., and Williams, D. F., *J. Chem. Soc. A* p. 184 (1967).
95. Lunazzi, L., *Determination Org. Struct. Phys. Methods* **6**, 335 (1976).
96. Lutz, O., Nolle, A., and Kroneck, P., *Z. Naturforsch., Teil A* **31**, 454 (1976).
- 96a. Lyubimov, V. S., and Ionov, S. P., *Russ. J. Phys. Chem. (Engl. Transl.)* **46**, 486 (1972), and references therein.
97. Maciel, G. E., in "NMR Spectroscopy of Nuclei other than Protons" (T. Axenrod and G. A. Webb, eds.) p. 347. Wiley, New York, 1974.
98. McFarlane, W., *J. Chem. Soc., Dalton Trans.* p. 324 (1974).
- 98a. McFarlane, H. C. E., and McFarlane, W., *J. Chem. Soc. Dalton Trans.* p. 2416 (1973).
99. McFarlane, H. C. E., McFarlane, W., and Rycroft, D. S., *J. Chem. Soc., Dalton Trans.* p. 1616 (1976).
100. McFarlane, W., Noble, A. M., and Winfield, J. M., *J. Chem. Soc. A* p. 948 (1971).
101. McFarlane, W., Wrackmeyer, B., and Nöth, H., *Chem. Ber.* **108**, 3831 (1975).
102. McLachlan, A. D., *J. Chem. Phys.* **32**, 1263 (1960).
103. McLean, A. D., and Yoshimine, M., *J. Chem. Phys.* **47**, 3256 (1967).
104. Malli, G., and Fraga, S., *Theor. Chim. Acta* **5**, 275 (1966).
105. Mansfield, P., *Prog. NMR Spectrosc.* **8**, 41 (1971).
106. Martin, R. L., and White, A. H., *Nature (London)* **223**, 394 (1969).
107. Mason, J., *J. Chem. Soc., Dalton Trans.* p. 19 (1975).
108. Mason, J., *J. Chem. Soc., Dalton Trans.* p. 1422 (1975).
109. Mason, J., *J. Chem. Soc., Dalton Trans.* p. 1426 (1975).
110. Mason, J., *J. Chem. Soc., Perkin Trans. 2* p. 1671 (1976).
111. Mason, J., *J. Chem. Soc., Faraday Trans. 2* **72**, 2064 (1976).
- 111a. Mason, J., *Adv. Inorg. Chem. Radiochem.* **18**, 197 (1976).
112. Mason, J., *Org. Magn. Reson.* **10**, 188 (1977).
113. Mason, J., *J. Chem. Soc., Faraday Trans. 2* **73**, 1464 (1977).
- 113a. Mason, J., *J. Chem. Soc., Faraday Trans. 2*, in press.
114. Mason, J., and van Bronswijk, W., *J. Chem. Soc. A* p. 791 (1971).
115. Masuda, Y., *J. Phys. Soc. Jpn.* **11**, 670 (1956).

116. Mateescu, G. D., and Riemenschneider, J. L., in "Electron Spectroscopy" (D. A. Shirley, ed.), p. 661. North-Holland Publ., Amsterdam, 1972.
117. Mavel, G., *Ann. Rep. NMR Spectrosc.* **5B**, 1 (1973).
118. Mooberry, E. S., Pupp, M., Slater, J. L., and Sheline, R. K., *J. Chem. Phys.* **55**, 3655 (1971).
119. Mooberry, E. S., and Sheline, R. K., *J. Chem. Phys.* **56**, 1852 (1972).
120. Mooberry, E. S., Spiess, H. W., and Sheline, R. K., *J. Chem. Phys.* **57**, 813 (1972).
- 120a. Morishima, I., Mizuno, A., and Yonezawa, T., *Chem. Phys. Lett.* **7**, 633 (1970).
121. Muller, N., and Carr, D. T., *J. Phys. Chem.* **67**, 112 (1963).
- 121a. Nakano, T., *Bull. Chem. Soc. Jpn.* **50**, 661 (1977).
122. Nöth, H., and Vahrenkamp, H., *Chem. Ber.* **99**, 1049 (1966).
123. Nöth, H., and Wrackmeyer, B., *Chem. Ber.* **107**, 3070 and 3089 (1974).
124. Onak, T. P., Landesman, H., Williams, R. E., and Shapiro, I., *J. Am. Chem. Soc.* **81**, 1533 (1959).
125. Onaka, S., Miyamoto, T., and Sasaki, Y., *Bull. Chem. Soc. Jpn.* **44**, 1851 (1971).
126. Onaka, S., Sasaki, Y., and Sano, H., *Bull. Chem. Soc. Jpn.* **44**, 726 (1971).
127. O'Reilly, D. E., *J. Phys. Chem.* **32**, 1007 (1960).
128. Orgel, L. E., *J. Chem. Soc., London* p. 4186 (1958).
129. Orgel, L. E., *Mol. Phys.* **1**, 322 (1958).
130. Owen, J., and Thornley, F. H. M., *Rep. Prog. Phys.* **29**, 676 (1966).
131. Parish, R. V., *Prog. Inorg. Chem.* **15**, 101 (1972).
132. Pidcock, A., Richards, R. E., and Venanzi, L. M., *J. Chem. Soc. A* p. 1970 (1968).
133. Piette, L. H., and Weaver, H. E., *J. Chem. Phys.* **28**, 735 (1958).
134. Pines, A., Gibby, M. G., and Waugh, J. S., *J. Chem. Phys.* **56**, 1776 (1972).
135. Pines, A., Gibby, M. G., and Waugh, J. S., *J. Chem. Phys.* **59**, 569 (1973).
136. Pitcher, E., Buckingham, A. D., and Stone, F. G. A., *J. Chem. Phys.* **36**, 124 (1962).
137. Politzer, P., Reuther, J., and Kasten, G. T., *J. Chem. Phys.* **67**, 2385 (1977).
138. Pople, J. A., *J. Chem. Phys.* **37**, 53 and 60 (1962).
139. Pople, J. A., *Discuss. Faraday Soc.* **34**, 7 (1962); *Mol. Phys.* **7**, 301 (1963-1964).
140. Pople, J. A., and Santry, D. P., *Mol. Phys.* **8**, 1 (1964).
141. Pople, J. A., McIver, J. W., and Ostlund, N. S., *J. Chem. Phys.* **49**, 2960 (1968).
142. Pople, J. A., Schneider, W. G., and Bernstein, H. J., "High Resolution NMR." McGraw-Hill, New York, 1959.
143. Ramsey, N. F., *Phys. Rev.* **78**, 699 (1950); **86**, 243 (1952).
144. Ramsey, N. F., "Molecular Beams." Oxford Univ. Press, London and New York, 1963.
145. Raymonda, J., and Klemperer, W., *J. Chem. Phys.* **55**, 232 (1971).
146. Raynes, W. T., *NMR Spec. Period. Rep. Chem. Soc.* **2**, 2 (1973).
- 146a. Rehder, D., *J. Magn. Reson.* **25**, 177 (1977).
147. Reichert, B. E., and West, B. O., *J. Chem. Soc. Chem. Commun.* p. 177 (1974).
148. Reinartz, J. M. L. J., and Dymanus, A., *Chem. Phys. Lett.* **24**, 346 (1974).
149. Retcofsky, H. L., and Friedel, R. A., *J. Am. Chem. Soc.* **94**, 6579 (1972).
150. Sadlej, A. J., *Chem. Phys. Lett.* **36**, 129 (1975).
151. Saika, A., and Slichter, C. P., *J. Chem. Phys.* **22**, 26 (1954).
152. Saito, Y., *Can. J. Chem.* **43**, 2530 (1965).
- 152a. Santry, D. P., "Theoretical Chemical Research at the Carnegie Inst. of Technology" 1965.
153. Schneider, W. G., and Buckingham, A. D., *Discuss. Faraday Soc.* **34**, 147 (1962).
- 153a. Schraml, J., and Bellama, J. M., *Determination Org. Struct. Phys. Methods* **6**, 203 (1976).
154. Schwartz, M. E., *Chem. Phys. Lett.* **6**, 631 (1970).

155. Schwenk, A., *J. Magn. Reson.* **5**, 376 (1971).
156. Sears, R. E. J., *J. Chem. Phys.* **66**, 5250 (1977), and references therein.
157. Selwood, P. W., "Magnetochemistry." Wiley (Interscience), New York, 1956.
158. Sheldrick, G. M., *Trans. Faraday Soc.* **63**, 1077 (1967).
159. Shirley, D. A., *Adv. Chem. Phys.* **23**, 85 (1973).
160. Siegbahn, K., Nordling, C., Johansson, G., Hedman, J., Hedén, P. F., Hamrin, K., Gelius, U., Bergman, T., Werme, L. O., Manne, R., and Baer, Y., "ESCA Applied to Free Molecules." North-Holland Publ., Amsterdam, 1969.
161. Slater, J. L., Pupp, M., and Sheline, R. K., *J. Chem. Phys.* **57**, 2105 (1972).
162. Smith, P. J., and Smith, L., *Inorg. Chim. Acta., Rev.* **7**, 11 (1973).
163. Spiess, H. W., Haas, H., and Hartmann, H., *J. Chem. Phys.* **50**, 3057 (1969).
164. Spiess, H. W., and Sheline, R. K., *J. Chem. Phys.* **53**, 3036 (1970).
165. Spiess, H. W., and Sheline, R. K., *J. Chem. Phys.* **54**, 1099 (1971).
166. Stevens, R. M., Pitzer, R. M., and Lipscomb, W. N., *J. Chem. Phys.* **38**, 550 (1963).
167. Stoll, M. E., Vaughan, R. W., Saillant, R. B., and Cole, T., *J. Chem. Phys.* **61**, 2896 (1974).
168. Stoll, M. E., Vega, A. J., and Vaughan, R. W., *J. Chem. Phys.* **65**, 4093 (1976).
169. Van Vleck, J. H., "Theory of Electric and Magnetic Susceptibilities." Oxford Univ. Press, London and New York, 1932.
170. Vaughan, R. W., Elleman, D. D., Rhim, W.-K., and Stacey, L. M., *J. Chem. Phys.* **57**, 5383 (1972).
171. Waugh, J. S., Huber, L. M., and Haeberlen, U., *Phys. Rev. Lett.* **20**, 180 (1968).
172. Wells, A. F., "Structural Inorganic Chemistry." Oxford Univ. Press, London and New York, 1962.
173. Wells, P. R., *Determination Org. Struct. Phys. Methods* **4**, 233 (1971).
174. Wuyts, L. G., and Van der Kelen, G. P., *J. Mol. Struct.* **23**, 73 (1974).
175. Yamasaki, A., Yajima, F., and Fujiwara, S., *Inorg. Chim. Acta* **2**, 39 (1968).
176. Zelewsky, A. v., *Helv. Chim. Acta* **51**, 803 (1968).
177. Zeroka, D., *Chem. Phys. Lett.* **14**, 471 (1972).

NOTE ADDED IN PROOF

Now that definitive studies of ^{129}Xe resonance in the element and its compounds are available (1A,2A), it is interesting to examine the pattern of chemical shifts for this heavy atom. The familiar effects of local symmetry and effective nuclear charge are evident in the sequence of the fluoride species in xenon resonance. The xenon shielding decreases $\text{Xe} \gg \text{XeF}_2 > (\text{FXe} \cdots \text{F} \cdots \text{XeF})^+ > \text{XeF}^+ > (\text{XeF}_6)_4 > \text{XeF}_5^+ > \text{XeF}_4 > \text{XeF}_3^+$, with the free atom and then the linear molecule XeF_2 at highest field, and at lowest field the T-shaped ion XeF_3^+ and then the square planar molecule XeF_4 . The shielding decreases also with increase in oxidation number of xenon from 0 to VIII (increasing the $\langle r^{-3} \rangle_{\text{sp,d}}$ terms), with XeF_4 and XeF_3^+ out of line, because of their lower symmetry.

Xenon is strongly deshielded with increase in oxygen substitution in the sequence $\text{XeF}_5^+ > \text{XeOF}_4 > \text{XeO}_2\text{F}_2 > \text{XeO}_3 > \text{XeOF}_3^+ > \text{XeF}_4 > \text{XeF}_3^+ > \text{XeO}_2\text{F}^+ \gg \text{XeO}_6^{4-}$. Interestingly, the highly symmetrical perxenate ion resonates at very low field. This is found for other oxyanions [such as ClO_4^- (64)] and may be associated with low excitation energies.

In the series of linear complexes of XeF_2 with Lewis acids (A) of increasing acid strength, from F-Xe-F via $\text{AF} \cdots \text{Xe} \cdots \text{F}$ to $^+\text{Xe-F}$, the xenon line goes downfield as the (terminal) fluorine line goes upfield, as the terminal Xe-F bond shortens, and with increase in $^1J(\text{XeF})$.

In these results the theory of Jameson and Gutowsky (3A,63) for the xenon fluorides and XeOF_4 , in terms of localized bonds using xenon s , p , and d orbitals, is well confirmed. It seems that the "atom in a molecule" description is rather well suited to the shielding of a heavy atom with lighter ligands, as ligand atom contributions can then more safely be neglected.

REFERENCES

- 1A. Schrobilgen, G. J., Holloway, J. H., Granger, P., and Brevard, C., *Inorg. Chem.* **17**, 980 (1978).
- 2A. Seppelt, K., and Rupp, H. H., *Z. Anorg. Allg. Chem.* **409**, 331 and 338 (1974).
- 3A. Jameson, C. J., and Gutowsky, H. S., *J. Chem. Phys.* **40**, 2285 (1964).

CYCLIC SULFUR-NITROGEN COMPOUNDS

H. W. ROESKY

Institute of Inorganic Chemistry, University of Frankfurt, Frankfurt, West Germany

I. Introduction	240
II. Three-Membered Rings	240
III. Description of Sulfur-Nitrogen Compounds with Coordination Number Two at the Sulfur and Nitrogen Atoms	242
IV. Four-Membered Rings	243
A. Doubly Coordinated Sulfur	243
B. Three- and Four-Coordinated Sulfur	244
C. Four-Membered Rings Containing One Element Other Than Sulfur and Nitrogen	245
V. Five-Membered Rings	248
A. Radical Cations	248
B. Compounds Related to $N_2S_3^+$	250
C. Five-Membered Rings Containing One Element Other Than Sulfur and Nitrogen	253
D. The Function of N_2S_2 , HN_2S_2 , and NS_3 as Bidentate Ligands.	261
VI. Six-Membered Rings.	264
A. Doubly Coordinated Sulfur and Nitrogen	264
B. Structural Investigations of Six-Membered Rings with the Coordina- tion Number Two at the Sulfur and Nitrogen Atoms	265
C. Sulfur and Nitrogen with Coordination Numbers Two and/or Three	266
D. Compounds of Coordination Number Two at Nitrogen and Four at Sulfur	269
E. Bonding Properties of Sulfur with Coordination Numbers Three and Four	272
F. Doubly Coordinated Nitrogen, Three- and/or Four-Coordinated Sulfur	273
G. Two- and Four-Coordinated Sulfur	274
H. Threefold Coordinated Nitrogen and Four-Coordinated Sulfur	276
I. Compounds Having One Element in the Ring Other Than Sulfur and Nitrogen.	276
VII. Seven-Membered Rings.	280
A. Doubly Coordinated Sulfur and Nitrogen	280
B. Compounds Having One Element within the Ring Other Than Sulfur and Nitrogen	281
VIII. Eight-Membered Rings	281
A. Structure and Bonding in N_4S_4 , Its Adducts with Lewis Acids and in $N_4S_4^{2+}$	281
B. Compounds with Coordination Numbers Two and Three	284
C. Compounds with Coordination Numbers Two, Three, and Four	290
IX. Ten-Membered Rings	292

X. Twelve-Membered Rings	293
References	294

I. Introduction

In the following article an attempt has been made to bring together recent data on cyclic sulfur–nitrogen compounds. The major sections of the review are organized on the basis of ring size. Within each section the versatility of the sulfur–nitrogen compounds is simplified by using coordination numbers. In other words, the focal point is the sulfur atom which can be classified on the basis of the number of surrounding substituents. In addition, the coordination numbers two and three at the nitrogen atoms will also be taken in account for the ordering principle. Finally, sulfur–nitrogen compounds which contain one other element will be discussed in each section. The numerous reports, wherein three- or four-membered rings are formulated as intermediates, will not be considered.

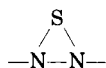
The literature has been surveyed up to the end of 1977. In many cases, the examples cited are meant to be representative and indicative rather than to be all-inclusive. In general, for the cohesion of this article the alphabetical order was used for writing the formulas.

II. Three-Membered Rings

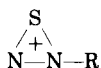
As stated in the introduction, the sulfur–nitrogen rings are classified according to the groups directly bonded to the sulfur atom. Thus, the coordination of the sulfur atom will be a reflection of the number of substituents rather than of the various oxidation states of sulfur.

There are 13 possible arrangements of sulfur with coordination numbers two, three, and four, which are shown in Table I. The sulfur ring compounds may contain these building blocks.

Three-membered rings with bivalent sulfur have so far not been reported. Several theoretical arrangements are possible [see structures



(I)



(II)



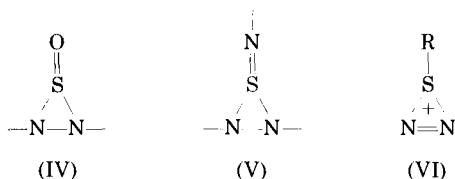
(III)

(I)–(III)]. Although the oxygen analog of (I) has been isolated (96, 110, 239), the repulsion between lone-pair electrons is probably the reason for the instability of these three-membered rings. On paper we would

TABLE I
ARRANGEMENTS OF SULFUR WITH COORDINATION
NUMBERS TWO, THREE, AND FOUR

cn2	cn3	cn4

expect that compounds of types (IV) and (V) might be more stable, but they are not mentioned in the literature (230).



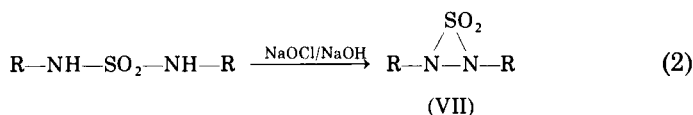
Compound (V) presents a real challenge for the synthetic chemist. The groups attached to the nitrogens should have strong electron-withdrawing properties, so that the interaction of the lone pairs will be diminished.

It was reported that the benzenesulfenium cation adds molecular nitrogen to form a cyclic adduct of type (VI) (177). Whether the



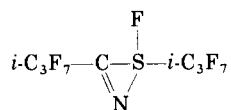
nitrogen forms a side-on or end-on adduct was not shown with certainty.

In the dioxide (VII) the sulfur extends its coordination number to four (46*a*, 187*b*).



Dioxide (VII) is prepared from the diamide with sodium hydroxide (63, 245) and hypochlorite. The structure was determined on the basis of an X-ray analysis (248). It is interesting to point out that the increasing size of substituents R is responsible for the stability of (VII). This observation is significant and could prove to be general and extremely useful for synthesis of other small ring systems. The R groups are in the trans configuration. This was found with ^1H NMR as well as by crystallography. The N—N bond (167 pm) is significantly longer than any analogous distance (for example, 147 pm in H_2NNH_2) and is, in fact, bracketed between the value for hydrazine and 175 pm found for the admittedly lengthened N—N bond in N_2O_4 (2).

When $\text{CF}_3\text{N}=\text{SF}_2$ and perfluoropropene were allowed to react at 83°C for 115 hours at autogenous pressure, a 4% yield of the three-membered compound,



which boiled at 75.5°C , was found (117). An analogous compound was isolated, when $\text{CF}_3\text{CF}=\text{CF}_2$ and $\text{C}_3\text{F}_7\text{N}=\text{SF}_2$ were allowed to react at 100°C in the presence of cesium fluoride (58). No structural proof is given for these two compounds.

III. Description of Sulfur–Nitrogen Compounds with Coordination Number Two at the Sulfur and Nitrogen Atoms

In the periodic table nitrogen and sulfur are located in a diagonal position. Therefore the ratio of radius to charge for both elements is nearly the same. As a result, the polar character of the S—N— bond is low and the electronegativity difference is small. These criteria are fulfilled for a S—N bond under the assumption that sulfur and nitrogen both have a coordination number of two. If we assume that only

p electrons are involved, we can ignore the electronegativity difference between sulfur and nitrogen. The calculations for electronegativities by Hinze and Jaffé (112) gave for both elements the same value of 2.28 for the p electrons. In the application of simple Hückel molecular orbital (MO) theory, we treat SN rings as though they were homonuclear. The effect of this approximation is to assign nonbonding character to some orbitals, which otherwise would be weakly bonding (80). Johnson, Blyholder, and Cordes (118) concluded from Hückel MO calculations that the electronic spectrum of N_3S_4^+ is consistent with a 10π -electron system. This suggests that in addition to the σ -framework electrons and the lone-pair electrons each sulfur atom provides two π electrons and each nitrogen provides one π electron. In cyclic S—N systems with coordination number two, the Hückel $4n + 2$ rule can be applied. A planar structure with delocalized bonding is favored when n , the number of π electrons, is 2, 6, 10, or 14. The method is justified by its simplicity, the agreement with valence bond formulation, and its success in structure correlation.

IV. Four-Membered Rings

A. DOUBLY COORDINATED SULFUR

The simplest known sulfur-nitrogen ring compound is N_2S_2 (54, 162). It was shown by X-ray analysis that the molecule has a square-planar configuration with nearly equal S—N bond lengths. N_2S_2 is isoelectronic with S_4^{2+} . According to simple Hückel MO theory, the bonding properties can be described in the following way, that the molecule has one pair of bonding π electrons, 4 electrons are in nonbonding orbitals, and the π^* orbital is unoccupied.

The square-planar configuration with D_{4h} symmetry for the S_4^{2+} cation is lowered to D_{2h} symmetry for N_2S_2 (Fig. 1). According to MO theory, the molecule has only one pair of bonding π electrons. This is in agreement with a valence bond description (78, 119, 237).

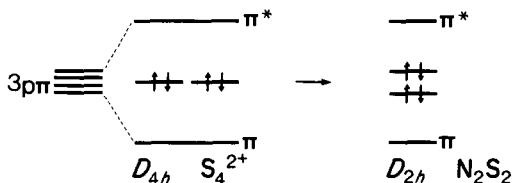


FIG. 1. Splitting of the four $3p\pi$ atomic orbitals.

On the other hand the structure of N_2S_2 can be compared with cyclobutadiene, but having two filled, instead of two half-filled, π nonbonding degenerate molecular orbitals (Fig. 2).

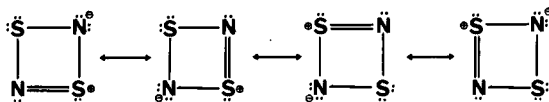
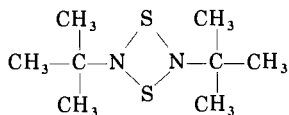


FIG. 2. Resonance structures for N_2S_2 .

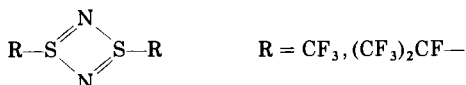
Further support for these bonding properties can be drawn from the structures of $N_2S_2(SbCl_5)_2$ and $N_2S_2BCl_3$. As a result, there is no appreciable lengthening of the S—N bonds (180). $N_2S_2(SbCl_5)_2$ and $N_2S_2SbCl_5$ are formed from N_2S_2 and $SbCl_5$ (178). The hitherto unknown $N_2S_2^{2+}$ is isoelectronic with P_4 ; whether, by analogy, it has a planar or tetrahedral structure, is an interesting question.

A nitrogen-substituted four-membered ring was obtained as a product of the reaction between *tert*-BuNH₂ and SCl₂ in diethyl ether (51). It was claimed that compounds of this type are useful fungicides and inhibitors for corrosion.

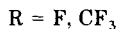
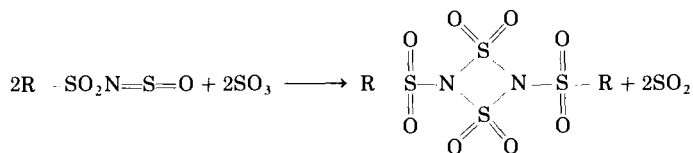


B. THREE- AND FOUR-COORDINATED SULFUR

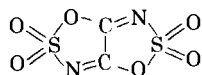
A short report claimed that $(CF_3S)_3N$ reacts under UV irradiation to give traces of $(CF_3SN)_2$ (38). An analogous compound was found by the reaction of $S_3N_3F_3$ with $CF_3CF=CF_2$ (84). The cyclic structure for these compounds was assigned on the basis of physical measurements.



It was found that $FSO_2N=S=O$ and $CF_3SO_2N=S=O$ react with SO_3 with formation of SO_2 to give a stable four-membered ring (197, 229).



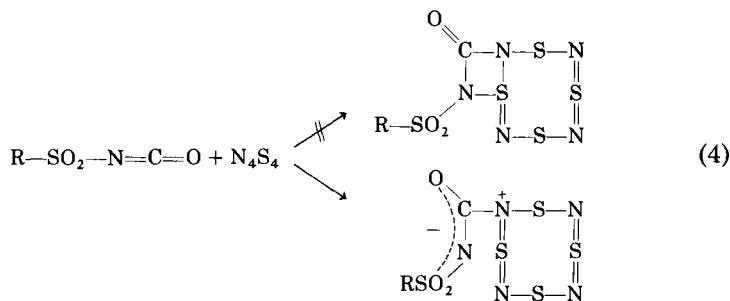
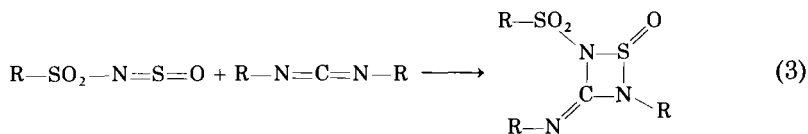
The monomer species $R-SO_2NSO_2$ could be stabilized with pyridine or N_4S_4 with formation of the 1:1 adducts. When the ring is treated with C_6H_5CN , a new six-membered ring is formed, containing two nitrile and one NSO_2 group. Cyanogen and SO_3 give a bicyclic ring when allowed to react in a ratio of 1:2 (196).

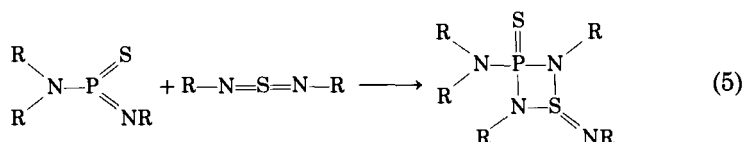


It is not a Lewis-acid Lewis-base adduct as stated earlier (133b), but it was found that $(CN)_2$ and SO_3 undergo a crisscross cycloaddition.

C. FOUR-MEMBERED RINGS CONTAINING ONE ELEMENT OTHER THAN SULFUR AND NITROGEN

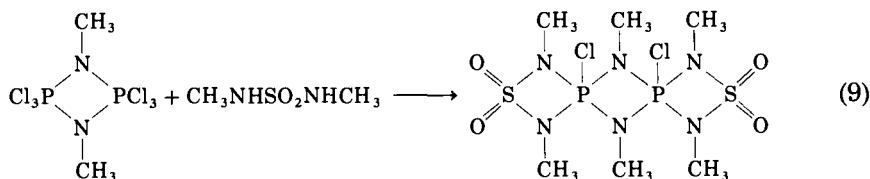
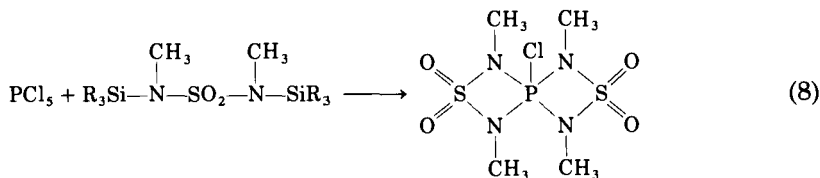
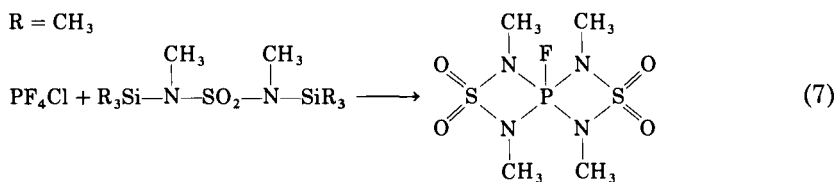
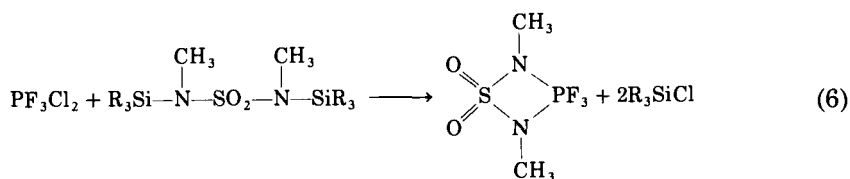
There are several papers that claim that four-membered rings are formed by the addition of iminosulfuroxides, isocyanates, ketene-imides, or phosphorus imides to $S-N$ multiple bonds (11, 131, 163, 164).

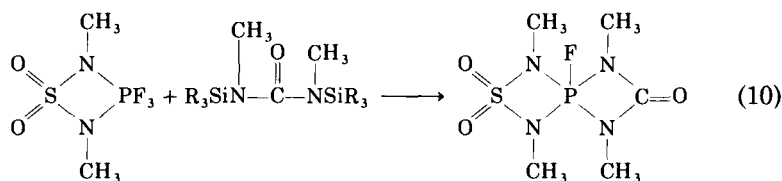




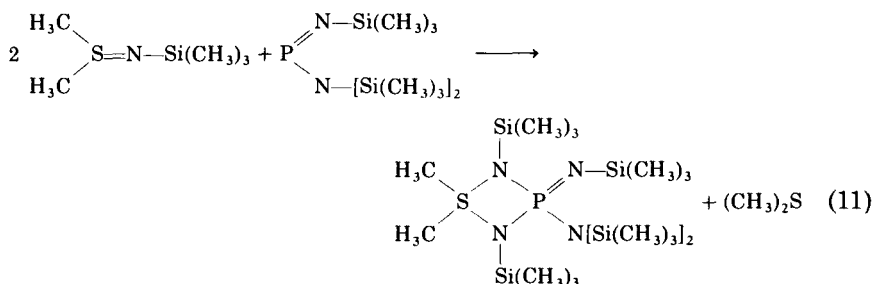
In all cases it was not shown whether cyclic compounds or zwitterionic species are formed. For the adduct of FSO_2NCO with N_4S_4 it was proved by an X-ray structure analysis that a dipolar cycloaddition did not occur, but a dipolar structure was observed, in which the carbon of the isocyanate group coordinates to a nitrogen atom of the N_4S_4 skeleton (195).

Becke-Goehring and co-workers have synthesized a number of four-membered rings with four-coordinated sulfur, which are summarized in Eqs. (6)–(10) (35, 36).



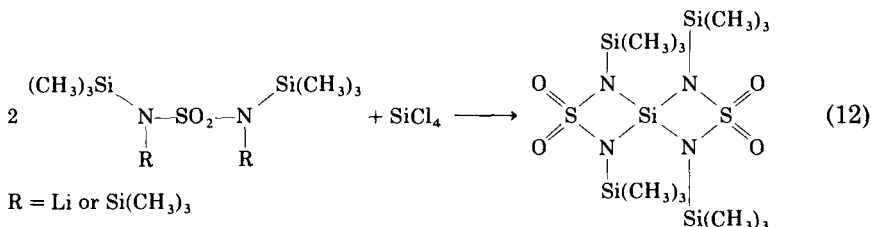


A condensation of iminosulfone and amino-iminophosphane results

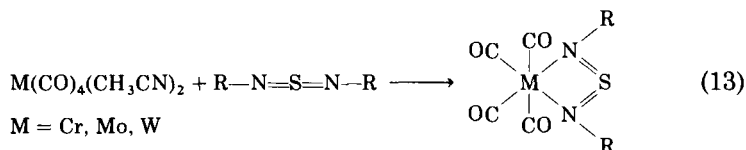


in the formation of a dimethyl sulfur-substituted four-membered ring, which is also obtained by the reaction of $[(\text{CH}_3)_3\text{Si}]_2\text{N}-\text{P}[\text{NSi}(\text{CH}_3)_3]_2$ with $(\text{CH}_3)_2\text{S}=\text{NSi}(\text{CH}_3)_3$ (9).

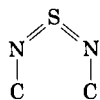
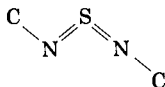
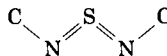
A spiro silazane has been obtained by the following reaction (10).



The reaction of carbonyls with sulfur diimides leads to metal containing four-membered rings (140, 155).



The sulfur diimides function as bidentate ligands. The structure of sulfur diimides has been a matter of dispute, because three possible planar conformations of the CNSNC skeleton may occur.

*cis-cis**trans-cis**trans-trans*

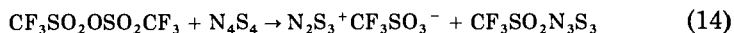
X-Ray data for bis(*p*-tolyl)sulfur diimide have shown this compound to have the *trans-cis* form in the solid state, and complete neglect of differential overlap (CNDO) calculations on similar compounds also lead to the conclusion that this conformation is the most stable one (98, 133). From the NMR and other results the most plausible structure for the above metal complexes involves a *trans-trans*-sulfur diimide bonded to the $M(CO)_4$ fragment.

V. Five-Membered Rings

A. RADICAL CATIONS

At this point, it is necessary to survey the reactions of radical cations that have been studied. Working with sulfur-nitrogen compounds it was found that the reactions take place with formation of radicals.

The intensive change in color during the reactions may be caused by radical formation or solvatochromie (37). In 1962 Chapman and Massey observed a radical cation (47) when they treated N_4S_4 with concentrated sulfuric acid, which they supposed to be N_2S^+ . Later Jolly and co-workers and other workers (11, 147, 154) found on the basis of electron spin resonance (ESR) measurements that the species was more probably $N_2S_2^+$ with a square-planar structure. According to the acid concentration proton-containing radicals were also detected. It is well known that strong acids such as FSO_3H or CF_3SO_3H easily form carbenium ions. This method cannot be applied in the sulfur-nitrogen field because the nitrogen will be protonated under these conditions. Therefore, we used the corresponding anhydrides, and, in fact, the reactions occur according to the following equation (205).



$\text{N}_2\text{S}_3^+\text{CF}_3\text{SO}_3^-$ can be isolated in high yield. It is a black-brown crystalline solid that is very sensitive to oxygen. ESR measurements gave a spectrum of five lines with an intensity ratio of 1:2:3:2:1 and a separation of 3.15 G. This spectrum is consistent with a radical containing two equivalent nitrogen atoms and is clearly the same spectrum as that obtained from the solution of N_4S_4 in sulfuric acid and from a solution of N_4S_4 in SbF_5 . However, the X-ray structural investigations (77, 126) clearly demonstrated that the hitherto recognized N_2S_2^+ radical is in reality the N_2S_3^+ radical.

Gillespie and co-workers (77) have shown that N_4S_4 is oxidized by AsF_5 and leads to the formation of $\text{N}_2\text{S}_3^+\text{AsF}_6^-$ in small quantities. The N_2S_3^+ radical is unusual in that it is a stable radical ion and is the only known sulfur-nitrogen radical that has been obtained as a stable crystalline salt.

The N_2S_3^+ cation is a planar five-membered ring (Fig. 3). The average bond length in the N_2S_3^+ ion is 158.7 pm. This is comparable to the average S—N distance in the S—N ring compounds. As an isolated N_2S_3^+ ion would be expected to have C_{2v} symmetry, the different lengths of the $\text{S}_1\text{—N}_1$ and $\text{S}_1\text{—N}_2$ bonds may be due to distortion of the ion in the crystal. Indeed, the difference in $\text{N}_2\text{S}_3^+\text{CF}_3\text{SO}_3^-$ is 2 pm, and in $\text{N}_2\text{S}_3^+\text{AsF}_6^-$ 3 pm.

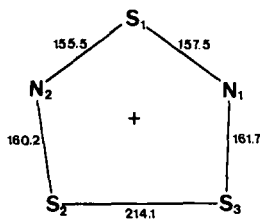
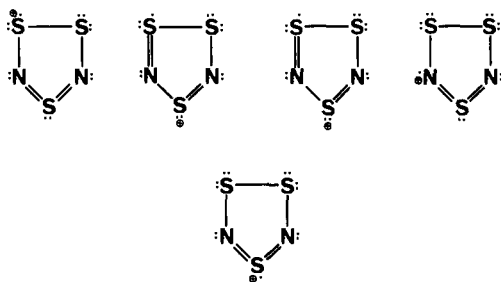


FIG. 3. Structure of the N_2S_3^+ radical.

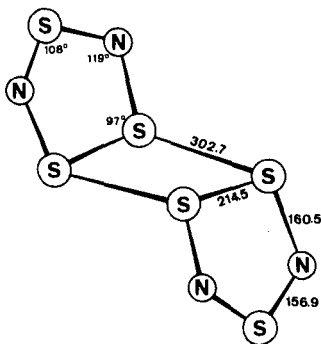
Experimental error and the influence of temperature appear to be not significant, because the determination of the structure by X-ray crystallography at -120°C showed no significant differences. N_2S_3^+ would be a 7π -electron ring. However, the difference in bond lengths of the average $\text{S}_1\text{—N}_1$ and $\text{S}_1\text{—N}_2$ as well as $\text{N}_1\text{—S}_3$ and $\text{N}_2\text{—S}_2$ is 156.5 and 160.9 pm, respectively. It appears that these differences can be explained on the basis of simple valence bond structures. If it is assumed that structures in which there is more than one charged atom and an S—S double bond are relatively unimportant and may be ignored, there are nine possible structures. In Fig. 4 the first four figures

FIG. 4. Resonance structures of N_2S_3^+ .

represent two structures as a consequence of the presence of the C_2 axis. Assuming that each of these structures has equal weight leads to the differences in bond lengths as they were found. The N_2S_3^+ structures can also be described as $\text{N}_4\text{S}_6^{2+}$ cations with two extremely long S—S bonds.

B. COMPOUNDS RELATED TO N_2S_3^+

The $\text{N}_4\text{S}_6^{2+}$ cation consists of two symmetry-related planar N_2S_3^+ rings held together by two very long S—S bonds of 302.7 pm. Therefore the bonding in $\text{N}_4\text{S}_6^{2+}$ can be regarded as consisting of two N_2S_3^+ rings linked together in a 4-center 6-electron bond (Fig. 5).

FIG. 5. Structure of $\text{N}_4\text{S}_6^{2+}$.

The compound was prepared in low yield from $\text{N}_2\text{S}_3\text{Cl}$ and chlorosulfonic acid and isolated as $\text{N}_4\text{S}_6^{2+} (\text{ClSO}_3\text{OSO}_3)_2^{2-}$ (21). $\text{N}_2\text{S}_3\text{Cl}$ has been known since 1880 (57), but very little is known about its

chemistry and its structure. It can be prepared from N_4S_4 , S_2Cl_2 or $NOCl$, $N_3S_3Cl_3$, and NO or, more conveniently, from $N_2S_3Cl_2$ either by heating in vacuum or by reduction with anhydrous formic acid (21, 30, 120).

$N_3S_3Cl^+Cl^-$ is another example of a five-membered ring (277) that is closely related to the $N_2S_3^+$ radical. It is interesting to compare the geometry of $N_2S_3^+$ with that of $N_2S_3Cl^+$. The latter is slightly puckered, but nevertheless the bond angles are very similar, as are the bond distances. Using the same criteria as mentioned above, only three reasonable valence bond structures can be written (Fig. 6).

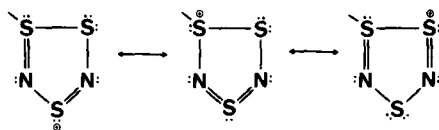
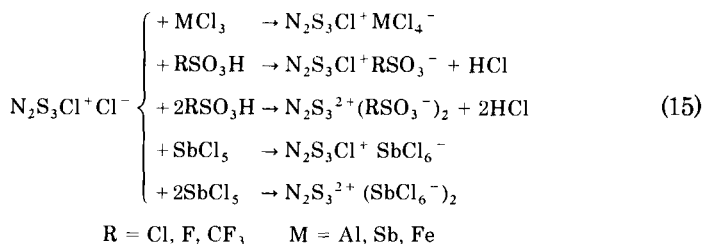


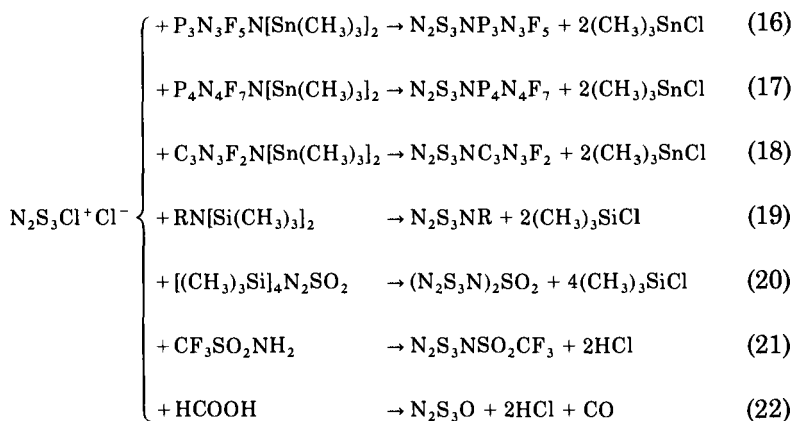
FIG. 6. Resonance structures of $N_2S_3Cl^+$.

Because of the inability of the three-coordinated sulfur atom to engage in π bonding, π bonding is restricted to the NSNS skeleton attached to the SCl group. The structure of $N_2S_3Cl^+Cl^-$ is rather unusual; one of the chlorine atoms is ionized, and the second is covalently bound to a sulfur atom of the ring. The different nature of the two chlorine atoms in $N_2S_3Cl^+Cl^-$ is also apparent in its reactions, the ionically bound chlorine being exchanged under milder conditions than the covalently bound chlorine (22, 159, 202).



$N_2S_3Cl^+Cl^-$ itself can be prepared from ammonium chloride or urea and S_2Cl_2 at reflux temperature (120, 214).

In the reaction of $N_2S_3Cl^+Cl^-$ with amino compounds it was observed that it is possible to replace the two chlorine atoms by one imino group, $=N-R$, when R is an electron-withdrawing substituent (167, 207, 214) or by an oxygen atom.



The question whether the five-membered 6- π -electron ring is preserved in the products or a six-membered 8- π -electron ring is formed could be established by X-ray investigations (206, 208, 238).

The data for the structures demonstrate that neither the bond angles nor the bond lengths within the five-membered rings are markedly influenced by the different substituents (Fig. 7). By comparing the average bond lengths of $\text{N}_2\text{S}_3\text{Cl}^+$ 169.8 with $\text{P}_3\text{N}_3\text{F}_5\text{NS}_3\text{N}_2$ 172.1, and $\text{FSO}_2\text{NS}_3\text{N}_2$ 172.4 pm, respectively, it is clearly shown that a decrease in electron density results in a shorter average bond length within the five-membered ring.

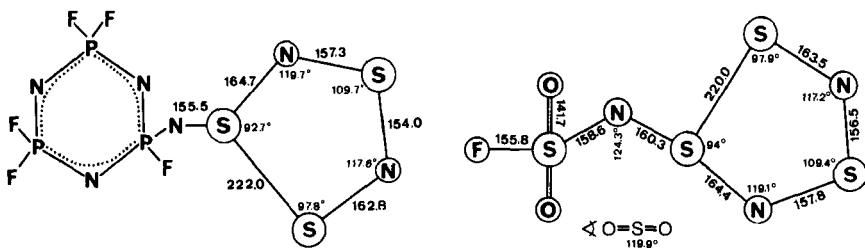
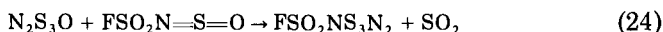
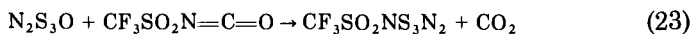
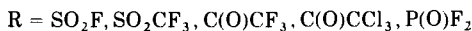
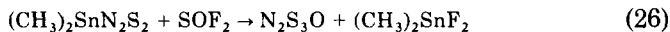


FIG. 7. Structure of $\text{P}_3\text{N}_3\text{F}_5\text{NS}_3\text{N}_2$ (left) and $\text{FSO}_2\text{NS}_3\text{N}_2$ (right).

In addition to the above-mentioned method, five other routes are so far known for the preparation of substituted N_2S_3 rings (44, 134, 203, 205, 214, 217, 238).

1. The reaction of isocyanates or iminosulfuroxides with $\text{N}_2\text{S}_3\text{O}$



2. The reaction of N_4S_4 with anhydrides3. The reaction of $(CH_3)_2SnN_2S_2$ with SOF_2 

4. The reaction of $(CH_3)_3SiNSNSi(CH_3)_3$ with $CF_3C(O)Cl$ yields $CF_3C(O)NS_3N_2$.

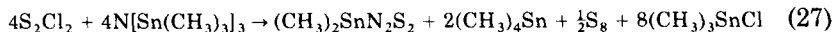
5. The reaction of $(CH_3)_3SiNSO$ with FSO_2NSCl_2 gives $FSO_2NS_3N_2$. $CF_3C(O)NS_3N_2$ was originally formulated as a six-membered ring (134).

N_2S_3O is the only oxide of a five-membered sulfur nitrogen ring so far known. It is a red oily liquid that can be distilled under vacuum without decomposition. The versatility of N_2S_3O for the preparation of N_2S_3 -containing ring systems was shown. A fluorine compound with a composition of $N_2S_3F_2$ has been reported in the literature. It has, however, been assigned the acyclic structure $FSN=S=NSF$; a closer study has yet to be made (88, 89).

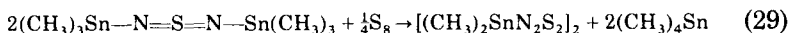
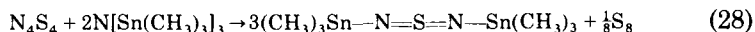
$N_2S_3Br_2$ was reported to be one of the products by the reaction of N_4S_4 with bromine in carbon disulfide. It decomposes already at room temperature. Whether this compound has a linear or cyclic structure is not known (278).

C. FIVE-MEMBERED RINGS CONTAINING ONE ELEMENT OTHER THAN SULFUR AND NITROGEN

Tetrasulfur tetranitride was prepared in 1835 by the reaction of disulfur dichloride with ammonia, although its composition was not established until 1850 (60, 81, 82, 90). For kinetically controlled reactions we used, instead of ammonia, a tin-substituted derivative of ammonia, and we allowed this to react with S_2Cl_2 . Instead of N_4S_4 we obtained a cyclic five-membered ring.



The same compound is formed when N_4S_4 and $N[Sn(CH_3)_3]_3$ are allowed to react at elevated temperatures; at lower temperatures a sulfur diimide could be isolated as an intermediate (190, 193, 218, 219).



Structural investigations show clearly that the molecule in the solid state consists of two five-membered and one four-membered ring (Fig. 8). The tin atoms have coordination number five. The molecule has C_i symmetry. By the way, this is the first example of a four-membered tin nitrogen ring whose structure was determined by X-ray analysis. This molecule is also a dimer in solution but monomeric in the gas phase. Another interesting feature of the structure is that the molecule has nearly a planar form in the solid state. All the S—N bonds are of different length; they will be discussed in detail later.

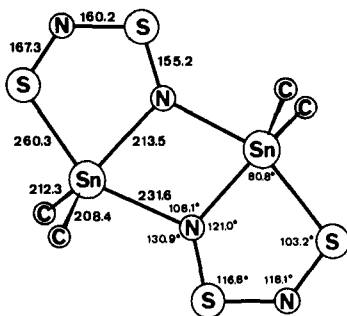
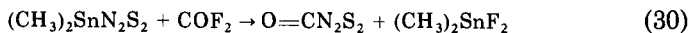


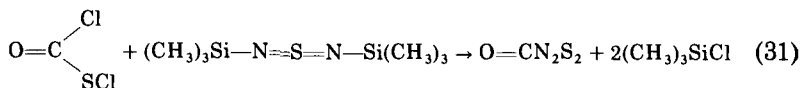
FIG. 8. Structure of $(\text{CH}_3)_2\text{SnN}_2\text{S}_2$.

SOF_2 and COF_2 react at room temperature with the tin compound with insertion and elimination of dimethyltin difluoride (215). COCl_2

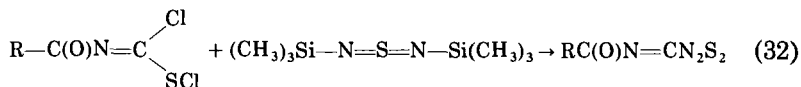


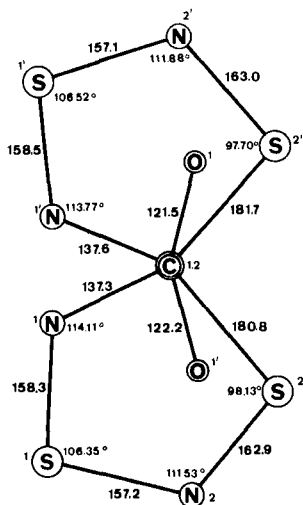
reacts similarly, but separation of the cyclic ketone from the dimethyltin dichloride proves to be difficult. The use of fluoro derivatives is favored by forming solid nonvolatile tin fluorides.

OCN_2S_2 (Fig. 9) is a yellow crystalline solid that melts at 40.5°C and can be sublimed under vacuum at room temperature. It may also be prepared from $\text{ClC}(\text{O})\text{SCl}$ and a silylated sulfur diimide (168).

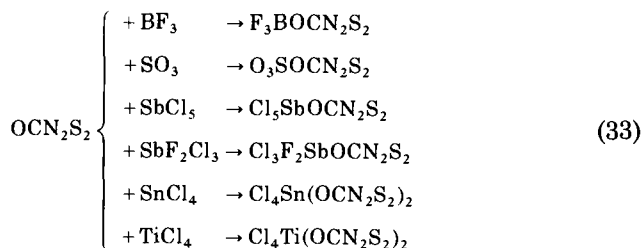


According to this reaction scheme benzoyl-substituted isonitriles were prepared (168, 169).

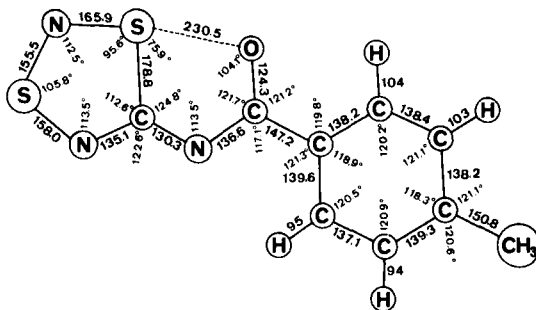


FIG. 9. Structure of OCN_2S_2 .

OCN_2S_2 forms adducts with various Lewis acids (216)

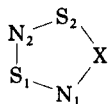


Infrared (IR) and Raman investigations support that the coordination of the Lewis acid to the ring occurs via the oxygen atom of the carbonyl group rather than a nitrogen atom of the ring. The adducts are decomposed on heating at elevated temperatures.

FIG. 10. Structure of $\text{CH}_3\text{C}_6\text{H}_4\text{C}(\text{O})\text{N}=\text{CN}_2\text{S}_2$.

The molecule $\text{CH}_3\text{C}_6\text{H}_4\text{C}(\text{O})\text{N}=\text{CN}_2\text{S}_2$, except for the hydrogen atoms of the methyl group, is planar (Fig. 10). The most noticeable feature of the structure is the S—O distance of 230.5 pm. It is a rare example of an SO bond longer than the "single bond" distance calculated from either Pauling's covalent radii (170 pm) or the Schomaker-Stevenson rule (169 pm) (185, 231), but on the other hand the SO distance is appreciably shorter than a van der Waals contact (325 pm). This can be considered as a "frozen" nucleophilic attack of the carbonyl oxygen on the sulfur atom.

For the discussion of the sulfur-nitrogen bonding properties within the five-membered rings, the structural data are collected in the accompanying tabulation.



X	S ₁ N ₁	S ₁ N ₂	S ₂ N ₂	Average SN	Angle N ₁ S ₁ N ₂
(CH ₃) ₂ Sn	155.2	160.2	167.3	160.9	116.8°
FSO ₂ NS	157.8	156.5	163.5	159.3	109.4°
P ₃ N ₃ F ₃ NS	157.3	154.0	162.8	158.0	109.7°
O=C	158.3	157.2	162.9	159.5	106.4°
CH ₃ C ₆ H ₄ C(O)NC	158.0	155.5	165.9	159.8	105.8°

It is quite obvious that, with decreasing size of X, the angle $\text{N}_1\text{S}_1\text{N}_2$ also should be diminished. A value of 116° is found for the tin compound, compared to 109° for the sulfur derivatives and 106° for the carbon compounds. Therefore the *s* character of S_1 should decrease when the angle increases and the bond length of the adjacent bonds $\text{N}_1\text{—S}_1$ and $\text{S}_1\text{—N}_2$ should become shorter. This trend cannot be observed because the N_2S_2 skeleton is a delocalized 6π -electron system, as is demonstrated by the nearly equal average S—N bond distance of the various compounds. This means that a change in electron density in the SN_2 part of the ring will be compensated by the remaining sulfur atom. The different S—N bond length can be explained best by resonance structures.

Calculations for S—N compounds have so far not given an answer to the different bond orders whereas resonance structures (Fig. 11)

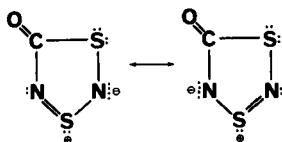
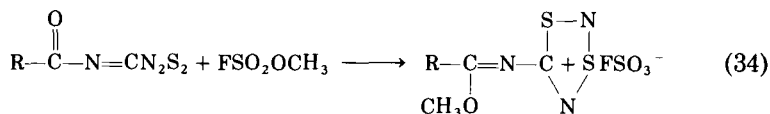
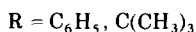
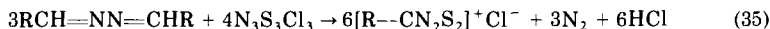


FIG. 11. Resonance structures of OCN_2S_2 .

show a fairly good agreement (1, 18, 65, 71, 164a). The alkylation of $R-C(O)-N=CN_2S_2$ with the methyl ester of fluorosulfonic acid yields a cation with the following structure:



The easy alkylation of the carbonyl oxygen is a support for the argument of a partial negative charge on the oxygen atom. An alkylation of the nitrogen atom was not observed (169). $N_3S_3Cl_3$ reacts with nitriles or azines to give dithiadiazolium chlorides, $RCN_2S_2^+Cl^-$ (5, 211).



According to this equation, the yield of the phenyl derivative is quantitative. The reaction with nitriles was not completely investigated; no equation or by-products were reported. The compounds contain a cation, confirmed by an X-ray structure determination (6), which has an S—S bond instead of an alternating NS arrangement shown in OCN_2S_2 and $RC(O)-N=CN_2S_2$ (Fig. 12).

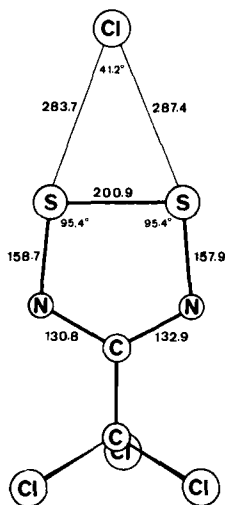
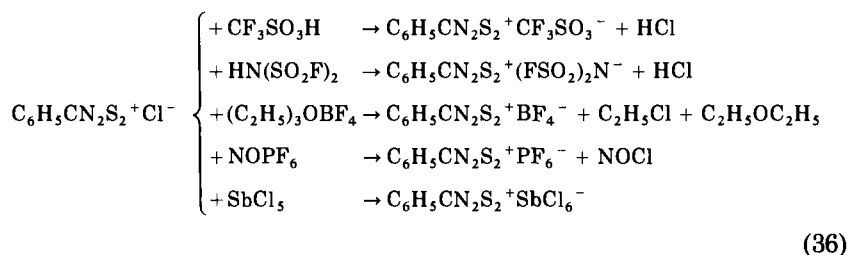


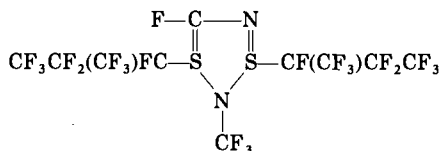
FIG. 12. Molecular structure of $[CCl_3CN_2S]^+Cl^-$.

To some extent this is surprising, because in such a structure it is not possible to write a resonance form with a carbenium center. Another striking feature is the close approach of the Cl^- ion to both sulfur atoms of the S_2 group. This triangular arrangement may be an important factor for the present structure. In $[\text{C}_6\text{H}_5\text{CN}_2\text{S}_2]^+\text{Cl}^-$ the chlorine ion can be replaced by various anions, and this is another proof of the ionic nature of this compound (211).

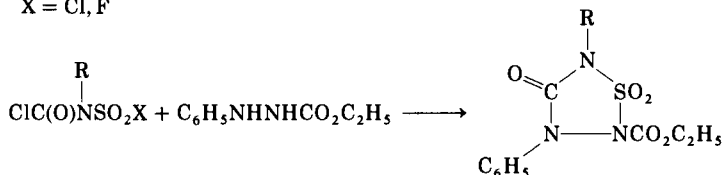
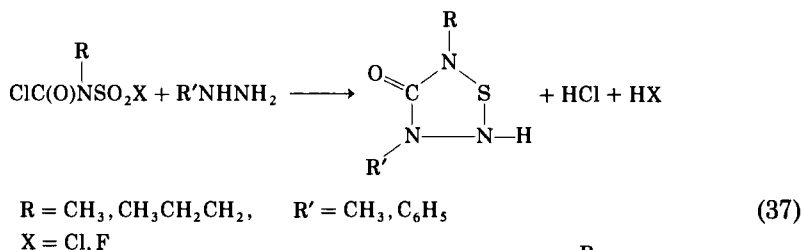


The complexes can be recrystallized from acetonitrile, and all are intensely yellow or red.

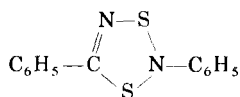
A five-membered dithiadiazole is formed, when $\text{CF}_3\text{C}\equiv\text{CCF}_3$ and $\text{CF}_3\text{N}=\text{SF}_2$ react in the presence of CsF (117).



It was shown recently that chloro- and fluorosulfonylcarbamoyl chlorides undergo exclusive attack at the carbonyl group to give with hydrazines clean condensation products (29).

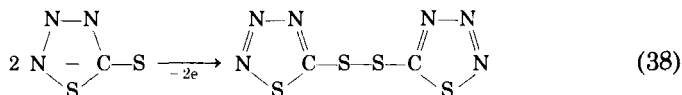


Thioarylisocyanates and diphenylsulfur diimide react to several products among which

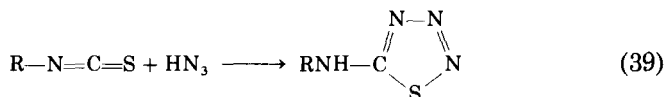


was isolated (248a).

Free dithiocarbonic acid azide, $\text{N}_3\text{CS}(\text{SH})$, was first described in 1915 (73, 234). It has been prepared by treating concentrated solutions of sodium azidodithioformate with hydrochloric acid at low temperatures. The complete absence of the strong absorptions characteristic of azide groups suggests that this acid has the structure of a thiatriazole (136). All alkali salts of N_3CS_2^- are known (73, 174) and many heavy-metal salts. They are sensitive to mechanical shock. Much more stable are the salts of the thiatriazoles that are complexed with phosphines, π -allyl, or dienes. They can be prepared either by insertion of carbon disulfide into the azido complex of transition metals or by reaction of a mixture of the corresponding metal nitrate, NaN_3CS_2 , and the phosphine (73). One of the major characteristics of N_3CS_2^- anions is their susceptibility to oxidation, resulting in the formation of the disulfide (73)

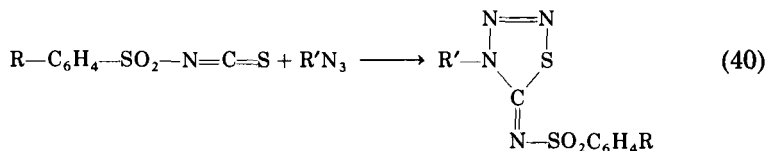


When N_3CS_2^- is allowed to react with various organic dihalides of the type $\text{X}-\text{R}-\text{X}$, compounds of the following structure were prepared: $\text{N}_3\text{CS}_2-\text{R}-\text{S}_2\text{CN}_3$ (186). Esters of the type N_3CSSR are known (73). Attempts to obtain alkyl and aryl esters by direct condensation of the organic azides with carbon disulfide failed. The general method adopted for the preparation of the esters involves reaction of alkyl or aryl halide with NaN_3CS_2 . The esters are crystalline solids that decompose more or less rapidly at elevated temperatures. The reaction of hydrazoic acid with isothiocyanates furnishes thiatriazoles (116).

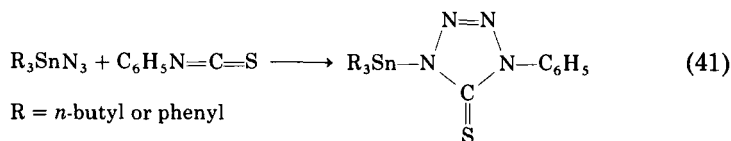


Despite the large number of investigations carried out with thiatriazoles, thiatriazolines have been mentioned in only a few reports (135, 170).

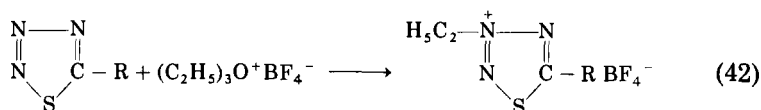
Arylsulfonylisothiocyanates react directly with organic azides to form thiatriazolines exclusively (132, 253).



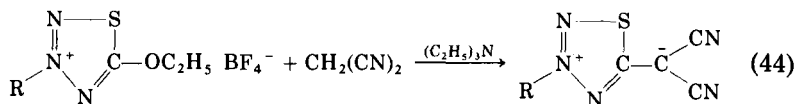
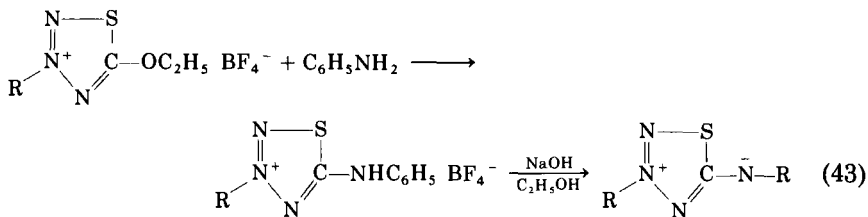
The reaction of tri-*n*-butyltin azide and triphenyltin azide with phenylisothiocyanate gives the 1:1 adduct (128).



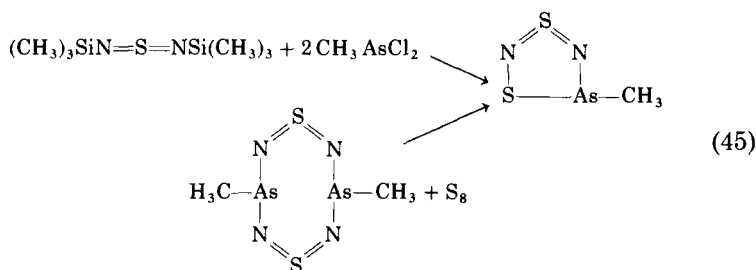
Other organometallic azides also produced $\text{C}=\text{N}$ but not $\text{C}=\text{S}$, adducts. Esters of thiatriazoles can be alkylated with $(\text{C}_2\text{H}_5)_3\text{O}^+\text{BF}_4^-$ with formation of thiatriazolium salts (103, 113).



The conversion of the thiatriazolium salts with amines or $\text{CH}_2(\text{CN})_2$ leads to new mesoionic heterocycles (103).



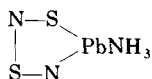
One five-membered sulfur-nitrogen-arsenic ring is known. The ring is obtained when *N,N'*-bis(trimethylsilyl)sulfur diimide is treated with CH_3AsCl_2 in the molar ratio of 1:2 (225). By using a different ratio of reactants, it is also possible to get a second product, in which there is a eight-membered ring (224). The eight-membered ring can be converted by elemental sulfur to the five-membered ring.



The product at room temperature is a red liquid that boils at $33^\circ\text{--}35^\circ\text{C}/0.05 \text{ Torr}$.

D. THE FUNCTION OF N_2S_2 , HN_2S_2 , AND NS_3 AS BIDENTATE LIGANDS

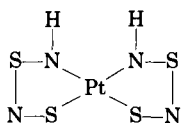
Already in 1904 Ruff and Geisel (222) observed a fragmentation of N_4S_4 when it is treated with lead iodide or nitrate in liquid ammonia. The product is an ammoniate of the composition $\text{Pb}(\text{N}_2\text{S}_2)\text{NH}_3$. The ammonia can be removed by heating. The structure was established by X-ray analysis (264).



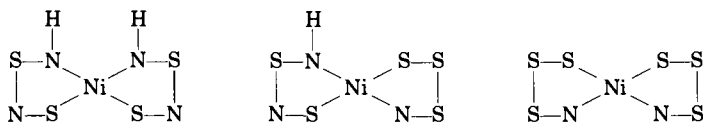
The thionitrosyl complexes of composition $\text{Me}(\text{HN}_2\text{S}_2)_2$, $\text{M} = \text{Ni}, \text{Co}, \text{Pt}, \text{Pd}, \text{Fe}$, are prepared from N_4S_4 and the metal chlorides, in the case of Pt from H_2PtCl_6 (104a). The iron, cobalt, and nickel derivatives can also be obtained from the tetranitride and the carbonyls $\text{Fe}(\text{CO})_5$, $\text{Co}_2(\text{CO})_8$, and $\text{Ni}(\text{CO})_4$ in a solvent (43, 267).

Compounds of this type were initially formulated as $\text{M}(\text{SN})_4$, but later it was found on the basis of IR measurements that they contain hydrogen and should be formulated as $\text{Me}(\text{HN}_2\text{S}_2)_2$ (187, 268). These products are formed only in the presence of a solvent containing

hydrogen, such as ethanol. The structure of the platinum complex was investigated by X-ray analysis.



The molecule was found to be planar (139). The hydrogens are bonded to the nitrogen atoms next to the platinum, and the two chelate ligands are in cis configuration. The products of the reaction of N_4S_4 and nickel chloride in ethanol solution were separated by using alumina column chromatography. Three different compounds were isolated.



$Ni(HN_2S_2)(NS_3)$ and $Ni(NS_3)_2$ are readily soluble, but $Ni(HN_2S_2)_2$ is less soluble in benzene. Structural investigations by Weiss and Thewalt for $Ni(HN_2S_2)_2$ (Fig. 13) and $Pd(HN_2S_2)_2$ gave results similar to those for the platinum complex (271).

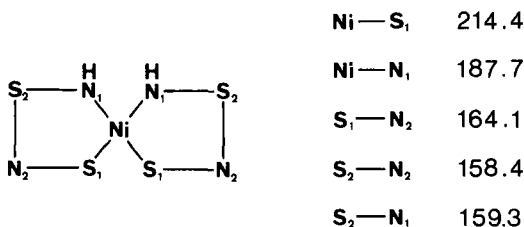
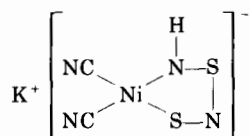


FIG. 13. Molecular structure of $Ni(HN_2S_2)_2$.

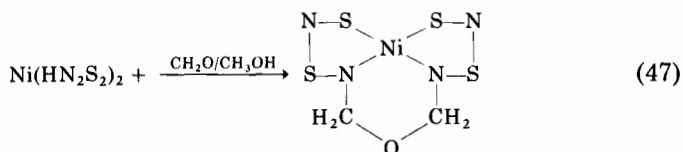
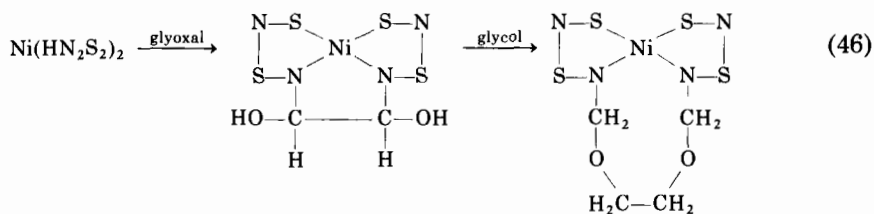
A sulfur atom is isoelectronic with an NH group. Therefore the replacement of the imido group by sulfur should not lead to a change in structure. It can be assumed that the other two derivatives are also planar. In contrast, the dimethyl derivative of $Ni(HN_2S_2)_2$, obtained by causing $Ni(HN_2S_2)_2$ to react with methyl iodide, possesses a trans configuration (272). The reason for this might be steric hindrance, because the monosubstituted methyl derivative has also a cis configuration. Of special interest is the mixed complex salt $K[Ni(CN)_2HN_2S_2]$, which can be prepared from $K_4[Ni_2(CN)_6]$ and N_4S_4 in alcoholic solu-

tion. It seems highly probable that the HN_2S_2 and NS_3 ligands could be used in a wider range for the preparation of metallic complexes (267).

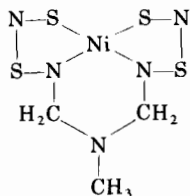


The chemistry of the $\text{Ni}(\text{HN}_2\text{S}_2)_2$ compound is essentially that associated with the two imido groups, which undergo a number of cyclization reactions (267).

The NH group can be metallated with silver nitrate or organolithium reagents and caused to react further with organic halides. The reaction of $\text{Ni}(\text{HN}_2\text{S}_2)_2$ with glyoxal and a mixture of formaldehyde and methanol leads to cyclic derivatives (102).

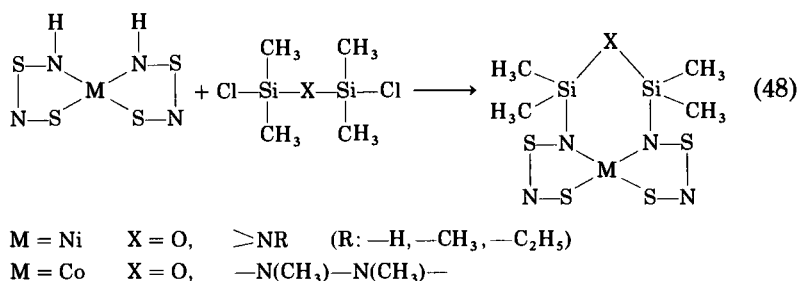


If methylamine is added in the reaction with formaldehyde, $\text{Ni}[\text{C}_3\text{H}_7\text{N}_5\text{S}_4]$ is formed.



New inorganic ring systems were obtained by the reaction of $\text{Ni}[\text{HN}_2\text{S}_2]_2$ and $\text{Co}[\text{HN}_2\text{S}_2]_2$ with 1,3-dichloropentamethyldisilazane

and 1,3-dichlorotetramethyldisiloxane in tetrahydrofuran and in the presence of triethylamine (261).

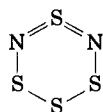


The tricyclic structure has been confirmed by X-ray analysis for a nickel as well as for a cobalt derivative (242). The complexes are very soluble in organic solvents.

VI. Six-Membered Rings

A. DOUBLY COORDINATED SULFUR AND NITROGEN

Tetrasulfur dinitride has been known for over 70 years, and the molecular formula N_2S_4 has been accepted since Meuwesen's determination of the molecular weight in 1951 (158). Its dipole moment, ^{14}N -NMR spectrum, mass spectrum, IR spectrum, electronic spectrum, and Raman spectrum have been determined. This physical evidence shows that the compound has a cyclic structure with the nitrogen atoms in the 1,3-position (172). No evidence for other isomers was reported.



The compound can be prepared by several routes:

1. Heating N_4S_4 with sulfur in CS_2 at 120°C in an autoclave (91)
2. Causing $\text{Hg}_5(\text{NS})_8$ to react with disulfur dichloride in CS_2 (158)



3. Reaction of disulfur dichloride with aqueous ammonia (175)
4. Reduction of $[\text{N}_3\text{S}_4]\text{Cl}$ with metallic zinc (102)

5. Treating S_7NH with $N_3S_3Cl_3$ in benzene at $80^\circ C$ in the presence of pyridine (94)



6. Decomposition of $Hg(NS_7)_2$ at room temperature (107a)

The reaction according to route 3 seems to be a simple route to tetrasulfur dinitride. The yield is 8.2%, and isolated by-products are S_7NH and N_4S_4 . N_2S_4 is a red-brown liquid with an unpleasant odor, mp. $23.5^\circ C$. The pure liquid decomposes within a few hours at room temperature. N_2S_4 is reduced with $LiAlH_4$ or $SnCl_2$ in ether, which results in the formation of $N_2S_4H_2$ (72). A product of the composition $N_3S_3SbCl_6$ was reported from the reaction of N_4S_4 with $SOCl_2$ and $SbCl_5$. The structure of $N_3S_3^+$ is not known (26). N_3S_3Cl was obtained from the reaction of chlorine with excess N_4S_4 (278). $N_3S_3^-$, a 10- π -electron system, was prepared from N_4S_4 and a tetraalkylammonium azide or CsN_3 in ethanol. On the basis of spectroscopic investigations a cyclic structure with C_{3v} symmetry was assigned for this anion (39a).

B. STRUCTURAL INVESTIGATIONS OF SIX-MEMBERED RINGS WITH THE COORDINATION NUMBER TWO AT THE SULFUR AND NITROGEN ATOMS

The structures of six-membered rings with an NSN unit have been established with the emphasis on investigating the influence of adjacent atoms with high coordination numbers. In detail, compounds with carbon and phosphorus (209) of coordination number four and compounds of sulfur with coordination numbers three and four were studied (75, 76, 204, 270) (Fig. 14).

The first three compounds demonstrate that the N—S bond (153 pm) as well as the NSN angle in all compounds is, within experimental error, the same. The π -electron density of the NSN-unit is not influenced by the adjacent atoms when they have a high coordination number. Atoms with high coordination numbers function as a barrier for π electrons, even if there is an additional charge, as demonstrated in $SN_2NS_2O_4^-$. The negative charge is localized on the SO_2-N-SO_2 part of the molecule. Also the electron-withdrawing property of a fluorine atom in $SN_2N_4P_4F_6$ does not influence the electron density. Although conjugation is not observed, hyperconjugation might be possible. In $SN_2S_2N_3PF_2$ the adjacent sulfur atoms to the NSN unit have a coordination number three. In this case it has already been seen that a small change in the NS-bond distance (155 pm) occurred. The

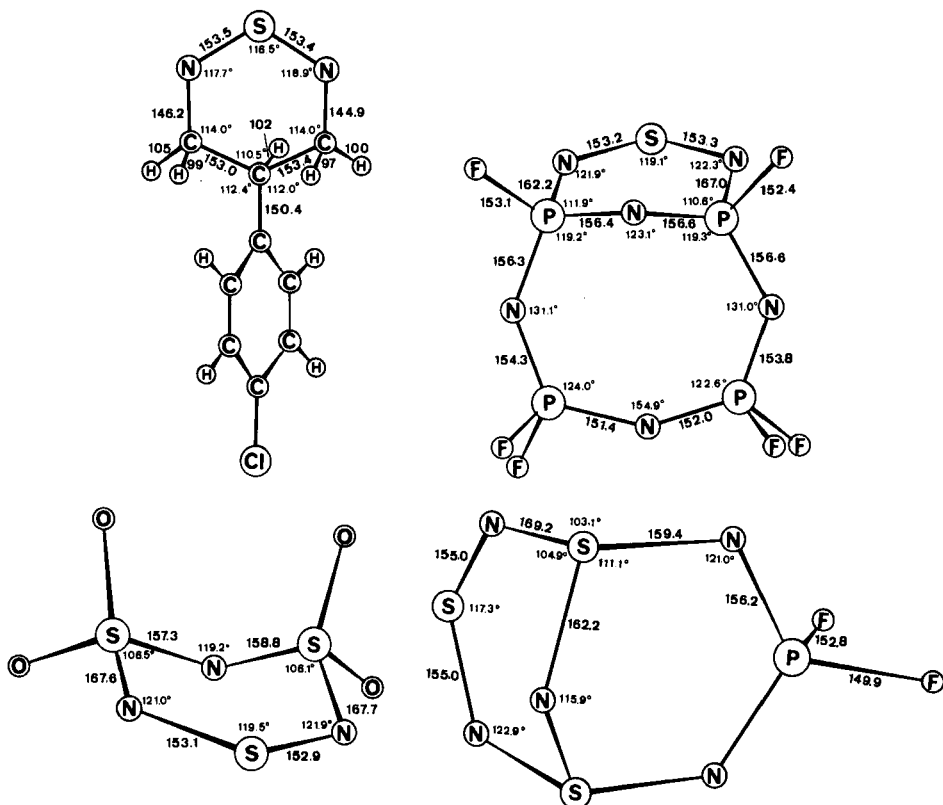


FIG. 14. Molecular structures of (a) $\text{SN}_2\text{C}_9\text{H}_9\text{Cl}$; (b) $\text{SN}_2\text{N}_4\text{P}_4\text{F}_6$; (c) $\text{SN}_2\text{NS}_2\text{O}_4^-$; (d) $\text{SN}_2\text{S}_2\text{N}_3\text{PF}_2$.

electron density of the NSN part is to a small extent influenced by sulfur atoms of coordination number three. In addition, it might be interesting to note that $\text{SN}_2\text{S}_2\text{N}_3\text{PF}_2$ and phenyl-substituted derivatives are prepared from $(\text{CH}_3)_3\text{SiNSNSi}(\text{CH}_3)_3$ and fluorophosphoranes (12, 131, 212).

A combination of the thirteen building units of sulfur in Table I results in 180 different six-membered rings. Only a small number of them have so far been synthesized (102a).

C. SULFUR AND NITROGEN WITH COORDINATION NUMBERS TWO AND/OR THREE

$\text{N}_3\text{S}_3\text{Cl}_3$ is obtained as large yellow needles when N_4S_4 is dissolved in CCl_4 and treated with chlorine. Instead of chlorine, SO_2Cl_2 can be

used as a chlorinating agent. Another method uses $\text{N}_2\text{S}_3\text{Cl}_2$ and SO_2Cl_2 for the preparation of $\text{N}_3\text{S}_3\text{Cl}_3$ (4, 91). On heating $\text{N}_3\text{S}_3\text{Cl}_3$ to 110° under high vacuum, NSCl may be obtained as a greenish-yellow gas. NSCl polymerizes again to $\text{N}_3\text{S}_3\text{Cl}_3$. The compound (Fig. 15) is freely soluble in organic solvents and is stable in dry air. It is a nearly flat ring where all N—S bonds are of the same length. The addition of SO_3 to $\text{N}_3\text{S}_3\text{Cl}_3$ leads to the adduct $\text{N}_3\text{S}_3\text{Cl}_3 \cdot 6\text{SO}_3$, which decomposes at 100°C to give $\text{N}_3\text{S}_3\text{Cl}_3 \cdot 3\text{SO}_3$; at higher temperatures $(\text{NSOCl})_3$ is formed (93).

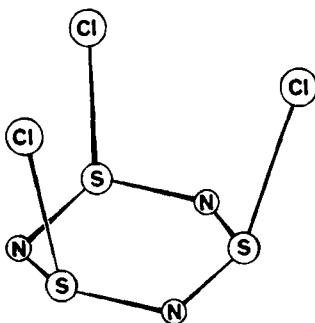
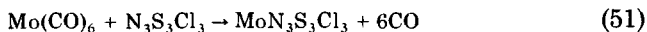
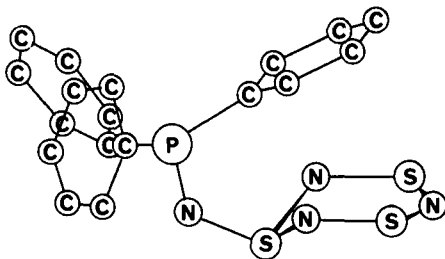


FIG. 15. Molecular structure of $\text{N}_3\text{S}_3\text{Cl}_3$.

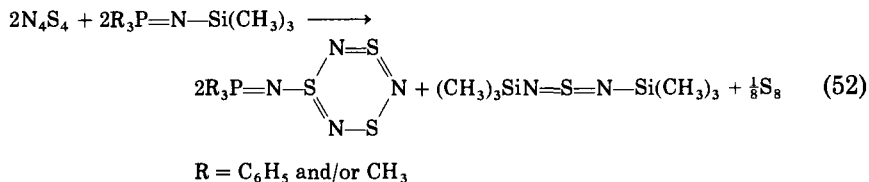
$\text{Mo}(\text{CO})_6$ and $\text{N}_3\text{S}_3\text{Cl}_3$ react in dichloromethane with formation of a brown crystalline solid.



The pyrolysis of $\text{MoN}_3\text{S}_3\text{Cl}_3$ under vacuum yields a sublimable solid of composition $\text{MoN}_3\text{S}_9\text{Cl}_6$. The structures of both compounds are unknown (276). The corresponding fluorine compound $\text{N}_3\text{S}_3\text{F}_3$ is obtained either from the fluorination of $\text{N}_3\text{S}_3\text{Cl}_3$ with AgF_2 or the direct fluorination of N_4S_4 with elemental fluorine at low temperatures (82, 83, 151). X-ray determination shows a slightly puckered six-membered N—S ring with bond distances of 158.7 and 159.8 pm, respectively. All fluorine atoms are in axial positions similar to $\text{N}_3\text{S}_3\text{Cl}_3$ (127). The Lewis acids BF_3 , SbF_5 , and AsF_5 form stable adducts with $\text{N}_3\text{S}_3\text{F}_3$ (161) with formation of the cation $\text{N}_3\text{S}_3\text{F}_2^+$. Three adducts of $\text{N}_3\text{S}_3\text{Cl}_3$ are known with the following composition: $\text{N}_3\text{S}_3\text{Cl}_3 \cdot \text{SbCl}_5$, $\text{N}_3\text{S}_3\text{Cl}_3 \cdot \text{TiCl}_4$, and $(\text{N}_3\text{S}_3\text{Cl}_3)_2 \cdot \text{SnCl}_4$ (161). Nitrogen-substituted organic derivatives of N_2S_4 are known. The 1,3-diaza as well as the 1,4-diaza isomers have been prepared.

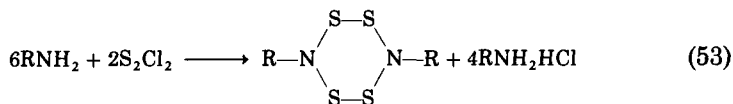
FIG. 16. Molecular structure of $(\text{C}_6\text{H}_5)_3\text{PN}_4\text{S}_3$.

The compound $(\text{C}_6\text{H}_5)_3\text{PN}_4\text{S}_3$ has been shown by X-ray single-crystal studies to have a six-membered N_3S_3 ring, five members of which are coplanar (N_3S_2) (Fig. 16). The third sulfur of the ring is tervalent and 139° out of the plane. The bonds between sulfur and nitrogen are not equal (114). $(\text{C}_6\text{H}_5)_3\text{PN}_4\text{S}_3$ is prepared from N_4S_4 and triphenylphosphine or methyltriphenylphosphorane or triorganylimino-*N*-(trimethylsilyl)phosphorane, respectively (67, 125, 223).

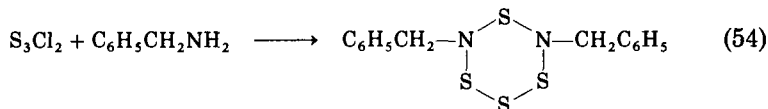


The structure of triphenylarsine trisulfur tetranitride is similar to that of the analogous phosphine compound. The triphenyl substituent group is bonded through nitrogen to the sulfur of an N_3S_3 group, the remaining five members of which are planar (115).

The 1,4-diazatetrasulfanes are prepared from primary amines and disulfur dichloride (102, 244).

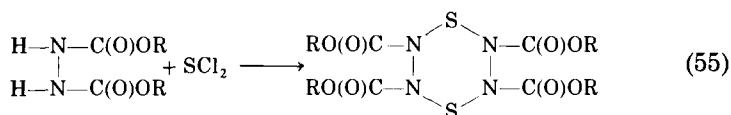


The 1,3-isomer has been obtained from S_3Cl_2 and benzylamine (41).

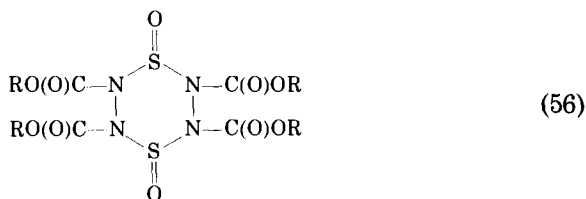


The cyclic structure of these compounds is assumed on the basis of molecular weight determinations. Their kinetic stability depends upon the nature of the organic substituents.

Six-membered hydrazine compounds were obtained by the condensation of sulfur dichloride with esters of hydrazine dicarbonic acid (263).



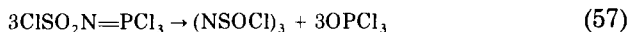
These compounds react with *m*-chloroperbenzoic acid. Among the products isolated, a bissulfoxide was found.



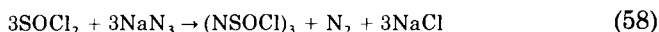
D. COMPOUNDS OF COORDINATION NUMBER TWO AT NITROGEN AND FOUR AT SULFUR

The sulfanuryl chlorides and fluorides belong to this class of compounds. There are four different possibilities for the preparation of $\text{N}_3\text{S}_3\text{O}_3\text{Cl}_3$:

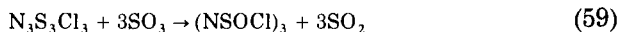
1. Pyrolysis of $\text{ClSO}_2\text{N}=\text{PCl}_3$, obtained from the reaction of PCl_5 and $\text{H}_2\text{NSO}_3\text{H}$ (122)



2. Reaction of thionyl chloride with sodium azide (124)



3. Oxidation of $\text{N}_3\text{S}_3\text{Cl}_3$ with SO_3 (93)



4. Ammonolysis of SO_2Cl_2 in the presence of SOCl_2 (92).

Kirsanov obtained two products by pyrolysis, the α - and β -isomers (m.p. 144° – 145° and 46° – 47°C). Separation could be achieved by vacuum sublimation. The structure of the α -isomer is known (24, 274). All N—S bonds were found to be of the same length (156.4 pm), the molecule exhibiting a chair form. All chlorine atoms are in axial positions. $(\text{NSOCl})_3$ is converted to the corresponding fluoride by means of KF in carbon tetrachloride (232) or under reduced pressure with SbF_3 (137). The two isomers differ in the position of their fluorine and oxygen atoms with respect to the nonplanar ring (86).

PHYSICAL PROPERTIES OF THE *cis*- AND *trans*-ISOMER

	<i>cis</i> -(NSOF) ₃	<i>trans</i> -(NSOF) ₃
Melting point	17.4°C	-12.5°C
Boiling point	138.4°C	130.3°C
Density (g/ml)	1.92	1.92
Heat of vaporization (joule/mol)	39.8	40.7
^{19}F NMR	A type	AB_2 type

Numerous sulfur oxide difluorides, such as CsNSOF_2 , $\text{Hg}(\text{NSOF}_2)_2$, $(\text{CH}_3)_3\text{SnNSOF}_2$, and $\text{B}(\text{NSOF}_2)_3$, have been found to decompose with liberation of $(\text{NSOF})_3$ (83).

Substitution reactions of sulfanuryl halides have been described in the literature (19, 86, 166, 259a). $\text{N}_3\text{S}_3\text{O}_3(\text{C}_6\text{H}_5)_3$ is accessible both from $\text{C}_6\text{H}_5\text{SOCl}$ and azide (152) and from $(\text{NSOF})_3$ and C_6H_6 in the presence of AlCl_3 (166).

Mixed chloro, fluoro compounds have been obtained by the fluorination with SbF_3 under reduced pressure (137). $(\text{NSOF})_2(\text{NSOCl})$ as well as $(\text{NSOCl})_2\text{NSOF}$ form mixtures of three isomers each, which can be separated by gas chromatography. Assuming the ring to be planar, the isomers of $(\text{NSOF})_2(\text{NSOCl})$ might be pictured as shown in Fig. 17 (83, 137).

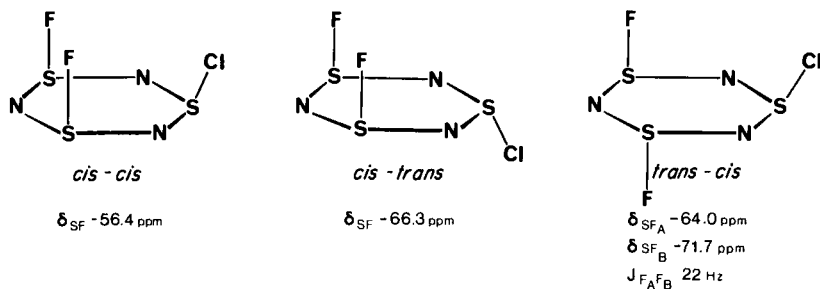
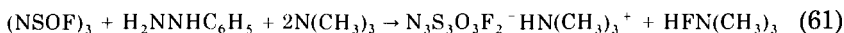
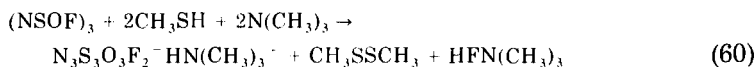


FIG. 17. Isomers of $(\text{NSOF})_2(\text{NSOCl})$.

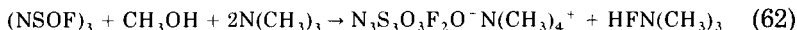
An interesting compound is $\text{N}_3\text{S}_3\text{O}_3\text{F}_2\text{NH}_2\text{NH}_3$, which is prepared from $(\text{NSOF})_3$ and ammonia in diethyl ether. $\text{N}_3\text{S}_3\text{O}_3\text{F}_2\text{NH}_2$ is formed by treatment of the ammoniate with HCl gas. $\text{N}_3\text{S}_3\text{O}_3\text{F}_2\text{NH}_2\text{NH}_3$ can be used to prepare a series of derivatives where the two protons of the amino group have been replaced by $=\text{SF}_2$, $=\text{SCL}_2$, $=\text{SOF}_2$, $=\text{PCl}_3$, and $=\text{CHC}_6\text{H}_5$. Oxalyl chloride forms a bridged derivative, $(\text{N}_3\text{S}_3\text{F}_2\text{NHCO})_2$ (138, 240, 260). The reaction of $(\text{NSF})_3$ with various amines was studied in detail (260).

With N,N' -dimethylethylenediamine, a bridged as well as a bicyclic compound is obtained (260). The anion $\text{N}_3\text{S}_3\text{O}_3\text{F}_2^-$ has been prepared by reaction of $(\text{NSOF})_3$ with CH_3SH (255) and $\text{C}_6\text{H}_5\text{NHNH}_2$ (260).

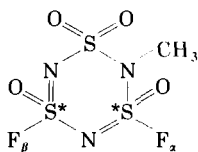


$\text{N}_3\text{S}_3\text{O}_3\text{F}_2\text{N}(\text{CH}_3)_2$ reacts with $\text{H}_2\text{NNHC}_6\text{H}_5$ with formation of the $\text{N}_3\text{S}_3\text{O}_3\text{FN}(\text{CH}_3)_2^-$ anion.

The use of CH_3OH instead of CH_3SH leads to the anion $\text{N}_3\text{S}_3\text{O}_3\text{F}_2\text{O}^-$ (255).

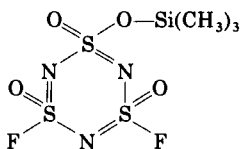


The free acid can be isolated by means of a cation exchanger, evaporation of the aqueous solutions yields the monohydrate $\text{N}_3\text{S}_3\text{O}_3\text{F}_2\text{OH} \cdot \text{H}_2\text{O}$. The silver salt and two alkylated products were reported (255–257). On the basis of ^{19}F NMR for the methyl derivate, the following structure was proposed:



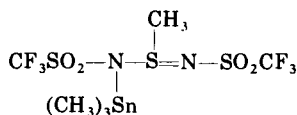
This compound has two asymmetric sulfur atoms, which are marked by asterisks (*). The optical activity was demonstrated by ^{19}F NMR in the presence of butanol-2 in an inert solvent. The alcohol coordinates to the sulfur atom adjacent to the α -fluorine, thus forming a pair of diastereoisomers. As a result, in the ^{19}F NMR spectrum all resonance lines are doubled (83). $\text{N}_3\text{S}_3\text{O}_3\text{FN}(\text{CH}_3)_2\text{O}^-$ was prepared from $\text{N}_3\text{S}_3\text{O}_3\text{F}_2\text{N}(\text{CH}_3)_2$ and methanol in the presence of triethylamine

(258). If $\text{N}_3\text{S}_3\text{O}_3\text{F}_2\text{O}^- \text{Ag}^+$ is subjected to reaction with $(\text{CH}_3)_3\text{SiCl}$ or $(\text{CH}_3)_3\text{SnCl}$, then the metal adds to an oxygen atom of the anion (258)



E. BONDING PROPERTIES OF SULFUR WITH COORDINATION NUMBERS THREE AND FOUR

From bond angles and bond lengths (Fig. 18) it is understandable that the >SX can be exchanged for an >SOX group (83). Within experimental error the bond angles at nitrogen are identical. The same applies to the angles at sulfur. The differences in bond length can be interpreted on the basis of different coordination numbers. Recently it was found that coordination numbers and bond lengths can be correlated. In the case of



it was found that the shortest SN bond ($\text{S}_2\text{—N}_2$: 155 pm) belongs to sulfur of coordination number four and nitrogen of coordination

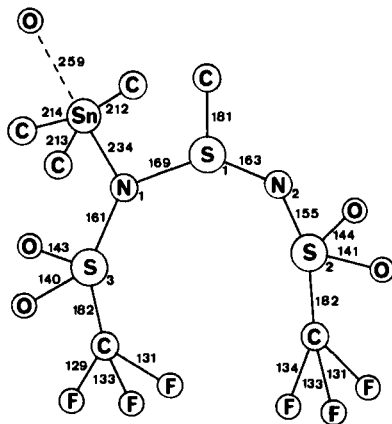


FIG. 18. Molecular structure of $\text{CF}_3\text{SO}_2(\text{CH}_3)_3\text{SnNSNSO}_2\text{CF}_3$.

CH₃

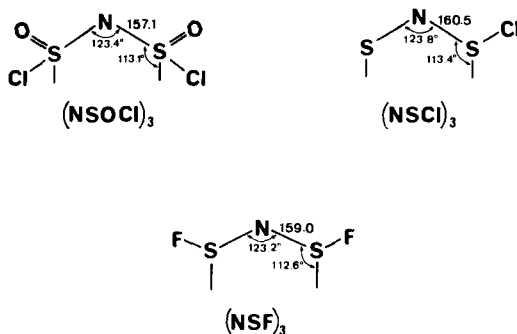


FIG. 19. Bond angles and bond lengths of (NSOCl)₃, (NSCl)₃, and (NSF)₃.

number two. An increase in coordination number of the atom N₁ leads to a lengthening of the S₃—N₁ distance to 161 pm (Fig. 18).

A similar effect is observed for the sulfur atom S₁ having coordination number three. S₁—N₂ is shorter than S₁—N₁ (198). In general, for sulfur of coordination numbers (CN) three and four, the following series of increasing bond lengths may be valid:

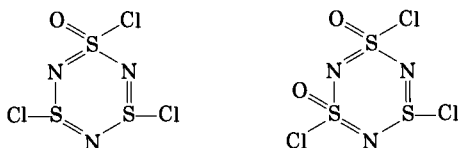
$$\begin{aligned} \text{S}(\text{CN} = 4) - \text{N}(\text{CN} = 1) &< \text{S}(\text{CN} = 4) - \text{N}(\text{CN} = 2) < \text{S}(\text{CN} = 4) - \text{N}(\text{CN} = 3) \\ &\approx \text{S}(\text{CN} = 3) - \text{N} - (\text{CN} = 2) < \text{S}(\text{CN} = 3) - \text{N}(\text{CN} = 3) \end{aligned}$$

Sulfurs of coordination number two cannot be included, because, as shown earlier, these compounds take part in the delocalization. According to this series, the shortest SN-bond will be observed when the difference of the coordination numbers is high. In fact, the polarity of such a bond is high, and this results in a decrease of the bond length. Therefore, the change in the SN-bond length from —N—S(=O)—Cl (157.1 pm) to N—S—Cl (160.5 pm) is understandable (Fig. 19). Another example is N≡SF and N≡SF₃ with NS bond lengths of 144.6 and 141.6 pm, respectively.

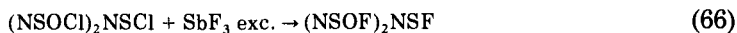
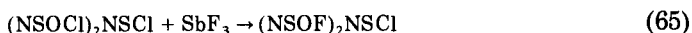
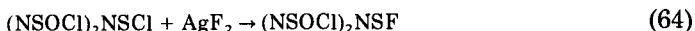
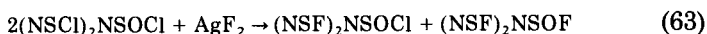
F. DOUBLY COORDINATED NITROGEN, THREE- AND/OR FOUR-COORDINATED SULFUR

The interconversion of NS(O)X and NSX results in the formation of various ring compounds. The chlorination of S(NSO)₂ yields (NSOCl)₃

and (228, 269) two compounds with mixed coordination numbers at sulfur.



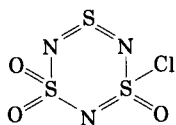
By means of AgF_2 or SbF_3 the chlorine atoms can be exchanged for fluorine under proper conditions



All compounds are distillable liquids without decomposition in vacuum. $(\text{NSOF})_2\text{NSCl}$ was also obtained from the reaction of $\text{N}_3\text{S}_3\text{O}_3\text{F}_2\text{NH}_2$ with SOCl_2 (138) and from the reaction of $\text{N}_3\text{S}_3\text{O}_3\text{F}_2\text{O}^-$ with PCl_5 (255). The corresponding $(\text{NSOF})_2\text{NSF}$ is accessible from $\text{N}_3\text{S}_3\text{O}_3\text{F}_2\text{O}^-$ and PF_5 (255).

G. TWO- AND FOUR-COORDINATED SULFUR

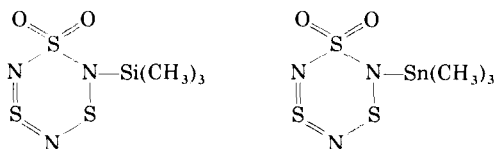
Compounds of this class are rare. The reaction of $\text{FSO}_2\text{N}=\text{S}=\text{O}$ and BCl_3 yields $\text{ClSO}_2\text{N}=\text{S}=\text{O}$ which is not stable and eliminates SO_2 . The resulting $\text{ClSO}_2\text{N}=\text{S}=\text{NSO}_2\text{Cl}$ could not be isolated and made to react with excess $\text{ClSO}_2\text{N}=\text{S}=\text{O}$ with formation (191, 192) of $\text{N}_3\text{S}_3\text{O}_3\text{Cl}$.



m.p. $105^\circ - 108^\circ\text{C}$

The yield of $\text{N}_3\text{S}_3\text{O}_3\text{Cl}$ is increased, when $\text{ClSO}_2\text{N}=\text{S}=\text{NSO}_2\text{Cl}$ is irradiated with ultraviolet light. If $\text{N}_4\text{S}_4\text{O}_2$ is treated with $\text{N}[\text{Si}(\text{CH}_3)_3]_3$

or $\text{N}[\text{Sn}(\text{CH}_3)_3]_3$,



$(\text{CH}_3)_3\text{SiN}_3\text{S}_3\text{O}_2$ as well as $(\text{CH}_3)_3\text{SnN}_3\text{S}_3\text{O}_2$ were isolated as red crystalline compounds (221). The same compounds were obtained from the reaction of FSO_2NSO with the sulfur diimides of trimethyl tin and trimethyl silicon; whether these compounds are six-membered or five-membered rings was established by X-ray analysis. These compounds are the first examples containing three different sulfur atoms of formal oxidation numbers two, four, and six (Fig. 20).

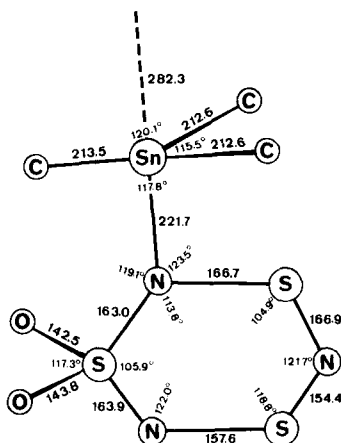
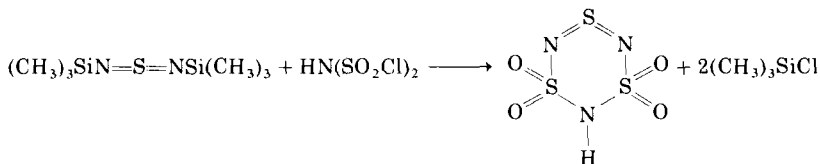


FIG. 20. Molecular structure of $(\text{CH}_3)_3\text{SnN}_3\text{S}_3\text{O}_2$.

It has been shown that $(\text{CH}_3)_3\text{SiN}=\text{S}=\text{NSi}(\text{CH}_3)_3$ and $\text{HN}(\text{SO}_2\text{Cl})_2$ reacted to form $\text{HN}_3\text{O}_4\text{S}_3$.



The structure was established by means of the mass spectrum (210). The same compound is formed when $\text{HN}(\text{SO}_2\text{Cl})_2$ is treated with $(\text{CH}_3)_3\text{SiNSO}$ (44).

H. THREEFOLD COORDINATED NITROGEN AND FOUR-COORDINATED SULFUR

Compounds of this type have been known since 1892 (102, 247). Recent X-ray analysis confirmed the six-membered cyclic structure (56, 105). $(\text{CH}_3\text{NSO}_2)_3$ reacts with trimethylamine to form the tetramethylammonium salt, which can be converted to the acid by means of an ion-exchange resin; this is caused to react with silver-carbonate to yield $(\text{CH}_3\text{NSO}_2)_2(\text{NSO}_2)^- \text{Ag}^+$. The reaction of the silver salt with $\text{C}_2\text{H}_5\text{I}$ gave $(\text{CH}_3\text{NSO}_2)_2(\text{NSO}_2\text{C}_2\text{H}_5)$ (259).

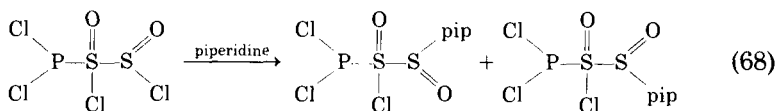
I. COMPOUNDS HAVING ONE ELEMENT IN THE RING OTHER THAN SULFUR AND NITROGEN

From the preparation of $(\text{NSOCl})_3$ and $(\text{NPCl}_2)_3$ it follows that ring systems containing both NPCl_2 and NSOCl units should also exist. If the thermolysis of $\text{ClSO}_2\text{N}=\text{PCl}_3$ is carried out under ultraviolet light, the mixed ring *cis*-(NPCl_2)-(NSOCl)₂ is formed (251). This compound and $(\text{NPCl}_2)_2\text{NSOCl}$ can be synthesized by thermolysis of the reaction mixture of $[\text{Cl}_3\text{PNPCl}_3]^+[\text{PCl}_6]^-$ and sulfamic acid (16, 17, 52, 104). Fluorination of (*cis*- NPCl_2)-(NSOCl)₂ by AgF_2 yields the fluorine analog. By allowing $(\text{NPCl}_2)(\text{NSOCl})_2$ to react with SbF_3 , a mixture of two isomers of $(\text{NPCl}_2)(\text{NSOF})_2$ is obtained (16, 123). The crystal structures of (*cis*- NPCl_2)-(NSOCl)₂ and of the fluorine analog $(\text{NPCl}_2) \cdot (\text{NSOF})_2$ (249, 252) have been investigated by X-ray analysis. Both molecules are six-membered rings, which show some deviation from planarity. The rings possess a chair conformation. The oxygen atoms are in equatorial position with respect to the mean plane of the ring. The sulfur-bonded halogen atoms are in an axial position. In contrast to $(\text{NSOCl})_3$, the N—S bond lengths in the mixed systems appear to be different:

	NS (pm)
(<i>cis</i> - NPCl_2)-(NSOCl) ₂	154.0; 157.8
(<i>cis</i> - NPCl_2)(NSOF) ₂	152.7; 156.8
(<i>cis</i> -NSOCl) ₃	157.1

In contrast to the aminolysis of $(\text{NPCl}_2)_2\text{NSOCl}$ by morpholine and pyrrolidine, it is observed that in the reaction of *cis*- $\text{NPCl}_2(\text{NSOCl})_2$

with piperidine in acetonitrile the first substitution takes place at one of the sulfur atoms. This results in a 1:1 mixture of two isomers (250).

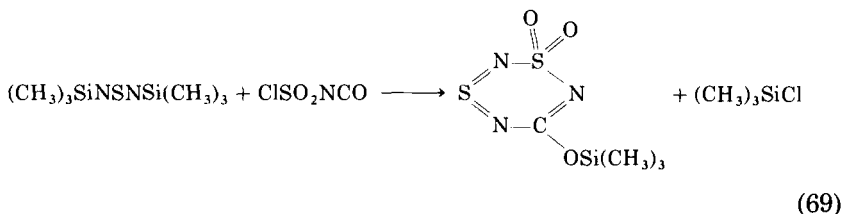


In both isomers, the PCl_2 center appears to be more reactive toward further substitution than the SOCl center.

In ether, if the reaction takes place the phosphorus atom is attacked predominantly. This has been observed for the amines NH_3 , CH_3NH_2 , $\text{C}_2\text{H}_5\text{NH}_2$, *n*- and *i*-propylamine. Introducing a relatively small amino group, the reaction in acetonitrile also takes place at phosphorus. However, in acetonitrile the substitution at phosphorus decreases with increasing bulk of the nucleophile, whereas the substitution at sulfur increases (123).

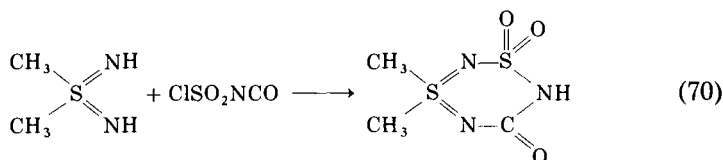
The substitution at sulfur requires a very polar solvent. Tetrakis- as well as tris-substituted piperidine derivatives of $\text{NPCl}_2(\text{NSOCl})_2$ are known (250). $\text{NPCl}_2(\text{NSOF})_2$ reacted with silicon-nitrogen compounds and ammonia with monosubstitution at the phosphorus (111).

When equimolar amounts of chlorosulfonyl isocyanate and $(\text{CH}_3)_3\text{SiNSNSi}(\text{CH}_3)_3$ are combined, a carbon-containing six-membered ring is formed (13, 210).

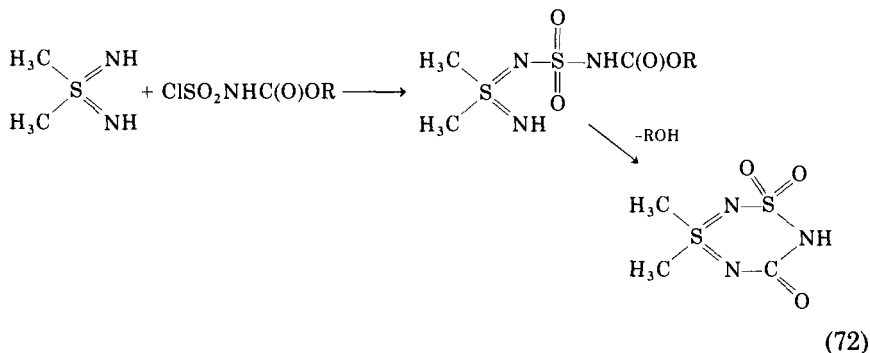
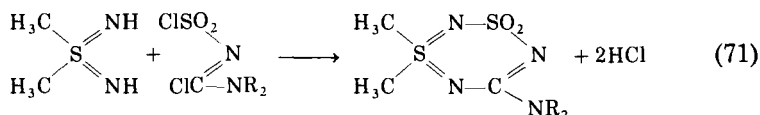


Using $(\text{CH}_3)_3\text{SiNS(O)NSi}(\text{CH}_3)_3$ in the reaction with chlorosulfonyl isocyanate leads to the analogous oxidized compound with coordination number three at one of the sulfur atoms (13).

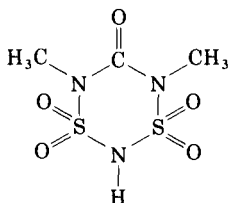
S,S-Dimethyl sulfodiimide has been reported to give in a condensation addition reaction with the bifunctional chlorosulfonylisocyanate a cyclic compound in low yield (99).



A series of such compounds have been synthesized either by the reaction of bifunctional imidoyl halides or *N*-chlorosulfonyl carbamates with *S,S*-dimethyl sulfodiimide (100).

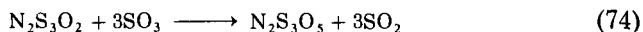
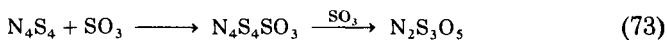


When $\text{HN}(\text{SO}_2\text{Cl})_2$ reacts with *N,N'*-dimethylurea, a compound with two SO_2 groups and one carbonyl group is isolated (243).

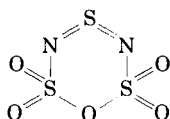


This compound can be converted to the silver salt, which reacts with CH_3I to yield the corresponding methyl derivative.

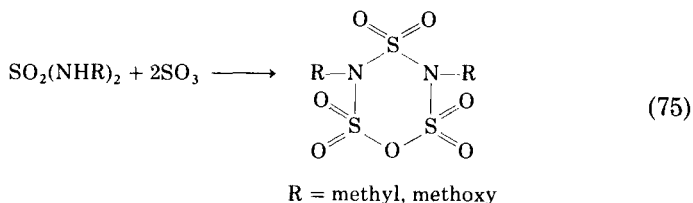
An oxygen-containing six membered ring of composition $\text{N}_2\text{S}_3\text{O}_5$ is readily available by reaction of either N_4S_4 or $\text{N}_2\text{S}_3\text{O}_2$ with excess of SO_3 (102).



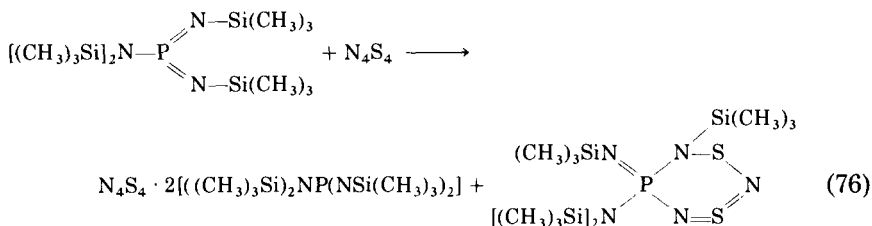
The following structure was found by X-ray analysis (189a):



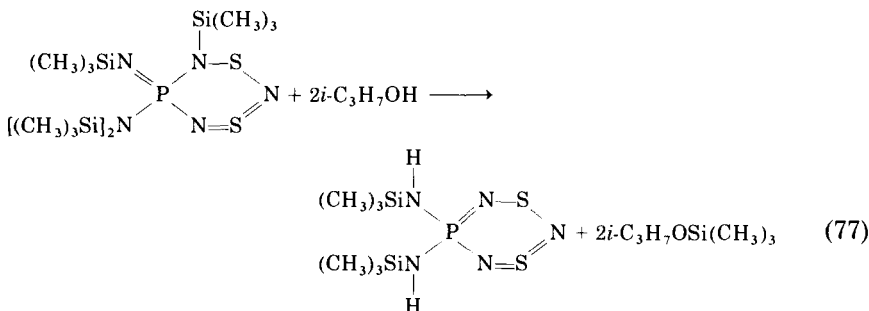
A cyclic six-membered ring is also formed when *N,N*-dimethyl sulfamide or *N,N*-dimethoxy sulfamide is made to react with SO_3 (102).



Probably a phosphorus-containing six-membered S—N ring is formed according to the following reactions:



In addition to the six-membered ring, a 1:2 adduct was isolated. When the six-membered ring is allowed to react with 2 mol of isopropanol, two of the four trimethylsilyl groups are replaced by hydrogen.



$[(\text{CH}_3)_3\text{SiNH}]_2\text{PN}_3\text{S}_2$ is blue-violet in color and melts at 104°C . An alternative four-membered ring has been discussed (8).

VII. Seven-Membered Rings

A. DOUBLY COORDINATED SULFUR AND NITROGEN

The N_3S_4^+ ion has been known for a long time. It is an almost planar seven-membered ring as shown in Fig. 21 (55, 118, 265, 266). The calculated charge distribution for this ion clearly indicates that the positive charge is extensively delocalized and largely located on the sulfur atoms. The fact that the S—N bond distances (155.0 pm) are equal within experimental error indicates that there is delocalization of the π bonding in this ring. N_3S_4^+ can be described as a 10- π -electron system. The question of the σ - and π -contribution in the sulfur-sulfur bond and the possibility of long-range S—S interactions are other points of interest in the structure of this cation (1).

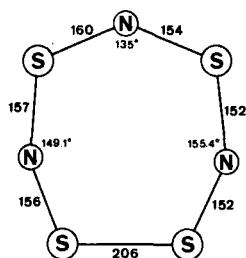
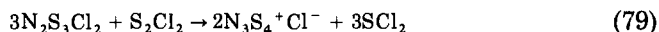
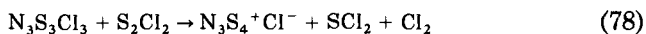
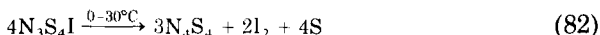
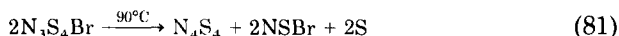
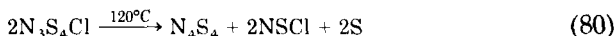


FIG. 21. Molecular structure of N_3S_4^+ .

A number of methods used to prepare N_3S_4^+ are based on ring contraction of N_4S_4 , which may be caused by S_2Cl_2 , SOCl_2 , $\text{CH}_3\text{C(O)Cl}$, HCl , and other acid chlorides (102). N_3S_4^+ may be obtained also by ring expansion of $\text{N}_3\text{S}_3\text{Cl}_3$ and $\text{N}_2\text{S}_3\text{Cl}_2$ with S_2Cl_2 .



If S_2Cl_2 is allowed to react with ammonia, lithium azide, or ammonium chloride under controlled conditions, $\text{N}_3\text{S}_4^+\text{Cl}^-$ is also formed. The bromide of N_3S_4^+ is prepared by metathesis of the chloride with potassium bromide in formic acid, and the corresponding fluoride is produced by fluorination of the bromide with hydrogen fluoride. It has been found that these halides undergo both oxidation and reduction reactions (102). Both $\text{N}_3\text{S}_4\text{Cl}$ and $\text{N}_3\text{S}_4\text{Br}$ give N_4S_4 and NSCl and NSBr , respectively, on thermal decomposition. No NSI is formed on decomposition of $\text{N}_3\text{S}_4\text{I}$ (83).

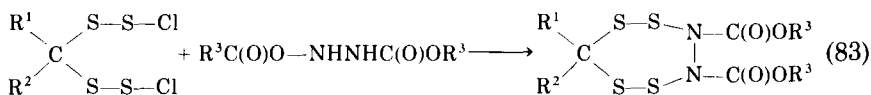


In $\text{N}_3\text{S}_4^+\text{Cl}^-$ the chloride can be replaced by various anions, SO_3F^- (182), SO_3CF_3^- , $\text{N}(\text{SO}_2\text{F})_2^-$, $\text{N}(\text{SO}_2\text{CF}_3)\text{SO}_2\text{Cl}^-$, $\text{N}(\text{SO}_2\text{CF}_3)\text{SO}_2\text{F}^-$ (201), $\text{N}(\text{SO}_2\text{Cl})_2^-$ (32, 102). $\text{N}_3\text{S}_4^+\text{Cl}^-$ forms adducts with CuCl_2 , NiCl_2 , CoCl_2 , TeBr_4 , SbCl_3 , BiCl_3 , ICl , ICl_3 (25, 130, 183, 184), SbCl_5 (129), InCl_3 (279), and HgCl_2 (262).

B. COMPOUNDS HAVING ONE ELEMENT WITHIN THE RING OTHER THAN SULFUR AND NITROGEN

It is of interest that N_4S_4 and SeCl_2 react to give $\text{N}_3\text{S}_3\text{Se}^+$. A seven-membered ring was proposed (25), but no structural investigations were reported.

A seven-membered ring with a nitrogen-nitrogen bond was isolated from the following reaction (144).



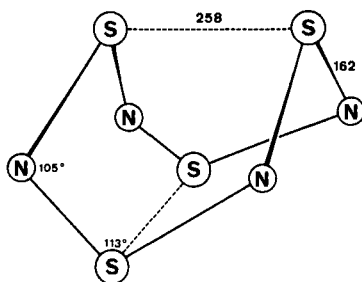
The structure of the methyl compound was determined by X-ray analysis. The seven-membered ring exists in a twist conformation (145).

VIII. Eight-Membered Rings

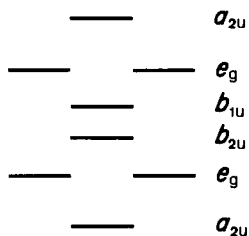
Although the chemistry of N_4S_4 has been fully discussed in recent articles (30, 60, 81, 82, 90, 91, 192), for the general cohesion of this chapter it is necessary that its chemistry be dealt with briefly here. The main emphasis is placed on more recent work.

A. STRUCTURE AND BONDING IN N_4S_4 , ITS ADDUCTS WITH LEWIS ACIDS AND IN $\text{N}_4\text{S}_4^{2+}$

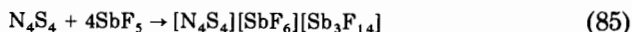
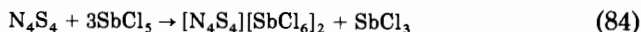
The spatial arrangement shown (Fig. 22) was proved by X-ray and electron diffraction (50, 148, 233). The cradlelike conformation showed that all sulfur atoms have coordination number three instead of two for a planar ring. An explanation for this was given on the basis

FIG. 22. Molecular structure of N_4S_4 .

of an HMO model. The resultant π -orbital scheme is shown in Fig. 23. The π -system of the planar N_4S_4 model is occupied by 12 electrons. Therefore, the lowest five π -orbitals are doubly occupied, and the two higher e_g -orbitals each accommodate a single electron, according to Hund's rule. Thus, the D_{4h} model predicts a triplet ground state. It was shown that symmetry reduction by bond alternation or angle deformation does not yield a significant split of the originally degenerate levels and will not change the multiplicity. The cradle conformation can be described by bending the planar system in such a way that two opposite atoms are brought into close transannular contact. Their interaction is too small to yield a stable singlet ground state and therefore a second σ -bond is necessary to create a 4-centered 8π -system in the plane of the molecule and two σ -bonds, one below and one above this plane. These symmetry considerations show that only the cradle conformation gives a singlet ground state. Whether the nitrogen or sulfur atoms form this transannular interaction is not a question of symmetry, but rather of the total energy of the system. With the help of MO calculations it was shown that the stabilization of the singlet ground state is caused by the effective interaction of the $3p$ -orbitals of sulfur over a distance of 258 pm. The $3p\sigma$ - $3p\sigma$ overlap of

FIG. 23. Hückel molecular orbital diagram for planar N_4S_4 with D_{4h} symmetry.

or N_4S_4 with $SbCl_5$ and of N_4S_4 with SbF_5 , respectively, in SO_2 solution (79).



The cell of $[N_4S_4][SbF_6][Sb_3F_{14}]$ contains two crystallographically nonequivalent $N_4S_4^{2+}$ ions (A) and (B). Structure (A) is planar and has equal bond lengths and bond angles; structure (B) is also planar but has alternating bond lengths; and structure (C) is nonplanar and has S_4 symmetry and a very pronounced alternation in bond lengths, while the bond angles are all equal (Fig. 26). All three forms have similar energies and the presumably weak interactions with neighboring ions in the crystal lattice appear to be sufficient to cause a rather drastic change in the structure of the cation.

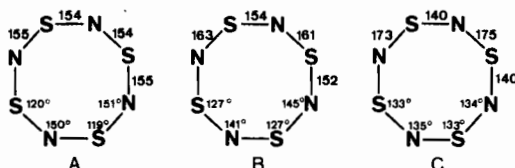


Fig. 26. Molecular structures of $N_4S_4^{2+}$. Structure of ring (A) in $[N_4S_4][SbF_6][Sb_3F_{14}]$; (B) structure of ring (B) in $[N_4S_4][SbF_6][Sb_3F_{14}]$; (C) structure of ring (C) in $[N_4S_4][SbCl_6]_2$, viewed down the S_4 axis.

B. COMPOUNDS WITH COORDINATION NUMBERS TWO AND THREE

N_4S_4 reacts in inert solvents with a wide variety of Lewis acids. Adducts with stoichiometries 2:1, 1:1, 1:2, and 1:4 have been isolated that contain, per mole of N_4S_4 : $C_6H_5BCl_2$, TiI_4 , $HfCl_4$, WCl_4 , WBr_4 (3), BF_3 (179, 275), X-ray structure (59), 1 or 2 BCl_3 (14, 179, 181, 275), 1 or 2 $AlCl_3$ (3, 46), 1 or 2 $AlBr_3$ (3, 46), $GaCl_3$ (3), $InCl_3$ (3), $FeCl_3$ (3), 4 TiF_4 (3), 0.5 $SnCl_4$ (14, 102), 0.5 $SnBr_4$ (27), 2 or 4 SbF_5 (53), 1 or 2 $SbCl_5$ (14, 173, 275), $SbBr_3$ (106), SbI_3 (106), 1,2, or 4 SO_3 (74), $SeCl_4$ (181), $TeCl_4$ (181), $TeBr_4$ (15), 1 or 2 $TiCl_4$ (102), $TiBr_4$ (14), $ZrCl_4$ (14), VCl_4 (14), $NbCl_5$ (14), $TaCl_5$ (14), $MoCl_5$ (173), WCl_4 (3), $CuCl$ (241), $CuBr$ (241), $CuCl_2$ (241).

Diadducts: $N_4S_4BCl_3SbCl_5$ (275), $N_4S_4AlCl_3SbCl_5$ (46), $N_4S_4SnCl_4POCl_3$ (23), $N_4S_4BCl_3SO_3$ (181), $N_4S_4SbCl_5SO_3$ (181), $N_4S_4TeCl_4SO_3$, $N_4S_4TeCl_4BCl_3$ (181), $N_4S_4TeCl_4SbCl_5$, $N_4S_4TeCl_4SO_3$ (181).

Structural investigations of the adducts are rare (59, 173, 241). In the structure of CuClN_4S_4 (241), N_4S_4 functions as a bridging ligand. It is surprising that the N_4S_4 group in CuClN_4S_4 does not change its conformation. Bond distances and angles are close to those of the free N_4S_4 molecule. The complex $\text{IrCl}(\text{CO})\text{P}(\text{C}_6\text{H}_5)_3\text{N}_4\text{S}_4$ is formed, together with other products, when N_4S_4 is treated with $\text{IrCl}(\text{CO})[\text{P}(\text{C}_6\text{H}_5)_3]_2$. This complex is diamagnetic; the structure is not known (153).

Originally, it was reported that N_4S_4 in a Diels-Alder type of reaction functions as a diene, when it forms 1:2 adducts with cyclopentadiene, bicycloheptene, or bicycloheptadiene (33). A structural investigation showed that the organic ligands are not bonded to sulfur and nitrogen, but only to the sulfur atoms of the N_4S_4 ring. Therefore, these reactions cannot be formulated as Diels-Alder-type additions. The average SN distance is 162 pm (Fig. 27), the same as is that found in N_4S_4 (64, 97). The transannular S—S-bond lengths are 400 pm compared to 258 pm in N_4S_4 . The N_4S_4 ring also remained intact with adducts of *trans*-cyclooctene (165), norbornene, norbornadiene, and dicyclopentadiene (42).

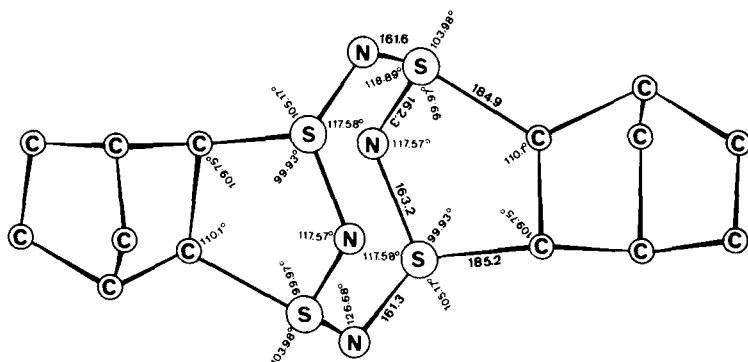


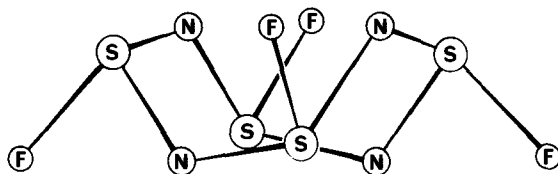
FIG. 27. Molecular structure of $\text{N}_4\text{S}_4 \cdot 2\text{C}_7\text{H}_8$, without hydrogen atoms.

Recently N_4S_4 has been used as an insertion reagent in metal-nonmetal bonds (101, 200, 218, 219, 223).



The resulting products are interesting starting materials for the reaction with halides.

$\text{N}_4\text{S}_4\text{F}_4$ was prepared by the direct fluorination of N_4S_4 with either elemental fluorine (151) or with AgF_2 in carbon tetrachloride (87). $\text{N}_4\text{S}_4\text{F}_4$ has a puckered compact structure (Fig. 28) with almost identical bond angles at the sulfur and nitrogen and a very pronounced

FIG. 28. Molecular structure of $N_4S_4F_4$.

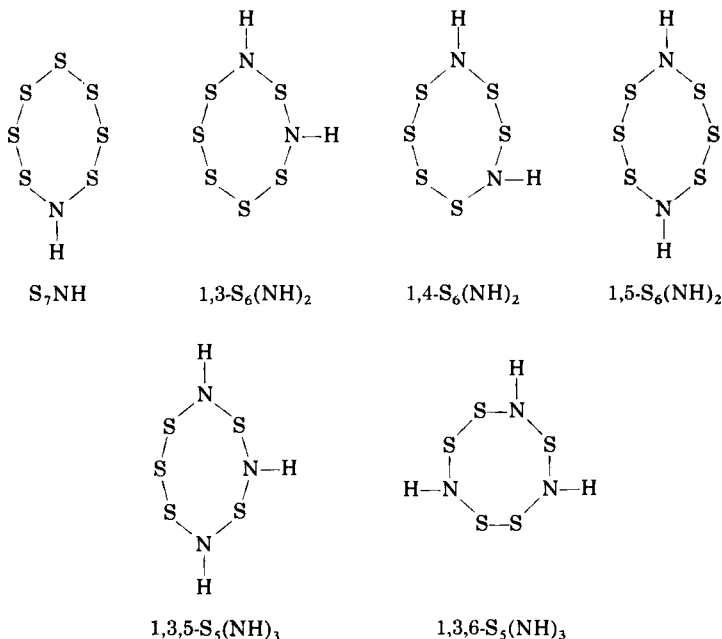
alternation in bond lengths of 154 and 166 pm. In contrast to the chair-shaped six-membered ring of $N_3S_3F_3$, only two fluorine atoms occupy axial positions (273). The electronic structure of $N_4S_4F_4$ and other cyclothiazenes has been investigated within the framework of the CNDO/2 approximation. The stability and preferred conformation of the molecules studied were discussed in terms of transannular energy bonding and antibonding terms. The results support Dewar's islands model (45). However, the average bond lengths in $N_4S_4F_4$ (160 pm) is essentially the same as in $N_3S_3F_3$ (159 pm) or $N_3S_3Cl_3$ (160 pm). The bond lengths of 160 pm seems to be characteristic of molecules having sulfur with coordination number three and nitrogen with coordination number two. Therefore, the energy differences of molecules with strongly alternating bond lengths and equal bond lengths should be small.

When $N_4S_4F_4$ is treated with the Lewis acids AsF_5 or SbF_5 , a mixture of $N_3S_3F_2^+MF_6^-$ and $NS^+MF_6^-$ ($M = As, Sb$) is obtained (161). The $N_4S_4F_3^+$ cation seems not to be a stable one, but it is reported that BF_3 forms a stable adduct with $N_4S_4F_4$ (85).

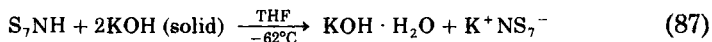
A chlorine analog of $N_4S_4F_4$ was detected as an unstable intermediate in the chlorination of N_4S_4 with elemental chlorine. $N_4S_4Cl_4$ is readily transformed into $N_3S_3Cl_3$ (4, 171). $N_4S_4[ON(CF_3)_2]_4$ is obtained when the stable bistrifluoromethylnitroxide radical, $(CF_3)_2NO$, reacts with N_4S_4 . A ring expansion is observed when $N_3S_3Cl_3$ reacts with $(CF_3)_2NO$ or with $Hg[(CF_3)_2NO]_2$ to give $N_4S_4[ON(CF_3)_2]_4$ (61, 62). The SN ring structure can be compared with that of $N_4S_4F_4$ having SN bond distances of 156 and 162 pm (70). These data result in an average S—N bond length of 159 pm, which is characteristic for three-coordinated sulfur and two-coordinated nitrogen.

The reduction of N_4S_4 with alcoholic tin(II) chloride gives the tetraimide $N_4S_4H_4$. The ring of this molecule has a crown-shaped configuration very similar to that of the S_8 molecule. The sulfur bond angles in $N_4S_4H_4$ and S_8 are very close, being 108.4° in $N_4S_4H_4$ and 107.8° in S_8 (102). The NH group is isoelectronic with a sulfur atom (106). The ammonolysis of S_2Cl_2 in dimethylformamide produced a mixture of products, which may be regarded as derivatives of S_8

by replacing atoms of sulfur by the imino group. Separations were achieved by fractional crystallization and column chromatography (106). A convenient route to S_7NH is the reaction of elemental sulfur with sodium azide (39b, 39c)

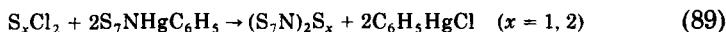
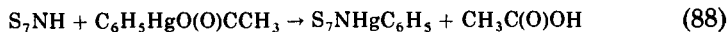


Structures have been confirmed by X-ray analysis (187a, 252a, 254) and also by a study of infrared, Raman (170a, 234a, 237a), and photoelectron spectra (27a). In the crown-shaped S_7NH molecule the nitrogen atom is nearly planar coordinated (109). The structure contains no $N \cdots H$ bond, but a weak $S \cdots H$ interaction. The similarities of $N_4S_4H_4$ along with S_7NH , $S_6(NH)_2$, and $S_5(NH)_3$ have led to their designation as pseudosulfurs. The chemistry of these compounds is mainly that associated with the imido group, which undergoes a number of normal reactions, such as metallization or substitution by inorganic and organic halides. S_7NH and $N_4S_4H_4$ have been studied in the greatest detail, as they are more accessible. NS_7^- was first reported as its sodium salt (34). It is a rather unstable yellow ion, best made by reaction (87) (156, 176).



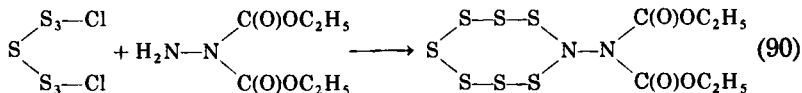
It reacts as a strong nucleophile, e.g., with methyl iodide.

S_7NH was coupled with various sulfur dichlorides, SCl_2 , S_2Cl_2 , S_3Cl_2 , and S_5Cl_2 in the presence of a stoichiometric amount of pyridine, giving $(S_7N)_2S$, $(S_7N)_2S_2$, $(S_7N)_2S_3$, and $(S_7N)_2S_5$, respectively (106). The same compounds were obtained according by following reactions (107, 188):

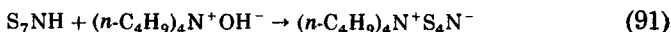


S_7NH and $[(CH_3)_2N]_3PO$ form a 2:1 adduct (238a) which is only stable below $-25^\circ C$.

The mercury derivative $S_7NHgC_6H_5$ can also be caused to react with $(CH_3)_3SnCl$, BCl_3 and BBr_3 to yield $S_7NSn(CH_3)_3$ and $(S_7N)_mBX_{n-m}$, where $X = Cl$, $m = 2, 3$ and $X = Br$, $m = 1, 2$ (107). According to this route, pyridine· $B(NS_7)_3$, $CO(NS_7)_2$, $(C_6H_5)_2P(S)NS_7$, and R_3MNS_7 ($M = Sn, Pb$; $R = CH_3, C_2H_5$) were prepared (189). $(C_6H_5)_2P(S)NS_7$ was also obtained from $(C_6H_5)_2P(S)Cl$ and S_7NH (121). The reaction between diborane and S_7NH gives S_7NBH_2 and $(S_7N)_2BH$ (157). A hydrazine derivative of the S_7N ring was prepared from S_7Cl_2 and the hydrazine dicarbonic acid ester in the presence of triethylamine (146).

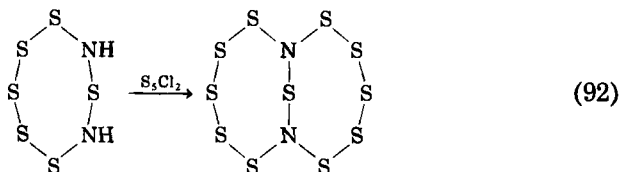


The X-ray structures of $S_7NC(O)CH_3$ and $1,3,5-S_5(NCH_2OH)_3$ were investigated (254). The S_7N ring is cleaved when S_7NH is treated with tetra-*n*-butylammonium hydroxide:

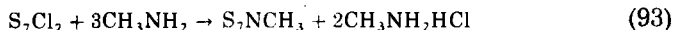


and the perthionitrate is formed (48, 49).

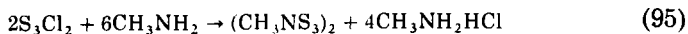
Anions of $1,5-S_6(NH)_2$ are obtained, when this compound is treated with C_2H_5Li . The resulting anions $S_6N_2H^-$ and $S_6N_2^{2-}$ may be allowed to react with alkyl iodides (246). The reaction between the 1,3-isomer and sulfur chlorides gives the first known fused-ring sulfur nitride, $S_{11}N_2$ (106, 108).



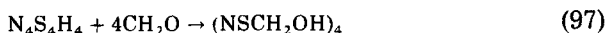
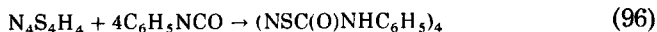
X-Ray analysis has shown that there are two puckered eight-membered rings with three coplanar bonds around each nitrogen. Organic derivatives of the eight-membered sulfur nitrogen ring may be obtained by the reaction of S_xCl_2 ($x = 1, 2, 3, 5, 7$) with primary amines (5a, 40, 95):



where $R = CH_3, C_2H_5, C_6H_5CH_2, C_6H_5CH_2CH_2,$

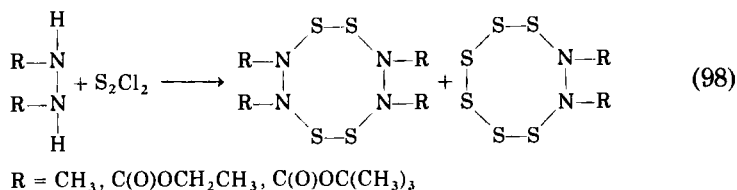


or by the reaction of tetrasulfurimide with organic reagents that react with secondary amines (102):



The most fully investigated was the tetramethyl derivative, for which infrared, Raman, and NMR spectra and an X-ray investigation were reported in support of its cyclic structure (150).

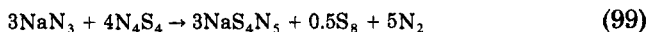
Hydrazine and disulfur dichloride in ether produce nitrogen and elemental sulfur. However, a more intensive study of the reaction of 1,2-dimethylhydrazine and other substituted hydrazines with S_2Cl_2 showed two types of compounds to be formed (141, 142):



The latter is obtained also from $RNHNHR$ and S_6Cl_2 (143). $(OSNH)_4$ has been prepared by air oxidation of $N_4S_4H_4$ or by heating a mixture of 80% elemental sulfur and 20% $N_4S_4H_4$ in the presence of air as an oxidant. $(OSNH)_4$ can be stored at room temperature for several days, but it slowly polymerizes to $(OSNH)_x$ (66, 68).

A short note has been published on the preparation of $(NSOF)_4$, which was obtained by pyrolysis of $Hg(NSOF)_2$ (137).

The syntheses of $S_4N_5^-$ was achieved by methanolysis of *N*-trimethylsilyl-*N'*-*tert*-butyl sulfodiimide or by reaction of sodium azide with N_4S_4 (39, 39d, 226).



$NH_4S_4N_5$ is formed by the reaction of S_2Cl_2 , SCl_2 , SCl_4 , $(NSCl)_3$, and N_4S_4 with ammonia (227).

The geometric structure (Fig. 29) of the $S_4N_5^-$ anion may be compared with that of N_4S_4 , where in one S—S bond a nitrogen has been inserted. This nitrogen bridge levels the distances between the sulfur atoms in such a way that each nitrogen has a nearly undistorted tetrahedral surrounding (69).

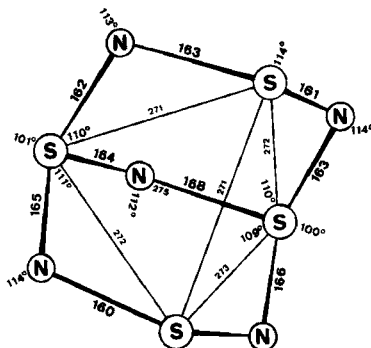
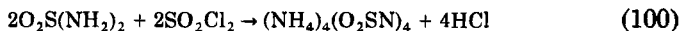


FIG. 29. Molecular structure of $S_4N_5^-$.

C. COMPOUNDS WITH COORDINATION NUMBERS TWO, THREE, AND FOUR

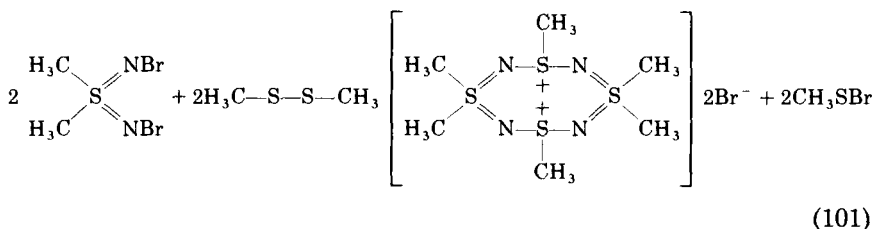
One of the products of the reaction of thionyl chloride with liquid ammonia is the salt $NH_4^+S_4N_5O^-$. This anion is clearly related to $S_4N_5^-$, but one sulfur atom has an additional oxygen atom, which was shown by an X-ray analysis (31, 149, 235, 236).

There have been several attempts to prepare the neutral compound $(O_2SNH)_4$ (102). The best method of preparing derivatives of the tetrameric ring appears to be the condensation of sulfamide with sulfonyl chloride in acetonitrile.



The ammonium salt can easily be converted into barium, potassium, or silver salts. The ammonium salt is only slightly soluble in water and can be recrystallized from it. A characteristic reaction is the substitution of the metal attached to the nitrogen sites by an organic group (37, 102).

When *N,N'*-dibromo-*S,S*-dimethyl sulfodiimines and dialkyl disulfides react in nitromethane, methanol, or methylene chloride, an eight-membered ionic ring system is formed containing alternating sulfur and nitrogen atoms (7, 194):



The saltlike compounds can be derived from N_4S_4 by adding two methyl groups each to two sulfur atoms, and one methyl group each to the two remaining sulfur atoms.

Oxides of N_4S_4 may be prepared from *N,N'*-bis(trimethylsilyl) sulfodiimide and $\text{FSO}_2\text{N}=\text{S}=\text{O}$, $\text{FSO}_2\text{N}=\text{S}=\text{NSO}_2\text{F}$, or $\text{FSO}_2\text{OSO}_2\text{F}$. However, the yields of $\text{N}_4\text{S}_4\text{O}_2$ and $\text{N}_4\text{S}_4\text{O}_4$ are low. $\text{N}_4\text{S}_4\text{O}_2$ is best prepared from condensation of sulfamide with $\text{N}_2\text{S}_3\text{Cl}_2$ (204, 213, 214, 220, 221). This procedure gives $\text{N}_4\text{S}_4\text{O}_2$ in yields of 80%. The unit cell contains two crystallographically independent sets of molecules. One set is situated on the mirror planes at $y = \frac{1}{4}$ and $\frac{3}{4}$, and the other around 2-fold axes. Individual molecules do not possess 2-fold shaped symmetry, and disordering of the molecules is required to give rise to the observed symmetry. The dimensions shown in Fig. 30 refer to the

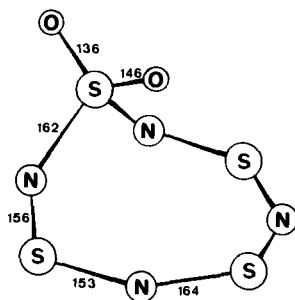
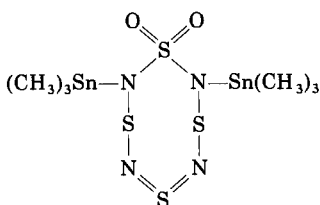


FIG. 30. Molecular structure of $\text{N}_4\text{S}_4\text{O}_2$.

ordered molecule lying on the mirror plane. The molecule contains an eight-membered N_4S_4 ring with both oxygens attached to the same sulfur atom. This atom lies 152 pm and the two adjacent nitrogen atoms 41 pm above the mean plane of the other ring atoms, which are coplanar to within 1.4 pm. The bonding can be described in terms of two sulfo-diimide fragments linked by S and SO_2 bridges or, in view of the approach to planarity of the N_4S_3 part of the ring, as a $10-\pi$ delocalized system linked into a ring by the SO_2 group.

$N_4S_4O_2$ reacts with $N[Sn(CH_3)_3]_3$ without ring contraction. The formula for this product, shown below, is recognizably related to that of $N_4S_4O_2$ (220). The structure was investigated by an X-ray analysis.



IX. Ten-Membered Rings

One of the compounds known so far in this class is the $N_5S_5^+$ cation. Salts of this cation have been prepared by three different methods: (a) from the reaction between $S[NSi(CH_3)_3]_2$ and FSO_2NSO ; (b) from N_4S_4 or $N_3S_3Cl_3$ with a metal chloride in $SOCl_2$; (c) by insertion of the thionitrosyl cation, NS^+ , into one NS bond of N_4S_4 (20, 22, 23, 160, 204).

On the basis of X-ray structural investigations two different structures were reported for the $N_5S_5^+$ cation: A heart-shaped configuration

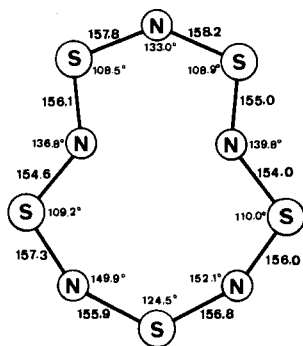
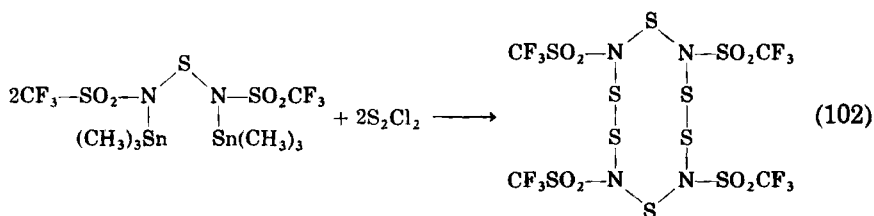


FIG. 31. Molecular structure of $N_5S_5^+$.

and an azulene-like configuration. In a localized picture (Fig. 31) the bonding of $N_5S_5^+$ can be described as follows. The σ -skeleton consists of 10 N—S σ -bonds, each center is furthermore carrying a lone pair, n . This accounts for 10 σ - and 20 n -electrons and leaves 14 π -electrons. Semiempirical calculations on the heart-shaped structure of $N_5S_5^+$ confirm this picture (1). X-Ray data from other SN rings indicate that the sulfur centers adopt angles between 90° and 120° while for the nitrogen centers values between 115° and 125° are found. On the average we obtain about the same value as for carbon π -systems, namely 120° . Taking angle strain and lone-pair interactions into account, it is hard to understand why a heart-shaped structure should be preferred over the others. The comparison of six possible structural isomers of $N_5S_5^+$ within an MO framework leads to the conclusion that an azulene-like structure of $N_5S_5^+$ is to be preferred (28). A ten-membered ring can be prepared by the action of S_2Cl_2 on $[CF_3SO_2NSn \cdot (CH_3)_3]_2S$ in the molar ratio of 1:1.



¹⁹F-NMR studies show all the fluorine atoms to be in the same environment. A proof for the ring size was given by mass spectra (199).

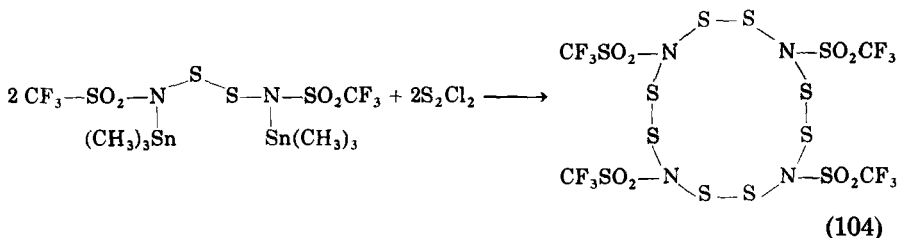
It seems highly probable that larger S—N rings could be made in a similar way, when electron-withdrawing groups are attached to nitrogen and other heteroatoms are incorporated into the rings. There is thus the prospect of considerable development of this particular aspect of sulfur–nitrogen chemistry in the future.

X. Twelve-Membered Rings

A twelve-membered ring has been reported, as a product of thermal condensation of ClSO_2NH_2 (133a):



$[\text{CF}_3\text{SO}_2\text{NSn}(\text{CH}_3)_3\text{S}]_2$ reacts with S_2Cl_2 to yield the twelve-membered ring $[\text{CF}_3\text{SO}_2\text{NS}_2]_4$.



It was shown by X-ray analysis that the molecule has a chair conformation (126a), which is different in structure from the isoelectronic S_{12} skeleton (237).

REFERENCES

1. Adams, D. B., Banister, A. J., Clark, D. T., and Kilcast, D., *Int. J. Sulfur Chem., Part A* **1**, 143 (1971).
2. Ahlrichs, R., and Keil, F., *J. Am. Chem. Soc.* **96**, 7615 (1974).
3. Alange, G. G., and Banister, A. J., private communication.
4. Alange, G. G., Banister, A. J., and Bell, B., *J. Chem. Soc., Dalton Trans.* p. 2399 (1972).
5. Alange, G. G., Banister, A. J., Bell, B., and Millen, P. W., *Inorg. Nucl. Chem. Lett.* **13**, 143 (1977).
- 5a. Allen, C. W., *J. Chem. Educ.* **44**, 38 (1967).
6. Andreasen, O., Hazell, A. C., and Hazell, R. G., *Acta Crystallogr., Sect. B* **33**, 1109 (1977).
7. Appel, R., Hänssgen, D., and Müller, W., *Chem. Ber.* **101**, 2855 (1968).
8. Appel, R., and Halstenberg, M., *Angew. Chem.* **88**, 763 (1976); *Angew. Chem., Int. Ed. Engl.* **15**, 695 (1976).
9. Appel, R., and Halstenberg, M., *Angew. Chem.* **87**, 810 (1975); *Angew. Chem., Int. Ed. Engl.* **14**, 769 (1975).
10. Appel, R., and Montenarh, M., *Z. Naturforsch., Teil B* **32**, 108 (1977).
11. Appel, R., Montenarh, M., and Ruppert, I., *Chem. Ber.* **108**, 582 (1975).
12. Appel, R., Ruppert, I., Milker, R., and Bastian, V., *Chem. Ber.* **107**, 380 (1974).
13. Appel, R., Uhlenhaut, H., and Montenarh, M., *Z. Naturforsch., Teil B* **29**, 799 (1974).
14. Ashley, P. J., and Torrible, E. G., *Can. J. Chem.* **47**, 2587 (1969).
15. Aynsley, E. E., and Campbell, W. A., *J. Chem. Soc.* p. 832 (1957).
16. Baalmann, H. H., and van de Grampel, J. C., *Recl. Trav. Chim. Pays-Bas* **92**, 716 (1973).
17. Baalmann, H. H., Velvis, H. P., and van de Grampel, J. C., *Recl. Trav. Chim. Pays-Bas* **91**, 935 (1972).
18. Banister, A. J., *Nature (London), Phys. Sci.* **237**, 92 (1972); **239**, 69 (1972).
19. Banister, A. J., and Bell, B., *J. Chem. Soc. A* p. 1659 (1970).
20. Banister, A. J., and Clarke, H. G., *J. Chem. Soc., Dalton Trans.* p. 2661 (1972).
21. Banister, A. J., Clarke, H. G., Rayment, I., and Shearer, H. M. M., *Inorg. Nucl. Chem. Lett.* **10**, 647 (1974).
22. Banister, A. J., and Dainty, P. J., *J. Chem. Soc., Dalton Trans.* p. 2658 (1972).
23. Banister, A. J., Durrant, J. A., Rayment, I., and Shearer, H. M. M., *J. Chem. Soc., Dalton Trans.* p. 928 (1976).
24. Banister, A. J., and Hazell, A. C., *Proc. Chem. Soc., London* p. 282 (1962).
25. Banister, A. J., and Padley, J. S., *J. Chem. Soc. A* p. 1437 (1967).

26. Banister, A. J., and Padley, J. S., *J. Chem. Soc. A* p. 658 (1969).
27. Banister, A. J., and Younger, D., *J. Inorg. Nucl. Chem.* **32**, 3763 (1970).
- 27a. Barrie, A., Garcia-Fernandez, H., Heal, H. G., and Ramsay, R. J., *J. Inorg. Nucl. Chem.* **37**, 311 (1975).
28. Bartetzko, R., and Gleiter, R., *Inorg. Chem.* **17**, 995 (1978).
29. Bartholomew, D., and Kay, I. T., *J. Chem. Res. (S)* p. 238 (1977); *J. Chem. Res. (M)* p. 2813 (1977).
30. Becke-Goehring, M., *Prog. Inorg. Chem.* **1**, 221 (1959).
31. Becke-Goehring, M., and Erhardt, K., *Naturwissenschaften* **56**, 415 (1969).
32. Becke-Goehring, M., and Leinenweber, P., *Z. Naturforsch. Teil. B* **24**, 1661 (1969).
33. Becke-Goehring, M., and Schläfer, D., *Z. Anorg. Allg. Chem.* **356**, 234 (1968).
34. Becke-Goehring, M., and Schwarz, R., *Z. Anorg. Allg. Chem.* **296**, 3 (1958).
35. Becke-Goehring, M., Wald, H. J., and Weber, H., *Naturwissenschaften* **55**, 491 (1968).
36. Becke-Goehring, M., and Weber, H., *Z. Anorg. Allg. Chem.* **365**, 185 (1969).
37. Bencker, K., Leiderer, G., and Meuwesen, A., *Z. Anorg. Allg. Chem.* **324**, 202 (1963).
38. Benseler, E., and Haas, A., *Chem. Ztg.* **95**, 757 (1971).
39. Bojes, J., Boorman, P. M., and Chivers, T., *Inorg. Nucl. Chem. Lett.* **12**, 551 (1976).
- 39a. Bojes, J., and Chivers, T., *J. Chem. Soc., Chem. Commun.* p. 453 (1977).
- 39b. Bojes, J., and Chivers, T., *Inorg. Nucl. Chem. Letters*, **10**, 735 (1974).
- 39c. Bojes, J., and Chivers, T., *J. Chem. Soc. Dalton Trans.* p. 1715 (1975).
- 39d. Bojes, J., and Chivers, T., *Inorg. Chem.* **17**, 318 (1978).
40. Brasted, R. C., and Pond, J. S., *Inorg. Chem.* **4**, 1163 (1965).
41. Brasted, R. C., Pond, J. S., Kanamueller, J., and Richter, G. P., *Prepr., Div. Pet. Chem. Am. Chem. Soc.* **19**, 277 (1974).
42. Brinkman, M. R., and Allen, C. W., *J. Am. Chem. Soc.* **94**, 1550 (1972).
43. Brown, D. A., and Frimmel, F., *J. Chem. Soc., Chem. Commun.* p. 579 (1971).
44. Buckendahl, W., and Glemser, O., *Chem. Ber.* **110**, 1154 (1977).
45. Cassoux, P., Glemser, O., and Labarre, J. F., *Z. Naturforsch., Teil B* **32**, 41 (1977).
46. Chan, C. H., and Olsen, F. P., *Inorg. Chem.* **11**, 2836 (1972).
- 46a. Chang, H.-H., and Weinstein, B., *J. Chem. Soc. Perkin Trans.* p. 1601 (1977).
47. Chapman, D., and Massey, A. G., *Trans. Faraday Soc.* **58**, 1291 (1962).
48. Chivers, T., and Drummond, I., *J. Chem. Soc., Chem. Commun.* p. 19 (1973).
49. Chivers, T., and Drummond, I., *Inorg. Chem.* **13**, 1222 (1974).
50. Clark, D., *J. Chem. Soc.* p. 1615 (1952).
51. Clements, D. A., U.S. Patent 3,365,495 (1968); *Chem. Abstr.* **69**, 27408 (1968).
52. Clipsham, R. M., Hart, R. M., and Whitehead, M. A., *Inorg. Chem.* **8**, 2431 (1969).
53. Cohen, B., Hooper, T. R., Hugill, D., and Peacock, R. D., *Nature (London)* **207**, 748 (1965).
54. Cohen, M. J., Garito, A. F., Heeger, A. J., MacDiarmid, A. G., Mikulski, C. M., Saran, M. S., and Kleppinger, J., *J. Am. Chem. Soc.* **98**, 3844 (1976).
55. Cordes, A. W., Kruh, R. F., and Gordon, E. K., *Inorg. Chem.* **4**, 681 (1965).
56. Daalgard, G. A. P., Hazell, A. C., and Hazell, R. G., *Acta Crystallogr., Sect. B* **30**, 2721 (1974).
57. Demarcay, E., *C. R. Hebd. Seances Acad. Sci.* **91**, 854 (1880).
58. Dresdner, R. D., Johar, J. S., Merritt, J., and Patterson, C. S., *Inorg. Chem.* **4**, 678 (1965).
59. Drew, M. G. B., Templeton, D. H., and Zalkin, A., *Inorg. Chem.* **6**, 1906 (1967).
60. Emeléus, H. J., *Endeavour* **32**, 76 (1973).
61. Emeléus, H. J., Fordes, R. A., Poulet, R. J., and Sheldrick, G. M., *Chem. Commun.* p. 1483 (1970).
62. Emeléus, H. J., and Poulet, R. J., *J. Fluorine Chem.* **1**, 13 (1971, 1972).

63. Engel, P. S., *Tetrahedron Lett.* **26**, 2301 (1974).
64. Ertl, G., and Weiss, J., *Z. Anorg. Allg. Chem.* **420**, 155 (1976).
65. Faucher, J. P., Labarre, J. F., and Shaw, R. A., *Z. Naturforsch., Teil B* **31**, 677 (1976).
66. Fluck, E., and Becke-Goehring, M., *Z. Anorg. Allg. Chem.* **292**, 229 (1957).
67. Fluck, E., Becke-Goehring, M., and Dehoust, G., *Z. Anorg. Allg. Chem.* **312**, 60 (1961).
68. Fluck, E., and Böing, H., *Chem.-Ztg.* **94**, 331 (1970).
69. Flues, W., Scherer, O. J., Weiss, J., and Wolmershäuser, G., *Angew. Chem.* **88**, 411 (1976); *Angew. Chem., Int. Ed. Engl.* **15**, 379 (1976).
70. Fordes, R. A., and Sheldrick, G. M., *J. Fluorine Chem.* **1**, 23 (1971, 1972).
71. Friedman, P., *Inorg. Chem.* **8**, 692 (1969).
72. Garcia-Fernandez, H., *Bull. Soc. Chim. Fr.* p. 760 (1959).
73. Gattow, G., and Behrendt, W., "Topics in Sulfur Chemistry," Vol. 2. Thieme, Stuttgart, 1977.
74. Gieren, A., Dederer, B., Roesky, H. W., Amin, N., and Petersen, O., *Z. Anorg. Allg. Chem.* **440**, 119 (1978).
75. Gieren, A., Dederer, B., Roesky, H. W., and Janssen, E., *Angew. Chem.* **88**, 853 (1976); *Angew. Chem., Int. Ed. Engl.* **15**, 783 (1976).
76. Gieren, A., and Pertlik, F., *Angew. Chem.* **88**, 852 (1976); *Angew. Chem., Int. Ed. Engl.* **15**, 782 (1976).
77. Gillespie, R. J., Ireland, P. R., and Vekris, J. E., *Can. J. Chem.* **53**, 3147 (1975).
78. Gillespie, R. J., Passmore, J., Ummat, P. K., and Vaidya, O. C., *Inorg. Chem.* **10**, 1327 (1971).
79. Gillespie, R. J., Slim, D. R., and Tyrer, J. D., *J. Chem. Soc., Chem. Commun.* p. 253 (1977).
80. Gleiter, R., *J. Chem. Soc. A* p. 3174 (1970).
81. Glemser, O., *Endeavour* **28**, 86 (1969).
82. Glemser, O., *Angew. Chem.* **75**, 697 (1963); *Angew. Chem., Int. Ed. Engl.* **2**, 530 (1963).
83. Glemser, O., *Z. Naturforsch., Teil B* **31**, 610 (1976).
84. Glemser, O., Klingebiel, U., Lin, T. B., Mews, R., Wagner, H., and Weiss, J., *Int. Fluorine Symp. 7th*, 1973 (1973).
85. Glemser, O., and Lüdemann, H., *Angew. Chem.* **70**, 190 (1958).
86. Glemser, O., and Mews, R., *Adv. Inorg. Chem. Radiochem.* **14**, 333 (1972).
87. Glemser, O., Schröder, H., and Haeseler, H., *Z. Anorg. Allg. Chem.* **279**, 28 (1955).
88. Glemser, O., Schröder, H., and Wyszomirski, E., *Z. Anorg. Allg. Chem.* **298**, 72 (1959).
89. Glemser, O., and Wyszomirski, E., *Angew. Chem.* **69**, 534 (1957).
90. Gmelins Handbuch der anorganischen Chemie, 8th ed. Part B, Sect. 3. Verlag Chemie, Weinheim, 1963.
91. Goehring, M., "Ergebnisse und Probleme der Chemie der Schwefelstickstoffverbindungen. Akademie-Verlag, Berlin, 1957.
92. Goehring, M., Heinke, J., Malz, H., and Ross, G., *Z. Anorg. Allg. Chem.* **273**, 200 (1953).
93. Goehring, M., and Malz, H., *Z. Naturforsch., Teil B* **9**, 567 (1954).
94. Golloch, A., and Kuss, M., *Z. Naturforsch., Teil B* **29**, 320 (1974).
95. Gordon, W. I., and Heal, H. G., *J. Inorg. Nucl. Chem.* **32**, 1863 (1970).
96. Greene, F. D., and Hecht, S. S., *J. Org. Chem.* **35**, 2482 (1970).
97. Griffin, A. M., and Sheldrick, G. M., *Acta Crystallogr., Sect. B* **31**, 895 (1975).
98. Grunwell, J. R., and Danison, W. C., *Tetrahedron* **27**, 5315 (1971).
99. Haake, M., *Angew. Chem.* **83**, 256 (1971); *Angew. Chem., Int. Ed. Engl.* **10**, 264 (1971).

100. Haake, M., "Topics in Sulfur Chemistry." Thieme, Stuttgart, 1976.
101. Haenssger, D., and Roelle, W., *J. Organomet. Chem.* **56**, C14 (1973).
102. Haiduc, I., "The Chemistry of Inorganic Ring Systems." Wiley (Interscience), New York, 1970.
- 102a. Haiduc, I., *Chem. Inorg. Heteroatom Ring Syst.*, 1977 p. 356 (1977).
103. Hanley, R. N., Ollis, W. D., and Ramsden, C. A., *J. Chem. Soc., Chem. Commun.* p. 307 (1976).
104. Haubold, W., Fluck, E., and Becke-Goehring, M., *Z. Anorg. Allg. Chem.* **397**, 269 (1973).
- 104a. Haworth, D. T., and Lin, G. Y., *J. Inorg. Nucl. Chem.* **39**, 1838 (1977).
105. Hazell, A. C., *Acta Crystallogr., Sect. B* **30**, 2724 (1974); *Acta Chem. Scand.* **26**, 2542 (1972).
106. Heal, H. G., *Adv. Inorg. Chem. Radiochem.* **15**, 375 (1972).
107. Heal, H. G., and Ramsay, R. J., *J. Inorg. Nucl. Chem.* **36**, 950 (1974).
- 107a. Heal, H. G., and Ramsay, R. J., *J. Inorg. Nucl. Chem.* **37**, 286 (1975).
108. Heal, H. G., Shahid, M. S., and Garcia-Fernandez, H., *J. Chem. Soc. A* p. 3846 (1971).
109. Hecht, H. J., Reinhardt, R., Steudel, R., and Bradaczek, H., *Z. Anorg. Allg. Chem.* **426**, 43 (1976).
110. Hecht, S. S., and Greene, F. D., *J. Am. Chem. Soc.* **89**, 6761 (1967).
111. Heider, W., Klingebiel, U., Lin, T. P., and Glemser, O., *Chem. Ber.* **107**, 592 (1974).
112. Hinze, J., and Jaffé, H. H., *J. Am. Chem. Soc.* **84**, 540 (1962).
113. Holm, A., Schaumburg, K., Dahlberg, N., Christophersen, C., and Snyder, J. P., *J. Org. Chem.* **40**, 431 (1975).
114. Holt, E. M., and Holt, S. L., *J. Chem. Soc., Chem. Commun.* p. 1704 (1970).
115. Holt, E. M., Holt, S. L., and Watson, K. J., *J. Chem. Soc., Dalton Trans.* p. 514 (1977).
116. Jensen, K. A., and Pedersen, C., *Adv. Heterocycl. Chem.* **3**, 263 (1964).
117. Johar, J. S., and Dresdner, R. D., *Inorg. Chem.* **7**, 683 (1968).
118. Johnson, D. A., Blyholder, G. D., and Cordes, A. W., *Inorg. Chem.* **4**, 1970 (1965).
119. Jolly, W. L., *Adv. Chem. Ser.* **110**, 92 (1972).
120. Jolly, W. L., and Maguire, K. D., *Inorg. Synth.* **9**, 102 (1967).
121. Kanamüller, J. M., *J. Inorg. Nucl. Chem.* **36**, 3855 (1974).
122. Kirsanov, A. V., *Zh. Obshch. Khim.* **22**, 93 (1952); *Chem. Abstr.* **46**, 6984b (1952).
123. Klingebiel, U., Lin, T. P., Buss, B., and Glemser, O., *Chem. Ber.* **106**, 2969 (1973).
124. Klüver, H., and Glemser, O., *Z. Naturforsch., Teil B* **32**, 1209 (1977).
125. Krauss, H. L., and Jung, H., *Z. Naturforsch., Teil B* **16**, 624 (1961).
126. Krebs, B., to be published.
- 126a. Krebs, B., Hein, M., Diehl, M., and Roesky, H. W., *Angew. Chem.* **90**, 825 (1978).
127. Krebs, B., and Pohl, S., *Chem. Ber.* **106**, 1069 (1973).
128. Kreutzer, P., Weis, C., Boehme, H., Kemmerich, T., Beck, W., Spencer, C., and Mason, R., *Z. Naturforsch., Teil B* **27**, 745 (1972).
129. Kruss, B., and Ziegler, M. L., *Z. Anorg. Allg. Chem.* **388**, 158 (1972).
130. Kruss, B., and Ziegler, M. L., *Z. Naturforsch., Teil B* **27**, 1282 (1972).
131. Kulbach, N. T., and Scherer, O. J., *Tetrahedron Lett.* **27**, 2297 (1975).
132. L'abbé, G., van Loock, E., Albert, R., Toppet, S., Verhelst, G., and Smets, G., *J. Am. Chem. Soc.* **96**, 3973 (1974).
133. Leandri, G., Busetti, V., Valle, G., and Mammi, M., *J. Chem. Soc., Chem. Commun.* p. 413 (1970).
- 133a. Lehmann, H. A., Schneider, W., and Hiller, R., *Z. Anorg. Allg. Chem.* **365**, 157 (1969).
- 133b. Lehmann, H. A., Riesel, L., Hoehne, K., and Maier, E., *Z. Anorg. Allg. Chem.* **310**, 298 (1961).

134. Lidy, W., Sundermeyer, W., and Verbeek, W., *Z. Anorg. Allg. Chem.* **406**, 288 (1974).
135. Lieber, E., Oftedahl, E., and Rao, C. N. R., *J. Org. Chem.* **28**, 194 (1963).
136. Lieber, E., Pillai, C. N., Ramachandran, J., and Hites, R. D., *J. Org. Chem.* **22**, 1750 (1957).
137. Lin, T.-P., Klingebiel, U., and Glemser, O., *Angew. Chem.* **84**, 1149 (1972); *Angew. Chem., Int. Ed. Engl.* **11**, 1095 (1972).
138. Lin, T.-P., and Glemser, O., *Chem. Ber.* **109**, 3537 (1976).
139. Lindquist, I., and Weiss, J., *J. Inorg. Nucl. Chem.* **6**, 184 (1958).
140. Lindsell, W. E., and Faulds, G. R., *J. Chem. Soc., Dalton Trans.* p. 40 (1975).
141. Lingmann, H., and Linke, K. H., *Angew. Chem.* **82**, 954 (1970); *Angew. Chem., Int. Ed. Engl.* **9**, 956 (1970).
142. Lingmann, H., and Linke, K. H., *Z. Naturforsch., Teil B* **26**, 1207 (1971).
143. Lingmann, H., and Linke, K. H., *Chem. Ber.* **104**, 3723 (1971).
144. Linke, K. H., and Bimczok, R., *Chem. Ber.* **107**, 771 (1974).
145. Linke, K. H., and Kalker, H. G., *Chem. Ber.* **109**, 76 (1976); *Z. Anorg. Allg. Chem.* **432**, 193 (1977).
146. Linke, K. H., and Skupin, D., *Z. Naturforsch., Teil B* **26**, 1371 (1971).
147. Lipp, S. A., Chang, J. J., and Jolly, W. L., *Inorg. Chem.* **9**, 1970 (1970).
148. Lu, G. S., and Donohue, J., *J. Am. Chem. Soc.* **66**, 818 (1944).
149. Luger, P., Bradaczek, H., and Steudel, R., *Chem. Ber.* **109**, 3441 (1976).
150. MacDonald, A. L., and Trotter, J., *Can. J. Chem.* **51**, 2504 (1973).
151. Maraschin, N. J., and Lagow, R. L., *J. Am. Chem. Soc.* **94**, 8601 (1972).
152. Marichich, T. J., *J. Am. Chem. Soc.* **90**, 7179 (1968).
153. McCormick, B. J., and Anderson, B. M., *J. Inorg. Nucl. Chem.* **32**, 3414 (1970).
154. McNeil, D. A. C., Murray, M., and Symons, M. C. R., *J. Chem. Soc. A* p. 1019 (1967).
155. Meij, R., Kuyper, J., Stufkens, D. J., and Vrieze, K., *J. Organomet. Chem.* **110**, 219 (1976).
156. Mendelsohn, M. H., and Jolly, W. L., *J. Inorg. Nucl. Chem.* **35**, 95 (1973).
157. Mendelsohn, M. H., and Jolly, W. L., *Inorg. Chem.* **11**, 1944 (1972).
158. Meuwisen, A., *Z. Anorg. Allg. Chem.* **266**, 250 (1951).
159. Mews, R., *Adv. Inorg. Chem. Radiochem.* **19**, 185 (1976).
160. Mews, R., *Angew. Chem.* **88**, 757 (1976); *Angew. Chem., Int. Ed. Engl.* **15**, 691 (1976).
161. Mews, R., Wagner, D. L., and Glemser, O., *Z. Anorg. Allg. Chem.* **412**, 148 (1975).
162. Mikulski, C. M., Russo, P. J., Saran, M. S., MacDiarmid, A. G., Garito, A. F., and Heeger, A. J., *J. Am. Chem. Soc.* **97**, 6358 (1975).
163. Minami, T., Fukuda, M., Abe, M., and Agawa, T., *Bull. Chem. Soc. Jpn.* **46**, 2156 (1973).
164. Minami, T., Takimota, F., and Agawa, T., *Bull. Chem. Soc. Jpn.* **48**, 3259 (1975).
164a. Mingos, D. M. P., *Nature (London), Phys. Sci.* **236**, 99 (1972); **239**, 16 (1972).
165. Mock, W. L., and Mehrotra, I., *J. Chem. Soc., Chem. Commun.* p. 123 (1976).
166. Moeller, T., and Dieck, R. L., *Prep. Inorg. React.* **6**, 63 (1971).
167. Montenarh, M., and Appel, R., *Z. Naturforsch., Teil B* **31**, 902 (1976).
168. Neidlein, R., and Leinberger, P., *Chem.-Ztg.* **99**, 433 (1975).
169. Neidlein, R., Leinberger, P., Gieren, A., and Dederer, B., *Chem. Ber.* **111**, 698 (1978).
170. Neidlein, R., and Tauber, J., *Arch. Pharm. (Weinheim)* **304**, 687 (1971).
170a. Nelson, J., *Spectrochim. Acta. Part A* **27**, 1105 (1971).
171. Nelson, J., and Heal, H. G., *Inorg. Nucl. Chem. Lett.* **6**, 429 (1970).
172. Nelson, J., and Heal, H. G., *J. Chem. Soc. A* p. 136 (1971).
173. Neubauer, D., and Weiss, J., *Z. Anorg. Allg. Chem.* **303**, 28 (1960).
174. Neves, E. A., and Franco, D. W., *J. Inorg. Nucl. Chem.* **36**, 3851 (1974).
175. Niinisto, L., and Laitinen, R., *Inorg. Nucl. Chem. Lett.* **12**, 191 (1976).

176. Olsen, B. A., and Olsen, F. P., *Inorg. Chem.* **8**, 1736 (1969).
177. Owsley, D. C., and Helmkamp, G. K., *J. Am. Chem. Soc.* **89**, 4558 (1967).
178. Patton, R. L., and Jolly, W. L., *Inorg. Chem.* **8**, 1389 (1969).
179. Patton, R. L., and Jolly, W. L., *Inorg. Chem.* **8**, 1392 (1969).
180. Patton, R. L., and Raymond, K. N., *Inorg. Chem.* **8**, 2426 (1969).
181. Paul, R. C., Arora, C. L., Kishore, J., and Malhotra, K. C., *Aust. J. Chem.* **24**, 1637 (1971).
182. Paul, R. C., Arora, C. L., and Malhotra, K. C., *Chem. Ind. (London)* **51**, 1810 (1968).
183. Paul, R. C., Sharma, R. P., and Verma, R., *Indian J. Chem., Sect. A* **14**, 48 (1976); **13**, 403 (1975).
184. Paul, R. C., Sharma, R. P. and Verma, R., *Indian J. Chem., Sect. A* **12**, 418 and 761 (1974).
185. Pauling, L. C., "The Nature of the Chemical Bond," 3rd ed. Cornell Univ. Press, Ithaca, New York, 1960.
186. Pilgram, K., and Görgen, F., *J. Heterocycl. Chem.* **8**, 899 (1971).
187. Piper, T. S., *J. Am. Chem. Soc.* **80**, 30 (1958).
- 187a. Postma, H. J., van Bolhuis, F., and Vos. A., *Acta Crystallogr., Sect. B* **27**, 2480 (1971); **29**, 915 (1973).
- 187b. Quast, H., and Kees, F., *Chem. Ber.* **110**, 1780 (1977).
188. Ramsay, R. J., Heal, H. G. and Garcia-Fernandez, H., *J. Chem. Soc., Dalton Trans.* p. 234 (1976).
189. Ramsay, R. J., Heal, H. G., and Garcia-Fernandez, H., *J. Chem. Soc., Dalton Trans.* p. 237 (1976).
- 189a. Rodek, E., Amin, N. and Roesky, H. W., *Z. Anorg. Allg. Chem.* (in press).
190. Roesky, H. W., *Angew. Chem.* **91**, 112 (1979).
191. Roesky, H. W., *Angew. Chem.* **83**, 253 (1971); *Angew. Chem., Int. Ed. Engl.* **10**, 266 (1971).
192. Roesky, H. W., *Chem.-Ztg.* **98**, 121 (1974).
193. Roesky, H. W., *Z. Naturforsch., Teil B* **31**, 680 (1976).
194. Roesky, H. W., "The Sulfur-Nitrogen Bond in A. Senning. Dekker, New York, 1971.
195. Roesky, H. W., Amin, N., and Gieren, A., unpublished results.
196. Roesky, H. W., Amin, N. Remmers, G., Gieren, A., Riemann, U., and Dederer, B., *Angew. Chem.* **91**, 243 (1979).
197. Roesky, H. W., and Aramaki, M., *Angew. Chem.* **90**, 127 (1978); *Angew. Chem., Int. Ed. Engl.* **17**, 129 (1978).
198. Roesky, H. W., Diehl, M., Fuess, H., and Bats, J. W., *Angew. Chem.* **90**, 73 (1978); *Angew. Chem., Int. Ed. Engl.* **17**, 58 (1978).
199. Roesky, H. W., Diehl, M., Krebs, B., and Hein, M., *Z. Naturforsch.* (in press).
200. Roesky, H. W., and Dietl, M., *Angew. Chem.* **85**, 453 (1973); *Angew. Chem., Int. Ed. Engl.* **12**, 424 (1973).
201. Roesky, H. W., and Dietl, M., *Z. Naturforsch., Teil B* **26**, 977 (1971).
202. Roesky, H. W., and Dietl, M., *Chem. Ber.* **106**, 3101 (1973).
203. Roesky, H. W., and Grimm, L., *Angew. Chem.* **84**, 684 (1972); *Angew. Chem., Int. Ed. Engl.* **11**, 642 (1972).
204. Roesky, H. W., Grosse-Böwing, W., Rayment, I., and Shearer, H. M. M., *J. Chem. Soc., Chem. Commun.* p. 735 (1975).
205. Roesky, H. W., and Hamza, A., *Angew. Chem.* **88**, 226 (1976); *Angew. Chem., Int. Ed. Engl.* **15**, 226 (1976).
206. Roesky, H. W., Holtschneider, G., Wiezer, H., and Krebs, B., *Chem. Ber.* **109**, 1358 (1976).

207. Roesky, H. W., and Janssen, E., *Chem.-Ztg.* **98**, 260 (1974).
208. Roesky, H. W., and Janssen, E., *Chem. Ber.* **108**, 2531 (1975).
209. Roesky, H. W., and Janssen, E., *Angew. Chem.* **88**, 24 (1976); *Angew. Chem., Int. Ed. Engl.* **15**, 39 (1976).
210. Roesky, H. W., and Kuhtz, B., *Chem. Ber.* **107**, 1 (1974).
211. Roesky, H. W., and Müller, T., *Chem. Ber.* **111**, 2960 (1978).
212. Roesky, H. W., and Petersen, O., *Angew. Chem.* **85**, 413 (1973); *Angew. Chem., Int. Ed. Engl.* **12**, 415 (1973).
213. Roesky, H. W., and Petersen, O., *Angew. Chem.* **84**, 946 (1972); *Angew. Chem., Int. Ed. Engl.* **11**, 918 (1972).
214. Roesky, H. W., Schaper, W., Petersen, O., and Müller, T., *Chem. Ber.* **110**, 2695 (1977).
215. Roesky, H. W., and Wehner, E., *Angew. Chem.* **87**, 521 (1975); *Angew. Chem., Int. Ed. Engl.* **14**, 498 (1975).
216. Roesky, H. W., Wehner, E., Zehnder, E. J., Deiseroth, H.-J., and Simon, A., *Chem. Ber.* **111**, 1670 (1978).
217. Roesky, H. W., and Wiezer, H., *Angew. Chem.* **87**, 254 (1975); *Angew. Chem., Int. Ed. Engl.* **14**, 258 (1975).
218. Roesky, H. W., and Wiezer, H., *Angew. Chem.* **85**, 722 (1973); *Angew. Chem., Int. Ed. Engl.* **12**, 674 (1973).
219. Roesky, H. W., and Wiezer, H., *Chem. Ber.* **107**, 3186 (1974).
220. Roesky, H. W., and Witt, M., to be published.
221. Roesky, H. W., and Witt, M., *Chem. Ber.* (to be published).
222. Ruff, O., and Geisel, E., *Ber. Dtsch. Chem. Ges.* **37**, 1573 (1904).
223. Ruppert, I., Bastian, V., and Appel, R., *Chem. Ber.* **107**, 3426 (1974).
224. Scherer, O. J., and Wies, R., *Angew. Chem.* **83**, 882 (1971); *Angew. Chem., Int. Ed. Engl.* **10**, 812 (1971).
225. Scherer, O. J., and Wies, R., *Angew. Chem.* **84**, 585 (1972); *Angew. Chem., Int. Ed. Engl.* **11**, 529 (1972).
226. Scherer, O. J., and Wolmershäuser, G., *Angew. Chem.* **87**, 485 (1975); *Angew. Chem., Int. Ed. Engl.* **14**, 485 (1975).
227. Scherer, O. J., and Wolmershäuser, G., *Chem. Ber.* **110**, 3241 (1977).
228. Schläfer, D., and Becke-Goehring, M., *Z. Anorg. Allg. Chem.* **362**, 1 (1968).
229. Schmidt, K.-D., Mews, R., and Glemser, O., *Angew. Chem.* **88**, 646 (1976); *Angew. Chem., Int. Engl.* **15**, 614 (1976).
230. Schmitz, E., "Dreiringe mit zwei Heteroatomen." Springer-Verlag, Berlin and New York, 1967.
231. Schomaker, V., and Stevenson, D. P., *J. Am. Chem. Soc.* **63**, 37 (1941).
232. Seel, F., and Simon, G., *Z. Naturforsch., Teil B* **19**, 354 (1964).
233. Sharma, B. D., and Donohue, J., *Acta Crystallogr.* **16**, 891 (1963).
234. Sommer, F., *Ber. Dtsch. Chem. Ges.* **48**, 1833 (1915).
234a. Steudel, R., *J. Phys. Chem.* **81**, 343 (1977).
235. Steudel, R., Luger, P., and Bradaczek, H., *Angew. Chem.* **85**, 307 (1973); *Angew. Chem., Int. Ed. Engl.* **12**, 316 (1973).
236. Steudel, R., *Z. Naturforsch., Teil B* **24**, 934 (1969).
237. Steudel, R., *Angew. Chem.* **87**, 683 (1975); *Angew. Chem., Int. Ed. Engl.* **14**, 655 (1975).
237a. Steudel, R., and Rose, F., *Spectrochim. Acta.* **33A**, 979 (1977).
238. Steudel, R., Rose, F., Reinhardt, R., and Bradaczek, H., *Z. Naturforsch., Teil B* **32**, 488 (1977).
238a. Steudel, R., Rose, F., and Pickardt, J., *Z. Anorg. Allg. Chem.* **434**, 99 (1977).

239. Swigert, J., and Taylor, K. G., *J. Am. Chem. Soc.* **93**, 7337 (1971).
240. Thamm, H., Lin, T. P., Niecke, E., and Glemser, O., *Z. Naturforsch., Teil B* **27**, 1431 (1972).
241. Thewalt, U., *Angew. Chem.* **88**, 807 (1976); *Angew. Chem., Int. Ed. Engl.* **15**, 765 (1976).
242. Thewalt, U., and Schlingmann, M., *Z. Anorg. Allg. Chem.* **406**, 319 (1974).
243. Thielemann, H., Schlotter, H. A., and Becke-Goehring, M., *Z. Anorg. Allg. Chem.* **329**, 235 (1964).
244. Thompson, Q. E., *Q. Rep. Sulfur Chem.* **5**, 245 (1970).
245. Timberlake, J. W., and Hodges, M. L., *J. Am. Chem. Soc.* **95**, 634 (1973).
246. Tingle, E. M., and Olsen, F. P., *Inorg. Chem.* **8**, 1741 (1969).
247. Traube, W., *Ber. Dtsch. Chem. Ges.* **25**, 2472 (1892).
248. Trefonas, L. M., and Cheung, L. D., *J. Am. Chem. Soc.* **95**, 636 (1973).
- 248a. Tsuge, O., Urano, S., and Mataka, S., *Heterocycles*, **5**, 189 (1976).
249. Tucker, P. A., and van de Grampel, J. C., *Acta Crystallogr., Sect. B* **30**, 2795 (1974).
250. van de Grampel, J. C., *Chem. Inorg. Heteroatom Ring Syst.*, 1977 p. 363 (1977).
251. van de Grampel, J. C., and Vos, A., *Recl. Trav. Chim. Pays-Bas* **82**, 246 (1963).
252. van de Grampel, J. C., and Vos, A., *Acta Crystallogr., Sect. B* **25**, 651 (1969).
- 252a. van de Grampel, J. C., and Vos, A., *Acta Crystallogr., Sect. B* **25**, 611 (1969).
253. van Loock, E., Vandensavel, J. M., L'abbé, G., and Smets, G. *J. Org. Chem.* **38**, 2916 (1973).
254. Vegas Molina, A., Martinez-Ripoll, M., Garcia-Blanco, S., and Garcia-Fernandez, H., *Chem. Inorg. Heteroatom Ring Syst.*, 1977 p. 328 (1977).
255. Wagner, D. L., Wagner, H., and Glemser, O., *Chem. Ber.* **108**, 2469 (1975).
256. Wagner, D. L., Wagner, H., and Glemser, O., *Z. Naturforsch., Teil B* **30**, 88 (1975).
257. Wagner, D. L., Wagner, H., and Glemser, O., *Z. Naturforsch., Teil B* **30**, 279 (1975).
258. Wagner, D. L., Wagner, H., and Glemser, O., *Chem. Ber.* **109**, 1424 (1976).
259. Wagner, D. L., Wagner, H., and Glemser, O., *Z. Naturforsch., Teil B* **32**, 265 (1977).
- 259a. Wagner, H., Mews, R., Lin, T. P., and Glemser, O., *Chem. Ber.* **107**, 584 (1974).
260. Wagner, H., Wagner, D. L., and Glemser, O., *Chem. Ber.* **110**, 683 (1977).
261. Wannagat, U., and Schlingmann, M., *Z. Anorg. Allg. Chem.* **406**, 312 (1974).
262. Weidenhammer, K., and Ziegler, M. L., *Z. Anorg. Allg. Chem.* **434**, 152 (1977).
263. Weinstein, B., and Hsien-Hsin, C., *J. Heterocycl. Chem.* **11**, 99 (1974).
264. Weiss, J., *Z. Naturforsch., Teil B* **12**, 481 (1957).
265. Weiss, J., *Angew. Chem.* **74**, 216 (1962); *Angew. Chem., Int. Ed. Engl.* **1**, 214 (1962).
266. Weiss, J., *Z. Anorg. Allg. Chem.* **333**, 314 (1964).
267. Weiss, J., *Fortschr. Chem. Forsch.* **5**, 635 (1966).
268. Weiss, J., and Becke-Goehring, M., *Z. Naturforsch., Teil B* **13**, 198 (1958).
269. Weiss, J., Mews, R., and Glemser, O., *J. Inorg. Nucl. Chem., Suppl.* p. 213 (1976).
270. Weiss, J., Ruppert, I., and Appel, R., *Z. Anorg. Allg. Chem.* **406**, 329 (1974).
271. Weiss, J., and Thewalt, U., *Z. Anorg. Allg. Chem.* **363**, 159 (1968).
272. Weiss, J., and Ziegler, M., *Z. Anorg. Allg. Chem.* **322**, 184 (1962).
273. Wiegers, G. A., and Vos, A., *Acta Crystallogr.* **14**, 562, (1962); **16**, 152 (1963).
274. Wiegers, G. A., and Vos, A., *Proc. Chem. Soc., London* p. 387 (1962).
275. Wynne, K. J., and Jolly, W. L., *Inorg. Chem.* **6**, 107 (1967).
276. Wynne, K. J., and Jolly, W. L., *J. Inorg. Nucl. Chem.* **30**, 2851 (1968).
277. Zalkin, A., Hopkins, T. E., and Templeton, D. H., *Inorg. Chem.* **5**, 1767 (1966).
278. Zborilova, L., Touzin, J., Navratilova, D., and Mrkosova, J., *Z. Chem.* **12**, 27 (1972).
279. Ziegler, M., Schlimper, H. U., Nuber, B., Weiss, J., and Ertl, G., *Z. Anorg. Allg. Chem.* **415**, 193 (1975).

1,2-DITHIOLENE COMPLEXES OF TRANSITION METALS

R. P. BURNS AND C. A. MCAULIFFE

Chemistry Department, University of Manchester Institute of Science
and Technology, Manchester, United Kingdom

I. Introduction	303
II. 1,2-Dithiolate Ligands and Synthetic Routes	304
III. Transition-Metal Complexes	310
A. Titanium, Zirconium, and Hafnium	310
B. Vanadium, Niobium, and Tantalum	312
C. Chromium, Molybdenum, and Tungsten	313
D. Manganese, Rhenium, and Technetium	316
E. Iron, Ruthenium, and Osmium	317
F. Cobalt, Rhodium, and Iridium	323
G. Nickel, Palladium, and Platinum	327
H. Copper, Silver, and Gold	333
IV. Physical Studies	335
A. X-Ray Structural Studies	336
B. Infrared Spectral Studies	337
C. ESR Spectral and Magnetic Studies	338
D. Electronic Spectral Studies	339
E. X-Ray Photoelectron Spectral (XPS) Studies	339
F. Mössbauer Spectral Studies	341
G. Electrochemical Studies	342
References	343

I. Introduction

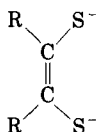
Over the past two decades there has been a phenomenal increase in the study of the chemistry of transition metal complexes containing sulfur ligands. There are a number of reasons for this, the major one being the revitalization of the chemistry of the unsaturated sulfur donor chelates. These were used as early as the 1930s as analytical reagents for various metals (32, 154). The interest in complexes of these ligand systems now embraces areas ranging from purely academic syntheses to large-scale industrial production. Almost every available physical technique has been utilized for the elucidation of the molecular and electronic structures and the kinetics manifested in these systems.

The spiraling interest in the complexes of sulfur donor ligands has prompted number of excellent and frequently exhaustive reviews. Discussions by Livingstone (127), Harris and Livingstone (128), and Jørgensen (95) cover sulfur ligands in general. Reviews by Gray (69), McCleverty (139), Schrauzer (175), and Hoyer (77) have dealt with the chemistry of 1,2-dithiolene complexes in great depth.

Other reasons for the expansion of the field of dithiochelate chemistry have undoubtedly included the correlations of model complexes with biological systems containing transition metal-to-sulfur bonds and the numerous commercial uses of the compounds. The patent literature abounds with examples of the uses of these compounds, and they include applications as vulcanization accelerators for rubbers, highly specific analytical reagents, chromatographic supports, high-temperature wear-inhibiting additives in lubricants, polarizers in sunglasses, polymerization catalysts, catalytic inhibitors, oxidation catalysts, semiconductors, fungicides, pesticides, mode-locking additives in neodymium lasers, and fingerprint developers in criminal investigations. This list is by no means exhaustive, but exemplifies the diversity of the applications of these complexes.

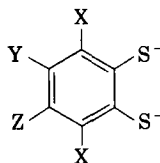
II. 1,2-Dithiolate Ligands and Synthetic Routes

One of the main reasons for the vast increase of interest in the chemistry of transition metal-sulfur complexes over the past 15 years has been the discovery of the novel complexes formed from the unsaturated 1,2-dithiols. These ligands form five-membered unsaturated chelate rings in the metal complexes. There are two main types of ligand that fall into the category of 1,2-dithiolates: the substituted and unsubstituted ethane-1,2-dithiolates (I) and the substituted and unsubstituted benzene-1,2-dithiolates (II).



(I)

R = H, CF₃, CN, alkyl, aryl



(II)

X = Y = Z = H, CH₃, F, Cl

X = Y = H

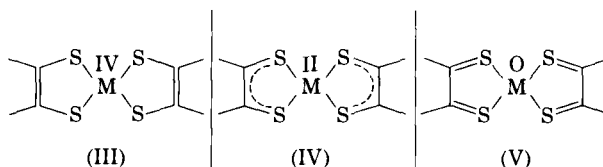
X = H

Z = CH₃

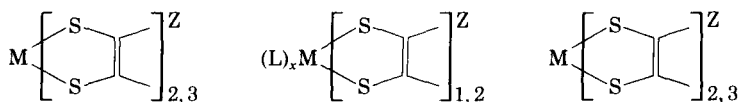
Y = Z = CH₃

The interest in these complexes has sprung mainly from the inability to assign formal oxidation states to the transition metal, the discovery of a very rare structural form, the trigonal prism, in the tris complexes, the facile one- and two-electron transfer reactions they undergo, and the five- and six-coordinate and organometallic adducts that they form.

The difficulty of assigning formal oxidation states in these complexes according to the traditional rules of valence has introduced conflicting nomenclature, e.g., in the planar $MS_4C_4R_4$ complexes (III)–(V). Three different limiting structures are possible in which the metal could have the formal oxidation states shown:



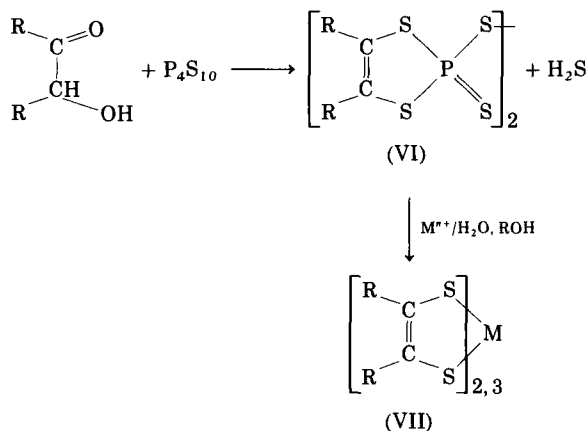
Structure (V), the bis dithioketone, is unlikely to be stable, as zero-valent metal complexes are not usually planar. Dithiolate dianions were previously considered to stabilize high valence states (124, 131), but this has since been discounted (172). Ligands in complexes of type (III), the dithiolato dianions, exist in complex anions, such as $Pt[S_2C_2(CN)_2]_2^{2-}$. In the neutral complexes, however, the ligand is usually considered to be in a state intermediate between (III) and (V), having a delocalized ground state. Schrauzer (172) has proposed that complexes regarded as having delocalized ground states, i.e., the intermediate structure (IV), be termed "dithienes" and the dianions "dithiolates." McCleverty (139), however, used "dithiolene" to denote metal complexes of the type:



This terminology, although vague at times, does not imply any particular formal oxidation state or structure.

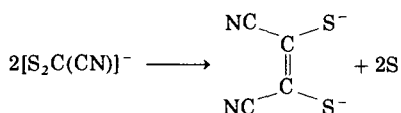
The 1,2-dithiolene complexes were first reported in the 1930s in the analytical studies of Clark and co-workers, who used toluene-3,4-dithiol and chlorobenzene-3,4-dithiol as reagents for zinc, cadmium, mercury, and tin (32, 154). It was not until the late 1950s and the early 1960s that the interest in 1,2-dithiol ligands moved most markedly from their analytical uses to their coordination chemistry.

In 1962, Schrauzer and Mayweg (175), while attempting to catalytically produce thioaromatics, carried out a reaction between solid nickel sulfide and diphenylacetylene. From this they isolated an unusual, intensely green solid, the nickel dithiolene, $[\text{Ni}(\text{S}_2\text{C}_2\text{Ph}_2)_2]$. This method gave low yields, and the synthesis of dialkyl and diaryl-dithiolenes was later accomplished by allowing an acyloin or a benzoin to react with phosphorus pentasulfide in refluxing xylene or dioxane to produce a dithiophosphoric ester (VI). Addition of a solution (usually aqueous or alcoholic) of a metal salt and subsequent heating produces the dithiolene complex (VII).

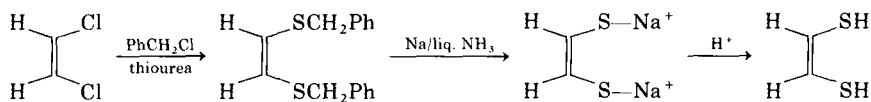


This provides a very versatile synthetic route to the neutral dithiolene complexes, as many acyloins are available commercially or can readily be produced, but the unsubstituted complex ($\text{R} = \text{H}$) could not be obtained by this method (196).

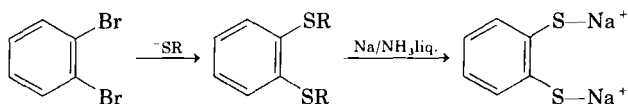
Also in 1962, Gray and co-workers (70) reported metal complexes derived from the *cis*-1,2-dicyano-1,2-dithiolate (maleonitriledithiolate, mnt) dianion. The latter was previously synthesized by Bähr and Schleitzer (5, 6) by dimerization of sodium dicyanodithioformate in water for 24 hours via a spontaneous desulfurization. Improved yields were reported for the same reaction in refluxing chloroform for 8 hours (128).



Many metal complexes derived from the mnt ligand have been prepared and studied. This introduced the second major synthetic route to dithiolene complexes, i.e., from the dianionic 1,2-dithiolates. Thus, the parent unsubstituted ligand *cis*-1,2-ethylenedithiol was prepared by Schrath and Peschel (171). They obtained the dibenzylidithioether from *cis*-1,2-dichloroethylene, benzyl chloride, and thiourea in refluxing ethanol. By making the dithioether react with sodium in liquid ammonia, the benzyl groups were cleaved, forming the disodium salt of the dianion. Acidification produced the free dithiol:



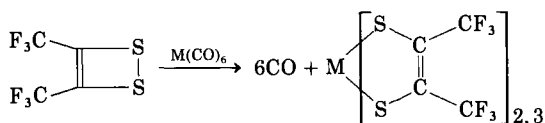
Metal complexes are easily produced by reaction of the dianion with the respective metal salts (23). The aryl-1,2-dithiolenes have also been prepared by reaction of the dianions with metal salts. Toluene-3,4-dithiol and quinoxaline-2,3-dithiol are available commercially, and treatment with potassium in alcohol liberates the dianion. Benzene-1,2-dithiol and its derivatives have been prepared in a similar manner to the *cis*-1,2-ethylenedithiol. *o*-Dibromobenzene is treated with copper ethyl- or *n*-butylmercaptide to yield the 1,2-dithioethers. Sodium/liquid ammonia cleavage of the alkyl groups produces the disodium dithiolate salt (1).



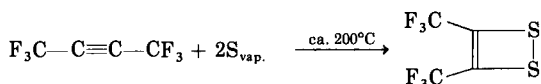
More recently, benzene-1,2-dithiol has been obtained in high yield from the diazotization of *o*-aminophenol in glacial acetic acid, which gives 1,2,3-benzodithiazole, followed by heating with carbon disulfide in an autoclave to give 1,3-benzodithiol-2-thione, which is decomposed in alkaline solution to give the product (82). The tetrachlorobenzene-1,2-dithiol is obtained via an iron complex. Hexachlorobenzene is made to react with iron powder and sodium sulfide in refluxing DMF, and $[\text{Fe}(\text{S}_2\text{C}_6\text{Cl}_4)_2]_n^0$ is precipitated by treatment with base. The free dithiol is liberated by boiling the complex with zinc oxide (145).

The third major synthetic route to dithiolene complexes is via the reaction of low-valent metal compounds (usually containing carbonyl

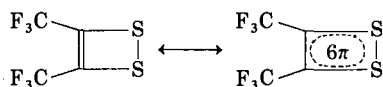
or phosphine ligands) with the heterocyclic bistrifluoromethyldithiete (108),



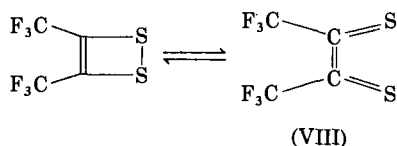
The ligand was first produced by the reaction of 1,1,1,4,4,4-hexafluorobut-2-yne with boiling sulfur (119) to yield a yellow liquid that boils at 95°–96°C. It is in equilibrium with a dimer that is more stable at room temperature; at the temperature of the reaction, however, the monomer is more stable:



The high thermal stability of the dithiete is explained by partial aromaticity as the ring system has 6 π -electrons (120):



The formation of metal complexes from bistrifluoromethyldithiete probably takes place via the very reactive dithioketonic form (VIII), as molecular orbital calculations (172) suggest that the difference in stability between the two forms is quite small and they could exist in equilibrium.

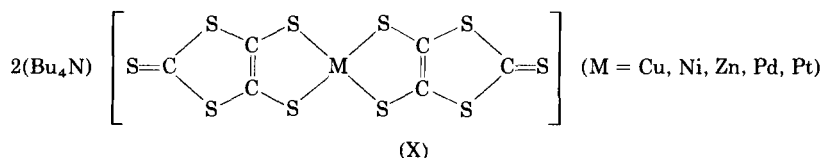
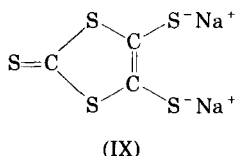


An electron diffraction study of the molecular structure of the dithiete in the vapor phase (73) has shown insignificant difference between it and its transition-metal complexes. This does not suggest that complex formation is accompanied by any great change in bond

character in the $\text{S}-\text{C}\equiv\text{C}-\text{S}$ moiety. The driving force for the rupture of the $\text{S}-\text{S}$ bond in complexation must be the formation of two $\text{M}-\text{S}$ bonds.

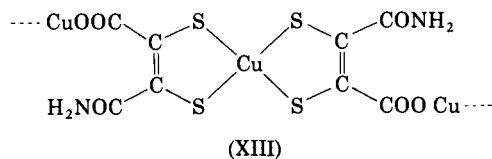
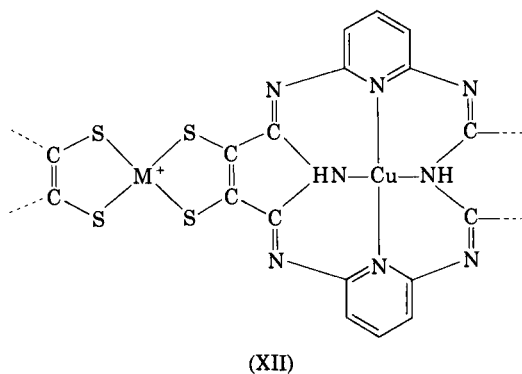
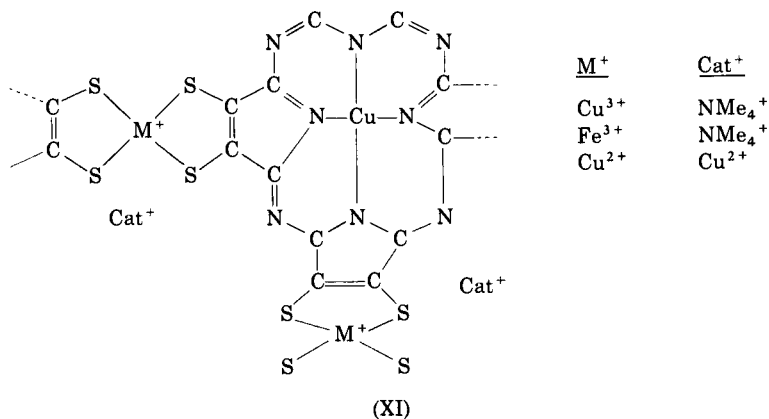
The discovery that facile one- and two-electron transfer reactions are major properties of the dithiolene complexes led to the syntheses of the various reduced and oxidized forms of existing complexes. The wealth of electrochemical redox data available for these complexes has been used to determine redox methods of synthesis. Oxidation and reduction have been achieved by a number of different oxidizing and reducing agents or by electrochemical methods. The commonest oxidizing agents are air, oxygen, iodine, and in special cases the powerful one-electron oxidizing agents $[\text{Ni}(\text{tfd})_2]^0$ or $[\text{Fe}(\text{tfd})_2]^0$. Common reducing agents include hydrazine, borohydride, zinc in pyridine, *o*- and *p*-phenylenediamine, alkali metal alkoxides, amalgams, and sometimes even weakly basic solvents, such as ketones and alcohols, have reduced the complexes, such as $[\text{Ni}(\text{tfd})_2]^0$.

A number of interesting and novel dithiolene ligand systems have been developed recently. Of these, the dimercaptodithiolene (IX) is of interest, as there is potential for forming mixed 1,1- and 1,2-dithiolate polymeric complexes even though, to date, only the 1,2-dithiolene metal complexes (X) have been prepared (184). The ligand (IX) is obtained together with $\text{SC}(\text{SNa})_2$ by treating carbon disulfide with sodium in DMF. Benzylation of the ligand has also been carried out.



Mixed-ligand complexes have been obtained by refluxing a neutral complex with a dianionic species or two equivalent monoanions. The rate of ligand exchange is found to be dependent upon the solvent, the temperature, and the nature of the ligands (52). Very interesting and novel mixed-metal polymeric catalyst matrices have been evolved

that contain dithiolene, porphorin, acetamide, and carboxylate units (XI–XIII) (99).



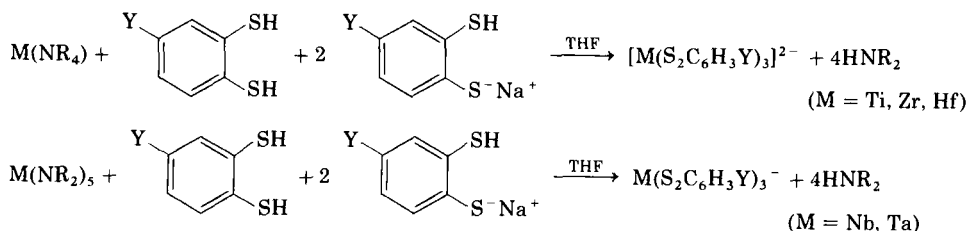
These systems possess unique chemical and physical properties.

III. Transition-Metal Complexes

A. TITANIUM, ZIRCONIUM, AND HAFNIUM

Few complexes of the early transition metals, apart from vanadium, have been reported (129, 151). The inability to synthesize these complexes can be traced to the lack of a suitable preparative method. Early

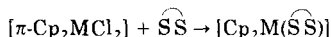
attempts to obtain dithiolene complexes of the early transition metals by known synthetic procedures invariably led to failures except in several notable cases (183, 202). The difficulties were eventually overcome by Takats and Martin, who used the metal amides, $[M(NR_2)_x]$, as starting materials (13, 134). Thus, $(R_4E)_x[M(S_2C_6H_3Y)_{3,2}]$ ($R_4E = Ph_4As, Et_4N, Et_2H_2N, Bu_4N$; $M = Ti, Zr, Hf$ and $x = 2$; $M = Ta$ or Nb and $x = 1$; $Y = H$ or CH_3) were prepared by the following reactions:



A variety of coordination geometries have been noted, and structural studies (13, 42) indicate that the niobium complex is trigonal prismatic and the isoelectronic zirconium complex has a structure intermediate between trigonal prismatic and antiprismatic or octahedral. The exceptions mentioned above are the successful preparations of $[Ti(S_2C_6Cl_4)_3]^{2-}$ (202) and $[Ti(mnt)_3]^{2-}$ (183). A distorted trigonal prismatic geometry has been suggested for $[Ti(mnt)_3]^{2-}$, and this complex is unstable in solution.

Polarographic results (134) show that the dithiolene complexes of the early transition metals undergo facile one-electron transfer reactions, but their electron transfer properties are more limited than in previously studied compounds (179). The ligands in these complexes are described as being close to the dithiolate structure, $C_6H_4S_2^{2-}$ and can be considered to be stabilizing a net highly positive charge on the metal ions (134).

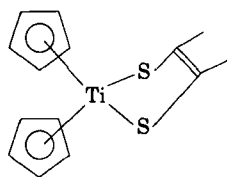
Although the unsubstituted complexes of the early transition metals with the 1,2-dithiolenes have proved to be difficult to isolate, the cyclopentadiene-substituted complexes have been prepared quite easily by several workers (109, 115–117, 128, 141, 142). The generalized reaction is:



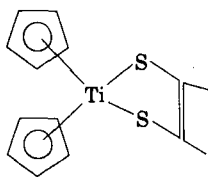
where $M = Ti, Zr, Co, Rh, Fe, W, Mn$; and $\widehat{SS} = mnt^{2-}, S_2C_2H_2^{2-}, S_2C_6H_4^{2-}, S_2C_6Cl_4^{2-}, S_2C_2H_3Me^{2-}$.

Some monocyclopentadiene- and nitrosyl-containing products have also been obtained by varying the starting material and the amount of

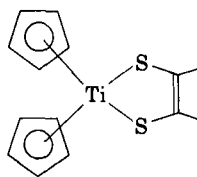
ligand. Thus, $\pi\text{-Cp}_2\text{TiCl}_2$ reacts with 1, 2, and 3 mol of $(\text{S}_2\text{C}_6\text{Cl}_4)^{2-}$ to give $(\pi\text{-Cp}_2\text{Ti}(\text{S}_2\text{C}_6\text{Cl}_4))$, $[\pi\text{-CpTi}(\text{S}_2\text{C}_6\text{Cl}_4)_2]^-$, and $[\text{Ti}(\text{S}_2\text{C}_6\text{Cl}_4)_3]^{2-}$, respectively (141). A crystal structure determination of $[\pi\text{-Cp}_2\text{Ti}(\text{S}_2\text{C}_2\text{H}_2)]$ showed that the central titanium atom was tetrahedrally coordinated by the two sulfur atoms and the cyclopentadiene centroids with the TiS_2 plane folded out of the $\text{S}_2\text{C}_2\text{H}_2$ plane at an angle of 46.1° (121). The ^1H NMR spectra of $[\pi\text{-Cp}_2\text{Ti}(\text{S}-\text{S})]$ ($\text{S}-\text{S} = \text{S}_2\text{C}_2\text{H}_2^{2-}$, $\text{S}_2\text{C}_6\text{H}_4^{2-}$, $\text{S}_2\text{C}_6\text{H}_3\text{Me}^{2-}$) complexes are temperature dependent (116), possibly representing the interconversion of the two identical conformers (XIV) and (XV) via an excited structure (XVI) in which the chelate ring is planar.



(XIV)



(XV)



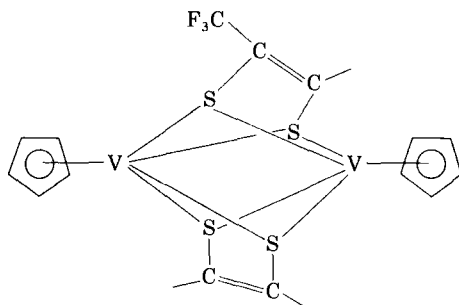
(XVI)

This is contrary to the planar structure generally proposed for metallocene dithiolene derivatives as characterized from NMR spectroscopic data (139).

B. VANADIUM, NIOBIUM, AND TANTALUM

In the past few years very few reports concerning the chemistry of complexes of the vanadium triad with 1,2-dithiolene ligands have appeared. The new complexes of niobium and tantalum were described in the preceding section. The preparation of violet-colored $(\text{Ph}_4\text{As})_2[\text{V}(\text{mnt})_3]$ have been reported and the $[\text{V}(\text{mnt})_3]^{2-}$ dianion possess a distorted octahedral coordination geometry (183). Reaction of VO^{2+} and VO_3^{2-} with $\text{Na}_2(\text{mnt})$ in hot water produces five-coordinate $\text{VO}(\text{mnt})_2^{2-}$ and a small amount of $[\text{V}(\text{mnt})_3]^{2-}$ (201). Yields of the latter were improved by boiling the mixture for several hours. Reduction with hydrazine produces $[\text{V}(\text{mnt})_3]^{3-}$ which reverts to $[\text{VO}(\text{mnt})_2]^{2-}$ on aerial oxidation. $[\text{V}(\text{S}_2\text{C}_6\text{Cl}_4)_2]^{2-}$ was isolated from the reaction of VCl_3 or $\text{VO}(\text{SO}_4)_2$ with $\text{K}_2\text{S}_2\text{C}_6\text{Cl}_4$ in aqueous solution (201). As with titanium, a number of cyclopentadiene-substituted complexes of vanadium with 1,2-dithiolene ligands have been synthesized. The simplest and most common method employs the use of $[\pi\text{-Cp}_2\text{VCl}_2]$ and an alkali metal salt of the ligand in polar solvents (28, 118). The patent

literature contains the synthesis of neutral metal chelates containing one, two, or three $S_2C_2(CF_3)_2$ groups (107), and a series of π -cyclopentadiene-substituted complexes, $[\pi-CpM(tfd)]$ ($M = V, Cr, Mo, Co, Ni$) have been prepared by refluxing the bistrifluorodithiete with a suitable π -cyclopentadiene metal carbonyl complex in a hydrocarbon solvent. These compounds, and the $[M(tfd)_3]$ complexes, were found to be effective antiknock additives in petrol and oxidizers and were used in criminal investigations for the development of fingerprints. An exploration of the electrochemistry of bridged bimetallic species reveals examples of systems that reduce or oxidize to give stable radical anions or cations, respectively (54). Included in this study is $[\pi-CpV(tfd)]_2$ which has the proposed dimeric structure:



A saturated dichloromethane solution containing $NbOL_3$ ($HL = 8$ -hydroxyquinoline) treated with $S_2C_6H_3Me^{2-}$ produces $O[NbL_2(S_2C_6H_3Me)]_2$ (84).

The electron spin resonance (ESR) spectra of magnetically dilute samples of $[VO(mnt)_2]^{2-}$ and $[V(mnt)_3]^{2-}$ have been analyzed in terms of molecular orbital descriptions of the electronic structures of the complexes (4, 123). The results indicate that in both dianions the metal have more electron density than the formal oxidation state of (IV) would imply. One study proposed a reassignment of the ground state of $[V(mnt)_3]^{2-}$ dianion, the unpaired electron being in the metal's $3d_{xy}$ orbital. Steifel and Kwik, however, proposed that the ESR parameters for $[V(mnt)_3]^{2-}$ could be interpreted in terms of a 2A_1 ground state in D_3 symmetry, the unpaired having substantial d_{z^2} orbital character.

C. CHROMIUM, MOLYBDENUM, AND TUNGSTEN

Complexes of this group of elements with 1,2-dithiolenes have been prepared and studied extensively: Molybdenum, in particular, has

received much attention because of the use of molybdenum-sulfur complexes in modeling biological systems, such as xanthine oxidase and nitrogenase. The early work on these complexes has been covered in detail (139).

The simple, stoichiometric complexes of the elements that are formed under normal conditions are usually the tris species. With the ligands $(mnt)^{2-}$, $(S_2C_6Cl_4)^{2-}$, and $(S_2C_6H_3Me)^{2-}$, the tris complexes of chromium, molybdenum, and tungsten have been prepared as part of the series described in the preceding section (183, 202). From physical measurements $[Cr(mnt)_3]^{3-}$ has octahedral symmetry and $[Cr(mnt)_3]^{2-}$ has distorted octahedral symmetry. Assignment of geometry of the dianionic complexes of molybdenum and tungsten is in doubt, and the possibility of trigonal prismatic coordination cannot be eliminated. In addition, Nyholm and co-workers prepared a series of complexes derived from tetrafluorobenzene-1,2-dithiol (26): $(Bu_4N)[Cr(S_2C_6F_4)_2]$ and $(Et_4N)_2[Mo(S_2C_6F_4)_3]$, for example. The diamagnetism of the formally assigned Mo(IV) complex suggests a trigonal prismatic structure. The four-coordinate geometry of the Cr(III) complex contrasts with the preferred octahedral geometry and is rather unusual. Hoyer and co-workers described the molybdenum and tungsten tris complexes of the ligand *o*-xylene-3,4-dithiol (59, 81) and with $S_2C_2H_2^{2-}$ and mnt^{2-} , during studies of the electronic and X-ray photoelectron spectra of the complexes. The known $Cr(tfd)_3$ complex has been found to be useful in cathode depolarization compositions for electrochemical cells (133). Methylation of $[W(S_2C_2Ph_2)_3]^{2-}$ with CH_3I results in $[W(S_2C_2Ph_2)_2] \cdot (S(Me)S(Me)C_2Ph_2)^{2-}$ being formed as an olive-green solid (178). The complex was characterized by physical measurements and by reaction with *cis*- $Ph_2PCH=CHPh_2(Vpp)$ and sulfur-alkylated $PhSMeC=CMeSPh$. Further methylation proved to be unsuccessful. The chromium, molybdenum, and vanadium complexes could not be isolated, and the $[Re(S_2C_2Ph_2)_3]^-$ complex was only methylated at one sulfur atom, i.e., purple $[Re(S_2C_2Ph_2)_2(S(Me)SC_2Ph_2)]$ was formed. The outcome of this reaction has been discussed in terms of the electronic structure of the trisdithiolene complexes.

Crystal and molecular structures of $(Ph_4As)_2[M(mnt)_3]$ ($M = Mo, W$) reveal that the complexes are isomorphous and almost isostructural (21). They are among the few examples that, by all criteria, find themselves close to midway between octahedral and trigonal prismatic limiting geometries. The structural dimensions reveal a closeness to "dithiolate" character.

A number of oxomolybdenum complexes containing 1,2-dithiolene ligands have been formulated and studied. From the reaction of oxyan-

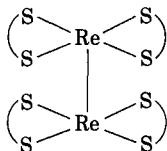
ion salts of molybdenum with $\text{Na}_2(\text{mnt})$, five-coordinate $[\text{MoO}(\text{mnt})_2]^{2-}$ has been isolated (201), and voltammetric studies indicate the presence of a monoanionic species. The six-coordinate nitrosyls $[\text{M}(\text{NO})_2(\text{mnt})_2]^{2-}$ ($\text{M} = \text{Mo}, \text{W}$), which were shown to have *cis*-octahedral structures (35), are prepared by treatment of $[\text{M}(\text{NO})_2\text{Cl}_2]_n$ with Na_2mnt . The chromium analog is obtained by similar treatment of $[\text{Cr}(\text{NO})_2(\text{NCMe})_4]^{2+}$ (33). The related complexes $[\text{M}(\text{NO})_2(\text{S}_2\text{C}_6\text{Cl}_4)_2]^{2-}$ are prepared similarly. All the complexes undergo a one-electron oxidation to the corresponding monoanions.

As with the other early transition metals, the complexes of the chromium triad containing π -cyclopentadiene groups and 1,2-dithiolene ligands have been studied in some detail (109, 128, 141). Thus, Köpf and Kutoglu (117, 122) prepared $\pi\text{-Cp}_2\text{M}(\text{S}_2\text{C}_2\text{H}_2)$ and $[\pi\text{-Cp}_2\text{M}(\text{S}_2\text{C}_6\text{H}_4)]$ ($\text{M} = \text{Mo}, \text{W}$) from Cp_2MCl_2 and $\text{NaS}_2\text{C}_2\text{H}_2$ in ethanol and $\text{C}_6\text{H}_4\text{S}(\text{H})\text{S}(\text{H})$ with Et_3N in benzene. $[\pi\text{-Cp}_2\text{M}(\text{S}_2\text{C}_6\text{H}_4)]$ was found to exist in two conformations statistically distributed in the crystals and differing by the staggered and eclipsed arrangement of the two π -cyclopentadiene rings. In both cases the molecule possesses a mirror plane bisecting the two cyclopentadiene rings as well as the chelate and benzene rings. The geometry about the molybdenum atom is considered to be a distorted tetrahedron. π -Cyclopentadiene rings can be cleaved from the molybdenum atom, and this is used to synthesize $[\text{Mo}(\text{tfd})_3]^{2-}$ and $[\text{Mo}(\text{S}_2\text{C}_6\text{Cl}_4)_3]^-$ with $\text{S}_2\text{C}_2(\text{CF}_3)_2$ and $\text{S}_2\text{C}_6\text{Cl}_4^{2-}$. Analogous reactions with Na_2mnt and $(\text{tdf})^{2-}$ have been reported (90, 206). The reactions proceed in stages and $[\text{CpMo}(\text{S}-\text{S})]_2^-$, $[\text{CpMoI}(\text{NO})(\text{S}-\text{S})]$, and $[\text{CpMo}(\text{NO})(\text{S}-\text{S})_2]$ with $\text{P}(\text{OPh})_3$ afford $[\text{CpMo}(\text{NO})(\text{P}(\text{OPh})_3)(\text{S}-\text{S})]$, with $[\text{CpMo}(\text{S}-\text{S})(\text{NO})_2]$ being produced originally. Voltammetric studies reveal that all species except the dimers could be oxidized in a reversible one-electron step, but only $[\text{Mo}(\text{S}_2\text{C}_6\text{Cl}_4)_3]^-$ was isolated. A number of 1,1- and 1,2-dithio-mixed ligand complexes of molybdenum and tungsten may be prepared by oxidative decarbonylation of $(\text{Bu}_4\text{N})[\text{M}(\text{CO})_2\text{I}]$ in the presence of both ligands (18).

Crystal structure determinations of $[\pi\text{-CpM}(\text{S}_2\text{C}_6\text{H}_4)]$ ($\text{M} = \text{Mo}, \text{W}$) show much the same features, the $\text{S}_2\text{C}_6\text{H}_4$ groups being inclined at 8° in the WS_2 plane and 9° in the MoS_2 plane (53, 122). Knox and Prout determined the structure of $[\pi\text{-Cp}_2\text{Mo}(\text{tdt})]$ and found a similar structure with no evidence that the lone-pair of electrons on sulfur is involved in $\text{Mo}-\text{S}$ π -bonding (114). A detailed investigation of the structural geometry of $(\text{Ph}_4\text{As})_2[\text{CpMo}(\text{mnt})_2]$ revealed that the metal atom is seven-coordinate, being linked by two bidentate dithiolate ligands and a formally tridentate cyclopentadiene ligand (30).

D. MANGANESE, RHENIUM, AND TECHNIUM

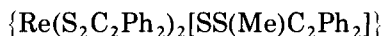
Until 1969 the only reported complexes of 1,2-dithiolene ligands with the manganese triad were $[\text{Mn}(\text{mnt})_2]^{2-}$, $[\text{Re}(\text{mnt})_2]_2^{2-}$ which was derived from $[\text{Re}_2\text{X}_8]^{2-}$ ($\text{X} = \text{Cl}^-$, Br^-) and believed to retain the Re-Re structure:



$[\text{Mn}(\text{mnt})_3]^{2-}$, $[\text{Re}(\text{S}_2\text{C}_6\text{H}_3\text{Y})_3]$ ($\text{Y} = \text{H}$, CH_3), $\text{Re}(\text{S}_2\text{C}_2\text{Ar})_3^-$ ($\text{Ar} = \text{Ph}$, $p\text{-MeC}_6\text{H}_4$), and $[\text{Re}(\text{S}_2\text{C}_2\text{H}_2)_3]$.

In recent years the number of complexes in this group has increased only slightly. Reports cited in previous sections (123, 183, 202) contain details of new complexes of the manganese triad with 1,2-dithiolenes. In addition, McCleverty and co-workers carried out a voltammetric study of the complex previously formulated as $[\text{Re}(\text{mnt})_2]_2^{2-}$ and reasigned it as a $[\text{Re}(\text{mnt})_2]_4^{4-}$ species that undergoes one-electron reduction and two-electron oxidation processes. Oxidation of $[\text{Re}(\text{mnt})_3]^{2-}$ with iodine afforded the new complex $[\text{Re}(\text{mnt})_2]^-$, which may be voltammetrically reduced to the dianion (36). Recently, very few papers concerning carbonyl derivatives of the manganese dithiolenes have appeared. A whole series of $[\text{Mn}(\text{CO})_4(\text{S}-\text{S})]^-$ ($\text{S}-\text{S} = \text{mnt}^2$, $i\text{-mnt}^2$, $\text{S}_2\text{C}_6\text{Cl}_4^{2-}$, tdt^{2-}) were originally prepared by McCleverty and co-workers (34) from reaction of $\text{Mn}(\text{CO})_5\text{Br}$ with the respective ligands. Action of phosphines on $[\text{Mn}(\text{CO})_4(\text{mnt})]^-$ produces $[\text{Mn}(\text{mnt})_3]^{2-}$ and some decomposition. A transient green color was observed when $[\text{Mn}(\text{CO})_4(\text{mnt})]^-$ was allowed to react with NO, but the product, which may have been $[\text{Mn}(\text{NO})(\text{mnt})_2]^{2-}$, was not isolated. With $\text{Na}_2\text{S}_2\text{C}_2\text{H}_2$ in acetone/methanol, $[\text{Mn}(\text{CO})_5\text{Br}]$ gives the deep-red, volatile complex $[\text{Mn}_2(\text{CO})_6(\text{S}_2\text{C}_2\text{H}_2)]$ (110). On addition of Lewis-base ligands in inert solvents, dark red-brown substitution products of the type $[\text{Mn}_2(\text{CO})_4\text{L}_2(\text{S}_2\text{C}_2\text{H}_2)]$ ($\text{L} = \text{PPh}_2$ or $\text{P}(\text{Me}_2\text{N})_3$) and yellow-brown monoadducts $[\text{Mn}_2(\text{CO})_6(\text{S}_2\text{C}_2\text{H}_2)\text{L}]$ [$\text{L} = \text{PR}_3$, $0.5(\text{Ph}_2\text{PCH}_2\text{CH}_2\text{PPh}_2)$, or NH_3] are formed. Hoyer and co-workers (78) have produced the monoanionic species $[\text{Mn}(\text{S}_2\text{C}_2\text{H}_2)\text{py}]^-$, $[\text{Mn}(\text{S}_2\text{C}_2\text{H}_2)]^-$, and $[\text{Mn}(\text{S}_2\text{C}_6\text{H}_2(\text{CH}_3)_2)_2\text{py}]^-$ as part of a general study of the mixed-ligand complexes of manganese, iron, cobalt, palladium, and platinum.

The methylation of $[\text{Re}(\text{S}_2\text{C}_2\text{Ph}_2)_3]$ to form



was described in the preceding section. Some interest has been shown in the π -cyclopentadiene-containing manganese dithiolene complexes. The novel complexes $[\pi\text{-C}_5\text{H}_4\text{RMn}(\text{NO})(\text{S}-\text{S})]^Z$ ($\text{R} = \text{H}$ or Me ; $Z = 0$ or -1 ; $\text{S}-\text{S} = \text{mnt}^{2-}$, tdt^{2-} , $\text{S}_2\text{C}_6\text{Cl}_4^{2-}$) have been prepared and investigated electrochemically (142). They were found to exist as part of a three-membered electron transfer series, $Z = +1, 0, -1$. Treatment of $[\pi\text{-CpMn}(\text{NO})(\text{CO})_2]\text{PF}_6$ the monoanionic species (143). With tdt^{2-} , $\text{S}_2\text{C}_6\text{Cl}_4^{2-}(\text{S}-\text{S})$, the neutral species $[\pi\text{-CpMn}(\text{NO})(\text{S}-\text{S})]$ were formed. Even in the presence of a large excess of the dithiolene ligands, the $\pi\text{-Cp}-\text{Mn}$ bond was not cleaved. Another report provides evidence for the formation of $[\text{Mn}(\text{NO})(\text{S}-\text{S})_2]^{2-}$ ($\text{S}-\text{S} = \text{Tdt}^{2-}$ or $\text{S}_2\text{C}_6\text{Cl}_4^{2-}$) and $[\text{Mn}(\text{NO})(\text{mnt})(\text{S}_2\text{C}_6\text{Cl}_4)]^{2-}$. $[\text{Mn}(\text{NO})(\text{mnt})_2]^{2-}$ is also produced by treating MnCl_2 with Na_2mnt and NO or by reaction of $[\text{Mn}(\text{mnt})_2]^{2-}$ with NO .

A recent application of $\text{Mn Mn}(\text{mnt})_2$ is as a catalyst in the formation of high-molecular-weight poly(phenylene oxides). The complex is usually produced and used *in situ* (96). A study of the spectrophotometric and voltammetric properties of $[\text{ML}_3]$ ($\text{M} = \text{Re}, \text{Mo}, \text{W}, \text{Te}$; $\text{L} = \text{tdt}^{2-}$) with organic basis appears to be the only account of a 1,2-dithiolene complex of technitium (104).

E. IRON, RUTHENIUM, AND OSMIUM

The chemistry of iron-1,2-dithiolene complexes has been studied exhaustively. In the past few years, however, interest has been channeled mainly into physicochemical studies of existing systems; as a result, literature concerning the synthetic chemistry of iron-dithiolene systems has become relatively sparse. The major concentration of synthetic effort has been directed toward the synthesis of carbonyl derivatives, ferredoxin models, and adducts of the existing complexes. Apart from early reports (139) of $[\text{Ru}(\text{S}_2\text{C}_2\text{Ph}_2)_2]$, $[\text{Ru}(\text{mnt})_3]^{3-}$, and $[\text{Os}(\text{S}_2\text{C}_2\text{Ph}_2)_2]$ the chemistry of ruthenium and osmium dithiolene complexes is relatively unknown. The only recent reports are of the reaction of $\text{Ru}_3(\text{CO})_{12}$ with $(\text{CF}_3)_2\text{C}_2\text{S}_2$ at 100°C to give an impure, orange-colored, carbonyl adduct and at higher temperatures to give a green, impure, carbonyl-free material (152). Addition of EPh_3 ($\text{E} = \text{P}, \text{As}, \text{or Sb}$) produces $[\text{Ru}(\text{CO})_n(\text{ER})_{3-n}(\text{tfd})]$ and

$[\text{Ru}(\text{EPH}_3)(\text{tfd})_2]$, respectively, suggesting that the green complex may be of the form $[\text{Ru}(\text{tfd})_2]_2$, which is similar to the iron analog. Two different molecular conformers are known for the orange and violet isomers of the square pyramidal $[(\text{Ph}_3\text{P})_2\text{Ru}(\text{CO})(\text{tfd})]$ and solution studies suggest that the former is thermodynamically favored (15). This isomerism is contrary to the usual behavior of pentacoordinate species (76). Osmium(VI) reacts with excess quinoxaline-2,3-dithiol in acidified DMF/ H_2O solutions to form 1:2 and 1:4 complexes (91).

The pure dithiolene complexes of iron, which were synthesized in the late 1960s consisted of those with $\text{S}_2\text{C}_6\text{Cl}_4^{2-}$ and $\text{S}_2\text{C}_6\text{F}_4^{2-}$. These, together with the mnt^{2-} complex, were prepared, as part of the series of complexes described in earlier sections (123, 183, 202). The novel complexes of several $[\text{M}(\text{mnt})_{2,3}]^{2-,3-}$ anions, $[\text{M} = \text{Fe}(\text{II}), \text{Fe}(\text{III}), \text{Co}(\text{II}), \text{Ni}(\text{II}), \text{Cu}(\text{II}), \text{Ag}(\text{II}), \text{and Sn}(\text{IV})]$ are readily precipitated with a polymeric cation prepared from *N*-methyllutidium iodide and terephthaldehyde (132, 186). The pure dithiolenes of iron and cobalt are normally dimeric, with the metal atom in a five-coordinate environment of sulfur atoms (Fig. 1). Holm and co-workers (10) interpreted the spectral, magnetic, and electrochemical properties of the $[\text{M}(\text{S}-\text{S})_2]_2$ ($\text{M} = \text{Co}, \text{Fe}; \text{S}-\text{S} = \text{tdt}^{2-}, \text{mnt}^{2-}, \text{and tfd}^{2-}$) complexes and systemized them as part of the series $[\text{M}(\text{S}-\text{S})_2]_2^0$, $[\text{M}(\text{S}-\text{S})_2]_2^-$, $[\text{M}(\text{S}-\text{S})_2]_2^{2-}$, and $[\text{M}(\text{S}-\text{S})_2]_2^{4-}$.

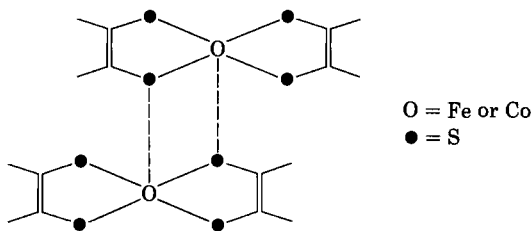
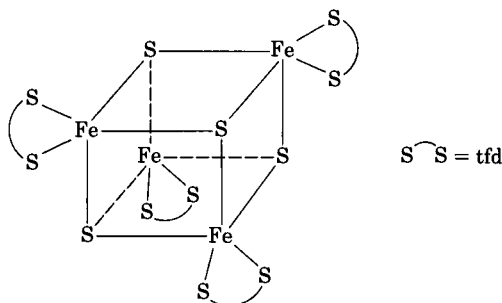


FIG. 1. Pure dithiolene of iron and cobalt.

The mixed dithiolate complexes $[\text{Fe}(\text{R}_2\text{dtc})(\text{mnt})_2]^{2-}$ ($\text{R} = \text{Me or Et}$), $[\text{Fe}(\text{R}_2\text{dtc})_2(\text{mnt})]^-$, and $[\text{Fe}(\text{S}_2\text{C}=\text{X})(\text{mnt})_2]^{3-}$ ($\text{X} = \text{C}(\text{CN})_2\cdot\text{C}(\text{CN})$, CO_2Et , CHNO_2 , $\text{N}(\text{CN})$, or $\text{C}(\text{CN})\text{CONH}_2$) have been prepared as salts of $(\text{Ph}_4\text{P})^+$ and studied polarographically (8). The trianions are oxidized in a one-electron step, the half-wave potentials showing a dependence on the nature of X. $[\text{Fe}(i\text{-mnt})(\text{mnt})_2]^{2-}$ may be further oxidized, and $[\text{Fe}(\text{R}_2\text{dtc})_2(\text{mnt})]$ may be irreversibly reduced to the dianion. Aerial oxidation of $[\text{Fe}(i\text{-mnt})(\text{mnt})_2]^{3-}$ produces the dianion. Mixed-ligand complexes, $[\text{Fe}(\text{S}_2\text{CNR}^1\text{R}^2)_2(\text{mnt})]$ ($\text{R}^1\text{R}^2 = \text{Et}_2$ and Et ,

Ph) result when $[\text{Fe}(\text{S}_2\text{CNR}^1\text{R}^2)_2]$ and Na_2mnt are mixed, followed by oxidation by air or Cu(II) in acetonitrile (162). Both complexes exhibit singlet-triplet equilibria and are stereochemically nonrigid, as shown by variable temperature $^1\text{H-NMR}$ spectroscopy. At lower temperatures there is an inversion process, the most likely mechanism for which is twisting about the pseudo-3-fold axis, and at higher temperatures the process of rotation about the C-N bond is observed.

The dimeric iron dithiolene complexes, $[\text{Fe}_2(\text{CO})_6(\text{S}_2\text{C}_2\text{R}_2)]$, have the ability to form sulfur-rich, tetrameric $[\text{FeS}(\text{S}_2\text{C}_2\text{R}_2)]_4$ complexes by reaction with S_8 in refluxing xylene. These complexes with $\text{R}=\text{CF}_3$ have been shown to undergo four voltammetric, one-electron processes (148), and on dissolution in basic solution the dianion is formed. Reaction of the dianion with the neutral species gives the paramagnetic monoanion $[\text{FeS}(\text{S}_2\text{C}_2(\text{CF}_3)_2)_2]_4^-$ and with PPh_3 affords $[\text{Fe}(\text{PPh}_3)(\text{S}_2\text{C}_2(\text{CF}_3)_2)_2]^-$. The corresponding diphenyldithiolene complex ($\text{R} = \text{Ph}$) is reducible in three one-electron steps, and the monoanion may be obtained from the neutral species by a hydrazine reduction. The trinuclear compound, $[\text{Fe}_3\text{S}_2(\text{tfd})_4]$ is a product of the sulfuration reaction, and it is reduced in two one-electron steps. Similarities have been drawn between these sulfur-rich complexes and ferredoxins, such as in the report of a nonenzymic model for nitrogen fixation (198). Significant amounts of ammonia are produced by treatment of $[\text{Mo}(\text{N}_2)(\text{Ph}_2\text{PCH}_2\text{CH}_2\text{PPh}_2)_2]$ with $[\text{FeS}(\text{S}_2\text{C}_2\text{Ph}_2)]_4^{n-}$ ($n \geq 4$). This is the first example of ammonia produced by direct reduction of a relatively stable nitrogenyl complex in a model system of the ferredoxin structural type. Reaction of $(\text{CF}_3)_2\text{C}_2\text{S}_2$ with $\text{Fe}(\text{CO})_5$ in the presence of H_2S yields a black crystalline complex of empirical formula $\text{Fe}_3(\text{tfd})_4\text{S}_6\text{H}_2$, which when dissolved in hydrocarbon solvents, exhibits many of the properties of reduced iron-sulfur proteins (166). ESR spectra of the compound in frozen solution, in the presence of isopropyl disulfide are similar to reduced adrenodoxin and putidaredoxin and indicate the presence of one unpaired electron per two iron atoms. ENDOR experiments show that the unpaired electron resides almost exclusively on an Fe-S center. In the series $[\text{Fe}_4\text{S}_4(\text{mnt})_4]^{n-}$ ($n = 0, 1, \text{ or } 2$), however, the overall electronic structure is very similar in all three cases, and magnetically perturbed Mössbauer spectra suggest that in the paramagnetic monanion the unpaired electron is highly delocalized over the dithiolene ligands and is not primarily associated with the (Fe_4S_4) core (17). The structure of $[\text{FeS}(\text{S-S})]_4^{2-}$ systems consists of a cubanelike iron sulfide array of Fe_4S_4 clusters (Fig. 2). Mössbauer data for this, and the monoanion and neutral species have been compared with data for various ferredoxins (16).

FIG. 2. Structure of $[\text{FeS}(\text{S}-\text{S})]_4^{2-}$.

The positive value of V_{zz} derived from the Mössbauer spectrum of $(\text{Ph}_4\text{As})_2 [\text{FeS}(\text{tfd})]_4$ is consistent with distorted trigonal bipyramidal coordination where the bonding electrons are probably the primary origin of the electric field gradient as is expected for in-plane bonding.

Considerable attention has been paid to the reactions of dimeric iron and cobalt dithiolenes with Lewis bases. The five- or six-coordinate products are formed by cleavage of the dimeric until followed by subsequent coordination of the Lewis base to the vacant coordination sites. The mechanism for the reaction is thought to proceed via an associative route (S_N2), but a small dissociative contribution cannot be ruled out (188). In acetonitrile, however, $[\text{Fe}(\text{mnt})_2]^-$ is believed to be monomeric (10), and reactions with bidentate ligands, e.g., phen, bipy, en, dmg, have been shown to yield low-spin six-coordinate products (140, 209). McCleverty and co-workers (140, 146, 150) have made a wide variety of iron and cobalt dithiolenes react with Lewis bases and nucleophiles, such as phosphines, arsines, stibines, amines, phosphites, phenylisocyanate, and azide, and have isolated a large number of complexes and identified several unstable species. Hoyer and co-workers (78) isolated a similar series of complexes with $\text{S}_2\text{C}_2\text{H}_2^{2-}$ and $o\text{-(CH}_3)_2\text{C}_6\text{H}_2\text{S}_2^{2-}$ as the dithiolene ligands. Novel complexes containing labile Mn—Fe and Mn—Co bonds are formed when $[\text{Fe}(\text{mnt})_2]^-$ and $[\text{Co}(\text{mnt})_2]^-$ are treated with $[\text{Mn}(\text{CO})_5]^-$ in THF (93) (Fig. 3).

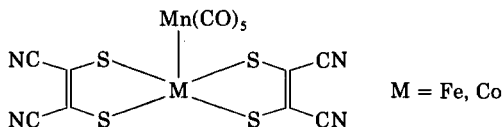


FIG. 3. Complexes containing labile Mn—Fe and Mn—Co bonds.

The adducts $[\text{Fe}(\text{diphos})(\text{S}-\text{S})_2]^Z$, $[\text{Fe}(\text{PEtPh}_2)(\text{S}-\text{S})_2]^Z$ [$Z = -1$; $\text{S}-\text{S} = \text{mnt}^{2-}$, tfd , $(\text{S}_2\text{C}_6\text{Cl}_4)^{2-}$; $Z = 0$, $\text{S}-\text{S} = \text{S}_2\text{C}_2\text{Ph}_2$, $\text{S}_2\text{C}_2(4\text{-MeC}_6\text{H}_4)_2$ or $\text{S}_2\text{C}_2(4\text{-MeOC}_6\text{H}_4)_2$], and $\text{Fe}(\text{diphos})(\text{mnt})_2$ are prepared by oxidation of the diiron with iodine (146). Complexes of Fe, Co, and Ni dithiolenes with chelating diarsine and diphosphines have also been reported (147). Holm and Eaton (55) used the carefully selected $p\text{-Ph}_2\text{PC}_6\text{H}_4\text{PPh}_2$, $\text{trans-Ph}_2\text{P}(\text{H})\text{C}=\text{C}(\text{H})\text{PPh}_2$ (DPPE), and $\text{Ph}_2\text{PCPPH}_2$ ligands to prepare a new series of diphosphine bridged binuclear complexes of iron and cobalt. $[\text{Fe}(\text{S}_2\text{C}_2\text{Ph}_2)_2]$ has been used as a completely artificial, nonenzymic catalyst, modeling ferredoxin activity. By the use of inorganic reductants, amino acids were synthesized via biogenic-type CO_2 fixation. The α -ketoacid products were successfully converted to the corresponding α -amino acids on treatment with pyridoxamine (156, 157).

$[\text{Fe}(\text{mnt})_2]^-$, $[\text{Fe}(\text{mnt})_3]^{2-}$, and $[\text{Fe}(\text{tfd})_2]^{2-}$ are found to activate molecular oxygen and are excellent catalysts for the autoxidation of PPh_3 by atmospheric oxygen (57, 140). Of the first two complexes $[\text{Fe}(\text{mnt})_3]^{2-}$ is found to be the most efficient catalyst (140). The $(\text{Bu}_4\text{N})[(\text{Ph}_3\text{PO})\text{Fe}(\text{tfd})_2]$ complex that was isolated in such a reaction had been previously formulated as a phosphine complex, and has the structure shown in Fig. 4.

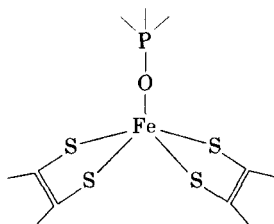
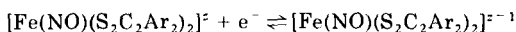


FIG. 4. Structure of $(\text{Bu}_4\text{N})[(\text{Ph}_3\text{PO})\text{Fe}(\text{tfd})_2]$ complex.

Electrochemical studies on a series of bis(diaryl-1,2-dithiolene) complexes indicate that the compounds are part of a four- and possibly five-membered electron transfer series, $[\text{Fe}(\text{NO})(\text{S}_2\text{C}_2\text{Ar}_2)_2]^Z$ ($Z = -2, -1, 0, +1, (+2)$) (149). The $E_{1/2}$ values of the couple depend upon the substituents Ar, but they have very little effect on the nitrosyle stretching frequency.

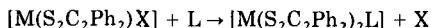


In recent years attention has been paid to the syntheses of novel carbonyl-containing complexes of iron dithiolenes. $[\text{Fe}_2(\text{CO})_6(\text{XR})_2]$

(X = S, R = Me, Ph; X = Se, R = Ph) reacts with $(S_2C_2(CF_3)_2)$ in pentane/benzene to yield a deep-green tetrameric $[Fe(XR)(CO)(tfd)_2]_4$ species in $CHCl_3$ and the dimer in acetone (144). The S-tetramer is shown by X-ray crystallography to be $[Fe_2(\mu-SMe)_3(CO)_6]^+ [Fe(tfd)_4]^-$ (94). Reaction of $Fe_2(CO)_9$ with $S_2C_2(CF_3)_2$ under carefully controlled conditions produce an extremely reactive volatile violet solid, $[Fe(CO)_3(tfd)_2]_2$, while $Fe_3(CO)_9S_2$, $Fe(CO)_5$, and $Fe_3(CO)_{12}$ with $S_2C_2(CF_3)_2$ yield $[Fe_3S_2(tfd)_2]_4$, $[Fe_2S_2(tfd)_2]_4$, $[Fe_2(CO)_6(tfd)_2]$, and $[Fe(tfd)_2]$, respectively. Physical characterization and chemical reactivity of $[Fe(CO)_3(tfd)]$, the initial product of the reaction between $Fe(CO)_5$ and $S_2C_2(CF_3)_2$, have been reported by Miller and Balch (152). Reaction of $Fe_2(CO)_9$ with *cis*-1,2-ethylenedithiolate in methanol solution results in the hydrogenation of the double bond of the ligand giving the saturated derivative $[Fe(CO)_6(S_2C_2H_4)]$ (110).

Reactions of aryldiazonium tetrafluoroborates with $[Fe(CO)_3(PR_3)_2]$, $[Fe(mnt)_2]^-$, $[Fe(cyst)H_2]^{2+}$, and $[Fe(CO)_2(cystH)_2]$ results in ligand abstraction yielding arenediazophosphonium salts and S-(arenediazo)-cysteine or the N_2 extrusion product or $ArS(CN)C \equiv C(CN)SAr$ (27). Nucleophilic sulfur is suggested as a site for the activation and reduction of complexed dinitrogen in biological nitrogen fixation. Evaporation of a filtered dichloromethane solution of $Fe(tfd)_2$ by a stream of CO gives a quantitative yield of square pyramidal $[Fe(tfd)_2(CO)]$ (153). Similarly structured $[(\pi-Cp)Fe(tfd)_2]$ results from the treatment of $[(Cp)-\mu_3-Fe(CO)]_4$ with bistrifluorodithiete.

The rapidity of substitution reactions at a metal atom surrounded by a porphyrin or corrin group seems to be connected with the π -delocalization and a strong in-plane ligand field. The substitution



reactions of five-coordinate neutral dithiolene complexes $[M = Fe \text{ or } Co; X \text{ and } L = PR_3 \text{ or } P(OR)_3]$ are likewise several orders of magnitude faster than normal. The kinetics of a series of reactions of this type are reported by Sweigart and co-workers (188). Although unusual for five-coordinate species, the mechanism followed by this reaction is probably mainly associative even though the existence of nonzero intercepts in the plots of $k_{obs} \nu S$ (nucleophile) in the cobalt series suggest a contribution from a dissociative pathway. Steric effects are apparently important in determining the relative rates of nucleophilic substitution in these compounds. For $[M(tfd)_2X]^Z$ complexes $[M = Fe, Co; X = PR_3, P(OR)_3; Z = 0, 1]$ the mechanism is associative for $Z = 0$ and dissociative for $Z = -1$ (187). The predominance of the associative

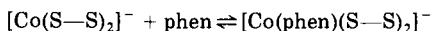
mechanism is noted in the substitution reactions of $[M(mnt)_2X]^-$ complexes [$M = Fe, Co$; $X = PR_3, P(OR)_3$], and a purely dissociative pathway is definitely excluded (190). Replacement of bidentate groups ($X = bipy, phen, diphos, vpp$) by PBu_3 proceeds via a dissociative mechanism. In each case the rates of reaction of the iron complexes are orders of magnitude faster than those of the corresponding cobalt species.

F. COBALT, RHODIUM, AND IRIIDIUM

The dithiolene complexes of cobalt and iron have frequently been studied in association. Much of the synthetic chemistry covered in previous sections (123, 183), like that of iron, has concentrated mainly on the syntheses of Lewis base, nitrosyl, and organometallic adducts. A new series of planar bis- and octahedral tris quinoxaline-2,3-dithiol (QDT) complexes of cobalt have been synthesized, and $Co(QDT)_3^{2-}$ is the first example of a trisdianionic cobalt dithiolene species to be isolated (61, 62). Hoyer and co-workers (79, 80) have presented an account of the synthesis and structural characterization of a series $R^+ M(S_2C_2H_2)_2^-$ ($M = Co, Ni, Pd, Cu$; $R = Et_4N$ or Ph_4As), the physical and chemical properties of which indicate considerable electronic delocalization in the ground state. The same workers have also studied cis- and trans-isomerism exhibited by the $Ni(II)$, $Pd(II)$, and $Pt(II)$ bis- and the $Co(III)$, $Rh(III)$, and $Ir(III)$ trisdithiolene complexes derived from the *S*-alkyl-2-alkyl mercaptoethylene ligands (71).

There have been a number of physicochemical studies, particularly using magnetic methods, on the square-planar benzene- and toluene-dithiolato cobalt(III) systems because of the unique spin-triplet ground states not previously observed in square-planar systems (159, 196). Many of the dithiolenes of cobalt, like those of iron, are dimeric and possess structures analogous to that shown in Fig. 1. In acetone solution the $[Co(mnt)_2]_2^{2-}$ exists in this dimeric form. Kinetic studies of the reaction of this species with PPh_3 , $AsPh_3$, py , and $phen$ have shown that the mechanism involves a rapid equilibrium between the dimer and the monomer, the reaction of Lewis base with the monomer being the rate-determining step (194). With the potentially bidentate $phen$ ligand, the kinetics correspond to a two-stage process in which the formation of a square-pyramidal adduct of $[Co(mnt)_2]^-$ and unidentate $phen$ is followed by concurrent chelate ring formation and the necessary stereochemical reorganization around the metal atom to permit cis-chelation. From a structural study of $[Co(S-S)_2(phen)]^-$ systems

(S—S = tdt, mnt), it is concluded that bonding in the two complexes appeared to be similar and that differences in the equilibrium for the



two complexes are primarily due to differences in the relative stabilities of the original bis-substituted complexes (105, 161). Another kinetic study investigated the reactions of $[\text{Co}(\text{mnt})_2\text{PPh}_3]^-$ with en, bipy, phen, mnt, 2^- -i-mnt, 2^- , and $\text{P}(\text{OPh})_3$ and of $[\text{Co}(\text{mnt})_2(\text{L—L})]^{n-}$ (L—L en, bipy, phen, mnt, 2^-) with Bu_3P and Ph_3P (83, 189), and indicate that associative and dissociative pathways contribute significantly to the overall mechanism as shown in Fig. 5.

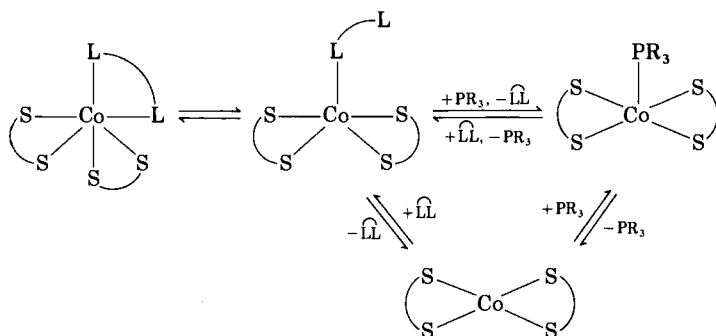
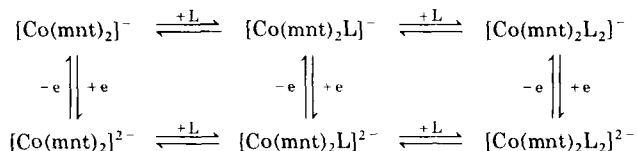


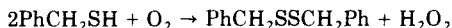
FIG. 5. Overall mechanism in the reactions of $[\text{Co}(\text{mnt})_2\text{PPh}_3]^-$ with en, bipy, phen, mnt, 2^- -i-mnt, 2^- and $\text{P}(\text{OPh})_3$ and of $[\text{Co}(\text{mnt})_2(\text{L—L})]^{n-}$ (L—L en, bipy, phen, mnt, 2^-) with Bu_3P and Ph_3P .

The formation of five- and six-coordinate complexes from Lewis-base addition to cobalt dithiolenes has followed much the same pattern as that outlined for iron (78, 83, 188). In addition, Balch (9) found that in ligand exchange of $[\text{Co}(\text{S—S})\text{L}]$ (S—S = tfd, mnt; L = PPh_3 , AsPh_3) the presence of additional base serves to retard the rate of attainment of equilibrium, but it does not affect the position of the equilibrium. Cobalt dithiolene systems have been the subject of kinetic investigations because of their relative kinetic inertness. An ESR study of the reaction of $[\text{Co}(\text{S}_2\text{C}_2\text{Ph}_2)_2]$ with $\text{P}(\text{OEt})_3$, $\text{PEt}(\text{OEt})_2$, and $\text{PET}_2(\text{OEt})$ in acetone indicates that one molecule of base is introduced into an axial position, and subsequently a second molecule enters trans to the first, followed by rearrangement to the cis structure (193). A similar series of reactions with PCl_3 , $\text{PCl}_2(\text{OR})$, $\text{PCl}(\text{OR})_2$, and $\text{P}(\text{OR})_3$ give only five-coordinate complexes. Dance (43) is responsible for an elabo-

rate voltammetric study of the coordination reactions of pyridine with $[\text{Co}(\text{mnt})_2]^Z$ ($Z = -2, -1$) complexes and proposes the following summary for the system:



Dance and Miller (48, 49) reported various amine adducts of $[\text{M}(\text{mnt})_2]^{2-}$ and $[\text{M}(\text{tfd})_2]_2^{2-}$ ($\text{M} = \text{Fe}, \text{Co}$). Monoadducts, $[\text{M}(\text{mnt})_2L]^-$, are high spin; $S = 3/2$ for Fe, $S = 1$ (possibly 0) for Co. At room temperature only Co forms six-coordinate bis-amine adducts, $[\text{Co}(\text{mnt})_2L_2]^-$, which are diamagnetic and exist as two stereoisomers, one of which is cis-octahedral; the one insoluble pyridine adduct is $[\text{Co}(\text{mnt})_2(\text{py})_2]^-$. $[\text{Fe}(\text{tfd})_2]_2^-$ with ethylenediamine and other bidentate amines produces amine-bridged binuclear species. $[\text{Co}(\text{mnt})_2(\text{amine})]^-$ readily forms $[\text{Co}(\text{mnt})_2(\text{amine})_2]^-$ provided there is minimal steric hindrance of the amine, while $\text{Fe}(\text{mnt})_2(\text{amine})^-$ shows no evidence of further coordination with any monodentate amine. Dance and co-workers have also made a detailed investigation of the catalysis by $[\text{Co}(\text{mnt})_2]_2^{2-}$ of the thiol autoxidation reaction



in acidic acetonitrile solution buffered with $\text{PhMe}_2\text{N}/\text{PhMe}_2\text{NH}^+\text{ClO}_4^-$ (45, 46). Results indicate that $[\text{Co}(\text{mnt})_2]_2^{2-}$ remains dimeric in the buffered system and does not coordinate to oxygen alone, but does coordinate to base-activated thiol, which then promotes oxygen coordination. The function of the dithiolene complex catalyst is to activate both reductant and oxidant by coordination and transmit one electron from the former to the latter.

The π -cyclopentadiene derivatives of cobalt and rhodium dithiolenes have been prepared by the methods described in previous sections. The crystal structure of $\pi\text{-CpCo}(\text{mnt})$ shows that the cobalt atom is penta-coordinate with a formally tridentate $\pi\text{-Cp}$ group and a bidentate mnt^{2-} group (193). Reaction of the $\text{Co}_3(\text{CO})_9\text{CY}$ ($\text{Y} = \text{Cl}$ or Me) cluster compound with $\text{S}_2\text{C}_2(\text{CF}_3)_2$ gives the novel cluster $[\text{Co}_3(\text{CO})_3(\text{tfd})_3\text{CY}]$ (144). Trinuclear $[\text{Co}(\text{CO})(\text{tfd})]_3$ is obtained by reaction of $\text{Co}_2(\text{CO})_8$ with $\text{S}_2\text{C}_2(\text{CF}_3)_2$ and undergoes one-electron reduction to the monoanion and oxidation to the monocation. This compound could exist as

some complex cationic/dianionic form similar to $[\text{Fe}_2(\mu\text{-SMe})(\text{CO})_6]^+$ $[\text{Fe}_2(\text{tfd})_4]^-$ described earlier.

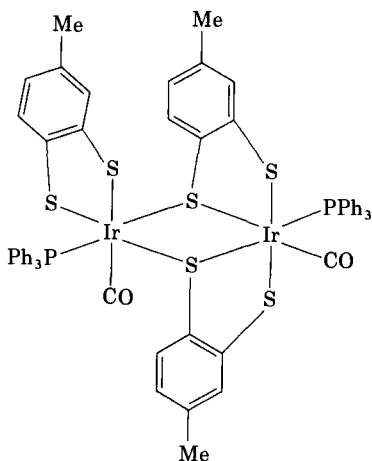
The synthetic chemistry of the pure and organometallic dithiolene complexes of rhodium and iridium has developed significantly in recent years. Both $[\text{Rh}(\text{mnt})_2]_n^{n-}$ ($n \geq 1$) and $\text{Rh}(\text{mnt})_3^{2-}$ have been isolated from the reaction of $\text{Rh}_2(\text{OAc})_4$ and $\text{Na}_2(\text{mnt})$ (37). *cis*-Dicarbonyls $[\text{Rh}(\text{CO})_2(\text{S-S})_2]^{2-}$ ($\text{S-S} = \text{mnt}^{2-}$, tdt^{2-} , *i*- mnt^{2-}) are prepared by treatment of $[\text{Rh}_2(\text{CO})_2\text{Cl}_2]_2$ with the appropriate dithiolate dianion and there is evidence for the existence of $[\text{Rh}(\text{CO})_2(\text{S}_2\text{C}_6\text{Cl}_4)]^-$. $[\text{Rh}(\text{CO})_2(\text{mnt}_2)]$ reacts with phosphines, phosphites, and $\text{S}_2\text{C}_2(\text{CF}_3)_2$ to form $[\text{Rh}(\text{CO})-(\text{PR}_3)(\text{mnt})]^-$, $[\text{RhP}(\text{OPh})_3\text{mnt}]^-$ and $[\text{Rh}(\text{mnt})(\text{tfd})]_n^{n-}$ ($n \geq 1$), respectively. Treatment of $[\text{M}(\text{CO})(\text{PPh}_3)_2\text{Cl}]$ ($\text{M} = \text{Rh}$ or Ir) with $\text{S}_2\text{C}_2(\text{CF}_3)_2$ affords $[\text{M}_2(\text{PPh}_3)_2(\text{tfd})_3]$.

The addition of alkyl halides to the Rh(I) complex $[\text{Rh}(\text{CO})(\text{PPh}_3)(\text{mnt})_2]$ produces Rh(III) acyl species:



and for $\text{RX} = \text{EtI}$ the structure of the product is square pyramidal (29). Heating solutions of the acyl species in THF or dichloromethane results in migration of the R group from acyl carbon to one of the sulfur donors of the mnt ligand to give S-alkylated rhodium(I) complexes.

Addition of toluene-3,4-dithiol (H_2L) to $[\text{IrHCl}(\text{HL})(\text{CO})]$, in which the ligand is bonded unidentately, and a novel dithiolene complex, $[\text{Ir}_2\text{L}_3(\text{CO})_2(\text{PPh}_3)_2]$ (181). X-Ray analysis (106) shows the last complex to have the novel structure:



Stiddard and Townsend (185) observed that reaction of tetrafluorobenzene-1,2-dithiol with *trans*-[IrX(CO)(PPh₃)₂] (X = Cl, Br) in benzene gives pale yellow [Ir(H)(X)(SC₆F₄SH)(CO)(PPh₃)₂] adducts. Refluxing the mixture, however, produces a deep red solution from which [IrH(S₂C₆F₄)(CO)PPh₃]₂ is eventually isolated. It is suggested for the [Ir(H)(X)C₆F₄CS(SH)(CO)(PPh₃)₂] complex that hydrogen bonding (Fig. 6) is involved and that elimination of HX under more vigorous conditions produces the dithiolene complexes.

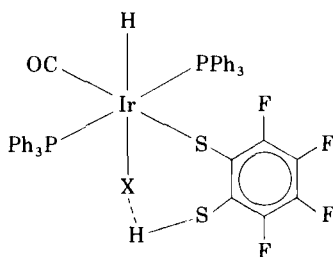


FIG. 6. Hydrogen bonding producing the dithiolene complex.

Recently, Eisenberg and Van Derveer produced a series of novel Rh(I) organometallic dithiolenes (197). Thus, reaction of [Rh(diene)(μ -Cl)]₂ (diene = cyclooctadiene or norbornadiene) with Na₂mnt in ethanolic hydrazine produces [Rh(diene)(mnt)]⁻, isolated as the Bu₄N⁺ salt. Reaction of this complex with CH₃I or PhCH₂X (X = Br or I) in ethanol produces [RH(diene)(mnt)R] (R = CH₃ or PhCH₂), and dynamic behavior is observed in the temperature-dependent ¹H-NMR spectra of the complexes. X-Ray structural analysis reveals that the complexes are methylated at the sulfur atoms and have pyramidal geometry and the ¹H-NMR spectral behavior is probably best explained by inversion about the pyramidal center.

G. NICKEL, PALLADIUM, AND PLATINUM

As with dithiolene complexes of other groups, the synthetic chemistry of the pure complexes of nickel, palladium, and platinum has been restricted in recent years, but some nickel complexes are shown in Table I. The square-planar species (Bu₄N)₂ [M(QDT)₂] (R = Ni, Pd, Pt, Cu, Zn) have been isolated by using the analytical reagent quinoxaline-2,3-dithiol (QDT) (Fig. 7) as a ligand (191). The physicochemical properties of the compounds closely resemble the related mnt complexes, and ESR spectral studies indicate that the ligand is S,S-bonded.

TABLE I
 RECENT DITHIOLENE COMPLEXES OF NICKEL

Complex ^a	Melting point (°C)	Color	References
(Bu ₄ N) ₂ [Ni(QDT) ₂]	204–5	Purple	(191)
(Et ₄ N)[Ni(S ₂ C ₂ H ₂) ₂]	176	Brown	(79)
(Ph ₄ As)[Ni(S ₂ C ₂ H ₂) ₂]	—	—	(79)
(Bu ₄ N)[Ni(S ₂ C ₆ F ₄) ₂]	144	Black	(123)
(M(PPh ₃) ₂) ₂ [Ni(mnt) ₂] (M = Cu, Ag)	—	—	(40)
(Ag(PPh ₂ Et) ₂) ₂ [Ni(mnt) ₂]	—	—	(40)
[Ni(mnt) ₂] ³⁻	—	Green	(155)
[Ni(tfd) ₃] ³⁻	—	—	(67)
(KOS) ₂ [Ni(mnt) ₂]	197.5–8.5	Black	(51)
(KOS) ₂ [Ni(tfd) ₂]	—	Brown	(51)
(KOS)[Ni(S ₂ C ₂ Ph ₂) ₂]	208.5–10.0	Red	(51)
(Ferrocenium)[Ni(tfd) ₂]	—	—	(130)
Cs[Ni(tfd) ₂]	150	—	(130)
(Perylene) ₂ [Ni(mnt) ₂]	—	Black	(204)
(Perylene)[Ni(tfd) ₂]	—	Black	(204)
(Pyrene)[Ni(tfd) ₂]	—	Black	(204)
(TTF)[Ni(tfd) ₂]	—	Black	(75, 103)
(TTF) ₂ [Ni(S ₂ C ₂ H ₂) ₂]	—	Black	(88)
(TTF)[Ni(mnt) ₂]	—	Black	(208)
(Phenoxazine)[Ni(tfd) ₂]	—	Brown	(64)
(Phenothiazine)[Ni(tfd) ₂]	—	Brown	(64)
(TCNQ)[Ni(tfd) ₂]	—	—	(22)
(Q)[Ni(tfd) ₂]	—	—	(22)
(C ₇ H ₇)[Ni(tfd) ₂]	189.5–191	Green-black	(205)

^a KOS = 1-ethyl-4-carbomethoxypyridinium cation; TTF = tetrathiafulvalene, i.e., 2,2'-bi-1,3-dithiolylium cation; TCNQ = 7,7,8,8-tetracyanoquinodimethane; Q = 2,3-Dichloro-5,6-dicyano-p-benzoquinone.

(Bu₄N)₂[Ni(QDT)₂], however, is more stable to oxidation than the corresponding (Bu₄N)₂[Cu(QDT)₂], which is the reverse trend to that observed in mnt²⁻ complexes. The monoanionic bistetrafluorobenzene-1,2-dithiolatonickelate complex has been isolated as the Bu₄N⁺ salt (123), and the dianionic tris complex of platinum with the same ligand was also prepared; slight antiferromagnetic behavior has been

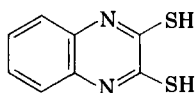


FIG. 7. The analytical reagent quinoxaline-2,3-dithiol (QDT).

noted for the nickel complex. Hoyer and co-workers (71, 79) have been responsible for the synthesis of the nickel, palladium, and platinum complexes of the parent ligand, ethylene-1,2-dithiol and its S-substituted derivatives. More recently, Coucouvanis and co-workers isolated the mixed metal complex $[M(PR_3)_2]_2[Ni(mnt)_2]$ ($M = Ag, Cu$; $R_3 = Ph_2Et, ph_3$) and have determined their structure (41). Wing and Herrmann (74) studied the reaction of $[Ni(tfd)_2]$ with several 1,1-dithiolates and found that centrosymmetric mixed-ligand dimers of the type shown in Fig. 8 are produced. The reactions appear to proceed via either a

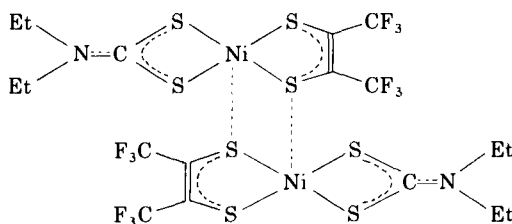


FIG. 8. Centrosymmetric mixed-ligand dimer.

preliminary redox process or formation of a highly polarized donor-acceptor complex. Dimers are also found to be formed in the mixed-ligand complexes of Cu, Zn, Co, Pd, and Pt with dithiocarbonates. Xanthates are also found to react in the same way as, but more slowly than, the dithiocarbonates.

The existence of more highly reduced species at large negative potentials in the electron-transfer series of metal-dithiolene systems has been largely overlooked. Recent reports by Geiger and co-workers, however, describe the generation of the green $[Ni(mnt)_2]^{3-}$ from the dianion by controlled-potential electrolysis at a mercury pool (63, 66, 67, 155). The green dimethoxymethane and acetonitrile solutions of the trianion are extremely air sensitive and revert to the organic dianion upon exposure to traces of oxygen. The solid complex has not been isolated, but the trianion is characterized electrochemically and by its ESR spectrum, which exhibits a single resonance with $g = 2.116$. The data favor a d^9 , or Ni(I) formulation for the metal in $[Ni(mnt)_2]^{3-}$. Similar results are reported for the $[Ni(tfd)_2]^{3-}$ complex, which has been generated electrochemically.

The kinetics of substitution reactions of nickel bisdithiolato complexes with dithiolate nucleophiles have been studied in aqueous solution at 25°C using stopped-flow techniques (160). Several five-coordinate intermediates are detected, and their stabilities have been

estimated. In order to substantiate model calculations that suggest considerable delocalization of negative charge onto the four sulfur atoms of the $[\text{Ni}(\text{S}_2\text{C}_2\text{R}_2)_2]^{2-}$ dianions, Schrauzer and Rabinowitz (177) have shown that the sulfur atoms in $[\text{M}(\text{S}_2\text{C}_2\text{R}_2)_2]^{2-}$ ($\text{M} = \text{Ni}$, Pd , or Pt) possess nucleophilic character. On reaction with alkylating agents new, neutral, diamagnetic 1,4-S,S-diakylated complexes of composition $[\text{M}[(\text{SR})\text{SC}_2\text{R}_2]_2]$ are obtained. The complexes show no tendency to undergo reversible oxidation or reduction and are remarkably resistant to attack by acids and bases.

During the course of investigating the physical properties of complexes containing the $(\text{S}_2\text{C}_2\text{H}_2)^{2-}$ ligand, a sharp contrast is observed between $[\text{Ni}(\text{S}_2\text{C}_2\text{H}_2)_2]$ and $[\text{M}(\text{S}_2\text{C}_2\text{R}_2)_2]$ ($\text{M} = \text{Pd}$ or Pt) both in the electrical conductivity in the solid state and in the nature of the powder X-ray diffraction patterns. Single-crystal X-ray structural determinations show the palladium and platinum complexes to be isostructural. The molecular units in each case are an approximately square-planar arrangement of sulfur atoms about the metal, with two $\text{MS}_4\text{C}_4\text{H}_4$ units in eclipsed relationship joined by a Pd-Pd (279 pm) and Pt-Pt (274.8 pm) bonds, respectively, in a dimeric structure (Fig. 9) (19). They represent the first proved examples of metal-metal bonded bisdithiolenes.

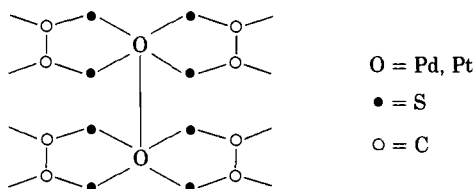


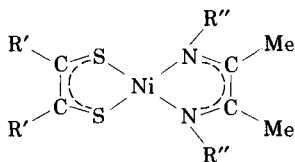
FIG. 9. Dimeric structure which represents the metal-metal bonded bisdithiolenes.

The X-ray photoelectron spectra of $(\text{Et}_4\text{N})[\text{M}(\text{mnt})_2]$, $(\text{Et}_4\text{N})_2[\text{M}(\text{mnt})_2]$, $[\text{M}(\text{S}_2\text{C}_2\text{Ph}_2)_2]$, $(\text{Et}_4\text{N})[\text{M}(\text{S}_2\text{C}_2\text{Ph}_2)_2]$, and $(\text{N}_2\text{H}_5)_2[\text{M}(\text{S}_2\text{C}_2\text{Ph}_2)_2]$ ($\text{M} = \text{Ni}$, Pd , or Pt) have been used to determine the binding energies of sulfur ($2p_{3/2,1/2}$), nickel ($2p_{3/2}$), palladium ($3d_{5/2}$) and platinum ($4f_{7/2}$) (136-138), and Hoyer and co-workers (125) have carried out a similar study on $[\text{Ni}(\text{S}_2\text{C}_2\text{H}_2)_2]^{0,-1}$ their S-alkylated derivatives, and their copper analogs. The results are discussed in a later section.

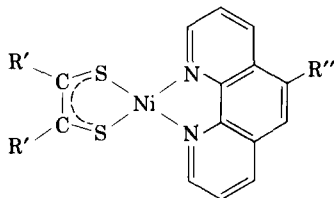
The semiconductor properties and piezoresistance of crystals of $[\text{M}(\text{S}_2\text{C}_2\text{R}_2)_2]$ complexes have been studied (11, 167). The resistivities lie between 10^3 and 10^5 cm at 25°C and depend upon the chelate

structure, the metal ion, and the ligand substituents. With the same R substituents a linear correlation was found to exist between the first half-wave polarographic potential and the resistivity. This suggested that electron transport takes place in the lowest unoccupied π -molecular orbitals of the complexes, in accord with the proposed electronic structure of the complexes. Hall-effect measurements identified the majority of charge carriers as being negative species. The corresponding rhenium complex ($R = \text{Ph}$) was found to be the best conductor of all, indicating that the unpaired electron must be in a molecular orbital delocalized over the whole molecular complex. Among the trigonal prismatic complexes studied, V, Cr, Mo, and W had resistivities between 10^{12} and 10^{14} cm.

McCleverty and Orchard synthesized a series of nickel dithiolene adducts, containing chelating diarsine, diphosphine, and related ligands (147). Miller and Dance (47-49) have studied the reactions of several iron, cobalt, and nickel dithiolenes with a wide variety of amines and diimmines. The following series of complexes have been prepared (47).

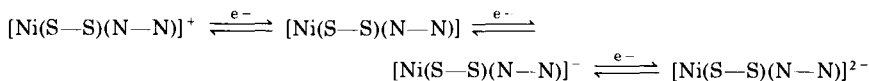


$R' = \text{CF}_3$; $R'' = \text{Ph}, p\text{-MeOC}_6\text{H}_4, m\text{-ClC}_6\text{H}_4$
 $R' = \text{CN}$; $R'' = \text{Ph}, p\text{-MeOC}_6\text{H}_4, \text{N} = \text{CHPh}$

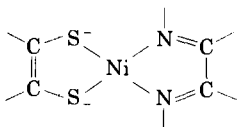


$R' = \text{CF}_3$; $R'' = \text{H}, \text{NO}_2$
 $R' = \text{Ph}$; $R'' = \text{H}$

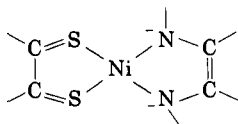
They are all intensely colored, diamagnetic, high-melting-point solids. Electrochemical studies reveal the following electron transfer series:



Electronic spectra show bands characteristic of the parent ligand complexes. The electronic ground state may be represented as



being the principal resonance form, and the excited state contains more of the form



Dance and Miller (50) have also allowed nickel, copper, and cobalt dithiolenes to react with weak nucleophiles and discovered the reaction to proceed by initial nucleophilic substitution of a dithiolene ligand followed by reduction of the oxidized complex leading to overall disproportionation stoichiometry.

Organometallic adducts of the nickel group dithiolenes have been thoroughly investigated. The cyclopentadiene complexes have been prepared and studied as for other metals (206). Wing and co-workers (7, 206) have been concerned with the oxidative addition of olefins, dienes, and cyclo-dienes to $[\text{Ni}(\text{tfd})_2]$. Structural studies of the adduct with norbornadiene suggests that the olefin suffers a two-electron oxidation, that two C—S bonds are formed between the reactants and that one of the norbornadiene double bonds had been transformed into a single bond. The sulfur atoms are in the exo-configuration (Fig. 10). A mechanism for the reaction was proposed after consideration of the Woodward–Hoffman rules (7). Schrauzer has also considered the addition of norbornadiene to $[\text{Ni}(\text{S}_2\text{C}_2\text{Ph}_2)_2]$ (174). Reactions of other olefins with other nickel triad dithiolenes have been reported. An X-ray study of the cycloaddition products of $[\text{Ni}(\text{S}_2\text{C}_2\text{H}_2)_2]$ with various dienes confirmed that the products formed by olefins and dienes are closed structural relatives and show a tetradentate ligand coordinated to square-planar nickel (3). Reactions of nickel and palladium olefin complexes with dithiolene ligands in the absence of oxygen has produced the metal dithiolene–olefin adducts (200). The crystal structure of the 1:1 adduct formed between $[\text{Pd}(\text{S}_2\text{C}_2\text{Ph}_2)_2]$ and cyclohexa-1,3-diene shows that a 1,8-cycloaddition

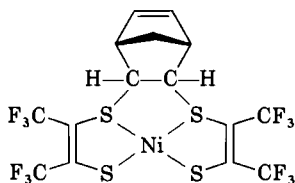
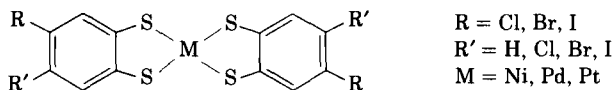


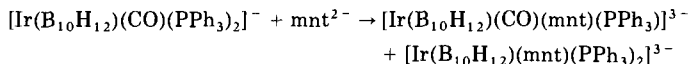
FIG. 10. Sulfur atoms in the exo-configuration.

reaction occurs between the donor and the acceptor, resulting in the two new C—S bonds (31).

Novel applications of the nickel group dithiolenes have been cited in the recent patent literature. The image dyes of color-photography recording materials and textile dyes can be stabilized to the effects of ultraviolet and visible radiation by use of $\{\text{Ni}[\text{S}_2\text{C}_2(\text{C}_6\text{H}_4\text{OMe})_2]_2\}$ as an additive (182). Coating materials containing the structure



have been used as selective absorbers of near-IR radiation (192). $[\text{Ni}(\text{S}_2\text{C}_2(\text{C}_6\text{H}_4\text{NMe}_2)_2)_2]$ is several times more stable than a standard iodopentacarbocyanine dye used for Q-switching and mode locking neodymium-glass lasers (165, 199). Novel complexes of the decaborane (172) ligand containing dithiolenes have been synthesized (180) by displacement reactions, e.g., $[\text{Pd}(\text{B}_{10}\text{H}_{12})(\text{mnt})]^{2-}$ from $[\text{Pd}(\text{B}_{10}\text{H}_{12})(\text{PPh}_3)_2]$ and



Complexes between electron acceptors and electron donors have been studied extensively. Electrically conducting donor-acceptor complexes between nickel dithiolenes and various organic cations, such as perylene, pyrene (204), tropylium ion (86), tetrathiofulvalene (24, 25, 85, 86, 88, 103, 207, 208), quinones (22), pyridinium cations (51), ferrocenium (130), phenoxazine (64), tetrathiotetracene (65), and others (20, 179) have been prepared and studied in considerable detail.

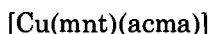
H. COPPER, SILVER, AND GOLD

The complexes of copper with 1,2-dithiolenes were studied extensively during the early intensive development of the chemistry of 1,2-dithiolenes. Since 1969, however, the literature on the synthesis of new copper-containing dithiolenes has become less abundant, probably because the complexes show little tendency to form Lewis-base or organometallic adducts. Complexes of copper have usually appeared only in general papers in which a series of first-row transition metal complexes have been prepared. Thus, $[\text{Cu}(\text{S}_2\text{C}_6\text{F}_4)_2]^{2-}$ (123), $[\text{Cu}(\text{S}_2\text{C}_2\text{H}_2)_2]^{2-}$ (79), $[\text{Cu}(\text{QDT})_2]^{2-}$, and $[\text{Cu}(\text{QDT})_2]^-$ (191) have

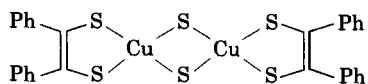
been prepared by methods outlined previously. The ESR spectrum of $(\text{Bu}_4\text{N})[\text{Cu}(\text{QDT})_2]$ indicates that the ligand is S,S-bonded.

The syntheses of mixed 1,1- and 1,2-dithiolates of copper have attracted some attention in recent years. An electron-transfer series of the complexes $[\text{M}(\text{mnt})(\text{S}_2\text{CNBu}^n)_2]^{2-}$ ($\text{M} = \text{Ni}, \text{Cu}, \text{or Au}$) has been investigated (195). The monoanionic ($Z = 1$) species have been obtained for nickel and copper, and the neutral species ($Z = 0$) for copper and gold. Voltammetric data show that these complexes exist as part of a two-membered, reversible, one-electron transfer series, $Z = 0$ or -1 . The $E_{1/2}$ values are intermediate between those for complexes with unmixed ligands. Hermann and Wing (74) produced similar mixed-ligand complexes of copper by ligand exchange reactions of $[\text{Cu}(\text{tfd})_2]$ and $[\text{Cu}(\text{S}_2\text{CX})_2]$ ($\text{X} = \text{NR}_2$ or OR) and with diethyldithiocarbamate as a ligand dimers are formed similar to the analogous nickel complex (Fig. 8). Reiche (164) has studied reactions of numerous ligands with the copper(I) species, $[\text{Cu}(\text{PPh}_3)_3\text{Cl}]$, and when the reaction is carried out using tdt^{2-} the stable $[\text{Cu}(\text{tdt})_2]^{2-}$ complexes are isolated, not the expected $[\text{Cu}(\text{tdt})(\text{PPh}_3)_2]^-$. Recent work on sulfur-containing copper complexes has been concerned mainly with physicochemical studies, particularly the ESR spectra and magnetic properties of copper(II), formally a d^9 system.

Maleonitriledithiolato-4-diacetyldi-(4-methoxyanil) copper



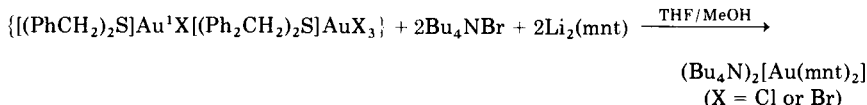
has been studied by ESR spectral methods in liquid and frozen solutions in order to explain the bonding situation in sulfur and nitrogen mixed chelates (122). Covalency parameters indicate that the unpaired electron is delocalized in the direction of the sulfur-containing ligands. Japanese workers (135) have prepared a sulfur-bridged copper dithiolene:



and characterized it by several physical methods. Like its manganese analog, $\text{Cu}[\text{Cu}(\text{tdt})_2]$ and other copper dithiolenes have been used as a catalyst for the oxidative polymerization of penols (97, 98, 100–102).

The chemistry of silver 1,2-dithiolenes is virtually nonexistent apart from one general report (72) of the production of $[\text{AgL}_2(\text{ClO}_4)]$ [$n = 1, 2$; $\text{L} =$ various thioethers and $\text{C}_2\text{H}_2(\text{SH})_2$, H_2mnt , H_2tdt , $\text{C}_6\text{H}_4(\text{SH})_2$,

and *o*-MeC₆H₃(SH)₂]. There is undoubted scope for expansion in this field. The 1,2-dithiolene complexes of gold, like those of copper, were synthesized in the 1960s. A new, higher-yield route has been developed to the formally gold(II) complex, [Au(mnt)₂]²⁻, which involves electron exchange between Au(I) and Au(III) (158). The reaction seems to be specific for mnt²⁻, since there is no evidence for a similar reaction with other unsaturated sulfur-donor ligands:



Bergendahl and Waters (14) have prepared and characterized the pseudo Au(II) complexes [(Ph₃E)Au(mnt)] (E = P, As) and describe their relationship with the authentic Au(mnt)₂²⁻ system. The complexes were reassigned as [(Ph₃E)₂Au]⁺[Au(mnt)₂]⁻, a mixed Au(I)-Au(III) complex. The green mixed-ligand complexes {Au(mnt)[S₂CN(Buⁿ)₂]} and {Au(tdt)[S₂CN(Buⁿ)₂]} have been prepared as described earlier (195), and the crystal structure of the former confirms the formulation as presented (14), the gold atom having approximately square-planar coordination.

Like the analogous copper complexes, the formally gold(II) 1,2-dithiolenes have been the subject of ESR spectral studies (170). This is of particular interest owing to the rarity of formal Au(II) complexes. Results indicate that the complex [Au(mnt)₂]²⁻ is best described as a gold(III) species with a radical anion ligand. The inability of most ligands to possess this form may explain the rarity of gold(II) complexes.

Complexes similar to those described in the nickel section have been formed from [M(tfd)₂] and [M(S₂C₂Ph₂)₂] (M = Cu, Au) and tetrathiofulvalene and magnetic and ESR studies provide the first unambiguous evidence for a spin-Pierels transition, a spin-lattice dimerization phenomenon, occurring below a transition temperature (87, 89).

IV. Physical Studies

A variety of physical techniques have been used to structurally and electronically characterize transition metal 1,1- and 1,2-dithio compounds. Much information has been documented in these numerous studies, and some examples of the kind of information that can be obtained are mentioned in the following sections.

A. X-RAY STRUCTURAL STUDIES

The structural systematics of the 1,1- and 1,2-dithiolato complexes of the transition metals has been the subject of an excellent review by Eisenberg (56). The wide variety of structural types exhibited by these compounds is quite remarkable, and as a result the interest in structural aspects of these species has maintained at a very intense level. The number of studies, varying in degrees of refinement, which have appeared in the literature since 1969 is appreciably large. In many cases these have been systematic confirmations of structures postulated from other physical techniques, but in some cases they have revealed new and totally unexpected stereochemistries. A number of structure determinations by X-ray methods have been discussed or mentioned in previous sections.

Four basic structural types are known for the "pure" dithiolenes (Fig. 11).

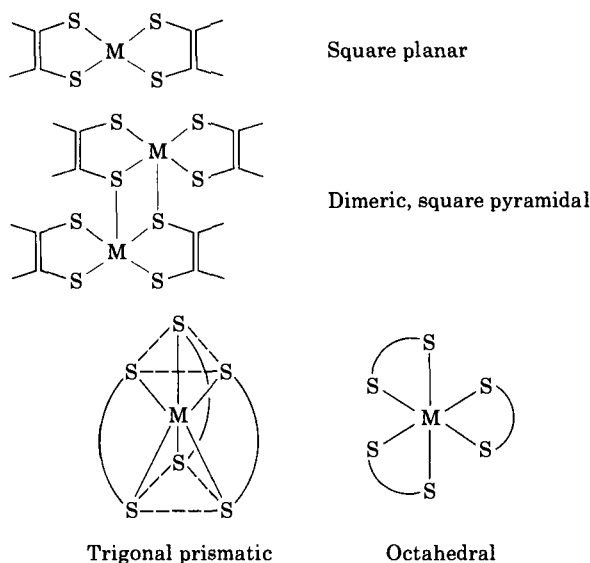


FIG. 11. "Pure" dithiolenes.

The neutral trisdithiolenes $M(S_2C_2R_2)_2$ ($M = V, Cr, Mo, W, Re$) are trigonal prismatic with delocalized electronic structures and the S—C bond distances indicate considerable multiple bond character. These complexes have the metal in its most oxidized form and the structure is ligand-preferred whereas the octahedral structure is metal preferred.

The intermediate oxidation states exhibit a recently discovered "in-between" geometry, e.g., $(\text{Ph}_4\text{As})_2[\text{M}(\text{mnt})_3]$ (21) ($\text{M} = \text{Mo}, \text{W}$). It is also significant that, amidst this great structural variety in the 1,2-dithiolene complexes, the bite of the ligand varies from only 303 to 315 pm. A study on the structures of an isoelectronic series of tris(benzenedithiolene) complexes of the early transition metals $[\text{Zr}(\text{S}_2\text{C}_6\text{H}_4)_3]^{2-}$, $[\text{Nb}(\text{S}_2\text{C}_6\text{H}_4)_3]^-$, and $[\text{Mo}(\text{S}_2\text{C}_6\text{H}_4)_3]$ revealed trigonal prismatic geometry for the Zr complex (134). The observed structural trends (Fig. 12) appear to be associated with the charge on the complex and the metal d -orbital energies.

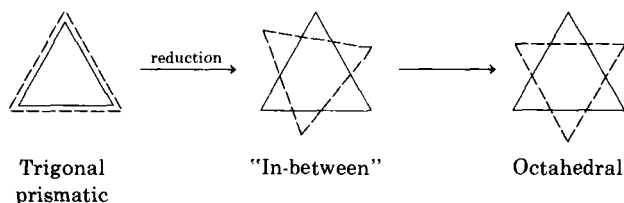


FIG. 12. Trigonal prismatic geometry.

Finally, the first examples of dimeric metal-metal bonded 1,2-dithiolenes were discovered by Browall and co-workers (19) in the complexes $[\text{M}(\text{S}_2\text{C}_2\text{H}_2)_2]_2$ ($\text{M} = \text{Pd}, \text{Pt}$). The arrangement of sulfur atoms about the metal is approximately square planar with two $\text{M}(\text{S}_2\text{C}_2\text{H}_2)_2$ eclipsed units joined by Pd-Pd (279 pm) or Pt-Pt (274.8 pm) bonds. The dimers have distorted cubic arrangement of sulfur atoms with the metal atoms pulled in toward each other from the centers of two opposite faces (Fig. 9). This is believed to be the first crystal structure determination of any bis-1,2-dithiolene complex of palladium or platinum.

B. INFRARED SPECTRAL STUDIES

Three absorption bands are usually characterized in the infrared spectra of the bis-1,2-dithiolenes; $\nu(\text{C}\equiv\text{C})$ at ca. 1400 cm^{-1} and $\nu(\text{C}\equiv\text{C})$ at ca. 1110 cm^{-1} and ca. 860 cm^{-1} . The frequencies vary little with the metal but do depend upon the nature of the substituents. On reduction of neutral species to the monoanion $\nu(\text{C}\equiv\text{C})$ increases and $\nu(\text{C}\equiv\text{S})$ decrease. In the dianions the dithiene, $\nu(\text{C}\equiv\text{S})$, bands usually disappear that can be considered to be a result of conversion of the ligand to the dithiolato dianions. The neutral dimeric cobalt and iron dithiolenes show lower-intensity bands, and the two $\nu(\text{C}\equiv\text{S})$ bands

are split. In the neutral tris complexes $\nu(\text{C}\cdots\text{C})$ occurs at higher frequencies than in the bis complexes, and $\nu(\text{C}\cdots\text{S})$ has a more complicated structure. As the dithioketonic nature of the ligands is decreased $\nu(\text{C}\cdots\text{C})$ increases and $\nu(\text{C}\cdots\text{S})$ decreases. Fresco and Siemann discussed anomalies in the assignment of IR active vibrations, from normal coordinate analysis, of $[\text{M}(\text{S}_2\text{C}_2\text{Me}_2)_2]$ ($\text{M} = \text{Ni}, \text{Pd}, \text{Pt}$), $[\text{Ni}(\text{S}_2\text{C}_2\text{H}_2)_2]$, and $[\text{Ni}(\text{S}_2\text{C}_2\text{Ph}_2)_2]$, and bonding in the chelate rings is interpreted on the basis of stretching-force constants (60). Isotopic substitution of nickel has been used in ten complexes of the type $[\text{Ni}(\text{S}_2\text{C}_2\text{R}_2)_2]^x$ ($\text{R} = \text{H}, \text{Ph}, \text{CF}_3, \text{CN}$; $x = 0, -1, -2$) in order to assign Ni—S stretching modes. Normal coordinate analysis on all ten complexes gives force constants as well as providing theoretical band assignments (169).

C. ESR SPECTRAL AND MAGNETIC STUDIES

These techniques have been used extensively for the electronic and structural characterization of paramagnetic, ferromagnetic, and anti-ferromagnetic complexes. The amount of work that has been undertaken and the various implications derived from the experimental data are very extensive, and for brevity this section will consider only selected examples of the use of the techniques in the field of transition metal-sulfur chemistry. In many cases the ESR and magnetic parameters have been used to give preliminary structure and bonding evidence.

McCleverty has outlined the ESR spectral properties of the transition metal dithiolenes in considerable detail (139). Complexes having a doublet ground state are particularly amenable to study by ESR, although the assignment of a ground state may not be a trivial operation. Recently, two ESR studies of the $\text{V}(\text{mnt})_3^{2-}$ complex as single crystals in diamagnetic hosts have led to a reassignment of the ground state in terms of 2A_2 state in D_3 symmetry (4, 84). The orbital bearing the unpaired electron has been shown to have substantial metal d_{z^2} character although the covalency is quite high. In complexes containing unpaired electrons that are delocalized onto orbitals primarily of ligand character, the ESR technique has been immensely useful. The ESR spectrum of the formally gold(II) complex, $\text{Au}(\text{mnt})_2^{2-}$, has been measured in several host crystals over a range of temperatures (158), and these results are consistent with a ground-state hole configuration $(B_{1g})^2(\text{Ag})$ in D_{2h} symmetry. The B_{1g} orbital in square-planar d^9 complexes is normally half-filled; the Ag orbital is primarily ligand-based. The complex was therefore better described

as a gold(III) complex with a radical anion ligand. Unusual antiferromagnetic exchange interactions have been observed from isotropic magnetic susceptibility data of the dimeric $[\text{Fe}(\text{tfd})_2]_2$ (44). A recent study of the trigonal prismatic $[\text{Re}(\text{S}_2\text{C}_2\text{Ph}_2)_3]$ and $[\text{Re}(\text{tdt})_3]$ have shown that they are characteristic of S-containing organic radicals and that the unpaired electron resides in a nonbonding orbital derived from the ligand π -orbitals. An electronic ground-state configuration of $(3a_1^{-1})(4e_1^{-1})(2a_2^{-1})$ has been derived for these complexes (2).

A large asymmetry parameter observed for $[\text{Cu}(\text{mnt})_2]^{2-}$ is due to a strong in-plane π -bond (203). A single-crystal ESR study of $\text{Bu}_4\text{N}[\text{Pd}(\text{mnt})_2]$ interprets ^{105}Pd and ^{33}S hyperfine splitting in terms of a $^2B_{3g}$ electronic ground state in which the half-filled out-of-plane molecular orbital is extensively delocalized over the ligands (111–113). The covalent character of the cobalt sulfur bond in phosphine adducts of $[\text{Co}(\text{S}_2\text{C}_2\text{Ph}_2)_2]$ is unaffected by the substituents on phosphorus (168).

D. ELECTRONIC SPECTRAL STUDIES

Electronic spectral studies of bidentate S-containing ligands have been reviewed in considerable detail (39, 95, 139), and the major use of the technique is in assignment of electronic and stereochemical structures to the complexes. In spite of the numerous studies in this field, the interpretation of the spectra are still far from being totally clear. π -bonding and electronic delocalization have wide and varying effects on the results, and high nephelauxetic effects are invariably observed. Another cause of the difficulty in assigning spectra is the presence of low-lying high intensity charge-transfer bonds (metal–ligand or ligand–ligand), which frequently mask the d – d bands. When d – d bands have been assigned, they usually have had anomalously high intensities due to borrowing of intensity from the charge-transfer bands.

E. X-RAY PHOTOELECTRON SPECTRAL (XPS) STUDIES

The ionization energies of electrons can be determined by XPS by means of the Einstein relationship,

$$E_i = h\nu - E_e$$

where E_i is the ionization energy, $h\nu$ is the X-ray energy, and E_e is the kinetic energy of the ejected photoelectron. The actual core

electron-binding energy, which is closely related to the ionization energy, is influenced by the local electron density surrounding the atom and by the structural arrangement of other atoms within the solid. The core electron-binding energies of a central atom varies as the valence electron density of the atom is charged through a series of different bonding conditions. XPS has been used to gain new physical data of substantial significance for understanding the bonding in transition metal dithiolenes, as the metal and sulfur binding energies can be related to the charges on the atoms. Grim and co-workers (136-138) have determined binding energies for the metal and sulfur atoms in $[M(mnt)_2]^{-1,-2}$ and $[M(S_2C_2Ph_2)_2]^{0,-1,-2}$ ($M = Ni, Pd, Pt$). Their results are shown in Table II.

TABLE II
METAL AND SULFUR BINDING ENERGIES (EV) IN $[M(S_2C_2R_2)_2]^{z-}$

R	Z	M = Ni		M = Pd		M = Pt	
		Ni(2p _{3/2})	S(2p _{1/2} 3/2)	Pd(3d _{5/2})	S(2p _{1/2} 3/2)	Pt(4f _{7/2})	S(2p _{1/2} 3/2)
Ph	0	852.9	161.1	336.4	161.9	71.5	161.8
Ph	-1	852.5	160.8	335.9	161.2	71.2	161.1
Ph	-2	852.8	160.5	335.8	161.3	71.1	161.3
CN	-1	853.1	161.3	335.3	161.1	71.2	161.8
CN	-2	853.1	161.4	335.8	161.2	71.5	161.8

Initially the data were interpreted in terms of Ni being assigned a formal oxidation state of 0 with the additional charge residing on the ligands (136); originally postulated from a comparison with the binding energies of other Ni(0) species. A study of over 100 Ni compounds (138) showed that the binding energies of the Ni(II) compounds overlap with those of Ni(0) compounds and that the electronegativity of the ligand can affect the binding energies significantly. The $S(2p_{1/2}, \frac{3}{2})$ binding energies decrease in the series $[Ni(S_2C_2Ph_2)_2]^z$ ($z = 0, -1, -2$), which indicates that the charge resides largely on the sulfur atoms. The trend in the Pd and Pt complexes begins in the same way but then remains essentially constant. The sulfur binding energies are very low, indicating high electron density on the sulfur atoms. In the mnt complexes, however, metal and sulfur binding energies are essentially constant, which may indicate that in gaining an electron the extra negative charged is delocalized over the electronegative cyanide group. The absence of fine structure in the XPS of the paramagnetic mono-anions is additional evidence for the unpaired electron residing primarily on the ligand, as other paramagnetic Ni compounds show

broad lines and shake-up satellites in their XPS. The overall results provide additional weight to the argument for considering the metal as formally M(II) with the extra negative charge residing essentially on the ligands and demonstrates the valence electron delocalization in the complexes.

Hoyer and co-workers (125) measured the XPS of $[M(S_2C_2H_2)_2]^n$ ($M = Cu$ or Ni ; $n = 0$ or -1) and found the charge at the sulfur atoms dependent on the total charge on the complexes. Alkylation at the S atoms caused a decrease of the charge density at the coordinated atom. The same group also drew similar conclusions for the tris-dithiolenes of Mo (58). It appears from the binding energies that the greater the localization of charge on the S atoms, the lower the binding energy.

F. MÖSSBAUER SPECTRAL STUDIES

To date, Mössbauer spectral studies of the bidentate S-chelates have been limited to the iron complexes. Complexes containing other Mössbauer-active nuclides have yet to be studied even though the Au^I systems present unique opportunities for studying pure trans effects of sulfur ligands in two-coordinate species.

Correlations of Mössbauer data with stereochemical rearrangements in the mixed-ligand complexes $[Fe(R_2dtc)_2(S_2C_2R_2)]^z$ have been studied recently (163), and the spectra of the $z = -1, 0$ complexes consist of a symmetrical quadrupole doublet, suggestive of spin interconversion rates in excess of 10^7 S^{-1} for the neutral species. Temperature-dependent Mössbauer techniques have been used in a study of $(Ph_4P)[Fe(mnt)_3]$ over a wide range of temperatures (12); a large quadrupole splitting was observed, indicating strong distortion from cubic symmetry. Conclusions concerning the ground-state formalization showed it to be an almost pure d_{xy} hole, well separated from higher states, contrary to previous assignments derived from ESR data (38).

The cluster compounds $(Ph_4As)^{n+}[Fe_4S_4(tfd)_4]^{n-}$ ($n = 0, 1$, or 2) are characterized by positive electric field gradients and near-zero asymmetry parameters. Furthermore, in each case the flux densities at the ^{57}Fe nuclear sites are similar to applied field values, demonstrating the delocalization of the additional electrons onto the dithiolene ligands (17) and the equivalence of the four iron atoms. Useful data derived from the Mössbauer spectra of iron dithiolene complexes has been related to empirical bonding parameters (75).

G. ELECTROCHEMICAL STUDIES

The growth of the chemistry of 1,2-dithiolene complexes is partly due to the discovery of facile reversible one- and two-electron transfer reactions exhibited by these species. A systemization of the pertinent electrochemical data has greatly extended the synthetic chemistry of this class of compounds. McCleverty (139) considered the electrochemistry of the 1,2-dithiolene complexes in great detail and attempted to standardize the $E_{1/2}$ values with respect to a standard acetonitrile-Standard Calomel Electrode (SCE) scale. Electrochemical studies have used most techniques available to investigate these reactions. These include ac, dc, and pulse polarography, linear sweep, pulse and cyclic voltammetry, chronopotentiometry, controlled potential, and exhaustive electrolysis.

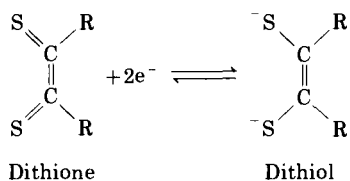
The interest in the electrochemistry of 1,2-dithiolenes has been maintained at an intense level in recent years, particularly in synthetic and characterization studies (47, 54, 55, 142, 191). Chronopotentiometry and linear-scan voltammetry have been used to demonstrate that the oxidation of $[\text{Ni}(\text{mnt})_2]^{2-}$ and the reduction of $[\text{Ni}(\text{mnt})_2]^-$ were diffusion controlled in the presence of Et_4NClO_4 and that neither species was electroactively adsorbed onto the Pt electrodes (126). Electron transfer series have been shown to exist in the mixed-ligand complexes containing, 1,1- and 1,2-dithio ligands (195). The $E_{1/2}$ values were intermediate between those for the complexes with unmixed ligands.

A series of previously unreported gold(III) bisdithiolene complexes have been generated by polarography, and controlled potential electrolysis and the half-wave potentials of the reactions were correlated with the variations in the ESR parameters (92).

Paramagnetic $[\text{M}(\text{mnt})_2]^{3-}$ complexes ($\text{M} = \text{Ni}, \text{Pd}, \text{Pt}$), have been generated by reversible cyclic voltammetry and ac polarography of the corresponding $[\text{M}(\text{mnt})_2]^{2-}$ species (66, 67, 155). They are characterized as d^9 metals with the unpaired electron consisting of contribution from the d_{xy} metal orbitals and in-plane s-orbitals with the palladium complex showing greater covalent character than the nickel species. The reduction of $[\text{Pt}(\text{mnt})_2]^{2-}$ proceeds by two successive one-electron processes, and arguments are presented that suggest an electronic ground state differing from the nickel and palladium analogs. This is just one example of the uniqueness of dithiolene systems and how they must be examined individually.

The recent discoveries that 1,1- and 1,3-dithiochelates undergo successive reversible one-electron transfer reactions have established that reversible behavior is not confined to those metal chelates with

what Schrauzer (173) termed "even" π -electron character, notably the 1,2-dithiene systems. It had been suggested that the "odd" π -electron systems, which cannot exhibit dithione and dithiol forms, e.g., 1,1- and 1,3-dithiochelates, would possess slightly different properties and structures from those of 1,2-dithiolene, which can exhibit such structures, viz.



In the case of the "odd" ligands the electrochemical processes appear to be mainly metal-centered; even though Golding and Lehlonen (68) have suggested that the redox processes in the dithiocarbamates take place through the nitrogen atom of the ligand, the orbitals involved are primarily of metal character. In the "even" 1,1-electron systems the redox processes appear to involve orbitals of predominantly ligand character.

REFERENCES

1. Adams, R., and Feretti, A., *J. Am. Chem. Soc.* **81**, 4927 (1959).
2. Al-Mawali, A. H., and Poreter, A. L., *J. Chem. Soc., Dalton Trans.* 250 (1975).
3. Alvin, H., and Wing, R. M., *J. Organomet. Chem.* **63**, 441 (1973).
4. Atherton, N. M., and Winson, C. J., *Inorg. Chem.* **12**, 383 (1973).
5. Bähr, G., *Angew. Chem.* **68**, 525 (1956).
6. Bahr, G., Schleitzer, G., *Chem. Ber.* **88**, 438 (1957).
7. Baker, J. R., Hermann, A., and Wing, R. M., *J. Am. Chem. Soc.* **93**, 6486 (1971).
8. Balch, A. L., *J. Am. Chem. Soc.* **91**, 6962 (1969).
9. Balch, A. L., *Inorg. Chem.* **10**, 388 (1971).
10. Balch, A. L., Dance, I. G., and Holm, R. H., *J. Am. Chem. Soc.* **93**, 707 (1971).
11. Ballard, L. F., and Wortman, J. J., *J. Appl. Phys.* **41**, 4232 (1970).
12. Bastow, T., and Whitefield, W. J., *J. Inorg. Nucl. Chem.* **36**, 97 (1974).
13. Bennett, M. J., Cowie, M., Martin, J. L., and Takats, J., *J. Am. Chem. Soc.* **95**, 7504 (1973).
14. Bergendahl, T. J., and Waters, J. H., *Inorg. Chem.* **14**, 2556 (1975).
15. Bernal, I., Clearfield, A., Epstein, E. F., Ricci, J. S., Jr., Balch, A., and Miller, J. S., *Chem. Commun.* p. 39 (1973).
16. Bernal, I., Davies, B. R., Good, M. L., and Chandra, S., *J. Coord. Chem.* **2**, 61 (1972).
17. Bernal, I., Frankel, R. B., Reiff, W. M., and Good, M. L., *Inorg. Chem.* **13**, 493 (1974).
18. Bosman, W. P., and Nieuwpoort, A., *Inorg. Chem.* **15**, 775 (1976).
19. Browall, K. W., Bursh, T., Interrante, L. V., and Kasper, J. S., *Inorg. Chem.* **11**, 1800 (1972).
20. Browall, K. W., and Interrante, L. V., *J. Coord. Chem.* **3**, 27 (1973).

21. Brown, G. F., and Steifel, E. I., *Inorg. Chem.* **12**, 2140 (1973); *Chem. Commun.* p. 728 (1970).
22. Burgess, J., Davies, K. M. C., Kemmitt, R. D. W., Raynor, J. R., and Stocks, J., *Inorg. Chem. Acta* **4**, 129 (1970).
23. Lo, L. H., M. Sc. Dissertation, University of Manchester (1976).
24. Cadas, P., Fabre, J. M., El-Khalife, M. S., Mas, A., Torreilles, E., and Giral, L., *Tetrahedron Lett.* p. 4475 (1975).
25. Cadas, P., Fabre, J. M., El-Khalife, M. S., Mas, A., Torreilles, E., Giral, L., and Cot, L., *Mol. Cryst. Liq. Cryst.* **32**, 151 (1976).
26. Callaghan, A., Leyton, A. J., and Nyholm, R. S., *Chem. Commun.* p. 399 (1969).
27. Caroll, J. A., Fisher, D. R., Raynor-Canham, G., and Sutton, D., *Can. J. Chem.* **52**, 194 (1974).
28. Casey, A. T., and Thakeray, J. R., *Aust. J. Chem.* **28**, 471 (1975).
29. Cheng, C. H., Spivack, B. D., and Eisenberg, R., *J. Am. Chem. Soc.* **99**, 3003 (1977).
30. Churchull, M. R., and Cooke, J., *J. Chem. Soc. A* p. 712 (1971).
31. Clark, G. R., Waters, J. M., and Whittle, K. R., *J. Chem. Soc., Dalton Trans.* 821 (1973).
32. Clark, R. E. D., *Analyst* **60**, 242 (1936).
33. Connelly, N. G., and Dahl, F., *Chem. Commun.* p. 880 (1970).
34. Connelly, N. G., Locke, J., and McCleverty, J. A., *Inorg. Chim. Acta* **2**, 41 (1968).
35. Connelly, N. G., Locke, J., McCleverty, J. A., Phillips, D. A., and Ratcliff, B., *Inorg. Chem.* **9**, 278 (1970).
36. Connelly, N. G., Locke, J., and McCleverty, J. A., *J. Chem. Soc. A* p. 712 (1971).
37. Connelly, N. G., and McCleverty, J. A., *J. Chem. Soc. A* p. 1621 (1970).
38. Cotton, S. A., Gibson, J. F., *J. Chem. Soc. A* p. 803 (1971).
39. Coucouvanis, D., *Prog. Inorg. Chem.* **11**, 233 (1970).
40. Coucouvanis, D., Baenziger, N. C., and Johnson, S. M., *Inorg. Chem.* **13**, 1191 (1974).
41. Coucouvanis, D., Baenziger, N. C., and Johnson, S. M., *J. Am. Chem. Soc.* **96**, 4882 (1974).
42. Cowie, M., and Bennet, M. J., *Inorg. Chem.* **15**, 1584, 1589, and 1595 (1976).
43. Dance, I. G., *J. Am. Chem. Soc.* **95**, 6970 (1973).
44. Dance, I. G., *Inorg. Chem.* **12**, 2748 (1973).
45. Dance, I. G., and Conrad, R. C., *Aust. J. Chem.* **30**, 305 (1977).
46. Dance, I. G., Conrad, R. C., and Cline, J. E., *Chem. Commun.* p. 13 (1974).
47. Dance, I. G., and Miller, T. R., *Chem. Commun.* p. 439 (1971).
48. Dance, I. G., and Miller, T. R., *J. Am. Chem. Soc.* **95**, 6970 (1973).
49. Dance, I. G., and Miller, T. R., *Inorg. Chem.* **13**, 525 (1974).
50. Dance, I. G., and Miller, T. R., *Chem. Commun.* p. 112 (1976).
51. Dance, I. G., and Solstad, P. J., *J. Am. Chem. Soc.* **95**, 7256 (1973).
52. Davison, A., McCleverty, J. A., Shawl, E. T., and Wharton, E. J., *J. Am. Chem. Soc.* **89**, 830 (1967).
53. Debaerdemaeker, T., and Kutoglu, A., *Acta Crystallogr., Sect. B* **29**, 2664 (1973).
54. Dessy, R. E., Kammann, P., Smith, C., and Haytor, R., *J. Am. Chem. Soc.* **90**, 2001 (1968).
55. Eaton, G. R., and Holm, R. H., *Inorg. Chem.* **10**, 805 (1971).
56. Eisenberg, R., *Prog. Inorg. Chem.* **12**, 295 (1970).
57. Epstein, E. V., and Bernal, I., *Chem. Commun.* p. 136 (1970).
58. Finster, J., Meusel, N., Müller, P., Dietzsh, W., Meisel, A., and Hoyer, E., *Z. Chem.* **13**, 146 (1973).
60. Fresco, J., and Sümann, O., *Inorg. Chem.* **10**, 297 (1971).
61. Ganguli, K. F., Ph.D. Thesis, North Texas State University, Denton (1969).

62. Ganguli, K. F., Carlisle, G. O., Lu, H. J., Thériot, L. J., and Bemal, I., *J. Inorg. Nucl. Chem.* **33**, 3579 (1971).
63. Geiger, W. E., Jr., Allen, C. S., Mines, T. E., and Seuftleber, F. C., *Inorg. Chem.* **16**, 2003 (1977).
64. Geiger, W. E., Jr., and Maki, A. H., *J. Phys. Chem.* **75**, 2387 (1971).
65. Geiger, W. E., Jr., and Maki, A. H., *J. Phys. Chem.* **77**, 1862 (1973).
66. Geiger, W. E., Jr., Mines, T. E., and Seuftleber, F. C., *Inorg. Chem.* **14**, 2141 (1975).
67. Geiger, W. E., Jr., and Seuftleber, F. C., *J. Am. Chem. Soc.* **97**, 5018 (1975).
68. Golding, R. M., and Lehlonen, H., *Aust. J. Chem.* **27**, 2083 (1974).
69. Gray, H. B., *Transition Met. Chem.* **1**, 240 (1965).
70. Gray, H. B., Williams, R., Bernaland, I., and Billig, E., *J. Am. Chem. Soc.* **84**, 4756 (1962).
71. Heber, R., and Hoyer, E., *J. Prakt. Chem.* **315**, 106 (1973).
72. Heber, R., and Hoyer, E., *J. Prakt. Chem.* **318**, 19 (1976).
73. Hencher, J. L., Shen, Q., and Tuck, D. G., *J. Am. Chem. Soc.* **98**, 899 (1976).
74. Herrmann, A., and Wing, R. M., *Inorg. Chem.* **11**, 1415 (1972).
75. Hoggins, J. T., and Steinfink, H., *Inorg. Chem.* **15**, 1682 (1976).
76. Holmes, R. R., *Acc. Chem. Res.* **5**, 296 (1972).
77. Hoyer, E., *Z. Chem.* **11**, 41 (1971).
78. Hoyer, E., Dietzsch, W., and Heber, H., *Proc. Symp. Coord. Chem.*, 3rd, 1970 Vol. 1, p. 259 (1970).
79. Hoyer, E., Dietzsch, W., Hennig, H., and Schroth, W., *Chem. Ber.* **102**, 603 (1969).
80. Hoyer, E., Dietzsch, W., and Schroth, W., *Proc. Int. Conf. Coord. Chem.* 9th, 1966 p. 316 (1966).
81. Hoyer, E., Müller, H., and Wagler, H., *Wiss. Z. Karl-Marx-Univ., Leipzig, Math.-Naturwiss. Reihe* **21**, 47 (1972).
82. Hunig, S., and Fleckenstein, E., *Justus Liebigs Ann. Chem.* **738**, 192 (1970).
83. Hynes, M., Sweigart, D. A., and De Wit, D. G., *Inorg. Chem.* **10**, 196 (1971).
84. Ilmaier, B., *Monatsh. Chem.* **106**, 657 (1975).
85. Interrante, L. V., *Adv. Chem. Ser.* **150**, 1 (1976).
86. Interrante, L. V., Browall, K. W., Hart, H. R., Jr., Jacobs, I. S., Watkins, G., and Wee, S. H., *J. Am. Chem. Soc.* **97**, 889 (1975).
87. Interrante, L. V., Kasper, J. S., Watkins, G. D., Prober, D. E., Bonner, J. C., Jacobs, J. S., Bray, J. W., and Hart, H. R., Jr., *Phys. Rev. B*, 312 (1975).
88. Jacobs, I. S., Interrante, L. V., and Hart, H. R., Jr., *Gen. Elec. Tech. Inf. Ser. Rep.* No. 75CRD009 (1975).
89. Jacobs, J. S., Kasper, J. S., Watkins, G. D., Bonner, J. C., Bray, J. W., Hart, H. R., Jr., Interrante, L. V., and Wee, S. H., *AIP Conf. Proc.* **29**, 504 (1976); *Phys. Rev. Lett.* **35**, 744 (1975).
90. James, T. A., and McCleverty, J. A., *J. Chem. Soc. A* 3308 (1970).
91. Janota, H. F., and Choy, S. B., *Anal. Chem.* **46**, 670 (1974).
92. Jenkins, J. J., and Williams, R. F., *Abstr. Pap. 17 Meet., Am. Chem. Soc.* INOR, p. 160 (1976).
93. Johnson, R. W., Muir, R. W., and Sweigart, D. A., *Chem. Commun.* 643 (1970).
94. Jones, C. J., and McCleverty, J. A., *J. Chem. Soc., Dalton Trans.* 701 (1975).
95. Jørgenson, C. K., *Inorg. Chim. Acta* **2**, 65 (1968).
96. Kaneko, M., *Japan Kokai* 75/126,097; 75/126,098; 76/79,199.
97. Kaneko, M., *Japan Kokai* 75/145, 497.
98. Kaneko, M., *Makromol. Chem.* **178**, 723 and 733 (1977).
99. Kaneko, M., and Maneck, G., *Makromol. Chem.* **174**, 2795 (1974).
100. Kaneko, M., and Manecke, G., *Makromol. Chem.* **175**, 2811 (1974).

101. Kaneko, M., and Manecke, G., *Makromol. Chem.* **174**, 2795 (1974).
102. Kaneko, M., and Manecke, G., *Ger. Offen.* **2**, 350, 312 (1975).
103. Kasper, J. S., Interrante, L. V., and Secaur, C. A., *J. Am. Chem. Soc.* **97**, 890 (1975).
104. Kawashima, M., Kogama, M., and Fujinaga, T., *J. Inorg. Nucl. Chem.* **38** 801 (1976).
105. Khare, G. P., and Eisenberg, R., *Inorg. Chem.* **9**, 2211 (1970).
106. Khare, G. P., and Eisenberg, R., *Inorg. Chem.* **11**, 1385 (1972).
107. King, R. B., *U.S. Patent* 3,361,777 (1968).
108. King, R. B., *Inorg. Chem.* **2**, 641 (1963).
109. King, R. B., and Eggars, C. A., *Inorg. Chem.* **7**, 340 (1968).
110. King, R. B., and Eggars, C. A., *Inorg. Chem.* **7**, 1214 (1968).
111. Kirmse, R., and Dietzsch, W., *J. Inorg. Nucl. Chem.* **38**, 255 (1976).
112. Kirmse, R., Dietzsch, W., and Rehorek, D., *Z. Chem.* **17**, 33 (1977).
113. Kirmse, R., Dietzsch, W., and Solov'ev, B., *J. Inorg. Nucl. Chem.* **39**, 1157 (1976).
114. Knox, J. R., and Prout, C. K., *Acta Crystallogr., Sect. B* **25**, 2013 (1969); *Chem. Commun.* p. 1277 (1967).
115. Köpf, H., *J. Organomet. Chem.* **14**, 353 (1968).
116. Köpf, H., *Angew. Chem., Int. Ed. Engl.* **10**, 134 (1971).
117. Köpf, H., *Z. Naturforsch., Teil B* **23**, 1531 (1968).
118. Kramolowsky, R., and Hackelberg, O., *Z. Naturforsch., Teil B* **30**, 219 (1975).
119. Krespan, C. G., McKusick, B. C., and Cairns, T. L., *J. Am. Chem. Soc.* **82**, 1515 (1960).
120. Krespan, C. G., *J. Am. Chem. Soc.* **83**, 3434 (1961).
121. Kutoglu, V. A., *Acta Crystallogr. Sect. B* **29**, 2891 (1973).
122. Kutoglu, V. A., and Köpf, H., *J. Organomet. Chem.* **25**, 455 (1970).
123. Kwik, W. L., and Steifel, E. I., *Inorg. Chem.* **12**, 2337 (1973).
124. Lalor, F., Hawthorne, M. F., Maki, A. H., Darlington, K., Davison, A., Gray, H. B., Dori, Z., and Steifel, E. I., *J. Am. Chem. Soc.* **89**, 2278 (1967).
125. Leonhardt, G., Dietzsch, W., Heber, R., Hoyer, E., Hedman, J., Berntsson, A., and Klasson, M., *Z. Chem.* **13**, 24 (1973).
126. Lingane, P., *Inorg. Chem.* **9**, 1162 (1970).
127. Livingstone, S. E., *Rev., Chem. Soc.* **19**, 38b (1965).
128. Livingstone, S. E., and Harris, C. M., in "Chelating Agents and Metal Chelates" (F. P. Dwyer and D. P. Mellor, eds.), p. 95, Academic Press, New York, 1964.
129. Locke, J., and McCleverty, J. A., *Inorg. Chem.* **5**, 1157 (1966).
130. Mahler, W., *U.S. Patent* 3,398,167 (1968).
131. Maki, A. H., Edelstein, N., Davison, A., and Holm, R. H., *J. Am. Chem. Soc.* **86**, 4580 (1964).
132. Manecke, G., and Woehrle, D., *Makromol. Chem.* **116**, 36 (1968).
133. Maride, D., and Hoffmann, A. K., *Fr. Demande* 2,014,532 (1970).
134. Martin, J. L., and Takats, J., *Inorg. Chem.* **14**, 73 (1975).
135. Masuda, Y., Koya, K., and Misumi, S., *Nippon Kagaku Kaishi* p. 636 (1975).
136. Mateinzo, L. J., Grim, S. O., and Swartz, W. E., *J. Am. Chem. Soc.* **94**, 5116 (1972).
137. Mateinzo, L. J., Yin, Lo. I., Grim, S. O., and Swartz, W. E., Jr., *Inorg. Chem.* **12**, 2762 (1973).
138. Matienzo, L. J., Yin, Lo. I., Grim, S. O., and Swartz, W. E., Jr., *Inorg. Chem.* **13**, 447 (1974).
139. McCleverty, J. A., *Prog. Inorg. Chem.* **10**, 49 (1968).
140. McCleverty, J. A., Atherton, N. M., Connelly, N. G., and Ainscom, C. J., *J. Chem. Soc. A* p. 2242 (1969).
141. McCleverty, J. A., and James, T. A., *J. Chem. Soc. A* p. 3318 (1971).
142. McCleverty, J. A., James, T. A., and Wharton, E. J., *Inorg. Chem.* **8**, 1340 (1969).

143. McCleverty, J. A., James, T. A., Wharton, E. J., and Winscom, C. J., *Chem. Commun.* p. 933 (1968).
144. McCleverty, J. A., Jones, C. J., and Orchard, D. G., *J. Organomet. Chem.* **26**, C19 (1971).
145. McCleverty, J. A., Locke, J., Wharton, E. J., and Winscom, C. J., *J. Am. Chem. Soc.* **89**, 6082 (1967).
146. McCleverty, J. A., and Orchard, D. G., *J. Chem. Soc. A* p. 626 (1971).
147. McCleverty, J. A., and Orchard, D. G., *J. Chem. Soc. A* p. 3784 (1971).
148. McCleverty, J. A., Orchard, D. G., and Smith, K., *J. Chem. Soc. A* p. 707 (1971).
149. McCleverty, J. A., and Ratcliff, B., *J. Chem. Soc. A* p. 1627 (1970).
150. McCleverty, J. A., and Ratcliff, B., *J. Chem. Soc. A* p. 1631 (1970).
151. Melson, G. A., and Statz, R. W., *Coord. Chem. Rev.* **7**, 133 (1971).
152. Miller, J., and Balch, A., *Inorg. Chem.* **10**, 1410 (1971).
153. Miller, J. S., *Inorg. Chem.* **14**, 2011 (1975).
154. Mills, W. H., and Clark, R. E. D., *J. Chem. Soc.* p. 175 (1936).
155. Mines, T. E., and Geiger, W. E., Jr., *Inorg. Chem.* **12**, 1189 (1973).
156. Nakajima, T., Tabushi, I., and Tabushi, I., *Nature (London)* **256**, 60 (1975).
157. Nakajima, T., Tabushi, I., and Tabushi, I., *Japan Kokai* 76/219.
158. Noordik, J. H., Hummelink, T. W., and Van der Linden, J. G. M., *J. Coord. Chem.* **2**, 185 (1973).
159. Ollis, C. R., Jeter, D. Y., and Hatfield, W. E., *J. Am. Chem. Soc.* **93**, 547 (1971).
160. Pearson, R. G., and Sweigart, D., *Inorg. Chem.* **9**, 1167 (1970).
161. Pierpont, C. G., and Eisenberg, R., *Inorg. Chem.* **9**, 2218 (1970).
162. Pignolet, L. H., Lewis, R. A., and Holm, R. H., *Inorg. Chem.* **11**, 99 (1972).
163. Pignolet, L. H., Patterson, G. S., Weiher, J. F., and Holm, R. H., *Inorg. Chem.* **13**, 1263 (1974).
164. Reiche, W., *Inorg. Chim. Acta* **5**, 321 (1971).
165. Reynolds, G. A., and Drexhage, K., *J. Appl. Phys.* **46**, 4852 (1975).
166. Robinson, K. A., and Palmer, J., *J. Am. Chem. Soc.* **94**, 8375 (1972).
167. Rosa, E. J., and Schrauzer, G. N., *J. Phys. Chem.* **73**, 3132 (1969).
168. Ryzhmanova, A. V., Troitskaya, A. D., Yablokov, Yu. Y. and Kudryavtsev, B. V., *Zh. Neorg. Khim.* **20**, 165, 1191, and 131 (1975).
169. Schlaepfer, C. W., and Nakamoto, K., *Inorg. Chem.* **14**, 1338 (1975).
170. Schlupp, R., and Maki, A. H., *Inorg. Chem.* **13**, 44 (1974).
171. Schrath, W., and Peschel, J., *Chimia* **18**, 171 (1964).
172. Schrauzer, G. N., *Transition Met. Chem.* **4**, 299 (1968).
173. Schrauzer, G. N., *Acc. Chem. Res.* **2**, 72 (1969).
174. Schrauzer, G. N., Ho, R. K. Y., and Murilio, R. P., *J. Am. Chem. Soc.* **92**, 3508 (1970).
175. Schrauzer, G. N., and Mayweg, V. P., *J. Am. Chem. Soc.* **84**, 3221 (1962).
176. Schrauzer, G. N., and Mayweg, V. P., *J. Am. Chem. Soc.* **87**, 3585 (1965).
177. Schrauzer, G. N., and Rabinowitz, H. N., *J. Am. Chem. Soc.* **90**, 4297 (1968).
178. Schrauzer, G. N., and Rabinowitz, H. N., *J. Am. Chem. Soc.* **91**, 6522 (1969).
179. Sholanik, G. M., and Geiger, W. E., Jr., *Inorg. Chem.* **14**, 313 (1975).
180. Siedle, A. R., and Todd, L. J., *Inorg. Chem.* **15**, 2838 (1976).
181. Singer, H., and Wilkinson, G., *J. Chem. Soc. A* p. 2516 (1968).
182. Smith, W. F., and Reynolds, G. A., *Ger. Offen.* 2,456,075 (1975).
183. Steifel, E. I., Bennett, L. E., Don, Z., Crawford, T. H., Sima, C., and Gray, H. B., *Inorg. Chem.* **9**, 281 (1970).
184. Steinmetre, G., Kirmse, R., and Hayer, E., *Z. Chem.* **15**, 28 (1975).
185. Stiddard, M. H. B., and Townsend, R. E., *J. Chem. Soc. A* **96**, 4994 (1970).
186. Sutin, N., and Yandell, J. K., *J. Am. Chem. Soc.* **95**, 4847 (1973).

187. Sweigart, D. A., *Inorg. Chim. Acta* **8**, 317 (1974).
188. Sweigart, D. A., Cooper, D. E., and Millican, J., *Inorg. Chem.* **13**, 1272 (1974).
189. Sweigart, D. A., and De Wit, D. G., *Inorg. Chem.* **9**, 1582 (1970).
190. Sweigart, D. A., De Wit, D. G., and Hynes, M. J., *Inorg. Chem.* **10**, 196 (1971).
191. Thériot, L. J., Ganguli, K. F., Kavanos, S., and Bernal, I., *J. Inorg. Nucl. Chem.* **31**, 3133.
192. Toatsu, M., *Japan Kokai* 75/45,027.
193. Troitskaya, A. D., Yablokova, Y. V., Ryzhmanova, A. V., Razumav, A. I., and Gurevich, P. A., *Russ. J. Inorg. Chem. (Engl. Transl.)* **17**, 1640 (1972).
194. Tsiang, H. G., and Langford, C. H., *Can. J. Chem.* **48**, 2776 (1970).
195. Van der Linden, J. G. M., and Van der Roer, H. G. J., *Inorg. Chim. Acta* **5**, 524 (1971).
196. Van der Put, P. J., and Schilperoord, A. A., *Inorg. Chem.* **13**, 2476 (1974).
197. Van Derveer, D. G., and Eisenberg, R., *J. Am. Chem. Soc.* **96**, 4994 (1974).
198. Van Tamelen, E. E., Galdysz, J. A., and Miller, J. S., *J. Am. Chem. Soc.* **95**, 1347 (1973).
199. Vasina, S. A., Gryaznov, Yu. M., Kirsanova, T. I., Savelova, V. K., and Shamshin, R. E., *Zh. Prikl. Spektrosk.* **24**, 113 (1976).
200. Wharton, E. J., *Inorg. Nucl. Chem. Lett.* **7**, 307 (1971).
201. Wharton, E. J., and McCleverty, J. A., *J. Chem. Soc. A* p. 2258 (1969).
202. Wharton, E. J., and McCleverty, J. A., *J. Chem. Soc. A* p. 2258 (1969).
203. White, L. K., and Belford, R. L., *J. Am. Chem. Soc.* **98**, 4428 (1976).
204. Wing, R. M., Maki, A. H., and Schmidt, R. D., *J. Am. Chem. Soc.* **91**, 4394 (1969).
205. Wing, R. M., and Schlupp, R. L., *Inorg. Chem.* **9**, 471 (1970).
206. Wing, R. M., Tustin, G. S., and Okamura, W. H., *J. Am. Chem. Soc.* **92**, 193 (1970).
207. Wüdl, F., *J. Am. Chem. Soc.* **97**, 1962 (1975).
208. Wüdl, F., Ho, C. H., and Nagel, A., *Chem. Commun.* p. 923 (1973).
209. Yandell, J. K., and Sutin, N., *Inorg. Chem.* **11**, 448 (1972).

SOME ASPECTS OF THE BIOINORGANIC CHEMISTRY OF ZINC

REG H. PRINCE

University Chemical Laboratory, Cambridge, United Kingdom

I. Introduction	349
A. Importance of Zinc in Biological Systems.	349
B. Zinc Coordination and Metalloenzyme Function	351
C. Characterization of Zinc Metalloenzymes	354
D. Range of Reactions Catalyzed by Zinc(II) Metalloenzymes.	355
II. Carbonic Anhydrase	356
A. Introduction	356
B. Structure	357
C. Metallocarbonic Anhydrases	361
D. Catalytic Properties of Carbonic Anhydrase	365
E. The Activity-Linked Group at the Active Site	372
F. Inhibition by Sulfonamides.	375
G. Inhibition by Anions	379
H. Mechanism of Action	387
III. Zinc-Based Alcohol Dehydrogenases	390
A. Introduction	390
B. Enzymes	390
C. Metal Ion-Reactivity Relationships	392
D. Coenzyme-Enzyme Interactions	394
E. Substrate-Enzyme Interactions	402
F. LADH and YADH: Metal Ion-Enzyme Interaction	408
IV. Carboxypeptidase A	409
A. Introduction	409
B. Structure of Carboxypeptidase A; Coordination of Zinc and Interaction with Substrate	413
C. Role of Zinc and Enzyme Side Chain-Substrate Interactions in the Catalytic Mechanism	416
V. Conclusions	421
VI. Glossary	423
References	431

I. Introduction

A. IMPORTANCE OF ZINC IN BIOLOGICAL SYSTEMS

Zinc is present at a relatively high concentration in the cells of most organisms, indeed among the $3d^n$ elements its concentration is second

only to that of iron. As study of the various biological functions of zinc proceeds, its extreme importance in life processes is constantly being emphasized.

It is an essential element for the normal functioning of most organisms, and its deficiency can lead to reduction of normal growth, impaired bone development, hindered maturation and function of reproductive organs and processes, impaired protein and carbohydrate metabolism, and retardation of learning capacity. The metal is thought to be effective in promoting wound healing and to be of therapeutic value in the treatment of atherosclerosis. It is probably involved in the photochemistry of vision (1).

Although nutritional studies of zinc were made as early as the nineteenth century (2) it was not until 1940 that carbonic anhydrase was isolated from mammalian red blood cells (erythrocytes) by Keilin and Mann (3) and the protein was shown to contain 0.33% of zinc, which was essential for activity.

As the number of zinc metalloenzymes that have been studied in considerable detail approaches 20, it is becoming clear that probably at least a further 60 or 70 await detailed characterization.

Recently it has been found that zinc may also have a role in genetics: studies of the zinc content of nucleic acid preparations and chromatin by sensitive analytical methods (4) suggest that zinc may have a function in DNA replication and transcription as well as in protein synthesis. A striking demonstration of a role for zinc in this area is exemplified by the finding that zinc deficiency in the growth medium of *Euglena gracilis* causes arrest of cell division (5, 6): there is a drop in the protein RNA content of the cell, and growth is arrested at a stage where the DNA content of each cell is doubled (5); considerable work has been done recently on DNA-dependent RNA-polymerases that bind zinc, but these fascinating studies are as yet in their early stages (6-11).

We shall be concerned here with three zinc-containing enzymes that have been subjected to the most detailed study (carbonic anhydrase, liver and yeast alcohol dehydrogenases, and carboxypeptidase A) to see how chemical and physical techniques are employed to unravel some of the mysteries of, or at least to limit the number of alternatives possible for, the mechanism of action at the zinc center of these enzymes.

We shall see how nature uses unusual and distorted low coordination numbers of the metal ion to achieve catalytic activity and how the metal works in unison with delicately positioned groups on the ligand protein to optimize its catalytic efficiency: the metal ion itself is not sufficient, nor are the ligand groups alone.

To assist readers who may not be familiar with some of the biochemical terminology used, a glossary (Section VI) is included. Abbreviations used in this chapter are listed below.

Abbreviations

ADP	adenosine diphosphate
ADP-R'	adenosine-5'-diphosphate-4-(2,2,6,6-tetramethyl-4-phosphopiperidine-1-oxyl)
AP	alkaline phosphatase
BGGP	benzoylglycylglycyl-L-phenylalanine
BGP	benzoylglycyl-L-phenylalanine
BovCA, BCA	bovine carbonic anhydrase
BovCAB	bovine carbonic anhydrase, B isozyme
CA	carbonic anhydrase
CD	circular dichroism
CDTA	cyclohexenediaminetetraacetic acid
CGP	carbobenzoxylglycyl-L-phenylalanine
CPA	carboxypeptidase, isozyme A
dipy	2,2'-dipyridyl
DNA	deoxyribonucleic acid
ESR	electron spin resonance
FAD	flavine adenine dinucleotide
HCAB	human carbonic anhydrase, B isozyme
HCAC	human carbonic anhydrase, C isozyme
HPLA	benzoylglycyl-L-phenyllactate
LADH	liver alcohol dehydrogenase
MCA	metal-substituted carbonic anhydrase
MCD	magnetic circular dichroism
NADH, NAD ⁺	the β -isomer of nicotinamide adenine dinucleotide, reduced and oxidized forms, respectively
NMR	nuclear magnetic resonance
NTA	nitrilotriacetic acid
ORD	optical rotatory dispersion
RNA	ribonucleic acid
tren	2,2',2''-triaminotriethylamine
tris	tris(hydroxymethyl)methylammonium
UV	ultraviolet
YADH	yeast alcohol dehydrogenase

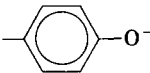
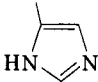
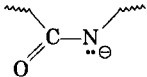
Abbreviations for amino acids are to be found in Section VI.

B. ZINC COORDINATION AND METALLOENZYME FUNCTION

Amino acid side chains with donor groups are potential binding groups for zinc in metalloproteins, and the most likely candidates are shown in Table I.

Three amino acid side chains, those of His, Glu, and Cys-SH, are often concerned in zinc metalloenzymes in general and in the three we

TABLE I
 DONOR GROUPS OF AMINO ACID SIDE CHAINS

	O-donors	N-donors	Heteroatom donors
Asp	$-\text{CH}_2\text{COO}^-$	Lys- $(\text{CH}_2)_4\text{NH}_2$	Cys $-\text{SH}$
Glu	$-(\text{CH}_2)_2\text{COO}^-$	Arg- $(\text{CH}_2)_3\text{NH}-\overset{\oplus}{\text{C}}\begin{matrix} \text{NH}_2 \\ \text{NH}_2 \end{matrix}$	
Tyr		His  N-terminal α -amino acid $-\text{NH}_2$ Deprotonated peptide 	

consider here. Thus CA has three His imidazole ligands, ADH has two SH groups of Cys-SH ligands and one His ligand, and CPA has two His ligands and one carboxy from a Glu residue. In all three, a further coordination site is occupied by a water molecule, the acid dissociation of which, as we shall see, has a marked effect on the pH behavior of the system.

Studies of simpler complexes of ligands having the same donor groups and metal ion as those of the active center in metalloenzymes are numerous and can be helpful in revealing possible new chemistry that the complex has in common with the metal center of the enzyme. Such studies can lead to the discovery of novel reactions that mimic those found in the modeled enzyme, although these reactions usually differ in substrate specificity and mechanism from those of the enzyme (see, for example, 12-14, and references therein). However, a key feature of metalloenzyme catalysis is the concerted action of a metal ion with other noncoordinating groups of the protein, and the synthesis of such a "pendant active group" model is usually difficult. Also, if the model is too simple it will tend to adopt a metal-controlled stereochemistry, whereas in the metalloenzyme it is now clear that the stereochemistry is dictated by the ligand geometry, a fact that can, for example, have profound effects on the affinity of the protein ligand for various metal ions. The bond lengths and angles at the multidentate metal coordination site in enzymes are dictated as much by the stereo-

chemistry of the relatively inflexible protein ligands as by the electron distribution of the metal ion (15).

Furthermore, models are often studied in aqueous solution, whereas the metal ion with its coordinating groups in an enzyme is usually in a cleft in the protein structure, the environment of which more closely resembles an oil drop than water; the cleft itself may also consist of regions of greater and lesser polarity. These are profoundly important features (16), where the substrate is attacked by a charged or partially charged nucleophile at the active site. It is significant that catalytically active metalloproteins have highly distorted and unusual coordination geometries; there has been much interesting discussion on the influence of such distortion on catalytic activity (17), but there seems to be little doubt that strain induced by distortion is intimately connected with activity.

Again, thermodynamic behavior, which appears unusual in terms of the behavior of simple complexes, is found with metalloenzymes: highly purified zinc metalloenzymes, for which the relative affinities of several first-transition series and group IIB metal ions for the metal binding site have been determined, show a remarkable preference for zinc compared with cobalt(II), nickel(II), and copper(II), although the sites are mostly made up of N,O ligands that in simple models have greater affinity for the other ions. Sulfur ligands also might be expected from models to have an especially high affinity for zinc (18, 19) and to be a common ligand. Such is not the case, and His, for instance, is a more common ligand than Cys-SH.

It is natural to ask whether the metal induces in the protein during its assembly the particular configuration of groups necessary to give the unusual stereochemistry of the active site. If so, the metal ion would have to be present during the synthesis of the ligand, i.e., the enzyme apoprotein. This point has been investigated in some detail for *Escherichia coli* alkaline phosphatase (AP). The apoenzyme forms readily in a zinc-free medium: it has physicochemical characteristics identical with those of the apoenzyme formed by zinc removal from *E. coli* AP and is completely reactivated by the addition of zinc (20). This is firm evidence that the presence of the Zn(II) ion is not necessary for the synthesis of the apoprotein. An intriguing finding is that *E. coli* will synthesize AP containing Co(II), Cu(II), and Cd(II) if these metals are added to the growth medium, but Zn(II) will displace these ions, and it does so at relative concentrations well below those expected for competitive binding to analogous model complexes (20). Clearly the configuration of active site groups imparts a high and specific affinity for zinc. The reason for this is again the subject of speculation, but,

like all complex formation processes in solution, the free energy of formation will be composite and contain differences between large quantities, e.g., the hydration energies of the ions and the total binding energy of the metal ion to the active site ligands. It is noteworthy that entropy changes are important in the control of affinity and can be overwhelmingly so; thus, the binding of $\text{Zn}^{2+}(\text{aq})$ to the apoenzyme of CA is accompanied by an enthalpy *increase* that is more than offset by a very large entropy increase, the entropy increase dominating the affinity of the apoenzyme for $\text{Zn}(\text{II})$ (see below). In a very real sense mammalian respiration is allowed to occur by courtesy of entropy.

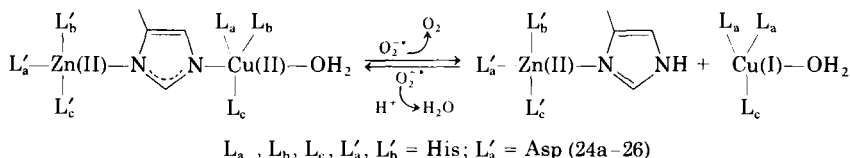
C. CHARACTERIZATION OF ZINC(II) METALLOENZYMES

Enzymes that require ions for activity are divided operationally into two classes: metal-activated and metalloenzymes, a division—somewhat arbitrary—determined by the tightness of binding of the metal ion to the protein (21, 22). A zinc metalloenzyme is assigned to the latter class if it satisfies certain criteria first put forward by Vallee (21, 21a). These criteria avoid ambiguities found with inhibition and activation studies and include the demonstrations of (a) an increase in the metal: protein ratio as the enzyme is purified and (b) a direct correlation between specific activity and metal content for the isolated homogeneous protein. If these requirements are met, then the metal ion is tightly bound to the protein. For several metal-protein complexes that may be classified as metalloenzymes the dissociation constant of the complex is found to be of the order of $10^{-10} M$ or less. As Chlebowski and Coleman (15) have pointed out, the definition means that the binding constant of the metal for the protein site is large enough to ensure that the metal is carried with the protein through the isolation procedures. Enzymes meeting the metalloenzyme criteria have been much easier to work with and have been the more intensively investigated. Since the stability of metal-protein complexes may be expected, like the stabilities of model coordination complexes, to cover a wide range, many important enzymes may be $\text{Zn}(\text{II})$ activated in that the metal is bound loosely enough to dissociate, at least partially, during isolation procedures. As well as analytical difficulties there is also the problem that, with such systems, activation may not be specific for a given metal ion; it may not, even in some $\text{Zn}(\text{II})$ metalloenzymes (see Sections II,C,1, III,C, and IV,A), and it may then be difficult to determine which, among the several divalent ions [$\text{Mg}(\text{II})$, $\text{Ca}(\text{II})$, $\text{Mn}(\text{II})$, $\text{Fe}(\text{II})$, $\text{Cu}(\text{II})$, and $\text{Zn}(\text{II})$] occurring in significant concentration in biological systems, is the natural activator. Some forty or so enzymes have been

listed that are activated by Zn(II), or are believed to contain zinc, but have not yet had the rigorous metalloenzyme criteria applied to them [see, for example, Chlebowski and Coleman (15)].

D. RANGE OF REACTIONS CATALYZED BY ZINC(II) METALLOENZYMES

Nine of the well-characterized Zn(II) metalloenzymes catalyze hydrolysis or hydration reactions. In these cases, acid-base catalysis is probably involved and the Zn(II) can be pictured as functioning in its capacity as a Lewis acid. Two of the zinc metalloenzymes catalyze oxidation reactions, alcohol dehydrogenase (see Section III), and superoxide dismutase. The function of the zinc ion in these proteins is, at first sight, different, and it may at first seem strange that zinc should have a catalytic role in a redox process: the chemistry of Zn(II) certainly does not suggest a role for it as an electron acceptor. The hydride (or 2-proton plus 2-electron) shift in the NAD⁺-dependent dehydrogenases is to the C-4 position of the nicotinamide ring of the coenzyme (see Fig. 14), and we note that many NAD-dependent dehydrogenases are not Zn(II) enzymes. The Zn(II) may function by inducing the proper positioning or polarization of the substrate with respect to the coenzyme, although it is not necessary for coenzyme binding (see Section III,D). Superoxide dismutase* is also a copper metalloenzyme and catalyzes an apparently diffusion-controlled oxidation of the superoxide radical ion at the Cu(II) ion center of this enzyme (23). There is evidence that an imidazole ring of a histidine bridges the Zn(II) and Cu(II) centers (23a), and a rapid protonation and deprotonation of the bridging group takes place (24, 24a) when it reacts with the O₂⁻ ion with change in oxidation state of the copper:



Proton NMR studies show that 4-6 histidine imidazoles are ligands for the metals (25), and histidine modification studies suggest that the zinc function here is to organize the structure of the active site (26).

* This enzyme catalyzes the conversion of O₂⁻ into molecular oxygen and hydrogen peroxide. It is found in most, if not all, organisms that use oxygen.

Zinc metalloenzymes also catalyze group-transfer reactions. Mechanisms for these may be postulated in which Zn(II) withdraws electrons from a group on the substrate by forming a coordinate bond in a mixed enzyme-metal-substrate complex. An interesting case is that of yeast aldolase, in which Zn(II) polarizes the carbonyl (and phosphoryl group) of the substrate $\text{CH}_3\cdot\text{C}(\text{O})\cdot\text{CH}_2\text{O}(\text{PO}_3\text{H}_2)$, facilitating substrate deprotonation and enolization and thus substituting for the positive lysyl- NH_3^+ group involved in the *nonmetal* mammalian aldolases (27). On the other hand, the Zn(II) ion in aspartate transcarbamylase has proved not to be the substrate binding site, but is located in the regulatory subunits (28). It seems clear that zinc may have a role both as an acceptor (Lewis acid) at an active site and in maintaining structure as well.

We shall now look for other subtleties in the function of zinc as we consider the examples of three zinc metalloenzymes—carbonic anhydrase, the alcohol dehydrogenases LADH and YADH, and carboxypeptidase A. Carbonic anhydrase and its isozymes are considered in rather more detail than the others to illustrate broadly how physical techniques are used to gain insight into the metal function and its role in the overall picture of the enzyme mechanism. The other enzymes will be considered more briefly, with emphasis on metal coordination and its relation to function.

II. Carbonic Anhydrase

A. INTRODUCTION

Meldrum and Roughton in 1933 isolated from blood an enzyme that catalyzed the reversible hydration of carbon dioxide; they named it carbonic anhydrase (EC 4.2.1.1, carbonate hydro-lyase) (29). The enzyme is present in most organisms, and is found in many different tissues of plants and animals (30). The literature concerned with the chemical and physiological aspects of carbonic anhydrase has been reviewed up to 1971 (31–34), and comprehensive reviews dealing with more biochemical and kinetic detail than we shall consider here are available (15, 35). The enzyme is involved in a variety of physiological functions, including photosynthesis, calcification, pH maintenance, ion transport, and CO_2 exchange, where its specific catalytic role is the interconversion of carbon dioxide and bicarbonate (30) at a rate which is one of the fastest known for enzymic catalysis.

The most widely studied carbonic anhydrases are those from human and bovine erythrocytes, the enzymes being the major protein component after hemoglobin. The mammalian enzymes consist of a single-

chain protein of molecular weight about 30,000, each chain coiling and forming a ligand binding a zinc ion that is essential for catalysis (36).

There are two isozymes of carbonic anhydrase, designated B (or I) and C (or II), in the erythrocytes of most mammalian species that have been studied (37–40). Reports have appeared of further distinct variants (41–44), but we shall be concerned here with the human carbonic anhydrases B and C, and with the bovine isozyme B (although labeled B, in its activity this isozyme belongs to class C).

The isozymes are antigenically distinct; compared with the B form, the C isozymes generally show higher specific activities, higher thermal stabilities (45, 46), different affinities for inhibitors (44), different chemical reactivity toward modifying agents (43, 47–49), a lower abundance in the red cell (50), different rates of biosynthesis and a difference in physical properties, some of which are shown in Table II. These differences indicate that each isozyme has a different physiological role, and this is discussed elsewhere (33, 51).

B. STRUCTURE

1. General Features

Studies of the complete primary structures of the human B (53–56) and C (57–59) isozymes and of the bovine B isozyme (60) show that each isozyme has a distinct amino acid composition. HCAB consists of 260 amino acid residues, and HCAC has 259 residues. It is interesting that the 60% sequence homology suggests that the two isoenzymes arose through gene duplication and subsequent independent evolution some 150 million years ago, before the divergence of marsupials, but after the divergence of birds, from the mammalian line (30). It is interesting also that carbonic anhydrase has evolved to a stage of maximum catalytic efficiency (see Section V).

2. Structure of the Isozymes and the Coordination of Zinc

The complete structures of the human isozymes B and C have been deduced from high-resolution X-ray studies on enzyme crystals obtained from 50 mM tris-sulfate buffer solutions, pH 8.5 (61–65). The tertiary structures of the two isozymes are very similar.

The enzymes are ellipsoids of dimensions $4.1 \times 4.2 \times 5.5$ nm, and the zinc ion is near the center of the molecule at the bottom of a 1.2 nm-deep conical cavity, which is 2 nm wide at the mouth (66); the general

TABLE II
COMPARISON OF THE CARBONIC ANHYDRASE ISOZYMES FROM HUMAN AND BOVINE RED BLOOD CELLS

Source	Activity type	CO ₂ turnover number (mol/min ^a × 10 ⁶)	Molecular weight ^b	Isoelectric point	Molar absorptivity ₂₈₀ × 10 ⁻⁴ mol ⁻¹ cm ⁻¹	Relative abundance
Human erythrocytes	B, low	1.2	28,800	5.85	4.69	7 /
	C, high	36	29,300	7.25	5.47	1
Bovine erythrocytes	A, high	30	30,000	—	5.7	1 /
	B, high	30	30,000	5.65	5.7	4

^a pH 7, 25°C (34,52).

^b The molecular weights for the human isozymes were calculated from the amino acid sequences.

features of this cavity have been confirmed by spin-label probe techniques (66–68). A large region of rigid β -structure extends through the center of the molecule, and the zinc ion is bound to this through the nitrogen atoms of three histidine imidazole ligands (His 94, 96, and 119); this is consistent with the results of both proton NMR (69, 70) and ESR (71) studies.

The zinc ion has distorted tetrahedral coordination (72), the fourth ligand being a water molecule or a hydroxide ion (Table III); the largest deviation from a tetrahedral angle is 20° .

TABLE III
ZINC LIGANDS IN HUMAN CARBONIC
ANHYDRASE C (72)

Ligand	Zinc–ligand distance (Å)
His 94 (3'N)	2.4
His 96 (3'N)	2.0
His 119 (1'N)	2.0
H ₂ O/HO	1.9

The coordination by His 94 is unusual; of the three coordinating histidines, it has the largest electron density and the position of this imidazole ring varies between two extremes (cf. Section II,H), which differ by 0.07 nm (the shortest Zn–N distance is 0.24 nm) and is also the most exposed ligand—features that may be important in the reaction mechanism (72).

Details of the active site cavity are shown in Fig. 1. The cavity can be divided into hydrophobic and hydrophilic regions. Threonine 199 in HCAC is hydrogen-bonded to the metal-bound water and interacts with most inhibitors. Apart from the histidine ligands, other residues in the active site that have not changed during evolution are Thr 199, Pro 201, Pro 202, His 64, Gln 92, and those involved in a hydrogen-bonded sequence: His 119–Glu 117–His 107–Tyr 194–Ser 29–Trp 209 (Figs. 1 and 2); these residues may be important also in the catalytic mechanism; for example, it has been suggested that the above hydrogen-bonded sequence may be a charge (proton) relay system of the kind that has been suggested for chymotrypsin and the serine proteases (73).

There are 11 amino acid differences between HCAC and HCAB, at the active site (66); for example, Tyr 202 is oriented away from the cavity in HCAB serving to make the cavity more open than in HCAC, where the residue is Leu 202. However, the region close to zinc is more

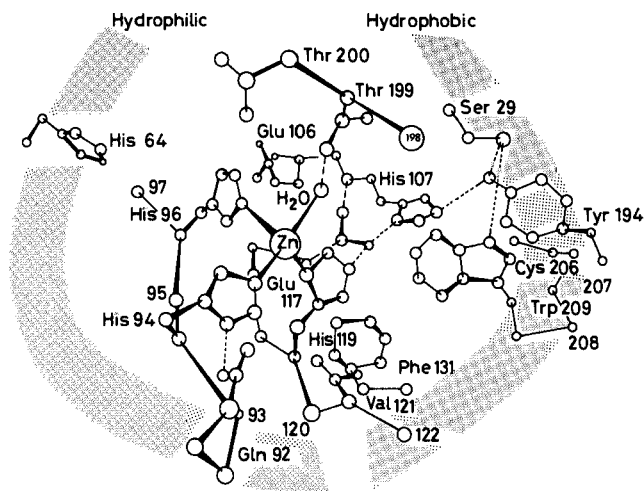


FIG. 1. Part of the active site of human carbonic anhydrase C (35).

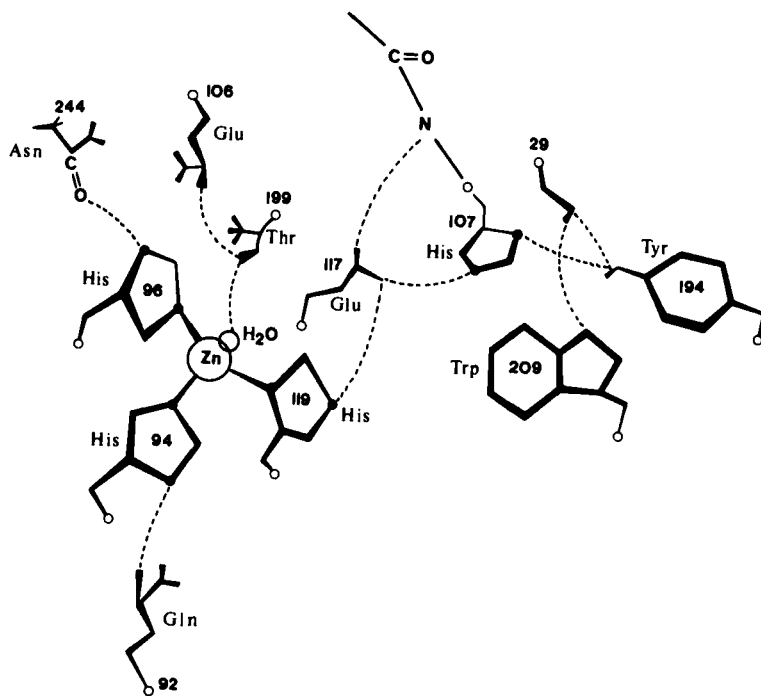


FIG. 2. The hydrogen bond network at the active site of human carbonic anhydrase B. [Redrawn from Wyeth and Prince (35) and Nostrand *et al.* (63)].

restricted in HCAB, owing to the substitution of Asn 67, Val 121, and Thr 200 in HCAC for His 67, Ala 121, and His 200 in HCAB; these differences may be connected with the lower catalytic efficiency of the B isozyme.

There are three pronounced aromatic clusters that may, *inter alia*, have a structural role, maintaining the stability of the active site cavity. The existence of a hydrophobic region is probably also important in determining catalytic activity. Although refinement of the crystal structure has led to the disappearance of what was once thought to be an icelike arrangement of water molecules within the active-site cavity (62), γ - γ correlation spectroscopy has recently indicated that, as might be expected, water at the protein-solution interface is highly ordered (74). It appears also that there remains sufficient space within the cavity for an icelike structure to exist; since proton transfer is more rapid through ice than through water, such a structure could provide a device for efficient proton transfer, a point to which we shall return later.

Although protein crystals differ from those familiar to inorganic chemists, such crystals are usually spongy and bathed in buffer, a cautionary note, not unfamiliar to inorganic chemists, must be sounded about the relevance of the structures of such crystals to the enzyme conformation in solution; X-ray resonance absorption measurements have indicated that a slow conformational change may occur upon dissolution (75) and a number of other cases are known where the behavior of the protein crystal is different from that of the protein in solution (76).

C. METALLOCARBONIC ANHYDRASES

1. *Metal Substitution Studies*

The zinc ion in carbonic anhydrase, although tightly bound (77), can be removed at low pH. The half-time for the metal dissociation is 80 hours for HCAC and 30 hours for HCAB at pH 5.3, 4°C, in the presence of 20 mM dipyrldyl (78). While the apoenzyme undergoes no gross structural changes relative to the holoenzyme, it is catalytically inactive; the metal also confers conformational stability (79).

The apoenzyme can be reconstituted with other divalent metal ions, and these occupy the zinc site (34); significant restoration of catalytic activity is brought about only by Zn(II) and Co(II)* (32) (Table IV) (80);

* Recently the Cd derivative has been shown to have some activity (79a).

TABLE IV
RELATIVE ACTIVITIES OF SOME M(II)-SUBSTITUTED
HUMAN B AND C CARBONIC ANHYDRASE DERIVATIVES^a

Metal ion derivative	Relative CO ₂ hydration activity	Relative rate of <i>p</i> -nitrophenylacetate hydrolysis
Apoenzyme	1.3	1.2
Mn(II)B	1.3	5
Co(II)B	20	120
Co(II)C	55	100
Ni(II)B	2	4.5
Cu(II)B	0.4	6.9
Zn(II)B	30	37
Zn(II)C	100	100
Cd(II)B	1.4	2.7
Hg(II)B	0.02	1.2

^a Modified from Dunn (80).

despite this, a number of investigations have concerned the Mn(II)- and Cu(II)-substituted enzymes, and it should be stressed that data obtained from these experiments may not be relevant to the native enzyme. The relative inactivity of these metallocarbonic anhydrases may be due to several factors, including changes in coordination geometry, rates of ligand exchange, and coordination flexibility.

In all carbonic anhydrases, the catalytic activity and other processes related to the active site appear to be controlled by a group titrating around neutrality; the apparent pK_a of this group in the low-activity isozyme B is about 1 unit higher than that in the high-activity variant (32). The introduction of cobalt rather than zinc does not cause a large change in the pK_a of this group (81–83); this substitution also has a negligible effect on the UV optical rotatory dispersion curves of the bovine (84) and human B (85, 86) enzymes, and on the ESR spectra of spin-labeled sulfonamide inhibitors bound to HCAB (34). This suggests that Co(II) and Zn(II) coordination is similar. However, substitution with cobalt does appear to induce some changes at the active site of HCAB (87); e.g., marked changes in the pH-dependence of anion binding at low pH are observed.

Cobalt(II) is the most valuable of the substituting ions because it serves as an ESR, optical spectral, and nuclear resonance probe as well as a relaxation probe for nuclei in its environment. The visible absorption and MCD spectra of Co(II) BovCAB are shown in Fig. 3; the pH dependence of the spectra reflects the ionization of the activity-linked group. The MCD spectra are particularly useful since they are

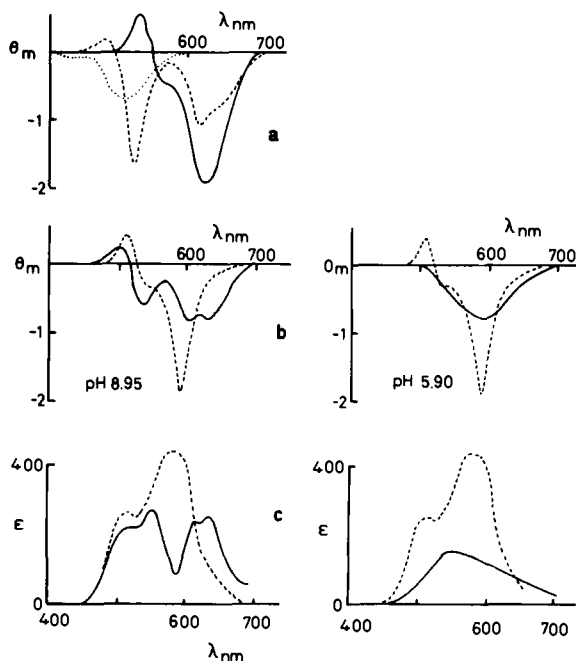


FIG. 3. (a) The magnetic circular dichroism (MCD) spectra of some Co(II) complexes of known geometry: \cdots , $\text{Co}(\text{H}_2\text{O})_6^{2+}$ octahedral; $---$, $\text{Co}(\text{Me}_6\text{tren})\text{Br}_2$ penta-coordinate; $---$, $\text{Co}(\text{OH})_4^{2-}$ tetrahedral. (b) The MCD spectra and (c) the optical spectra of Co(II) BovCAB at pH 8.5, 5.9, and in the presence of 1.5 equivalents of the sulfonamide inhibitor acetazolamide ($---$). Enzyme concentration = 2.5×10^{-4} M. MCD spectra were measured at 40 kG. [Reproduced from Wyeth and Prince (35), with permission.]

less sensitive to coordination distortion and give a clear indication of the cobalt coordination geometry. The metal is tetrahedrally coordinate at low pH and probably pentacoordinate at alkaline pH (88); the addition of the sulfonamide inhibitor acetazolamide again appears to induce tetrahedral coordination. Magnetic susceptibility data are in accord with this interpretation of the coordination geometry of high-spin Co(II) (89); however, the analysis appears to be at variance with X-ray crystallographic results for the zinc enzyme, which show a tetrahedrally coordinated zinc ion in enzymes crystallized at pH 8.5.

2. Binding of Zinc to the Enzyme Protein

The kinetics and thermodynamics of the binding of zinc to the carbonic anhydrase apoenzyme have been investigated (91, 92), and Table V shows the second-order rate constants, activation parameters,

TABLE V
SOME RATE AND EQUILIBRIUM PARAMETERS FOR THE REACTION
 $\text{Zn}^{2+} + \text{LIGAND} + \text{M}^{2+} + \text{apoCA} \rightarrow \text{MCA}^a$

	k ($1 \text{ mol}^{-1} \text{ sec}^{-1}$)	ΔH^* (kcal/mol)	ΔS^* (e.u.)	ΔH (kcal/mol)	ΔS (e.u.)
Zn typical small unidentate	10^{7-8}	—	—	—	—
Zn typical small bidentate (bipyridyl)	10^6	+6	-9	-10	+8
Zn typical small tridentate (terpyridyl)	10^6	+8	-4	—	—
Zn apoCA, pH 5.5	$<10^4$	+21	+28	+3.9	+61
Zn apoCA, pH 7.0	10^4	+21	+30	+9.8	+88
Co apoCA, pH 7.0	—	—	—	+9.4	—
Ni apoCA, pH 7.0	—	—	—	+3.2	—
Cu apoCA, pH 7.0	—	—	—	+3.4	—
Cd apoCA, pH 7.0	—	—	—	+4.4	—
Zn CDTA (cyclohexenediamine tetracetate)	—	—	—	+4.7	+82

^a Data from Henkens and Sturtevant (91) and Henkens *et al.* (92).

and thermodynamic constants of binding. They are compared with those for smaller ligands giving complexes of various coordination numbers. Both rate process and equilibrium are entropy-dominated, in spite of a smaller opposing enthalpy. The entropy terms are substantial, and the only ligand comparable in this respect is CDTA, a formally hexadentate ligand. While it is most unlikely that apocarbonic anhydrase is a hexadentate ligand, the similarity between carbonic anhydrase and CDTA probably has the same origin: the expulsion of a large number of water molecules. The effect in the case of CDTA is due to charge neutralization, and in carbonic anhydrase the binding of the metal may also result in charge neutralization in the active site region.

Further evidence for this may be cited [see literature quoted in Henkens *et al.* (92)]: the difference UV spectrum of ZnCA minus apoCA is similar to the difference spectra produced when a tyrosine or a tryptophan derivative is transferred from water to a less polar solvent. This similarity suggests that one or more tyrosine and/or tryptophan groups (residues 194, 209 perhaps?) are in a more polar environment in the apoenzyme than in the holoenzyme. Other workers concluded on the basis of studies with fluorescent sulfonamides that the active site of the native enzyme is nonpolar. It is interesting to note that structural work on the holoenzyme shows the active site to possess a polar and nonpolar environment (cf. Fig. 1).

The positive binding enthalpy may well indicate a small coordination number, so that during the reaction more M—L bonds are broken than formed, as expected if the zinc is three or four coordinate (aquated zinc is hexacoordinate). It is interesting that the metals zinc and cobalt, whose binding gives an active enzyme, are those with the most endothermic binding to carbonic anhydrase. Dennard and Williams (93) have pointed out that a catalytically active metal must not bind too strongly to its apoenzyme or it will lose coordination flexibility.

D. CATALYTIC PROPERTIES OF CARBONIC ANHYDRASE

Carbonic anhydrase, *in vitro*, catalyzes a range of reactions in which nucleophilic attack of oxygen at an electrophilic center occurs; these include the hydration of carbon dioxide and some aldehydes and the hydrolysis of some carboxylic, sulfonic, and carbonic esters (94–96). The reaction of importance in biological systems is the reversible hydration of CO_2 . One may expect that, if there exists among a variety of possible mechanisms for the catalysis of a given reaction one that is particularly effective, then an enzyme which also catalyzes that reaction may, in the course of evolution, have incorporated it. We shall therefore first consider some general aspects of the catalysis of the carbonyl hydration reaction to see what features are shown by an effective catalyst.

1. Some General Features of the Catalysis of Carbonyl Hydration

A number of studies have been made of the catalysis of CO_2 hydration (93, 97, 98), and several interesting features are revealed. The reaction has been shown not to be proton-catalyzed by studies of ^{18}O exchange between gaseous CO_2 and water in acidified solutions. Purely general base catalysis can be rejected because the Brønsted dependence on acid dissociation constant is not observed, e.g., $(\text{CH}_3\text{CO})_2\text{CH}^-$ is not catalytically active whereas the ion AsO_3H_2^- is active although they both have about the same $\text{p}K$ values, 9.18 and 9.26, respectively. The anions germanate, arsenite, sulfite, selenite, tellurite, and tellurate are active whereas phosphite, phosphate, arsenate, sulfate, and selenate have very small or no catalytic activity. The essential feature appears to be that the most effective catalysts have a *dual* Lewis acid–proton-acceptor function, suggesting a mechanism of the kind shown in Fig. 4, where X—O is part of the catalyst structure. It is interesting in this context that hypohalites are very effective catalysts; e.g., Caplow (99) has found that HOBr is a powerful

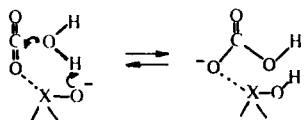
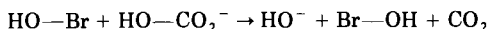


FIG. 4. Lewis acid-Brønsted base features of the most effective catalysts of CO_2 hydration.

catalyst of the dehydration reaction and concluded that a concerted electrophilic displacement occurred:



The bromine atom is here acting as the Lewis acid, X.

Table VI summarizes data on the catalytic efficiency of various catalysts for CO_2 hydration (99a).

TABLE VI
EFFICIENCIES OF VARIOUS CATALYSTS
IN CO_2 HYDRATION^{a,b}

Catalyst	Efficiency ($\text{mol}^{-1} \text{sec}^{-1}$)
H_2AsO_3^-	0.9
HAsO_4^-	0.0002
BrO^-	2
SeO_3^{2-}	1.2
SO_3^{2-}	0.2
$\text{Cu}(\text{glycylglycinate})\text{OH}$	20
ZnCROH^{+c}	25
Carbonic anhydrase	~ 10,000

^a From Woolley (99a).

^b If the forward reaction has velocity constant k , then efficiency is defined as $dk/d[\text{catalyst}]$ (99a). The anions NO_2^- , NO_3^- , CO_3^{2-} , SO_4^{2-} , and the complexes MX_n , where $\text{M} = \text{Mn, Fe, Co, Ni, Cu, Zn}$, and $\text{X} = \text{EDTA, NTA, dipy, Cys, mercaptoethylamine}$, and CN^- have zero efficiency.

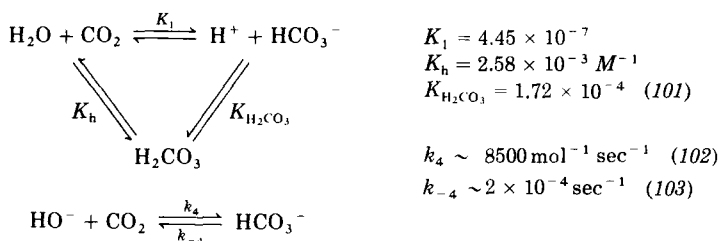
^c The structure of CR is shown in Fig. 6.

Several studies have been made of carbonyl hydration reactions; of particular interest are the hydrations of pyridine 2-aldehyde and pyridine 4-aldehyde using Zn^{2+}aq and Co^{2+}aq solutions and the Zn^{2+} - and Co^{2+} -activated bovine CA (124, 125). The enzyme is about 10^8 more effective than water for both 2- and 4-aldehydes; Zn^{2+} and Co^{2+} are about 10^7 times as effective as water in the case of the 2-aldehyde, but much less effective for the 4-aldehyde. This suggests that there is

no pyridine nitrogen-to-metal coordination in the enzyme, and the metal in the enzyme either directly polarizes the carbonyl group or does so through a bridging water molecule.

2. The Enzyme-Catalyzed Reversible Hydration of CO₂

In the absence of a catalyst the hydration proceeds at a relatively slow rate (0.037 sec^{-1} , 25°C) (34), and a catalyst is therefore necessary in the capillary circulation of mammals, where the rapid transfer of CO₂ is essential (90). In the absence of a catalyst the reversible hydration can be written as shown in Scheme 1 (101–103).



SCHEME 1

The enzyme accelerates CO₂ hydration by a factor of 10^7 at neutral pH. The carbonic anhydrases follow a simple Michaelis–Menten behavior with respect to both CO₂ hydration and HCO₃[−] dehydration; the Haldane relationship is also obeyed. Some selected values of the Michaelis parameters are given in Table VII (104–106).

TABLE VII
MICHAELIS PARAMETERS FOR THE CARBONIC
ANHYDRASE-CATALYZED REVERSIBLE HYDRATION OF CARBON
DIOXIDE (104–106)

Isozyme	pH	CO ₂ hydration		HCO ₃ [−] dehydration	
		k_{cat} (sec ^{−1})	K_m (mM)	k_{cat} (sec ^{−1})	K_m (mM)
Zn(II) HCAC	7.05	6.2×10^5	14	3.7×10^5	68
Co(II) HCAC	7.05	2.6×10^5	5.9		
Zn(II) HCAB	7.05	1.5×10^4	2.6	2.3×10^4	32
Co(II) HCAB	7.05	9×10^3	1.8		
Zn(II) BovCA	7.05			8.9×10^{6a}	
Co(II) BovCA	7.05	1.7×10^5	2.4		

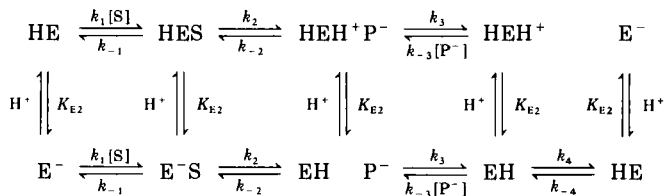
^a $k_{\text{cat}}/K_m \text{ mol}^{-1} \text{ sec}^{-1}$.

We have seen that a group in the active site with a pK_a near neutrality controls the catalytic activity, so that hydration requires the basic form and the rate of hydration increases with pH and that of dehydration decreases. The pH-rate profile takes the form of a simple sigmoid titration curve in the case of HCAC (35). We may note that although BovCAB and HCAC are kinetically similar in some respects (107–109), for the B isozyme the situation is more complicated because the state of ionization of additional groups appears to influence the rate (107), and this has been confirmed by bromoacetate binding studies (110, 111).

These studies use the fact that BrCH_2COOH carboxymethylates His 200, which is near the zinc ion. (The carboxymethylated HCAB has its own CO_2 -hydration and esterase activity, 2.5–20% that of unmodified HCAB, depending upon substrate). When 90% ^{13}C -labeled bromoacetate is used, only one ^{13}C -NMR peak not found in HCAB or in unenriched carboxymethylated HCAB is found: therefore the ^{13}C label is functioning as a probe. The probe signal shifts with pH, and the shift-pH data can be fitted to a curve with two pK_a 's of 6.0 and 9.2, but not to a curve with a single pK_a . The former value could be due to the imidazole side chain of His 200, and the latter to a zinc-bound water molecule.

It is interesting that modification of His 200 may also increase the rate of exchange of anions at zinc (133).

This is discussed in detail elsewhere (35) but, to summarize, a general mechanistic scheme (Scheme 2) (78, 112, 113, 115) assumes that two ionizing groups are present. One of these is the catalytically active group, and the enzyme with this group protonated is represented as EH; the other ionizing group is responsible for transferring protons between the solution and the catalytically active group: the enzyme with this group protonated is represented as HE.



SCHEME 2

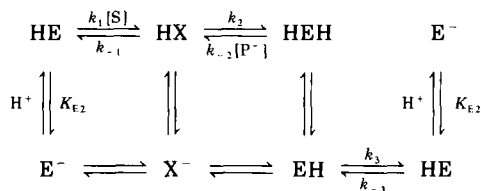
This scheme replaces an earlier one (116) which is unable to account satisfactorily for the pH dependence of the Michaelis parameters.

The scheme also assumes that the basic form of the catalytic group is required for the binding of CO_2 , and the acidic form for the binding of HCO_3^- ; however, product-inhibition studies indicate that CO_2 does bind weakly to the acidic form (113).

An important feature is that proton transport occurs in two stages; there is an intramolecular transfer between the two active-site groups, and the transfer to solvent, which is necessarily buffer mediated (117–119), occurs independently of the rest of the catalytic cycle (112). At sufficiently low buffer concentrations, this latter step limits the rate of the catalyzed reaction (115, 120, 121), and there is also some buffer dependence for $k_{\text{cat max}}$; this may indicate that the proton-transfer group represents a specifically bound buffer molecule rather than an amino acid residue. In this connection a specific interaction of imidazole with HCAB has been noted (69). Indeed, the X-ray analysis of the HCAB–imidazole complex has been determined: the imidazole lies in a hydrophobic pocket binding directly to the metal at a fifth coordination site (122).

The analysis has been applied to the interpretation of the kinetics of reaction in $^1\text{H}_2\text{O}$ and $^2\text{H}_2\text{O}$ (112, 113, 115), of product inhibition, and of the results of a ^{13}C -NMR study (78).

The rate constants in Scheme 2 cannot all be obtained from accessible kinetic data, but the scheme may be simplified to give Scheme 3, where



SCHEME 3

again EH represents the protonated catalytic group ($K_{\text{E}1}$) and HE represents the protonated transfer group ($K_{\text{E}2}$) in Scheme 2. ES^- and EHP^- , the transitory complexes, are symbolized by X^- . While this is an oversimplification, rate constants and pK_a values can now be found that are in accord with all the experimental data (Table VIII).

We note that $K_{\text{E}1}$, the dissociation constant of the protonated catalytic group, is related to that of the proton transfer group and is given by: $K_{\text{E}1} = k_3 K_{\text{E}2} / k_{-3}$. An interesting feature of the data in Table VIII is the large isotope effect on k_3 and to a lesser extent on k_{-3} corresponding to the proton transfers between the catalytically active group and the proton transfer group of the enzyme. The intramolecular

TABLE VIII
RATE CONSTANTS ($\pm 20\%$)
FOR THE HCAC-CATALYZED INTERCONVERSION
OF CO_2 AND HCO_3^- AT 25°C IN 50 mM
TRIS-SULFATE BUFFER^a

Constant ^a	Solvent	
	$^1\text{H}_2\text{O}$	$^2\text{H}_2\text{O}$
$k_1 (\text{mol}^{-1}\text{sec}^{-1})$	3×10^8	3×10^8
$k_{-1} (\text{sec}^{-1})$	2.5×10^6	2.5×10^6
$k_2 (\text{sec}^{-1})$	1.5×10^6	1.5×10^6
$k_{-2} (\text{mol}^{-1}\text{sec}^{-1})$	3×10^7	3×10^7
$k_3 (\text{sec}^{-1})$	3×10^6	0.3×10^6
$k_{-3} (\text{sec}^{-1})$	0.7×10^6	0.2×10^6
$\text{p}K_{\text{E1}}$	6.9	7.5
$\text{p}K_{\text{E2}}$	7.5	7.7

^a From Scheme 3 (113).

proton transfer step is not quite rate-limiting in $^1\text{H}_2\text{O}$ but becomes so in $^2\text{H}_2\text{O}$.

3. Hydrolytic Reactions

Carbonic anhydrase, as well as catalyzing the hydration of the carbonyl group (123–125), can also function as an esterase (126), and a well studied substrate, used in activity assay, is *p*-nitrophenyl acetate (Table IX) (44, 78, 106, 127). The pH-rate profile of *p*-nitrophenyl acetate hydrolysis is sigmoidal for BovCAB, HCAB, and HCAC, and there appears to be a close correspondence with the pH-dependence of the CO_2 hydration reaction (32). The complex behavior of HCAB becomes more marked during anionic inhibition of the esterase

TABLE IX
MICHAELIS PARAMETERS FOR *p*-NITROPHENYL ACETATE HYDROLYSIS AT 25°C

Isozyme	pH	k_{cat} (min^{-1})	K_{m} (mM)	$k_{\text{cat}}/K_{\text{m}}$ ($\text{min}^{-1}\text{mmol}^{-1}$)	Ref- erence
Zn(II) HCAC	8.1	1300 ± 100	8.7 ± 0.2	150	(127)
Co(II) HCAC	8.1			130	(78)
Zn(II) HCAB	8.2	150 ± 10	4.5 ± 0.2	33	(127)
Co(II) HCAB	8.2	200	4	50	(127)
Zn(II) BovCAB	7.0	7.8	1.4	5.6	(106)
	9.0	66	8.6	7.6	(44)

activity; there are at least two independent ionizing groups (87), one with pK_a 7.3 and another with pK_a 6.1, and the latter group affects only the *p*-nitrophenyl acetate K_m value. Linear free-energy relationships indicate that the hydrolysis mechanism is similar for Zn(II) HCAC and Zn(II) HCAB and probably also for Co(II) HCAB (127).

A biphasic pH-activity profile is observed in the case of long-chain and branched alkyl esters of *p*-nitrophenol (128, 129) (Fig. 5).

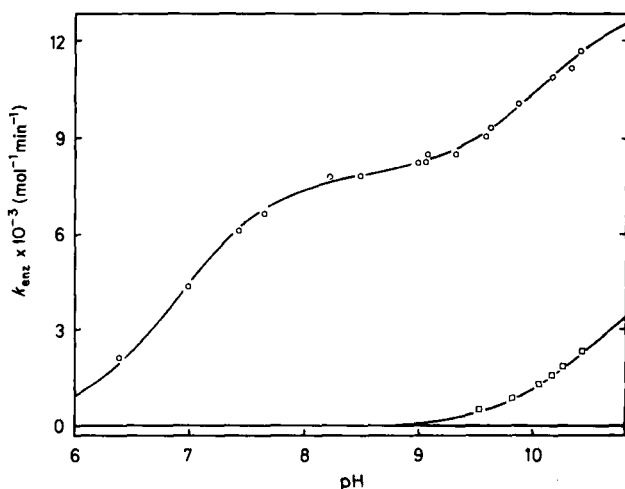


FIG. 5. pH dependence of k_{enz} for the enzymic hydrolysis of *p*-nitrophenyl propionate at 25°C. \circ , BCAB; \square , alkylated BCAB. k_{enz} is defined, for the ester hydrolysis in presence of buffer, B, by the equation

$$k_{obs} = k_o + k_{H_3O^+} [H_3O^+] + k_{OH^-} [OH^-] + k_{HB} [HB] + k_B [B^-] + k_{enz} [E]$$

Reproduced from Wells *et al.*, (129).

There are two points of inflection, one around neutrality, reflecting ionization of the active-site catalytic group(s), and the second above pH 10. A detailed analysis of this high-pH activity, which involved a study of acetazolamide-inhibited HCAB and mono- and dialkylated derivatives of HCAB, indicated that the second site, represented by the high-pH ionization, is outside the active site cavity (130). Other substrates hydrolyzed catalytically by carbonic anhydrase include methylpyridyl carbonates (96), *p*-substituted phenylesters (131), 3-pyridyl and nitro-3-pyridyl acetates (132) and mono- and disubstituted derivatives of carbonic acid (96).

E. THE ACTIVITY-LINKED GROUP AT THE ACTIVE SITE

1. *Possible Candidates*

The results of modification studies have indicated that His 64, once implicated in the catalytic mechanism (112), is not the ionizable catalytic group since there is residual activity in HCAC carboxyketo-methylated at His 64 (134). However, the group could be another active-site histidine (135–137). Another possibility is that the metal-bound water molecule ionizes to provide the necessary nucleophile in the form of zinc-bound hydroxide ion (117, 119, 137, 138) and recently a third candidate for the ionizable group was suggested, viz., the carboxyl group of Glu 106, which occurs in a hydrogen-bonded sequence: Glu 106–Thr 199–H₂O · Zn (122).

Detailed NMR studies on the protons of the histidine residues in zinc and cobalt HCAB (69, 139, 140) and HCAC (70, 139, 140) indicate that the catalytic group is Zn—OH₂ rather than an active-site histidine. However, His 64 may be the proton transfer group (112) so that in Schemes 2 and 3 EH could contain $\equiv \text{ZnOH}_2$ as the active group and HE could have His 64 as the proton transfer group. The $\text{p}K_a$ derived from the NMR studies on HCAC is consistent with this (70), and the X-ray crystallographic results indicate that the residue is ideally set up for this role. In HCAB, however, the $\text{p}K_a$ of His 64 is at least 2 units below that of the catalytic group, and this casts some doubt on its proposed role in proton transfer in this isozyme.

It has been suggested that the enzyme may employ two catalytic groups, depending upon the substrate; for example, the zinc-bound hydroxide could be active in CO₂ hydration, and an imidazole site could be active in ester hydrolysis (141).

2. *Relaxation Measurements on Solvent Water*

Observations of the increased relaxation rate of protons in the coordination sphere of a paramagnetic ion in a metallocarbonic anhydrase have allowed the determination of proton exchange rates and metal-to-proton distances (142, 143).

The results on the cobalt-substituted enzymes can be explained, approximately, in terms of an alkaline form of the enzyme, in which the cobalt binds a water molecule or a hydroxide ion, the protons of which have residence times $\ll 34 \mu\text{sec}$ or $17 \mu\text{sec}$ and distances of 0.285 nm and 0.25 nm from the metal, respectively; and in terms of an acid form of the enzyme in which, it was previously thought, the cobalt either has a bound water molecule, the protons of which have a residence time $> 0.2 \text{ msec}$ (perhaps due to strong hydrogen bonding), or has no bound

group possessing exchangeable protons (144). Bertini and co-workers (145), however, have recently demonstrated the presence of these exchangeable protons. It is suggested that earlier studies may be in error owing to the presence of sulfate that interacts with the metal ion and reduces the proton exchange rate. More detailed observations also indicate that at least two ionizations with pK_a values between 6 and 8 are revealed in the relaxivity measurements on Co(II) BovCAB (146). The pH dependence up to pH 9 is similar to that of the enzymic activity. The data are inconsistent with the location of the exchangeable proton on a histidine ligand, but consistent with an ionizable metal-bound water molecule.

^{13}C and ^{18}O tracer studies of the carbon dioxide-bicarbonate interconversion and of the labeling of H_2O are consistent with NMR data (120); from the results of these experiments it was concluded that the metal-bound hydroxide has a long lifetime at low pH.

The sulfonamide inhibitors acetazolamide and ethoxazolamide (see Section F) abolish the proton relaxation enhancement, and this is also true for the monobromacetazolamide-alkylated Co(II)BovCAB. There is an increase in the relaxation enhancement at high pH (>9), which may imply a conformational change of the enzyme (146).

The results of the relaxation studies in the presence of Mn(II)-BovCAB can also be interpreted in terms of a metal-bound H_2O or OH^- . A peculiarity in these results is that while sulfonamides reduce the enhancement to the order of that observed at low pH values, the anions N_3^- and NO_3^- , which are also inhibitors of the native enzyme, have no effect. In this case the anions may enter a fifth coordination position, so that a metal-bound water molecule with exchangeable protons remains (143).

The protons of the water ligand could exchange by whole-molecule exchange, or by a cyclic proton-exchange mechanism. While the exchange rates of ^{17}O and ^1H of H_2O coordinated to simple transition-metal complexes are identical, indicating whole-molecule exchange (147, 148), a complex possessing a bound water molecule with a low pK_a has not yet been studied, in this case the cyclic exchange mechanism may dominate.

3. An Ionizable Water Ligand

It is interesting that studies on model systems such as that shown in Fig. 6 demonstrate that the pK of the zinc-bound water may approach 7 if the coordination number of zinc in the complex is 4 or 5 (99a) (Table X). The metal-bound hydroxide has sufficient nucleophilic power to account for the enzyme's activity in acetaldehyde hydration, although

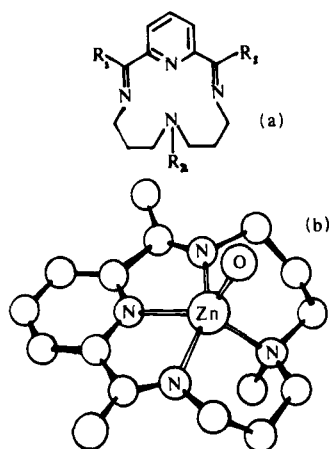


FIG. 6. Macrocyclic ligands based on 2,6-dicarbonyl pyridines. (a) The free ligand. (b) In the complex the four nitrogen atoms coordinate to a metal ion, Zn^{2+} , Cu^{2+} , Ni^{2+} , or Co^{2+} , which also binds a water molecule. The skeleton of the $\text{Zn}(\text{N-MeCR})(\text{H}_2\text{O})^{2+}$ complex is shown (H omitted; unlabeled atoms are C). CR: $\text{R}_1 = \text{CH}_3$, $\text{R}_2 = \text{H}$; N-MeCR: $\text{R}_1 = \text{R}_2 = \text{CH}_3$; *desdi*MeCR: $\text{R}_1 = \text{R}_2 = \text{H}$ (99a).

not in carbon dioxide hydration *if* the zinc environment were the same in the enzyme as in CR complexes (99a, 149); however, a poorly solvated nucleophile would, in a nonpolar environment, be more reactive (141), a point we shall return to later. Certain other inactive metallocarbonic anhydrases, e.g., those containing copper and vanadyl ions (150), show

TABLE X
IONIZATION OF WATER BOUND TO METAL IONS (M) IN MACROCYCLIC COMPLEXES^a
 $\text{p}K_a$'s FOR THE PROCESS^b: $\text{M}(\text{ligand})\text{OH}_2^{2+} \rightleftharpoons \text{M}(\text{ligand})\text{OH}^+ + \text{H}^+$

Ligand ^c	M	Temperature (°C)	$\text{p}K_a$	Approx. heat of ionization (kcal mol ⁻¹)
CR	Zn	25	8.69	7.1 ± 1
CR	Zn	0	9.17	
CR	Cu	25	11	
CR	Ni	25	11	
CR	Co	25	8 ^d	
N-MeCR	Zn	25	8.12	8.3 ± 1
N-MeCR	Zn	0	8.68	
N-MeCR	Cu	25	11	
<i>desdi</i> MeCR	Zn	25	8.13	6.0 ± 1
<i>desdi</i> MeCR	Zn	0	8.53	
(H ₂ O) ₅	Zn, Co	—	10	
Apocarbonic anhydrase	Zn, Co	—	7	

^a From Woolley (99a).

^b Aqueous solutions; ionic strengths in the range 0.002–0.04 M.

^c Ligand nomenclature is given in Fig. 6.

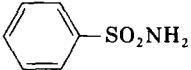
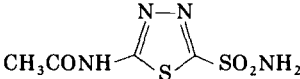
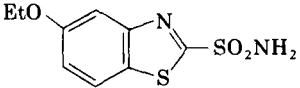
^d An approximate value only; cluster formation prevented a more accurate determination.

an ionization having a pK_a around neutrality and *provided that the active site structure of the two metalloenzymes does not differ significantly from that of the Zn holoenzyme* (which is not very likely), it must be shown that this does not represent a metal-bound water before the zinc-bound hydroxide nucleophile mechanism is accepted unequivocally (99a).

F. INHIBITION BY SULFONAMIDES

Sulfonamides are the most potent and selective inhibitors of animal and bacterial carbonic anhydrase (31, 32, 151), and inhibition by the sulfonamide acetazolamide (pK_i 7-8, Table XI) has become an accepted criterion for the active-site-directed nature of any process associated with the enzyme (130).

TABLE XI
INHIBITION CONSTANTS OF HCAC FOR VARIOUS SULFONAMIDES

Sulfonamide	K_i (M)	References
Benzene sulfonamide 	2×10^{-5}	(153)
<i>p</i> -NO ₂ benzene sulfonamide	5×10^{-7}	(154, 155)
<i>p</i> -NH ₂ benzene sulfonamide (sulfanilamide)	8×10^{-6}	(154, 155)
<i>p</i> -CH ₃ benzene sulfonamide	8×10^{-6}	(153)
Acetazolamide 	6×10^{-8}	(34)
Ethoxzolamide 	10^{-9}	(34)

Coleman (152) has reviewed physical studies on the interaction of sulfonamides with carbonic anhydrase, and the structure-inhibition relationships have been reviewed by Maren (31); the most powerful inhibition is found when an aromatic ring is substituted with a free sulfonamide group (Table XI) (34, 153-155).

The strong binding of the sulfonamides has been used as the basis of a convenient method of determining the enzyme concentration: the

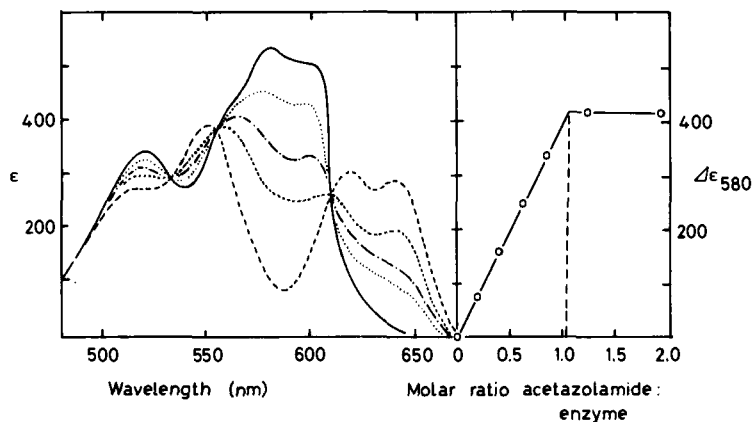


FIG. 7. The visible absorption spectrum of Co^{2+} carbonic anhydrase at different concentrations of acetazolamide, measured at 25°C, pH 8.0. The enzyme concentration was $6.9 \times 10^{-5} \text{ M}$. The curves on the left represent the spectra at acetazolamide concentrations of 0 M, $2.8 \times 10^{-5} \text{ M}$, $4.2 \times 10^{-5} \text{ M}$, $5.6 \times 10^{-5} \text{ M}$, respectively. The diagram on the right shows the increment in extinction coefficient at 580 nm ($\Delta\epsilon_{580}$) as a function of the molar ratio of inhibitor to enzyme. [Reproduced from Lindskog (157).]

activity of the carbonic anhydrase solution is titrated with acetazolamide or ethoxazolamide (156); the visible absorption spectrum of the cobalt enzyme can be titrated in a similar manner (Fig. 7).

Both Co(II) and Zn(II) BovCAB bind acetazolamide stoichiometrically; however, the affinity is reduced by at least two orders of magnitude in other metallocarbonic anhydrases and is comparable with binding to the apoenzyme (157, 158).

Sulfonamide complexes of Zn(II) HCAC and Zn(II) HCAB have been studied by X-ray crystallography; the sulfonamide nitrogen or oxygen binds the zinc (62), and a second atom of the sulfonamide group may form an additional long bond with the metal (159). This rather irregular coordination geometry is consistent with recent magnetic susceptibility measurements (160). A distorted tetrahedral coordination is also suggested by absorption and MCD spectroscopic studies (88, 161) and by ESR studies on the cobalt enzymes in the presence of various sulfonamides (52).

Further hydrogen bond and van der Waals's interactions with the hydrophobic part of the active site cavity (159) restrict sulfonamide motion (162, 163) (Fig. 8).

The nonpolar nature of the sulfonamide binding site is consistent with the changes observed in the fluorescence and absorption spectra of certain sulfonamides (34, 156); evidence for the involvement of tryptophan and tyrosine residues in the interaction is provided by UV

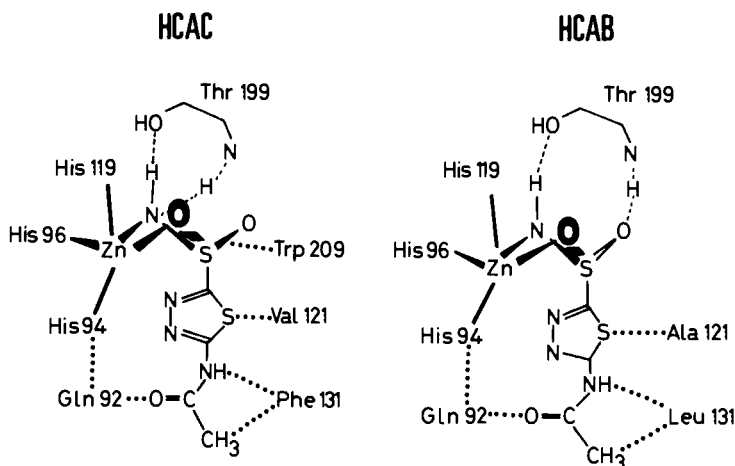
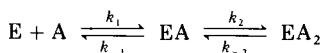
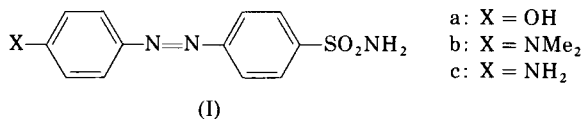


FIG. 8. Protein-sulfonamide interactions: the acetazolamide complexes of HCAC and HCAB. The sulfonamides are coordinated in the anionic form. ---, hydrogen bonds; ·····, van der Waals contacts. [Details from Kannan *et al.* (159).]

difference spectroscopy experiments (164) and triplet-triplet energy transfer studies (165, 166). The apoenzyme retains a significant affinity for the sulfonamides (K_1 acetazolamide = 10^{-4} M), which indicates that van der Waals and hydrogen bond interactions may play a large part in stabilizing the holoenzyme complexes—indeed it has been concluded from the results of NMR and fast-binding kinetic studies that sulfonamides initially bind to the enzyme without coordinating the metal (153, 167) and that this initial complex then isomerizes into one in which the sulfonamide group is so coordinated; i.e., kinetic studies require a scheme of the type:

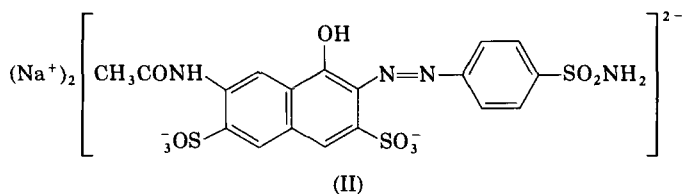


On the other hand, the kinetics may depend on the sulfonamide structure, thus, in the binding of the azosulfonamide (I) to bovCA the rapid kinetics of the induced CD and difference spectra proceed in parallel, indicating that a single binding process is being observed (168).



NMR studies on several sulfonamide complexes of human CA indicate that enzyme conformational change is involved. It is suggested that

inhibition of CA involves the following: stabilization of an appropriately oriented initial complex through the hydrophobic binding of the aromatic ring of the inhibitor to residues of the active site cavity; ionization of the $\text{—SO}_2\text{NH}_2$ group, facilitated by the proximity of the zinc ion; protonation of the proton-accepting ligand controlling catalytic activity; and the formation by the SO_2NH^- group of an ionic bond to zinc and a hydrogen bond to the hydroxy group of serine (in HCAB) or threonine (in HCAC) (140). Evidence has been obtained from resonance Raman experiments for the presence of the $\text{—SO}_2\text{NH}^-$ group in the complexes of I(a-c) with various isozymes of CA, and it seems that in these cases hydrophobic binding can be ruled out (169). The affinity of the enzymes for sulfonamides varies with pH (82); it is the second association reaction that is affected (153, 167), the isomerization probably being selective for the ionized sulfonamide and the acid form of the catalytic group in the enzyme (153). A number of investigators have concluded that the sulfonamide is complexed as the anion (155, 156, 164, 171), although the results of a recent resonance Raman spectroscopic study indicate that neoprontosil [disodium 2-(4'-sulfamyl phenylazo)-7-acetamido-1-hydroxy naphthalene 3,6-disulfonate (II)], binds in the neutral form (172). The lifetime of the complex



at $\text{pH} < 10$ is dominated by k_{-2} , there is little hydrophobic dependence, the stability of the complex depending mainly upon the coordination energy of the metal-sulfonamide bond; at $\text{pH} > 10$, however, the affinity decreases markedly, indicating dependence upon a group in the enzyme with $\text{p}K_a > 11$ (153). In an homologous series of sulfonamides, the increase in binding constant at low and intermediate pH is therefore due mainly to an increase in the association rate constant [$k_{\text{ass}}(\text{acetazolamide}) = 10^5\text{--}10^7 \text{ mol}^{-1}\text{sec}^{-1}$].

Amino acid differences at the active sites result in different modes of sulfonamide interaction with HCAC and HCAB (Fig. 8), and this can result in marked differences in association and dissociation rates (Table XII), for example, benzene sulfonamides substituted at the ortho position show a relative decrease in affinity for HCAC compared to HCAB (152).

TABLE XII
ASSOCIATION (k_a) AND DISSOCIATION
(k_d) RATES FOR DANSYLAMIDE BINDING
TO THE HUMAN CARBONIC ANHYDRASE
ISOZYMES^a

	k_a (mol ⁻¹ sec ⁻¹)	k_d (sec ⁻¹)
HCAC	2.4×10^5	0.390
HCAB	1.34×10^5	0.030

^a From Coleman (152).

The interactions in the acetazolamide complexes are different from those in the sulfanilamide complexes; in particular, there is an additional interaction with Gln 92 on the hydrophobic side of the cavity (Fig. 8). Mutual inhibition experiments indicate that acetazolamide and HCO_3^- compete for a binding site which is the same as that for aldehyde hydrates but different from that used by esters (173). Since the dissociation from the complex is slow, preequilibration of acetazolamide with the enzyme results in pseudoirreversible inhibition (82) so that, for example, inhibition of CO_2 hydration is apparently non-competitive.

G. INHIBITION BY ANIONS

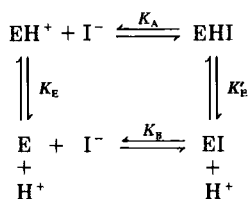
1. General Features

The manner in which anions bind to a metalloenzyme is a question of great interest to the inorganic chemist.

Monovalent anions are inhibitors of carbonic anhydrase (174), but divalent anions are not (105, 157)*; some apparent anion inhibition constants are given in Table XIII (44, 82, 86, 153, 174a).

The reversible inhibition of the CO_2 hydration activity of Co(II) and Zn(II) carbonic anhydrase by anions is noncompetitive (44, 175) whereas the dehydration reaction is inhibited competitively (32); the inhibition of the esterase activity is also noncompetitive (82, 173). The anionic inhibition is pH-dependent, being controlled predominantly by the ionization of the catalytic group; for the salts of relatively strong acids ($\text{p}K_a < 5$), the interaction with HCAC can be described approximately by Scheme 4, with $K_A \ll K_B$, that is, the interaction with the acid form of the enzyme is favored.

* Although, we have seen, there is evidence (145) that the SO_4^{2-} ion is not innocuous.



SCHEME 4

A more complex situation exists for H_2S and HCN , where HX also interacts with the alkaline form of the enzyme to yield $\text{EH} \cdot \text{X}$ (176). In the presence of anions, the $\text{p}K_a$ of the activity-linked group is shifted to higher pH values, the stronger binding anions causing the greater shifts (89).

Studies of mutual inhibition (81, 110, 173, 175, 176), $[\text{}^3\text{H}]$ acetazolamide binding (158, 177), and $^{35}\text{Cl}^-$ NMR line broadening (178, 179)

TABLE XIII
APPARENT ANION INHIBITION CONSTANTS FOR CARBONIC
ANHYDRASE, MEASURED FROM THE INHIBITION OF THE
CATALYZED HYDROLYSIS OF *p*-NITROPHENYL ACETATE (35)

Anion	K_i	M	
		BovCA ^a	HCAC ^{b,c}
HS ⁻	1.9×10^{-6}	—	—
CN ⁻	3.2×10^{-6}	—	—
OCN ⁻	3.9×10^{-5}	—	—
NCS ⁻	5.9×10^{-4}	8×10^{-4}	7×10^{-4}
N ₃ ⁻	5.9×10^{-4}	—	—
I ⁻	8.7×10^{-3}	3.1×10^{-3}	2×10^{-3}
ClO ₄ ⁻	1.6×10^{-2}	1.5×10^{-3}	1.3×10^{-3}
HCO ₃ ⁻	2.6×10^{-2}	—	—
HSO ₃ ⁻	3.0×10^{-2}	—	—
NO ₃ ⁻	4.8×10^{-2}	1.8×10^{-2}	1.5×10^{-2}
Br ⁻	6.6×10^{-2}	2.7×10^{-2}	2.3×10^{-2}
CH ₃ COO ⁻	8.5×10^{-2}	3.4×10^{-2}	2.6×10^{-2}
Cl ⁻	1.9×10^{-1}	2.0×10^{-1}	3.0×10^{-3}
F ⁻	1.2	—	0.4

^a pH 7.55, 25°C. Data from King and Burgen (153) except for HS⁻, CN⁻, OCN⁻ (82); the values for HS⁻ and CN⁻ are calculated on the basis of total sulfide and cyanide ($\text{HX} + \text{X}^-$).

^b 25°C. Data are from Verpoorte *et al.* (44) for HCAC, pH 6.8, and HCAB, pH 7.3, except for $K_i(\text{Cl}^-)$.

^c Data for $K_i(\text{Cl}^-)$: from Whitney (174a) for HCAC, pH 6.5; from Whitney and Brandt (87) for HCAB \lesssim 6.

show that the anions compete with each other as well as with acetazolamide for the same or overlapping sites in the zinc and cobalt enzymes. The inhibition may not be so simple, however, for while the strength of inhibition appears to reflect a binding to the metal for the more potent anionic inhibitors, the weaker inhibitors ($K_i \geq 10^{-3} M$) conform to the Hofmeister lyotropic series (180), which reflects the effects that the anion has upon the water structure at the binding site (181); this could be taken as evidence of ion-pair formation.

The different modes of anion-metal interaction are also reflected in the visible absorption, ORD, and CD spectra of the Co(II) carbonic anhydrase-anion complexes (32, 175, 182) (Fig. 9).

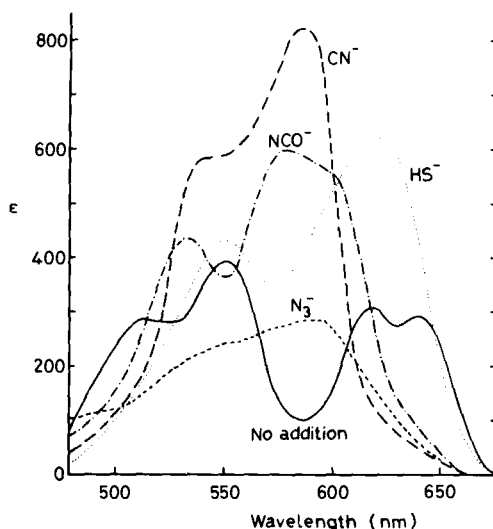


FIG. 9. The visible absorption spectra of Co^{2+} -bovine carbonic anhydrase saturated with different inhibitors, pH 8.0, 22°C. Enzyme: $3.5 \times 10^{-4} M$ to $4.2 \times 10^{-4} M$ giving absorbances of 0.1–0.29. Inhibitor: cyanide, $8.4 \times 10^{-3} M$; cyanate, $4.2 \times 10^{-3} M$; sulfide, $4.8 \times 10^{-4} M$; azide, $8.4 \times 10^{-3} M$. [From Lindskog (157).]

The metal in the cyanide complex is tetrahedrally coordinated, but the other complexes show distinct distortions from this geometry and may have pentacoordination. The changes in the absorption spectra parallel the inhibition of CO_2 hydration (175, 183) and ester hydrolysis (110) at low pH; however, unlike the inhibitory effects, the spectral changes of Co(II) BovCAB give no indication of a weak association between the anions and the basic form of the enzyme (175).

In some cases the anion is directly bound to the metal; this has been confirmed for N_3^- by infrared studies (184) and for CN^- by NMR (176)

and ESR (71, 185) studies. The results of $^{35}\text{Cl}^-$ (178, 186, 187) and $^{81}\text{Br}^-$ (133) NMR relaxation enhancement studies in the presence of the zinc and cobalt carbonic anhydrases also indicate a metal-halide interaction. It has been suggested, however, that this interaction is more like that of a charge-transfer complex, since $\log K_1$ values of the Zn(II), Co(II), and Cu(II) BovCAB halides depend linearly on the redox potential of the X_2/X^- couple (188). Charge-transfer bands are indeed observed, in particular for the iodide complex, and the zinc-halide distances determined from X-ray crystallography (Br^- , 3.0 Å; I^- , 3.4 Å) (72) are consistent with this interpretation.

2. The Question of Two-Anion Binding Sites

The X-ray studies indicate that there are two anion binding sites within the active site cavity. The anion binding positions were derived exclusively by difference techniques from crystals of HCAC prepared in 20 mM Cl^- ; since it has been reported that one Cl^- binds to the native enzyme in 5 mM KCl (44), the results of these investigations must be treated with some caution. However, any chloride binding interference would result only in the observation of fewer binding sites than are actually present, for those anions which bind less tightly than Cl^- or are about as electron dense as Cl^- ; thus for the enzyme-iodide complex, both the binding sites may be observed.

The first site represents a direct interaction with the metal (Fig. 10) to give an inner sphere complex. In this site chloride is bound to zinc

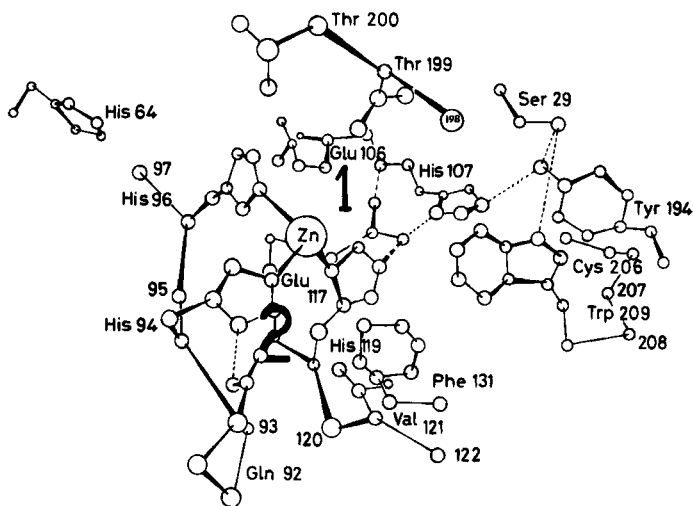


FIG. 10. The anion binding sites of HCAC, as reported by Vaara (72).

while the larger iodide interacts significantly with Thr 199; this hydrogen bond interaction may account for the marked stability of the anionic complexes and for the fact that *both* the holo- and apoenzymes bind the same numbers of anions at high salt concentrations (44).

The second site (Fig. 10) was demonstrated clearly for $\text{Pt}(\text{CN})_4^{2-}$, AuCl_4^- , and $\text{Au}(\text{CN})_2^-$ (Fig. 11). Iodide was also found at this site. The interaction appears to be with Gln 92, Phe 131, and with the zinc-bound water; i.e., it represents a metal outer-sphere site. The behavior of His 64 is also affected by occupancy of this site; in the presence of $\text{Au}(\text{CN})_2^-$ this residue shows an increased reactivity toward bromopyruvate (134) and methylmercurithioglycolic acid (72), although there is no apparent rearrangement of the amino acid residues.

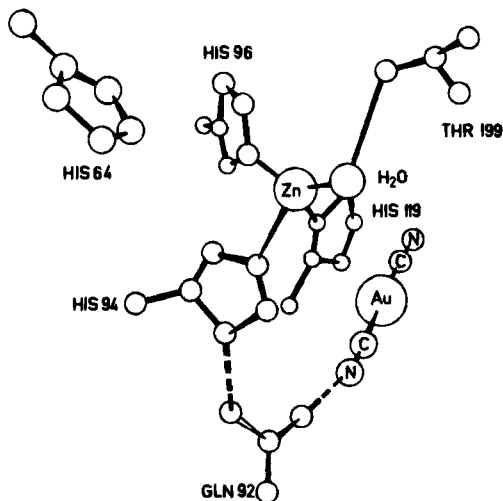


FIG. 11. The binding of $\text{Au}(\text{CN})_2^-$ at site 2 of HCAC. [From Vaara (72).]

We may note that iodide binding to the human B isozyme is influenced by a group with a $\text{p}K_a$ of 6.1, and this has been identified (189) as His 200. The results of X-ray crystallographic studies had indicated that a water molecule may separate the zinc and iodide ions in the enzyme-iodide complex, but X-ray absorption studies suggest that the iodide binds directly to the metal ion with a Zn-I distance of $2.65 \pm 0.06 \text{ \AA}$ (190). However, both studies required solid samples, and the behavior in solution may be different; the different pH values of the solutions from which the solids were isolated may have some bearing on these results. Under appropriate conditions there is little doubt that the iodide ion may occupy either of the two anion binding sites.

A third anion binding site is present on the surface of the enzyme and involves the amino acid residues Lys 24, Arg 246, Pro 13, Pro 247, and Glu 14.

The results from the crystal structures and NMR dispersion experiments indicate that sulfonamides and CN^- enter site 1 and displace the metal-bound water. However, in other cases, for example the halides or carboxylate anions (191–194), the anion may enter as a fifth ligand; the formation of a dicyanide complex of Co(II) carbonic anhydrase at very low temperatures indicates that five coordinate complexes do form (71, 185). The associative nature of this interaction has been invoked to explain the apparently high rates of formation of the anion complexes (195), although, as discussed below, this may not be necessary.

The anion $\text{Au}(\text{CN})_2^-$ reduces drastically the $^{35}\text{Cl}^-$ NMR line width induced by carbonic anhydrase (196); since the relaxation enhancement is due to binding at site 1, while $\text{Au}(\text{CN})_2^-$ binds at site 2, there must be significant cross-site interactions. For smaller anions, however, it has been suggested that the two anion binding sites in the active site cavity can be occupied simultaneously (197, 198); the primary evidence for this comes from the relaxation enhancement of the methyl protons of acetate induced by Zn(II) and Mn(II) BovCAB (197).

With *p*-toluene sulfonamide bound (i.e., site 1 occupied) a relaxation enhancement of the acetate protons is still observed, but this can be titrated with N_3^- ; azide on its own will titrate both sites independently

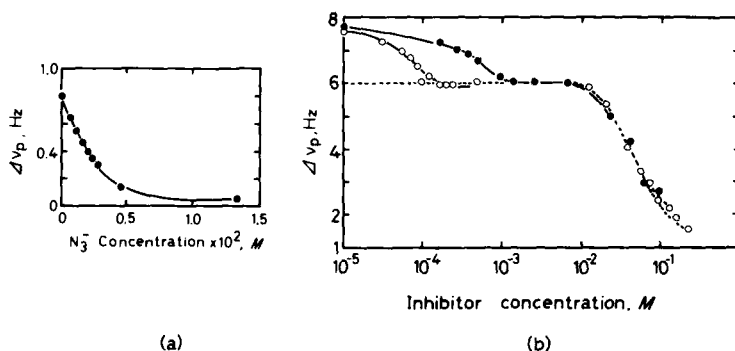


FIG. 12. (a) The net line broadening of acetate ion bound to bovine carbonic anhydrase B, upon titration with N_3^- . Enzyme concentration 0.98×10^{-3} M, and acetate 0.033 M. Tris-sulfate buffer in $^2\text{H}_2\text{O}$, pH 7.0, 30°C. (b) Titration of 0.5 M acetate bound to 2.07×10^{-4} M Mn(II) bovine carbonic anhydrase B by: ○—○, *p*-toluene sulfonamide; ●—●, N_3^- ; □—□, N_3^- to solution of enzyme containing 6.5×10^{-4} M *p*-toluene sulfonamide. All the $^2\text{H}_2\text{O}$ solutions contained 2×10^{-4} M MnCl_2 in 0.01 M Tris-sulfate buffer, pH 7.5. [Reproduced from Lanir and Navon (197).]

(Fig. 12). Acetazolamide, which interacts significantly with Gln 92 at site 2 (Fig. 8) may be expected to inhibit the relaxation enhancement completely if this represents the second site detected by NMR. The conclusion, based on the NMR and esterase inhibition results, must be that there are two anion-binding sites and that the first represents a weak-binding inhibitory, metal inner-sphere site, and the second a stronger, but noninhibitory, interaction with the protein, not necessarily within the active-site cavity (Table XIV). However, the results are consistent with binding at sites 1 and 2.

TABLE XIV
INHIBITOR BINDING CONSTANT FOR BOVCA (197)

Metal	$K_1 M^{-1}$				
	Inhibitory site			Noninhibitory site	
	CH_3COO^-	N_3^-	$p\text{-CH}_3\text{-sulfonamide}$	CH_3COO^-	N_3^-
Zn	9	$\sim 1.2 \times 10^3$	2.1×10^6	35	$\sim 1.2 \times 10^3$
Mn	0.8	2.8×10^3	2.6×10^4	29	2.8×10^2

Although an earlier study of the interaction of acetate and mono-, di- and trifluoroacetate with Co(II) HCAC, using ^1H and ^{19}F NMR (190), gave no evidence for two binding sites, this may not be at variance with the above conclusions since in this case control spectra were run with *p*-carboxybenzene sulfonamide; this sulfonamide may not displace acetate at the second site so that the difference between the control and observed spectra represent a specific site 1 effect. In the case of Co(II) HCAC the linewidth in the presence of the sulfonamide was comparable with that in the presence of the zinc enzyme; however, the linewidth broadening was only of the order of a few Hertz and the effect of binding at site 2 may not be observable within the experimental error. For Co(II) HCAB a complete return to the natural linewidth was not always observed, and this was attributed to the presence of paramagnetic impurities; however, it could arise from significant second-site contributions. A second acetate binding site, titratable with azide but not with *p*-toluene sulfonamide, has been found in Co(II) BovCAB (194).

While azide binds to the second site with an affinity similar to that for the metal-binding site, it is interesting to note that a radiolabeled cyanide binding study indicates that if a second site exists for CN^- the concomitant dissociation constant is $> 2 \text{ mM}$, three orders of magnitude higher than that for site 1 (78).

The affinity of acetate ions for the noninhibitory site of Zn(II) Bov-CAB is pH dependent, the related enzymic ionizations having a similar pK_a to that which controls activity (197), as expected if the second site was site 2 and there was a site-site interaction; the binding to the noninhibitory site is not nullified in the basic form of the enzyme. The pH-dependent $^{35}\text{Cl}^-$ NMR relaxation in the presence of bovine carbonic anhydrase (Fig. 13) is also consistent with the two-site hypothesis provided that the binding to site 2 is very weak ($K_1 \gg 0.5\text{ M}$) in the basic form of the enzyme, or that binding in site 2 does not produce a significant effect on the line width. Both of these assumptions are reasonable. The titrations of the proton resonances of histidine with iodide (69, 70) also indicate that there are two anion binding sites in the cavity of Zn(II) HCAC and Zn(II) HCAB.

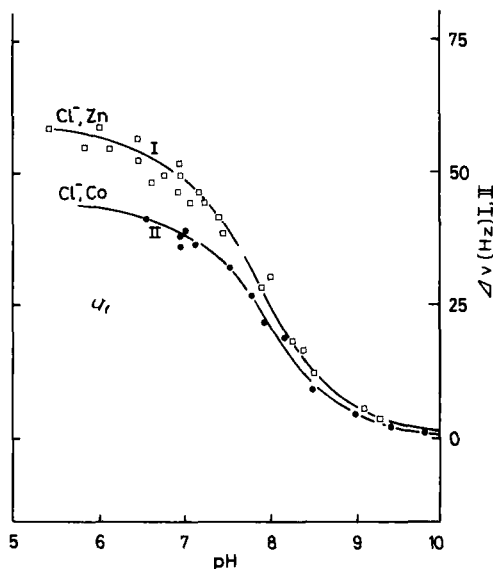


FIG. 13. Variation with pH of: (I) the increase in linewidth of the resonance of $^{35}\text{Cl}^-$ ions in a solution containing 0.5 M NaCl , upon addition of $23\text{ }\mu\text{M}$ native bovine carbonic anhydrase; (II) similar data for addition of $29\text{ }\mu\text{M}$ cobalt-substituted carbonic anhydrase. [Reproduced from Lindskog *et al.* (32); original data from Ward (178) and Ward and Fritz (187).]

Further evidence for the two-site hypothesis has been adduced from the observation of a binding constant, determined from $\text{H}^{13}\text{CO}_3^-$ NMR studies in the presence of Co(II) BovCAB, which is much less than that determined from esterase inhibition measurements (198); the deri-

vation of this binding constant is valid only if the $\text{H}^{13}\text{CO}_3^- - ^{13}\text{CO}_2$ system is in slow exchange on the NMR time scale (T_2) or there is a relatively small exchange contribution to the line width. Although further experimental data were analyzed in terms of two sites (198), it being suggested that the second site was an outer sphere site (i.e., site 2), the data can be analyzed in terms of single-site occupation; in this case a dissociation constant of 100 mM for the $\text{Co(II) BovCA-HCO}_3^-$ complex would yield a metal- $^{13}\text{C}(\text{HCO}_3^-)$ distance of 3.9 Å, consistent with inner-sphere coordination.

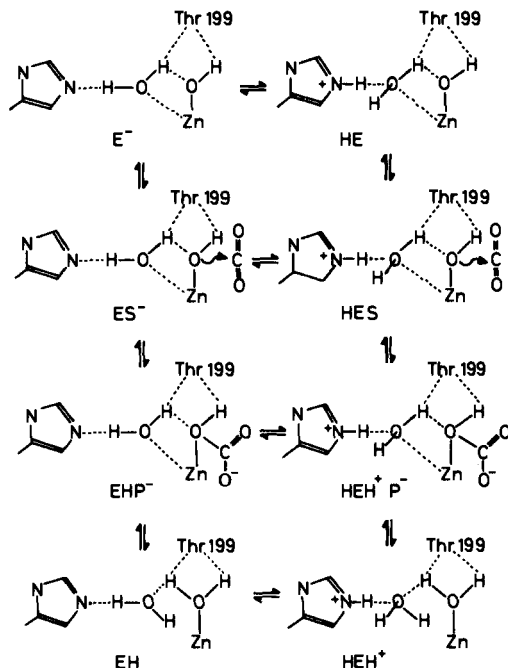
An investigation of the interaction of HCO_3^- with Co(II) HCAC , by ^{13}C NMR, has given no evidence for a second bicarbonate binding site (78), and proof of a second anion binding site on the enzyme, in solution. similar to that found for Co(II) BovCA (194, 197), is awaited. We see that from evidence at present available it appears that there may be two anion binding sites within the active-site cavity, a noninhibitory tight binding site and a weaker-binding inhibitory site. The anion interacts most strongly with the enzyme when the catalytic group is in its acidic form, but it also interacts, at both sites, with the alkaline form of the enzyme, but with reduced affinity. However, the question should probably not be regarded as closed; for example, since occupancy of the anion binding site affects the behavior of His 64, it would be expected that ionization of His 64 [i.e., ionization of the possible proton transfer group (112)] would affect anion binding; however, no evidence for this is found from the pH dependence of the anionic inhibition. For a deeper discussion of the kinetic aspects of anionic inhibition the reader is referred to Wyeth and Prince (35).

H. MECHANISM OF ACTION

Various physical techniques have shown us so far that the active site contains a proton-transfer group that may be an amino acid residue, possibly His 64, or a specifically bound buffer molecule, as well as a catalytic group that is probably an ionizable zinc-bound water molecule. The metal is four-coordinate at low pH and probably five-coordinate when the bound water molecule is ionized; this change in coordination may result in more mobile histidine ligands [the histidine proton resonances sharpen when the pH is raised (69, 70)] consistent with a small zinc displacement, possibly required to achieve the higher coordination number. This could explain the anomalous X-ray crystallography results for His 94. The relaxation spectra of complexes of the human carbonic anhydrases with aromatic sulfonamides are consistent with the view that the catalytic activity may be associated with the

capacity of the metal to undergo fast changes in coordination geometry (199).

The dehydration of ^{18}O -labeled HCO_3^- leaves an ^{18}O atom in the active site (120), and with this vital piece of experimental evidence in mind a plausible mechanism (Scheme 5) for the reversible hydration of



SCHEME 5

CO_2 may be proposed (46), in which the imidazole ring of His 64 is drawn as the proton-transfer group. Note that we may regard the active nucleophile not simply as an OH^- ligand bound to zinc, but as a co-ordinated H_3O_2^- ligand hydrogen-bonded to a proton acceptor group, His 64.

The bicarbonate ion does not displace the metal-bound water. However, more strongly binding anions, for example, CN^- and N_3^- , will do so, resulting in tetrahedral coordination about zinc. Significant hydrogen bond interactions with Thr 199 must be invoked, at low pH, to account for the results of the solvent proton relaxation studies.

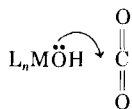
The results of the labeling studies indicate that the metal-bound hydroxide has a long lifetime at low pH, but that exchange is rapid at high pH (120). The high-pH form is E^- but the protonated form HE

also has the metal-bound hydroxide ion. His 64 (or the specifically bound buffer molecule) can assist the hydroxide displacement in E^- , or it may reduce the hydroxide dissociation rate in HE by virtue of the adjacent positive charge.

An increase in buffer concentration does increase the hydroxide-exchange rate (120). This scheme could also account for the fluctuations observed in the magnetic axis of cobalt in Co(II) HCAC (70), but fluctuating coordination of His 94 could also account for this.

Since hydroxide displacement from E^- is faster than from HE it might be expected that the rate for $ES^- \rightarrow EHP^-$ would be faster than $HES \rightarrow HEH^+P^-$, i.e., Scheme 2 is a poor description of the real system.

It is interesting that the nucleophilic power of a metal-coordinated hydroxide ion is considerably larger than would be expected from the pK_a of the corresponding aquo complex in inert d^3 and d^6 complexes (149), an effect reminiscent of the α -effect in general mechanistic chemistry (and possibly having a similar origin but with filled, or partially filled, d orbitals of T_2 symmetry playing the role of filled p orbitals). However, the zinc-bound hydroxide-nucleophile mechanism (99a, 149), in which the essential process is

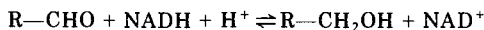


is unlikely to account for the full catalytic activity of the enzyme in CO_2 hydration (149), but an assisted attack with a hydrogen-bonded $H_3O_2^-$ ligand may do so. Also, the zinc ion may act as a Lewis acid, polarizing the CO_2 molecule; and the CO_2 molecule could be distorted toward the transition state conformation in its binding site: we have already seen (Section II,D1) that a Lewis acid-proton acceptor combination is particularly effective in the catalysis of CO_2 hydration. The infrared studies of Riepe and Wang (184), while indicating that CO_2 binds near the metal, give no indication of a conformational or polarization change. The difficulty is that these studies were performed at low pH and may represent CO_2 bound to HEH^+ (Scheme 2) which is *inactive* in CO_2 hydration; there may be subtle changes in the binding site as the pH is raised that result in a distortion of the CO_2 molecule. This illustrates the difficulty in determining the mode of CO_2 binding in the *active* form of the enzyme. It has been suggested, from the results of a ^{13}C NMR study, that the CO_2 binding site in HCAB is about 3.4 Å from the metal (200), although this result requires certain assumptions and could again represent binding to HEH^+ .

III. Zinc-Based Alcohol Dehydrogenases

A. INTRODUCTION

Alcohol dehydrogenases from various sources catalyze the reaction:



where NAD is nicotinamide adenine dinucleotide.

Reports of the oxidation of alcohols by different animal tissues appeared toward the end of the 19th century, and since that time the dehydrogenases, the cofactors NADH and NAD^+ , their analogs, and the various substrates have been the subject of an extensive literature. This survey is therefore confined to the metal ion involvement in the enzyme reaction, together with a brief resumé of the relevant background. More comprehensive reviews, particularly on the biochemical and structural aspects, are available. The dehydrogenases, such as LADH and YADH, illustrate again how knowledge of the involvement of the metal ion in an enzymic reaction may be sought: the effect of varying metal ion or metal ion content; the effect of metal-chelating agents; variation of cofactor, substrate, and inhibitors, together with X-ray, spectrophotometric, kinetic and equilibrium studies are all possible tools. There is again the added possibility of observing analogous nonenzymic reactions of simpler complexes, which may throw light on the possibilities open to the metal ion as it functions in the enzyme.

B. ENZYMES

Alcohol dehydrogenase activity occurs widely in natural systems (201, 201a) for example, in the livers of humans, fishes, horses, and rats, in plant tissues, in microorganisms, and in yeast. The enzymes do not possess pronounced substrate specificity and can react with a large number of normal and branched-chain aliphatic and aromatic primary and secondary alcohols and carbonyl compounds. The transfer of the formal hydride is direct between coenzyme and substrate and is stereospecific.

The first successful crystallization of a pure alcohol dehydrogenase was that from yeast (YADH) in 1937 (202), and that of LADH was reported in 1948 (203). Of all the reported dehydrogenases, LADH and YADH have been the most widely studied (the former somewhat more

than the latter) and are the two with which we are concerned here. LADH has a molecular weight now thought to be about 80,000 (204). Initial investigations, based on an incorrect molecular weight of $\sim 73,000$ (205), gave the number of gram atoms of zinc per mole of enzyme as 2 (206, 207). More recent studies, using purified enzyme, have shown the true value to be 4 (208).

The enzyme itself is a dimer (209) consisting of two identical subunits (210). Each subunit binds two zinc ions (210) and has one site at which to bind the coenzyme NADH in reductions, or NAD^+ in oxidations. The structure of the coenzyme is shown in Fig. 14.

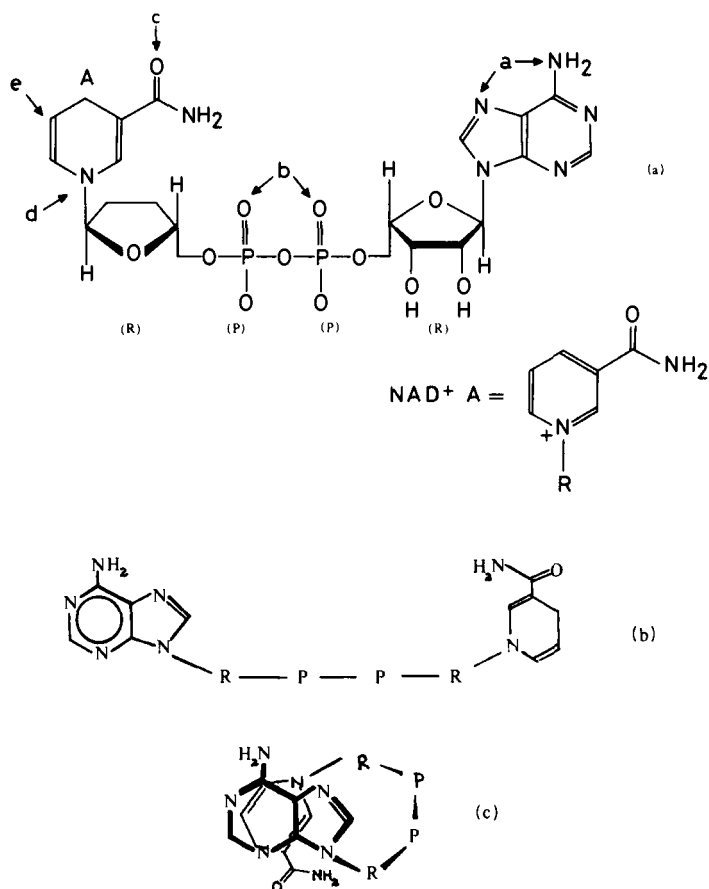


FIG. 14. (a) NADH, the coenzyme used by LADH and YADH; loss of a formal H^- from the 4-position of the nicotinamide ring gives NAD^+ the coenzyme for dehydrogenations. (b) The extended form of the coenzyme. (c) The coiled form of the coenzyme.

Improvements (211*a*) in crystallization techniques (211*b*) were needed for X-ray studies.

The primary sequence of 374 amino acids in each residue has been described (210) and X-ray structural studies of the whole enzyme (212) at 2.9 Å resolution and of the active site at 2.4 Å (213) have confirmed the dimeric natures and the presence of two coenzyme binding sites and have identified the positions of the four zinc ions. The X-ray studies are discussed further below: the gross features of LADH are that it is a dimer, with four zinc ions and two active sites.

YADH, on the other hand, is a tetramer (214) of molecular weight ~140,000, which contains four zinc ions (215). Initial work indicated that the enzyme bound 4 mol of cofactor per mole of enzyme (216), but more recent work by Dickinson (217) has suggested that the number is more probably 2.

C. METAL ION-REACTIVITY RELATIONSHIPS

1. LADH

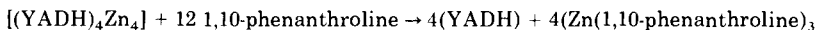
The evidence for zinc ion involvement in both a catalytic and a structural role in LADH has been reviewed (204, 217*a*). The enzyme is inhibited by metal-chelating agents, such as 1,10-phenanthroline and 2,2'-dipyridyl; the metal can be removed from the enzyme by dialysis against such metal-chelating agents, and the resulting apo- or "half-apo"-enzyme, depending on the system (204, and see below), is inactive. The activity can be regenerated by replacement of the metal ion using either zinc itself or cobalt.

The evidence for both a structural and a catalytic role for the metal ion comes from several sources. In phosphate buffer, for example, all the zinc ions will exchange with $^{65}\text{Zn}^{2+}$ within 24 hours (204), whereas in acetate buffer only two of the four do so, which indicates two different "types" of zinc. Inhibition by 1,10-phenanthroline is total at a ratio of 2 mol of 1,10-phenanthroline per mole of enzyme, and 1,10-phenanthroline binds to the "catalytic" zinc (212). Dialysis of the enzyme against EDTA can give an enzyme containing only two zinc ions, and this "half-apo" enzyme is inactive, 1,10-phenanthroline does not interact with the "buried" zinc (i.e., noncatalytic or not easily dialyzable) (212), which presumably plays a part in maintaining the enzyme

structure (204, 212). It is the detailed function of the catalytic zinc that is of interest here.

2. YADH

The inhibition of YADH by 1,10-phenanthroline differs from that of LADH in that the metal-free apoenzyme cannot be prepared by dialysis: rather the tetramer dissociates into monomer when 1,10-phenanthroline is present in large excess. The dissociation, which is irreversible, may be represented as



Progressive inhibition by nonexcess amounts of 1,10-phenanthroline (or 8-hydroxyquinoline-5-sulfonic acid) produces a linear dependence of the activity and structural integrity of the enzyme on inhibitor concentration (215).

Inhibition by these reagents results in solutions having UV spectra very similar to those of the ligand and free zinc salts in aqueous solution (219). An interesting feature is that the inhibition is prevented by the coenzyme, NADH or NAD⁺ (215). Thus, both ligands are competitive inhibitors, and both bind at or near the metal site.

The foregoing is a very brief resumé of the evidence for metal ion involvement in the enzyme. More detailed reviews may be found in Sund and Theorell (201, 201a), Brändén *et al.* (219), Ulmer and Vallee (204), and Scrutton (220). The specific point of interest in this instance is whether, when catalysis occurs, the metal ion binds the coenzyme, the substrate, both simultaneously, or neither. Figure 15 shows the possibilities schematically. We shall see in Section III,D how this problem can be approached.

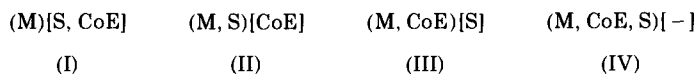


FIG. 15. A schematic representation of the possible modes of interaction of an alcohol dehydrogenase enzyme with its coenzyme (CoE) and substrate (S): () represents a catalytic metal binding site, and [] an alternative site or sites capable of binding coenzyme, or substrate, or both. If the coenzyme can bind in either a coiled or extended conformation, the number of possibilities is doubled. There is also the possibility that CoE and CoE⁺ may select different binding sites.

D. COENZYME-ENZYME INTERACTIONS

There are two considerations in the binding of the coenzymes to the two dehydrogenases: where the coenzyme binds the enzyme, and where the enzyme binds the coenzyme. The possible metal binding sites on NADH are illustrated in Fig. 14a. The metal ion may bind at the adenine (a), the pyrophosphate (b), the nicotinamide carbonyl group (c), the pyridine ring nitrogen (d), or the nicotinamide C-5 position (e). In NAD^+ , only a, b and c are possible candidates.

The five possibilities for NADH have been reviewed by Mildvan (221), who pointed out that a and b are unlikely, since 1,10-phenanthroline and ADP-ribose (Fig. 16) (both NADH-competitive inhibitors) are not mutually competitive and, furthermore ADP-R' (a paramagnetic analog of NADH; see Fig. 24 and Section III,E below) has been found to bind with the same stoichiometry to both native and apo-LADH (222). (This latter point must be treated with caution, however. As discussed below, that there is ligand-enzyme and ligand-apoenzyme interaction does not necessarily reveal anything about metal-ligand binding.)

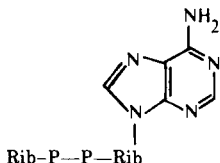


FIG. 16. ADP-R, an NADH-competitive inhibitor.

Mildvan (221) also pointed out that it is "not apparent how coordination at 'c' and 'e' would facilitate hydride transfer, although coordination at 'd' remains a possibility." In terms of simultaneously coordinated substrate, however, there would seem to be no reason why coordination at c should not facilitate reaction [and there is evidence that this may occur in model systems (222a)]; coordination at e (besides being intuitively unlikely) might be seen to raise certain steric difficulties. If a simultaneously coordinated substrate is not proposed, then it might be thought that each of the possibilities a to e is equally unlikely.

Within this context the UV spectrum of NADH is of interest. NADH in aqueous solution has $\lambda_{\text{max}} = 340 \text{ nm}$, $\epsilon = 6.2 \times 10^3 \text{ cm}^2 \text{ mol}^{-1}$ (223). The transition has been visualized as shown in Fig. 17. On binding to LADH, the maximum is shifted to 325 nm. Kosower (224) has shown

that such a shift may be explained by the interaction of a positively charged nitrogen (in the form of an ammonium ion) situated $\sim 3 \text{ \AA}$ from the increasingly positive nitrogen of the pyridine ring.

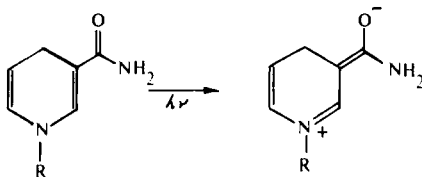


FIG. 17. Electronic transition of β -NADH. [From 224.]

We may note here that coordination of a metal ion to the amide carbonyl would be expected to promote the transition and lower the energy, leading to a shift to longer wavelengths. Kosower, however, included in his assumptions that the zinc ion bound the NADH via the pyrophosphate group and so could not constitute the positive charge responsible for the shift in absorbance. The zinc ion does not so coordinate (see above), and it may be argued that the zinc ion–dihydropyridine interaction [i.e., Mildvan's (221) "d"] is therefore possible. That this may not be the case is shown by differences and similarities between LADH and YADH. There is no shift in NADH absorbances on binding to YADH, and yet the metal ion function in both cases is very similar (Section III,F), indicating that in the LADH active site there may well be a positive nitrogen moiety that is absent in YADH.

There is a further consideration regarding the conformation of NADH on binding. Several investigators utilizing NMR (^1H , ^{13}C , and ^{31}P) spectroscopy (224a–d) have examined the conformations of NADH, NAD^+ and related dinucleotides and have shown, *inter alia*, that NADH exists in a stacked conformation in aqueous solution at pH 4.0 and 30°C . The stacking is such that there is interaction between the nicotinamide and the adenine (Fig. 14c). Barrio *et al.* (225), working on the related dinucleotide, ϵ -FAD, have pointed out that such a stacked or folded conformation results in a quenching of the nucleotide fluorescence. The binding of NADH to LADH or YADH results in an enhancement of the coenzyme fluorescence (226), indicating that the NADH is binding in an "open" conformation. This is confirmed by the X-ray structural study on the enzyme-ADP-ribose complex (212) and by NMR (227).

In the detailed X-ray study of the active site (213), the binding of the coenzyme analog is revealed to be primarily a result of an interaction of the adenine with a hydrophobic pocket on the enzyme. The adenine NH_2 points away from the enzyme (213), and the O_2 hydroxyl of the adenine ribose is hydrogen-bonded to Asp 223. The situation is represented in Fig. 18 (213, 228), where it is seen that there is also an ionic interaction between the guanidinium group of Arg 47 and the pyrophosphate group. This illustrates the rich variety of interactions to be found in the biological systems, for here we have a hydrophobic interaction, a hydrogen bond, and an electrostatic attraction acting in concert to bind a reactant, viz., the coenzyme.

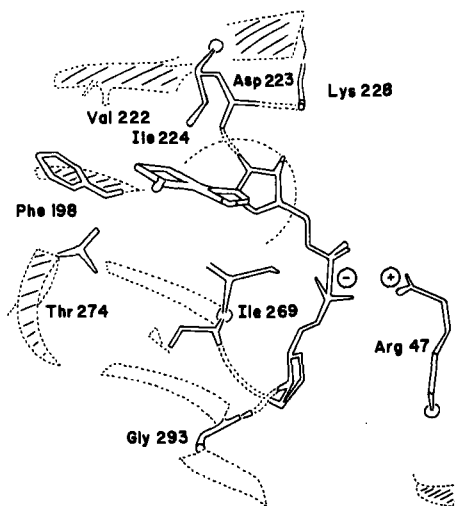


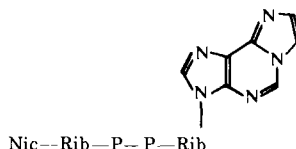
FIG. 18. Schematic representation of the interaction of LADH with ADP-ribose. [From Eklund *et al.* (213) and Hughes and Prince (228).]

An assumed position for the nicotinamide moiety can be deduced from the given structure (212, 213), and the C-4 atom of the nicotinamide ring is $\sim 4.5 \text{ \AA}$ from the catalytic zinc. It is also of interest that in all the dehydrogenase structures reported, the residue Asp is invariant in the coenzyme binding site (i.e., in lactate dehydrogenase, LADH, and glyceraldehyde-3-phosphate dehydrogenase), indicating that the ribose oxygen-Asp hydrogen bond is an important feature of coenzyme

binding (213, and references therein). This then narrows the number of possibilities to (I) and (II) of Fig. 15.

That such a situation exists in the solid is, of course, no guarantee that the same is true in solution [see, for example, Lipscomb (76)] since conformational changes may occur that alter the enzyme-coenzyme interaction. Luisi *et al.* (229) have reported, however, that the binding of the NAD^+ analog nicotinamide 1- N^6 -ethenoadenine dinucleotide ($\epsilon\text{-NAD}^+$) (Fig. 19), to various dehydrogenases results in an enhancement of the coenzyme fluorescence by a factor of 10–13 [indicating unfolding (225)] and in a blue shift of the fluorescence maximum, which the authors (229) interpret as the adenine "sensing" a hydrophobic region. This indicates that the solution enzyme-coenzyme interaction may well be the same as in the solid. [Indeed, the involvement of the adenine moiety in coenzyme binding may be inferred from the relative K_m 's and V_{\max} 's exhibited for several NADH analogs with modified adenine substituents (228, 228a).] It is clear from such studies that adenine-metal ion interaction is precluded.

FIG. 19. The structure of $\epsilon\text{-NAD}^+$.



The X-ray work puts the C-4 of the nicotinamide 4.5 Å from the zinc, a distance that may well be changed in solution, so that direct nicotinamide-metal ion interaction is possible. Shore and Santiago (230) recently reported coenzyme interactions with totally cobalt-substituted LADH. Binding of NADH causes a shift in the 655-nm peak of the heteroenzyme to 670 nm, and similar perturbations were observed on binding pyrazole and trifluoroethanol with NAD^+ , but not with NAD^+ alone. The authors interpreted this as indicating metal ion involvement in binding alcohol and NADH, but not NAD^+ .

On the other hand, Weiner *et al.* (231) and Iweibo and Weiner (232) have shown by the techniques of fluorescence enhancement, quenching, and polarization that the native zinc enzyme may bind as many as 6 or 8 mol of NADH per mole; that, of these, two are tightly bound; that apo-LADH binds 2 mol of NADH with the same affinity as the 2 that are tightly bound to the native enzyme, and that the apoenzyme also binds substrate with the same affinity as the native enzyme (232). The work confirms earlier studies involving a spin-labeled analog of the NAD

skeleton (Fig. 24), which was found to bind to both the native and apo-LADH with the same stoichiometry as that reported above (i.e., 8 to the native enzyme and 2 to the apoenzyme), although the binding of the analog to apo-LADH was slightly weaker than that to the native enzyme. Thus, there is an indication that zinc is not involved in interaction with either substrate or coenzyme.

There is, however, a further point to consider, in that it is not necessarily the case that the binding of the coenzyme (or the substrate) to apo-LADH occurs in the same way as to LADH. Weiner *et al.* (231) reported that they were prompted to use fluorescence polarization to search for additional binding sites for NADH on LADH since such binding sites may not enhance the coenzyme fluorescence, as was evidenced by *the binding of NADH to the apoenzyme*. Since (as was discussed above) the coenzyme binds to the enzyme in an open as opposed to a folded conformation, and the opening of the coenzyme enhances the fluorescence (225, 226, 229), the coenzyme cannot be binding to the apoenzyme in the same way as to the active enzyme. A comparison of binding strengths between native and apoenzyme therefore becomes invalid in considerations of metal ion involvement; rather, the mode of binding is of importance, and this is seen to be different. One possibility is that, in both cases, NADH binds via the adenine, but the metal promotes opening of the coenzyme (and fluorescence enhancement), either by conformational changes in the enzyme or by nicotinamide-metal interaction.

The use of ^{35}Cl NMR line-broadening experiments has yielded valuable information with regard to zinc ion function in the enzymes alkaline phosphatase (AP) (233) and carbonic anhydrase (CA) (Section II,G) (234). The addition of LADH to KCl solutions causes the ^{35}Cl resonance to broaden (235), and the subsequent addition of NADH decreases the broadening, which is consistent with the displacement of bound Cl^- (233-235). The metal ion in a metalloenzyme may be regarded as a possible chloride binding site [in AP and CA it is the actual site (233, 234)], but the addition of 1,10-phenanthroline, which binds to the zinc in LADH (212), cyanide, or 8-hydroxyquinoline derivatives, has no effect on the ^{35}Cl line width of an LADH/KCl solution (235), indicating that such ligands do not bind at the same place as NADH.

On the other hand, an analogous study involving ^{81}Br linewidths (236) showed that binding of bromide to LADH was insensitive to the addition of NAD^+ or NADH. The most likely explanation for this is a stronger enzyme-bromide interaction or the bromide ion binds at a different place from that of the chloride. Unfortunately, the effect of chelating agents, which might have indicated whether the bromide was bound to the zinc ion, was not studied. It is noteworthy that

chelated zinc, e.g., in the ligand CR (Fig. 6) is able to bind bromide ion strongly (237).

In a study of the effects of chloride on coenzyme binding, Coleman and Weiner (238, 239) established coenzyme-competitive inhibition at saturating substrate levels. With coenzyme saturating, however, the anion was found to be a noncompetitive inhibitor against either acetaldehyde reduction or isobutyramide binding (238). The authors interpreted this as evidence for the existence of at least two specific anion binding sites on the enzyme, since they observed the formation of an enzyme-NADH-aldehyde-chloride complex (239). They also reported that chloride ion diminishes the fluorescence of enzyme-bound NADH (238), other spectroscopic techniques (UV, ORD) showing the coenzyme to be still bound.

The latter observation suggests that the addition of chloride is similar in effect to the removal of metal ion (see above) in that both cause a different mode of binding of coenzyme. Whether the chloride ion effects mimic those of metal ion removal by blocking a positive charge on the zinc ion is a matter of conjecture; the ^{35}Cl -NMR results (235) militate against the suggestion, but the indication of multisite anion binding (238, 239), supported by the ^{81}Br -NMR results, suggests that there is some uncertainty about the mode of chloride binding.

The absence of any coenzyme-metal interaction has been proposed by Takahashi and Harvey (240) as a result of measurements of energy transfer between bound NADH, thionicotinamide NADH, or Rose Bengal and cobalt in a hybrid Co(II)Zn(II) -LADH. Measurements based on the fact that fluorescence enhancement is less with the hybrid than with the native enzyme result in a Co(II) -nicotinamide ring distance of $19 \pm 2 \text{ \AA}$ (240). This is in accord with the observation (241) that binding of azide, 1,10-phenanthroline, or pyrazole does not affect the absorption spectrum of a similar hybrid enzyme. Such hybrid enzymes are prepared by utilizing the known (204) (see above) rapid exchange of two of the four zinc ions in acetate buffer. Ulmer and Vallee (204, and references contained therein) originally equated the two rapidly exchanging zincs with catalytic activity, while the other two were equated with maintenance of structure. Therefore, the above observations indicate that the catalytic metal ion serves no substrate or coenzyme binding function.

There is, however, another explanation (242). If the two structural zincs, in fact, are rapidly exchanging ones, then their removal must necessarily affect the enzyme structure and hence the activity.

A recent report by Sytkowski and Vallee (217a) is of particular interest in this connection: using the ^{65}Zn and Co hybrid enzymes, they showed that the catalytic atoms are those which are reactive to

1,10-phenanthroline, while the noncatalytic pair are not affected by this reagent. But metal-metal exchange studies shows the converse to be true: the chemical reactivity of the noncatalytic atoms is much higher, and they exchange more rapidly.

The X-ray studies of Brändén *et al.* (212) have shown the two different zincs to be ~ 20 Å apart. There is one on the enzyme surface (212) and one at the bottom of the cleft that is the active site (213); 1,10-phenanthroline binds to this second, catalytic zinc (212), and 1,10-phenanthroline binding affects the absorption spectrum of the *totally* cobalt-substituted enzyme (230). The surface zinc might possibly exchange more rapidly than the zinc at the bottom of the cleft. One would therefore expect no evidence of any coenzyme-cobalt (or substrate-cobalt) interaction in the hybrid enzyme (240) and no indication of a metal-inhibition interaction with 1,10-phenanthroline (241), and a distance of ~ 20 Å (240) between the nicotinamide ring and the cobalt ion is to be expected. It is also significant in this context that ESR studies on the interaction of ADP-R' (see Fig. 24) with totally cobalt-substituted LADH (243) show the spin label to be ~ 6 Å away from the catalytic cobalt, although the NMR results of Mildvan *et al.* (244) on the same system (see below) indicate that this is the case in the hybrid enzyme, which does not agree with the work of Takahashi and Harvey (240) or the UV results on inhibitor binding (241). Thus, the work of Mildvan *et al.* (244) indicates that the two rapidly exchanging zincs are those at the bottom of the cleft, not the structural ones as argued above, although this offers no explanation of the other observations discussed above (230, 240, 241).

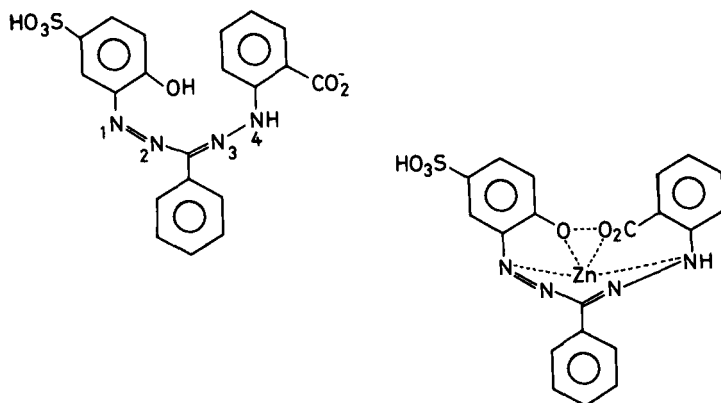


FIG. 20. The mode of binding of Zincon to zinc. [From McFarland *et al.* (246).]

Some further evidence for a direct metal ion/NADH interaction comes from pH effects on 1,10-phenanthroline binding (245) and resonance Raman investigations of binary complexation between 2-carboxy-2-hydroxy-5'-sulfoformazyl benzene (Zincon) (Fig. 20) (246) and LADH or zinc.

1,10-phenanthroline binds weakly to LADH at alkaline pH, and Reynolds *et al.* interpret this as resulting from displacement of zinc-bound hydroxide as opposed to more readily displaced zinc-bound water at pH < 7; i.e., the 1,10-phenanthroline binds directly to the metal ion. Since 1,10-phenanthroline is competitive with NADH, there is an intimation that this may also be one mode of NADH-enzyme interaction.

Zincon is also strictly competitive with NADH (246) and binds zinc as shown. The resonance Raman study shows that in the enzyme the binding at pH 8.75 is to the zinc, but not via the carboxylate and N-4, only via the phenolate and N-1. Thus, there is a further indication of coenzyme-metal ion interaction.

To summarize, on the basis of the evidence available no definite conclusion can be drawn regarding *direct* coenzyme-metal ion interaction: The inhibition results indicate an interaction, since chelating agents (204, 215, 217a, 246) are competitive; the X-ray data indicate the opposite (212, 213); spectroscopic evidence is contradictory (214, 230, 240, 247); NMR and the effect of anions are inconclusive (235, 236, 238, 239) (and see above) while the results of resonance Raman experiments are more positive (246). Although doubt remains it seems that (III) and (IV) (Fig. 15) can be eliminated.

It is interesting that the 3-amido group of the nicotinamide ring in NAD⁺ appears to be necessary for the correct positioning of the coenzyme molecule in the active site (248), but activity is not confined to the 3-amido derivative: 3-halogeno (Cl, Br, I) analogs are active as well (249), but the unsubstituted pyridine derivative is not. However, in a structural study of the adducts of 3-iodo and the unsubstituted pyridine adenine dinucleotides with equine LADH, Samama and co-workers (248), have found that, although the binding of the adenosine part of the molecule is very similar to that of NADH or its analog ADP-ribose (Fig. 16), the conformations of the remaining parts of the analog are quite different (Fig. 21).

The striking fact is that, mainly owing to a difference in the orientation and position of the pyrophosphate group, the pyridine rings of the 3-substituted analog are at the surface of the molecule, well removed from the zinc ion at the active site. Moreover, a conformational change in LADH is induced by coenzyme binding (248, 249), and the CONH₂

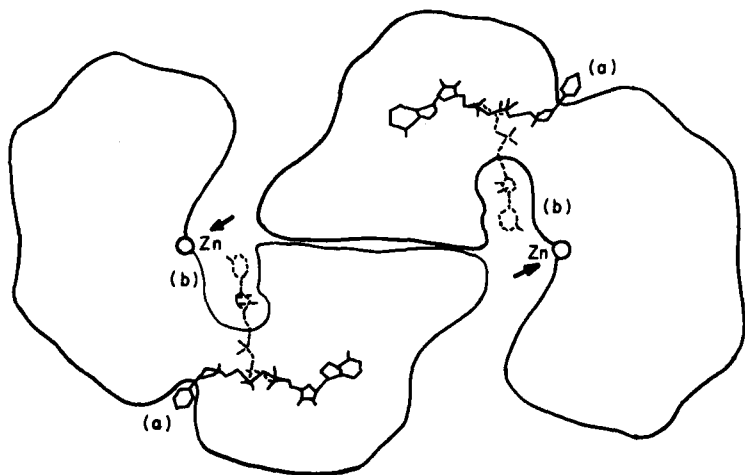


FIG. 21. Schematic diagram of a section through the alcohol dehydrogenase molecule with bound nucleotides projected onto this section. [after Samama *et al.* (248).] The pyridine and 3-halogeno pyridine adenine dinucleotides take up position (a); the nicotinamide adenine dinucleotide, position (b). The swing about the pyrophosphate group is clearly indicated. Substrate can take up the arrowed positions [cf. also Brändén (100).]

group appears to be essential for this change to occur (e.g., ADP-ribose does not induce it). The 3-iodo and pyridine analogs also do not induce the change.

The question then arises how it is possible for the 3-iodo analog to be an active coenzyme: if the mechanism remains essentially the same as with NAD^+ the iodopyridine ring must swing through a considerable distance, using the pyrophosphate group as a hinge to position itself near the zinc ion in the active site. (We have not met such a large group movement with CA, but we shall come across a rather similar and remarkable movement of a phenolic side chain with CPA).

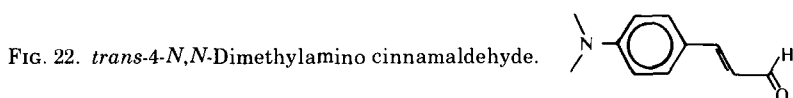
It is likely that there are two different conformations of the 3-iodo derivative in solution; one of them is active, and the other has the inactive binding mode described. However, if such a contortion is possible for the 3-iodo compound, it should also be possible for the (inactive) unsubstituted pyridine derivative. The origin of the activity difference is at present unknown.

E. SUBSTRATE-ENZYME INTERACTIONS

The suggestion that the function of the zinc ion in alcohol dehydrogenases was to act as a Lewis acid in polarizing the carbonyl group

of coordinated aldehydes was first made by Abeles *et al.* (247) after studies on model reactions with NADH analogs and thioketones. Supporting evidence based on the stereospecificity of the transferred hydrogen and the deuterium isotope effect on the YADH-catalyzed reaction led Sund and Theorell (201, and references contained therein) to suggest a mechanism in which both coenzyme and substrate were bound to zinc, the coenzyme binding through adenine and the substrate through oxygen. The nicotinamide ring was pictured as interacting both with groups in the active site cavity wall and with the substrate ligand on the side remote from zinc.

A number of recent investigations have supported the suggestion of a direct carbonyl-zinc ion interaction. Jacobs *et al.* (250) compared the rates of reduction of several benzaldehydes under both enzymic and nonenzymic conditions. The ratio of *p*-chloro to *p*-methoxy benzaldehyde was 100 for reduction by sodium borohydride, whereas for reduction by NADH with LADH as catalyst the ratio was 2. This lack of substituent effect on the enzymic reaction was thought (250) to be a result of polarization of the carbonyl bond by zinc coordination. Dunn and Hutchinson, in a kinetic study of the stable intermediate formed between *trans*-4-*N,N*-dimethylamino cinnamaldehyde (Fig. 22), NADH, and LADH at $\text{pH} \geq 9.0$, concluded that the zinc ion in the enzyme played a Lewis acid role by binding through the carbonyl oxygen. The YADH-catalyzed reduction of substituted benzaldehydes has been shown to involve a general acid in the active site (264), and, in subsequent work on the pH dependence of the reaction, Klinman (265) concluded that the ionizing group (which has a pK of ~ 8.6) could be either an imidazole, a cysteine, a lysine, or a zinc-bound water molecule. In similar studies on the reduction of acetaldehyde and butyraldehyde (251) and the oxidation of butan-1-ol and propan-2-ol (252), Dickenson and Dickinson (251, 252) reached the same conclusion.



Shore *et al.* (253), in a study of proton liberation during the steady-state turnover of LADH, concluded that there was on the enzyme a group X with a pK of 9.6 and that this pK was perturbed by the binding of NAD^+ to 7.6 (253). The scheme is depicted in Fig. 23.

The group plays a significant part in the binding of the substrate and was thought to be either an amino group or a zinc-bound water molecule (253).

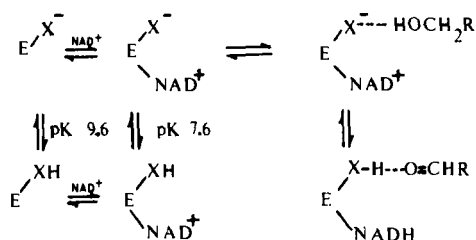


FIG. 23. Schematic representation of the mechanism of alcohol dehydrogenase catalysis (253).

McFarland and Chu (254), however, have shown that in the LADH-catalyzed reduction of an aromatic aldehyde (β -naphthaldehyde or benzaldehyde) to an alcohol, or oxidation of alcohol to aldehyde, the only pH-dependent parameters are the kinetic binding constant for ternary complex formation and the rate of dissociation for alcohols. The other parameters (catalytic step and isotope effect) are pH independent. This is consistent only with *direct* carbonyl-zinc ion coordination. The same direct coordination has been deduced (213) from X-ray studies.

Some of the most detailed solution studies on the nature of the metal ion-substrate interactions have been performed by Mildvan and Weiner (255, 256) and Mildvan *et al.* (244) using NMR techniques involving spin-labeled ligands. The NAD^+ analog adenosine-5'-diphosphate-4-(2,2,6,6-tetramethyl-4-phosphopiperidine-1-oxy) (ADP-R')

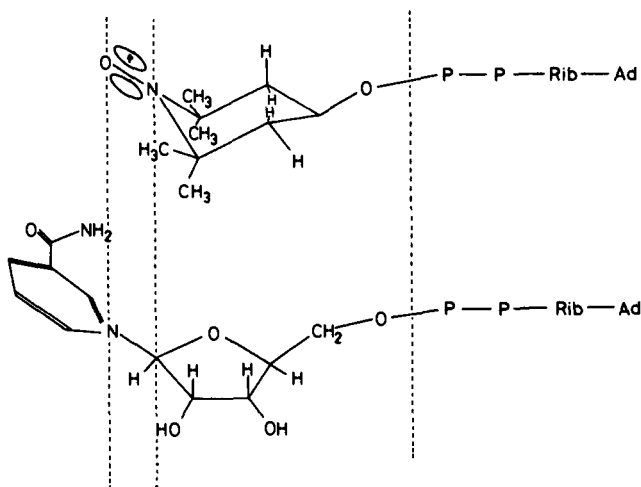


FIG. 24. The equivalence of ADP-R' and NAD. [From Mildvan and Weiner (255).]

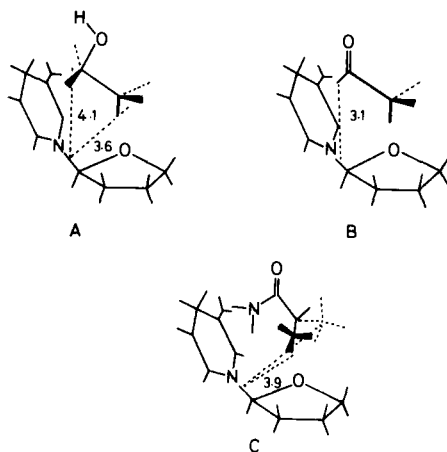


FIG. 25. Coenzyme-substrate (or inhibitor) distances in LADH: (A) ethanol; (B) acetaldehyde; (C) (isobutyramide).

Figure 24, first prepared by Weiner (222), has its unpaired electron located in a position equivalent to the nicotinamide nitrogen-ribose carbon bond in NAD^+ (Fig. 24) (255). The binding of ADP-R' to LADH is found to enhance the effect of the unpaired electron on the proton relaxation rate of water (255). The addition of ethanol to the binary ADP-R'-enzyme complex reduces the enhancement, leading to the suggestion that the ethanol binds to the solvent side of the bound coenzyme and lies over the ribosidic bond to pyridine (255). The relative positions of the appropriate coenzymes and ethanol, acetaldehyde, and isobutyramide (a substrate-competitive inhibitor) as calculated from the enhancement of proton relaxation rates are shown in Fig. 25 (256).

A suggestion regarding the involvement of the metal ion is shown (221, 244) in Fig. 26. The use of a spin-labeled iodoacetamide analog

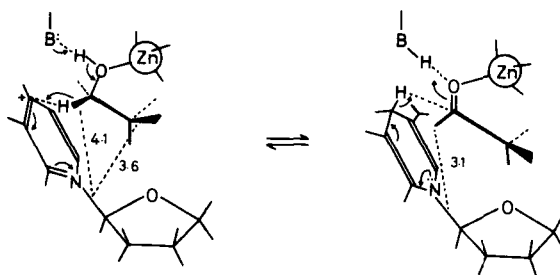


FIG. 26. Mechanism of LADH reaction based on calculated distances between the enzyme-bound substrates and enzyme-bound ADP-R'. [From Mildvan *et al.* (244).]

[4-(2-iodoacetamido)-2,2,6,6-tetramethylpiperidino oxyl] (Z) in similar studies on the yeast enzyme (256) revealed the close similarities between zinc ion function in LADH and in YADH through comparison with NMR (244) and X-ray (212, 213) data. The calculated distances between the spin label, NADH, and isobutyramide (*i-b*) in the ternary complex EZ(*i-b*) are shown in Fig. 27. [The locations of zinc and Cys 43 are taken from Eklund *et al.* (213) and the YADH primary amino acid sequence (257) which is discussed below.] The substrate is thought to be *directly* coordinated to the zinc (258); i.e., we have an interaction approaching (II) in Fig. 15 with the coenzyme in an extended conformation.

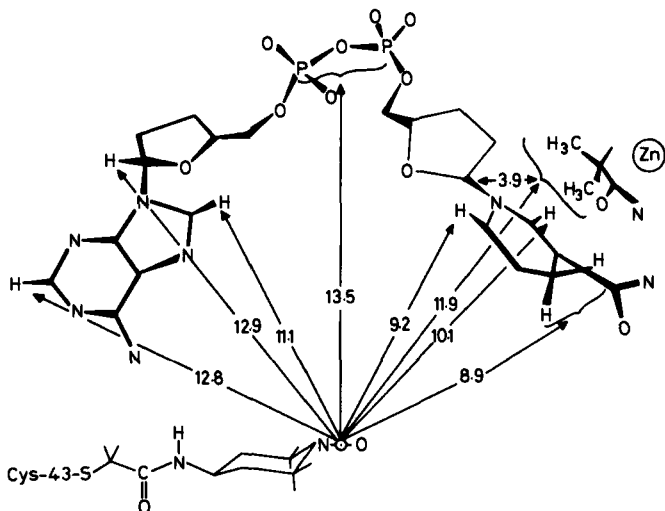


FIG. 27. Metal ion-substrate interaction in YADH. [From Sloan and Mildvan (258).]

In similar studies using the hybrid Co(II)Zn(II)-LADH enzyme and the totally cobalt-substituted enzyme, Sloan *et al.* (227) have found that binding of isobutyramide occurs with the methyl protons 9.1 Å from the "catalytic" Co(II). The distance shortens to 6.9 Å on binding NADH, and the metal-methylene distance is 6.6 Å (227). The construction of the active site that may be reached by consideration of Mildvan *et al.* (227, 244, 257, 258) is shown in Fig. 28.

Again we see that a metal-bound water molecule is involved. Eklund *et al.* (213), concluded, however, that the water molecule bound to the catalytic zinc was displaced by substrate (see below). This seeming discrepancy may possibly be an effect of substituting Co(II) for Zn(II),

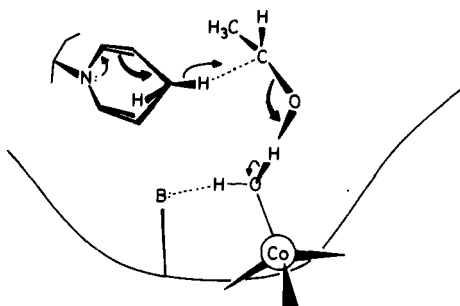


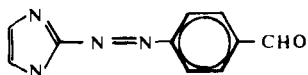
FIG. 28. Metal ion function in Co(II)-LADH. [From Sloan *et al.* (227).]

which involves a contraction in metal ion radius of some 0.16 Å and may cause some conformational changes. When 1,10-phenanthroline binds, the water molecule is displaced (219).

That there is *no* metal ion–substrate interaction has been suggested recently by Iweibo and Weiner (232, and references contained therein) based on studies of apoenzyme–substrate interactions, although there is, of course, no certainty that substrate binding to the apoenzyme occurs at the same site as with the zinc enzyme. In contrast, using spectrophotometric studies on the totally cobalt-substituted enzyme, Shore and Santiago (230) suggested direct metal–substrate interaction.

The binding of 4-(2'-imidazolylazo)benzaldehyde (Fig. 29) to LADH results in an unproductive binary complex (259, 260) which has a UV spectrum very similar to that of the zinc(II)-azoaldehyde complexes (260).

FIG. 29. 4-(2'-Imidazolylazo)benzaldehyde.



Both substrate- and coenzyme-competitive inhibitors displaced the aldehyde, indicating that it overlaps both binding sites. If the azoaldehyde is added to an enzyme–NADH mixture, then reaction occurs (259, 260), indicating that, under these circumstances, a productive ternary complex is produced that involves a different interaction with the azoaldehyde. It is not impossible that the initial unproductive binding is via the imidazole to the zinc, whereas in the productive complex the interaction is via the aldehyde. There are also indications that pyrazole, a substrate-competitive inhibitor (261), acts by binding directly to the zinc (262).

Thus, as with coenzyme binding, there is uncertainty about the mode of metal ion-substrate interaction: NMR indicates an involvement (227, 244, 255-258); some kinetics suggest direct coordination (201, 201a, 219, 250, 254, 262, 263), and others suggest that there may be an alternative ionizable active site group involved in substrate binding (251, 252, 264, 265); fluorescence studies and the apoenzyme-substrate interaction suggest (232) no involvement, while spectrophotometric (230) and X-ray (212, 213) studies indicate the opposite.

F. LADH AND YADH: METAL ION-ENZYME INTERACTION

Although there are certain differences between YADH and LADH [specifically, subunit structure, the effect of metal ion removal, and activity toward certain substrates (Table XV) (see Section III,C)], the metal ion catalytic function has been treated here as virtually identical in the two enzymes. The basis for this is the following: Sloan and Mildvan (258) have established that the metal ion location and function in LADH are the same as in YADH; Jörnval (257) has shown that, in the active site region, the principal amino acid residues are the same in YADH as in LADH. It is of interest here to speculate that it is a difference in amino acid residues that causes the difference in spectral shifts of NADH on binding to the two enzymes. As was discussed in Section III,D, Kosower (224) has shown that a shift from 340 to 325 nm on NADH binding by LADH may result from an ammonium ion-pyridine nitrogen interaction; Fig. 18 shows (213) an interaction between the ammonium group of Arg 47 and the pyrophosphate of ADP ribose in LADH. In YADH, the residue equivalent to Arg 47 is a histidine (257). Furthermore, the kinetic descriptions of the reactions of the two enzymes is the same [ordered bi-bi in both

TABLE XV
SOME DIFFERENCES IN SUBSTRATE SPECIFICITY
BETWEEN LADH AND YADH^a

LADH (relative rate)	Substrate	YADH (relative rate)
100	Ethanol	100
0	Methanol	0.8
108	<i>n</i> -Propanol	65
159	<i>n</i> -Butanol	60
125	<i>n</i> -Hexanol	30
135	<i>n</i> -Octanol	40

^a Data from Sund and Theorell (201).

cases (266, 267); the sequence is NADH first and then aldehyde; alcohol leaves first and then NAD^+ , and the inhibition patterns are identical, Section III, C].

In LADH, the metal ion is coordinated by two cysteine sulfurs and a histidine nitrogen (Cys 46, Cys 174, and His 67) with a water molecule or hydroxyl ion completing a distorted tetrahedron (213). In YADH, the equivalent residues in the active site are identical (257). It is felt, therefore, that the basic assumption of a similar catalytic function of the metal ion is justified.

It is of interest that the visible spectrum of cobalt-LADH has been interpreted as possibly representing an "entatic" state (268); i.e., the metal may be regarded as being in a distorted or "strained" configuration. The spectrum is represented in Fig. 30. Such phenomena are common in cobalt-substituted zinc metalloenzymes as well as in others and have been reviewed by Williams (269). The question of whether such a strained configuration enhances catalysis has been the subject of debate (268-270), but surely is evidence of some distortion from the more stable octahedral or tetrahedral environment, and such distortion is commonly associated with catalytic activity.

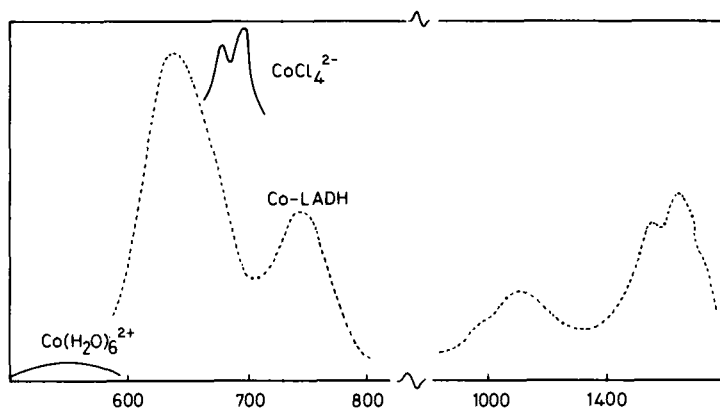


FIG. 30. The visible spectrum of Co(II)-LADH compared with those of the $\text{Co}(\text{OH}_2)_6^{2+}$ and CoCl_4^{2-} ions (268).

IV. Carboxypeptidase A

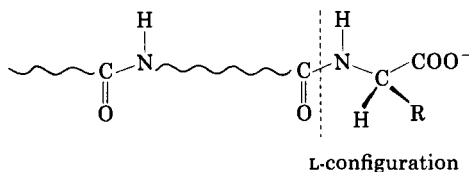
A. INTRODUCTION

Carboxypeptidase A, discovered in 1931 by Waldschmidt-Leitz (271) has been isolated from the pancreas of several animal species and shown to contain one zinc ion per molecule. It catalyzes the hydrolysis

of a variety of substrates ranging from *N*-acyl amino acids and dipeptides to large proteins. Its molecular weight is 30,000–35,000 depending upon the source and the form of the CPA from a given source. There are four forms of bovine CPA formed by enzymic release from the pancreatic CPA precursor, procarboxypeptidase (272). All have comparable specific enzymic activity; the three important forms are designated CPA_α, CPA_γ, and CPA_δ (CPA_β is a contaminant). CPA_α has different crystal cell constants from those of CPA_γ; CPA_δ has the same constants as CPA_α, but it has seven fewer amino acid residues and a different N-terminal residue (Asn instead of Ala). Conformational differences probably exist between CPA_γ and CPA_δ, both of which have 300 residues. These two forms differ in solubility and in the reversible removal of zinc: the γ form is more readily reactivated than the δ. The γ and δ forms have the same sedimentation and electrophoretic mobility.

The main features of the solution chemistry are as follows (272, 273):

i. The substrate must have a free COO⁻ group at the C-terminal end (III),



(III)

ii. The C-terminal residue must have the L-configuration (but the penultimate residue does not have strict stereospecificity).

iii. The rate of hydrolysis is increased if R (see III) is an aromatic or a branched aliphatic group.

iv. The rate decreases if the NH group is alkylated.

v. At least five residues influence K_m and are therefore probably at a binding site about 18 Å long.

vi. CPA shows esterase as well as peptidase activity, but the sequence of metal ions replacing zinc to give an active enzyme is not the same: the order for peptidase activity is $\text{Co} > \text{Zn} = \text{Ni} > \text{Mn} > \text{Cu(zero)}$, whereas the order for esterase activity is $\text{Cd} > \text{Mn} > \text{Co} > \text{Zn} = \text{Ni} > \text{Hg} > \text{Cu(zero)}$. This is illustrated quantitatively in Table XVI (272, 273a). A Co(III) derivative of CPA can be prepared; although there is controversy concerning its catalytic activity (274), it appears that the activity of the derivative depends upon the method of metal

TABLE XVI
 STABILITY AND KINETIC CONSTANTS FOR METALLOCARBOXYPEPTIDASES^a

Metal ion	Log K^b	Substrate							
		(a) BGGP		(b) BGP		(c) CGP		(d) HPLA	
		K_m	k_{cat}	K_m	k_{cat}	K_m	k_{cat}	K_m	k_{cat}
Zn	10.5	8.0	1.2	8.1	5.6	19.5	5.5	0.76	28.6
Ni	8.2	7.4	1.1	—	—	—	—	2.1	27.6
Co	7.0	6.0	5.9	4.8	7.4	11.7	12.3	0.98	37.7
Mn	5.6	2.9	0.23	1.1	0.45	22.9	2.3	3.2	56.8
Cd	10.8	—	—	—	—	—	—	5.5	61.5
Hg ^c	21.0	—	—	—	—	—	—	—	—
Cu	10.6	—	—	—	—	—	—	—	—

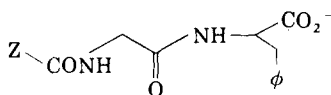
^a From Quijcho and Lipscomb (272).

^b K is corrected for competition by 1 M Cl^- and 0.05 M Tris buffer, pH 8.

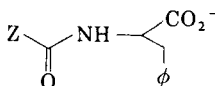
^c K_m values are $M \times 10^4$; k_{cat} values are $\text{min}^{-1} \times 10^{-3}$.

^d In the following designation of substrates (a)–(d), $Z = \phi\text{CONH-CH}_2^-$ and $W = \phi\text{CH}_2\text{OCONH-CH}_2^-$:

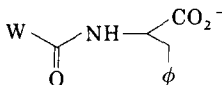
(a) benzoylglycylglycyl-L-phenylalanine



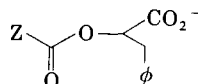
(b) benzoylglycyl-L-phenylalanine



(c) carbobenzoxyglycyl-L-phenylalanine



(d) benzoylglycyl-L-phenyllactate
(hippuryl-L-phenyllactate)



^e Some peptidase activity in crystals of CPA₇ has been reported (273a).

substitution (275), direct metal exchange and subsequent oxidation of Co(II) to Co(III) yielding a Co(III)-PCA, which has esterase activity.

vii. Peptide substrates bind to the apoenzyme and then prevent access of $^{65}\text{Zn}^{2+}$, suggesting that the substrate binding site is close to the metal ion.

viii. The binding of various substrates depends upon whether or not the zinc ion is present. Table XVII summarizes the experimental findings (273). It is interesting that substrates 3, 4, and 5 will bind if metal ion is present, and then metal exchange is prevented. This suggests that

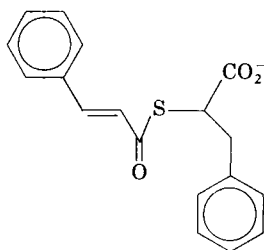
binding to the apoenzyme is cooperative and a C-terminal side chain in the L configuration, a free NH of the C-terminal residue, and a free NH of the penultimate residue are all required. Metal substitution gives derivatives that bind the substrates in Table XVII, but as the metal at the active site is changed it is found that the substrate binding tendency does not correlate with metal activity (e.g., Cu(II) induces substrate binding but the Cu(II)-ES complex is inactive). This is a good illustration of the distinction between binding and activity.

Again, caution must be exercised before one states that a metal-substituted metalloenzyme is inactive because the copper derivative,

TABLE XVII
BINDING OF SUBSTRATES TO CARBOXYPEPTIDASE A
HOLO- AND APOENZYME

Substrate	Binding to holoenzyme	Binding to apoenzyme
1. Acylated dipeptide	Bound	Bound
$ \begin{array}{c} \text{[H]} \qquad \qquad \text{O} \qquad \qquad \text{CO}_2^- \\ \qquad \qquad // \qquad \qquad / \\ \text{R}_3\text{---N---CH}_2\text{---C---N---CH (L)} \\ \qquad \qquad \\ \text{[H]} \qquad \qquad \text{[R]} \end{array} $		
2. Dipeptide	Bound	Bound
$ \begin{array}{c} \text{[H]} \quad \text{R}_2 \qquad \text{O} \qquad \qquad \text{CO}_2^- \\ \quad / \quad // \quad / \\ \text{H---N---CH---C---N---CH (L)} \\ \quad \quad \\ \text{(L)} \quad \quad \text{[H]} \quad \text{[R]} \end{array} $		
3. Same as 2, but configurations are (D)-(L)	Bound	Not bound
4. N-Acyl amino acid	Bound	Not bound
$ \begin{array}{c} \text{O} \qquad \qquad \text{CO}_2^- \\ \qquad \qquad / \\ \text{CH}_3\text{---C---NH---CH (L)} \\ \qquad \qquad \\ \qquad \qquad \text{[R]} \end{array} $		
5. Ester analog of acylated dipeptide	Bound	Not bound
$ \begin{array}{c} \text{[H]} \qquad \qquad \text{O} \qquad \qquad \text{CO}_2^- \\ \qquad \qquad // \qquad \qquad / \\ \text{R}_3\text{---N---CH}_2\text{---C---O---CH (L)} \\ \qquad \qquad \\ \qquad \qquad \text{[R]} \end{array} $		

although inactive for the hydrolysis of the normal peptide and carboxylic ester substrates, will catalyze the hydrolysis of the thiol ester IV.



(IV)

The Cu(II)-PCA is about 45% as active as the zinc enzyme, but there is an intriguing stereospecificity difference between the zinc and copper enzymes: the former catalyzes the hydrolysis of both the D and L forms, the latter that of the L form only (276).

ix. Organic groups on the protein ligand are also involved in the catalytic function; thus acetylation with *N*-acetylimidazole causes peptidase activity to decrease and esterase activity to increase. The spectrum of the acylated enzyme shows that two tyrosine residues have formed *O*-acetyl derivatives. One of the two tyrosines can be selectively nitrated with $C(NO_2)_4$, and peptidase activity is then destroyed.

x. Esters and peptides inhibit each other competitively; therefore the peptidase and esterase sites must at least overlap, even if they are not the same.

The structure and function of carboxypeptidase A have been the subject of a number of reviews (272-273a), and we focus briefly here on some recent developments and on those aspects concerned with the role of the zinc ion.

B. STRUCTURE OF CARBOXYPEPTIDASE A; COORDINATION OF ZINC AND INTERACTION WITH SUBSTRATE

The structure of bovine CPA has been determined at a resolution of 2 Å (277, 278). It is an ellipsoidal molecule of approximate dimensions $50 \times 42 \times 38$ Å. About 48% of the protein ligand has a random-coil structure that undergoes conformational changes on substrate binding.

The zinc ion is coordinated to the protein by two imidazole side chains and a carboxyl group of the three residues: His 69, Glu 72,

and His 196. A water molecule completes distorted tetrahedral coordination of the zinc ion, which lies in a groove and pocket in the enzyme surface.

Ideas on the possible mechanism of action in terms of the structure were aided by the determination of the structure of a Gly-L-Tyr complex with the native enzyme (277). The dipeptide is hydrolyzed 10^3 times more slowly than the best substrates and more slowly still if the crystals are cross-linked with glutaraldehyde (279, 280). In this way a sufficiently durable binding of the Gly-L-Tyr at the active site was obtained to enable the structure of the complex to be determined (277).

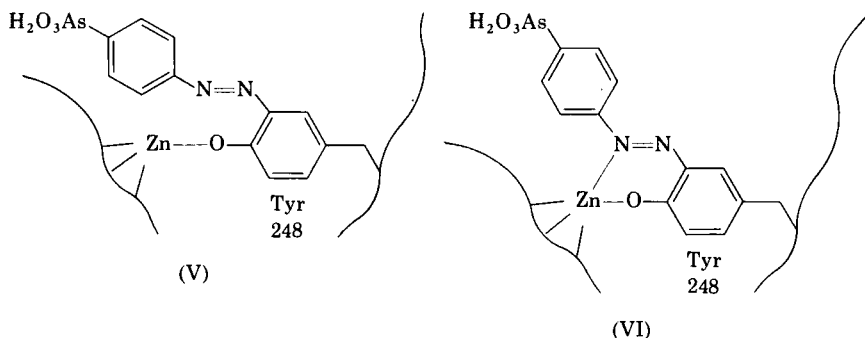
The substrate lies in the groove containing the zinc ion. The aromatic side chain of the substrate falls in a pocket that contains no specific binding groups and is large enough to accommodate a tryptophan side chain. This feature accounts for the observed specificity for the side chain of the C-terminal amino acid of the substrate, since the best substrates for carboxypeptidase A are those that have an aromatic or branched aliphatic side chain at the C-terminal residue (281). The most commonly used peptide substrate is carbobenzoxy-Gly-L-Phe (CGP) (cf. Table XVI). The free carboxyl group interacts with the positively charged guanidinium group of Arg 145. The carbonyl oxygen of the —CONH bond undergoing attack replaces the water molecule coordinated to the zinc ion. The carboxyl group of Glu 270 binds through a water molecule to the free amino group, an interaction possible only with dipeptide substrates with a free N-terminal amino group. The hydroxyl group of Tyr 248 is ~ 2.7 Å away from the nitrogen of the attacked peptide bond and ~ 3.5 Å from the α -amino group.

Figure 31A depicts the substrate (heavy bonds) interacting with the zinc ion and the active groups of the protein ligand. This quite complex interaction is brought about by some interesting conformational changes in the molecule induced by the binding of Gly-L-Tyr (see Fig. 31B) (278). Thus, the guanidinium group of Arg 145 moves 2 Å owing to rotation about the C_β — C_γ bond of the side chain, and the carboxylate of Glu 270 also moves by about 2 Å owing to rotations about both the C_α — C_β and C_β — C_γ bonds. Most spectacular of all, the phenolic group of Tyr 248 swings through 12 Å, mainly by rotation about the C_α — C_β bond to bring its —OH to bear on the peptide nitrogen. There are, also, some related movements of the peptide backbone and a system of hydrogen bonds in the region between Arg 145 and Tyr 248. These conformational changes provide an example of Koshland's "induced fit" theory (282, 283): this proposes that substrate interaction leads to conformational changes in the protein that are related to the electronic changes in the enzyme-substrate complex needed to effect catalysis. Binding of the C-terminal side chain

of the substrate in the pocket at the active site ejects the H_2O from this cavity, and the movement of Tyr-248 effectively closes off the active site from the solvent.

From the viewpoint of zinc coordination the question arises whether or not the hydroxyl group of Tyr 248 is coordinated to the zinc ion in the resting enzyme and has to be displaced when the substrate binds. Information on this is obtained in an interesting way by labeling the phenolic side chain of this residue with the arsanilazo group: arsanilazophenols show a marked color change on coordination to a metal ion, and coordination of the phenolic group may be monitored by observing such changes. The color change observed with CPA crystals depends upon the crystal modification: A_α , A_γ , and A_δ . In solution, the arsanilazo derivatives of all three are red, and the visible spectrum is similar to that of metal complexes of the azoaromatic ligand (284). When the A_γ arsanilazo derivative is crystallized, the crystals are yellow, suggesting that the modified Tyr 248 no longer coordinates zinc at the active site (285). On the other hand, the crystals of arsanilazo-carboxypeptidase A_α of the type used for the crystal structure determination remain red (286). Crystals of carboxypeptidase A_α , elongated along the a axis, were those on which the crystal structure was done, so that the crystal packing in the A_γ derivative must prevent the orientation of the modified residue for coordination to the metal ion.

In solution then, arsanilazotyrosine-248 carboxypeptidase A forms a complex with the Zn(II) at the active site probably by coordination of the free phenolic hydroxyl group of the modified tyrosine as shown in structures (V) or (VI) (284, 287–289).



The absorption characteristic of the zinc(II)–arsanilazotyrosine complex is observed only with the zinc(II) enzyme, and it is stable only near neutral pH (284). Its formation and dissociation have two apparent $\text{p}K_a$ values, 7.7 and 9.5 (284). The curve leading up to the

lower pK_a may be regarded as a formation curve for the complex, as the proton is displaced from the azophenolic hydroxyl group to form the zinc complex. The upper pK_a corresponds to dissociation of the anionic form from the zinc(II) ion: possibly hydroxide ion competes for the zinc(II) coordination site (284). The arsanilazo enzyme is still catalytically active, and addition of the dipeptide Gly-L-Tyr causes dissociation of the complex of zinc(II) with the arsanilazotyrosine group (284), the substrate displacing the coordinated phenolic hydroxyl group. The solution studies indicate that the phenolic OH is in a position to coordinate the zinc ion, and it may do this at least some of the time in the native enzyme (284), although the electron density map suggests that the side chain is mobile and free to rotate in solution. However, it becomes fixed near the peptide bond in the Gly-L-Tyr complex, and the phenolic hydroxyl group of the arsanilazotyrosine 248 may also behave similarly.

Resonance Raman studies (290) of arsanilazocarboxypeptidase A have shown that azophenol coordination can occur as shown in (VI), a type of coordination well established for azophenol ligands (291, 292). Resonance Raman spectroscopy is a particularly useful tool since it is applicable to both solids and solutions; its application to both states of carboxypeptidases A (and also B) will be particularly interesting since the kinetic properties of the enzymes are significantly altered upon crystallization (293, 294).

C. ROLE OF ZINC AND ENZYME SIDE CHAIN-SUBSTRATE INTERACTIONS IN THE CATALYTIC MECHANISM

1. *Structural Implications for the Mechanism*

We have seen that the coordinated Zn(II) ion, the side chains of Glu 270, and Tyr 248 are close enough to the substrate to suggest direct assistance in catalysis. Zinc can clearly function as a Lewis acid and polarize the carbonyl of the peptide bond. Although the complex is unipositive (a carboxylate and two neutral donors as ligands), the single formal net positive charge (which, of course, says nothing of the actual site charge distribution, which may be more or less diffuse) may exert a powerful polarizing effect by finding itself in a relatively nonpolar environment when water is ejected from the side-chain binding cavity and the Tyr 248 side chain partially closes the cavity (278). The interaction between the free carboxylate of the substrate and Arg 145 may assist in locating the phenolic hydroxyl of Tyr 248 in the vicinity of the peptide bond. This could clearly explain the absolute necessity for a free carboxyl group if the hydroxyl of

Tyr 248 near the peptide bond is necessary for peptide hydrolysis (278, 295).

The carboxyl group of Glu 270 may engage in nucleophilic attack on the peptide carbonyl carbon so forming a (labile) anhydride, or may function as a general base catalyst by accepting a proton from a water molecule poised near the carbonyl group. Tyr 248 may then, by a proton shift in a hydrogen bond, donate a proton to the incipient amino group as the peptide bond breaks. With dipeptide substrates another hydrogen bond may be made between the tyrosyl oxygen and the terminal NH_2 (or NH in substituted dipeptides) and such hydrogen bonds could help to produce strain at the substrate peptide bond. These postulated mechanistic features are summarized in Fig. 31. Of the two possible mechanisms, general base catalysis (Fig. 31C) and the specific nucleophilic attack by Glu 270 with anhydride formation (Fig. 31D), the latter has recently been favored (278, 296).

The features shown in Fig. 31 are based on structural information from a relatively nonproductive complex, and, although the key structural features in an active enzyme-substrate complex may closely resemble those shown, the prediction of mechanism from structural information alone is hazardous. It is necessary to examine how far the extensive physicochemical and kinetic data on CPA are consistent with the mechanistic implications of Fig. 31, which we have just discussed.

2. *Comparison of Chemical Properties with the Structural Features*

The zinc ion has been shown to be essential for both peptidase and esterase activity (295, 297–299). Substrate-binding studies showed that the metal ion was not, however, necessary for the *binding* of dipeptide or N-substituted dipeptide substrates: both form stable complexes with the apoenzyme and then prevent binding of the metal ion (300, 301). A series of comparative binding studies with a variety of substrates, (see, for example, Section IV,A) established that the groups on the substrate necessary for binding to the apoenzyme were the side chain on the C-terminal residue (aromatic or branched aliphatic), the NH of the susceptible peptide bond, and the NH or NH_2 of the penultimate residue. That these three substrate groups have specific interactions with the protein is clear from Fig. 31A. However, the analogous ester substrates or N-acylamino acids do require a metal ion for binding, presumably because the former lack the NH on the C-terminal residue and the latter the penultimate NH or NH_2 . Thus, the metal may have a substrate orientation effect besides polarizing the substrate carbonyl group. Such an effect may also occur with peptide substrates, although

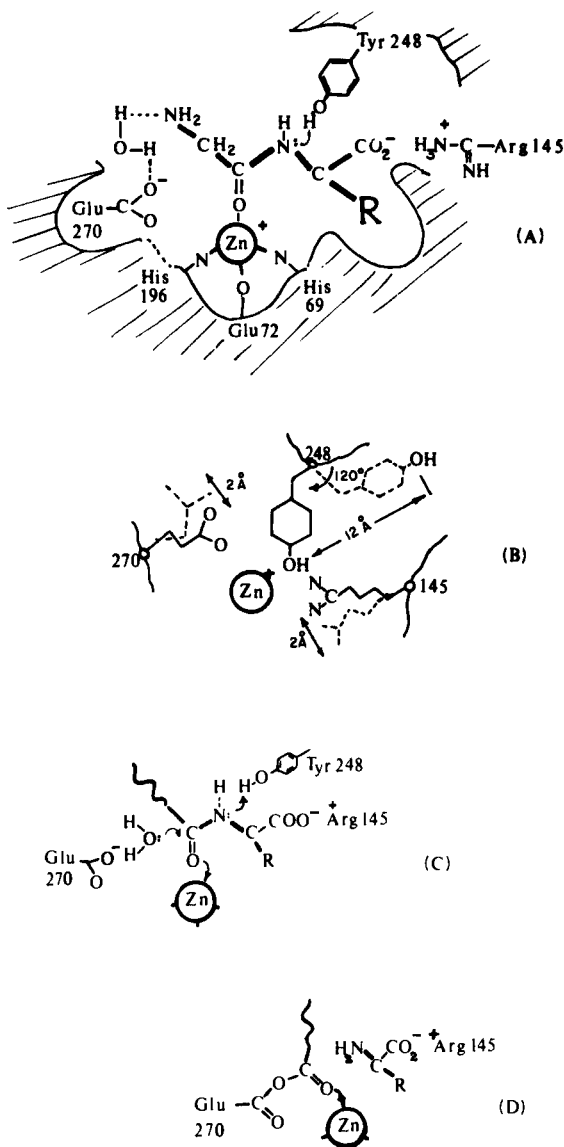


FIG. 31. The active site of carboxypeptidase A. (A) Schematic diagram showing side-chain interactions with substrate, the bonds of which are shown with heavy lines. (B) Side-chain movements on substrate binding. (C) General base-catalyzed attack on the peptide bond. (D) Nucleophilic attack by the carboxyl group of Glu 270 giving a labile anhydride.

the stronger interaction of the latter with the protein side groups provides for complex formation with the apoenzyme. The free C-terminal carboxyl is not absolutely necessary for binding, since amides will bind, but it is an absolute requirement for catalysis, possibly because its interaction with Arg-145 triggers conformational changes necessary for catalysis (278).

Chemical modifications, particularly those involving Tyr 248 (and at least one other tyrosyl residue) have been illuminating. Modifications involving Glu 270 and Arg 145 unfortunately have given less definite results (302). The chemical modifications and their effects on peptidase and esterase activity are extensive and are summarized by Chlebowski and Coleman (15). Briefly, most acylations appear to acylate the hydroxyl groups of tyrosyl residues (302, 303). When acetylimidazole and acetic anhydride are the acylating agents, the O-acetylation of two tyrosyl residues is indicated from the spectroscopic changes (303, 304). One of these residues is probably Tyr 248, although in only two of the modifications, iodination and reaction with diazotized arsanilic acid, has reaction with Tyr 248 been directly identified by the key experiment of isolation of the peptide containing the modified residue (305, 306).

The most significant result of the tyrosyl modifications is the loss of peptidase activity and remarkable enhancement of esterase activity accompanying the apparent modification of Tyr 248. Thus, Tyr 248 would appear to be required for peptide hydrolysis, but not for the hydrolysis of the substrate ester used in these studies, hippuryl- β -phenyllactate (see Table XVI). The modification appears to decrease the affinity of peptide binding to the apoenzyme (307), as might be expected from the loss of the hydrogen bond interaction of Tyr 248 with the C-terminal NH (Fig. 31A).

The nitration of one tyrosyl residue with tetranitromethane abolishes most of the peptidase activity, so that residue 248 is probably nitrated (308).

3. Comparison of Kinetic Behavior with the Structural Features

Carboxypeptidase A kinetics are not simple, and substrate inhibition and product inhibition and activation have caused difficulties (309–311). However the pH–rate profile for CPA-catalyzed peptide hydrolysis is bell-shaped with an apparent pK_a on the acid side of ~ 6.5 and one on the alkaline side near 9.4, the optimum occurring at about pH 7.5 (311). Although the pH–rate profile for the ester substrate, hippuryl- β -phenyllactate, is not bell-shaped, a series of esters, including O-acetyl-L-mandelate and O-(transcinnamoyl)-L- β -phenyllactate, show

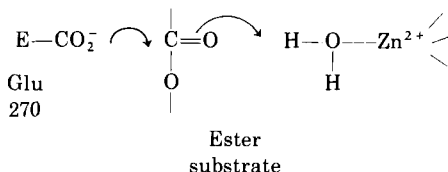
bell-shaped pH-rate profiles. The apparent pK_a values of ionizations on the free enzyme that affect activity are one of 6.5 ± 0.4 and another that varies from 9.4 to 7.5 (296). The pK_a of 6.5 could be attributed to Glu-270, required in its carboxylate form. This pK_a is rather different from those usually observed for β - or γ -carboxylic acid groups, but may be shifted by the environment in the protein. The observed shifts in the value of the alkaline pK_a , 9.4–7.5, and the fact that acetylation of Tyr-248 stops peptide hydrolysis and the hydrolysis of certain esters (e.g., *O*-acetyl-L-mandelate), but not others (e.g., the β -phenyllactate esters), make it less certain that the alkaline pK_a is that of Tyr 248 (296). It has recently been suggested that the alkaline pK_a is that of a Zn-coordinated H_2O molecule (296) and the observed pK_a is then a composite value reflecting competition between the substrate carbonyl and OH^- for zinc coordination.

As we have seen, there are marked differences between peptide and ester hydrolysis, and it is likely that at least some features of the mechanism differ in each case. For CPA-catalyzed hydrolysis of peptides, for example, there is no kinetic solvent isotope effect on the value of $k_{cat}/K_{m\ app}$, and the effect on k_{cat} is small ($k_{cat} H_2O/k_{cat} D_2O = 1.33 \pm 0.15$) compared with that expected for a reaction in which proton transfer occurs in a rate-determining step (296). In contrast, the $k_{cat} H_2O/k_{cat} D_2O$ ratio for the reaction of the ester is about 2, suggesting that a catalytic step involving proton transfer becomes important in the enzyme-catalyzed hydrolysis of esters. Comparison of the CPA-catalyzed hydrolysis rates of a series of esters and peptides showing simple kinetic behavior reveals that esters are about 5×10^3 times more reactive than the corresponding peptides (296).

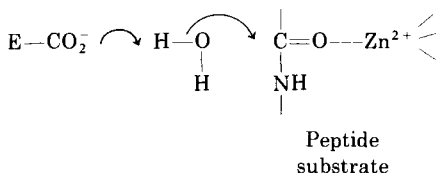
The lack of a solvent isotope effect in peptide hydrolysis and the existence of one in ester hydrolysis may be accommodated in terms of the mechanism involving anhydride formation with the carboxyl of Glu 270 (Fig. 31,D). It has been suggested that a tetrahedral intermediate (analogous to that observed in model ester hydrolyses) breaks down to give an anhydride species and the α -amino or α -hydroxy acid product (296). The lack of a solvent isotope effect in peptide hydrolysis suggests that anhydride *formation* may be rate-controlling, in which case an isotope effect would not be expected, whereas the solvent isotope effect on ester hydrolysis could be explained if *hydrolytic breakdown* of an anhydride intermediate were rate-controlling.

In this connection an experiment (312) on the esterase activity of CPA using the ester *o*-(*trans*-*p*-chlorocinnamoyl)-L- β -phenyllactate as substrate is particularly interesting. Reduced-temperature kinetics were used to demonstrate the formation of an acyl-enzyme intermediate that is sufficiently stable at $-60^\circ C$ for spectral characterization and

accounts for the biphasic kinetics of the hydrolysis. These results and knowledge of the active-site groups led to the conclusion that a mixed anhydride intermediate forms at Glu 270 during the reaction:



Again, a zinc-bound water molecule is implicated in the reaction.* It has been suggested that such is not the case in peptidase action, a different alignment existing at the active site (313):



Calculations on the electrostatic environment of the scissile peptide bond suggest that catalysis is enhanced by stabilization of the products rather than by an induced polarization by the Zn(II) ion (314).

It is interesting that extensive studies of the kinetics of CPA-catalyzed hydrolysis indicate the existence of deeper subtleties; e.g., more than one substrate or inhibitor binding site and productive and non-productive binding in one site have been proposed (309, 310, 315, 316), and the decay of an $E \cdot S$ complex followed fluorimetrically have indicated that, at least in some cases of noncompetitive inhibition, two sites must be involved (317). Thus, structural information enables us to glimpse some of the broad features of the catalytic mechanism, but much remains tantalizingly concealed.

V. Conclusions

For carbonic anhydrase we have seen how modern kinetic and physical techniques have revealed much about the mechanism of the CO_2 hydration reaction without revealing all the secrets of the process.

* The Co(III)-enzyme could readily retain esterase activity in an analogous way, since no Co(III)-ligand fission (likely to be a slow process) is required.

The specificity for zinc and cobalt emerges clearly. The question here is: how does the zinc (or cobalt) work? Evidence is not firm that CO_2 coordinates during reaction, but the possibility has not been disproved. Indeed, it has recently been proposed that CO_2 binds weakly to the fifth coordination site of the zinc ion in the hydrophobic region of the active site; this suggestion is based on the results of a crystal structure study of the HCAB-imidazole complex (122), previous studies having indicated that imidazole is a competitive inhibitor of CO_2 hydration (107). The general chemistry of CO_2 hydration catalysis shows the interesting feature that a combined Lewis acid-proton acceptor is the most effective catalyst. Again, there is some evidence that a zinc-bound water molecule dissociates to give the effective nucleophile, but it is reasonably clear that a hydroxo complex, $\text{M}-\text{OH}$, *by itself*, is inadequate for the high enzyme reactivity. However, coupled with a proton-transfer group or groups at the active site an $(\text{His})_x\text{M}-\text{OH}$ complex bears a strong resemblance to the effective inorganic catalysts of CO_2 hydration.

The high reactivity of the carbonic anhydrases raises the intriguing question whether, in the course of evolution, maximum reactivity has been achieved. In contrast to the other two enzymes we have been considering, it is not difficult to answer this question for carbonic anhydrase. It can be shown [see, for example, Fersht (318)] that where the organism requires maximum rate [although this is true for most enzymes, there are cases where the rate is subordinate to control (318)] a criterion of the state of progress in evolution has two parts: (a) that k_{cat}/K_m is maximized, and (b) that K_m is greater than $[\text{S}]$.

The maximum value of k_{cat}/K_m is 10^8 – $10^9 \text{ sec}^{-1} \text{ mol}^{-1}$, and a perfectly evolved enzyme should have a value for this ratio in this range and the additional feature that $K_m > [\text{S}]$. For carbonic anhydrase criterion (a) is met, and under physiological conditions the concentrations of CO_2 and HCO_3^- are such that the enzyme is only 6% saturated with each substrate and the K_m for CO_2 is too large to be measured. By these criteria then, carbonic anhydrase has already reached the stage of evolution of maximum rate.

The evidence on the role of zinc in the dehydrogenases, LADH and YADH, indicates that the coenzyme has an adenine binding site well removed from the catalytic zinc ion: NADH and NAD^+ bind in an extended conformation with the nicotinamide ring projecting near to the catalytic zinc but not coordinated to it, although as we have seen there is conflicting evidence on the latter point. The substrate is probably able to coordinate to the zinc in the enzyme-coenzyme complex, but again there is uncertainty about the precise mode of enzyme-coenzyme-substrate interaction.

Carboxypeptidase A, the first metalloenzyme to have its structure determined, shows remarkable conformational changes of large magnitude on substrate binding, and there is no better illustration of the key factor in the functioning of a metalloenzyme, viz., a cooperative process involving the metal ion and groups on the ligand protein functioning in concert to attack the substrate at several points. It seems likely that a zinc-bound water molecule plays a role in the esterase activity of CPA, but probably not in its peptidase activity.

VI. Glossary

Amino acids and protein structure: The essentials (318a, 318b) are indicated in Charts 1 and 2.

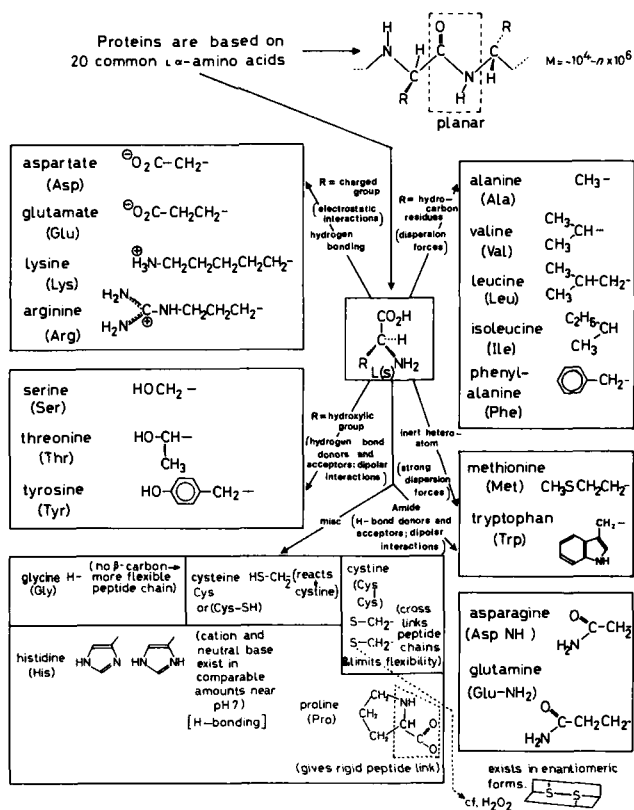


CHART 1. Amino acids. In writing a polypeptide, for instance, Gly-Glu-Arg—etc.—Ala, hyphens mean that the sequence is known (if it is not, commas are used). The free amino group is at the left (on Gly) and the free carboxyl at the right (on Ala).

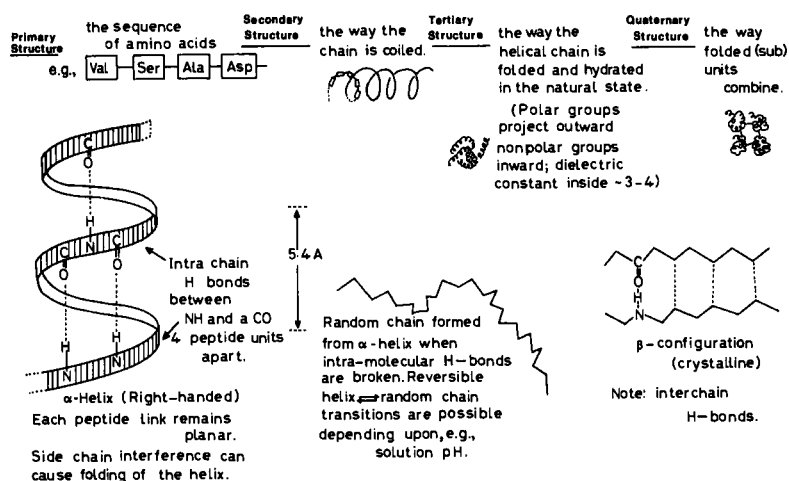


CHART 2. Protein structure. The properties of a protein are governed by its amino acid sequence, which is determined genetically, and by its structure.

Apoenzyme and holoenzyme: The apoenzyme is the protein part of the enzyme, e.g., a metalloenzyme from which the metal ion has been removed; more generally the term is used for an enzyme-coenzyme system without the coenzyme. The term holoenzyme refers to the enzyme complete with its metal ion or coenzyme. Some confusion is possible; e.g., in literature on dehydrogenases which use NAD^+ or the phosphate derivative, NADP^+ , as coenzyme, the complex of the enzyme and coenzyme is called the holoenzyme and the free enzyme is called the apoenzyme, although with YADH and LADH it would contain zinc ions. The context usually makes clear the meaning intended.

Conformational change: A conformational change is a change in the average positions of the atomic nuclei, but does not include covalent bond changes. Thus, unfolding or rotation about the bonds of a protein is a conformational change, but the dissociation of a proton is not, although it may accompany a conformational change. Polarizations of electrons without change in the positions of the atomic nuclei are not conformational changes.

Enzyme kinetics (318c), a resumé: Experimentally, the concentration of enzyme, E , at least in most *in vitro* experiments, is negligible compared with that of the substrate, S , and as the concentration of the substrate is increased a saturation effect on the initial reaction velocity, v , is observed (Fig. 32a). Analysis of the experimental data shows that the variation of initial rate with substrate concentration is

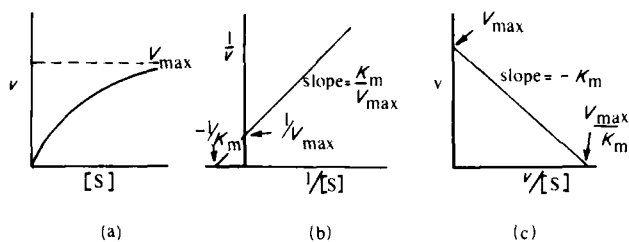


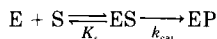
FIG. 32. The typical behavior of an enzyme-catalyzed reaction: (a) initial velocity, v , is plotted against substrate concentration $[S]$; (b) Lineweaver-Burk plot; (c) Eadie-Hofstee plot.

given by

$$v = \frac{V_{\max}[S]}{([S] + K_m)} \quad (1)$$

and $V_{\max} = k_0 E_0$. Equation (1) is called the Michaelis-Menten or Henri equation. K_m is called the Michaelis constant; k_0 , which is V_{\max}/E_0 , is called the *turnover number* of the enzyme, the number of moles of substrate converted per mole of enzyme per unit time. Thus, the turnover number (sec^{-1}) of carboxypeptidase A is about 10^2 , that of carbonic anhydrase 10^4 – 10^5 , depending on the isozyme. Most turnover numbers are in the region of 10^2 – 10^4 , although that of catalase is exceptionally high at 10^7 . The rate observations are sometimes plotted in reciprocal form as a Lineweaver-Burk (Fig. 32b) or Eadie-Hofstee plot (Fig. 32c).

Michaelis and Menten, developing earlier ideas, proposed a mechanism in which E and S were in thermodynamic equilibrium with an enzyme-substrate complex, ES:



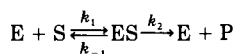
This scheme leads simply to the equation

$$v = \frac{[E_0][S]k_{\text{cat}}}{([S] + K_s)} \quad (2)$$

where $K_s = [E][S]/[ES]$. K_m is clearly the equilibrium constant in this scheme, i.e., the dissociation constant of the ES complex; the larger the K_m , the lower the stability of the ES complex.

The *mechanism* is only appropriate when k_{cat} is very much less than the rate of dissociation of ES. The Eq. (1) holds for many mechanisms,

but the particular mechanism of Michaelis and Menten is not always a correct description of the processes actually occurring in the system. Equation (1) can also be derived from a steady-state approach in which $d[\text{ES}]/dt = 0$, the Briggs-Haldane treatment; writing the mechanism as



it is readily shown that

$$v = \frac{[\text{E}_0][\text{S}]k_2}{[\text{S}] + \frac{(k_2 + k_{-1})}{k_1}}$$

which is identical with Eq. (1), where $K_m = (k_2 + k_{-1})/k_1$. Clearly if $k_{-1} \gg k_2$, $K_m = K_s$.

A mechanism using any number of intermediates, a two-step consecutive reaction ($k_{-1} \ll k_2$) and one involving a nonproductive ES complex, all lead to rate equations of the form of (1). K_m and k_0 are then composite. This question is discussed more fully in reference 318, but we may note two points. First, although $K_m = K_s$ only for the Michaelis-Menten mechanism, K_m may be treated for some purposes as an apparent dissociation constant. For instance, the free enzyme concentration may be calculated from the relation

$$\frac{[\text{E}][\text{S}]}{\sum [\text{ES}]} = K_m$$

where $\sum \text{ES}$ is the sum of all the bound enzyme species (318). Care is needed in interpreting the effects of temperature, pH, etc., on an apparent K_m because the rate constants contained in this composite term are also affected. Similar remarks also apply to k_{cat} , which again is a composite function of rate constants of individual steps in mechanisms more complex than that corresponding to the Briggs-Haldane scheme. As Fersht has pointed out (318), there are examples in the literature where breaks in the temperature dependence of k_{cat} have been interpreted as conformational changes in the enzyme when they are really due to a different temperature dependence of the individual rate constants comprising k_{cat} . Second, although it would appear that little mechanistic information can be obtained by kinetic measurements per se, a diagnostic test of the Briggs-Haldane mechanism is possible using rapid reaction techniques to measure k_1 , the rate of association between E and S. It can be shown (318) that association rate constants

should be of the order of $10^8 \text{ mol}^{-1} \text{ sec}^{-1}$. Where $k_2 \gg k_1$ then $k_1 = k_{\text{cat}}/K_m$; if the latter ratio is $\sim 10^7$ – 10^8 , then the Briggs–Haldane mechanism operates. This is true for a variety of enzymes, including, for instance, carbonic anhydrases (318).

From a purely mechanistic viewpoint it is unlikely that a simple scheme, such as the Michaelis–Menten or Briggs–Haldane scheme, will work without modification since each has basically three deficiencies. These are: (i) enzyme reactions are reversible so the step $E + P \rightarrow ES$ must be considered (but in steady-state conditions $[S] \gg [P]$, so that this is not serious); (ii) there should be at least one other step in which EP, product bound to enzyme, is considered; (iii) if there is a conformational change, e.g., when S combines with E, it is not usually possible to measure this kinetically (except when $[E]$ is stoichiometric, not catalytic).

The most useful general picture is probably to regard an enzyme-catalyzed reaction as being made up of three elementary steps:



Step 1 is the formation and dissociation of an enzyme/reactant complex; step 2 is a conformational change in the complex; and step 3 is the chemical transformation, bond making or rupture, or electron or proton transfer.

As we have seen, combination rates for step 1 are often close to 10^8 and most fall in the range 10^6 – 10^8 ; however, dissociation rates of ES vary over many orders of magnitude. There is a parallel here with metal complex formation (rates of complex formation for a given metal with various ligands show relatively small variation whereas rates of dissociation vary widely and control stability), and the dissociation constants of acids ($HA \xrightleftharpoons{a} H^+ + A^-$ varies widely, k_b relatively little).

For a description of the issue of the pH dependence of K_m and k_{cat} , the reader is referred to reference 318.

Enzyme inhibition: Enzymes may be irreversibly inactivated by heat or chemical reagents; active-site-directed irreversible inhibitors or *affinity labels* are important in identifying catalytically important residues (318, 319), and hundreds of them have been synthesized. They involve covalent bonding to active residues in the protein, and some of them are important in chemotherapy. The inhibitor may, however, bind reversibly and noncovalently: there are four main types of such inhibition.

1. Competitive inhibition: If the inhibitor, I, binds reversibly at the active site of the enzyme and prevents S binding and vice versa, I is

said to be a competitive inhibitor. For enzymes conforming to Eq. (1) this appears on a Lineweaver–Burk or Eadie–Hofstee plot as shown in Fig. 33a (318, 320). V_{\max} is unaffected but K_m is increased. Results are often expressed in terms of an inhibition constant, K_i (see, for example, Tables XI and XIII) where K_i is $[E][I]/[EI]$, i.e., the dissociation constant of the EI complex.

2. Noncompetitive inhibition: If the inhibitor binds at a site other than the active site, but such binding decreases the reactivity of the ES complex, the inhibitor is said to be noncompetitive because there is no competition with substrate for the active site. This behavior gives rise to the plots shown in Fig. 33b. Here V_{\max} is decreased, but K_m is unaffected. Provided that the mechanism of the catalysis is two step, noncompetitive inhibition can indicate the existence of an equilibrium between S, E, and ES ($k_{-1} \gg k_2$): the observation of noncompetitive inhibition (k_0 varies, but K_m remains constant) shows that k_2 must be much less than k_{-1} for K_m to be constant because $K_m = (k_{-1} + k_2)/k_1$. The hydrogen ion is a typical noncompetitive inhibitor.

3. Mixed inhibition: For a Michaelis–Menten mechanism, it is readily shown that noncompetitive inhibition is observed when the

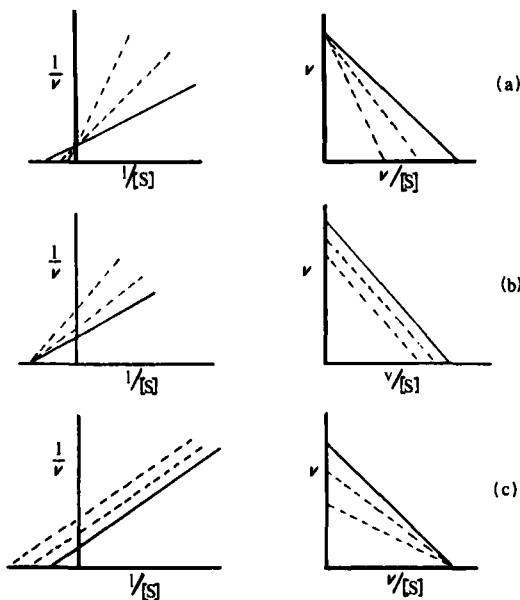


FIG. 33. Types of enzyme inhibition and their effects on Lineweaver–Burk (left) and Eadie–Hofstee (right) plots. The solid line is the plot with zero inhibitor concentration; the dashed lines are plots with inhibitor present at successively larger concentrations. (a) Competitive inhibition. (b) Noncompetitive inhibition. (c) Uncompetitive inhibition.

inhibitor has the same affinity for E as for ES (318); where this affinity differs, both K_m and k_{cat} are altered and the inhibition is described as mixed, with obvious consequences for the Lineweaver–Burk and Eadie–Hofstee plots.

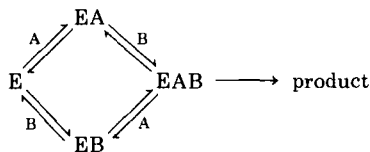
4. Uncompetitive inhibition: Here the inhibitor binds to ES, but not to E, and gives the behavior shown in Fig. 33c. This behavior can also arise (321) in the case where K_m approaches k_2/k_1 ; i.e., k_{-1} is small and the inhibitor has an effect on k_2 , so producing proportional changes in V_{max} and K_m .

For the effects of pH on enzyme inhibition the reader is referred to Fersht (318).

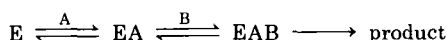
Enzyme–coenzyme kinetics: Dehydrogenases such as LADH, YADH, etc., have two substrates: one is NAD^+ the coenzyme; the other is the alcohol, the oxidation of which is to be catalyzed. In fact, in the study of isolated enzyme reactions the distinction between coenzymes and substrates is not meaningful (322). The general solutions of the steady-state equations for multisubstrate systems are involved, and the reader is referred to Fromm and other authors (323–326) and to shorter summaries (327, 327a, 328) for further information. The key experimental feature is the fact that most reactions obey Michaelis–Menten kinetics when the concentration of one substrate is held constant and the other is varied. It also appears that only a limited range of mechanisms is observed in practice. The terms used are as follows.

Reactions in which all the substrates bind to the enzyme before the first product is formed are called *sequential*. Reactions in which one or more products are released before all the substrates are added are called *Ping-Pong*. In an *ordered* sequential mechanism, the substrates combine with the enzyme and the products dissociate in an obligatory order. A *random* mechanism implies no obligatory order of combination or release.

If the two substrates are A and B, then EAB is a ternary complex and we then have the following cases.



1. RANDOM SEQUENTIAL MECHANISM



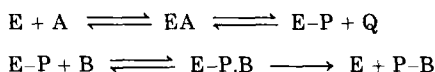
2. ORDERED MECHANISM

The ordered mechanism is the type observed with NAD^+ -linked dehydrogenases. A special case of this, the Theorell-Chance mechanism, is found with LADH; the ternary complex does not accumulate.



Here A is NAD^+ , B is EtOH, P is CH_3CHO , Q is NADH.

3. Ping-Pong mechanism: This is of the kind



It is found with phosphate-transferring enzymes; A might be a phosphate ester, E-P a phosphorylated enzyme, B is a second alcohol, and P-B the phosphate ester of the second alcohol.

Sequence homologies, mutations, and isozymes: There are three basic postulates of chemical palaeontology (329-331). (i) Polypeptide chains in present-day organisms have arisen by evolutionary divergence from similar polypeptide chains that existed in the past. The present and past chains would be similar in that many of their amino acid residues along the chain match; such chains are said to be homologous or to show sequence homology. (ii) A gene existing at some past epoch can occasionally be duplicated so that it appears at two or more sites in the total stock of genetic information of descendant organisms. Thus, a contemporary organism can have two or more homologous genes giving rise to homologous polypeptide chains *that have mutated independently* and are therefore no longer identical in structure. (iii) Mutational events that are most commonly retained through natural selection are those that lead to a replacement of a single amino acid residue in a polypeptide chain. Human carbonic anhydrases B and C contain a 60% sequence homology (Section II,B,1); i.e., 60% of the sequence of amino acids match in the B and C forms.

It may be wondered how one can assume that the chains of the B and C forms have common ancestry when there are so many differences. The justification is that it is most improbable that two different and unrelated polypeptide chains could evolve in such a way as to have qualitatively the same function, the same conformation, and a substantial number of amino acid residues at corresponding molecular sites. The marked difference in sequence is then taken as evidence that a long time has elapsed since the B and C forms diverged from a common ancestor. These molecules, such as HCAC and HCAB, which have been produced by gene duplication and mutation, are called isozymes. They differ quantitatively in reactivity as we have seen for the carbonic

anhydrases, and, since kinetic measurements should be made on a single characterized species, it is important at an early stage to see what isozymes of a metalloenzyme exist (e.g., by chromatographic and/or electrophoretic methods) and to use a pure isozyme. The use of mixtures of isozymes has led to difficulties of interpretation, for example, with carbonic anhydrase, before the discovery of its constituent isozymes and in other cases (332).

REFERENCES

1. Tam, S. W., Wilber, K. E., and Wagner, F. W., *Biochem. Biophys. Res. Commun.* **72**, 302 (1976).
2. Raulin, J., *Ann. Sci. Nat., Bot. Biol. Veg.* **11**, 93 (1869).
3. Keilin, D., and Mann, T., *Biochem. J.* **34**, 1163 (1940).
4. Eichhorn, G. L., *Inorg. Biochem.* **2**, 1191 and 1210 (1973). Cf. also, Auld, D. S., Kawaguchi, H., Livingston, D. M., and Vallee, B. L., *Proc. Natl. Acad. Sci. U.S.A.*, **71**, 2091 (1974).
5. Wacker, W. E. C., *Biochemistry* **1**, 859 (1962).
6. Falchuk, K. H., Mazus, B., Ulpino, L., and Vallee, B. L., *Biochemistry* **15**, 4468 (1976).
7. Wandzilak, T. M., and Benson, R. W., *Biochem. Biophys. Res. Commun.* **76**, 247 (1977).
8. Sabbioni, E., *FEBS Lett.* **71**, 233 (1976).
9. Springate, C. F., Mildvan, A. S., Abramson, R., Engle, J. L., and Loeb, L. A., *J. Biol. Chem.* **248**, 5987 (1973).
10. Scrutton, M. C., Wu, C. W., and Goldthwait, T. A., *Proc. Natl. Acad. Sci. U.S.A.* **68**, 2497 (1971).
11. Valenzuela, P., Morris, R. W., Faras, A., Levinson, W., and Rutter, J., *Biochem. Biophys. Res. Commun.* **53**, 1036 (1973).
12. Hughes, M. H., and Prince, R. H., *J. Inorg. Nucl. Chem., Bio-Inorg. Sect.* **40**, 703 (1978).
13. Hughes, M. H., and Prince, R. H., *J. Inorg. Nucl. Chem., Bio-Inorg. Sect.* **40**, 713 (1978).
14. Hughes, M. H., and Prince, R. H., *J. Inorg. Nucl. Chem., Bio-Inorg. Sect.* **40**, 719 (1978).
15. Chlebowski, J. F., and Coleman, J. E., *Met. Ions Biol. Syst.* **6**, p. 1 (1976).
16. Clark, I. D., and Wain, R. P., *Compr. Chem. Kinet.* **2**, 318, 329, and 334 (1969); cf. also Hix, J. E., and Jones, M. M., *Inorg. Biochem.* **1**, 361 (1973).
17. Vallee, B. L., and Williams, R. J. P., *Proc. Natl. Acad. Sci. U.S.A.* **59**, 498 (1968); Williams, R. J. P., *Inorg. Chim. Acta Rev.* **5**, 137 (1971).
18. Coleman, J. E., *Prog. Bioorg. Chem.* **1**, 159 (1971).
19. Coleman, J. E., in "Reactivities of Functional Groups of Proteins" (H. Gutfreund, ed.), MTP Int. Rev. Sci., p. 185. Med. Tech. Publ., Oxford, 1974.
20. Harris, M. I., and Coleman, J. E., *J. Biol. Chem.* **243**, 5063 (1968).
21. Vallee, B. L., *Adv. Protein Chem.* **16**, 401 (1961).
- 21a. Vallee, B. L., *Adv. Protein Chem.*, **10**, 317 (1955).
22. Malmström, B. G., and Rosenberg, A., *Adv. Enzymol.* **21**, 131 (1959).
23. Rotilio, G. R., Morpurgo, L., Giovagnoli, C., Calabrese, L., and Mondovi, B., *Biochemistry* **11**, 2187 (1972).

- 23a. Richardson, J. S., Thomas, K. A., Rubin, B. H., and Richardson, D. C., *Proc. Natl. Acad. Sci. U.S.A.* **72**, 1349 (1975).
24. Beem, K. M., Richardson, D. C., and Rajagopalan, K. V., *Biochemistry* **16**, 1930 (1977).
- 24a. McAdam, M. E., Fielden, E. M., Lavelle, P., Calabrese, L., Cocco, D., and Rotilio, G., *Biochem. J.* **167**, 271 (1977).
25. Cass, A. E. G., Hill, H. A. O., Smith, B. E., Bannister, J. V., and Bannister, W. H., *Biochemistry* **16**, 3061 (1977).
26. Lippard, S. J., Burger, A. R., Ugurbil, K., Pantoliano, M. W., and Valentine, J. S., *Biochemistry* **16**, 1136 (1977).
27. Mildvan, A. S., Kobes, R. D., and Rutter, W. J. *Biochemistry* **10**, 1191 (1971).
28. Nelbach, M. E., Pigiet, V. P., Gerhardt, J. C., and Schachman, H. K., *Biochemistry* **11**, 315 (1972).
29. Meldrum, N. U., and Roughton, F. J. W., *J. Physiol. (London)* **75**, 15 (1932).
30. Tashian, R. E., Goodman, M., Tanis, R. J., Ferre, R. E., and Osborne, W. R. A., in "The Isozymes" (C. L. Markert, ed.), Vol. 4, p. 207 et seq. Academic Press, New York, 1975.
31. Maren, T., *Physiol. Rev.* **47**, 595 (1967).
32. Lindskog, S., Henderson, L. E., Kannan, K. K., Liljas, A., Nyman, P. O., and Strandberg, B., in "The Enzymes" (P. D. Boyer, ed.) 3rd ed., Vol. 5, p. 587 et seq. Academic Press, New York, 1971.
33. Carter, M. J., *Biol. Rev. Cambridge Philos. Soc.* **47**, 465 (1972).
34. Coleman, J. E., *Inorg. Biochem.* **1**, 488 (1973).
35. Wyeth, P., and Prince, R. H., *Inorg. Perspect. Biol. Med.* **1**, 37 (1977).
36. Keilin, D., and Mann, R., *Nature (London)* **144**, 442 (1939); cf. also Keilin and Mann (3).
37. Tashian, R. E., Tanis, R. J., and Ferrell, R. E., *Oxygen Affinity Haemoglobin Red Cell Acid Base Status, Proc. 4th Alfred Benson Symp., 1971* Vol. 4, p. 353 et seq. (1972).
38. Lindskog, S., *Biochim. Biophys. Acta* **39**, 218 (1960).
39. Nielsen, S. A., and Frieden, E., *Comp. Biochem. Physiol. B* **41**, 461 (1972).
40. Sciaky, M., and Laurent, G., *FEBS Lett.* **63**, 141 (1976).
41. Nyman, P. O., *Biochim. Biophys. Acta* **52**, 1 (1961).
42. Nassi, L., Poggini, G., Borselli, L., and Galvan, P., *Quad. Sclavo. Diagn. Clin. Lab.* **11**, 594 (1975).
43. Whitney, P. L., Nyman, P. O., and Malmström B. G., *J. Biol. Chem.* **242**, 4212 (1967).
44. Verpoorte, J. A., Mehta, S., and Edsall, J. T., *J. Biol. Chem.* **242**, 4221 (1967).
45. Osborne, W. R. A., and Tashian, R. E., *Biochem. J.* **141**, 219 (1974).
46. Osborne, W. R. A., and Tashian, R. E., *Isozyme Bull.* **7**, 40 (1974).
47. Bradbury, S. L., *J. Biol. Chem.* **244**, 2002 and 2010 (1969).
48. Kandel, M., Gornall, A. G., Wong, S.-C. C., and Kandel, S. I., *J. Biol. Chem.* **245**, 2444 (1970).
49. Whitney, P. L., Fölsch, G., Nyman, P. O., and Malmström, B. G., *J. Biol. Chem.* **242**, 4206 (1967).
50. Tashian, R. E., *Adv. Exp. Med. Biol.* **28**, 167-168 (1972).
51. Maren, T. H., Rayburn, C. S., and Liddell, N. E., *Science* **191**, 469 (1976).
52. Cockle, S. A., Lindskog, S., and Grell, E., *Biochem. J.* **143**, 703 (1974).
53. Anderson, B., Nyman, P. O., and Strid, L., *Biochem. Biophys. Res. Commun.* **48**, 670 (1972).
54. Lin, K.-T. D., and Deutsch, H. F., *J. Biol. Chem.* **248**, 1885 (1973).
55. Marriq, C., Sciaky, G., Kiraud, N., Foveau, D., and Laurent-Tabusse, G., *Biochimie* **55**, 1361 (1973).

56. Giraud, N., Marriq, C., and Laurent-Tabusse, G., *Biochimie* **56**, 1031 (1974).
57. Henderson, L. E., Henriksson, D., and Nyman, P. O., *Biochem. Biophys. Res. Commun.* **52**, 1388 (1973).
58. Henderson, L. E., Henriksson, D., and Nyman, P. O., *J. Biol. Chem.* **251**, 5457 (1976).
59. Lin, K.-T. D., and Deutsch, H. F., *J. Biol. Chem.* **249**, 2329 (1974).
60. Sciaky, M., Limozin, N., Fillipi-Foveau, D., Gulian, M. J.-M., Dalmasso, C., and Laurent, G., *C.R. Habd. Scances Acad. Sci., Ser. D* **279**, 1217 (1974).
61. Kannan, K. K., Liljas, A., Vaara, I., Bergstén, P.-C., Lövgren, S., Strandberg, B., Bengtson, U., Carlbom, U., Fridborg, K., Järup, L., and Petef, M., *Cold Spring Harbor Symp. Quant. Biol.* **36**, 221 (1971).
62. Liljas, A., Kannan, K. K., Bergstén, P.-C., Vaara, I., Fridborg, K., Strandberg, B., Carlbom, U., Järup, L., Lövgren, S., and Petef, M., *Nature (London), New Biol.* **235**, 131 (1972).
63. Nostrand, B., Vaara, I., and Kannan, K. K., in "The Isozymes" (C.L. Markert, ed.), Vol. 1, p. 575 et seq. Academic Press, New York, 1975.
64. Kannan, K. K., Nostrand, B., Fridborg, K., Lövgren, S., Ohlsson, A., and Petef, M., *Proc. Natl. Acad. Sci. U.S.A.* **72**, 51 (1975).
65. Vaara, I., Lövgren, S., Liljas, A., Kannan, K. K., and Bergstén P.-C., *Adv. Exp. Med. Biol.* **28**, 169 (1972).
66. Wee, V. T., Feldmann, R. J., Tanis, R. J., and Chignell, C. F., *Mol. Pharmacol.* **12**, 832 (1976).
67. Erlich, R. H., Starkweather, D. K., and Chignell, C. F., *Mol. Pharmacol.* **9**, 61 (1973).
68. Hower, J. F., Henkens, R. W., and Chesnut, D. B., *J. Am. Chem. Soc.* **93**, 6665 (1971).
69. Campbell, I. D., Lindsog, S., and White, A. I., *J. Mol. Biol.* **90**, 469 (1974).
70. Campbell, I. D., Lindsog, S., and White, A. I., *J. Mol. Biol.* **98**, 597 (1975).
71. Cockle, S. A., *Biochem. J.* **137**, 587 (1974).
72. Vaara, I., Inaugural Dissertation, University of Uppsala, Sweden (1974).
73. Blow, D. M., Birktoft, J. J., and Hartley, B. S., *Nature (London)* **221**, 337 (1970).
74. Glass, J. C., and Graf, G., *U.S. N.T.I.S. PB Rep. PB-252 190* (1975); *Chem. Abstr.* **85**, 139365w (1976).
75. Diehn, B., Halpern, A., and Stöcklin, G., *J. Am. Chem. Soc.* **98**, 1077 (1976).
76. Lipscomb, W. N., *Chem. Soc. Rev.* **1**, 319 (1972).
77. Tupper, R., Watts, R. W. E., and Wormall, A., *Biochem. J.* **50**, 429 (1952).
78. Wyeth, P., Ph.D. Thesis, University of Cambridge, England (1976).
79. Závodsky, P., Johansen, J. T., and Hvidt, A., *Eur. J. Biochem.* **56**, 67 (1975).
- 79a. Bauer, R., Limkilde, P., and Johansen, J. T., *Biochemistry* **15**, 334 (1976).
80. Dunn, M. F., *Struct. Bonding (Berlin)* **23**, 61 (1975).
81. Thorsland, A., and Lindsog, S., *Eur. J. Biochem.* **3**, 117 (1967).
82. Lindsog, S., and Thorsland, A., *Eur. J. Biochem.* **3**, 453 (1968).
83. Taylor, P. W., King, R. W., and Burgen, A. S. V., *Biochemistry* **9**, 3894 (1970).
84. Lindsog, S., *Biochim. Biophys. Acta* **122**, 537 (1966).
85. Myers, D. V., and Edsall, J. T., *Proc. Natl. Acad. Sci. U.S.A.* **53**, 169 (1965).
86. Coleman, J. E., *Biochemistry* **4**, 2644 (1965).
87. Whitney, P. L., and Brandt, H., *J. Biol. Chem.* **251**, 3862 (1975).
88. Holmquist, B., Kaden, T. A., and Vallee, B. L., *Biochemistry* **14**, 1454 (1975).
89. Lindsog, S., and Ehrenberg, A., *J. Mol. Biol.* **24**, 133 (1967).
90. Edsall, J. T., *Harvey Lect.* **62**, 191 (1968).
91. Henkens, R. W., and Sturtevant, J. M., *J. Am. Chem. Soc.* **90**, 2669 (1968).
92. Henkens, R. W., Watt, G. D., and Sturtevant, J. M., *Biochemistry* **8**, 1874 (1969).
93. Dennard, A. E., and Williams, R. J. P., *Transition Met. Chem.* **2**, 116 (1966).
94. Pocker, Y., and Stone, J. T., *Biochemistry* **7**, 4139 (1968).

95. Lo, K., and Kaiser, E. T., *J. Am. Chem. Soc.* **91**, 4912 (1969).
96. Pocker, Y., and Guilbert, L. J., *Biochemistry* **13**, 4912 (1969).
97. Sharma, M. M., and Danckwerts, P. V., *Trans. Faraday Soc.* **59**, 386 (1963).
98. Dennard, A. E., and Williams, R. J. P., *J. Chem. Soc.* p. 812 (1966).
99. Caplow, M., *J. Am. Chem. Soc.* **93**, 230 (1971).
- 99a. Woolley, P. R., *Nature (London)* **258**, 677 (1975); *J. Chem. Soc., Perkin II*, 318, (1977).
100. Brändén, C.-I., *Biochem. Soc. Trans. 568th Meet.*, 1977 p. 612 (1977).
101. Edsall, J. T., and Wyman, J., "Biophysical Chemistry," Vol. 1, Chap. 10. Academic Press, New York, 1958.
102. Sirs, J. A., *Trans. Faraday Soc.* **54**, 201 (1957).
103. Gibbons, B. H., and Edsall, J. T., *J. Biol. Chem.* **238**, 3502 (1963).
104. Gibbons, B. H., and Edsall, J. T., *J. Biol. Chem.* **239**, 2539 (1964).
105. Kernohan, J. C., *Biochim. Biophys. Acta* **96**, 304 (1965).
106. Woolley, P. R., Ph.D. Thesis, University of Cambridge, England (1973).
107. Kalifah, R. G., *J. Biol. Chem.* **246**, 2561 (1971).
108. Magid, E., *Biochim. Biophys. Acta* **151**, 236 (1968).
109. Christiansen, E., and Magid, E., *Biochim. Biophys. Acta* **220**, 630 (1970).
110. Whitney, P. L., *Eur. J. Biochem.* **16**, 126 (1970).
111. Strader, D. G., and Khalifah, R. G., *J. Am. Chem. Soc.* **98**, 5043 (1976).
112. Steiner, H., Jonsson, B.-H., and Lindskog, S., *Eur. J. Biochem.* **59**, 253 (1975).
113. Steiner, H., Jonsson, B.-H., and Lindskog, S., *FEBS Lett.* **62**, 16 (1976).
114. Cleland, W. W., *Biochim. Biophys. Acta* **67**, 104 (1963).
115. Jonsson, B.-H., Steiner, H., and Lindskog, S., *FEBS Lett.* **64**, 310 (1976).
116. De Voe, H., and Kistiakowsky, G. B., *J. Am. Chem. Soc.* **83**, 274 (1961).
117. Lindskog, S., and Coleman, J. E., *Proc. Natl. Acad. Sci. U.S.A.* **70**, 2505 (1973).
118. Khalifah, R. G., *Proc. Natl. Acad. Sci. U.S.A.* **70**, 1986 (1973).
119. Prince, R. H., and Woolley, P. R., *Bioorg. Chem.* **2**, 337 (1973).
120. Silverman, D. N., and Tu, C. K., *J. Am. Chem. Soc.* **97**, 2263 (1975).
121. Tu, C. K., and Silverman, D. N., *J. Am. Chem. Soc.* **97**, 5935 (1975).
122. Kannan, K. K., Petef, M., Cid-Dresdner, H., and Lövgren, S., *FEBS Lett.* **73**, 115 (1977).
123. Pocker, Y., Meany, J. E., and Davis, B. C., *Biochemistry* **13**, 1411 (1974).
124. Pocker, Y., and Meany, J. E., *Biochemistry* **4**, 2535 (1965).
125. Pocker, Y., Meany, J. E., Dickerson, D. G., and Stone, J. T., *Science* **150**, 382 (1965).
126. Schneider, F., and Lieflander, M., *Hoppe-Seyler's Z. Physiol. Chem.* **334**, 279 (1963).
127. Lee, W. K., and Prince, R. H., unpublished data; Lee, W. K., Ph.D. Thesis, University of Cambridge, England (1977).
128. Pocker, Y., and Storm, D. R., *Biochemistry* **7**, 1202 (1968).
129. Wells, J. W., Kandel, S. I., Kandel, M., and Gornall, A. G., *J. Biol. Chem.* **250**, 3522 (1975).
130. Wells, J. W., Ph.D. Thesis, University of Toronto, Canada (1975).
131. Pocker, Y., and Beug, M. W., *Biochemistry* **11**, 698 (1972).
132. Pocker, Y., and Watamori, N., *Biochemistry* **12**, 2475 (1973).
133. Ward, R. L., and Whitney, P. L., *Biochem. Biophys. Res. Commun.* **51**, 343 (1973).
134. Göthe, P. O., and Nyman, P. O., *FEBS Lett.* **21**, 159 (1972).
135. Appleton, D. W., and Sarkar, B., *Proc. Natl. Acad. Sci. U.S.A.* **71**, 1686 (1974).
136. Gupta, R. K., and Pesando, J. M., *J. Biol. Chem.* **250**, 2630 (1975).
137. Davis, R. P., in "The Enzymes" (P. D. Boyer, H. Lardy, and K. Myrbäck, eds.), 2nd ed., Vol. 5, p. 545 et seq. Academic Press, New York, 1961.
138. Werber, M. M., *J. Theor. Biol.* **60**, 51 (1976).
139. Pesando, J. M., *Biochemistry* **14**, 675, 681 (1975).

140. Pesando, J. M., and Grollman, A. P., *Biochemistry* **14**, 689 (1975).
141. Harrowfield, J. M., Norris, V., and Sargeson, A. M., *J. Am. Chem. Soc.* **98**, 7282 (1976).
142. Fabry, M. E., Koenig, S. H., and Schillinger, W. E., *J. Biol. Chem.* **245**, 4256 (1970).
143. Lanir, A., Gradsztajn, S., and Navon, G., *FEBS Lett.* **30**, 351 (1973).
144. Koenig, S. H., and Brown, R. D., *Proc. Natl. Acad. Sci. U.S.A.* **69**, 2422 (1972).
145. Bertini, I., Canti, G., Luchinat, C., and Scozzafava, A., *Biochem. Biophys. Res. Commun.* **78**, 158 (1977).
146. Wells, J. W., personal communication; cf. also Wyeth and Prince (35).
147. Pearson, R. G., Palmer, J., Anderson, M. M., and Allred, A. L., *Z. Elektrochem.* **64**, 110 (1960).
148. Swift, T. J., and Connick, R. E., *J. Chem. Phys.* **37**, 307 (1962).
149. Martin, R. B., *J. Inorg. Nucl. Chem.* **38**, 511 (1976).
150. Fitzgerald, J. J., and Chasteen, N. D., *Biochemistry* **13**, 4338 (1974).
151. Mann, T., and Keilin, D., *Nature (London)* **146**, 164 (1940).
152. Coleman, J. E., *Annu. Rev. Pharmacol.* **15**, 221 (1975).
153. King, R. W., and Burgen, A. S. V., *Proc. R. Soc. London, Ser. B* **193**, 107 (1976).
154. Olander, J., Bosen, S. F., and Kaiser, E. T., *J. Am. Chem. Soc.* **95**, 1616 (1973).
155. Kakeya, N., Aoki, M., Kamada, A., and Yata, N., *Chem. Pharm. Bull.* **17**, 1010, (1969).
156. Chen, R. F., and Kernohan, J. C., *J. Biol. Chem.* **242**, 5813 (1967).
157. Lindsog, S., *J. Biol. Chem.* **238**, 945 (1963).
158. Coleman, J. E., *Nature (London)* **214**, 193 (1967).
159. Kannan, K. K., Vaara, I., Nostrand, B., Borell, A., Fridborg, K., and Petef, M., in "Proceedings, on Drug Action at the Molecular Level" (G. C. K. Roberts, ed.), p. 73. Macmillan, New York, 1976.
160. Aasa, R., Hanson, M., and Lindsog, S., *Biochim. Biophys. Acta* **453**, 211 (1976).
161. Coleman, J. E., and Coleman, R. V., *J. Biol. Chem.* **247**, 4718 (1972).
162. Taylor, J. S., Mushak, P., and Coleman, J. E., *Proc. Natl. Acad. Sci. U.S.A.* **67**, 1410 (1970).
163. Lanir, A., and Navon, G., *Biochemistry* **10**, 1024 (1971).
164. King, R. W., and Burgen, A. S. V., *Biochim. Biophys. Acta* **207**, 278 (1970).
165. Galley, W. C., and Stryer, M., *Proc. Natl. Acad. Sci. U.S.A.* **60**, 108 (1968).
166. Galley, W. C., and Strambini, G. B., *Nature (London)* **261**, 521 (1976).
167. Lanir, A., and Navon, G., *Biochemistry* **11**, 3536 (1972).
168. Kumar, K., King, R. W., and Carey, P. R., *Biochemistry* **15**, 2195 (1976).
169. Bayley, P., and Anson, M., *Biochem. Biophys. Res. Commun.* **62**, 717 (1975).
170. Taylor, P. W., King, R. W., and Burgen, A. S. V., *Biochemistry* **9**, 2638 (1970).
171. Mushak, P., and Coleman, J. E., *J. Biol. Chem.* **247**, 373 (1972).
172. Petersen, R. L., Li, T.-Y., McFarland, J. T., and Watters, K. L., *Biochemistry* **16**, 726 (1977).
173. Pocker, Y., and Stone, J. T., *Biochemistry* **7**, 2936 and 3021 (1968).
174. Meldrum, N. U., and Roughton, F. J. W., *J. Physiol. (London)* **80**, 113 (1933).
- 174a. Whitney, P. L., *Anal. Biochem.* **57**, 467 (1975).
175. Lindsog, S., *Biochemistry* **5**, 2641 (1966).
176. Feeney, J., Burgen, A. S. V., and Grell, E., *Eur. J. Biochem.* **34**, 107 (1973).
177. Coleman, J. E., *J. Biol. Chem.* **242**, 5212 (1967).
178. Ward, R. L., *Biochemistry* **9**, 2447 (1970).
179. Ward, R. L., and Cull, M. D., *Arch. Biochem. Biophys.* **150**, 436 (1972).
180. Hofmeister, F., *Arch. Exp. Pathol. Pharmacol.* **24**, 247 (1888).
181. Fridovich, I., *J. Biol. Chem.* **238**, 592 (1963).

182. Coleman, J. E., *NASA Spec. Publ.* **188**, 141 (1969).
183. Lindskog, S., *Struct. Bonding (Berlin)* **8**, 153 (1970).
184. Riepe, M. E., and Wang, J. H., *J. Biol. Chem.* **243**, 2779 (1968).
185. Taylor, J. S., and Coleman, J. E., *J. Biol. Chem.* **246**, 7058 (1971).
186. Ward, R. L., *Biochemistry* **8**, 1879 (1969).
187. Ward, R. L., and Fritz, K. J., *Biochem. Biophys. Res. Commun.* **39**, 707 (1970).
188. Morpurgo, L., Rotilio, G., Agró, A., and Mandovi, B., *Arch. Biochem. Biophys.* **170**, 360 (1975).
189. Khalifah, R. G., *Biochemistry* **16**, 2236 (1977).
190. Khalifah, R. G., Strader, D. J., Bryant, S. H., and Gibson, S. M., *Biochemistry* **16**, 2241 (1977).
191. Taylor, P. W., Feeney, J., and Burgen, A. S. V., *Biochemistry* **10**, 3866 (1971).
192. Taylor, P., *J. Pharm. Sci.* **64**, 501 (1975).
193. Bertini, I., Luchinat, C., and Scozzafava, A., *J. Am. Chem. Soc.* **99**, 581 (1977).
194. Bertini, I., Luchinat, C., and Scozzafava, A., *Biochim. Biophys. Acta* **452**, 239 (1976).
195. Gerber, K., Ng, F. T. T., Pizer, R., and Wilkins, R. G., *Biochemistry* **13**, 2663 (1974).
196. Norne, J. E., Lilja, H., Lindman, B., Einarsson, R., and Zeppezauer, M., *Eur. J. Biochem.* **59**, 463 (1975).
197. Lanir, A., and Navon, G., *Biochim. Biophys. Acta* **341**, 65 and 75 (1974).
198. Yeagle, P. L., Lochmüller, C. H., and Henkens, R. W., *Proc. Natl. Acad. Sci. U.S.A.* **72**, 454 (1975).
199. Giannini, I., and Sodini, G., *NATO Adv. Study Inst. Ser., Ser. C* **18**, 423 (1975).
200. Stein, P. J., Merrill, S. P., and Henkens, R. W., *J. Am. Chem. Soc.* **99**, 3194 (1977).
201. Sund, H., and Theorell, H., in "The Enzymes" (P. D. Boyer, ed.), 2nd ed., Vol. 7, p. 27. Academic Press, New York, 1963.
- 201a. Sund, H., in "Biological Oxidations" (T. P. Singer, ed.), p. 603. Wiley (Interscience), New York, 1968.
202. Negelein, E., and Wulff, H.-J., *Biochem. Z.* **293**, 351 (1937).
203. Bonnischen, R. K., and Wassen, A. M., *Arch. Biochem. Biophys.* **18**, 361 (1948).
204. Ulmer, D. D., and Vallee, B. L., *Adv. Chem. Ser.* **100**, 201 (1971).
205. Theorell, H., and Bonnischen, R., *Acta Chem. Scand.* **5**, 1105 (1951).
206. Theorell, H., Nygaard, P., and Bonnischen, R., *Acta Chem. Scand.* **9**, 1148 (1955).
207. Vallee, B. L., and Hoch, F. L., *J. Biol. Chem.* **225**, 185 (1957).
208. Drum, D. E., Li, T.-K., and Vallee, B. L., *Biochemistry* **8**, 3783 (1969).
209. Jörnvall, H., and Harris, J. I., *Eur. J. Biochem.* **13**, 565 (1970).
210. Jörnvall, H., *Eur. J. Biochem.* **16**, 25 (1970).
211. Åkeson, H., *Biochem. Biophys. Res. Commun.* **17**, 211 (1964).
- 211a. Zeppezauer, E., Söderberg, B.-O., Brändén, C.-I., Åkeson, Å., and Theorell, H., *Acta Chem. Scand.* **21**, 1099 (1967).
- 211b. Brändén, C.-I., *Arch. Biochem. Biophys.* **112**, 215 (1965).
212. Brändén, C.-I., Eklund, H., Nordström, B., Boiwe, T., Söderlund, G., Zeppezauer, E., Ohlsson, I., and Åkeson, A., *Proc. Natl. Acad. Sci. U.S.A.* **70**, 2439 (1973).
213. Eklund, H., Nordström, B., Zeppezauer, E., Söderlund, G., Ohlsson, I., Boiwe, T., and Brändén, C.-I., *FEBS Lett.* **44**, 200 (1974); Eklund, H., Nordström, B., Zeppezauer, E., Söderlund, G., Tapia, O., Brändén, C.-I., Ohlsson, I., Boiwe, T., Soderberg, B. O., and Åkeson, Å., *J. Mol. Biol.* **102**, 27 (1976).
214. Harris, I., *Nature (London)* **203**, 30 (1964).
215. Kagi, H. R., and Vallee, B. L., *J. Biol. Chem.* **235**, 3188 (1960).
216. Hayes, J. E., and Velick, S. F., *J. Biol. Chem.* **207**, 225 (1954).
217. Dickinson, M., *Eur. J. Biochem.* **41**, 31 (1974).
- 217a. Sytkowski, A. J., and Vallee, B. L., *Proc. Natl. Acad. Sci. U.S.A.* **73**, 344 (1976).

218. Vallee, B. L., Coombs, T. L., and Williams, R. J. P., *J. Am. Chem. Soc.* **80**, 401 (1958).
219. Brändén, C.-I., Jörnvall, H., Eklund, H., and Furugren, B., in "The Enzymes" (P. D. Boyer, ed.), 3rd ed., Vol. 11, Part A, p. 103. Academic Press, New York, 1975.
220. Scrutton, M. C., *Inorg. Biochem.*, **1**, 394 (1973).
221. Mildvan, A. S., in "The Enzymes" (P. D. Boyer, ed.), 3rd ed., Vol. 2, p. 526. Academic Press, New York, 1970.
222. Weiner, H., *Biochemistry* **8**, 526 (1969).
- 222a. Hughes, M., and Prince, R. H., *Chem. Ind. (London)* p. 648 (1975); *J. Inorg. Nucl. Chem., Bio-Inorg. Sec.* **40**, 703, 713, and 719 (1978).
223. Burton, K., and Wilson, T. H., *Biochem. J.* **54**, 86 (1953).
224. Kosower, E. M., *Biochim. Biophys. Acta* **56**, 474 (1962).
- 224a. Blumenstein, M., and Raftery, M. A., *Biochemistry* **11**, 1643 (1972).
- 224b. Birdsall, B., and Feeney, J., *J. Chem. Soc., Perkin Trans.* **2** p. 1643 (1972).
- 224c. Sarma, R. H., Moore, M., and Kaplan, N. O., *Biochemistry* **9**, 549 (1970).
- 224d. Sarma, R. H., and Kaplan, N. O., *Biochemistry* **9**, 557 (1970).
225. Barrio, J. R., Tolman, G. L., Leonard, N. J., Spencer, R. D., and Weber, G., *Proc. Natl. Acad. Sci. U.S.A.* **70**, 941 (1973).
226. Boyer, P. D., and Theorell, H., *Acta Chem. Scand.* **10**, 447 (1956).
227. Sloan, D. S., Maitland-Young, J., and Mildvan, A. S., *Biochemistry* **14**, 1998 (1975).
228. For summary, see M. Hughes and R. H. Prince, *Bioorg. Chem.* **6**, 137 (1977).
- 228a. Woenkhaus, C., and Zumpe, P., *Z. Naturforsch. B*, **23**, 484 (1968).
229. Luisi, P. L., Baici, A., Bonner, F. J., and Aboderini, A. A., *Biochemistry* **14**, 362 (1975).
230. Shore, J. D., and Santiago, D., *J. Biol. Chem.* **250**, 2008 (1975).
231. Weiner, H., Iweibo, I., and Coleman, P. L., *Wenner-Gren Cent. Int. Symp. Ser.* **18**, 619 (1972).
232. Iweibo, I., and Weiner, H., *J. Biol. Chem.* **250**, 1959 (1975).
233. Csopak, H., Lindman, B., and Lilja, H., *FEBS Lett.* **9**, 189 (1970).
234. Ward, R. L., *Biochemistry* **8**, 1879 (1969).
235. Lindman, B., Zeppezauer, M., and Å. Åkeson, *Wenner-Gren Cent. Int. Symp. Ser.* **18**, 603 (1972).
236. Zeppezauer, M., Lindman, B., Forsen, S., and Lindqvist, I., *Biochem. Biophys. Res. Commun.* **37**, 137 (1969).
237. Prince, R. H., and Woolley, P. R., unpublished work.
238. Coleman, P. L., and Weiner, H., *Biochemistry* **12**, 1707 (1973).
239. Coleman, P. L., and Weiner, H., *Biochemistry* **12**, 1705 (1973).
240. Takahashi, M., and Harvey, R. A., *Biochemistry* **12**, 4743 (1973).
241. Young, J. M., and Wang, J. H., *J. Biol. Chem.* **246**, 2815 (1971).
242. Hughes, M., Ph.D. Thesis, University of Cambridge, England (1975).
243. Drott, H. R., Santiago, D., and Shore, J. D., *FEBS Lett.* **39**, 21 (1974).
244. Mildvan, A. S., Waber, L., Villafranca, J. J., and Weiner, H., *Wenner-Gren Cent. Int. Symp. Ser.* **18**, 745 (1972).
245. Reynolds, C. H., Morris, D. L., and McKinley-McKee, J. S., *Eur. J. Biochem.* **14**, 14 (1970).
246. McFarland, J. T., Walters, K. L., and Petersen, R. L., *Biochemistry* **14**, 624 (1975).
247. Abeles, R. H., Hutton, R. F., and Westheimer, F. H., *J. Am. Chem. Soc.* **79**, 712 (1957).
248. Samama, J.-P., Zeppezauer, J.-F., Biellmann, J.-F., and Brändén, C.-I., *Eur. J. Biochem.* **81**, 403 (1977).

249. Abdallah, M. A., Biellmann, J.-F., Samama, J.-P., with Wrixon, A. D., *Eur. J. Biochem.* **64**, 351 (1976).
250. Jacobs, J. W., McFarland, J. T., Wainer, I., Jeanmaier, D., Ham, C., Hamm, K., Wnuk, M., and Lam, M., *Biochemistry* **13**, 60 (1974).
251. Dickenson, C. J., and Dickinson, F. M., *Biochem. J.* **147**, 303 (1975).
252. Dickinson, F. M., and Dickenson, C. J., *Biochem. J.* **147**, 541 (1975).
253. Shore, J. D., Gutfreund, H., Brooks, R. L., Santiago, D., and Santiago, P., *Biochemistry* **13**, 4185 (1974).
254. McFarland, J. T., and Chu, Y.-H., *Biochemistry* **14**, 1140 (1975).
255. Mildvan, A. S., and Weiner, H., *Biochemistry* **8**, 552 (1969).
256. Mildvan, A. S., and Weiner, H., *J. Biol. Chem.* **244**, 2465 (1969).
257. Jörnvall, H., *Proc. Natl. Acad. Sci. U.S.A.* **70**, 2295 (1973).
258. Sloan, D. L., and Mildvan, A. S., *Biochemistry* **13**, 1711 (1974).
259. McFarland, J. T., Chu, Y. H., and Jacobs, J. W., *Biochemistry* **13**, 65 (1974).
260. Bernhard, S. A., Dunn, M. F., Luisis, P. L., and Schack, P., *Biochemistry* **9**, 185 (1970).
261. Taniguchi, S., Yonetani, T., and Sjöberg, B., *Acta Chem. Scand.* **23**, 255 (1969).
262. Gilleland, M. L., and Shore, J. D., *Biochem. Biophys. Res. Commun.* **40**, 230 (1970).
263. Dunn, M. F., and Hutchinson, J. S., *Biochemistry* **12**, 4882 (1973).
264. Klinman, J. P., *J. Biol. Chem.* **247**, 7977 (1972).
265. Klinman, J. P., *J. Biol. Chem.* **250**, 2569 (1975).
266. Wratten, C. C., and Cleland, W. W., *Biochemistry* **4**, 2442 (1965).
267. Wratten, C. C., and Cleland, W. W., *Biochemistry* **2**, 935 (1963).
268. Ulmer, D. D., and Vallee, B. L., *Ad. Chem. Ser.* **100**, 195 (1971).
269. Williams, R. J. P., *Inorg. Chim. Acta Rev.* **5**, 137 (1971).
270. Mildvan, A. S., in "The Enzymes" (P. D. Boyer, ed.) 3rd ed., Vol. 2, p. 530 et seq. Academic Press, New York, 1970.
271. Waldschmidt-Leitz, E., *Physiol. Rev.* **11**, 358 (1931).
272. See, for example, Quiocho, F. A., and Lipscomb, W. N., *Adv. Protein Chem.* **25**, 1 (1971).
273. Coleman, J. E., *Prog. Bioorg. Chem.* **1**, 159 (1971); Ludwig, M. L., and Lipscomb, W. N., *Inorg. Biochem.* **1**, 438 (1973).
- 273a. Bishop, W. H., Quiocho, F. A., and Richards, F. M., *Biochemistry* **5**, 4077 (1966).
274. Van Wart, H. E., and Vallee, B. L., *Biochem. Biophys. Res. Commun.* **75**, 732 (1977).
275. Jones, M. M., Hunt, J. B., Storm, C. B., Evans, P. S., Carson, F. W., and Pauli, W. J., *Biochem. Biophys. Res. Commun.* **75**, 253 (1977).
276. Suh, J., and Kaiser, E. T., *Chem. Commun.* p. 106 (1976).
277. Lipscomb, W. N., Hartsuck, J. A., Quiocho, F. A., and Reeke, G. N., *Proc. Natl. Acad. Sci. U.S.A.* **64**, 28 (1969).
278. Hartsuck, J. A., and Lipscomb, W. N., *Enzymes* **3**, 1 (1971).
279. Quiocho, F. A., and Richards, F. M., *Biochemistry* **5**, 4062 (1966).
280. Bishop, W. H., Quiocho, F. A., and Richards, F. M., *Biochemistry* **5**, 4077 (1966).
281. Neurath, H., and Schwert, G. W., *Chem. Rev.* **46**, 69 (1950).
282. Koshland, D. E., *Proc. Natl. Acad. Sci. U.S.A.* **44**, 98 (1958).
283. Koshland, D. E., and Neet, K. E., *Annu. Rev. Biochem.* **37**, 359 (1968).
284. Johansen, J. T., and Vallee, B. L., *Proc. Natl. Acad. Sci. U.S.A.* **70**, 2006 (1973).
285. Johansen, J. T., and Vallee, B. L., *Proc. Natl. Acad. Sci. U.S.A.* **68**, 2532 (1971).
286. Riordan, J. F., and Vallee, B. L., *Biochemistry* **3**, 1768 (1964).
287. Johansen, J. T., and Vallee, B. L., *Proc. Natl. Acad. Sci. U.S.A.* **68**, 2532 (1971).
288. Quiocho, F. A., McMurray, C. H., and Lipscomb, W. N., *Proc. Natl. Acad. Sci. U.S.A.* **69**, 2850 (1972).
289. Johansen, J. T., Livingston, D. M., and Vallee, B. L., *Biochemistry* **11**, 2584 (1972).

290. Scheule, R. K., Van Wart, H. E., Vallee, B. L., and Scheraga, H. A., *Proc. Natl. Acad. Sci. U.S.A.* **74**, 3273 (1977).
291. Prince, R. H., and Spencer, R. C., *Inorg. Chim. Acta* **3**, 54 (1969).
292. Alcock, N. W., Prince, R. H., and Spencer, R. C., *J. Chem. Soc. A* p. 2383 (1968).
293. Spilburg, C. A., Bethune, J. L., and Vallee, B. L., *Biochemistry* **16**, 1142 (1977).
294. Alter, G. M., Leussing, D. L., Neurath, H., and Vallee, B. L., *Biochemistry* **16**, 1142 (1977).
295. Vallee, B. L., Riordan, J. F., and Coleman, J. E., *Proc. Natl. Acad. Sci. U.S.A.* **49**, 109 (1963).
296. Kaiser, E. T., and Kaiser, B. T., *Acc. Chem. Res.* **5**, 219 (1972).
297. Diamond, I., Swenerton, H., and Hurley, L. S., *J. Nutr.* **101**, 77 (1971).
298. Coleman, J. E., and Vallee, B. L., *J. Biol. Chem.* **235**, 390 (1960).
299. Coleman, J. E., and Vallee, B. L., *J. Biol. Chem.* **236**, 2244 (1961).
300. Coleman, J. E., and Vallee, B. L., *J. Biol. Chem.* **236**, 3430 (1962).
301. Coleman, J. E., and Vallee, B. L., *Biochemistry* **1**, 1083 (1962).
302. Vallee, B. L., and Riordan, J. F., *Brookhaven Symp. Biol.* **21**, 91 (1968).
303. Simpson, R. T., Riordan, J. F., and Vallee, B. L., *Biochemistry* **2**, 616 (1963).
304. Riordan, J. F., and Vallee, B. L., *Biochemistry* **2**, 1460 (1963).
305. Roholt, O. A., and Pressman, D., *Proc. Natl. Acad. Sci. U.S.A.* **58**, 280 (1967).
306. Johansen, J. T., and Vallee, B. L., *Proc. Natl. Acad. Sci. U.S.A.* **68**, 2532 (1971).
307. Wacker, H., Lehky, P., Fischer, E. H., and Stein, E. A., *Helv. Chim. Acta* **54**, 473 (1971).
308. Riordan, J. F., Sokolovsky, M., and Vallee, B. L., *Biochemistry* **6**, 3609 (1967).
309. Vallee, B. L., Riordan, J. F., Bethune, J. L., Coombs, T. L., Auld, D. S., and Sokolovsky, M., *Biochemistry* **7**, 3547 (1968).
310. Davies, R. C., Riordan, J. F., Auld, D. S., and Vallee, B. L., *Biochemistry* **7**, 1090 (1968).
311. Auld, D. S., and Vallee, B. L., *Biochemistry* **10**, 2892 (1971).
312. Makinen, M. W., Yamamura, K., and Kaiser, E. T., *Proc. Natl. Acad. Sci. U.S.A.* **73**, 3882 (1976).
313. Breslow, R., and Wernick, D. L., *Proc. Natl. Acad. Sci. U.S.A.* **74**, 1303 (1977).
314. Hayes, D. M., and Kollman, P. A., *J. Am. Chem. Soc.* **98**, 7811 (1976).
315. Barber, A. K., and Fischer, J. R., *Proc. Natl. Acad. Sci. U.S.A.* **69**, 2970 (1972).
316. Vallee, B. L., *Ann. N.Y. Acad. Sci.* **158**, 377 (1969).
317. Reck, G. R., Walsh, K. A., Hermodson, M. A., and Neurath, H., *Proc. Natl. Acad. Sci. U.S.A.* **68**, 1226 (1971).
318. Fersht, A., "Enzyme Structure and Mechanism" Freeman, San Francisco, California, 1977.
- 318a. Dickerson, R. E., and Geis, I., "Structure and Function of Proteins." Harper, New York, 1969.
- 318b. Elmore, D. J., "Peptides and Proteins." Cambridge Univ. Press, New York, 1968.
- 318c. Laidler, K. J., and Bunting, P. S., "The Chemical Kinetics of Enzyme Action," 2nd ed. Oxford Univ. Press, London and New York, 1973.
319. "Specialist Periodical Reports: Amino-acids, Peptides and Proteins" Chem. Soc. London.
320. Williams, A., "Introduction to the Chemistry of Enzyme Action" McGraw Hill, New York, 1969.
321. Dodgson, K. S., Spencer, B., and Williams, K., *Nature (London)* **177**, 432 (1956).
322. Gutfreund, H., "An Introduction to the Study of Enzymes." Blackwell, Oxford, 1965.

- 323. Fromm, H. J., "Initial Rate Enzyme Kinetics." Springer-Verlag, Berlin and New York, 1975.
- 324. Wong, J. T.-F., "Kinetics of Enzyme Mechanisms." Academic Press, New York, 1975.
- 325. Segel, I. H., "Enzyme Kinetics." Wiley, New York, 1975.
- 326. Cornish-Bowden, A., "Principles of Enzyme Kinetics." Butterworth, London, 1975.
- 327. Cleland, W. W., *Enzymes* 2, 1 (1970).
- 327a. Cleland, W. W., in "The Enzymes" (P. D. Boyer ed.), 2nd ed., Vol. 2, p. 8 et seq. Academic Press, New York, 1970.
- 328. Dalziel, K., *Enzymes* 10, 2 (1975).
- 329. For a readable account, see Zuckerkandl, E., in "Bioorganic Chemistry," p. 53, Freeman, San Francisco, California, 1968.
- 330. Zuckerkandl, E., and Pauling, L., in "Evolving Genes and Proteins" (V. Bryson and H. J. Vogel, eds.), p. 97. Academic Press, New York, 1965.
- 331. Zuckerkandl, E., and Pauling, L., in "Horizons in Biochemistry" (M. Kasha and B. Pullman, eds.), p. 189. Academic Press, New York, 1962.
- 332. See Gutfreund, H., "An Introduction to the Study of Enzymes," pp. 278, 279, and 289. Blackwell, Oxford, 1965.

Subject Index

A

Actinide, redox reactions, 152
 Actinide thiobromide, 176
 Alcohol dehydrogenase, 390–409
 catalysis, 355
 coenzyme–enzyme interactions, 394–402
 liver, 390
 metal ion–reactivity relationships, 392, 393
 structure, 392
 metal ion–enzyme interactions, 408, 409
 reactions, 390, 391
 substrate–enzyme interactions, 402–408
 visible spectrum, 409
 yeast, 390
 metal ion–reactivity relationships, 393, 394
 structure, 392
 zinc in, 350
 Alkaline phosphatase, zinc and, 353
 Aluminum, nuclear magnetic shielding, 222
 Americium, as oxidizing agent, 152
 Amino acid, structure, 423
 Ammonia, chlorination, 116
 Ammonium salt $[(\text{NH}_4)_2\text{MCl}_6]$, lattice energy, 23
 Angeli's salt, 140–143, *see also* Trioxodinitrate
 decomposition, 141–143
 Anisotropy, 203
 Antifluorite salts, 1–105, 107–111, *see also* specific substances
 charge distributions, 16, 17, 94, 95
 lattice energy, 1–5, 9
 calculation, 10–17
 estimated, 17–22
 Antimony(IV) salts, lattice energy and thermochemistry, 84
 Apoenzyme, 424
 Aspartate transcarbamylase, role of zinc, 356

Atherosclerosis, zinc in, 350
 Atomic orbitals, gauge-invariant (GIAO), 205

B

Binding energy, metal–sulfur, 340
 Bond energy, 6, 7, 98, 99
 diagram, 8
 Bond fission
 heterolytic, 6, 7
 homolytic, 6
 Bond strength, 6, 7
 lattice energy and, 103, 104, 107
 metal–halogen, 7, 10
 Born–Fajans–Haber cycle, 2, 6
 Boron, nuclear magnetic shielding, 218, 221, 222
 Bromate, as oxidizing agent, 132, 133

C

Cadmium, carbonic anhydrase substitution, 362
 Carbon dioxide hydration
 catalysis, 365–637
 reversible, enzyme-catalyzed, 367–370
 Carbonic anhydrase, 356–389
 active sites, 372–375
 anion binding sites, 382–387
 binding of zinc to, 363–365
 rate and equilibrium parameters, 364
 carbonyl hydration, 365–367
 reversible, 367–370
 catalytic properties, 365–371
 human
 vs bovine, 357, 358
 zinc ligands, 359
 hydrolysis, pH dependence, 371
 hydrolytic reactions, 370–372
 inhibition by anions, 379–387

- Carbonic anhydrase (*cont'd.*)
 by sulfonamides, 375–379
 inhibition constants, 380
 inhibitor binding constant, 385
 ionizable water ligand, 373–375
 isozymes, 357, 358
 structure, 357–361
 macrocyclic ligands, 374
 mechanism of action, 387–389
 relaxation measurements, 372, 373
 structure, 357–361
 visible absorption spectrum, 376, 381
 zinc in, 350, 357–361
 zinc coordination, 357–361
- Carbonic anhydrase B, 357
 human, hydrogen bonding, 360
- Carbonic anhydrase C, 357
 human, active site, 360
- Carbonyl hydration
 catalysis of, 365–367
 reversible, enzyme-catalyzed, 367–370
- Carboxypeptidase A, 409–421
 active site, 418
 catalytic mechanism, 416–421
 chemical properties vs. structure, 417–419
 enzyme–substrate interactions, 416–421
 kinetics vs. structure, 419–421
 structure, 413–416
 substrate binding, 412
 zinc in, 350, 409–421
- Cerium, as oxidizing agent, 120, 124, 132
- Cesium salt (Cs_2MCl_6), lattice energy, 22
- Charge distribution, 94, 95
- Chloramine, formation, 116, 117
- Chlorine, nuclear magnetic shielding, 224
- Chromium
 as oxidizing agent, 119, 127
 reaction with nitric acid, 162
 as reducing agent, 156
- Chromium complex, azide reactions, 134, 135
- Chromium-1,2-dithiolene complexes, 313–315
- Chromium(IV) salts, lattice energy and thermochemistry, 40
- Chromium selenoiodide, 180
- Chromium telluroiodide, 180
- Chromium thiobromide, 180
- Chromium thiodiodide, 180
- Cobaloxime, partial field gradients, 215, 216
- Cobalt
 carbonic anhydrase substitution, 361–363
 magnetic circular dichroism, 363
 NQR, 216, 217
 nuclear magnetic shielding, 225, 226, 228
 oxidation of nitrous acid, 152
 as oxidizing agent, 120, 124, 125, 131
- Cobalt complex, azide reactions, 134
- Cobalt–1,2-dithiolene complexes, 323–327
 reaction mechanisms, 324
 reactions with Lewis bases, 320
 structure, 318
- Cobalt(IV) salts, lattice energy and thermochemistry, 59, 60
- Copper
 carbonic anhydrase substitution, 362
 as oxidizing agent, 120, 126
- Copper chalcogenide halide, X-ray diffraction, 193
- Copper–1,2-dithiolene complexes, 333–335
 synthesis, 334
- Copper metalloenzyme, 355
- Copper peroxonitrite, decomposition of hydroxylamine, 122
- Copper selenohalide, 193, 194
- Copper tellurobromide, crystal structure, 194
- Copper tellurohalide, 193, 194
- Cornwell effect, 203
- Corrosion inhibition, 244
- Crystal field theory, nuclear magnetic shielding and, 225
- Cyclic sulfur–nitrogen compounds, *see* Sulfur–nitrogen compounds, cyclic

D

- Dansylamide, binding to carbonic anhydrase, 379
- Deshielding, 200, *see also* Nuclear magnetic shielding
- Diamagnetic current, 199–201
- Diamagnetic shielding, 200
- Diamagnetism
 terms, 207
 theory, 204
 Xps and, 207–210
- Diazene, *see* Diimide
- Diimide, reaction mechanisms, 121

Dinitrogen tetroxide, reaction mechanisms, 156–160
Dispersion energy, *see* Lattice energy
1,2-Dithiolate ligands, 304–310
1,2-Dithiolene, complexes of transition metals, 303–343, *see also* specific elements
 electrochemistry, 342, 343
 electronic spectra, 339
 ESR, 338, 339
 infrared spectra, 337, 338
 magnetic studies, 338, 339
 Mössbauer spectra, 341
 polarography, 311
 synthesis, 304–310
 X-ray photoelectron spectra, 339–341
 X-ray structure, 336, 337

E

Electric field gradient, 214–218
Electrochemistry, transition metal–1,2-dithiolene complexes, 342, 343
Electron spin resonance, transition metal–1,2-dithiolene complexes, 338, 339
Enthalpy
 of formation, lattice energy and, 96–100, 111
 of hydration of ions, 100, 101
Enzyme kinetics, 424–431
Erythrocytes
 carbonic anhydrase, 356
 human vs. bovine, 358
ESR, *see* Electron spin resonance
Excitation energy, 213, 214

F

Ferredoxin, 317, 319
Finite perturbation theory, 211, 212
Fischer–Hepp rearrangement, 151
Fluorine, nuclear magnetic shielding, 212, 223, 224, 227
Flygare method, 208
Fungicide, 244

G

Gallium, nuclear magnetic shielding, 222
Genetics, role of zinc in, 350
Germanium, nuclear magnetic shielding, 223

Germanium(IV) salts, lattice energy and thermochemistry, 73–76
Gold–1,2-dithiolene complexes, 333–335
Gold selenobromide, 194
Gold selenochloride, 194
Gold tellurobromide, 194
 preparation, 195
Gold tellurochloride, 194
 preparation, 195
Gold tellurohalide, 194, 195
Gold telluroiodide, 194
 preparation, 195

H

Hafnium–1,2-dithiolene complexes, 310–312
Hafnium(IV) salts, lattice energy and thermochemistry, 34–36
Halide ion affinity, 7, 9
 lattice energy and, 101–103, 109
Haloenzyme, 424
Hexabromohafnate ion, lattice energy and thermochemistry, 36
Hexabromoosmate ion
 charge distribution, 59
 lattice energy, 59
 radius, 57, 59
 structure, 58
Hexabromoplatinate ion
 charge distribution, 68
 enthalpy, 68, 69
 halide ion affinities, 69
 lattice energy, 68, 69
 radius, 66, 68
 structure, 68
Hexabromorhenate ion
 charge distribution, 92
 lattice energy, 92
 radius, 92
 structure, 91
Hexabromorhinate ion
 charge distribution, 55
 enthalpy, 55, 56
 halide ion affinities, 56
 lattice energy, 55, 56
 radius, 53, 55
 structure, 55
Hexabromoselenate ion
 charge distribution, 86

- Hexabromoselenate ion (*cont'd.*)
 lattice energy, 86
 radius, 85, 86
 structure, 85
- Hexabromostannate ion
 charge distribution, 80
 lattice energy, 81
 radius, 76, 81
 structure, 80
- Hexabromotellurate ion
 charge distribution, 89
 enthalpy, 90
 halide ion affinity, 90
 lattice energy, 90
 radius, 87, 90
 structure, 89
- Hexabromotitanate ion
 charge distribution, 29
 enthalpy, 29, 30
 halide ion affinity, 30, 31
 lattice energy, 29, 31
 radius, 27, 29
 structure, 29
- Hexabromotungstate ion
 charge distribution, 46
 electron affinity, 48
 enthalpy, 47, 48
 halide ion affinities, 48
 lattice energy, 47, 48
 radius, 44, 47
 structure, 46
- Hexabromozirconate ion, lattice energy and
 thermochemistry, 34
- Hexachlorogermanate ion
 charge distribution, 75
 enthalpy, 75, 76
 halide ion affinity, 75
 lattice energy, 75
 radius, 74, 75
 structure, 75
- Hexachlorohafnate ion
 charge distribution, 34
 enthalpy, 35
 halide ion affinities, 35
 lattice energy, 34–36
 radius, 35
 structure, 34, 35
- Hexachloroiridate ion
 charge distribution, 60
 enthalpy, 61
 lattice energy, 60–62
 radius, 60, 61
 structure, 60
- Hexachloromanganate ion
 charge distribution, 49
 lattice energy, 49–51
 radius, 50
 structure, 49, 51
- Hexachloromolybdate ion
 charge distribution, 41
 enthalpy, 41–43
 halide ion affinities, 41, 43
 lattice energy, 41–43
 radius, 41
 structure, 40, 42
- Hexachloroniobate ion
 enthalpy, 37
 halide ion affinities, 37
 lattice energy, 37, 38
 structure, 36
- Hexachloroosmate ion
 charge distribution, 57
 enthalpy, 58
 halide ion affinities, 58
 lattice energy, 57, 58
 radius, 57
 structure, 56, 58
- Hexachloropalladate ion
 charge distribution, 63
 enthalpy, 64, 65
 lattice energy, 63, 64
 radius, 63
 structure, 62, 64
- Hexachloroplatinate ion
 charge distribution, 65
 enthalpy, 66, 67
 halide ion affinities, 67
 lattice energy, 65, 67, 68
 radius, 65, 66
 structure, 65
- Hexachloroplumbate ion
 charge distribution, 82
 enthalpy, 82, 83
 halide ion affinities, 83, 84
 lattice energy, 82
 radius, 82, 83
 structure, 82
- Hexachloropolonate ion
 charge distribution, 91
 lattice energy, 91
 radius, 91, 92
 structure, 91

- Hexachlororhenate ion**
charge distribution, 52
enthalpy, 52, 53, 55
halide ion affinities, 53
lattice energy, 52, 54, 55
radius, 52, 53
structure, 52, 54
- Hexachlororuthenate ion**
lattice energy, 56
structure, 56
- Hexachloroselenate ion**
charge distribution, 84
lattice energy, 84
radius, 85
structure, 84
- Hexachlorostannate ion**
charge distribution, 77
enthalpy, 77–79
halide ion affinities, 79
lattice energy, 77, 80
radius, 76, 77
structure, 77
- Hexachlorotantalate**
enthalpy, 38, 39
halide ion affinities, 39
lattice energy, 38, 39
structure, 38
- Hexachlorotechnetate ion**
charge distribution, 51
lattice energy, 51, 52
radius, 51
structure, 51
- Hexachlorotellurate ion**
charge distribution, 86
enthalpy, 87–89
halide ion affinity, 88, 89
lattice energy, 86, 89
radius, 87
structure, 86, 89
- Hexachlorotitanate ion**
charge distribution, 26
enthalpy, 26, 27
halide ion affinities, 28
lattice energy, 26, 28, 29
radius, 26, 27
structure, 25
- Hexachlorotungstate ion**
charge distribution, 44
electron affinity, 46
enthalpy, 45, 46
halide ion affinities, 46
lattice energy, 44
radius, 44, 45
structure, 43
- Hexachlorozirconate ion**
charge distribution, 31
enthalpy, 32, 33
halide ion affinities, 33
lattice energy, 31, 33, 34
radius, 31, 32
structure, 31
- Hexafluorochromate ion**
charge distribution, 40
lattice energy, 40
radius, 40
structure, 40
- Hexafluorocobaltate ion**
charge distribution, 59
lattice energy, 59
radius, 59, 60
structure, 59
- Hexafluorogermanate ion**
charge distribution, 73
enthalpy, 73
halide ion affinity, 74
lattice energy, 73
radius, 73, 74
structure, 73
- Hexafluoromanganate ion**
charge distribution, 49
lattice energy, 49
radius, 49, 50
structure, 48
- Hexafluoronickelate ion**
charge distribution, 62
enthalpy, 62
lattice energy, 62
radius, 62, 63
structure, 62
- Hexafluorosilicate ion**
charge distribution, 70
enthalpy, 70–72
halide ion affinities, 72, 73
lattice energy, 70
radius, 70, 71
structure, 70
- Hexaiodotellurate ion**
charge distribution, 91
lattice energy, 91
structure, 90
- Hexaiodostannate ion**
charge distribution, 81

lattice energy, 81
radius, 76, 82
structure, 81
Hexahalometallate(IV) complexes, 1–105,
107–111, *see also* specific complexes
Hydrazine
 reaction mechanisms, 118–121
 oxidizing agents, 118–121
 protonation, 118
 reaction with nitrous acid, 151, 152
Hydrazoic acid, reaction mechanisms,
 131–135
 of coordinated azide ion, 133–135
 oxidation by metals, 131, 132
 by nonmetals, 132, 133
Hydrogen, nuclear magnetic shielding, 213,
 214
Hydroxylamine
 oxidation by nitric acid, 161
 reaction mechanisms, 122–128
 decomposition in alkaline solution, 122,
 123
 oxidizing agents, 124–128
 photolysis, 123
 radiolysis, 123
 reducing agents, 128
 sulfonic acids, 128–131, *see also* specific
 compounds
Hydroxylamine-*N*-monosulfonic acid, 129
Hydroxylamine-*O*-sulfonic acid, reaction
 mechanisms, 128, 129
Hyponitrous acid, reaction mechanisms,
 135–137
 decomposition, 136
 oxidation, 136, 137

I

Infrared spectroscopy, 177, 186, *see also*
 specific compounds
 transition metal–1,2-dithiolene com-
 plexes, 337, 338
Iodine, reaction with nitric acid, 161, 162
Iridium complex, azide reactions, 133
Iridium–1,2-dithiolene complexes, 323–327
 hydrogen bonding, 327
Iridium(IV) salts, lattice energy and ther-
 mochemistry, 60–62
Iron
 oxidation of hydroxylamine, 124–126

 as oxidizing agent, 152
 as reducing agent, 155
Iron–1,2-dithiolene complexes, 317–323
 reactions with Lewis bases, 320
 structure, 318

L

LADH, *see* Alcohol dehydrogenase, liver
Lanthanide thiobromide, 176
Lanthanum selenofluoride, 176
Lanthanum thiobromide, 176
Lanthanum thiochloride, 176
Lanthanum thiofluoride, 176
Lanthanum thiohalide, 176
Lanthanum thioiodide, 176
Lattice energy, *see also* specific species
 of antiferroite salts, 1–5, 9
 associated data, 24–92
 calculation, 10–17
 charge dependence, 15
 comparison with literature calculations,
 95, 96
 computations, 24–92
 derived estimates, 25, 93
 estimated, 17–22, 93
 format, 24
 of hexahalometallate(IV) complexes,
 1–105, 107–111
 potential, 10
 repulsion, 11
 theory, 10–16
 unit cell parameter, 11
LCAO-MO theory, 204
Lead, nuclear magnetic shielding, 224
Lead(IV) salts, lattice energy and ther-
 mochemistry, 82–84
Lewis acids, adduct with N_4S_4 , 283–287
Ligand, bidentate, S–N compounds, 261–
 264
Ligand field splitting, 200

M

Madelung constant, 12
Manganese
 carbonic anhydrase derivative, 362
 NQR, 216, 217
 nuclear magnetic shielding, 225

- oxidation of nitrous acid, 152, 153
 - as oxidizing agent, 120, 124, 132
 - Manganese-1,2-dithiolene complexes, 316, 317
 - Manganese(IV) salts, lattice energy and thermochemistry, 48-51
 - Manganese selenobromide, 192
 - Manganese selenochloride, 192
 - Manganese seleniodide, 192
 - Manganese thiochloride, 192
 - Mass spectrometry, 188, *see also* specific compounds
 - Mercury
 - carbonic anhydrase substitution, 362
 - nuclear magnetic shielding, 224, 225
 - Metal-halogen bond strength, 7, 10
 - Metallocarbonic anhydrase, 361-365
 - metal substitution, 361-363
 - Metallo-carboxypeptidase
 - kinetic constants, 411
 - stability constants, 411
 - Mössbauer effect, 214-218
 - Mössbauer spectroscopy, transition metal-1,2-dithiolene complexes, 341
 - Molybdenum
 - as oxidizing agent, 120
 - reaction with nitric acid, 162-164
 - as reducing agent, 156
 - Molybdenum-1,2-dithiolene complexes, 313-315
 - crystal structure, 315
 - Molybdenum(IV) salts, lattice energy and thermochemistry, 40-43
 - Molybdenum selenobromide, 185
 - Molybdenum selenochloride, 185
 - Molybdenum selenohalide, 180, 185, 186
 - Molybdenum tellurohalide, 186
 - Molybdenum thiobromide, 184
 - crystal structure, 181
 - Molybdenum thiochloride, 180-184
 - crystal structure, 184, 185
 - Molybdenum thiohalide, 180-185
 - IR spectra, 182, 186
 - magnetic moments, 182
 - Raman spectra, 186
- N**
- Neptunium
 - oxidation, 159
 - as oxidizing agent, 152
 - Nickel, carbonic anhydrase substitution, 362
 - Nickel cyanide complex, decomposition of hydroxylamine, 122, 123
 - Nickel-1,2-dithiolene complexes, 327-333
 - adduct formation, 331
 - commercial uses, 333
 - kinetics, 329, 330
 - structure, 329
 - Nickel(IV) salts, lattice energy and thermochemistry, 62
 - Nicotinamide adenine dinucleotide, LADH/YADH reactions, 391
 - Niobium dithiodichloride, 278
 - Niobium-1,2-dithiolene complexes, 312, 313
 - Niobium(IV) salts, lattice energy and thermochemistry, 36-38
 - Niobium thiobromide, 177
 - Niobium thiochloride, 177
 - Niobium thiodichloride, 176
 - Niobium thiohalide
 - IR spectra, 177-179
 - Raman spectra, 178, 179
 - Niobium selenobromide, 177
 - Niobium selenochloride, 177
 - Nitramide, reaction mechanisms, 138, 139
 - acid catalysis, 139
 - Nitrate reductase, 163
 - Nitration, 147
 - Nitric acid
 - as oxidizing reagent, 161-164
 - reaction mechanisms, 160-164
 - photolysis, 160, 161
 - radiolysis, 160, 161
 - Nitric oxide, reaction mechanisms, 139-141
 - pulse radiolysis, 140
 - Nitroamine, *see* Nitramide
 - Nitrogen
 - electronegativity, 242, 243
 - nuclear magnetic shielding, 214, 222
 - Nitrogen compounds, *see also* specific compounds
 - reaction mechanisms, 113-164
 - Nitrogen dioxide, reaction mechanisms, 156-160
 - Nitrogen-sulfur compounds, *see* Sulfur-nitrogen compounds
 - Nitrogen tribromide, reaction mechanism, decomposition, 117, 118

- Nitrogen trichloride, reaction mechanism
 chlorination, 116
 decomposition, 116, 117
Nitrogen trihalide, reaction mechanisms,
 116–118
p-Nitrophenyl acetate, enzymic hydrolysis,
 370, 371
Nitrosating agents, 144, 145
Nitrosation, electrophilic, 144–152
N-Nitrosohydroxylamine *N*-sulfonate, reac-
 tion mechanisms, 130, 131
Nitrosonium ion, 146
Nitrosyl compound, rate constants, 145
Nitrosyldisulfonic acid, reaction mecha-
 nisms, 129, 130
Nitrous acid
 decomposition, rate constants, 157
 as oxidizing agent, 133
 reaction mechanisms, 143–156
 electrophilic nitrosations, 144–152
 with inorganic species, 148, 149
 nitrite oxidation by metals, 152–154
 oxidation by halogens, 154, 155
 in solution, 143, 144
 reduction by metals, 155, 156
Nitroxyl, reaction mechanisms, 138
Nuclear fuel reprocessing, 151
Nuclear magnetic shielding, 199–231, 236,
 237, *see also* specific elements
 atom in a molecule approximation, 204–
 207
 correlations with spectroscopic and other
 properties, 230, 231
 electric field gradient, 214, 215
 excitation energies, 213, 214
 finite perturbation theory, 211, 212
 in inorganic molecules, 212–221
 local symmetry, 218–221
 main group elements, 221–225
 Mössbauer effect, 214, 216–218
 nuclear quadrupole coupling constant,
 214–216
 radial factor, 214, 215
 Ramsey theory, 201–204
 restricted term approximations, 210, 211
 shielding tensor, 218–221
 substituent effects, 218–221
 terms, 201–212
 theory, 201–204
 transition metals, 225–230
Nuclear quadrupole coupling constant,
 214–218
- O**
- Osmium–1,2-dithiolene complexes, 317–323
Osmium(IV) salts, lattice energy and ther-
 mochemistry, 56–59
Oxidizing agent, 124–128, *see also* specific
 substance
Oxygen
 decomposition of hydroxylamine, 123
 nuclear magnetic shielding, 214
- P**
- Palladium–1,2-dithiolene complexes, 327–
 333
 structure, 330
Palladium(IV) salts, lattice energy and
 thermochemistry, 62–65
Paramagnetic current, 199–201
Paramagnetism, temperature-independent,
 203
Pernitrous acid, 147
Phosphorus, nuclear magnetic shielding,
 218, 223
Photolysis, nitric acid, 160, 161
Platinum
 nuclear magnetic shielding, 226, 227, 229,
 230
 as oxidizing agent, 121, 128
Platinum–1,2-dithiolene complexes, 327–
 333
 structure, 330
Platinum(IV) salts, lattice energy and ther-
 mochemistry, 65
Platinum thiohalide, 193
Plutonium
 autocatalytic reoxidation, 151
 oxidation, 159
 as oxidizing agent, 124
Polarography, 342
Polonium(IV) salts, lattice energy and ther-
 mochemistry, 91, 92
Potassium salt (K_2MCl_6), lattice energy, 20
Potassium permanganate, oxidation of ni-
 trous acid, 153

Protein, structure, 423, 424
 Protein-sulfonamide interaction, 377
 Pulse radiolysis, 123, 140, 156, 157
 nitric acid, 160, 161

Q

Quinoxaline-2,3-dithiol, 328

R

Radial factor, 214–218
 Raman spectroscopy, 178, 179, 186, *see also*
 specific compounds
 Ramsey theory, 201–204
 Reaction mechanism of nitrogen com-
 pounds, 113–164
 Reducing agent, 128, *see also* specific sub-
 stance
 Relaxation process, 209
 Rhenium, NQR, 216
 Rhenium–1,2-dithiolene complexes, 316,
 317
 Rhenium(IV) salts, lattice energy and ther-
 mochemistry, 52–56
 Rhenium selenobromide, 192, 193
 Rhenium selenochloride, 192
 Rhenium selenohalide, 192, 193
 Rhenium thiobromide, 192
 Rhenium thiochloride, 192
 Rhodium–1,2-dithiolene complexes, 323–
 327
 synthesis, 326
 Rubidium salt (Rb_2MCl_6), lattice energy, 21
 Ruthenium complex, azide reactions, 133,
 135
 Ruthenium–1,2-dithiolene complexes,
 317–323
 Ruthenium(IV) salts, lattice energy and
 thermochemistry, 56

S

Selenium, nuclear magnetic shielding, 223
 Selenium(IV) salts, lattice energy and ther-
 mochemistry, 84–86
 Selenohalide, 171–195, *see also* specific
 compound
 Shielding, *see* Nuclear magnetic shielding

Shielding tensor, 218–221
 Silicon, nuclear magnetic shielding, 222
 Silicon(IV) salts, lattice energy and ther-
 mochemistry, 70–73
 Silver, as oxidizing agent, 124
 Silver–1,2-dithiolene complexes, 333–335
 Silver tellurobromide, 194
 Silver tellurochloride, 194
 Spin-rotation constant, 209, 210
 Sulfamic acid, reaction mechanism
 hydrolysis reactions, 115
 oxidation by nitric acid, 115, 116
 Sulfonamide
 inhibition of carbonic anhydrase, 375–379
 inhibition constants, 375
 Sulfonic acid, derived from hydroxylamine,
 128–131
 Sulfur
 bonding properties, coordination number
 three and four, 272, 273
 coordination numbers, 240, 241
 D_{4h} symmetry, 243
 electronegativity, 242, 243
 ligands with transition metals, 303
 Sulfur diimide, 247, 248
 X-ray data, 248
 Sulfur–metal binding energy, 340
 Sulfur–nitrogen–carbon–oxygen ring, 245
 Sulfur–nitrogen–carbon ring, 242, 245,
 255–260, 277, 278, 281
 Sulfur–nitrogen compounds, cyclic, 239–
 294
 coordination number two at S and N
 atom, 242, 243
 eight-membered ring, 281–292
 bonding in, 281–284
 coordination numbers two and three,
 284–290
 coordination numbers two, three, and
 four, 290–292
 structure, 281–284
 five-membered rings, 248–264
 bidentate ligands, 261–264
 containing one other element, 253–261
 structure, 254–257
 radical cations, 248–250
 structure, 249, 250
 related to N_2S_3^+ , 250–253
 structure, 250–252

- Sulfur-nitrogen compounds, cyclic (*cont'd.*)
 four-membered rings, 243–248
 containing one other element, 245–248
 doubly coordinated sulfur, 243, 244
 resonance structures, 244
 four-coordinated sulfur, 244, 245
 three-coordinated sulfur, 244, 245
 seven-membered ring, 280, 281
 containing one other element, 281
 doubly-coordinated S, N, 280, 281
 six-membered ring, 264–279
 containing one other element, 276–279
 coordination number two at N, four at S, 269–272
 coordination number two at S and N, 265, 266
 coordination number two and/or three at S and N, 266–269
 doubly coordinated N, three-and/or four-coordinated S, 273, 274
 doubly coordinated S and N, 264, 265
 sulfur bonding properties, 272, 273
 three-coordinated N, four-coordinated S, 276
 two-and four-coordinated S, 274–276
 ten-membered rings, 292, 293
 three-membered rings, 240–242
 twelve-membered rings, 293, 294
Sulfur–nitrogen–metal ring, 247, 253, 254, 261–264
Sulfur–nitrogen–oxygen ring, 276, 277, 279
Sulfur–nitrogen–phosphorus ring, 246, 247, 276, 277, 279
Sulfur–nitrogen–silicon ring, 246
Superoxide dismutase, catalysis, 355
Symmetry, nuclear magnetic shielding and, 218–221
- T**
- Tantalum dithiodichloride, 180
Tantalum–1,2-dithiolene complexes, 312, 313
Tantalum salts, lattice energy and thermochemistry, 38–40
Tantalum selenobromide, 180
Tantalum thiobromide, 180
Tantalum thiochloride, 179, 180
Tantalum thiohalide, 179, 180
 IR spectra, 177
Technetium–1,2-dithiolene complexes, 316, 317
Technetium(IV) salts, lattice energy and thermochemistry, 51, 52
Tellurium(IV) salts, lattice energy and thermochemistry, 86–91
Tellurohalide, 171–195, *see also* specific halide
Tetrazene, reaction mechanisms, 121, 122
Thallium
 nitrite oxidation, 153
 nuclear magnetic shielding, 224, 225
 as oxidizing agent, 119, 120, 124
Thermochemical cycle, 2, 6
Thermochemistry of hexahalometallate(IV) complexes, 1–105, 107–111
 standard data, 22–24
Thiocyanate, oxidation of, 149
Thiohalide, 171–195, *see also* specific compound
Thiourea, reaction with nitrous acid, 149, 150
Tin, nuclear magnetic shielding, 223
Tin(IV) salts, lattice energy and thermochemistry, 77–82
Titanium, as reducing agent, 128
Titanium–1,2-dithiolene complex, 310–312
 NMR, 312
Titanium(IV) salts, lattice energy and thermochemistry, 25–31
Titanium thiochloride, 176, 177
Townes–Dailey model, 216
Transition metal, *see also* specific element
 nuclear magnetic shielding, 225–230
Transition metal complexes, *see also* specific compound
 with 1,2-dithiolene, 303–343
 nuclear magnetic shielding, 218, 219
 with sulfur
 commercial uses, 304
 synthesis, 304–310
Transition metal selenohalide, 173
 preparation, 173
Transition metal tellurohalide, 173
 preparation, 174
Transition metal thiohalide 172
 preparation, 173
Trioxodinitrate, reaction mechanisms, 141–143
Tungsten–1,2-dithiolene complexes, 313–315

Tungsten(IV) salts, lattice energy and thermochemistry, 43–48
 Tungsten selenobromide, 188
 Tungsten selenochloride, 188–190
 Tungsten selenofluoride, 191
 Tungsten selenohalide, 186, 188
 Tungsten tellurohalide, 191
 Tungsten thiobromide, 188
 Tungsten thiochloride, 186–188
 crystal structure, 187, 189
 mass spectrum, 188
 Tungsten thiofluoride, 190, 191
 ¹⁹F NMR, 190
 Tungsten thiohalide, 186–188
 IR spectra, 182
 magnetic moments, 182

U

Uranium
 oxidation, 159
 as oxidizing agent, 132

V

Vanadium
 as oxidizing agent, 120, 126
 as reducing agent, 128
 Vanadium–1,2-dithiolene complexes, 312, 313
 ESR, 313
 Vanadium thiobromide, 177
 Vanadium thiochloride, 177
 Voltammetry, 342

W

Water
 ionization in macrocyclic complexes, 374
 zinc-bound, 373–375
 Wound healing, role of zinc in, 350

X

Xenon shielding, 236, 237

X-ray diffraction, 174, 175, 193, *see also* specific substances
 1,2-dithiolene complexes of transition metals, 336, 337
 of N–S compounds, 283
 X-ray photoelectron spectroscopy, 206
 core-binding energy, 207
 nuclear magnetic shielding, 207–210
 transition metal–1,2-dithiolene complexes, 339–341

Y

YADH, *see* Alcohol dehydrogenase, yeast
 Yttrium selenofluoride, 174
 crystal structure, 174–176
 Yttrium thiofluoride, 174
 crystal structure, 174
 Yttrium thiohalide, 174

Z

Zeeman effect, 204
 Zinc
 binding to carbonic anhydrase, 363–365
 rate and equilibrium parameters, 364
 bioinorganic chemistry of, 349–431
 in biological systems, 349–351
 coordination, 351–354
 in carbonic anhydrase, 357–361
 in carboxypeptidase, 413–416
 deficiency, 350
 in enzymes, *see* specific enzyme
 metal substitution, 361–363
 Zinc metalloenzymes, 350, *see also* specific enzymes
 amino acid side chains, 351, 352
 characterization of, 354, 355
 ligand geometry, 352
 reactions catalyzed by, 355, 356
 thermodynamics, 353
 Zirconium–1,2-dithiolene complexes, 310–312
 Zirconium(IV) salts, lattice energy and thermochemistry, 31–34